Final Technical Report

OTEC COLD WATER PIPE-PLATFORM SUBSYSTEM DYNAMIC INTERACTION VALIDATION

U.S. Department of Energy Award Number DE-EE0003637
September 2010 – December 2013

Prepared by:

Lockheed Martin Corporation
Mission Systems & Training
9500 Godwin Drive
Manassas, VA 20110-4147

Program Manager
Robert Varley
(703) 367-1955
robert.varley@lmco.com

Principal Investigator
John Halkyard, Sc. D., P.E.
John Halkyard & Associates, LLC
Houston, Texas

Peter Johnson
Rizwan Sheikh, PhD
BMT Scientific Marine Services, Inc.

Shan Shi, PhD, PE
Houston Offshore Engineering

Thiago Marinho
Universidade Federal do Rio de Janeiro
LabOceano

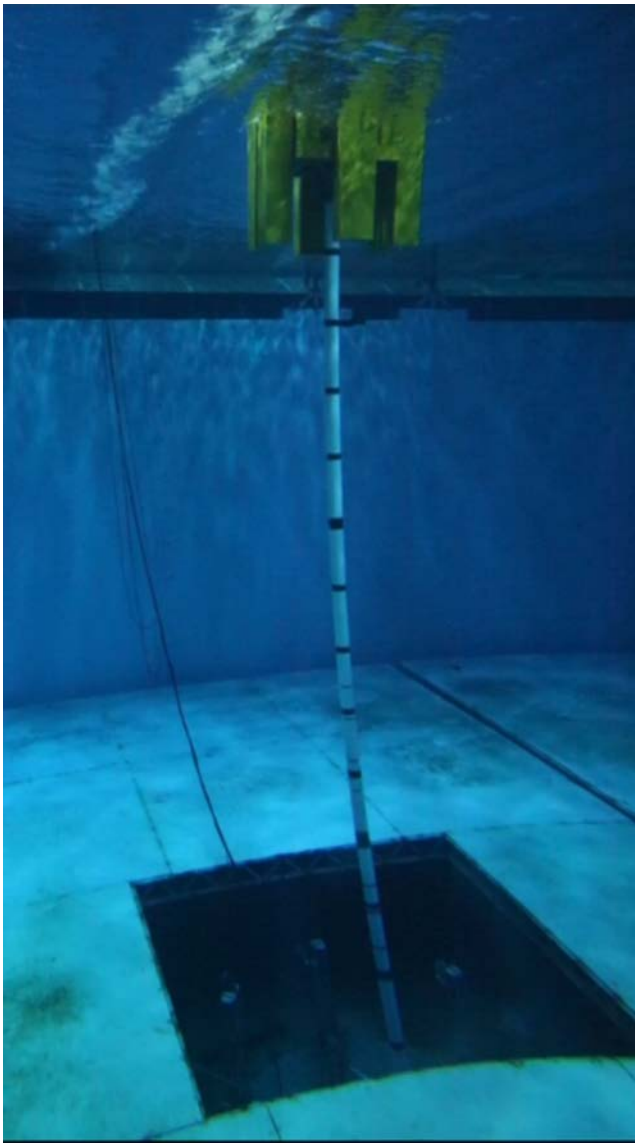

Revision 1 - 9 May 2014

ACKNOWLEDGEMENTS

This report is based upon work supported by the United States Department of Energy under Award Number DE-EE0003637.

Under the DE-EE0003637 cooperative agreement, Lockheed Martin Corporation provided internal research and development funding to support this work and report.

In addition, Petrobras provided many of the model basin test days allowing for an expanded number of configurations tested.

The success of this project was due to the teamwork of numerous contributors. Principal team member names and roles are:

Lockheed Martin Corporation	Robert Varley, Program Manager
	Matt Ascari, Prior Program Manager
	Lonnie Manns, Subcontracts Manager
John Halkyard & Associates, Inc.	Dr. John Halkyard, Principal Investigator
BMT Scientific Marine Services, Inc.	Rizwan Sheikh, Test Oversight & Data Collection
	Peter Johnson, Test Oversight & Data Collection
	James Ng, Test Oversight & Data Collection
Houston Offshore Engineering	Dr. Shan Shi, Numerical Analysis
LabOceano, COPPE-UFRJ	Thiago Marinho, Model Development & Test Conduct
	Joel Sena, Model Development & Test Conduct
Makai Ocean Engineering, Inc.	Nick Reese, Handling System Parameters

DISCLAIMER

CONTENTS

TABLE OF FIGURES

LIST OF TABLES

This page intentionally left blank.

EXECUTIVE SUMMARY

A commercial floating 100-megawatt (MW) ocean thermal energy conversion (OTEC) power plant will require a cold water pipe (CWP) with a diameter of 10-meter (m) and length of up to 1,000 m. The mass of the cold water pipe, including entrained water, can exceed the mass of the platform supporting it.

The offshore industry uses software-modeling tools to develop platform and riser (pipe) designs to survive the offshore environment. These tools are typically validated by scale model tests in facilities able to replicate real at-sea meteorological and ocean (metocean) conditions to provide the understanding and confidence to proceed to final design and full-scale fabrication.

However, today's offshore platforms (similar to and usually larger than those needed for OTEC applications) incorporate risers (or pipes) with diameters well under one meter. Secondly, the preferred construction method for large diameter OTEC CWPs is the use of composite materials, primarily a form of fiber-reinforced plastic (FRP). The use of these material results in relatively low pipe stiffness and large strains compared to steel construction. These factors suggest the need for further validation of offshore industry software tools.

The purpose of this project was to validate the ability to model numerically the dynamic interaction between a large cold water-filled fiberglass pipe and a floating OTEC platform excited by metocean weather conditions using measurements from a scale model tested in an ocean basin test facility.

A 1:50 scale model of a 100 MW commercial OTEC plant with an elastically modeled cold water pipe (CWP) was tested in six different configurations.

- Platform configured by itself
- Platform with six power modules
- Platform with ½ length CWP (CWP fabrication configuration)
- Platform with full length CWP (CWP fabrication configuration)
- Platform with power modules, full length CWP, and free gimbal (operational configuration)
- Platform with power modules, full length CWP, and stiff gimbal (operational configuration)

The platform in the operational configuration is illustrated in Figure 1 and Figure 2.

Environments tested included seven regular wave fields and five design seas, i.e. a 100-year cyclone, 10-year swell, 10-year sea, fatigue wave, and white noise wave spectrums. Currents were not available at the model basin facility.

Instrumentation consisted of 90 different sensors measuring all facets of the environment, platform, and pipe responses. The instruments included 20 strain sensors on the pipe to measure the critical modal responses of the pipe. Of these strain sensors, only two failed during the test series.

One hundred twenty two tests were performed over the test period. Runs included system identification (or wet calibration) and wave tests. In addition, numerous "dry test" calibrations were performed to measure model and pipe physical parameters to provide data for input to the numerical model.

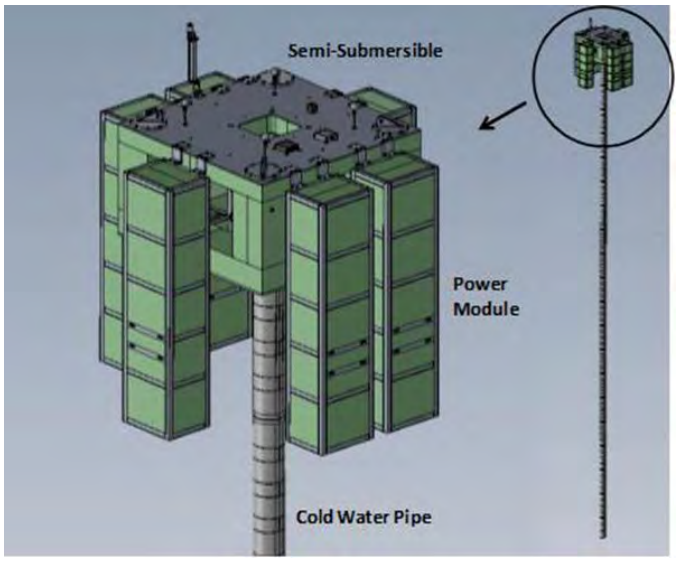

Figure 1 Platform in Operational Configuration with Power Modules & Full Length CWP

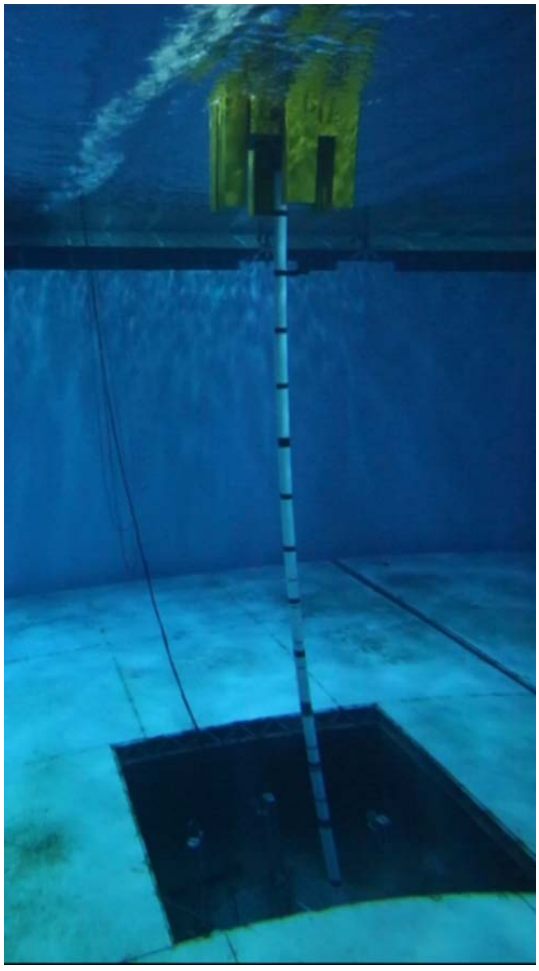

Figure 2 CWP Suspended from the Operational Platform
(Apparent CWP curvature due to visual distortion through model basin water and viewport)

The numerical model software was the coupled frequency and time domain program HARP. This state of the art program is one of the standard programs for analysis of offshore oil & gas floating platforms and risers. It is a fully "coupled" program, meaning the hydrodynamic forces and responses of the pipe and platform are solved simultaneously. Even though this analysis application has previously been calibrated against other standard industry programs for an OTEC application, comparison of results to model basin test data was required to provide confidence that analysis results were applicable to the much larger OTEC riser (pipe).

The numerical modeling approach was based on a "model the model" principle. That is, input to the numerical model was based on calibrated values from the model basin, including model platform dimensions, mass properties; model pipe mass and elastic properties, and the calibrated wave properties. Several simulations were performed using the actual wave traces from the tests for the numerical simulation.

Figure 3 and Figure 4 show the measured and computed pitch motions for the operational platform in a 10-year swell and 100-year cyclone environment, respectively. Figure 5 shows the measured and computed strain envelops along the CWP for one test run.

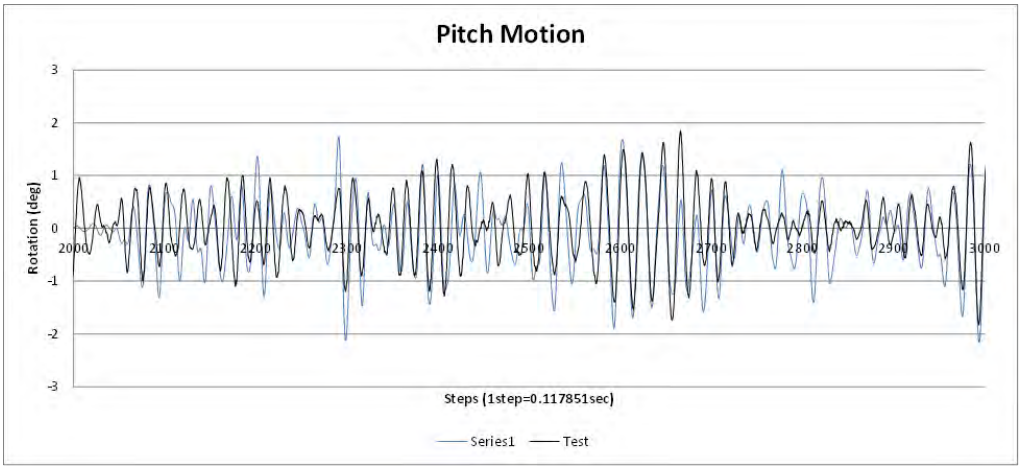

Figure 3 Measured and Computed Pitch Motions for the Operational Platform in 10-Year Swell

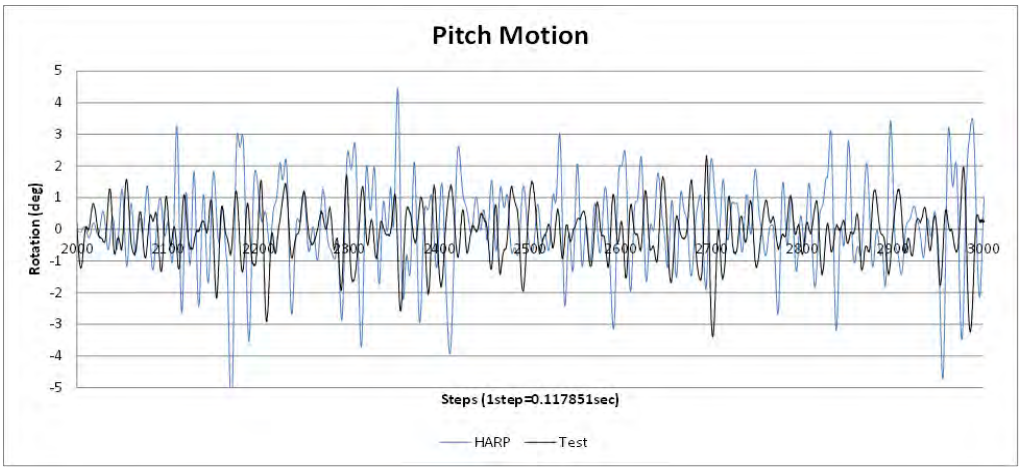

Figure 4 Measured and Computed Pitch Motions of the Operational Platform in a 100-Year Cyclone

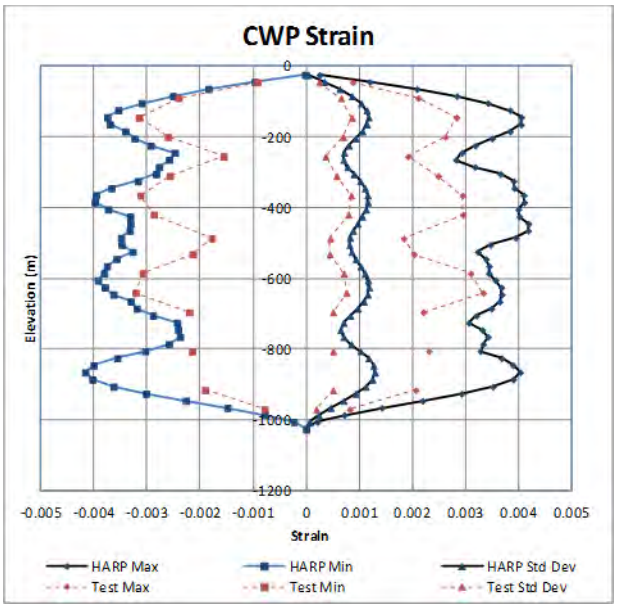

Figure 5 Measured and Computed Pipe Strain Envelopes along the Length of the CWP
(Operational Configuration, Free Gimbal, 100-Year Cyclone)

One of the most important parameters for the Lockheed Martin CWP design is the bending strain in the pipe at the platform interface during pipe fabrication. Analysis of the installation case indicated much greater numerically computed strains than measured.

> ***Results like those shown here have led to the overall conclusion that the numerical model provides a conservative estimation of motions and strains in the cold water pipe. In practically all cases analyzed, the numerically modeled motions and strains exceeded, sometimes by a large margin, the measured values. The team believes this validation of numerical modeling is sufficient to proceed with preliminary design of a commercial or pilot system.***

This document reports the more severe metocean weather cases. Much more data is available for future processing. Several recommendations for going forward, including further analysis using this test data, some post-test calibrations (mentioned above) and recommendations for future tests are provided.

Funding for this project was provided by a cooperative agreement between the United States Department of Energy and Lockheed Martin Corporation. Additional ocean-basin test days were provided by Petróleo Brasileiro (Petrobras) to expand the number of configurations evaluated.

1 INTRODUCTION

This document is the final technical report for the OTEC Cold Water Pipe-Platform Subsystem Dynamic Interaction Validation project. It presents the results of efforts to validate the ability to model numerically the dynamic interaction between a large cold-seawater filled pipe and a floating ocean thermal energy conversion (OTEC) platform excited by meteorological and ocean (metocean) weather conditions by comparing numerical results with measurements from a scale model exercised in an ocean-basin test facility. Understanding these dynamic interactions is a critical step toward commercializing large, reliable, utility-scaled OTEC power plants and thereby enabling the use of ocean thermal energy as a significant addition to renewable energy options.

The project was a cooperative agreement between the United States Department of Energy (DoE) and Lockheed Martin Corporation under Topic Area #2 of Funding Opportunity Announcement DE-FOA-0000293. The project is a logical extension of the cold water pipe development effort supported by DoE in the 1970s and the 2000s.

In addition to the DoE and Lockheed Martin funds, Petróleo Brasileiro (Petrobras) provided additional ocean-basin test time to expand the number of configurations evaluated.

1.1 OCEAN THERMAL ENERGY CONVERSION (OTEC)

Ocean thermal energy is a large untapped renewable energy resource that can potentially yield terawatts of power for human consumption [1]. This thermal energy is contained in an existing, vast energy storage mechanism, the tropical oceans. Ocean Thermal Energy Conversion or OTEC is a name for the technologies that can harness the temperature difference between warm surface seawater and cold deep seawater in a thermodynamic cycle to produce electricity. Because the ocean itself is such a large energy storage mechanism, from a utility perspective, OTEC is a baseload technology, i.e. provides power 24/7. Generated power can connect directly to a local grid from land-based facilities or via undersea cable from offshore facilities. Offshore facilities that are too distant for affordable undersea cable connections can produce energy carriers and other products for shipment to shore.

In geographic areas with warm surface seawater and deep cold seawater, the temperature difference can be utilized to drive a steam-like cycle that turns a turbine and produces power. See for example Figure 6 depicting a Rankine cycle. This temperature difference is the primary "fuel" for OTEC.

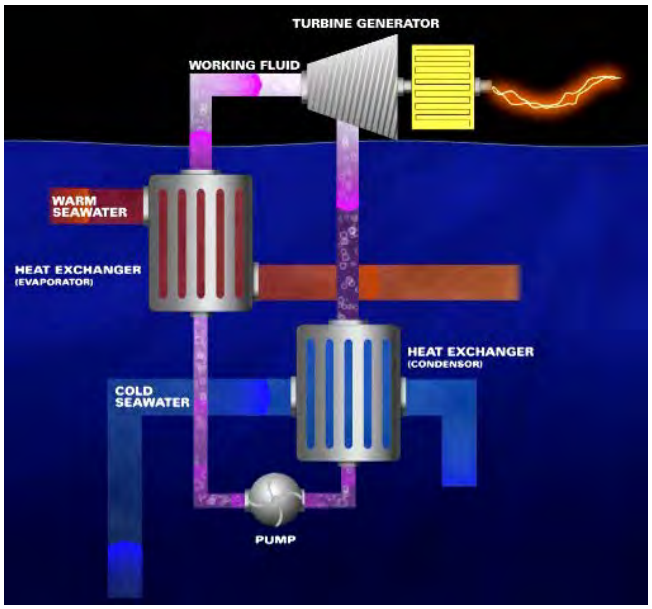

Figure 6 Rankine Thermodynamic Cycle

Warm surface seawater is pumped through a heat exchanger (evaporator), vaporizing a low boiling point working fluid (ammonia). The vapor expands through a turbine-generator, producing electricity. Deep seawater is pumped through another heat exchanger (condenser) to return the discharged vapor back to a liquid. Ammonia pumps re-pressurize the fluid, which is directed back to the evaporator to continue the cycle.

This process is very similar to that used in steam power plants today, just at a different temperature and pressure. The major components of a floating OTEC system include large heat exchangers, seawater pumps, turbine generators, an undersea cable to shore, a platform and mooring, and a long cold water pipe (CWP).

1.2 COLD WATER PIPE-PLATFORM CHALLENGE

A commercial floating 100-megawatt (MW) OTEC power plant will require a CWP with a diameter of 10-meter (m) and length of up to 1,000 m. Figure 7 shows a conceptual 100 MW OTEC power plant. Figure 8 shows a perspective of the CWP length. Cold water pipes for smaller plants will be about 4m in diameter to support 10MW production capacities. CWP diameters will scale as the square of the capacity. The interaction of these CWP-platform subsystems from combinations of metocean conditions must be understood to design a reliable OTEC system.

Figure 7 Lockheed Martin At-Sea 100 MW OTEC Power Plant Concept

Figure 8 CWP Length is Over Twice the Height of the Empire State Building (With Spire)

The offshore industry uses software-modeling tools validated by scale model tests in facilities able to replicate real at-sea metocean conditions to provide the understanding and confidence to proceed to final design and full-scale fabrication. However, today's offshore platforms (similar to and usually larger than those needed for OTEC applications) incorporate risers (or pipes) with diameters well under one meter.

In the case of the OTEC system, the mass of the cold water pipe, including entrained water, can exceed the mass of the platform supporting it. This situation is quite

different from that of most marine risers. Secondly, the preferred construction method for large diameter CWPs is the use of composite materials, primarily a form of fiber-reinforced plastic (FRP). The use of these material results in relatively low pipe stiffness and large strains compared to steel construction. These factors suggested the need for further validation of the software.

The composite CWP is a key component for an OTEC system. Challenges with this kind of pipe in this application are the construction and installation. Lockheed Martin is developing a method for fabricating and installing the pipe from the floating platform as a single piece, without connectors. A particular requirement of this installation process is that the pipe be "gripped" and guided below the manufacturing equipment as it is built. The grippers and guides must be able to suspend the pipe and minimize pipe deflections during resin curing periods [2]. The loads on the pipe at the lower guide and pipe motions from the platform control the design of the pipe core from the standpoint of bending. Proving the ability of existing numerical models to predict these loads is a key objective of these tests.

Once the pipe is manufactured, it is hung off the platform keel using a gimbal or other suspension mechanism with a given rotational stiffness. It is critical to be able to predict the pipe's axial and bending strains in this condition. Tests on fiberglass fatigue in seawater indicate that fatigue life is extremely sensitive to dynamic strain amplitudes.

Analysis of pipe response is complicated by several factors, e.g.:

1. The pipe has a major influence on platform motions; the pipe itself has a suspended mass about equal to the platform mass.

2. Pipe strains are dependent upon relative stiffness between the pipe and the platform.

3. Flow around the pipe may influence the hydrodynamic loads on the platform from waves and current.

Team members have previously benchmarked several industry standard numerical modeling software programs against one another and have been able to show agreement to about +/- 15% on the maximum pipe strains [1, 3]. This project is to validate the computational tools and establish "best practices" for the analysis by comparing analytical results to measurements from a comprehensive model basin test.

This page intentionally left blank.

2 BACKGROUND

2.1 PAST COLD WATER PIPE STRUCTURES

This project is not the first time that OTEC CWP responses have been studied. OTEC was the subject of great interest following the 1970s oil embargo [4, 5]. Between 1975 and 1980, the United States Department of Energy (DoE) funded a large CWP development program that included design, analysis, and testing of several concepts [6]. Figure 9 shows some of the leading pipe candidates.

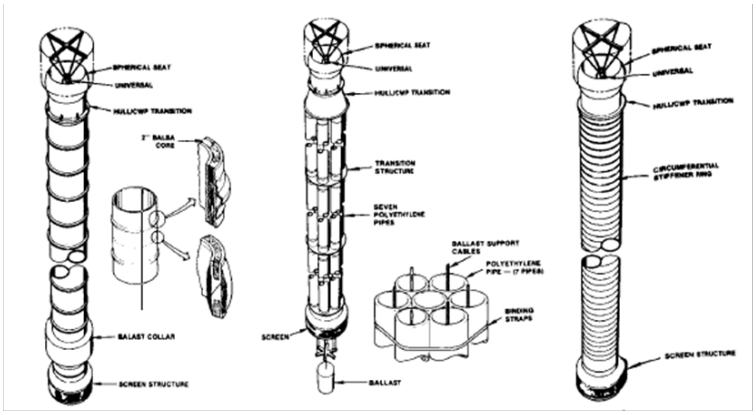

TRW-FRP Sandwich CWP **TRW-Polyethylene CWP** **TRW-Elastomer CWP**

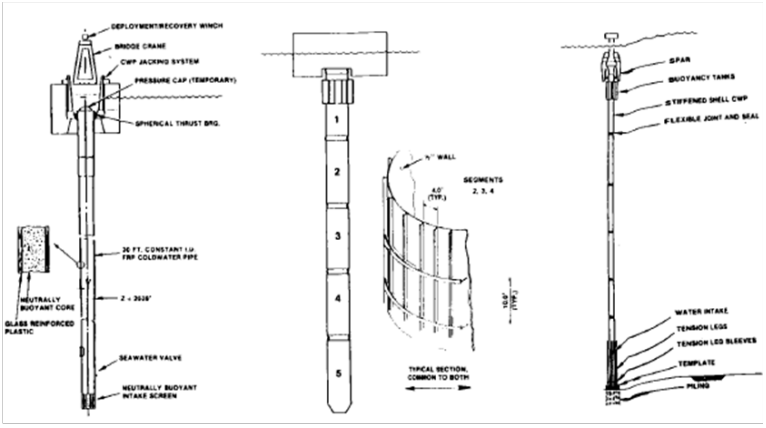

SAI-Fiberglass Sandwich CWP **SAI-Stiffened Steel CWP** **SAI-Bottom Mounted CWP**

Figure 9 Early CWP Designs for 10-40 MW OTEC Plant, 1980 [6]

The pipes studied during that time included steel, concrete, aluminum, FRP, bundled high-density polyethylene (HDPE) and elastomeric pipes. The studies also considered alternate schemes for installing the pipes, primarily two methods: tow-out and upend followed by keelhauling into place; and vertical assembly in place. The advantage of the tow-out and upending scenario is less at-sea time for installation. The disadvantage is difficult control of the operation and the risk of exceeding design loads. The advantage of the vertical assembly in-place is positive control over the operation at all times. The disadvantage is the longer length of time required for fabrication operations, and the longer weather

window required to complete an operation sensitive to sea states causing angular motions on the platform. Lockheed Martin has opted for the vertical assembly method [2]. During this fabrication phase, the increasingly longer pipe is rigidly connected to the platform for multiple months. Validating the ability to predict accurately pipe loads in this scenario is an important objective of this project.

Most of the early work focused on the rigid designs, which were found to require articulation between joints to survive the harsher environments in the operational condition. The FRP ultimately was selected as the favorite design. The DoE work, which was managed by the National Oceanic and Atmospheric Administration (NOAA), included three phases: analytical development, laboratory testing, and field-testing.

2.2 PREVIOUS MODELING AND VALIDATION EFFORTS

Note the distinction between the terms 'prototype' and 'model.' Prototype refers to full-scale version of the intended product and is relatively expensive to produce and test. Model refers to a smaller, scaled version of the prototype and is relatively less expensive to produce and test. The model design is focused on replicating desired parameters of the prototype.

Mathematical models were developed in the 1970s to analyze the cold water pipe. These included a coupled time domain program based in strip theory and two-dimensional pipe motion [7]; a linear program based on proportional damping (called "NOAA/DoE" Code) [8], and a coupled frequency domain code with non-proportional (viscous) damping included (called ROTEC Code) [9].

Several laboratory tests were conducted to validate the software. Hydronautics conducted tests of two different OTEC platforms in the 1970s [10, 11].

One set of tests was conducted using the "Hughes mining barge" which was a model of the barge planned for full-scale tests. The model scale was 1:50. Two cold water pipe models were tested: a 2" Schedule 40 PVC pipe (representing a steel CWP) and a 2" clear vinyl tubing pipe (representing a fiber reinforced CWP). These commercial pipes scaled the hydrodynamic and elastic properties of the prototype pipe reasonably well. It was pointed out that larger pipes or larger scale factors would make modeling these properties difficult with commercial pipe or tubing.

A second set of tests was conducted simulating a 400 MW OTEC Plant at a scale a 1:110, Figure 10 [10]. The platform was a spar type platform. The CWP pipe in prototype scale was 80-feet (ft) in diameter and 2,970 ft long (8.7" and 27 ft model scale, respectively).

This CWP was fabricated as four separate sections. Each section was laid up using epoxy resin and a single layer of fiberglass cloth. The sections were wrapped with a spiral pattern of fiberglass roving to increase the buckling strength, Figure 11. The elastic properties scaled a steel prototype pipe.

Comparison of measured with predicted values from the early Hydronautics tests was mixed. Platform motion predictions were generally good, but the bending moments showed mixed results, Figure 12.

A 1:30 scale model of a 40 MW barge based OTEC Plant was tested at the Offshore Model Basin tank in Escondido in 1981 [12], Figure 13. These tests were primarily concerned with the sea keeping behavior of the barge. The CWP was truncated and no measurements of its elastic responses were made.

Figure 10 1:110 Scale Model Tests of Spar and CWP, 1979 [10]

Another set of model tests were conducted at the Offshore Model Basin using a 1:110 scale model of a 40 MW plant ship and a 30 ft by 3,000 ft CWP. The CWP model in this case was a hybrid using a thin rod to scale the elastic properties of the 30 ft prototype FRP pipe, and an outer shell to capture the hydrodynamic forces, see Figure 14 [13].

This was the first test in which bending moments were measured along the length of the CWP. Pipe stress estimates using the NOAA/DoE code [8] greatly over predicted the stresses while the NOAA/ROTEC Code [15] gave a much better result, see Figure 15. The conclusion was that the difference in theoretical results was a consequence of damping [16]. The NOAA/DoE code used linear proportional damping. The ROTEC code used a linearized form of quadratic damping [17].

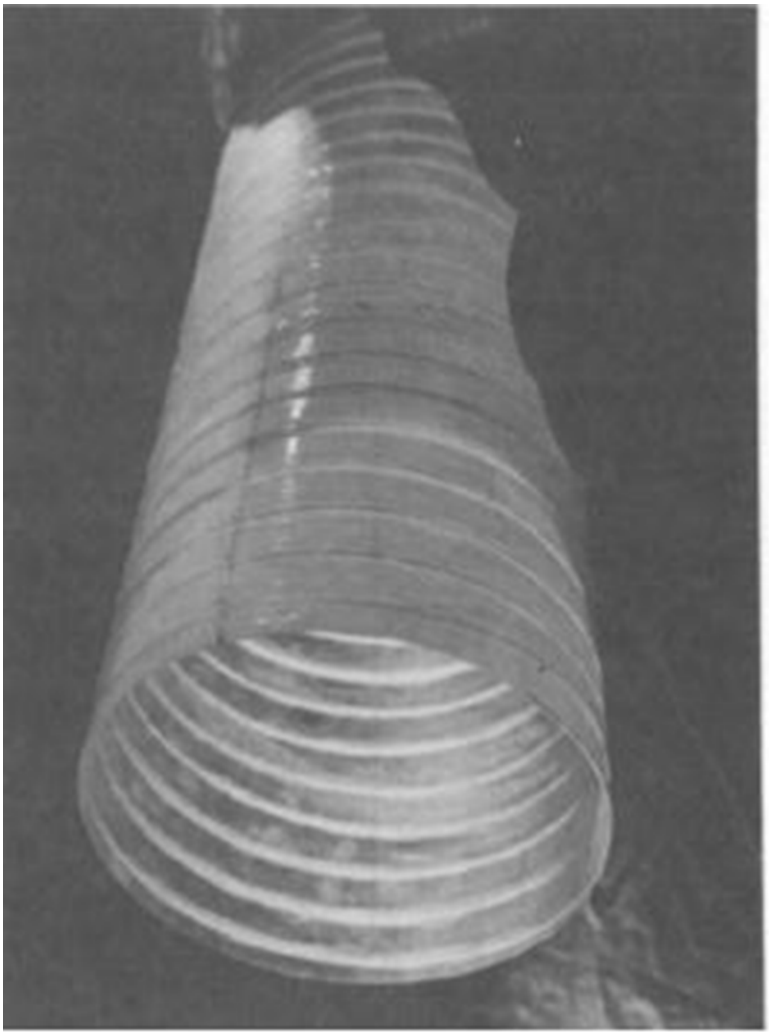

Figure 11 Section of CWP Model, 1979 [10]

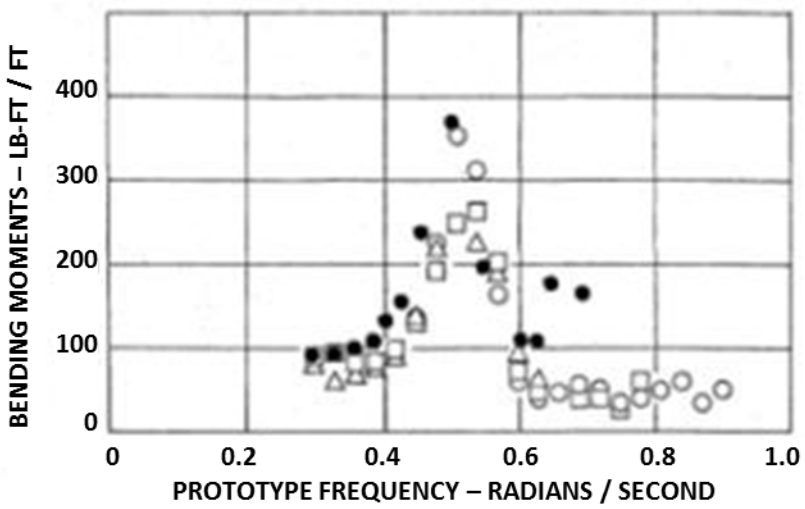

Fig. 8 – Comparison of bending moment 75% down spar with rigidly attached CWP.

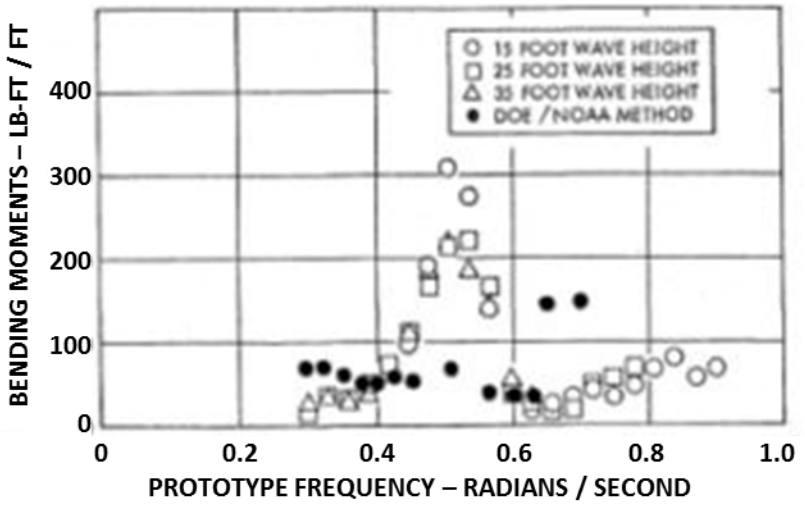

Fig. 9 – Comparison of bending moment at top of spar with rigidly attached CWP.

Figure 12 Comparison of CWP Bending Moments from 1:110 Scale Tests, 1980 [11]

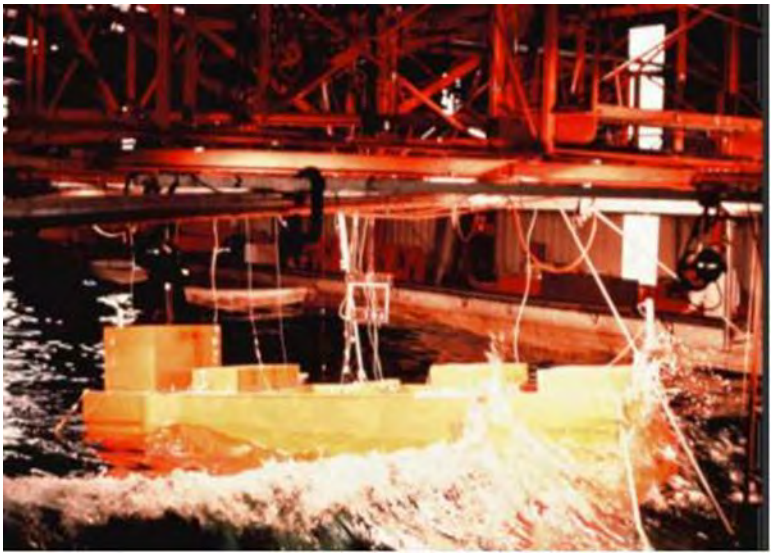

Figure 13 1:30 Scale Model of 40 MW OTEC Plant, 1982 [12]

Figure 14 1:110 Scale Model of 30 ft CWP, Offshore Model Basin Test, 1981 [14]

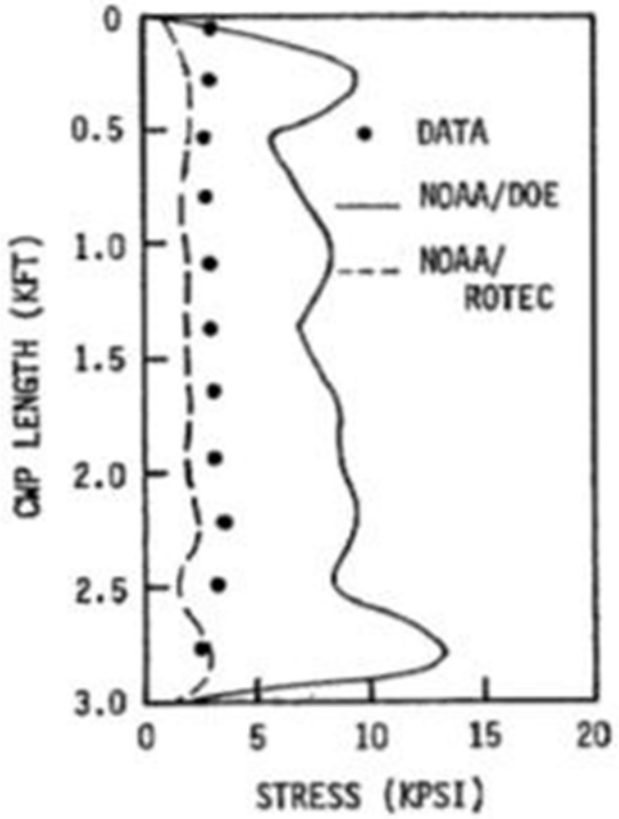

Figure 15 Comparison of Measured and Computed CWP Bending Moments [16]

Several at-sea cold water pipe tests were conducted in the 1970s and 1980s:

Mini-OTEC: Makai Ocean Engineering designed a 24" diameter HDPE cold-water pipeline that also served as the mooring line for the Mini-OTEC barge. The Lockheed demonstration operated successfully for over 600 hours during 1979 and was the world's first demonstration of net power production from a floating OTEC system.

OTEC-1: The DoE's "OTEC-1" heat exchanger test ship used a cold water pipe composed of a triple bundle of 48" diameter vertical HDPE pipes attached to the ship via a gimbal. The system operated successfully during 1980-81. Vessel heave caused difficulties affecting the pump's suction.

DoE 8 ft FRP Pipe At-Sea Test: This DoE funded test used results from both DoE pipe software programs (NOAA/DoE and ROTEC) and other calculations to design an FRP / syntactic foam pipe that was a 1/3 scale model of a size needed for a 40 MW OTEC structure. The instrumented, 400 ft long, 8 ft diameter, gimbal-suspended pipeline was used from April-May 1983 to collect and analyze hydrodynamic data.

It appears the only available CWP performance data from these tests is for the DoE 8 ft pipe [5]. Time histories of wave height, water velocity profile, barge motions, gimbal angles, and strains at nine positions along the pipe were measured. Drag coefficients derived from gimbal angles and velocity profiles, mainly from towing experiments, indicate the pipe drag coefficient was between 1.03 and 1.14 for a range of Reynolds's numbers of $1.2 – 1.8 \times 10^6$. These values are consistent with a cylinder of roughness between 0.02 and 0.07. Pipe data taken in waves and current was analyzed to determine drag and added mass coefficients. The variability of the current created some difficulties in interpreting the results; however, it was noted from the observation of modal frequencies that the added mass coefficients were in the range of 0.26 to 0.78, which is consistent with the results for high Keulegan-Carpenter (KC) numbers (indicating separated flow).

In 2007, Lockheed Martin reestablished an OTEC team and began development of a fiber-reinforced plastic (FRP) pipe, which may be manufactured vertically from the floating platform itself. Bending loads on the pipe at the platform during the fabrication phase drive pipe design.

3 MODEL TEST DESCRIPTION

Model test requirements are provided in Appendix B. Detailed descriptions of model tests are provided by the BMT Dry Model Tests Progress Report (Appendix C) and the LabOceano OTEC Final Report (Appendix D). Selected model specifications and as built, calibrated properties are provided in Appendix G through J and electronically on the DVD bound with the hard copies (Appendix L). This section presents the important modeling parameters and some discussion of the calibrations.

3.1 SEMI-SUBMERSIBLE PLATFORM

The Lockheed Martin OTEC platform consists of a four-column semi-submersible with detachable power modules. The power modules contain heat exchangers, pumps for warm and cold seawater, and pumps for ammonia. Turbines and generators are located on the semi-submersible deck. Figure 16 shows a rendering of an early 10 MW pilot plant. The semi-submersible has a draft of 20 m; the power module's draft is 73 m. The power modules are neutrally buoyant and, when detached from the platform, are similar to spar buoys. They are deployed horizontally and upended for attachment to the platform. The process is reversible, so the power modules may be replaced for service or upgrade. This facilitates servicing of the critical heat exchangers and upgrading as technology improves. Upending a power module is less complex relative to towing out and upending a 1,000 m CWP.

The other unique feature of the Lockheed Martin OTEC system compared to previous systems is the fabrication of the FRP cold water pipe on board the platform. This approach avoids the need for connectors in the large diameter pipe, and the pipe is fabricated as one single section, 1,000 m long. This approach also eliminates the need to float out a long FRP pipe from shore and upending it. Figure 17 illustrates how the fabricated pipe is supported by the platform. Two "grippers" use friction to hold the pipe and support its weight while it is being fabricated. The upper gripper is fixed. The lower gripper travels up and down to lower or raise the pipe. The upper and lower grippers alternately grip and un-grip the pipe. There is always one gripper engaged.

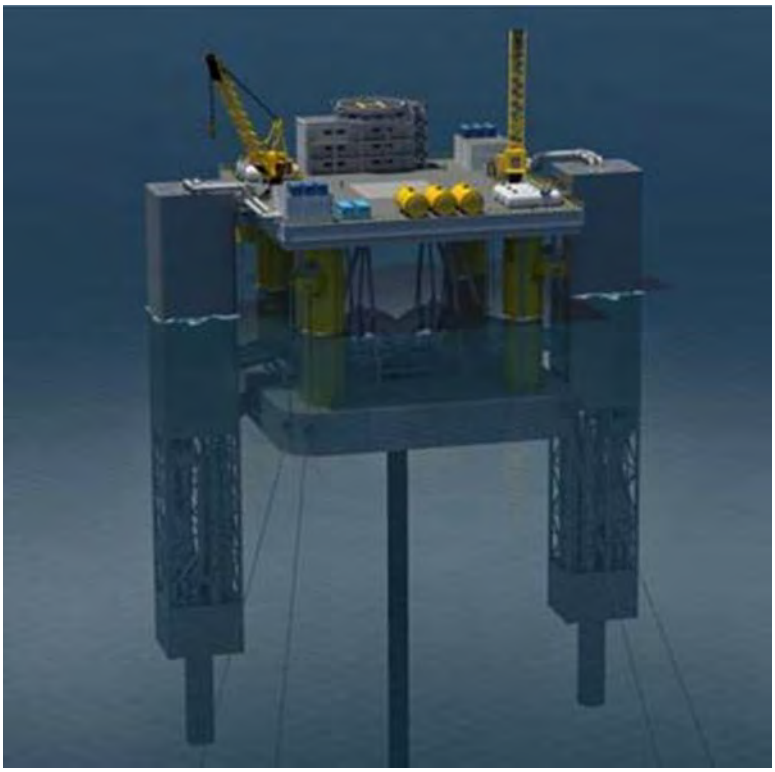

Figure 16 Lockheed Martin 10 MW OTEC Platform Concept

A pair of low friction guides positioned below the grippers restricts horizontal displacements to insure the pipe remains aligned with the grippers and the fabrication equipment.

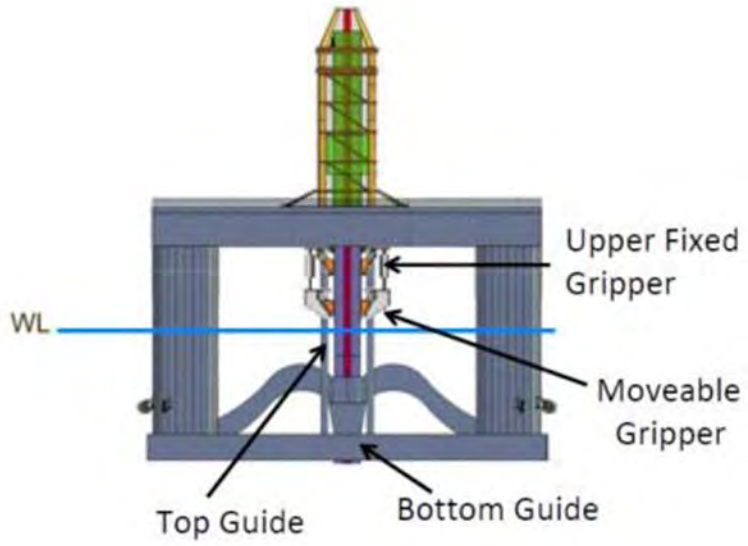

Figure 17 Installation Configuration with CWP in Grippers [1]

A challenge for this method of pipe installation is the fact that during the fabrication operation the pipe is rigidly constrained in roll and pitch. It is not possible to gimbal the pipe to relieve bending at the platform connection. Hence, the pipe is vulnerable to severe weather during this time.

A commercial version of this OTEC system designed to provide 100 MW requires a larger platform, six larger power modules, and a CWP with a 10 m diameter. This prototype 100 MW configuration is the basis for this latest model basin test reported in this document.

A test of a CWP-platform sub-system should be performed in as large a scale a practical and in as realistic an environment as possible. The DoE guideline for laboratory demonstration suggests a model scale of 1:1 – 1:5. This range is an impossible scale to achieve in a laboratory for a platform designed to operate in 1,100 m of water with a 1,000 m pipe. Based on industry experience, offshore platforms are never tested at such a large scale before commercial implementation. For example, the principal investigator for this project was a principal member of the team that developed the novel Spar offshore drilling and production platform. This effort took 10 years from concept design (and patent) to the first commercial order. A small team worked on the R&D effort that involved numerous desktop studies and model basin tests. At one point, potential oil company clients requested an offshore model test at a scale of 1:3–1:4. This large scale proved impractical. Instead, several oil companies jointly funded a comprehensive, fully integrated deep-water ocean basin test, similar in scope to the testing conducted here. The test scale was 1:55, but the key feature was that they could model the full depth in simulated "real" ocean environments. Based on these and subsequent more focused model tests they designed and built the first production spar.

This model test of the complete CWP-platform subsystem was conducted at a scale of 1:50. The depth of the main basin at the LabOceano facility is 15 m with a central pit providing an additional 10 m depth. At 1:50, the scaled CWP is 210 mm in outside diameter, and 20 m long.

Figure 18 shows an illustration of the model with the power modules attached, the "operational" configuration. Figure 19 shows a plan view of the platform at the upper guide. Figure 20 shows an elevation view and Table 1 shows the mass properties with and without the power modules.

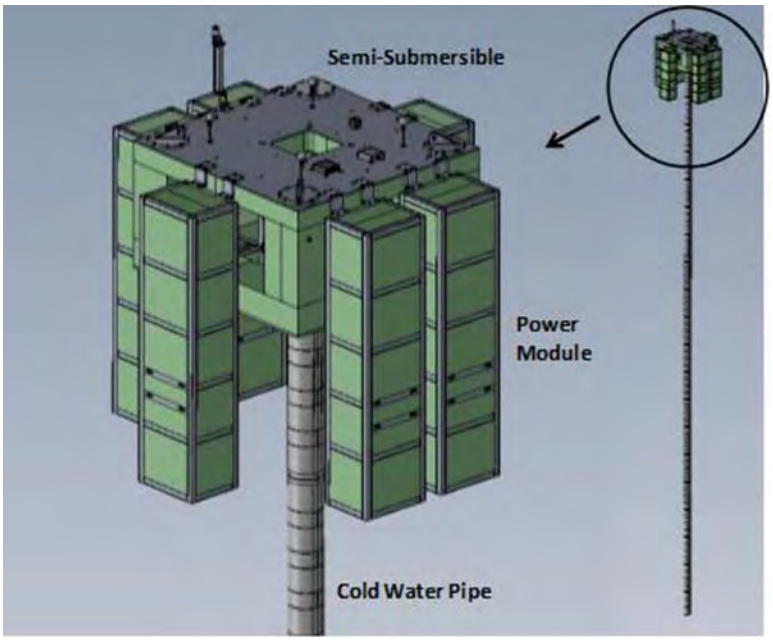

Figure 18 Illustration of the LabOceano OTEC Model in the Operational Configuration

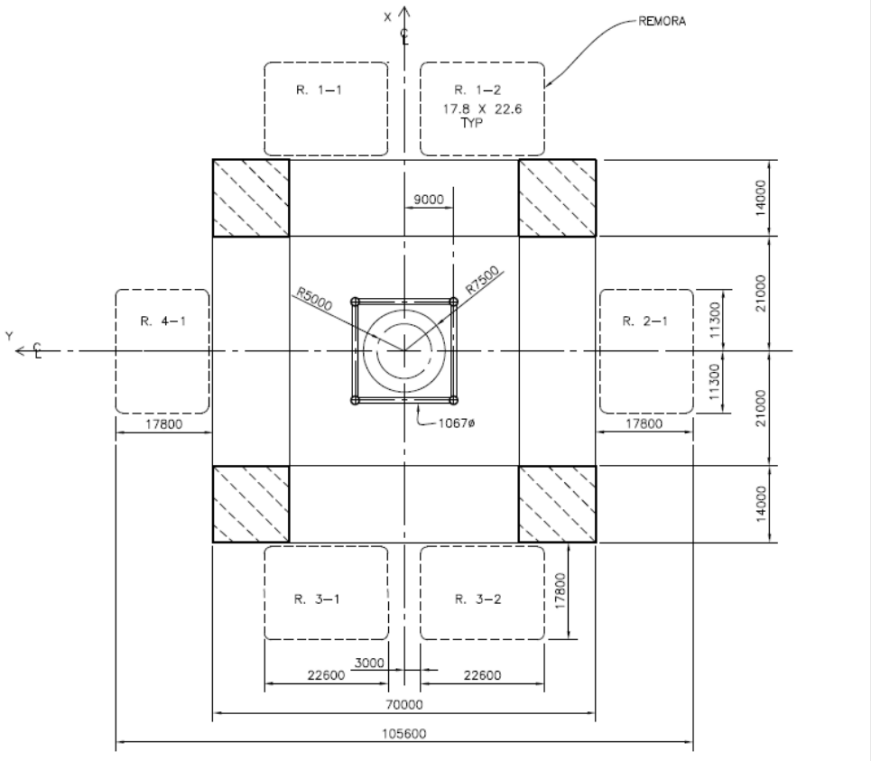

Figure 19 Plan View of Platform and Power Modules (aka Remoras)

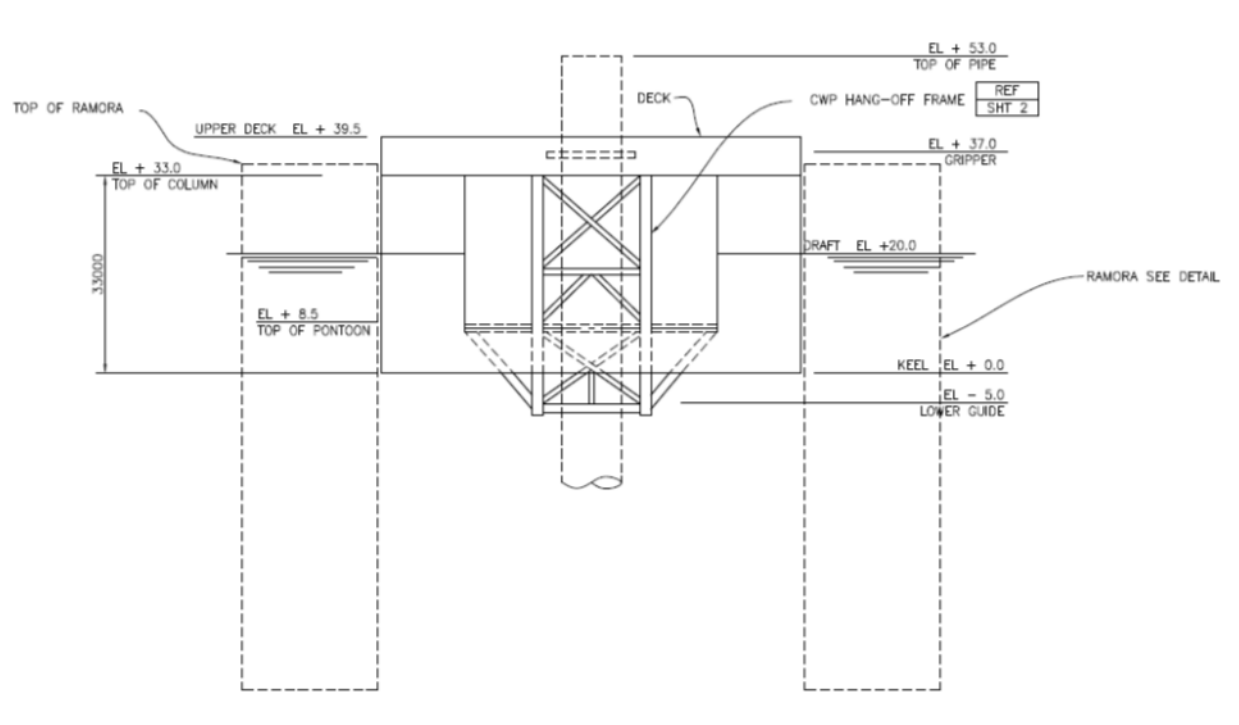

Figure 20 Elevation View of Platform with Power Modules (aka Remoras)

Table 1 As-Built Mass Properties with and without Power Modules

	Platform without Power Modules	Platform with Power Modules
m (t)	41,470.8	220,738.6
Rgx (m)	28.6	35.3
Rgy (m)	28.7	41.2
Rgz (m)	30.2	44.8
XCG (m)	0.1	0.0
YCG (m)	(0.2)	0.0
ZCG (m)	(1.99)	(34.00)
ZB (m)	(13.5)	(32.2)
GMx (m), longitudinal	3.9	20.3
GMy (m), lateral	3.9	14.1
Waterplane Area (m^2)	784.0	3,197.7

Figure 21 shows the semi-submersible model with the CWP support frame attached.

During the installation phase, the power modules would not be present. In this case, the lower displacement of the semi-submersible results in greater wave responses. The responses are also complicated by the fact that the mass of the pipe, including entrained water when fully deployed,

exceeds the mass of the platform. Table 2 illustrates the relative mass of the platform and pipe for the two installations and operational configuration.

Figure 21 Semi-Submersible Model with CWP Support Frame

Table 2 Relative Mass of Platform and CWP

Mass (t)	Installation	Operations
Semi-Submersible	36,627	36,627
Power Modules w/ entrained water		179,010
Total Platform w/ entrained water	36,627	215,637
CWP w/ internal water	135,680	135,680

Most of the mass in the pipe is from the internal water. Of the 136,000 t total mass, only 4,800 t is associated with the pipe structure. A good percentage of the power module mass is also entrained water within the power module structure (57% of the power module mass is entrained water). During operations, the internal water in the pipe will only affect the pipe's horizontal motion. Vertical motion of the platform and pipe will induce pressure fluctuations associated with relative velocity fluctuations in the pipe and ducting, as the mass of water in the pipe is unable to accelerate with the heave motions of the platform. These pressure fluctuations present an operational challenge for the pump controller and can lead to a restricted weather window for operations, especially for high heave platforms. See the earlier comment regarding the OTEC-1 tests, for example.

The issues with the relative mass of the pipe compared to the platform, and the very large diameter and high elasticity of the FRP pipe makes the dynamics of the OTEC system distinctly different from typical oil & gas riser problems. Model tests are critical to confirm the ability to compute accurate platform and pipe motions and loads.

3.2 COLD WATER PIPE SCALING

It was desirable to scale the mass, elasticity and hydrodynamic properties of the pipe along with the stiffness of the connection to the platform and the platform's mass and hydrodynamic properties to validate the analysis of the coupled platform and pipe. Froude scaling suffices for scaling the wave forces and responses of the platform, however for geometrically similar platform and CWP models, the modal periods and shapes of the CWP will only be preserved if these values for the pipe are preserved [11]:

$$\frac{wL^3}{EI} = \text{constant} \quad (1)$$

$$\frac{\rho \mathrm{A} \mathrm{U}^2 L^2}{EI} = \text{constant} \quad (2)$$

$$\frac{EI}{mL^4} = \text{constant} \quad (3)$$

Since the mass of the pipe is dominated by the entrained water, m/L^2 is approximately constant, and the scaling may be satisfied if

$$\frac{EI}{L^5} = \text{constant} \quad (4)$$

For a uniform pipe cross section and a scale factor λ, this yields

$$(EI)_m = (EI)_p \quad (5)$$

"*m*" and "*p*" refer to model and prototype values respectively. For CWP of geometrically similar wall thickness or with equal model and prototype E:

$$E_m = E_p \lambda^{-1} \text{ for } t_m = t_p \lambda^{-1} \quad (6)$$

$$t_m = t_p \lambda^{-2} \text{ for } \mathrm{E_m} = E_p \quad (7)$$

This means that for material of the same stiffness as the FRP pipe the model wall thickness will be about 96 microns. For a geometrically scaled pipe, the material elasticity would have to be 1/50th that of the fiberglass. As pointed out by Barr and Sheldon [11], this scaling is for all practical purposes impossible for scales smaller than about 1/10. For these tests, the CWP model employed a central rod with outer sheath, the hybrid approach shown in Figure 14.

The CWP model was manufactured as a compound model with an internal aluminum tube core (6351-T6 alloy) dimensioned to the proper-scaled flexural rigidity and segmented outer sheet sections to provide the correct outer diameter, Figure 22. The CWP core was divided into five parts connected to each

other by a solid aluminum connector with angularly distributed threaded holes for bolts to connect the tubes and a longitudinal hole.

The CWP outer sheet is segmented into 20 parts, roughly 50 m long (prototype scale), manufactured on a composite fiberglass woven mat and polyester resin structure with polyester gel coat finishing. The connection to the CWP core was made by end plates manufactured as a sandwich composite structure with fiberglass mat, PVC foam, and polyester resin and a center nylon glove with hose clamps to attach it to the core tube. The end plates rest on internal PVC foam with polyester resin finishing preventing water absorption. In order to contain entrained mass of water while not affecting the bending stiffness, the outer sheets were sealed with rubber sleeves as shown in Figure 22.

Figure 22 Cold Water Pipe Model

An instrumented section of pipe was suspended horizontally between two pivots to verify bending stiffness, Figure 23. Various loads were applied to a point in the middle of the pipe and the deflections and strains were recorded. Fitting this data to the beam equation gave verification of the stiffness.

Figure 23 Setup for Pipe Bending Calibration

Mass properties and stiffness of the pipe were verified by suspending a half section of pipe from the ceiling and weighing the section. The "dry" natural periods were measured by tapping the lower portion of the suspended pipe with a hammer and recording the strains. Wet mass properties including entrained water were estimated from the geometry. Impulse tests on the suspended pipe in water were performed to verify the modal properties including natural frequencies and damping.

3.3 GIMBAL AND CALIBRATION

The attachment of the pipe to the platform was a critical and challenging part of this project. The effect of rotational stiffness of the attachment point was particularly important, as the installation scenario required a high equivalent stiffness. Various gimbal designs are being considered for the operational scenario, which could have varying stiffness values. For these tests, three different rotational stiffness's were tested: a free (pinned) connection, a stiff connection representing the installation equivalent stiffness, and an intermediate value which represents a possible real gimbal design for a 10 m pipe.

The gimbal was attached to a dynamometer, which was mounted on a truss that was suspended below the deck and between the pontoons of the platform, Figure 24. The gimbal itself consisted of a Teflon semi-sphere supported in an aluminum cup, in effect a ball joint. The dynamometer consisted of four 6-degree of freedom load cells to measure forces and moments at the top of the gimbal as shown at the top of Figure 24

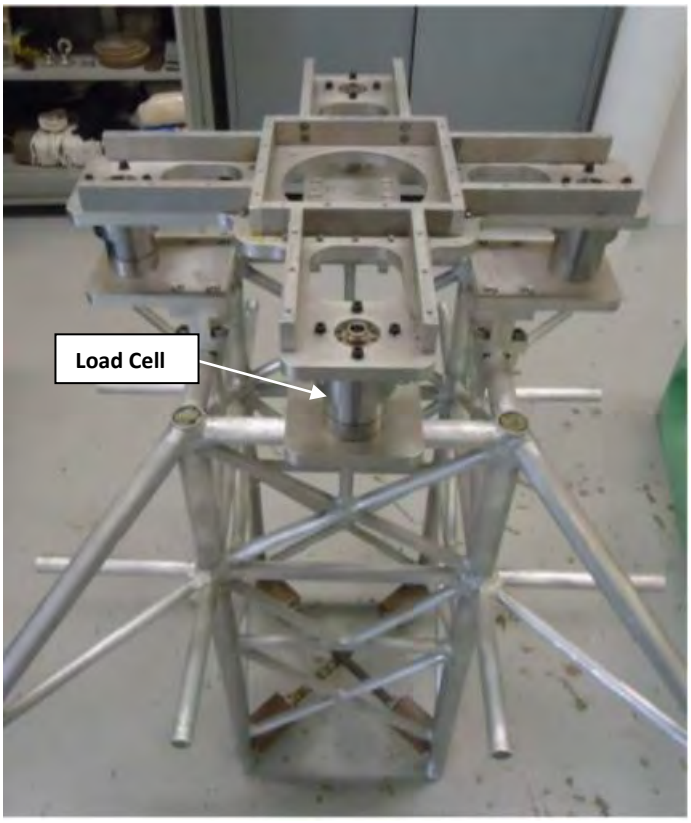

Figure 24 Gimbal on Hangoff Frame

The gimbal assembly itself is shown in Figure 25. It consists of a plate with the aluminum cup and ball joint suspended on six rods representing the lateral stiffness of the gimbal assembly in the prototype frame. An aluminum tube is supported on the gimbal. The lower end of the tube attaches to the CWP. The motion of the upper end of the tube is measured with four linear voltage displacement transducers (LVDTs) allowing angle determination angle and lateral deflection of the gimbal. Gimbal rotational stiffness is achieved by attaching springs between the upper end of the tube to the frame. For the installation stiffness, this is achieved by connecting the tube and plate attached to cantilevered rods. Intermediate stiffness is achieved by connecting four pre-tensioned coil springs between the upper tube and the frame. Dynamic pendulum tests were conducted to assess the frictional damping in the gimbal.

The gimbal angle measurements were calibrated by comparing derived angles from the LVDTs with measurements of a VECTOR-NAV VN-100 inclinometer. Stiffness values for the gimbal consist of a rotational stiffness and a lateral stiffness (representing deflection of the full-scale truss). Calibrations were performed with the gimbal assembly rigidly mounted to a fixture as shown in Figure 25. The resulting values are tabulated in Table 3. Of particular note is the “installation” stiffness, which was chosen to represent the equivalent stiffness of the pipe in the gripper, and guides during manufacturing, Figure 17. After the tests were completed, the results with the installation stiffness suggested that the actual stiffness of the gimbal was an order of magnitude less than the “calibrated” value (see discussion below). The team’s conclusion is that the dynamometer deflections were sufficient to change the effective stiffness of the gimbal in this case, although this was not measured.

A lesson learned for future testing is to calibrate the gimbal, particularly when testing very high stiffness values, with it attached to the actual model fixture with load cells installed.

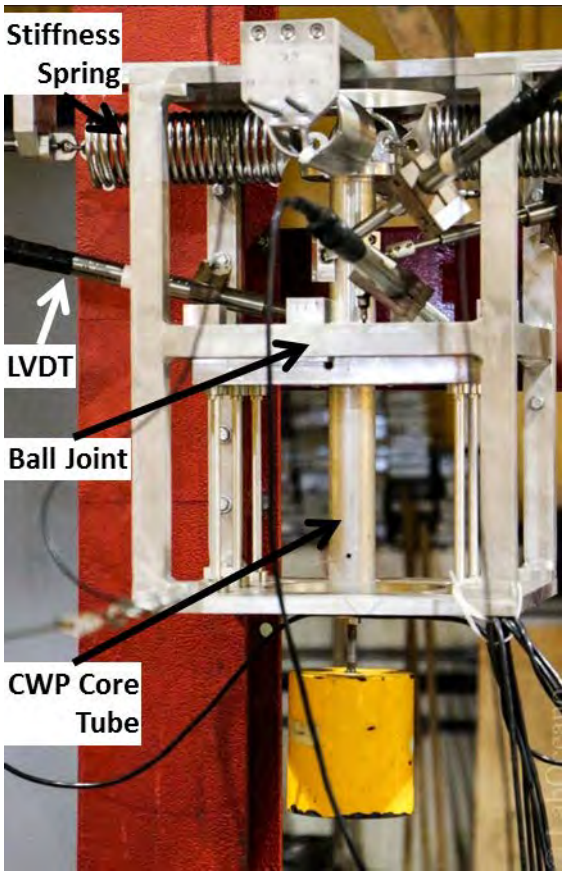

Figure 25 Gimbal Assembly

Table 3 Gimbal Stiffness

Gimbal stiffness and rotational properties			
Model Test Specification	**Installation**	**Operation A**	**Operation B**
Gimbal Angular Stiffness [N·m/rad]	4.93E+10	1.00E+09	0.00E+00
Gimbal Lateral Stiffness [N/m]	2.00E+08	2.00E+08	2.00E+08
Maximum angular offset [^{o}]	0.7	12	12
As built stiffness and gimbal rotation accuracy	**Installation**	**Operation A**	**Operation B**
Gimbal Angular Stiffness [N·m/rad]	9.55E+10	1.26E+09	0.00E+00
Gimbal Lateral Stiffness [N/m]	3.15E+08	3.36E+08	3.15E+08
Gimbal Rotation Accuracy [^{o}]	0.62^o	0.62^o	0.62^o
Δ (%)			
Gimbal Angular Stiffness	93.75%	25.84%	
Gimbal Lateral Stiffness	57.67%	67.87%	57.67%

3.4 TEST ENVIRONMENTS AND CONFIGURATIONS

The tests were conducted over the 25 m deep pit of the LabOceano facility, Figure 26. The deep facility allowed testing at the relative large scales of these experiments.

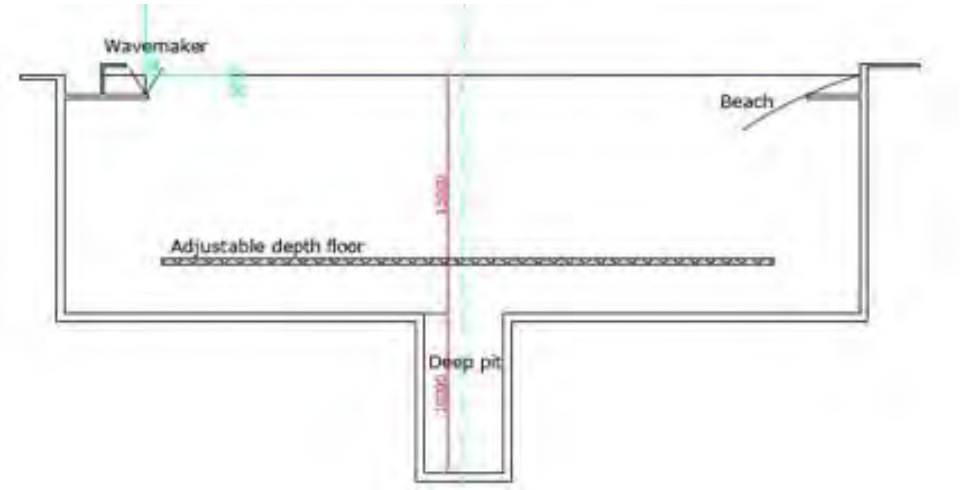

Figure 26 Cross Section of the LabOceano Basin

The test environments consisted of five irregular waves and seven regular waves. The wave environments are listed in Table 4.

Table 4 Test Environments

Irregular Waves	100-Year Cyclone	10-Year Sea	10-Year Swell	Fatigue Wave	White Noise
Uw, m/sec	33.8	15.7	14.6	8	8
Hs, m (measured)	10.2	4.2	3.8	2.5	2
Tp, sec (measured)	12.8	8.3	15.7	16.6	2-26
Gamma	2	1	6	6	
Wind Force, kN (w/PM)	2002.2	432	373.6	112.2	112.2
Center of Pressure (w/PM)	14.3	14.3	14.3	14.3	14.3
Wind Force, kN (w/o PM)	1547.2	333.8	288.7	86.7	86.7
Center of Pressure (w/o PM)	16.6	16.6	16.6	16.6	16.6

Regular Waves	Regular Wave 1	Regular Wave 2	Regular Wave 3	Regular Wave 4	Regular Wave 5	Regular Wave 6	Regular Wave 7
Hs, m (measured)	1.5	2.5	3.6	5	6.6	8.5	11.3
Tp, sec (measured)	5.5	7	8.5	10	11.5	13	15

Wind force was simulated with a steady force applied with a string and mass attached through a pulley. No current or current forces were simulated in this program. Current was initially specified but the

LabOceano facility current system had not been installed at the time of these tests so it was decided to proceed with software validation without current. Future tests should address current-CWP interactions.

The environments represent conditions expected for an OTEC facility in Hawaii. In particular, previous analysis has shown the CWP-platform combination to be particularly sensitive to long-period swell such as that found in the Hawaiian winter as represented by the 10-year swell and most damaging fatigue sea state. The 10-year sea and swell cases are considered survival cases for the installation scenario.

Table 5 Test Configurations[1]

							Gimbal Stiffness		
Configuration Description	**Basin Test Group**	**Test Specification Reference**	**Test Schedule Order**	**Semi**	**Six Power Modules**	**CWP Length (m)**	**Rotation (N-m/rad)**	**Lateral (N/m)**	**Comments**
Calibrations	T000	Dry Tests	0						
Semi Installation	T100	Group 3	1	Y	N	0			
Operational Semi & Remoras	T200	Group 1	2	Y	Y	0			
Operational A	T300	Group 1	4	Y	Y	1,000	0	3.15E+08	Free Gimbal
Operational B	T400	Group 2	3	Y	Y	1,000	1.26E+09	3.33E+08	Stiff Gimbal
CWP Installation 1	T500	Group 3	6	Y	N	500	9.55E+10	3.05E+08	
CWP Installation 2	T600	Group 4	5	Y	N	1,000	9.55E+10	3.15E+08	

Six different configurations were tested as shown in Table 5. Two configurations were tested without the CWP: The platform alone (T100) and platform with power modules (T200). Two operational cases were performed to represent different gimbal stiffness values. T300 is with a free gimbal and T400 is with an intermediate stiffness. Two installation cases were run with 500 m and 1000 m of pipe deployed (T500 and T600 respectively).

3.5 MOORING

The mooring system consisted of four taut horizontal lines attached to the model at the corners, 15.75 m from the waterline, Figure 27. The lines are arranged at 45° angles and extend 961 m to pulleys. There, they turn and are each connected to a pre-tensioned linear spring. The springs' design stiffness is 320 kN/m, 126.5 gf/cm, the pre-tension on the line is 13,735 kN and 10,862 gf in prototype and model scale respectively.

[1] Stiffness values are nominal calibrated values. The installation stiffness is indicated to be significantly lower in-place. See discussion in text.

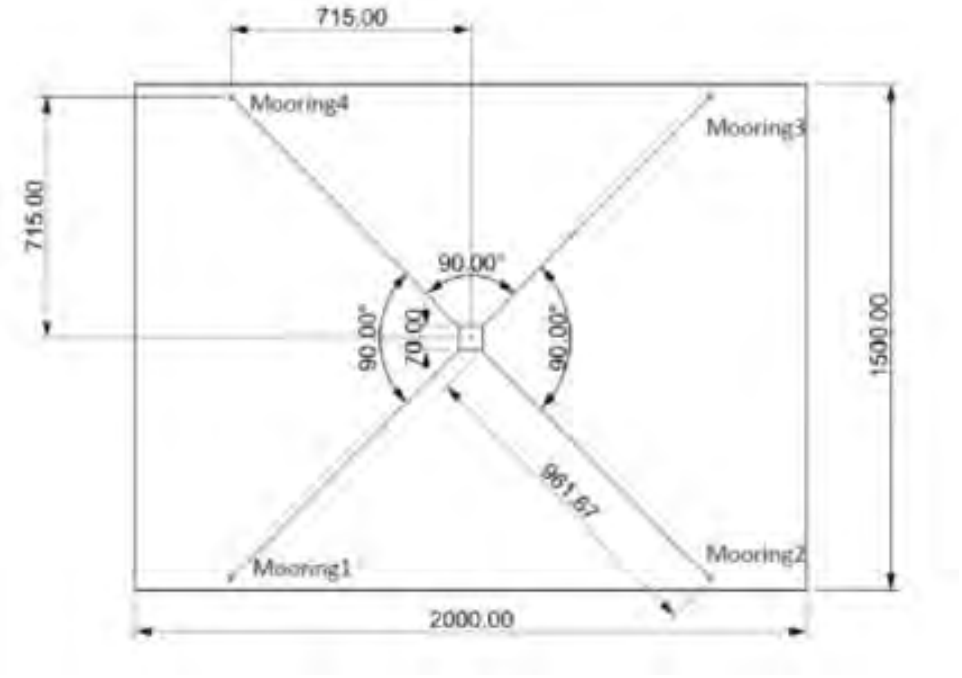

Figure 27 Mooring Layout (m, Prototype Scale)

This arrangement resulted in a linear mooring system stiffness of 650 kN/m.

The stiffness of the mooring lines was achieved by placing springs in line with the mooring cable. The arrangement is shown in Figure 28. Since a pulley was placed in the cable between the model and the fixed point, friction was introduced into the horizontal motions of the platform. This arrangement resulted in almost total elimination of surge and sway motions at resonance (slow drift), which were significant in the numerical simulations, even though free decay tests indicated similar damping.

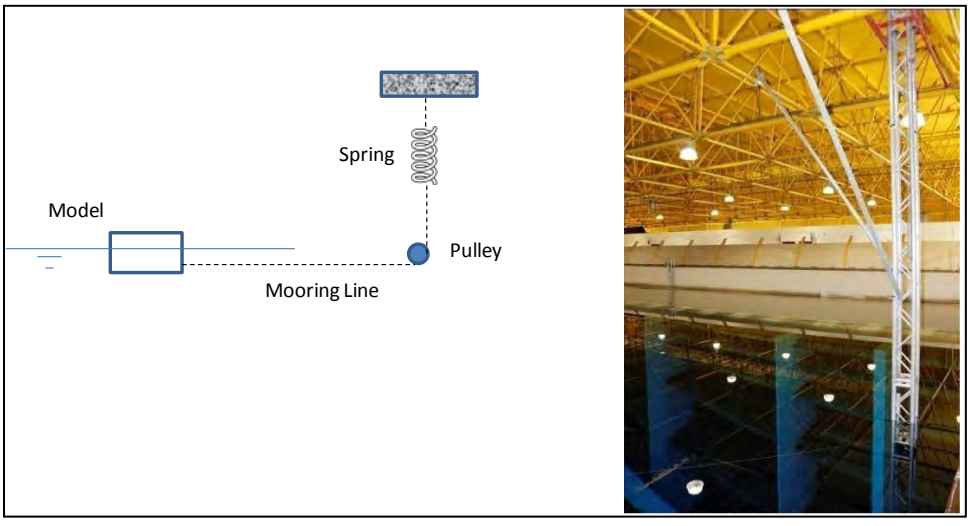

Figure 28 Mooring Line and Spring Arrangement

The springs should be placed in the horizontal lines and the pulleys eliminated in future tests.

Because pulleys were used between the springs and the mooring lines considerable damping was introduced into the surge and sway responses. Free decay tests indicated damping ratios of around 0.3 for the platform alone, and 0.2 for the platform with power modules.

3.6 INSTRUMENTATION

Measurements included 90 sensors and 5 derived channels as shown in Table 6. The VECTOR-NAV inclinometer was attached to the gimbal and values recorded, but they were not time synchronized and some observations indicated the readings were unreliable.

Measurement of the moment at the pipe attachment point was not required so the gimbal frame was not calibrated for moments (only x, y, z forces are derived). The moment at the attachment point may be derived from the measured angles and rotational stiffness of the gimbal, and the moments could be derived from the frame load cells.

Table 6 Sensors and Derived Channels

	Sensors	Derived
6-DOF Platform Motions (Qualisys)	6	
Underwater Qualisys (CWP XYZ @ 6 locations)	18	
CWP Strain Gages: In-Line	18	
CWP Strain Gages: Transverse	2	
Wave Probes	10	
Axial Load: Wind	1	
Axial Load: Mooring	4	
Axial Load: Pulling Forces	3	
Gimbal (LVDTs)	4	2
Gimbal Support Load Cells	24	3
Total	90	5

The 20 strain gage locations on the CWP are given in Table 7. Of the 20 gages installed for this test, only two failed: gages 14 and 16. The principal investigator has had bad experiences with underwater strain gages in the past, and the fact that all but two of the CWP strain gauges functioned throughout several weeks of testing was remarkable.

Table 7 Strain Gage Position on the CWP (Relative to CWP Top)

Strain Gage	Model Scale Position (mm)	Prototype Scale Position (m)	Direction
1	1120	56	X
2	2200	110	X
3	3300	165	X
4	4400	220	X
5	5500	275	X
6	6600	330	X
7	7700	385	X
8	8800	440	X
9	9880	494	X
10	10780	539	X
11	12120	606	X
12	13200	660	X
13	14300	715	X
14	15400	770	X
15	16500	825	X
16	17600	880	X
17	18700	935	X
18	19600	980	X
19	6670	333.5	Y
20	13330	666.5	Y

4 NUMERICAL MODEL DESCRIPTION

The numerical simulations were performed with HARP: "Hull and Riser/mooring Program" [18]. This software is a suite of integrated hydrodynamic and structural analysis modules for offshore engineering applications. The main solver is the fully coupled analysis program CHARM3D [19]. Hydrodynamic coefficients are derived using WAMIT [20]. The model includes Morison members to capture drag forces, and inertial forces on the gimbal frame. A static riser program, PROFLEX, is included to establish the initial configuration of the CWP. The theory of HARP/Charm3D is very similar to that of ROTEC with a few improvements. The platform model uses linear radiation diffraction and a modified Morison equation for wave loads. The second order forces make use of the full quadratic transfer function (QTF) results from WAMIT. The HARP CWP and mooring lines are modeled using an improved higher order tension-beam model [21]. This improvement reduces the number of nodes required for a given accuracy. HARP has also been specially modified for the OTEC project to employ a non-isometric added to the CWP. In the case of the CWP, the entrained water is treated as mass for transverse motions, but there is an option not to include it in the longitudinal direction. HARP does not include stiffness from internal flow. Finally, the simulations used here are time domain rather than frequency domain.

HARP was used to prepare "blind" analysis of the test results in order to verify the program and the assumed inputs. The blind runs were performed with calibrated mass properties for the platform and the calibrated mass and stiffness of the CWP. Post-processed results, particularly of the free decay tests, were used to "calibrate" the coefficients used in the analysis, especially CWP damping. The wave tests were again analyzed using these calibrated coefficients.

This page intentionally left blank.

5 RESULTS AND DISCUSSION

The following discussion describes key results and findings. Detailed numerical analysis results are provided in Appendix E. A summary listing of tests is provided in Appendix F.

5.1 FREE DECAY TESTS

Natural periods and damping values were derived from free decay tests on selected configurations.

Table 8 shows a tabulation of the natural periods measured. These results show remarkable differences between the surge periods of the platform with and without power modules (54.9 versus 167.6) however not so dramatic difference in heave and pitch periods where the added hydrostatic stiffness is offset by the added mass and inertia. Pitch periods observed for T300 and T400 indicate that the CWP has a large effect on pitch natural periods for the free gimbal case but not for the stiff gimbal case (T300 and T400 respectively). The mass of the pipe has a large impact on the heave periods of the platform alone in the installation configuration: T100 versus T600.

Table 8 Natural Periods

				Surge		Heave		Pitch	
Basin Test Group	Platform	CWP Length (m)	Gimbal	Test	Numerical	Test	Numerical	Test	Numerical
T100	Semi	None	n/a	54.9 (70.0)	70	22.4	21.8	27.6	27.7
T200	Semi+PM	None	n/a	167.6 (190)	175	20.3	20	21.9	21.8
T300	Semi+PM	1,000	Free					36.7	
T400	Semi+PM	1,000	Intermediate	191.3 (180)	185	20.7	20.4	21.3	21.4
T500	Semi	500	Stiff					39.7	
T600	Semi	1,000	Stiff			40.9		35.5	

Comparison of numerical and test free decay results for the T200 and T400 series are shown in Figure 29 and Figure 30 respectively. Numerical damping was added in the form of viscous damping between the platform and the fixed coordinate for surge motions to account for the friction in the pulley. No external damping was added for heave or pitch. The addition of the pipe has no apparent change in the natural period or damping of the platform with power modules, which is counter-intuitive.

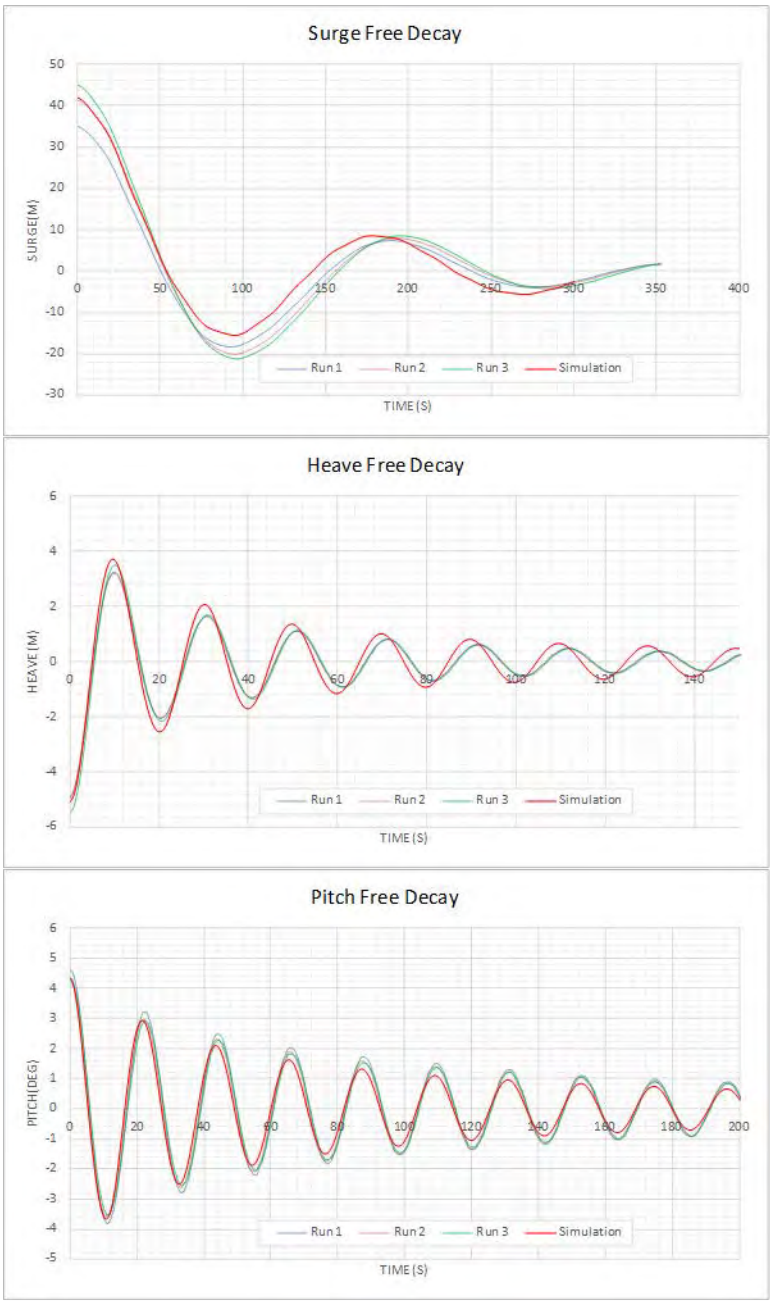

Figure 29 Comparison of Free Decay Results for T200

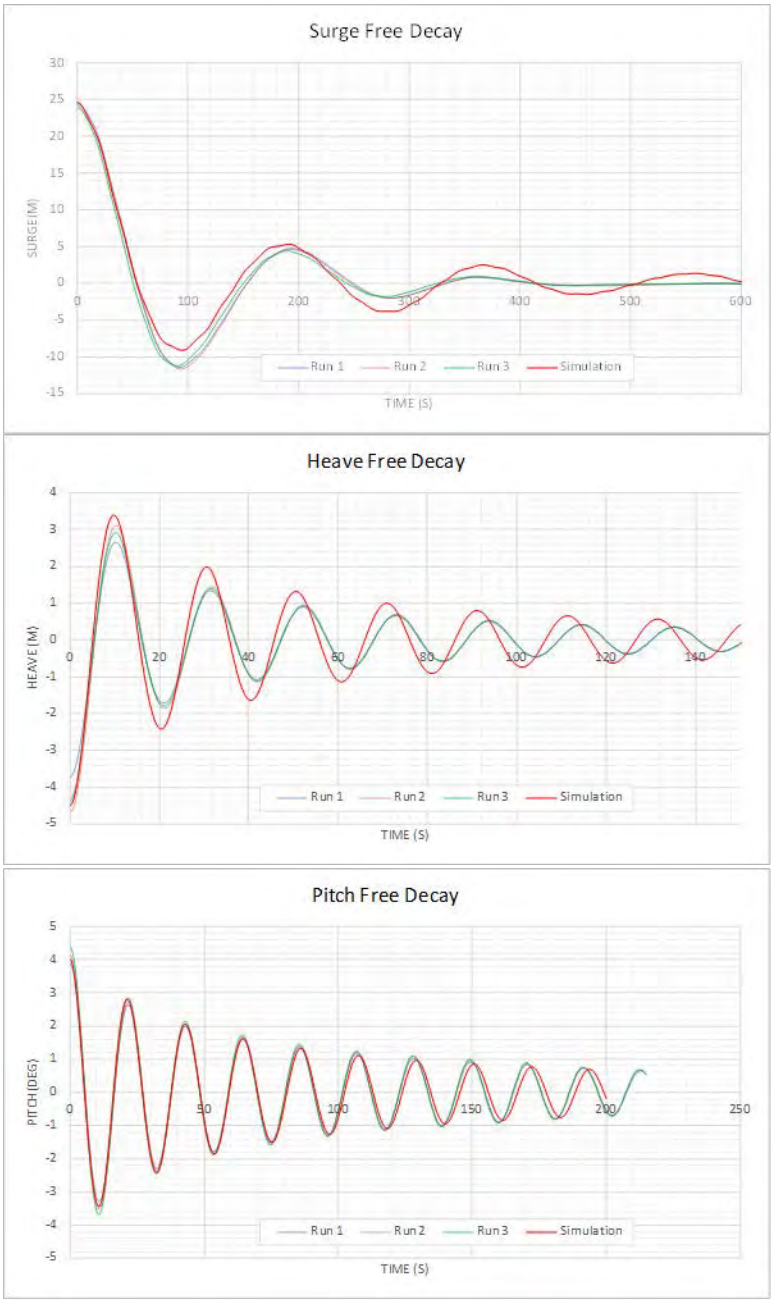

Figure 30 Comparison of Free Decay Results for T400

5.2 PLATFORM MOTION COMPARISONS

5.2.1 PLATFORM ALONE (TEST SERIES T100)

As might be expected the wave frequency results with the platform alone (T100) show good agreement with the radiation diffraction solution (WAMIT). Figure 31 - Figure 33 show the comparison of regular wave RAOs for surge, heave, and pitch respectively.

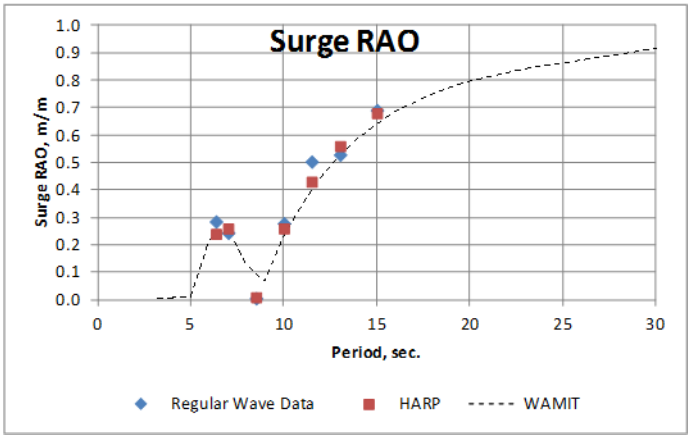

Figure 31 T100 Surge RAO Comparison

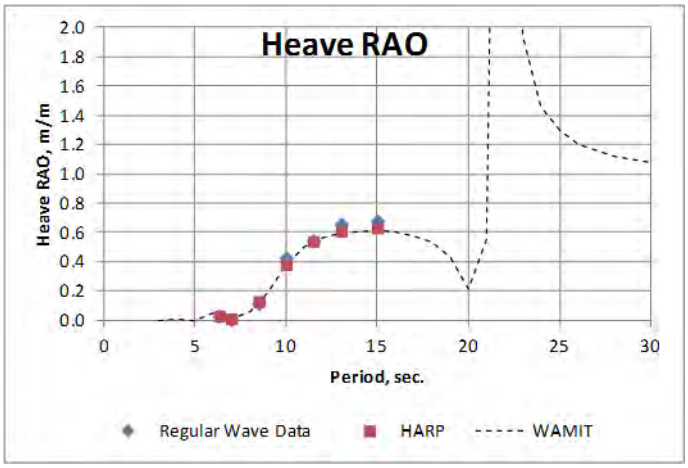

Figure 32 T100 Heave RAO Comparison

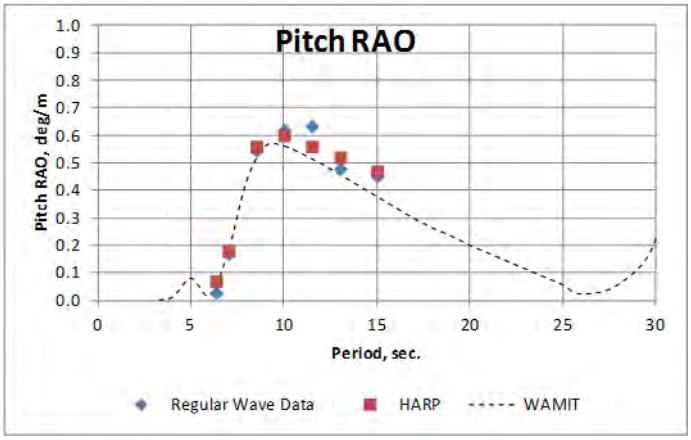

Figure 33 T100 Pitch RAO Comparison

Time domain simulations were performed for these tests utilizing the exact measured wave profile. A resulting comparison of surge motions is illustrated in Figure 34. The un-filtered results show clearly the damping of slow drift motions in the model test, presumably due to the mooring configuration (discussed earlier). Filtering the results and comparing only wave frequency responses shows excellent agreement, consistent with the RAOs shown above.

> Since the primary excitation of the cold water pipe is from the wave frequency motions, other motion comparisons shown in this report will only include the wave frequency responses, unless specifically stated.

CWP strain values shown later are unfiltered; however, the pipe itself acts as a kind of high pass filter. Heave and pitch responses for T100 show excellent agreement.

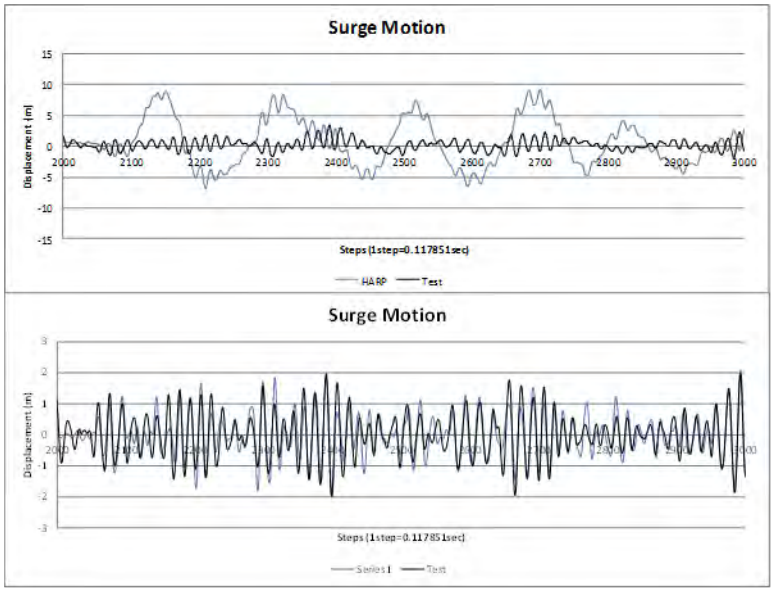

Figure 34 Total Surge Motions (upper) and Filtered Wave Frequency Motions (lower) for T100, 10 Year Swell

5.2.2 PLATFORM MOTIONS WITH POWER MODULES (T200)

Figure 35, Figure 36, and Figure 37 show similar good comparisons for the RAOs from the tests and numerical simulations of the platform with power modules. In these plots, the test RAOs were derived from irregular wave tests with a broad banded “white noise” spectrum.

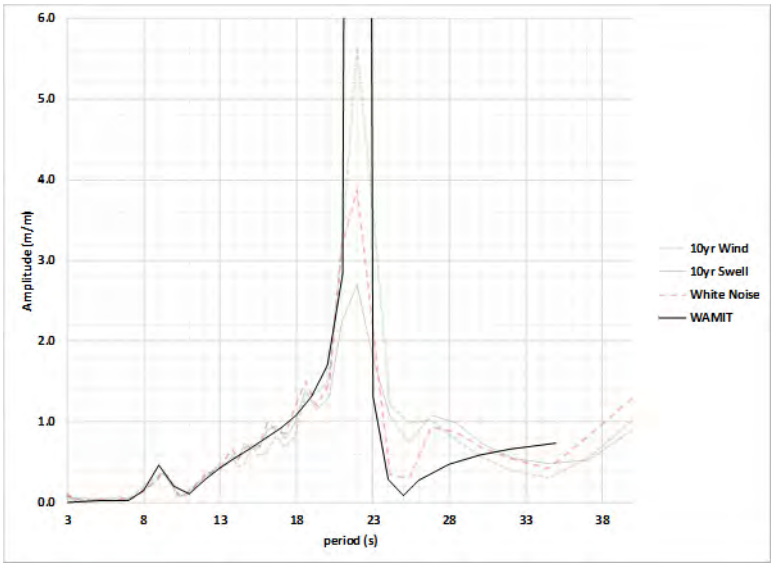

Figure 35 T200 Surge RAO Comparison

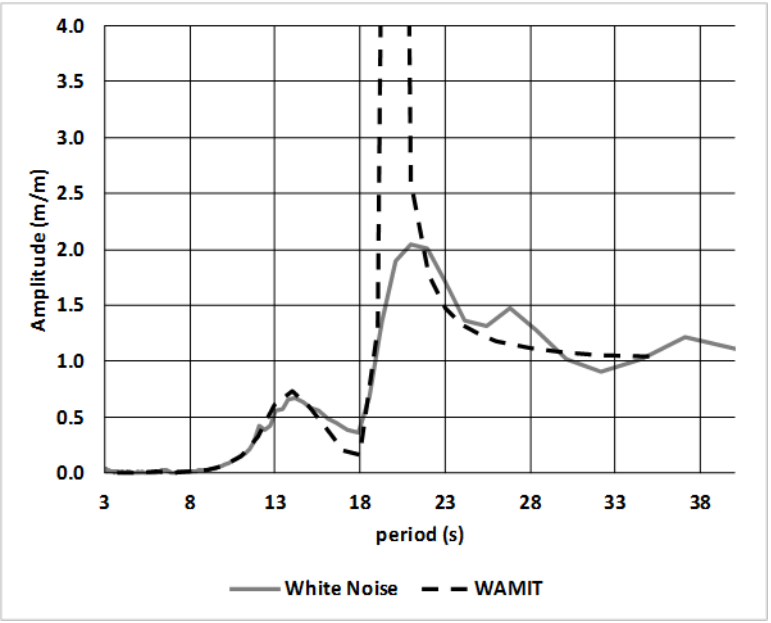

Figure 36 T200 Heave RAO Comparison

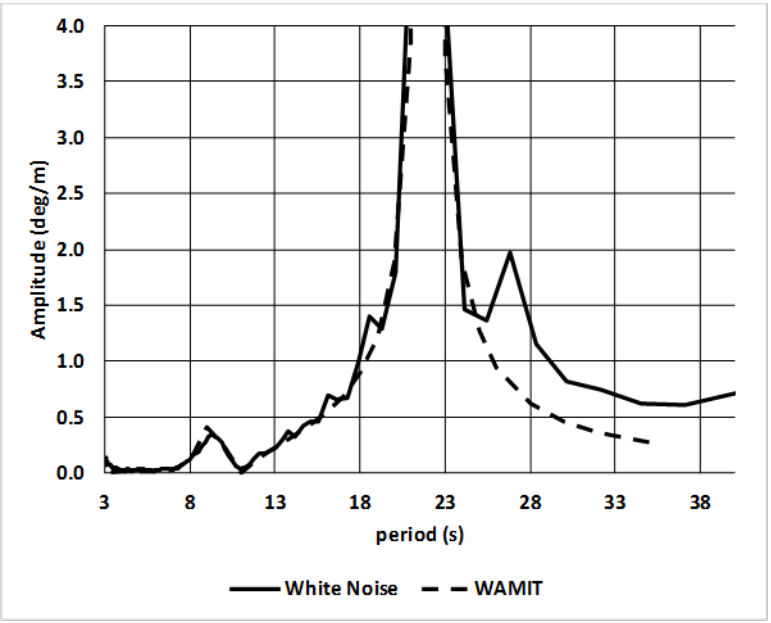

Figure 37 T200 Pitch RAO Comparison

The difference in RAOs between the platform with and without the power modules, based on WAMIT, is illustrated in Figure 38 and Figure 41. Figure 38 and Figure 39 show the surge motions at the waterline and the hangoff location of the CWP respectively. Motions at the hangoff are most critical to the CWP. Surge at the hangoff and pitch motions are both considerably lower in the range of wave energy (most importantly between 10 – 16 seconds where the greatest pipe responses are found) with the power modules in place. The reduction in the heave and pitch natural periods with the power modules added is evident.

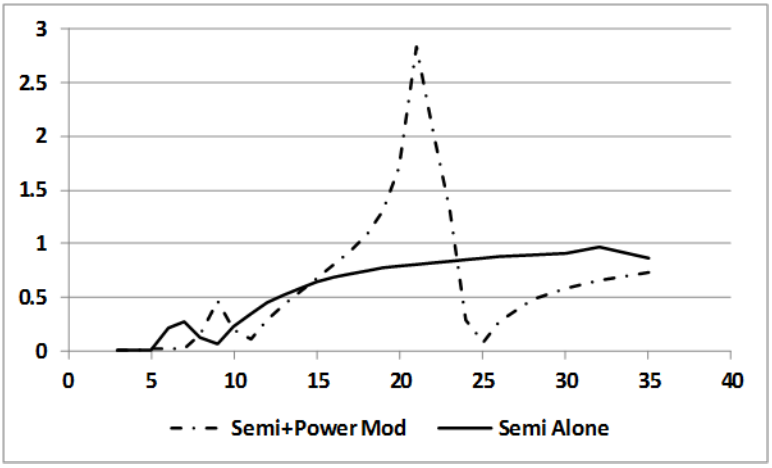

Figure 38 Surge at Waterline RAO Comparison with and without Power Modules

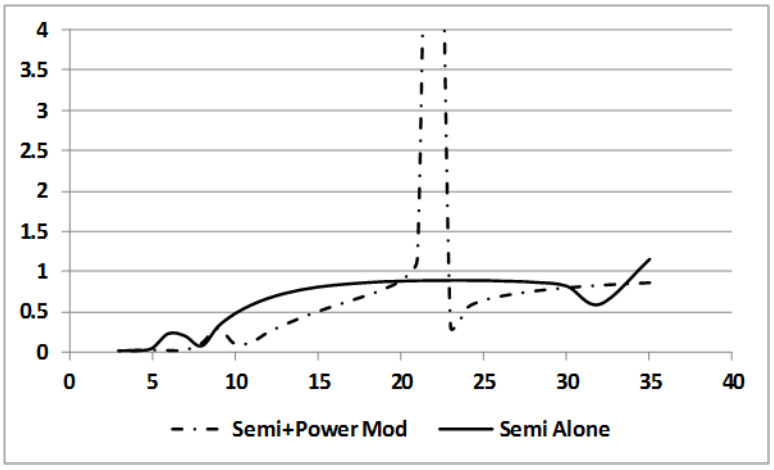

Figure 39 Surge at CWP Hangoff Location RAO Comparison with and without Power Modules

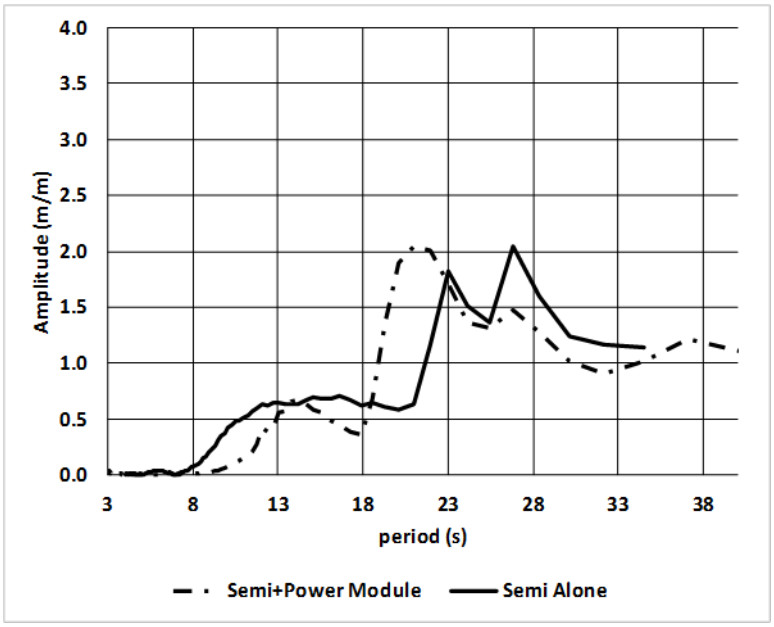

Figure 40 Heave RAO Comparison: Platform with and without Power Modules

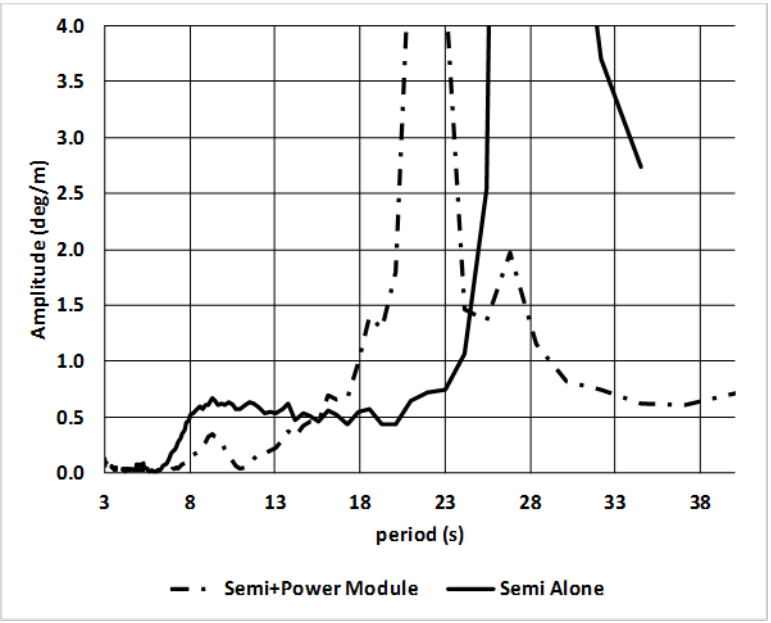

Figure 41 Pitch RAO Comparison: Platform with and without Power Modules

Results for time domain simulations, using the measured wave profile, are shown below. Figure 45 shows the standard deviation results (surge has been filtered to eliminate the slow drift responses as discussed above. Heave and responses include all frequencies. This approach is the same for all presentation of data unless indicated otherwise).

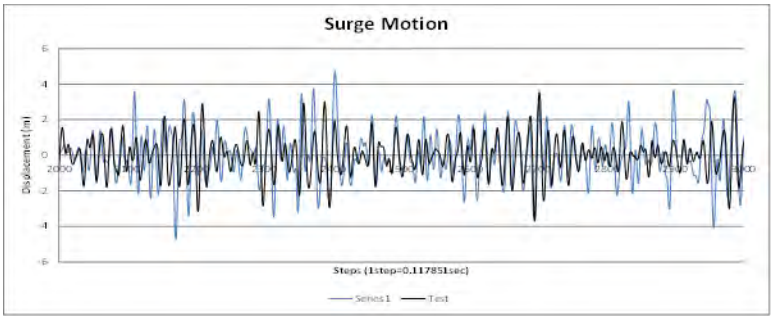

Figure 42 Surge Motion Comparison T200 Platform with Power Modules, 100-Year Cyclone

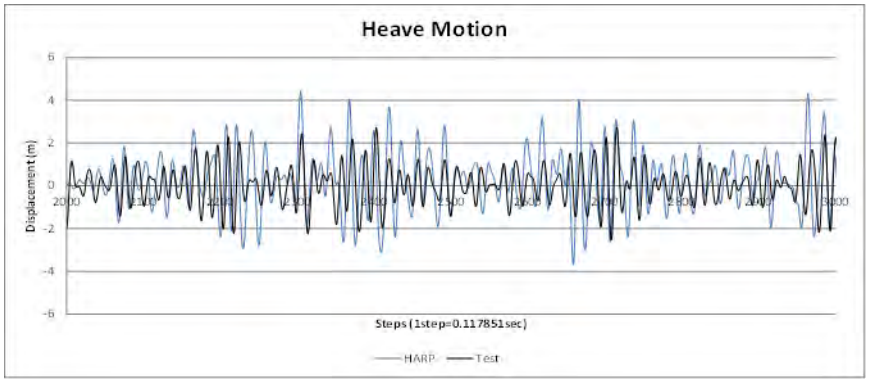

Figure 43 Surge Motion Comparison T200 Platform with Power Module, 100-Year Cyclone

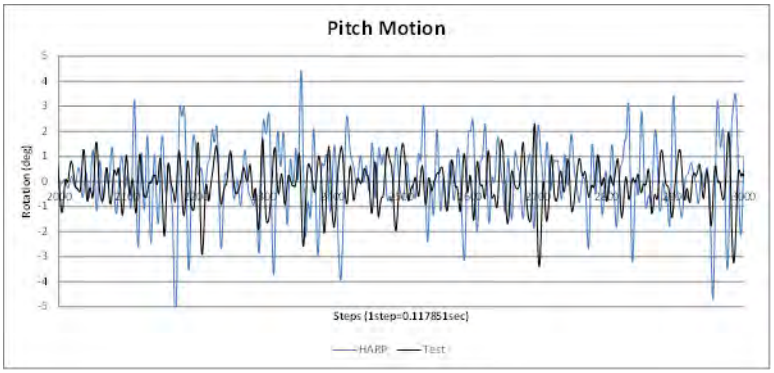

Figure 44 Pitch Motion Comparison T200 Platform with Power Module, 100-Year Cyclone

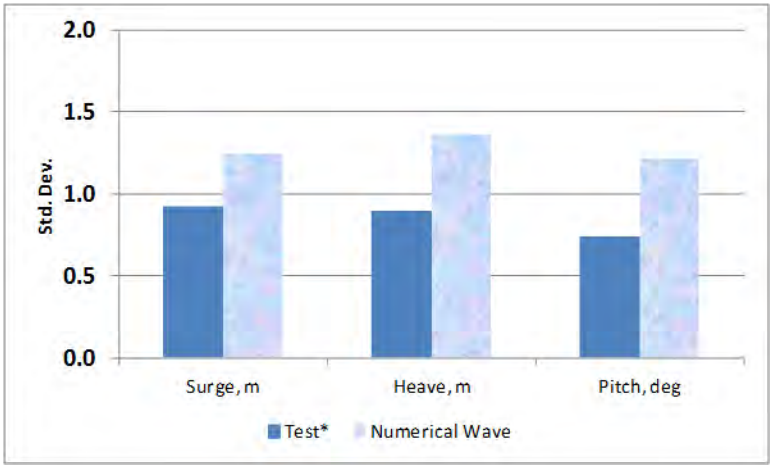

Figure 45 Statistics Comparison T200 100-Year Cyclone (* Surge motions filtered)

The above findings, that the numerical model consistently predicts higher motions than the tests, were found to be the case for all of the configurations tested.

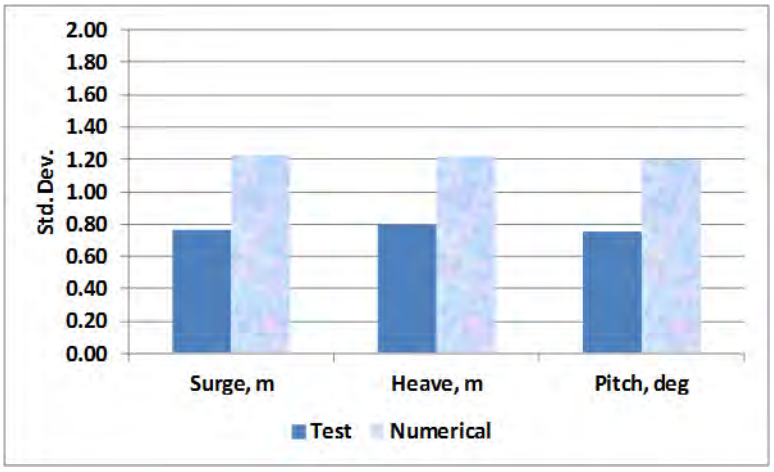

Figure 46 Statistics Comparison T300 Operational A, 100-Year Cyclone

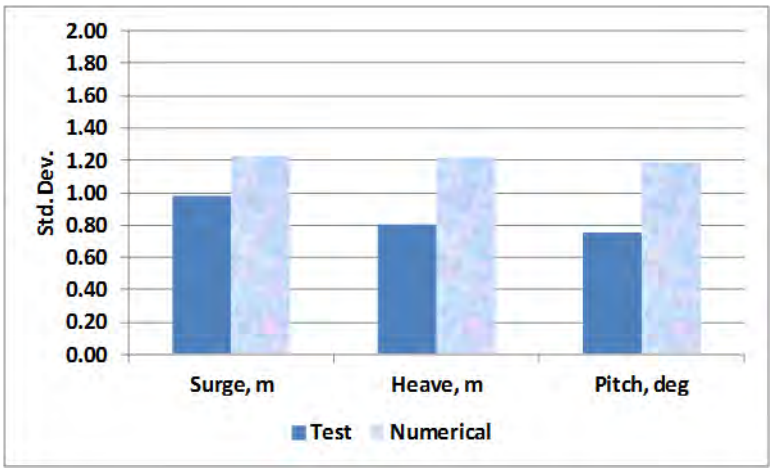

Figure 47 Statistics Comparison T400 Operational B, 100-Year Cyclone

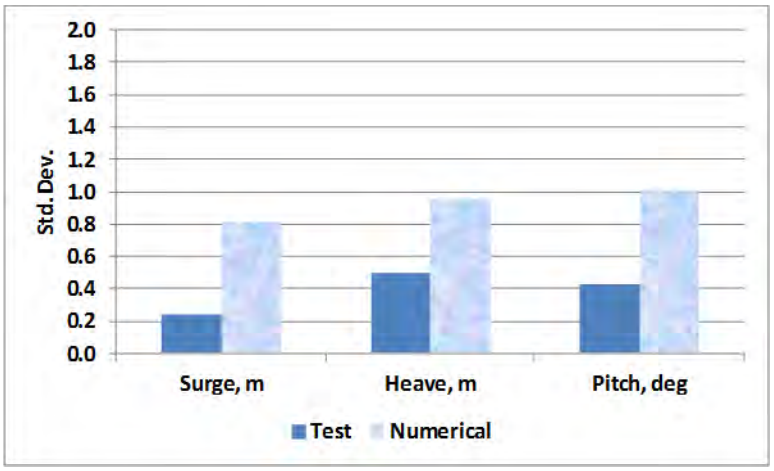

Figure 48 Statistics Comparison Installation A, 10-Year Swell

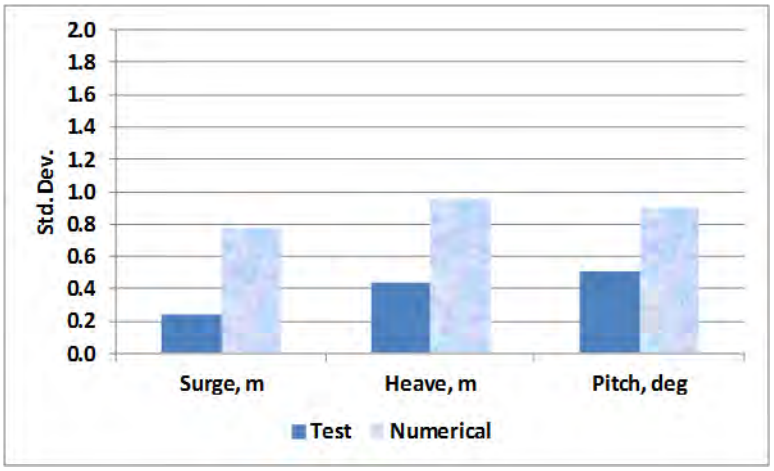

Figure 49 Statistic Comparison Installation B, 10-Year Swell

Motions in the installation configuration are of particular interest, as these might suggest that the numerical predictions are overly conservative concerning the installation scenario. Further discussion of this is included below with respect to the strain comparisons.

5.2.3 CWP EFFECT ON MOTIONS

As mentioned earlier (see Table 2), the mass of the CWP is the same order of magnitude of the platform alone. The RAOs of the platform + power modules with and without the CWP are shown in Figure 50 to Figure 52. The RAOs of the platform alone with and without CWP are shown in Figure 53 to Figure 55. It can be seen that the CWP does not have much effect on the platform motions with the power modules attached, but there is a remarkable difference on the responses of the platform alone. These results illustrate the importance of performing fully coupled analysis with the installation cases.

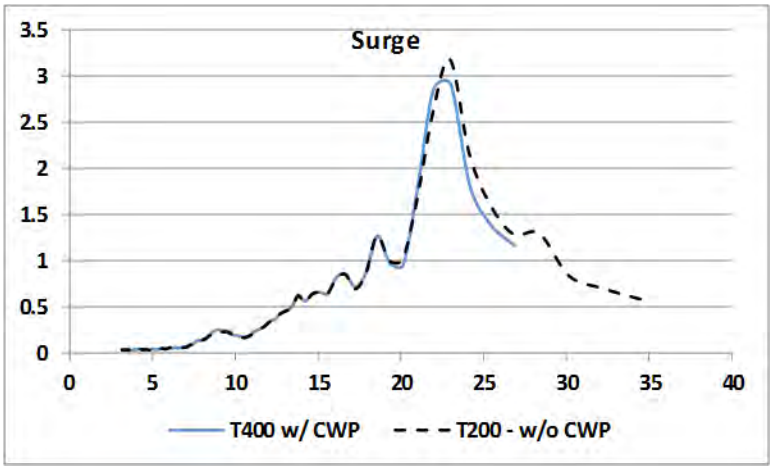

Figure 50 Effect of CWP on Surge RAO

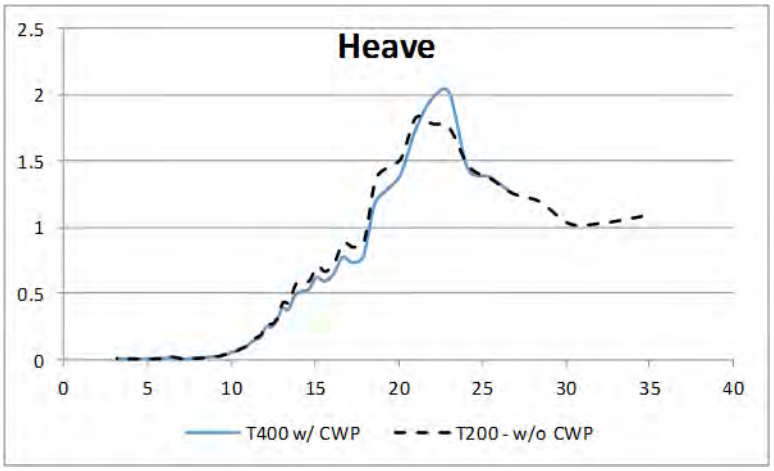

Figure 51 Effect of CWP on Heave RAO

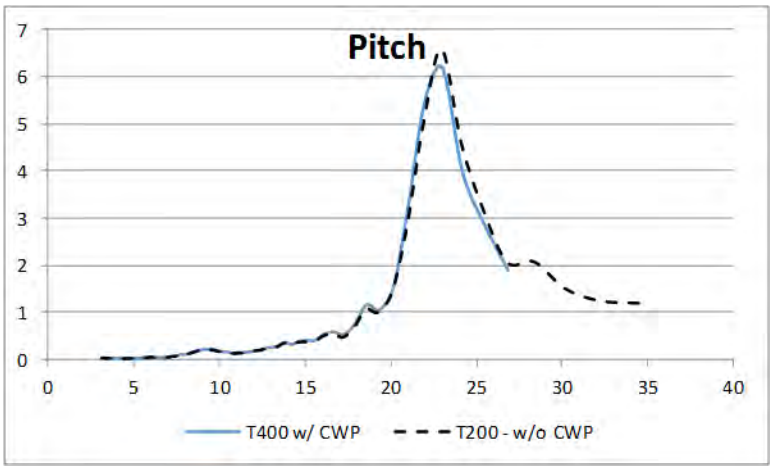

Figure 52 Effect of CWP on Pitch RAO

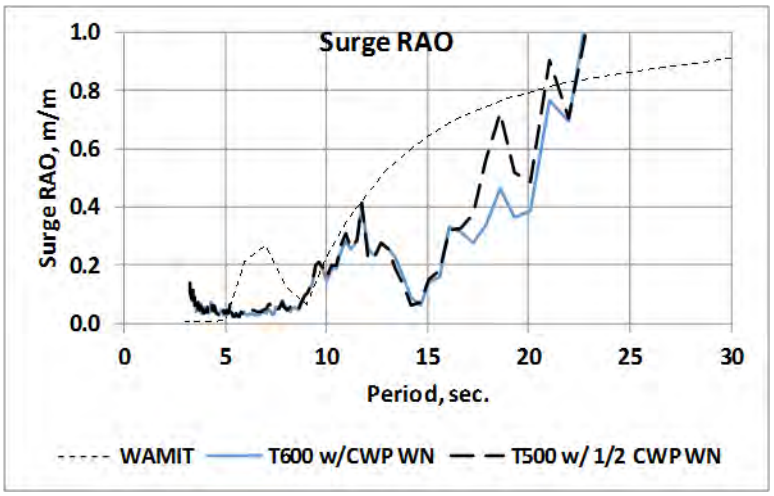

Figure 53 Effect of CWP on Surge RAO - Platform Alone

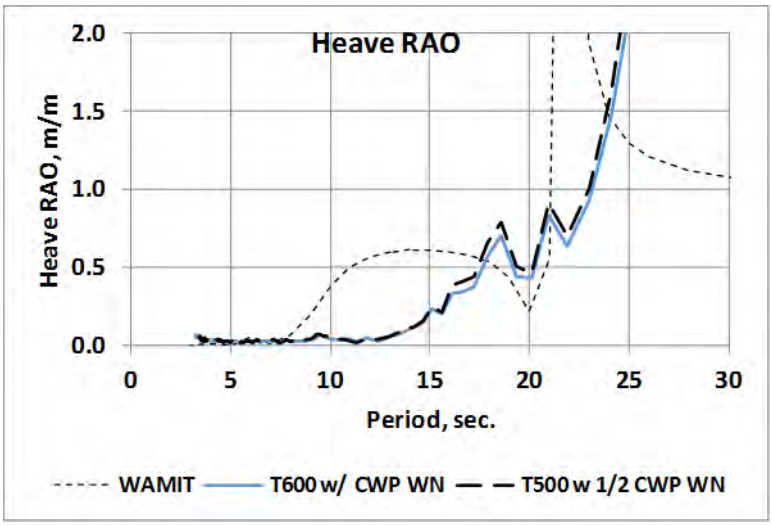

Figure 54 Effect of CWP on Heave RAO - Platform Alone

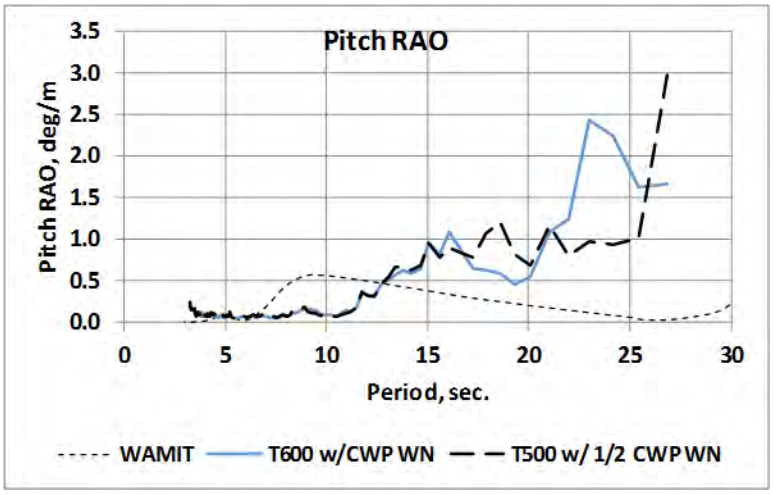

Figure 55 Effect of CWP on Pitch RAO - Platform Alone

5.3 CWP RESPONSES

The 1,000 m CWP model was instrumented with 20 strain gages: 18 were place along the pipe in the dominant wave direction (moments in the Y-axis) and two placed in the transverse direction. The gages proved reliable for the duration of the program. Only two of the gages failed. Comparisons of the measured strains with the numerical predictions are presented in this section.

The pipe has three vibration modes in the range of wave energy: modes 4, 5 and 6. See Table 9 and Figure 56 for the modal frequencies and dominant mode shapes for the operational configuration with intermediate stiffness. Mode 5 was observed to be the most actively excited mode for the important metocean cases. Spectral analysis of the strain gauge values indicates that the pipe responses are highly tuned to these frequencies.

Table 9 Predicted CWP Modal Frequencies

Mode No	Eigenvalue	Frequency (Hz)	Period (s)
1	0.0002	0.0021	465.3
2	0.0025	0.0079	126.4
3	0.0171	0.0208	48.0
4	0.0664	0.041	24.4
5	0.1854	0.0685	14.6
6	0.4217	0.1034	9.7
7	0.8359	0.1455	6.9
8	1.501	0.195	5.1
9	2.5031	0.2518	4.0
10	3.9406	0.3159	3.2
11	5.9251	0.3874	2.6

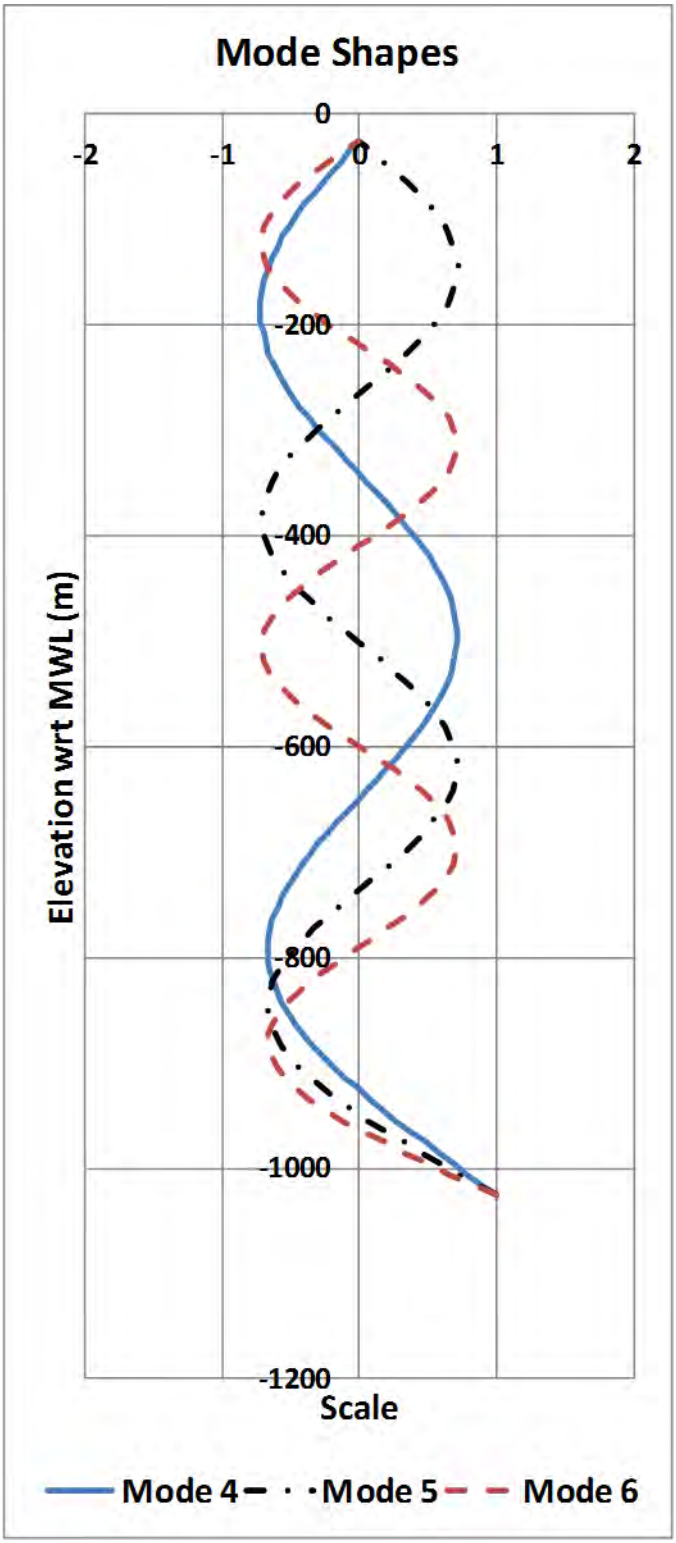

Figure 56 CWP Mode Shapes

5.3.1 CWP STRAINS

The following figures show comparisons of the computed and measured strains for some of the tests. The figures show the standard deviation, maximum and minimum strain values plotted against the position along the pipe. The hangoff point is 25 m below the free surface. The first test data point, strain gage 1, is 56 m below the hangoff point.

Figure 57 and Figure 58 show the results for the operational case with the free gimbal for the 10-year swell and 100-year cyclone conditions respectively. The results show the computations are slightly conservative, probably owing to the greater motions as discussed in the previous section. From examination of these figures, it is clear there the responses are dominated by the fifth mode (five anti-nodes) which is close to the peak spectral period.

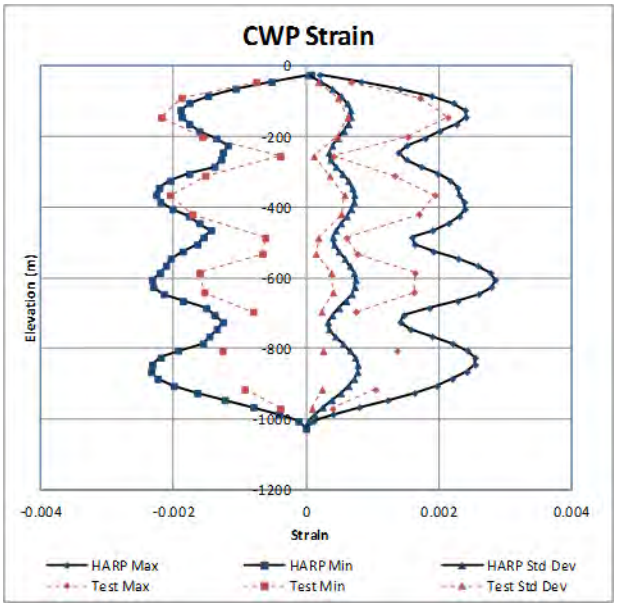

Figure 57 T300 – Operational A (pinned) 10-Year Swell

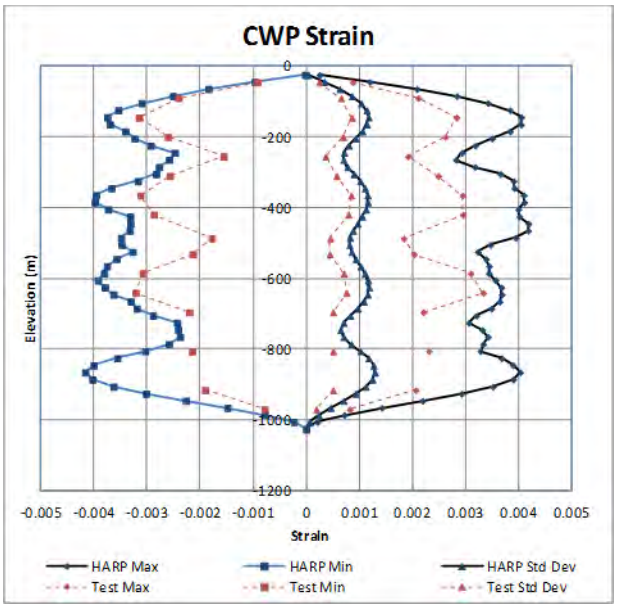

Figure 58 T300 Operational A (pinned) 100-Year Cyclone

Results for the intermediate stiffness operational configuration for the 100-year cyclone are shown in Figure 59. Comparing with Figure 58, the effect of adding a moderate amount of stiffness to the gimbal is insignificant.

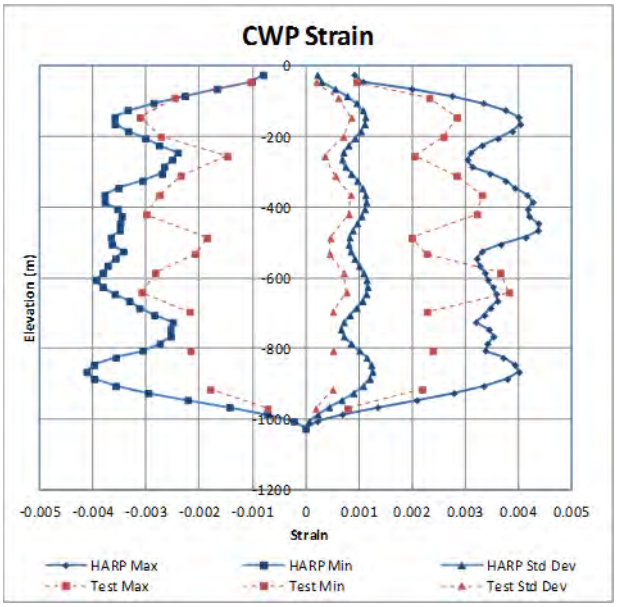

Figure 59 T400 Operational B (Intermediate Stiffness Gimbal) 100-Year Cyclone

5.3.2 INSTALLATION CASES

The strains with the stiff gimbal during an installation survival condition are of particular interest. Figure 60 and Figure 61 shows comparisons for the 10-year swell condition for the case of 500 m and 1,000 m pipe deployed with the stiff top connections respectively. These results are “blind” simulations based upon the calibrated gimbal stiffness, Table 3, 9.55E10 N-m/rad for the installation case. Both figures

show a divergent behavior near the top of the pipe. The computations show a growth in the strain near the top connection while this is not seen in the test results.

These results raised questions about the sensitivity to stiffness of the connection between the CWP and the platform. The team believes this discrepancy can be attributed to the flexural properties of the gimbal assembly. The gimbal fixture set up for calibration is shown in Figure 25. The gimbal frame is rigidly suspended from a structural beam for these calibrations. When the frame is installed in the model, it is attached with U-bolts to the dynamometer assembly and through the support frame to the platform. The load cell/dynamometer assembly is shown attached to the frame in Figure 24. There is flexibility in this setup, which was not accounted for in the calibration setup. Load cells are particularly flexible, and the truss frame and platform attachment have flexibility.

Figure 62 shows the comparison of tests and HARP results for the 500 m riser with platform alone for stiffness equal to 3.3% of the installation stiffness, 3.15E9 N-m/rad. The sensitivity of the T600 results (1,000 m pipe) also showed good agreement near the platform with about 5 – 10% of the prescribed installation stiffness.

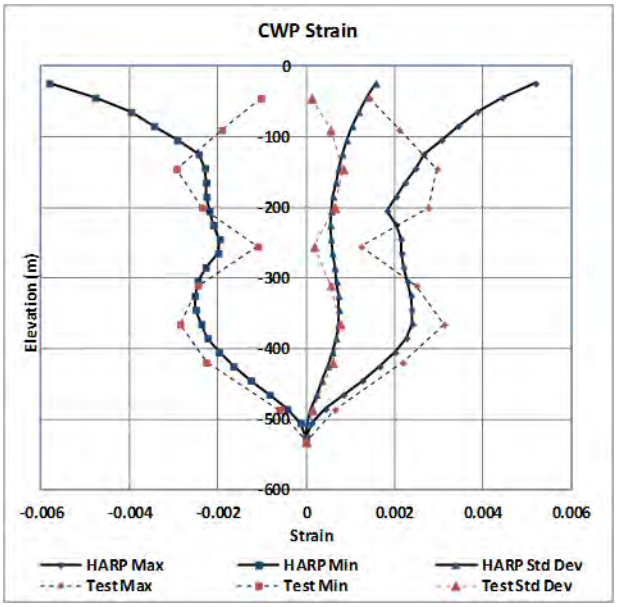

Figure 60 T500 Installation A (500 m Pipe) 10-Year Swell

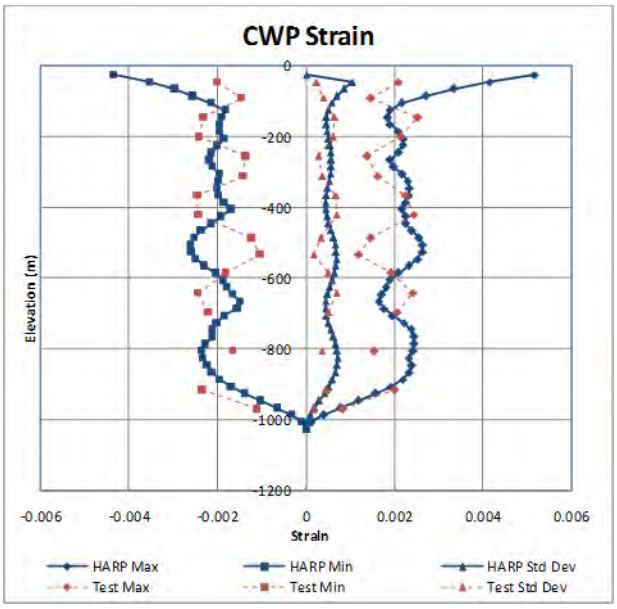

Figure 61 T600 Installation (1,000 m Pipe) 10-Year Swell

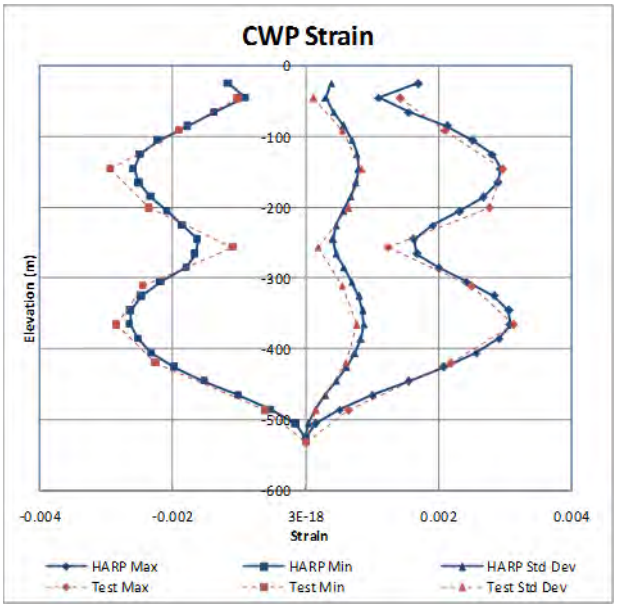

Figure 62 T500 Installation (500 m Pipe) with 3.3% of the Installation Stiffness 10-Year Swell

5.3.3 SENSITIVITY TO STIFFNESS AND CA

The above results led to an investigation of the effect of stiffness, and the pipe added mass parameter, Ca. The reason that stiffness was investigated was the result presented above for matching the measured bending strains at the upper end of the pipe. The lateral added mass of the pipe was investigated because it is known this parameter is sensitive to the Keulegan-Carpenter (KC) number [222]. The numerical simulations all used a value of Ca = one, however earlier CWP tests indicated the values might be closer to .3 - .8 [5].

The following plots, Figure 63 - Figure 68 present the results of these investigations for the full 1000 m pipe installation case, T600. In all cases, the 10-year swell environment was selected, as this is the survival environment for the installation scenario.

The lower Ca values resulted in slightly lower strains at the top of the pipe. In all cases, the magnitude of the strains along the pipe remained similar. The T600 results show a curious phase shift in the mode shapes: the antinodes for the measured responses appear where the nodes for the numerical results occur. In the results presented above for the operational cases, and the 500 m long installation cases, the nodes and antinodes for the numerical and test results generally were synchronized. The synchronization appears closer at the lower stiffness values, however.

Gimbal Stiffness = 9.55E+10
[Installation Stiffness, Ca = 1.0]

Gimbal Stiffness = 9.55E+10
[Installation Stiffness, Ca = 0.5]

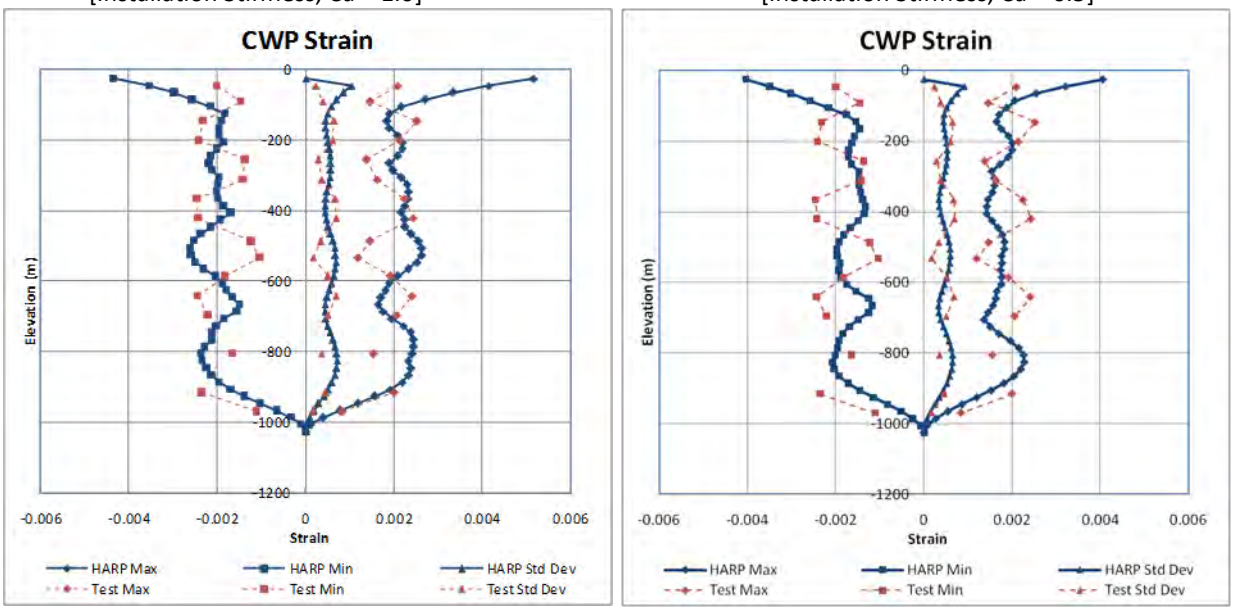

Figure 63 Ca Sensitivity: Ca=1, 0.5 T-600 10-Year Swell

Gimbal Stiffness = 9.55E+10
[Installation Stiffness, Ca = 0.3]

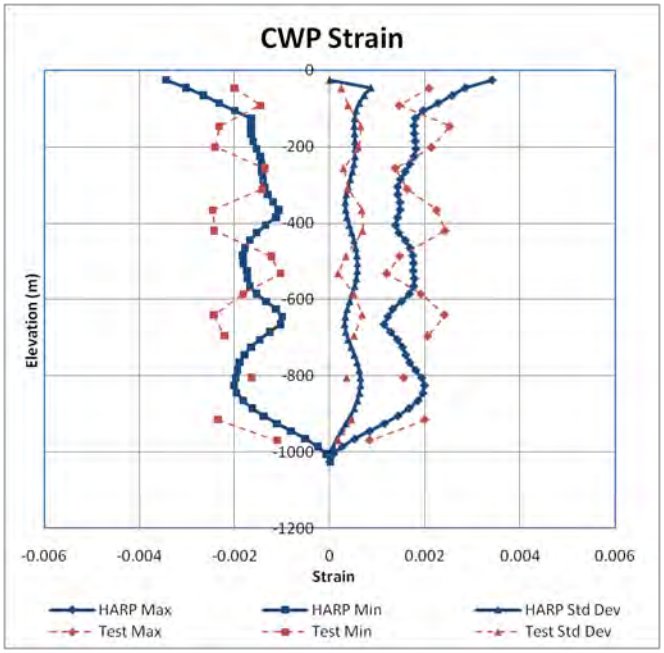

Figure 64 Ca Sensitivity Ca = 0.3 T600 10-Year Swell

Gimbal Stiffness = 9.55E+10
[Installation Stiffness]

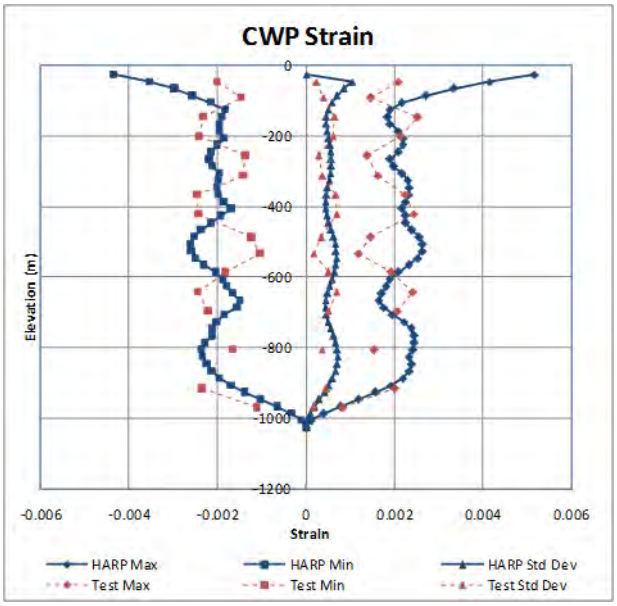

Gimbal Stiffness = 7.19E+10
[75.3% Installation Stiffness, 57.1x Operation Stiffness]

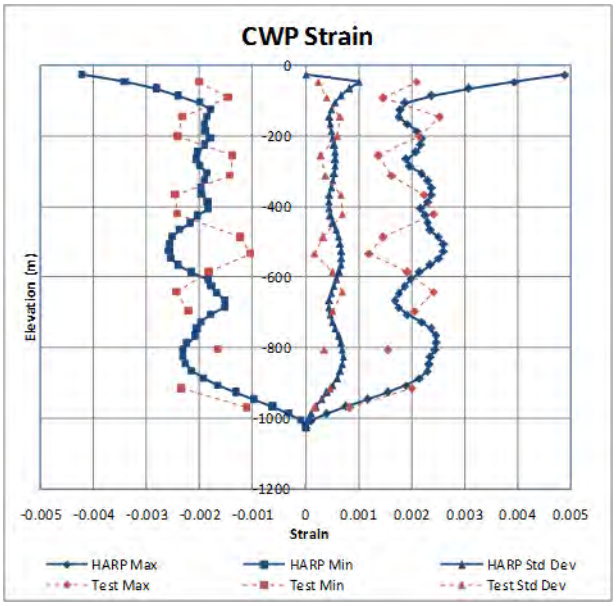

Figure 65 Stiffness Sensitivity (1) T600 10-Year Swell

Gimbal Stiffness = 4.84E+10
[50.7% Installation Stiffness, 38.4x Operation Stiffness]

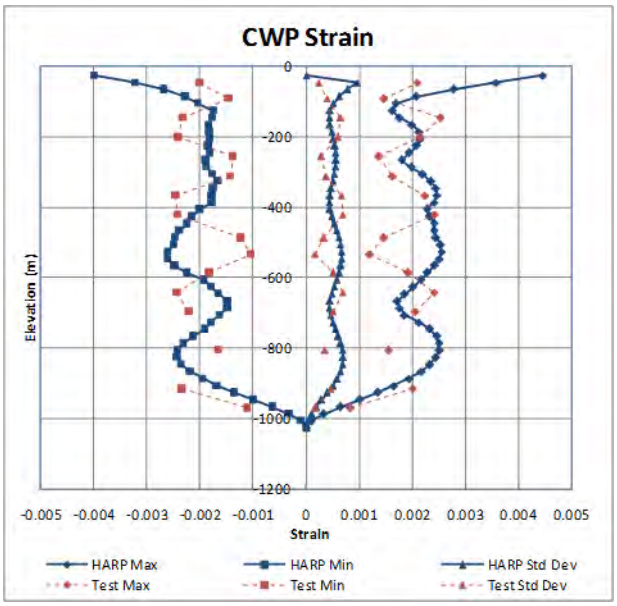

Gimbal Stiffness = 2.48E+10
[25.9% Installation Stiffness, 19.7x Operation Stiffness]

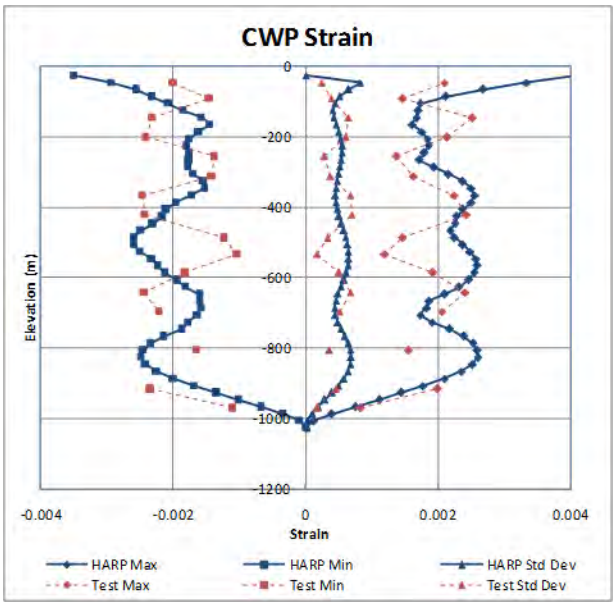

Figure 66 Stiffness Sensitivity (2) T600 10-Year Swell

Gimbal Stiffness = 1.89E+10
[19.8% Installation Stiffness, 15x Operation Stiffness]

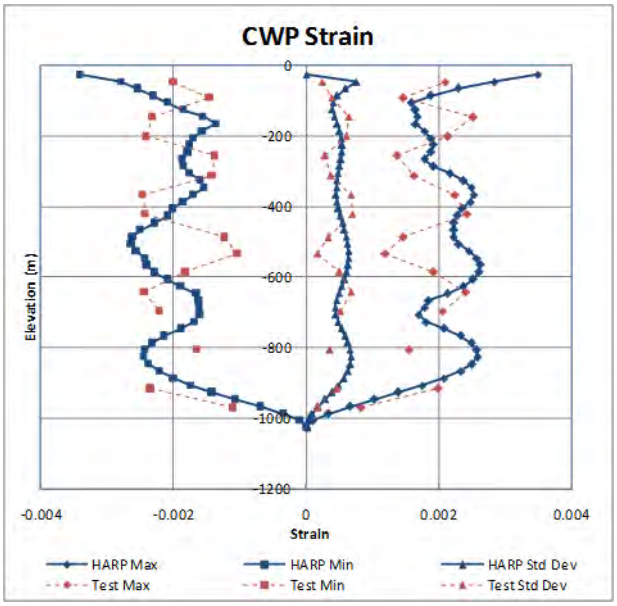

Gimbal Stiffness = 1.30E+10
[13.6% Installation Stiffness, 10.3x Operation Stiffness]

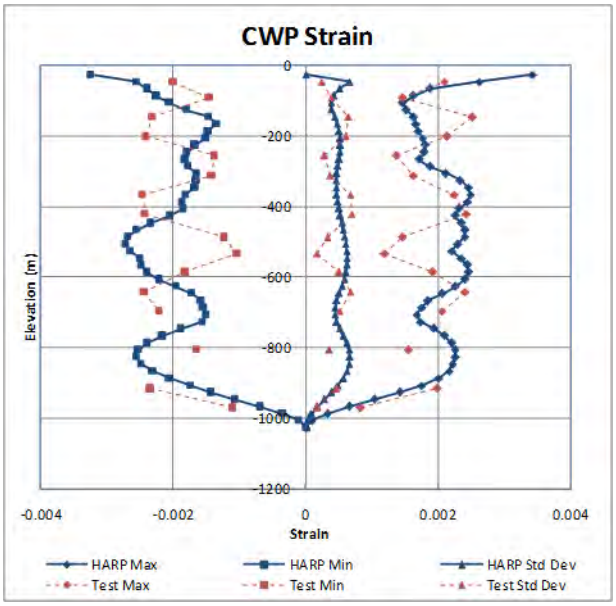

Figure 67 Stiffness Sensitivity (3) T600 10-Year Swell

Gimbal Stiffness = 7.15E+09
[7.5% Installation Stiffness, 5.7x Operation Stiffness]
(Selected for T500 Analysis)

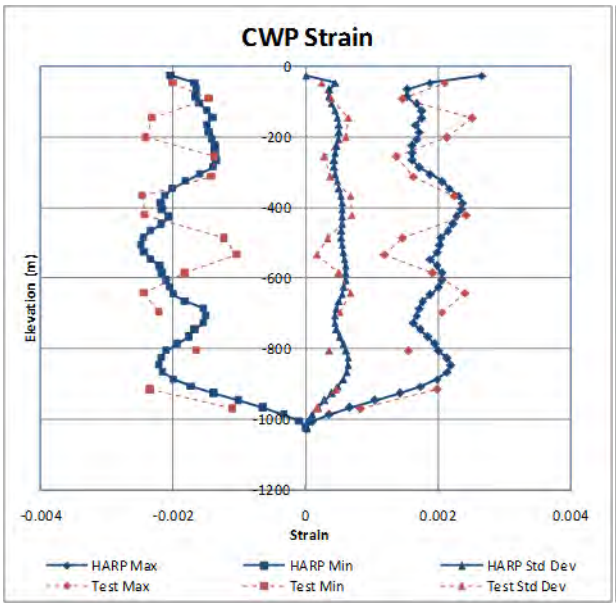

Gimbal Stiffness = 3.15E+09
[3.3% Installation Stiffness, 2.5x Operation Stiffness]
(Selected for T500 Analysis)

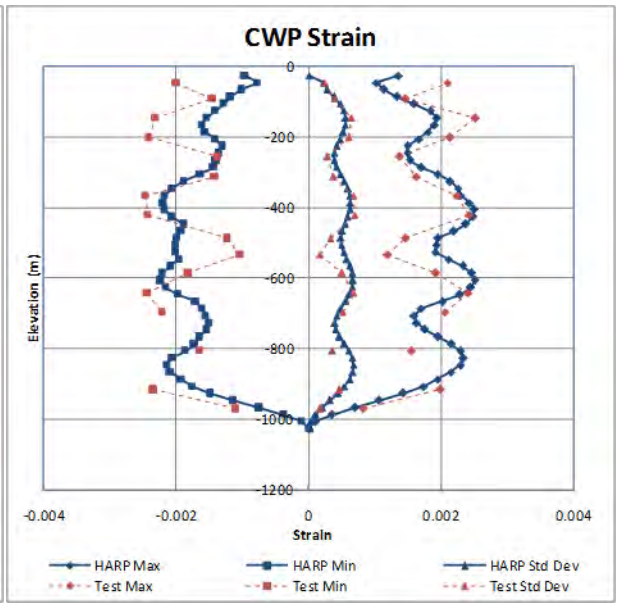

Figure 68 Stiffness Sensitivity (4) T600 10-Year Swell

6 CONCLUSIONS

The overall conclusion is that the numerical methods provide adequate, if not overly conservative results upon which to evaluate platform responses and pipe loads. The pipe response was observed to be highly tuned to the mode shapes closest to the peak wave energy. The numerical methods captured this effect very well.

Computed dynamic wave platform responses (surge, heave and pitch) based on time domain coupled analysis were generally 25 – 60% higher than those observed in the tests for the platform with power modules. The difference was even greater for the platform alone. This result is in spite of the fact that frequency domain comparisons, Response Amplitude Operators, showed very good agreement of the wave frequency responses.

Computed dynamic strain values were also higher than the measured values in most cases. For the operational cases, the computed strain values were roughly 50% higher than the measured values along the length of the pipe. The observed periods and mode shapes agreed very well with the computed results. The strains measured in for the installations cases suggested that the effective gimbal stiffness was significantly less than the specified and calibrated values. As a result, the nominal computed value of strain near the top of the pipe was significantly greater than the measured values. Calculations at varying stiffness values suggest the actual stiffness was about 3.3% of the nominal calibrated result is very close agreement between the dynamic strains along the length of the riser between calculated and measured values.

While it is comforting to find numerical solutions providing such conservative results, the differences in motions particularly are greater than would normally be expected from these types of tests. It may be that the numerical time domain methods used incorrect wave parameters, which might explain why the time domain results over predicted the motions, while regular wave results were consistent with numerical predictions. Further investigation of this is worthwhile.

In the case of the installation condition, the cold water pipe is shown in both experiments and calculations to have a major influence upon the platform motions. This is because the effective mass of the CWP is about equal to the mass of the platform. In this case fully coupled analysis should be performed. Coupling effects seems less pronounced in the case of the large platform: platform with power modules, however coupled analysis should still be used or the results will be even more conservative than indicated here.

It should be noted that these results were obtained for tests in waves only. The test facility could not produce a current; hence, the impact of wave-current interaction could not be validated. It is suspected that this would result in greater hydrodynamic damping.

The numerical model of the CWP did not include any mechanical damping. In reality, some might be expected, and this could be one reason the computed strains were higher than the measured values. Experience based on full-scale measurements of marine risers suggests that hydrodynamic damping is the dominant factor, however further investigation of its importance for the large CWP is worthwhile.

This page intentionally left blank.

7 RECOMMENDATIONS

These model tests produced a wealth of data. The analysis effort that has been performed within the scope of this study addresses a small part of the data collected. The following are recommendations for further work.

1) Perform further work to try to explain the reasons for the over prediction of platform motions:
    i) Perform numerical simulations of the regular wave tests with the calibrated regular waves.
    ii) Check the specified waves used for irregular wave simulations against the calibrated waves.
2) Perform a posttest calibration of the gimbal with the load cell frame to quantify the as-built rotational stiffness for the installation tests.
3) Compare spectral density and filtered statistics comparisons for all the irregular wave tests.

The team believes these tests provide sufficient confidence to proceed with project specific designs at the preliminary design phase, e.g. FEED engineering. However, during the FEED engineering and prior to detailed design the team believes further testing is prudent. This testing might include an integrated system like these tests, or there might be a few sub-system tests as suggested in the recommendations below.

1) The gimbal angle and bending moments at the CWP connection are critical measurements that should be included in future tests.
2) The strain measurements were invaluable in these tests. A similar density of gages is recommended. CWP displacement measurement was not utilized, but they would be more important if tests are conducted in a current.
3) The mooring system should not introduce external damping. It is recommended that springs be placed between the model and the anchor point.
4) Further calibration of pipe damping is suggested, especially with a current. It might be beneficial if a pipe test could be performed with the top fixed (through a gimbal) to a planar motion mechanism to introduced prescribed motions. Fully integrated tests introduce many unknowns related to platform motions and pipe responses.
5) The pipe model with a central tube and outer sheath seemed to capture the dynamic responses as tested. It would be worthwhile to perform separate tests with an elastically modeled pipe at some scale that would allow pumping of water to determine if there were any phenomena due to fluid flow, which are not being capturing.
6) Tests in a realistic current are recommended for the final design.

This page intentionally left blank.

8 ACCOMPLISHMENTS

- Analysis to-date indicates numerical modeling provides conservative estimates of cold water pipe loads in relevant environments. Therefore, cold water pipe designers can use numerical analysis results to continue CWP development.
- These results advanced the state-of-art understanding of FRP cold water pipe designs.
- Additional analysis of the data sets will provide additional confidence, which may allow cold water pipe designers to reduce pipe specification requirements, potentially lowering subsystem costs.
- Clear recommendations were generated to guide the next steps for analysis and tests. Lessons-learned allows refinements of test specifications, test plans, and test execution for future efforts.
- Project results will guide task, schedule, and cost estimates for the cold water pipe related design activities associated with the first, floating OTEC system development.
- Early results were submitted and accepted for inclusion in the OMAE 2014 conference in San Francisco, California, United States.
- A fifteen-minute video record describing the project and showing aspects of the test activity was developed. The script is provided as Appendix G and a version of the video is provided in a DVD attached to Appendix H.

This page intentionally left blank.

9 REFERENCES

1. Rajagopalan, K. and G.C. Nihous, (2013). "Estimates of Global Ocean Thermal Energy Conversion (OTEC) Resources using an Ocean General Circulation Model," Renewable Energy, 50, 532-540.
2. Naval Facilities Engineering Command, Engineering Service Center (2011), "NAVFAC Ocean Thermal Energy Conversion (OTEC) Project; OTEC Technology Development Report," Prepared by Lockheed Martin Corporation, Contract N62583-09-C-0083, CDRL A002, DTIC Accession Number ADA532390, (November 2010).
3. Houston Offshore Engineering, "Ocean Thermal Energy Conversion (OTEC) Plant Modeling Test - Numerical Modeling and Simulation Report" Report H12129-G-RPT-RI-00001, Rev. A, 26 Feb. 2014
4. Avery, W.H. & Wu, C., Renewable Energy from the Ocean – A Guide to OTEC, Oxford University Press, Oxford & NY, 1994.
5. Vega, L. A. and G. C. Nihous (1988) "At-Sea Test of the Structural Response of a Large-Diameter Pipe Attached to a Surface Vessel," *Offshore Technology Conference, OTC*-5798-MS, Houston, TX, (May 1988).
6. McGuiness, T. and Scotti, R.S., (1980) "OTEC Cold Water Pipe Program Status," *Offshore Technology Conference*, OTC-3685-MS, Houston, TX, (May 1980).
7. Chou, D.Y., Minner, W.F., Ragusa, L.Y. and Ho, R.T., 1978, "Dynamic Analysis of Coupled OTEC Platform-Cold Water Pipe System", *Offshore Technology Conference,* OTC-3338-MS, Houston, TX, (May 1978).
8. Barr, R. A., Chang P. Y., and Thasanatorn, C., (1978) "Methods for and Examples of Dynamic Load and Stress Analysis of OTEC Cold Water Pipe Designs," HYDRONAUTICS Inc. T.R. 7825-2 (2 Vols.), (November 1978).
9. Paulling, J. R., (1979), "Frequency-Domain Analysis of OTEC CW Pipe and Platform Dynamics," *Offshore Technology Conference*, OTC-3543-MS, Houston, TX, (May 1979).
10. Kowalyshyn, R. and Barr, R.A., (1979) "Seakeeping Model Tests of a 400 MW OTEC Spar Platform and Cold Water Pipe" Hydronautics, Inc., Technical Report COO-2681-4. United States Department of Energy.
11. Barr, R.A. and Sheldon, L.R., (1980) "Model Testing of OTEC Plant Platforms and Cold Water Pipe," *Offshore Technology Conference*, OTC-3687-MS, Houston, TX, (May 1980).
12. George, J. F. and Richards, D., (1982) "Model Basin Test of Ocean Wave Responses for a 40-MW OTEC Pilot Plant," Transactions of ASME, Vol. 104, pp. 46-51.
13. Vega, L.A. and Nihous, G.C., (1994), "Design of a 5MWe OTEC pre-Commercial Plant," Oceanology International '94 Conference, Brighton, UK, (March 1994).
14. Vega, Luis., "Ocean Thermal Energy Conversion History, Mostly about USA, 1980's to 1990's, and Bias Toward Vega's Experience," http://hinmrec.hnei.hawaii.edu/wp-content/uploads/2010/01/OTEC-History-with-Vega-bias.pdf
15. Paulling, J.R., (1980a), "Theory and User Manual for OTEC C W Pipe Program ROTECF and SEGPIP," J. Randolf Paulling Inc.

16. Hove, D.T., (1981) “OTEC Cold Water Pipe Design and Laboratory Testing”, Proceedings IEEE Conference
17. Paulling, J. R., (1980b), “An Equivalent Representation of the Forces Exerted on the OTEC CW Pipe by Combined Effects of Waves and Currents”, 1980 Energy-Sources Technology Conference and Exhibition, New Orleans, LA.
18. http://www.harponline.com
19. Ran, Z. and Kim, M.H., (1996), “Nonlinear Coupled Responses of a Tethered Spar Platform in Waves,” Proceedings of the Sixth International Offshore and Polar Engineering Conference, Vol. 1, pp281-288.
20. http://www.wamit.com
21. Garrett, D.L., (1982), “Dynamic Analysis of Slender Rods,” ASME Journal of Energy Resources Technology, Vol. 104, pp. 302-306.
22. Turgut Sarpkaya, Michael Isaacson (1981), Mechanics of wave forces on offshore structures, Van Nostrand Reinhold Co.

10 APPENDICES

This page intentionally left blank.

A. LIST OF ACRONYMS & DEFINITIONS

This page intentionally left blank.

Acronyms & Definitions

BMT	BMT Scientific Marine Services, Inc.
Ca	added mass parameter
CB	Center of Buoyancy
Charm3D	fully coupled analysis program
CG	Center of Gravity
CWP	cold water pipe
DoE	United States Department of Energy
FRP	fiberglass reinforced plastic
ft	feet
gf	grams-force
HARP	HARmonic Phase loads analysis software, used for numerical simulations
HDPE	high-density polyethylene
HOE	Houston Offshore Engineering, Inc.
Heave	linear vertical (up-down)translation motion, see Figure 69
Hs	Significant Wave Height
IR&D	Independent Research & Development
JHA	John Halkyard & Associates, Inc.
KC	Keulegan-Carpenter number, a dimensionless ratio describing the relative importance of the drag forces over inertia forces for bluff objects in an oscillatory fluid flow
kN	kilo-Newtons
LMC	Lockheed Martin Corporation
LVDT	linear voltage displacement transducer
metocean	an abbreviation of “meteorology" and "oceanography" to describe the physical environment of at-sea and coastal areas
model	the replica of the full sized platform, gimbal, and cold water pipe tested in the model basin, scaled at 50:1 for this project
MW	megawatt
NOAA	National Oceanic and Atmospheric Administration
OTEC	Ocean Thermal Energy Conversion
Pitch	rotation around transverse (side-side) axis, see Figure 70

prototype	reference to the full size platform, gimbal, and cold water pipe hardware
PVC	polyvinyl chloride
QTF	quadratic transfer function
RAO	Response Amplitude Operator - ratio of motion to the wave amplitude causing that motion, presented over a range of wave periods
Remoras	Another name for power modules
Roll	rotation around longitudinal (forward-aft) axis, see Figure 70
ROTEC	a quasi-linear frequency domain analysis of coupled cold water pipe and platform responses for continuous pipe designs
Semi	Semi-submersible
Surge	linear longitudinal (forward-aft) translation motion, see Figure 69
Sway	linear lateral (side-side) translation motion, see Figure 69
t	metric tonne
Tp	Peak Wave Period
w/	with
WAMIT	Wave Analysis Massachusetts Institute of Technology, used to derive hydrodynamic coefficients
Yaw	rotation around vertical axis, see Figure 70

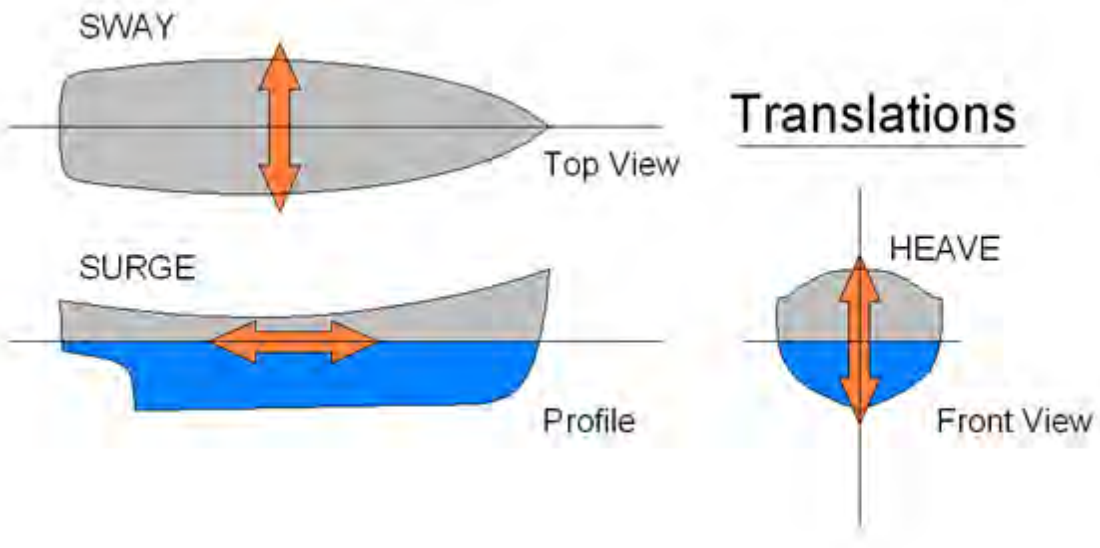

Appendix A - Figure 69 Linear Motion Definitions

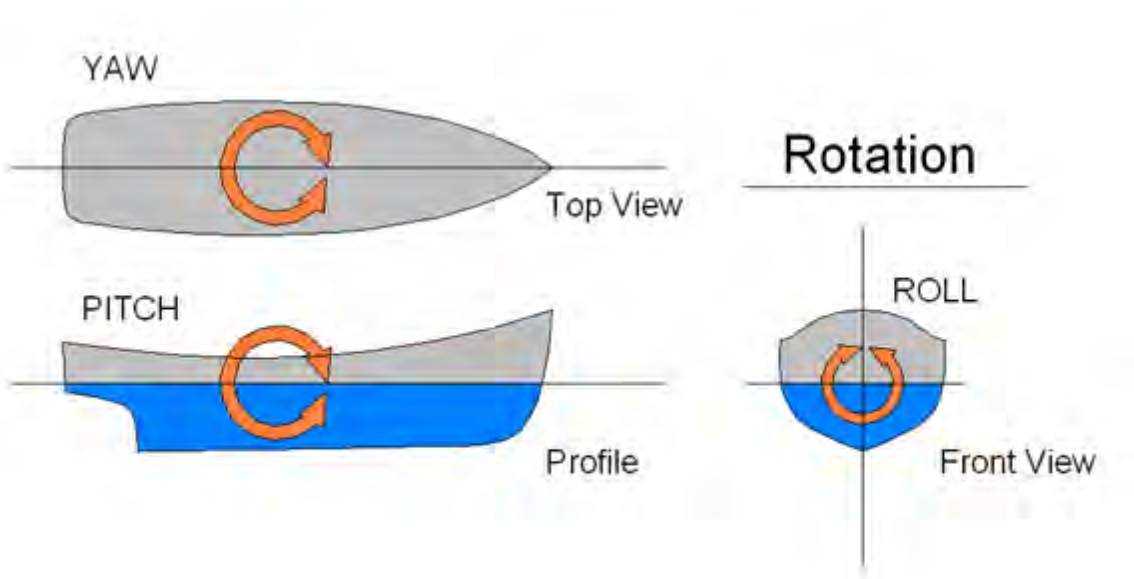

Appendix A - Figure 70 Rotational Motion Definitions

This page intentionally left blank.

B. MODEL BASIN TEST SPECIFICATION

This page intentionally left blank.

Ocean Thermal Energy Conversion (OTEC) Model Basin Test Specification

(Excerpts from Statement of Work)

25 July 2012

Table of Contents

List of Figures

List of Tables

1 Introduction

1.1 Objectives

This project will validate the ability to model numerically the dynamic interaction between a large cold water-filled fiberglass pipe and a floating ocean thermal energy conversion (OTEC) platform excited by meteorological and ocean (metocean) weather conditions using measurements from a scale model tested in an ocean basin test facility.

1.2 Background

An OTEC system generates electrical power by running a Rankine thermodynamic cycle supported on a moored, floating platform subsystem. Warm surface water evaporates a working fluid. The working fluid gas is expanded through a turbo-generator, producing electricity. The discharged gas is condensed using cold deep-sea water accessed through a large cold water pipe (CWP). For power plant capacities of 100 MW, the CWP may be 10 meters in diameter and up to 1,000 meters long.

The interaction of this CWP-platform subsystem from combinations of metocean conditions must be understood to design an OTEC system to survive for typical utility life cycles. The offshore industry uses software-modeling tools validated by scale model tests in facilities able to replicate real at-sea metocean conditions to provide the understanding and confidence to proceed to final design and full-scale fabrication. However, today's offshore platforms (similar to and usually larger than those needed for OTEC applications) incorporate risers (or pipes) with diameters well under one meter. Hence, existing offshore design tools are not validated for OTEC applications where the CWP has mass loading properties of the same magnitude as the rest of the platform.

The fiberglass CWP is a key component for an OTEC system. A commercial system requires a 10 m diameter pipe suspended to 1,000 m depth. A particular requirement of this CWP installation process is the pipe be "gripped" and guided below the manufacturing equipment as it is built. The grippers and guides must be able to suspend the pipe and minimize pipe deflections during curing. The loads on the pipe at the lower guide from platform and pipe motions control the design of the pipe core from the standpoint of bending loads. Application of existing numerical modeling methods to analyze the OTEC system needs to be validated to minimize the risk to a pipe. That is a key objective of this project. If motions and/or minimum deflections are exceeded a significant proportion of the time, the offshore manufacturing scheme may be impractical.

Once the pipe is manufactured, it is hung off from the keel of the platform using a gimbal or other suspension mechanism of a given rotational stiffness. It is critical to be able to predict the axial and bending strains in the pipe in this condition. Tests on fiberglass fatigue in seawater indicate that the fatigue life is VERY sensitive to the dynamic strain amplitudes.

Analysis of the pipe responses is complicated by several factors, e.g.:

1. The pipe has a major influence on platform motions, e.g. the pipe itself has a suspended mass about equal to the platform mass,
2. Pipe strains are dependent upon relative stiffness between the pipe and the platform
3. Flow around the pipe may influence the hydrodynamic loads on the platform from waves and current

We have benchmarked several industry standard numerical modeling software programs against one another and have been able to show agreement to about +/- 15% on the maximum pipe strains. In

order to proceed to the next level of development we need to verify the computational tools and establish “best practices” for the analysis in a comprehensive model basin test.

2 Description of the OTEC System

2.1 Hull – Installation Condition

The OTEC system will be supported on a four-column semisubmersible, shown in Figure 2-1and Figure 2-2. A “gripper” to hold the pipe is installed at elevation 37 m. This gripper supports the weight of the pipe by friction. The top of the pipe in this configuration is at elevation 53 m and is free standing above the gripper. The motion at the pipe at the top is important to the manufacturing process and should be measured.

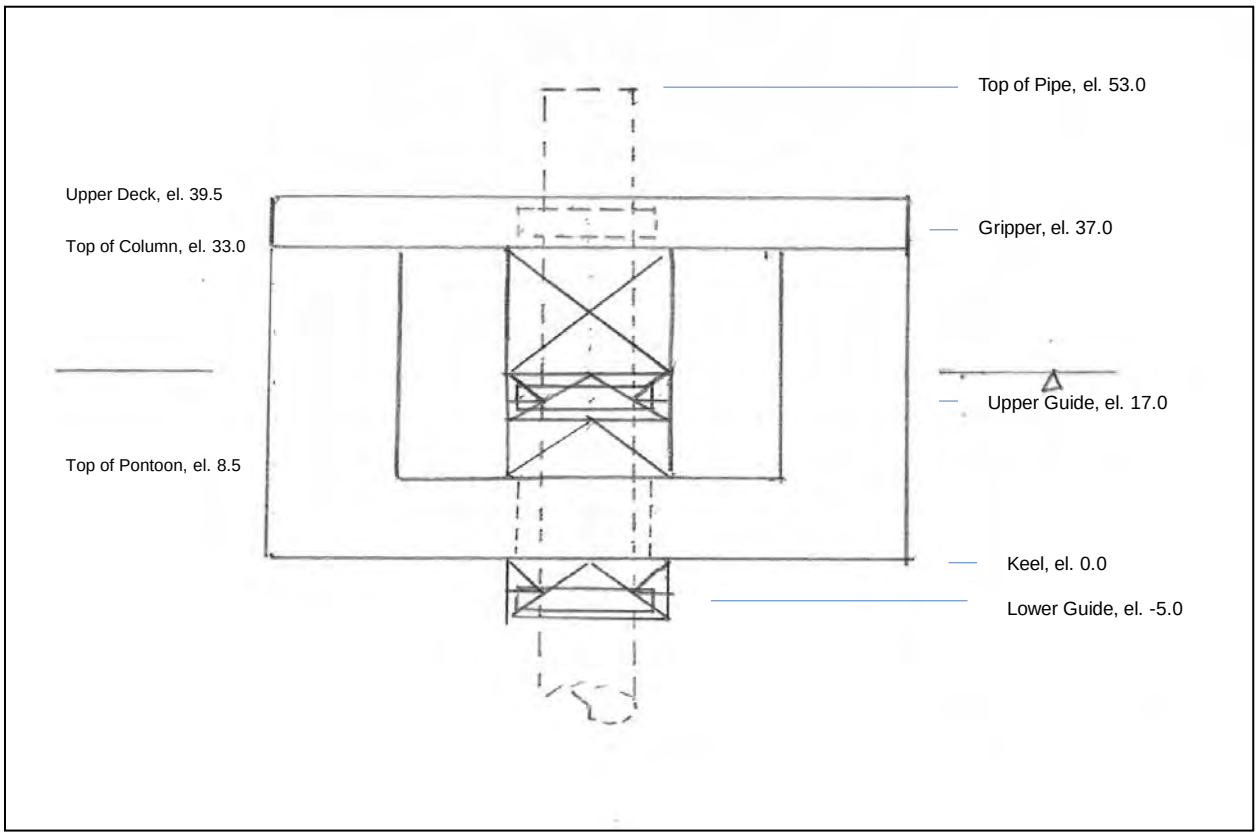

Figure 2-1 Platform Outboard Profile

Two guides constrain the pipe laterally at elevations -5 m and 17 m. The gripper and guides provide lateral stiffness, but allow the pipe to rotate. A truss framework is built into the hull to support the gripper and guide structures. Once the pipe is manufactured, it is hung off the lower guide and the other guides are removed. The lower guide is configured to allow the pipe to pivot relative to the hull. For test purposes, two rotational stiffness values will be specified for this gimbal.

The principal dimensions of the semisubmersible are listed in Table 2-1.

Mass properties are given in Table 2-3 and Table 2-4 for two conditions to be tested: 1000 m of pipe deployed and 500 m of pipe deployed. The length of pipe is measured from the top end suspended above the gripper. The “vertical loads” consist entirely of the hanging weight of the pipe. For these tests, the mooring system will consist of horizontal springs and will not impart any vertical loads in the calm water condition. Mass properties should be calibrated without the pipe.

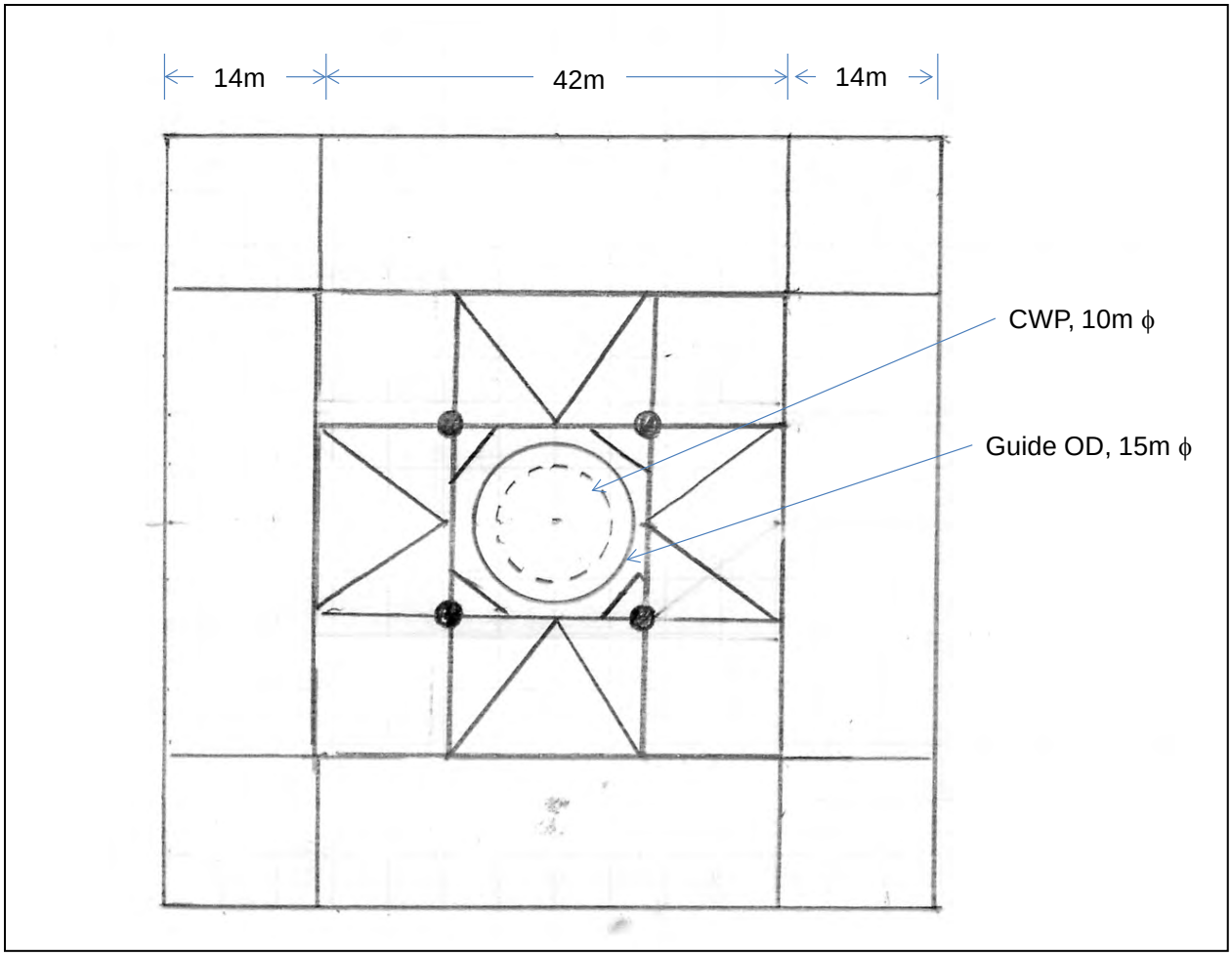

Figure 2-2 Plan at Pontoon Level

Table 2-1 Principle Dimensions of Hull

Item	Units	Value
Column height	m	33.0
Column depth	m	14.0
Column width	m	14.0
Column center to center spacing	m	56.0
Pontoon length	m	42.0
Pontoon height	m	8.5
Pontoon width	m	14.0
Deck length	m	70.0
Deck width	m	70.0
Upper deck elevation (TOS)	m	39.5
Lower deck elevation (BOS)	m	33.0
Installed draft	m	20.0

Table 2-2 Hull Buoyancy

Hull Buoyancy	B, t	KB, m
Columns	9241	14.3
Nodes	6831	4.3
Pontoons	20492	4.3
Guide Support	40	10.0
Guides	23	6.0
Total Buoyancy	36627	6.8

Table 2-3 Hull Weight & Mass Properties - 1000 m pipe deployed

	Weight, t	KG, m
Deck	11972	44.0
Hull	9761	9.3
Ballast	12805	4.3
Total Hull Weight	34538	19.5
Vertical Loads	2089	0.0
Total Weight+Vertical Loads	36627	18.3
Gyradii (kxx, kyy, kzz), m	(28.7, 28.7, 31.4)	

Table 2-4 Hull Weight & Mass Properties - 500 m Pipe deployed

Hull Weight	Weight, t	KG, m
Deck	11972	44.0
Hull	9761	9.3
Ballast	13850	4.3
Total Hull Weight	35583	19.0
Vertical Loads	1044	0.0
Total Weight+Vertical Loads	36627	18.5
Gyradii (kxx, kyy, kzz), m	(28.6, 28.6, 31.3)	

The model shall be ballasted with all instruments, electrical cables, mechanical fixtures and other items that may be present during testing that affect the mass properties. The model weight in air shall be within ±0.5% of the specification. The location of the model center of gravity, LCG, TCG and VCG, shall be within ±10 cm, full scale, of the specification. The model radii of gyration, k_{xx}, k_{yy} and k_{zz}, shall be within ±5% of the specification.

The Bidder shall describe the methods to be used for model fabrication. The Bidder shall describe the methods to be used for ballasting the model and the expected accuracy of the results for: weight in air, LCG, TCG, VCG, k_{xx}, $k_{yy,}$ and k_{zz}.

The semisubmersible model shall have a draft line drawn around all four columns at the design draft. Markers shall be placed on the outside surfaces of the columns at two-meter intervals, full scale, for visual estimation of wave run-up.

Structure on or above the upper deck need not be modeled.

2.2 Hull – Operational Condition

In the operational condition the gripper and guides are removed, and the pipe is suspended from a gimbal at elevation -5.0 (from the keel), see Figure 2-3. In the OTEC operation there will be large ducting connecting the cold water pipe to the remoras; however, for the purposes of this model test we are not including the ducting in the model.

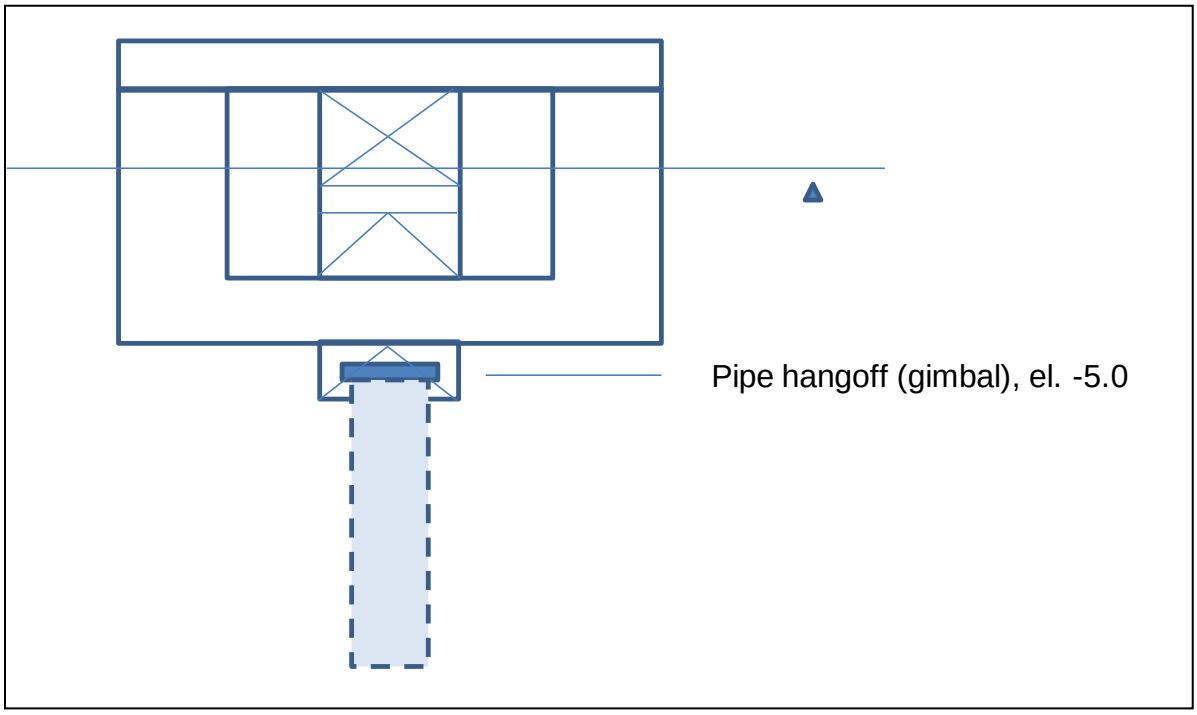

Figure 2-3 Profile in Operational Condition (Remoras not shown)

The hull in the operational condition will have six remoras rigidly fixed to the hull. Figure 2-4and Figure 2-5 show plan views at the deck and the pontoon with the remoras. Connections between the remoras and the hull are at the deck level and the pontoon level. For purposes of the model test, these connections should facilitate adding and removing remoras for testing, although the planned configurations only include zero and six remoras.

Figure 2-6 shows the outboard profile looking north.

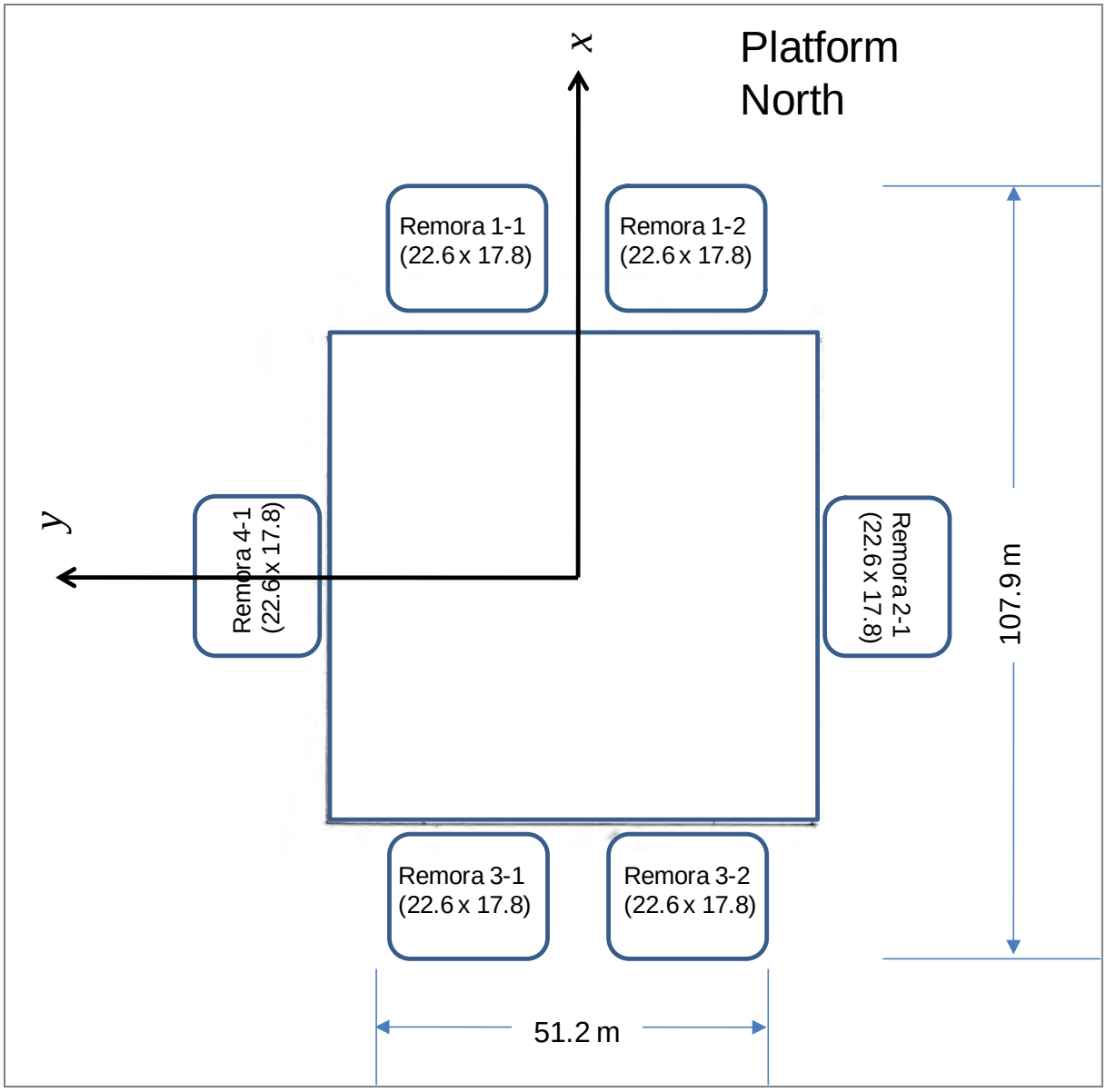

Figure 2-4 Deck Plan (elev. 33) with Remoras

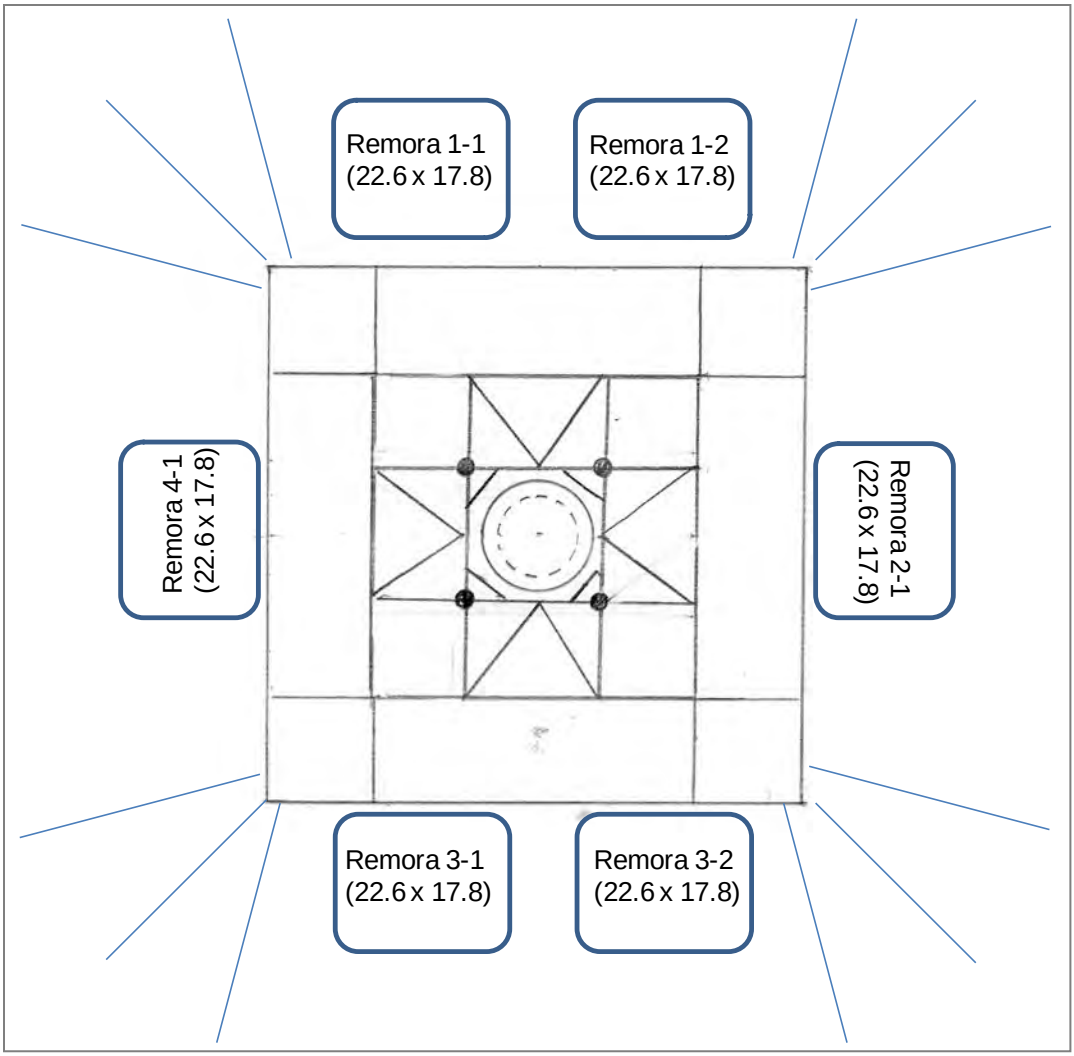

Figure 2-5 Plan at Pontoon with Remoras

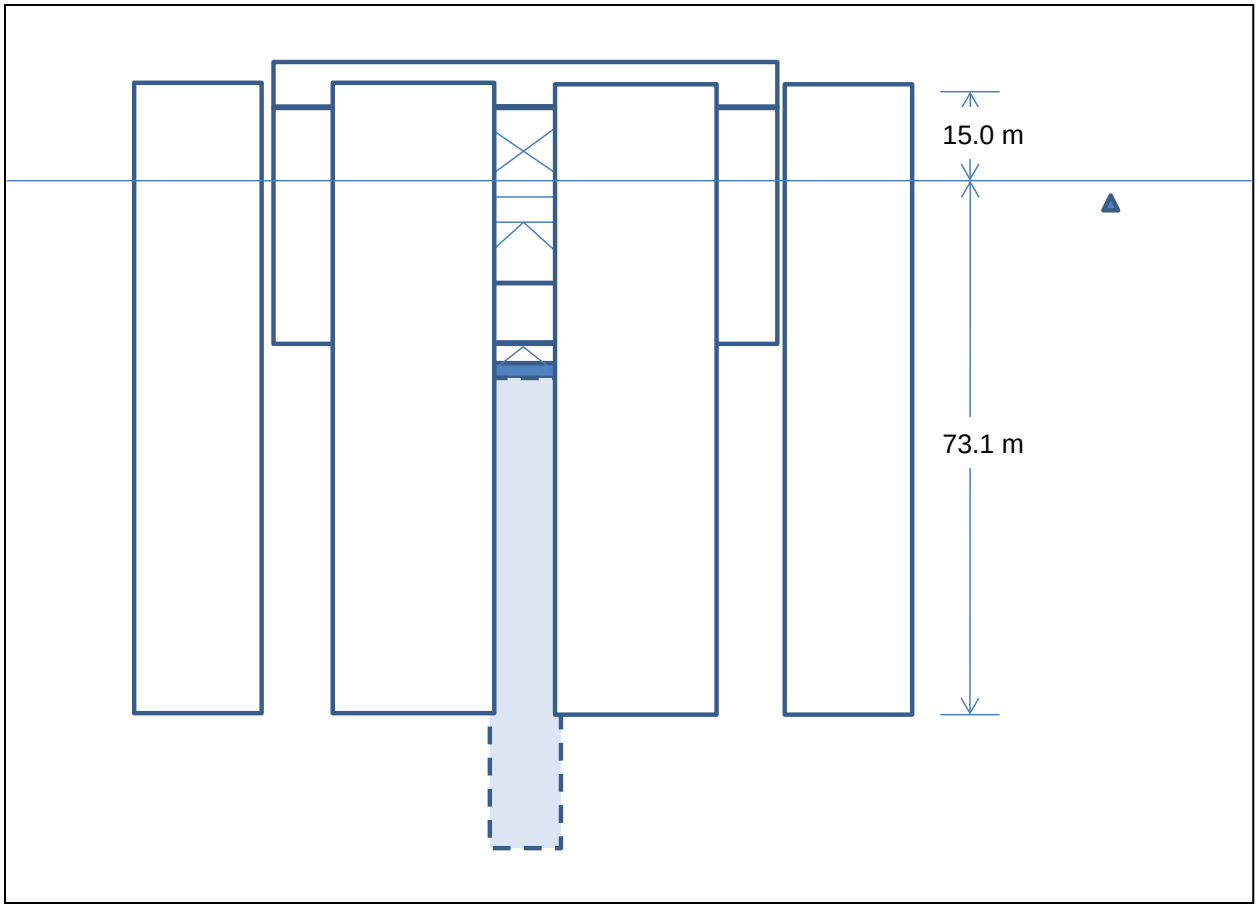

Figure 2-6 Outboard Profile looking North

2.3 Remoras

The remoras consist of an upper buoyant section and a flooded lower section, which contains the heat exchangers, pumps, and piping for the OTEC system. For the purposes of the model test program, the remoras may be considered closed, rigid bodies with no free surfaces. Alternately, the remoras may be flooded as shown in Figure 2-7. The mass properties of the individual remoras with and without entrained water are presented in Table 2-5, for information only. Using the alternate method reduces the total model weight; however, the volume and center of gravity of the entrained water will need to be calibrated to determine assemble model mass properties.

The mass and hydrostatic properties of the combined semisubmersible hull and the remoras are listed in Table 2-6. Only the mass and hydrostatic properties of the combined semisubmersible and the remoras are of direct interest in this model test program.

The combined model shall be ballasted with all instruments, electrical cables, mechanical fixtures and other items that may be present during testing that affect the mass properties. The combined model weight in air shall be within ±0.5% of the specification. The location of the combined model center of gravity, LCG, TCG and VCG, shall be within ±10 cm, full scale, of the specification. The combined model radii of gyration, k_{xx}, k_{yy} and k_{zz}, shall be within ±5% of the specification.

The Bidder shall describe the methods to be used for model fabrication. The Bidder shall describe the methods to be used for ballasting the model and the expected accuracy of the results for: weight in air,

LCG, TCG, VCG, k_{xx}, $k_{yy,}$ and k_{zz}. If the flooded remora option is chosen, the bidder shall describe the method for determining the volume and center of gravity of entrained water.

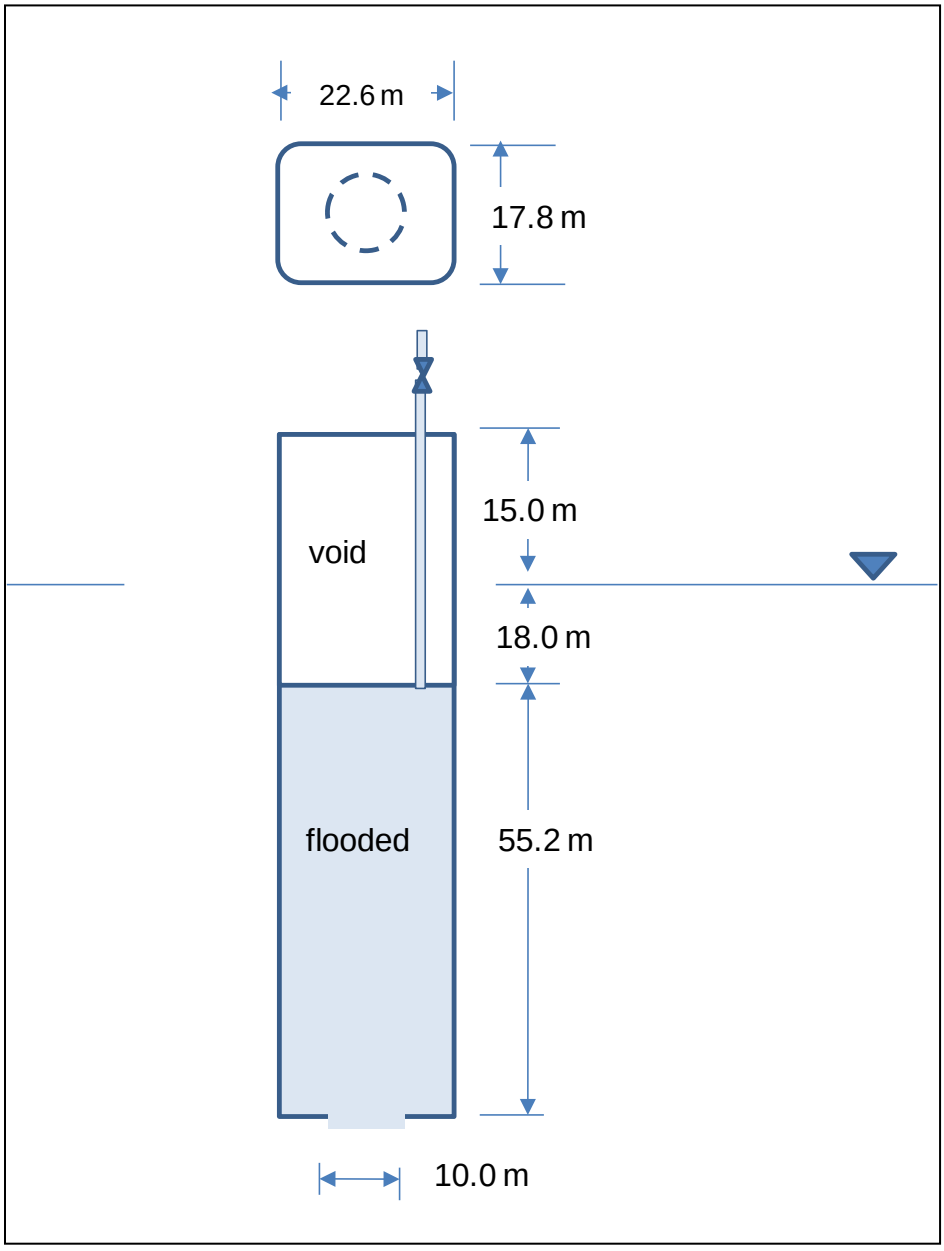

Figure 2-7 Remora with Flooded Volume (alternate arrangement)

Table 2-5 Individual Remora Mass Properties

	w/ Ent. Water	w/o Ent. Water
Total Weight, t	30183.1	9786.2
KG (ref base of Remora)	31.7	40.4
kxx, m	21.12	26.1
kyy, m	21.47	26.4
kzz, m	8.21	8.2

Table 2-6 Mass Properties and Hydrostatics for Combined Semi and Remoras

	w/ Ent. Water	w/o Ent. Water
Weight, t	215637	93256
Hull KG (ref to Semi draft)	-14.9	-0.87
kxx	35.7	38.1
kyy	42.2	34.1
kzz	45.0	42.0
Vertical Loads, t	2089	2089
Total Displacement	217725	95344
Effective KG w/ Loads	-14.8	-0.85
Semi Buoyancy	36627	36627
Semi KB	6.8	6.8
Remora Buoyancy	181098	58717
Remora KB	-16.6	2.2
Total Buoyancy	217725	95344
Total KB	-12.7	3.9
BMx, m	12.5	28.5
BMy, m	18.7	42.7
GMx, m	14.6	33.3
GMy, m	20.8	47.4

2.4 Cold Water Pipe

In the prototype, the fiberglass cold water pipe will be installed from the semisubmersible. In the model, two lengths of pipe will be tested in the installation configuration: half-length and full length.

The properties of the cold water pipe are listed in Table 2-7. The most important properties to model precisely are the length, diameter, bending stiffness, and wet weight. The model tolerance for length and diameter is ±10 cm, full scale. The tolerance for bending stiffness is ±10%. The tolerance for wet weight is ±0.5%. The as-built cold water pipe model axial stiffness should be provided, but need not be scaled precisely.

Pipe modal properties are illustrated in Figure 2-8 and Table 2-8

The estimated maximum strain moment envelope for the cold water pipe hanging from the gimbal in a 100-year cyclone, with the 1.00 E+09 N-m/radian gimbal, is shown in Figure 2-9. The bending strain envelope for the cold water pipe in the gripper is shown in Figure 2-10. The bending strain standard deviation for the cold water pipe in the gripper is shown in Figure 2-11. The bending strain is the outer fiber strain for the prototype pipe, 10 m diameter. If the bidder elects to model this pipe with a smaller diameter tube or rod with an equivalent value for EI, the bending strains will be reduced by the ratio of the tube/rod diameter to the prototype diameter.

The bidder should note that these are high strains for metallic structure. The shear and bending statistics for the 100-year cyclone case at the attachment to the gimbal are listed in Table 2-9.

The Bidder shall describe the proposed model cold water pipe design, instrumentation, and fabrication. Appendix A offers a discussion of possible design and fabrication approaches the Bidder may wish to consider. The model mooring cold water pipe design and instrumentation plan shall be provided prior to fabrication for review and approval by Lockheed Martin.

The as-built bending cold water pipe bending stiffness shall be provided for review and approval by Lockheed Martin at least one week prior to start of the model tests in the basin.

Table 2-7 Cold Water Pipe Properties

Summary CWP Characteristics	Units	Value
Inside diameter including Resin Distribution Layer	m	10.01
Outside Diameter including Resin Distribution Layer	m	10.49
Length *	m	1,000.8
Bottom Weight, wet weight	kN	-
Mass, CWP - no bottom weight - no internal water	kg	4,807,809
% wall that is void inc RDL	%	65.3
Total wet Weight including bottom weight	tonnes	2,077.3
EA	kN	7.35E+07
EI	kN-m^2	9.50E+08
Wet Weight per unit length of circumference:	tonnes/cm	0.63
Air Pressure to float:	atm	2.58
Natural frequency of CWP/pad interaction.	sec	1.21

Note (*): Alternate Pipe Length: The maximum model scale may be dictated by the pipe length and basin/pit depth. The preference is to test the full 1000 m length, however if because of basin limitations this results in what is considered too small a scale, a shorter pipe length may be proposed, but in no event less than 700 m. The values given above for total weight and top tension will change accordingly. In any event, numerical predictions will "model the model" and accurate pipe properties will need to be calibrated.

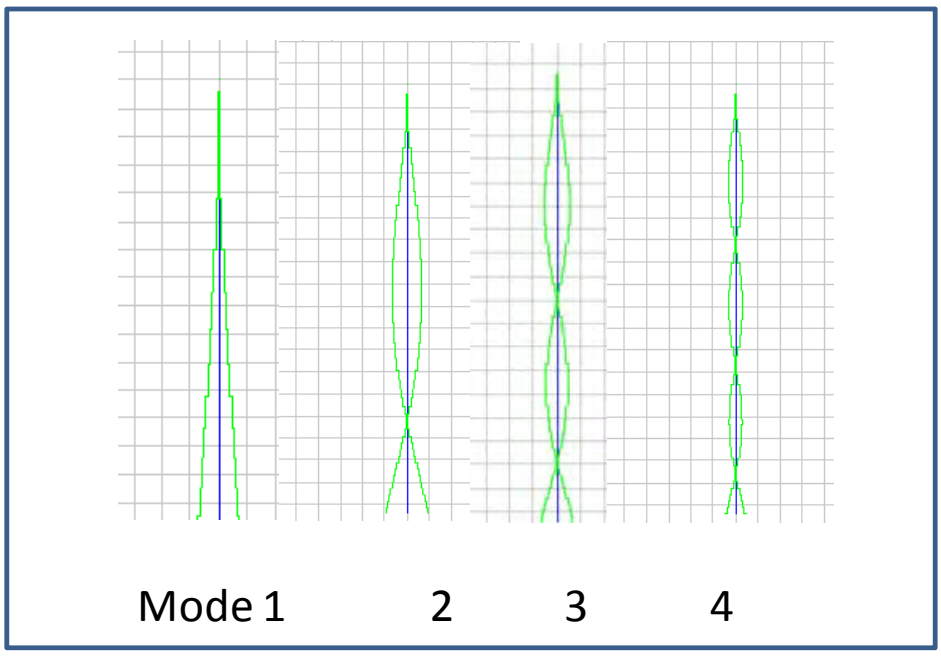

Figure 2-8 OTEC Pipe Computed Mode Shapes

Table 2-8 Computed Modal Periods for OTEC Pipe

Mode	Period
1	412
2	103
3	40
4	20.9
5	12.8
6	8.6
7	6.2

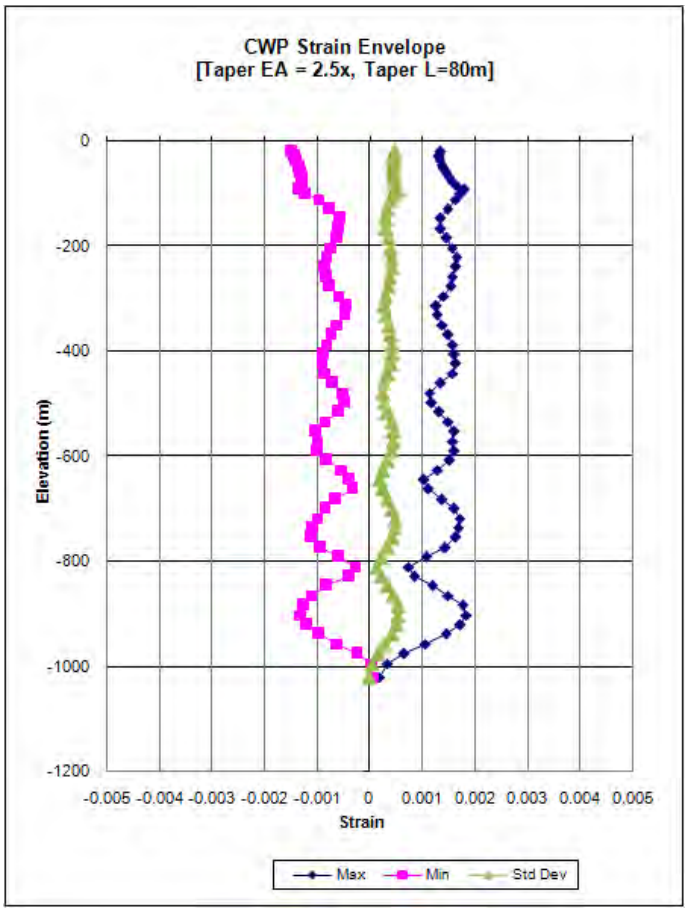

Figure 2-9 Bending Strain Envelope for Coldwater Pipe Hanging from Gimbal in 100 Year Cyclone

Table 2-9 Estimated Shear and Bending Statistics for Coldwater Pipe in 100 Year Cyclone

	Shear Force at Top	Bending Moment at Top	Rotation at Top
	(N)	(N-m)	(º)
	Gimbal Rotational Stiffness = 1.0 E+09 N-m/radian		
Maximum	6.32 E+06	6.29 E+07	3.60
Minimum	-4.77 E+06	-7.40 E+07	-4.24
Mean	5.24 E+05	-1.55 E+07	-0.89
Std Deviation	1.71 E+06	2.17 E+07	1.24

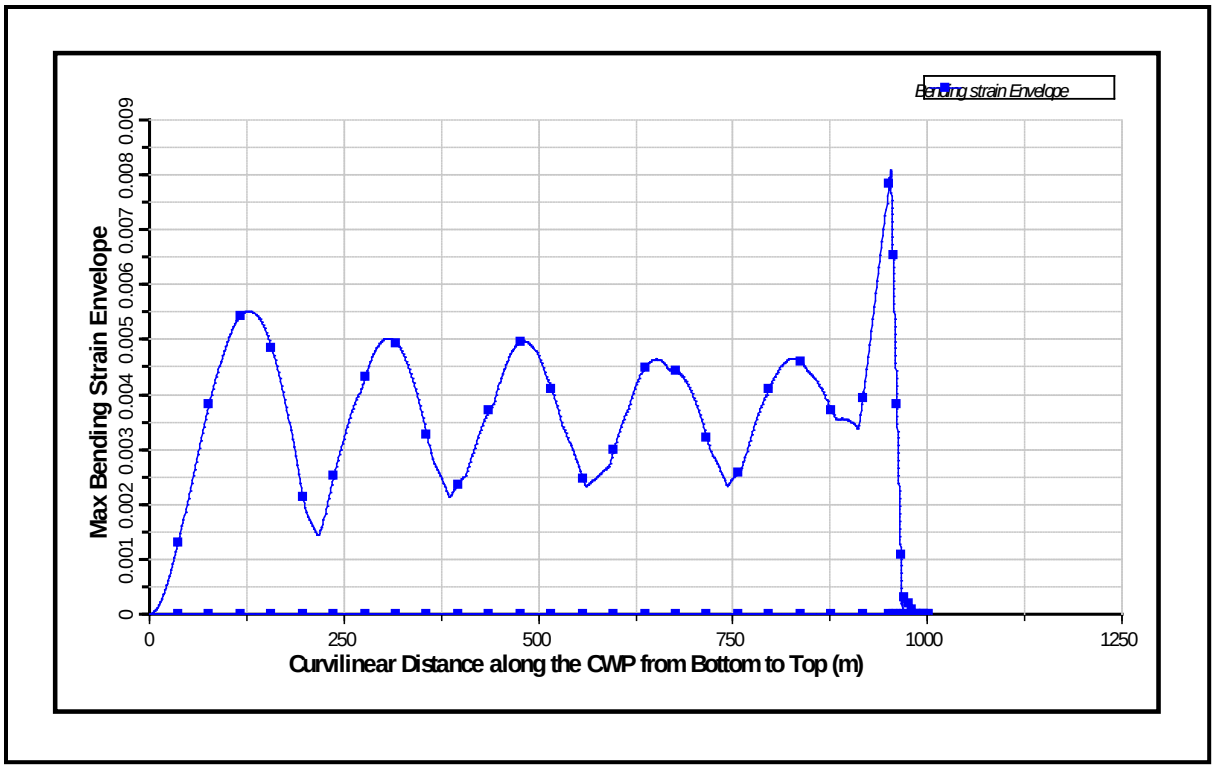

Figure 2-10 Bending Strain Envelope for Coldwater Pipe Hanging from Gripper in 10-yr Sea

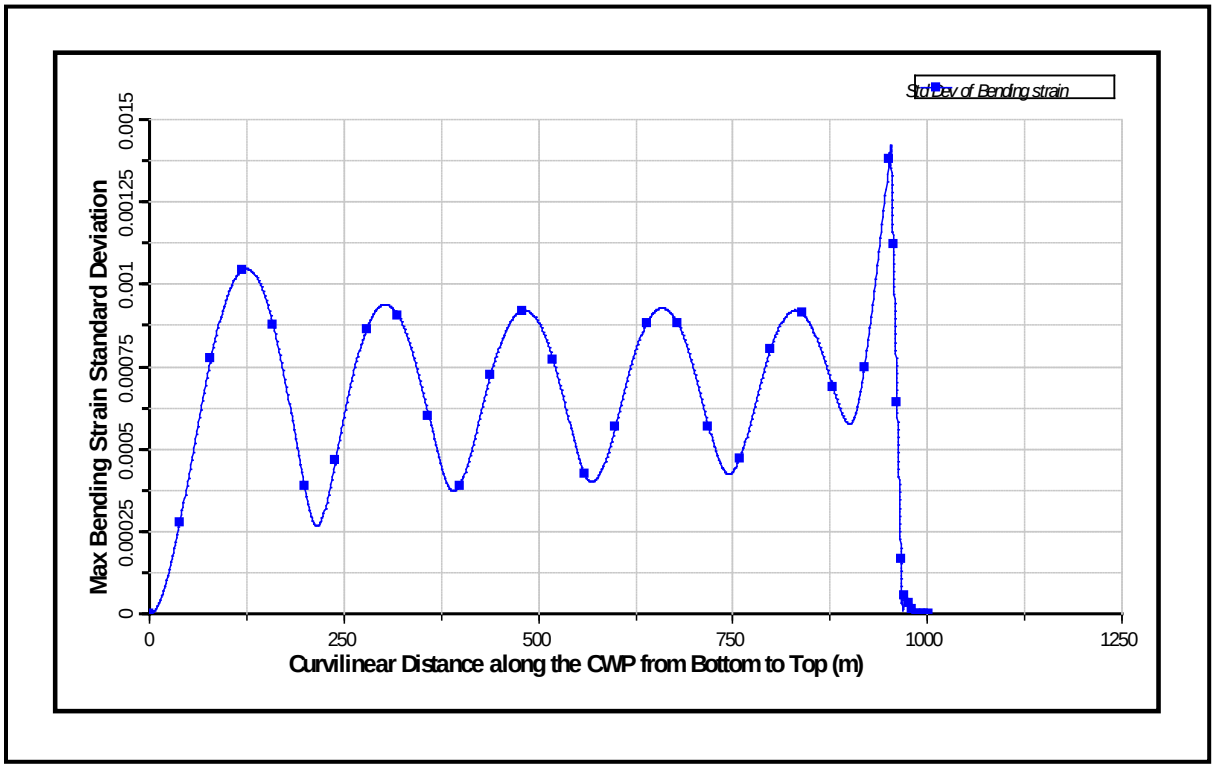

Figure 2-11 Bending Strain Standard Deviation Envelope for Coldwater Pipe Hanging from Gripper in 10-yr Sea

2.5 Gripper and Guides (pipe installation configuration only)

In the pipe installation configurations, the cold water pipe weight will be supported at the gripper location as shown in Figure 2-1, Section 2.1.

In the pipe installation configurations, the cold water pipe will pass through two (2) horizontally compliant guides as shown in Figure 2-1, Section 2.1. The guides shall have an inside diameter equivalent to the outside diameter of the pipe, and shall maintain a nominal preload to avoid "gap" effects. The amount of preload shall be less than that which would result in a longitudinal friction force greater than 5% of the hanging weight of the pipe, under the nominal preload.

Friction in the model guides will affect the loads measured at the gripper. The Bidder shall describe how they will quantify the friction force.

The horizontal stiffness of the gripper and pipe guides shall be:

Table 2-10 Lateral Stiffness of Grippers and Guides

	Lateral Stiffness (N/m)
Gripper	8.5E9
Guides (each)	2.0E8

The Bidder shall describe how the guide compliance will be accomplished and quantitatively demonstrated. The horizontal stiffness of the model guides shall be within ±15% of the specified value.

The guide design shall be submitted to Lockheed Martin for review and approval prior to model fabrication. The as-built model horizontal stiffness's along the x and y axes shall be submitted to Lockheed Martin for review and approval at least one week prior to commence of the model test program.

2.6 Gimbal (operational configuration only)

In the operational configurations, the cold water pipe will hang from the semisubmersible keel on a gimbal. The gimbal shall have a linear rotational stiffness, which will be equal in all directions. Two rotational stiffness's will be tested. The stiffness's are:

- 0.0 N-m/radian, and
- 1.00 E+09 N-m/radian.

The Bidder shall describe how the gimbal rotational stiffness's will be accomplished and quantitatively demonstrated. The model gimbal rotational stiffness shall be within ±10% of the specified value.

The gimbal support should be removable to accommodate the cold water pipe installation configuration, during which the pipe will be supported from the gripper. The gimbal design shall be submitted to Lockheed Martin for review and approval prior to model fabrication. The as-built model rotational stiffness's about the x and y axes shall be submitted to Lockheed Martin for review and approval at least one week prior to commence of the model test program.

2.7 Mooring

For purposes of this test, a horizontal mooring exerting no vertical force on the platform in the calm water condition shall be utilized. Mooring shall be connected at the corners of the pontoons at an

elevation of 4.25 m above the semi-submersible keel, and shall not make contact with the remoras in the operational case. Two mooring stiffness's are of interest corresponding to a catenary and taut mooring, respectively:

Catenary Mooring Stiffness: 194 kN/m (estimated maximum offset 78 m)
Taut Mooring stiffness: 650 kN/m (estimated maximum offset 27 m)

These are nominal stiffness values at zero offset. The bidder shall provide a description of the mooring and theoretical plots of force vs. offset up to the 150% of the maximum indicated offsets prior to fabricating the mooring components.

The base case mooring stiffness is the taut moorings stiffness. The bidder shall offer a cost for additional tests with the catenary mooring stiffness. The base case tests and optional tests are discussed later.

2.8 Test Configurations

The combinations of semisubmersible, cold water pipe and remoras to be tested in the model basin are listed in Table 2-11. All tests will be conducted at the 0º heading.

The semi alone configuration is without a cold water pipe or remoras. The purpose of the tests with the semi alone is to confirm the mass and hydrostatic properties of the vessel alone, as well as to validate the numerical models for the dynamic response vessel alone.

The cold water pipe will be fabricated and installed from the semisubmersible prior to mating the remoras. The installation configuration will be tested with a reduced length of pipe, nominally half the final length, as well as the full length of pipe.

The combination of semisubmersible and remoras is not expected to be a configuration that will occur in the field. This configuration will be tested to confirm the mass and hydrostatic properties of the hull-remora combination and well as to validate the numerical models for the dynamic response of the combination.

The combination of the semisubmersible with the full-length cold water pipe and the remoras represents the operational condition of the facility.

Table 2-11 Test Configurations

Description	Semi	CWP	Remoras	Gimbal Stiffness	Mooring
Semi Alone	x				Taut
CWP Installation 1	x	½			Taut
CWP Installation 2	x	1			Taut
Semi & Remoras	x		6		Taut
Operations A	x	1	6	0.00 N-m/rad	Taut
Operations B	x	1	6	1.00 E+09 N-m/rad	Taut

3 Description of the Environments

3.1 Water Depth

The full design water depth is 1100 meters. The bidder shall specify the full-scale equivalent depth to both the top of the pit and the bottom of the pit at the proposed scale.

3.2 Waves

3.2.1 Random Waves

The random waves and associated wind to be tested are listed in Table. All model sea states shall consist of long-crested waves. The Random Phase method shall be used to create the random wave drive signals. The wave elevation realization of any specified spectrum shall present true random characteristics (no periodicity of wave elevations). Irregular sea tests will be three hours, prototype, in length. Sufficient time shall be allowed between tests to avoid any distortion of the newly generated seas by a previous test. A sufficient "warm-up" period after the waves reach the model, just prior to the start of data acquisition, shall be allowed to minimize the effect on the data due to any "start-up" transient.

It is imperative that the waveform and test start time remain constant between tests and over the period between wave calibration and testing with the model so the time series analysis of the vessel responses may evaluated against the undisturbed wave field. The Bidder shall describe the means to be taken to ensure that the calibrated waves are replicated during the tests with the model.

The waves shall be calibrated without the model vessel in the basin and with the associated model currents listed in Table 3-3 and Table 3-4. The wave spectra generated in the basin shall present similar statistical properties throughout the whole test duration. Special attention shall be paid to avoid the generation of standing waves in the basin during the long duration irregular wave tests.

The calibrated model significant wave height (Hs) shall be within ±2% of the target value. The peak spectral period (Tp) shall be within ±0.2 seconds of the target values. Energy near the peak of the spectrum (80% of the area under spectrum target curve) shall not deviate more than ±10% from the target value. Excessive smoothing of the wave Power Spectral Density (PSD) plots shall not be allowed. The bandwidth of the smoothing function shall be noted on the plots and shall not exceed 0.005 Hz. Plots, in pdf format, of the target and measured wave spectra shall be submitted for approval prior to testing.

The cumulative non-exceedance distributions of wave height and wave crests shall be reasonably well behaved and smooth for all the calibrated random sea states, as presented on a Weibull plot. The most likely three-hour crest in the 100 Year Cyclone only shall be within 0 to +10 percent of the specified value. Similarly, the largest observed crest value shall be within 0 to +10 percent of the specified value. Extreme distribution Weibull plots of the wave heights and crest elevations shall also be presented, in pdf format, for each random wave realization.

The Bidder shall provide, in the proposal, data indicating the repeatability of the model waves, both in the presence of model currents and without currents, Hs, Tp, three hour extreme crest elevation, spectral shape, etc.

Calibrations of wave spectra in the model basin shall be performed and the results shall be provided at least 72 hours prior to commencement of installation of the model in the basin for review and approval by Lockheed Martin.

Table 3-1 Random Waves

	100 Year Cyclone	10-Yr Sea	10-Yr Swell	Fatigue Wave	White Noise
Uw, m/sec	33.8	15.7	14.6	8	8
Hs, m	10.2	4.2	3.8	2.5	2
Tp, sec	12.8	8.3	15.7	16.6	2-26
Gamma	2	1	6	6	
Hmax, m	16.9	8	7.1		
Amax, m	9.4	4.5	4		
Wind Force, kN (w/ remoras)	2002.2	432.0	373.6	112.2	112.2
Center of Pressure (w/ remoras)	14.3	14.3	14.3	14.3	14.3
Wind Force, kN (w/o remoras)	1547.2	333.8	288.7	86.7	86.7
Center of Pressure (w/o remoras)	16.6	16.6	16.6	16.6	16.6

Table 3-2 Regular Waves

Description	**H**	**T**
	(m)	**(s)**
Regular Wave 1	tbd	tbd
Regular Wave 2	tbd	tbd
Regular Wave 3	tbd	tbd
Regular Wave 4	tbd	tbd
Regular Wave 5	tbd	tbd
Regular Wave 6	tbd	tbd
Regular Wave 7	tbd	tbd

3.2.2 Regular Waves

The regular waves to be tested are listed in Table 3-2. As indicated, the wave height and period are unknown at this time. Lockheed Martin prefers not to specify the regular wave heights and period until after the first white noise test with the cold water pipe has been conducted and analyzed. However, it is understood that the calibration tests without the model would then need to be conducted after the model is removed from the basin. The Bidder shall provide costs for calibrating the regular waves prior to placing the model in the basin and for calibrating the regular waves after the model is removed at the end of the program.

In the regular wave tests uni-directional, monochromatic waves of known amplitude and frequency shall be generated in the basin. There are no associated currents or wind forces.

Wave probe placement during calibration shall be the same as the irregular wave tests. It is imperative that the waveform and test start time remain constant between tests and over the period between wave calibration and testing so the time series analysis of the vessel responses may evaluated against the undisturbed wave field. The Bidder shall describe the means to be taken to ensure that the calibrated waves are replicated during the tests with the model.

After the initial transient response of the vessel model has been estimated to die out, a continuous sequence of not less than ten (10) regular wave oscillations shall be analyzed for wave height (H) and

period (T). The wave height shall be within ±2% of the target value. The period shall be within ±0.2 seconds, full scale, of the target values.

The Bidder shall provide, in the proposal, data indicating the repeatability of the model regular wave statistics, wave height, and period.

Calibrations of regular waves in the model basin shall be performed and the results shall be provided at least 72 hours prior to commencement of installation of the model in the basin for review and approval by Lockheed Martin.

3.3 Currents

These tests will be run without current.

3.4 Winds

Wind shall be modeled as a constant force applied at the elevation of the wind center of pressure. The Bidder shall describe the means used to apply the constant wind force. Table 3-1 shows the wind speeds and associated forces & centers of pressure for configurations with and without remoras.

4 Model Tests

4.1 Scale

The Bidder shall propose a model scale.

4.2 Units and Coordinate System

All measurements are to be reported in full-scale equivalent units, unless otherwise specified. The units to be used are listed in Table 4-1.

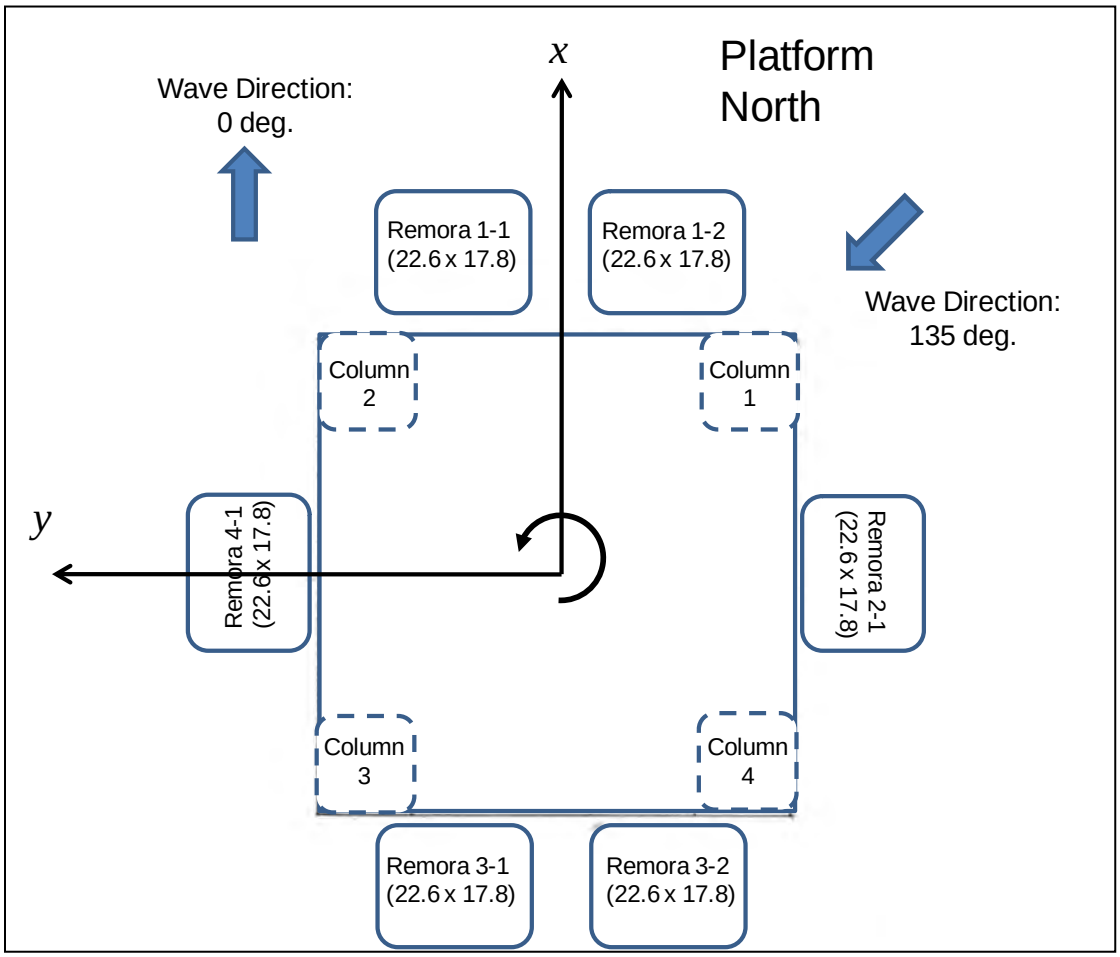

Figure 4-1 Coordinate System

The origin of the global coordinate system shall be the water surface at the center of the semisubmersible when moored without any external loads. The vessel coordinate system shall be a right-handed system. Positive x, surge, from the origin horizontally between columns 1 and 2 (see Figure 4-1). The vessel positive y, sway, shall be oriented 90 degrees counterclockwise from the x-axis, between columns two and three. The z-axis, heave, shall be positive up. Positive roll shall be rotation about the x-axis, in which columns 1 and 4 move down. Positive pitch shall be rotation about the y-axis, in which columns 1 and 2 down. Positive yaw shall be rotation in the horizontal plane about the z-axis, in a counterclockwise direction when viewed from above.

4.3 Measurements

Table 4-2 lists the proposed measurements for this test program and the preliminary range of measured values expected.

4.3.1 Sample Rate

The Bidder shall specify in the bid a sample rate, associated filter frequency and measurement resolution for each channel of data. The sample rate should not be less than the full-scale equivalent of four (4) Hz. The Bidder shall describe the filter to be employed.

4.3.2 Calibration of Instrumentation

Each instrument shall be calibrated over the full expected range of measurement. Calibration plots for each instrument shall be provided. The minimum of information on each plot shall be:

1) The name (and number if applicable) of the channel being calibrated,
2) The date and time of the calibration,
3) The values of the instrument output voltages and the corresponding full-scale engineering units,
4) The linear calibration coefficient,
5) The linear correlation coefficient of the data (R^2),
6) A plot of the output voltage versus engineering units and the least squares best fit line through the data,
7) A plot of the 95% confidence limits of the data,
8) The calibration range shall cover the complete range of possible values expected to be recorded in a test.

The accuracy of every instrument used shall be 1% of full range or better (computed by dividing the standard deviation of the errors by the full range).

Measurements will be reported in full-scale values following the Froude scaling law.

Any instrument suspected of being damaged or giving false readings shall be re-calibrated or replaced at any time throughout the project.

Table 4-1 Units

Quantity	Units
Length	meters
Rotation	degrees
Time	seconds
Mass	kilograms
Velocity	meters/seconds
Acceleration	meters/second^2
Force	kilo-Newtons
Strain	non-dimensional

4.3.3 Waves

During sea state calibration, the water surface elevation shall be measured at four locations. One location shall be the at-rest location of the hull while the other shall be the maximum estimated excursion in the 100-year cyclone. These probes shall be used for sea state calibration purposes only. The other two locations will be at an equal distances from the wave maker as the calibration measurements, but to the side of the model so as not to interfere with the model or the mooring. The two probes will remain throughout the test program for reference purposes.

During tests with the model, the calibration probes shall be removed.

4.3.4 Air Gap

The air gap beneath the deck of the semisubmersible shall be measured at one location. The location shall be at the up wave edge of the hull deck halfway between a remora and a column.

4.3.5 Run-up

Wave run-up on the up wave centerline of an up wave remora shall be measured.

4.3.6 Wind Load

The applied horizontal model wind load shall be measured at the point of application of the force.

4.3.7 Platform Motions

Platform motions in all six degrees of freedom shall be measured on the semisubmersible. The motions shall be reported at the geometric center of the vessel at the waterline.

4.3.8 Mooring Tensions

Tensions in each of the model mooring lines shall be measured. The Bidder shall specify whether the tension measurements are to be made at the vessel fairleads or at the anchors.

4.3.9 Gripper Loads

During the installation of the cold water pipe, it will be held rigidly by the gripper. In the tests of configurations “CWP Installation 1” and “CWP Installation 2,” the X, Y and Z forces on the model gripper shall be measured. The vector components of the measured force shall be aligned with the vessel coordinate system.

4.3.10 Top of pipe motion (CWP installation configurations only)

Referring to Figure 2-1, the horizontal surge and sway motion of the top of the pipe shall be measured.

4.3.11 Guide Loads

During tests in the “CWP Installation 1” and “CWP Installation 2” configurations, the cold water pipe will be restrained with compliant guides at two elevations. The horizontal X and Y forces on each of the model guides shall be measured. The vector components of the measured forces shall be aligned with the vessel coordinate system.

4.3.12 Hangoff Loads and Angles

During the tests in the “Operational” configuration, the cold water pipe will hang from the gimbal. The gimbal shall be instrumented to measure the X, Y and Z forces as well as the X, Y and Z moments. The

vector components of the measured forces and moments shall be aligned with the vessel coordinate system.

The roll and pitch angles of cold water pipe relative to the platform and relative to a global coordinate system shall be measured. These may be "computed" or "derived" channels based upon the measured forces.

4.3.13 Coldwater Pipe Bending

Bending strain in the cold water pipe shall be measured in twenty (20) locations. Ten (10) locations shall measure bending about the X-axis and ten (10) locations shall measure bending about the Y-axis. The vector components of the measured strains shall be aligned with the vessel coordinate system.

The Bidder shall propose the locations for the strain measurements to capture up to the 4th mode of bending as illustrated in Figure 2-10. The Bidder shall describe in detail in the bid:

- the means to be employed to measure pipe bending,
- the means for calibrating the sensors, and
- the means for demonstrating the accuracy of the sensors.

The Model Basin will deliver a Cold Water Pipe Model Design Report for review and approval by Lockheed Martin prior to fabrication of the model. This design report shall provide a detailed description of the instruments, their application to the model, their effect on the mass of the model, and their effect on the structural bending stiffness of the model.

4.3.14 Coldwater Pipe Motion

The horizontal X and Y translations of the cold water at a location near the middle of the pipe and at the bottom shall be measured. The Bidder shall describe the means by which these measurements will be made and the accuracy to be expected. The vector components of the measured motions shall be aligned with the vessel coordinate system. The translations shall be referenced to (0, 0), the "at rest" location when the vessel and the cold water pipe are not exposed to outside forces.

During the installation configuration tests, the horizontal motion, surge, and sway, of the top of the cold water pipe relative to the hull shall be measured.

Table 4-2 Measurement List

	Measurements	Units	Min	Max	Semi Only & Semi+Remoras	CWP Installation 500 m Pipe	CWP Installation 1000 m Pipe	Operations
1	Wave Calibration 1	m	-15	15				
2	Wave Calibration 2	m	-15	15				
3	Wave Reference 1	m	-15	15	x	x	x	x
4	Wave Reference 2	m	-15	15	x	x	x	x
5	Run-up	m	-15	30	X (remoras only)	x	x	x
6	Air gap	m	-10	20	x	x	x	x
7	Platform Surge	m	-50	100	x	x	x	x
8	Platform Sway	m	-50	50	x	x	x	x
9	Platform Heave	m	-20	20	x	x	x	x
10	Platform Roll	m	-15	15	x	x	x	x
11	Platform Pitch	m	-15	15	x	x	x	x
12	Platform Yaw	m	-20	20	x	x	x	x
13	Wind Force	kN	0	3000	x	x	x	x
14	Pipe Top Surge	m	-0.10	0.10		x	x	
15	Pipe Top Sway	m	-0.10	0.10		x	x	
16	Gripper X-Force	kN	-100	100		x	x	
17	Gripper Y-Force	kN	-100	100		x	x	
18	Gripper Z-Force	kN	0	2500		x	x	
19	Upper Guide X-Force	kN	-500	500		x	x	
20	Upper Guide Y-Force	kN	-500	500		x	x	
21	Lower Guide X-Force	kN	-1000	1000		x	x	
22	Lower Guide Y-Force	kN	-1000	1000		x	x	
23	Mooring 1 Tension	kN	0	25000	x	x	x	x
24	Mooring 2 Tension	kN	0	25000	x	x	x	x
25	Mooring 3 Tension	kN	0	25000	x	x	x	x
26	Mooring 4 Tension	kN	0	25000	x	x	x	x
27	Gimbal X-Force	kN	-1000	1000				x
28	Gimbal Y-Force	kN	-1000	1000				x
29	Gimbal Z-Force	kN	0	2500				x
30	Gimbal Roll Angle	deg	-15	15				x
31	Gimbal Pitch Angle	deg	-15	15				x
32	Pipe Bottom Surge	m	-50	150		x	x	x
33	Pipe Bottom Sway	m	-50	50		x	x	x
34	Pipe Mid Surge	m	-50	150			x	x
35	Pipe Mid Sway	m	-50	50			x	x

	Measurements	Units	Min	Max	Semi Only & Semi+Remoras	CWP Installation 500 m Pipe	CWP Installation 1000 m Pipe	Operations
36	Pipe Strain X 1		-0.02	0.02		x	x	x
37	Pipe Strain Y 1		-0.02	0.02		x	x	x
38	Pipe Strain X 2		-0.02	0.02		x	x	x
39	Pipe Strain Y 2		-0.02	0.02		x	x	x
40	Pipe Strain X 3		-0.02	0.02		x	x	x
41	Pipe Strain Y 3		-0.02	0.02		x	x	x
42	Pipe Strain X 4		-0.02	0.02		x	x	x
43	Pipe Strain Y 4		-0.02	0.02		x	x	x
44	Pipe Strain X 5		-0.02	0.02		x	x	x
45	Pipe Strain Y 5		-0.02	0.02		x	x	x
46	Pipe Strain X 6		-0.02	0.02			x	x
47	Pipe Strain Y 6		-0.02	0.02			x	x
48	Pipe Strain X 7		-0.02	0.02			x	x
49	Pipe Strain Y 7		-0.02	0.02			x	x
50	Pipe Strain X 8		-0.02	0.02			x	x
51	Pipe Strain Y 8		-0.02	0.02			x	x
52	Pipe Strain X 9		-0.02	0.02			x	x
54	Pipe Strain Y 9		-0.02	0.02			x	x
55	Pipe Strain X 10		-0.02	0.02			x	x
56	Pipe Strain Y 10		-0.02	0.02			x	x

4.4 Test Matrix

For bidding purposes, the matrix for the tests to be conducted in the model basin has been divided into five (5) groups.

- Group 1 tests include:
  - the semisubmersible in the operation configuration plus remoras plus cold water pipe with the gimbal rotational stiffness of 0.0N-m/radian,
  - taut mooring, and
  - all tests at 0º heading.
- Group 2 tests include:
  - the semisubmersible in the operation configuration plus remoras plus cold water pipe with the gimbal rotational stiffness of 1.0 E+09 N-m/radian,
  - taut mooring, and
  - all tests at 0º heading.
- Group 3 tests include:
  - the semisubmersible alone in the installation configuration,
  - the semisubmersible in the installation configuration plus half the installed cold water pipe,
  - taut mooring, and
  - all tests at 0º heading.

- Group 4 tests include:
    - the semisubmersible in the installation configuration plus the full length cold water pipe,
    - taut mooring, and
    - all tests at 0º heading.

The tests in the model basin shall include:

- Static offset tests,
- Incline tests,
- Free decay tests,
- Pipe impulse response tests,
- Regular wave tests, and
- Random wave tests.

These tests are described below.

4.4.1 System Identification Tests

4.4.1.1 Coldwater Pipe Structural Calibrations

The Bidder shall describe the means to measure and confirm the bending stiffness of the cold water pipe model.

The Bidder shall describe the means to calibrate the strain measurements in the cold water pipe model. The strain measurements in both the x and y direction shall be calibrated.

4.4.1.2 Static Offset Tests

The total offset force and vessel response shall be measured for at least five different offset positions over the anticipated range of motion. The vessel model shall be offset to minimize off-axis responses. The offset force and the vessel response shall be measured and recorded when the model has stopped moving.

Static offsets tests on the cold water pipe shall be conducted by offsetting the bottom of the cold water pipe. The horizontal offset force and the reaction of the pipe shall be measured. At least five different offset loads shall be applied.

4.4.1.3 Incline Tests

The purpose of the incline tests with the semi alone and the semi+remoras is to measure the hydrostatic stiffness of the model in roll and pitch. These incline tests will be conducted with the model in the mooring. The hydrostatic stiffness estimates shall be provided by the Model Basin for pitch and roll based on the measurements from these tests. The measured data shall be compared to target values provided by Lockheed Martin. Variances greater than 5% will require resolution prior to further testing.

Tests shall be conducted in which the hull with the coldwater pipe model will be inclined in order to confirm the bending stiffness of the coldwater pipe model, the lateral stiffness of the model gripper and guides and the rotational stiffness of the model gimbal. Lockheed Martin will specify the three desired incline values in roll and pitch. The measured data shall be compared to predicted values provided by Lockheed Martin. Variances greater than 5% will require resolution prior to further testing.

4.4.1.4 Free Decay Tests

The model is to be independently excited in all six degrees of freedom while the decaying resonant motions shall be recorded. A minimum of three excitations in each degree of freedom shall be performed and analyzed. Care shall be taken to ensure that the measured response of the vessel is not corrupted by the reflections from waves generated by previous model motions. The free decay tests will be performed with the mooring system.

The measured data shall be compared to target values provided by Lockheed Martin. Variances greater than 5% will require resolution prior to further testing.

4.4.1.5 Pipe Impulse Response

In order to characterize the pipe natural frequencies and mode shapes a test shall be conducted whereby the platform is moved suddenly (jerked) in order to introduce an impulse at the top of the pipe. Care shall be exercised that the jerk forces do not damage the pipe or the instrumentation.

4.4.2 Dynamic Environment Tests

Table 4-3 Group 1 Test Matrix

Configuration	Semi & Mooring	CWP	Remoras	Gimbal Compliance	Mooring
Operational Semi & Remoras	x	None	6	NA	Taut

Test Description	H or Hs	T or Tp	Current	Wind Force	
	(m)	(s)	(m/s)	(kN)	
GMl	NA	NA	0.00	0.00	
GMt	NA	NA	0.00	0.00	
Surge Static Offset	NA	NA	0.00	0.00	
Sway Static Offset	NA	NA	0.00	0.00	
Yaw Static Offset	NA	NA	0.00	0.00	
Surge Free Decay	NA	NA	0.00	0.00	
Sway Free Decay	NA	NA	0.00	0.00	
Heave Free Decay	NA	NA	0.00	0.00	
Roll Free Decay	NA	NA	0.00	0.00	
Pitch Free Decay	NA	NA	0.00	0.00	
Yaw Free Decay	NA	NA	0.00	0.00	
Regular Wave 1	tbd	tbd	0.00		Tests not performed if regular waves post-test calibrated
Regular Wave 3	tbd	tbd	0.00		
Regular Wave 5	tbd	tbd	0.00		
Regular Wave 7	tbd	tbd	0.00		
100 Year Cyclone	See Table 3-1				
10-yr Sea					
10-yr Swell					
White Noise					

Configuration	Semi & Mooring	CWP	Remoras	Gimbal Compliance	Mooring
Operations A	x	1	6	0.0 N-m/rad	Taut

Test Description	H or Hs	T or Tp	Current	Wind Force	
	(m)	(s)	(m/s)	(kN)	
GMl w/ Pipe	NA	NA	0.00	0.00	
GMt w/ Pipe	NA	NA	0.00	0.00	
Pipe Bottom Surge Static Offset	NA	NA	0.00	0.00	
Surge Free Decay	NA	NA	0.00	0.00	
Sway Free Decay	NA	NA	0.00	0.00	
Heave Free Decay	NA	NA	0.00	0.00	
Roll Free Decay	NA	NA	0.00	0.00	
Pitch Free Decay	NA	NA	0.00	0.00	
Yaw Free Decay	NA	NA	0.00	0.00	
Pipe Impulse	NA	NA	0.00	0.00	
Regular Wave 1	tbd	tbd	0.00	0.00	
Regular Wave 2	tbd	tbd	0.00	0.00	
Regular Wave 3	tbd	tbd	0.00	0.00	
Regular Wave 4	tbd	tbd	0.00	0.00	
Regular Wave 5	tbd	tbd	0.00	0.00	
Regular Wave 6	tbd	tbd	0.00	0.00	
Regular Wave 7	tbd	tbd	0.00	0.00	
100 Year Cyclone	See Table 3-1				
10-yr Sea					
10-yr Swell					
Fatigue Wave					
White Noise					

Table 4-4 Group 2 Test Matrix

Configuration	Semi & Mooring	CWP	Remoras	Gimbal Compliance	Mooring
Operations B	x	1	6	1.0 E+09 N-m/rad	Taut

Test Description	H or Hs	T or Tp	Current	Wind Force	
	(m)	(s)	(m/s)	(kN)	
GMl w/ Pipe	NA	NA	0.00	0.00	
GMt w/ Pipe	NA	NA	0.00	0.00	
Pipe Bottom Surge Static Offset	NA	NA	0.00	0.00	
Pipe Impulse	NA	NA	0.00	0.00	
Regular Wave 1	tbd	tbd	0.00	0.00	
Regular Wave 2	tbd	tbd	0.00	0.00	
Regular Wave 3	tbd	tbd	0.00	0.00	
Regular Wave 4	tbd	tbd	0.00	0.00	
Regular Wave 5	tbd	tbd	0.00	0.00	
Regular Wave 6	tbd	tbd	0.00	0.00	
Regular Wave 7	tbd	tbd	0.00	0.00	
100 Year Cyclone	See Table 3-1				
10-yr Sea					
10-yr Swell					
Fatigue Wave					
White Noise					

Table 4-5 Group 3 Test Matrix

Configuration	Semi & Mooring	CWP	Remoras	Gimbal Compliance	Mooring
Installation Semi Alone	x	None	None	NA	Taut

Test Description	H or Hs	T or Tp	Current	Wind Force	
	(m)	(s)	(m/s)	(kN)	
GMl	NA	NA	0.00	0.00	
GMt	NA	NA	0.00	0.00	
Surge Free Decay	NA	NA	0.00	0.00	
Sway Free Decay	NA	NA	0.00	0.00	
Heave Free Decay	NA	NA	0.00	0.00	
Roll Free Decay	NA	NA	0.00	0.00	
Pitch Free Decay	NA	NA	0.00	0.00	
Yaw Free Decay	NA	NA	0.00	0.00	
Regular Wave 1	tbd	tbd	0.00	0.00	
Regular Wave 2	tbd	tbd	0.00	0.00	
Regular Wave 3	tbd	tbd	0.00	0.00	
Regular Wave 4	tbd	tbd	0.00	0.00	
Regular Wave 5	tbd	tbd	0.00	0.00	
Regular Wave 6	tbd	tbd	0.00	0.00	
Regular Wave 7	tbd	tbd	0.00	0.00	
100 Year Cyclone	See Table 3-1				
10-yr Sea					
10-yr Swell					
White Noise					

Configuration	Semi & Mooring	CWP	Remoras	Gimbal Compliance	Mooring
CWP Installation 1	x	½	None	NA	Taut

Test Description	H or Hs	T or Tp	Current	Wind Force	
	(m)	(s)	(m/s)	(kN)	
GMl w/ Pipe	NA	NA	0.00	0.00	
GMt w/ Pipe	NA	NA	0.00	0.00	
Pipe Bottom Surge Static Offset	NA	NA	0.00	0.00	
Surge Free Decay	NA	NA	0.00	0.00	
Sway Free Decay	NA	NA	0.00	0.00	
Heave Free Decay	NA	NA	0.00	0.00	
Roll Free Decay	NA	NA	0.00	0.00	
Pitch Free Decay	NA	NA	0.00	0.00	
Yaw Free Decay	NA	NA	0.00	0.00	
Pipe Impulse	NA	NA	0.00	0.00	

Configuration	Semi & Mooring	CWP	Remoras	Gimbal Compliance	Mooring
CWP Installation 1	x	½	None	NA	Taut

Test Description	H or Hs	T or Tp	Current	Wind Force	
	(m)	(s)	(m/s)	(kN)	
Regular Wave 1	tbd	tbd	0.00	0.00	
Regular Wave 2	tbd	tbd	0.00	0.00	
Regular Wave 3	tbd	tbd	0.00	0.00	
Regular Wave 4	tbd	tbd	0.00	0.00	
Regular Wave 5	tbd	tbd	0.00	0.00	
Regular Wave 6	tbd	tbd	0.00	0.00	
Regular Wave 7	tbd	tbd	0.00	0.00	
10-yr Sea					
10-yr Swell					
White Noise					

Table 4-6 Group 4 Test Matrix

Configuration	Semi & Mooring	CWP	Remoras	Gimbal Compliance	Mooring
CWP Installation 2	x	1	None	NA	Taut

Test Description	H or Hs	T or Tp	Current	Wind Force	
	(m)	(s)	(m/s)	(kN)	
GMl w/ Pipe	NA	NA	0.00	0.00	
GMt w/ Pipe	NA	NA	0.00	0.00	
Pipe Bottom Surge Static Offset	NA	NA	0.00	0.00	
Pipe Impulse	NA	NA	0.00	0.00	
Regular Wave 1	tbd	tbd	0.00	0.00	
Regular Wave 2	tbd	tbd	0.00	0.00	
Regular Wave 3	tbd	tbd	0.00	0.00	
Regular Wave 4	tbd	tbd	0.00	0.00	
Regular Wave 5	tbd	tbd	0.00	0.00	
Regular Wave 6	tbd	tbd	0.00	0.00	
Regular Wave 7	tbd	tbd	0.00	0.00	
10-yr Sea					
10-yr Swell					
White Noise					

4.4.2.1 Regular Wave Tests

Regular wave tests will be conducted using the approved wave drive signals from the wave calibration tests. Sufficient time shall be allowed between tests to avoid any distortion of the newly generated seas

by a previous test. Data acquisition shall commence with the start of the wave maker so that the initial transient response of the vessel can be identified. Regular wave tests shall have a duration that allows a minimum of ten (10) regular wave cycles to be captured after the initial transient response has subsided.

4.4.2.2 Random Wave Tests

Random wave tests will be conducted using the approved wave drive signals from the wave calibration tests. Random wave tests with associated currents shall be conducted only after the current has achieved steady state. Sufficient time shall be allowed between tests to avoid any distortion of the newly generated seas by a previous test. The tests will be the full-scale equivalent of three hours in duration. Data acquisition will not commence until the initial transient response of the vessel to the startup of the waves is estimated to have died out.

4.4.3 Data Reduction and Processing

The Model Basin shall provide tabular results and de-multiplexed time series data in a text format that may be directly read by Microsoft Word, Microsoft Excel, and MatLab on a computer operating under the Microsoft Windows operating system. The Model Basin shall provide graphical analysis products in pdf format. All captions, labels, and text shall be in English. The Bidder shall provide typical examples of the analysis products requested below to ensure that all the necessary information will be provided as requested.

Example data files and analysis product files shall be provided at least two weeks prior to testing so that Lockheed Martin may be adequately prepared to accept, read and process the files made available after each test is conducted.

The Bidder shall state in the bid the amount of time after the completion of a test until the preliminary results, as described in this section, will be made available to Lockheed Martin. Preliminary test results, de-multiplexed time series files, and appropriate analysis products shall be made available to permit review by Lockheed Martin during regular business hours. Adequate time shall be allowed prior to completion of one test series and initiation of the next for Lockheed Martin to ensure completeness of the necessary data set and to permit changes to the test plan to be implemented with minimum impact on the project schedule and cost.

4.4.3.1 System Identification Tests

4.4.3.1.1 Coldwater Pipe, Guides and Gimbal Structural Calibrations

The Bidder shall describe the report and analysis products to be provided that document the cold water pipe, pipe guide and gimbal structural stiffness's.

4.4.3.1.2 Static Offset Tests

The Model Basin shall provide summary statistics and de-multiplexed time series files for each static test conducted in full-scale values. Summary statistics shall include:

- the maximum value recorded,
- the minimum value recorded,
- the average value, and
- the standard deviation.

Plots showing the imposed force vs. the response shall be provided, including both vessel displacement/rotation and model mooring tensions. The plots shall include the individual data points as well as the curve derived from the mooring design.

4.4.3.1.3 Incline Tests

The Model Basin shall provide summary statistics and de-multiplexed time series files for each static test conducted. The vessel GM shall be computed from the measured data and provided to Lockheed Martin.

4.4.3.1.4 Free Decay Tests

The Model Basin shall provide summary statistics and de-multiplexed time series files for each free decay test conducted. The Model Basin shall provide graphical analysis products showing the measured and best fit for equivalent linear damping. The best-fit amplitude, period, and damping coefficient shall be provided. The time window, i.e. start time and stop time for the analysis, shall be evident.

Time series plots of every acquired channel shall be provided to ensure that the tests excite a response primarily in the degree of freedom of interest.

4.4.3.2 Dynamic Environment Tests

4.4.3.2.1 Regular Wave Tests

Summary statistics and de-multiplexed time series files shall be provided for the each regular wave test covering the full duration of the test. Time series plots of every channel shall be provided.

Windowed data over an interval during which the regular wave RAOs may be computed shall be provided. The windowed data shall include summary statistics and time series plots for each channel. In addition, the Model Basin shall produce tables of regular wave statistics and regular wave RAOs, both amplitude and phase, for each channel using the calibrated wave record when the model was absent from the model basin. Regular wave statistics include:

- Wave height, and
- Wave period.

The time window, i.e. start time and stop time for the windowed analysis, shall be evident.

4.4.3.2.2 Random Wave Tests

Summary statistics and de-multiplexed time series files shall be provided for the each random wave test covering the full duration of the test. Time series plots of every channel shall be provided.

RAOs shall be computed, both amplitude and phase, for all channels in the white noise tests.

Extreme value statistics and Weibull plots shall be produced for all channels for tests in the 100-year cyclone, 25-year non-cyclone, and maximum current environments. Estimates of the three-hour extreme values shall be provided based upon a best fit of the Weibull distribution to the test data.

4.5 Access to Facility/Offices

The test program will be monitored by Lockheed Martin or a Lockheed Martin representative who will be responsible for reviewing the setup and the validity of each test nominated by the Model Basin as "good." Lockheed Martin, or a representative, is to be on site during execution of all dynamic tests with the model.

The Model Basin shall provide a workspace for these individuals, access to the basin and control room, a desk with facilities for using a portable computer with access to email and the internet. The Model Basin shall provide immediate access to data from each run judged by the Model Basin to be acceptable. At various other times during the test program, two to three additional observers from Lockheed Martin may be present.

Access to the model basin and model test control room shall be available to the Lockheed Martin representatives at all times during working hours when the test program set up and testing is under way.

5 Project Deliverables

All correspondence, reports, and analysis products shall be in English.

Data on the model design, mass properties and the Cold Water Pipe calibrations shall be provided as soon as practical prior to execution of in-place tests in order to allow numerical modeling of the model prior to the tests. This should be a minimum of one week prior to the execution of random or regular wave tests. The model basin shall provide

5.1 Model Design

The bidder shall provide drawings of the proposed models for the platform and remoras in sufficient detail to allow numerical hydrodynamic modeling.

5.2 Model Mass Properties

Mass properties including model weight in air, center of gravity, and gyradii about the center of gravity shall be provided for the semi alone and the semi with six remoras. If the flooded remora option is selected, the data shall include the properties without entrained water and a separate computed value with entrained water based on measurements of the amount of entrained water.

5.3 Inclining Test Results

Inclining test results shall be provided as soon as practical prior to the beginning of wave tests.

5.4 Cold Water Pipe and Gripper/Guide/Gimbal Model Design and Instrumentation Plan

The Model Basin shall provide a design and instrumentation plan for the cold water pipe model, the compliant guides, and the gimbal for review and approval by Lockheed Martin.

5.5 Cold Water Pipe and Gripper/Guide/Gimbal Structural Calibration Results

The Model Basin shall present a report complete with a description of the test method and analysis products that documents the cold water pipe, pipe guide and gimbal structural stiffness's.

5.6 Model Mooring Design

The model mooring design information shall be provided to Lockheed Martin for review and approval prior to fabrication. The model mooring design information package shall provide sufficient information so that a numerical model of the physical model may be programmed. At a minimum the pretension and the lengths, dry weight, wet weight, and axial stiffness of the model mooring components shall be provided. The three dimensional, earth fixed locations of the fairleads and anchor points shall be provided.

Upon fabrication of the model mooring, the as-built properties of the model lines shall be provided.

5.7 Wave Calibration Results

Summary statistics and de-multiplexed time series files shall be provided for the each calibrated wave tests covering the full duration of the test. It is possible that Lockheed Martin will not have a representative on-site for wave calibrations. Therefore, the Model Basin must be prepared to provide the result summaries remotely for review and approval.

5.7.1 Regular Waves

For regular wave calibration tests, summary statistics, and time series plots of every channel shall be provided. Windowed data over an interval during which the regular wave RAOs may be computed when the OTEC model is tested shall be provided. The windowed data shall include summary statistics and time series plots for each channel. In addition, the Model Basin shall produce tables of regular wave statistics. Regular wave statistics include:

- Wave height, and
- Wave period.

The time window, i.e. start time and stop time for the windowed analysis, shall be evident.

Calibrations of regular waves in the model basin shall be performed and the results shall be provided at least 72 hours prior to commencement of installation of the model in the basin for review and approval by Lockheed Martin.

5.7.2 Random Waves

For random wave calibration tests, time series plots of every channel shall be provided. Power spectral density plots showing both the measured and the target wave spectrum shall be provided. Extreme value statistics and Weibull plots shall be produced for all channels. Estimates of the three-hour extreme wave height and crest elevation shall be provided based upon a best fit of the Weibull distribution to the test data.

Calibrations of wave spectra in the model basin shall be performed and the results shall be provided at least 72 hours prior to commencement of installation of the model in the basin for review and approval by Lockheed Martin.

5.8 Preliminary Model Test Results

The Model Basin shall provide tabular results and de-multiplexed time series data in a text format that may be directly read by Microsoft Word, Microsoft Excel, and MatLab on a computer operating under the Microsoft Windows operating system. The Model Basin shall provide graphical analysis products in pdf format. The Model Basin shall provide immediate access to the preliminary data from each run judged by the Model Basin to be acceptable.

5.9 Final Report

A printed test report and copy of all electronic files is to be provided by the Model Basin. Three copies of the report are to be provided. At a minimum, the test report is to contain:

- Description of the facility, including basin resonant periods and results of absorber wave reflection tests. Results of basin calibration, especially with regard to cross-tank wave stability, are to be provided.
- Physical dimensions of tank, model, mooring lines, model installation, and location of wave sensors.
- Drawings of test setup and layout.
- Results of weighing, balancing, and swinging tests.
- Results of Cold Water Pipe calibration tests
- Documentation of instrument and sensor calibration, including results of pre and post testing calibration.
- List and identification of channels recorded in data sets.
- Results of wave calibration runs.

- Results of inclination tests.
- Results of static offset tests.
- Results of decay tests.
- List of test runs giving testing parameters for each run.
- Results of zero runs before and after wave runs are also to be tabulated.
- File names for data files are to be included in list.
- Tables of basic statistics of all data channels for all runs.
- Tables of dimension, mass, weight, stiffness characteristics, etc. of the as modeled system.
- Copy of test engineer's logbooks, showing test activities and providing record of conditions, tests, comments by test engineer, etc.
- Discussion of any significant uncertainties in the results, any difficulties encountered during the test, and recommendations for modifying similar future tests.

All files are also to be provided on a CD-ROM or DVD.

5.10 Still Photography

Selected still photographs shall be taken of the following items:

- The semisubmersible, remoras, cold water pipe and mooring elements model during and upon completion of construction,
- Close ups of the gripper, guides, gimbal and mooring fairleads,
- The semisubmersible with and without remoras during ballasting,
- The installed sensors,
- The model during wave tests,
- The tank basic setup,
- Any other relevant subjects.

It is required that a date stamp be included on each photograph. All photos shall be provided on a DVD or CD-ROM in JPEG format at the highest quality available.

5.11 Video

Video documentation of all dynamic tests shall be provided. The Model Basin shall provide the video on Zone 1 DVDs in NTSC format capable of being viewed on players in the USA.

At a minimum, a time and date stamp shall be synchronized on the video with the instrument data acquisition system. A detailed video log shall be kept which shall include at a minimum:

- test name,
- DVD number,
- Date and time,
- model configuration,
- test type and/or sea state.

A header with the above listed information recorded on the DVD prior to the test is desirable.

Three video views are required:

- One surface camera for viewing the motions of the vessel,
- One underwater camera for viewing the motions of the cold water pipe approximately half along its length, and
- One underwater camera for viewing the motions of the cold water pipe at the bottom.

A. Coldwater Pipe Modeling Techniques

The most challenging portion of the OTEC model to design and build is the cold water pipe. Figure 0-1 below shows a preliminary model design. The dimensions shown may not apply for the specified 10 m pipe. In order to model the important pipe properties, a composite structure with an aluminum, fiberglass, or other tube in the center to obtain the correctly scaled bending stiffness (EI). Care must be taken to select a material capable of withstanding the predicted strains. The cabling for the strain sensing devices must be taken into account in designing for the model mass and bending stiffness. An outer sheath of the right outside diameter is centralized on the tube. The outer shell is segmented so that it does not introduce bending stiffness.

The second picture, Figure 0-2, below shows a 1:110 scale CWP model used in an early model test. This picture shows the central rod and centralizers, and a split outer shell used on an earlier test.

The stiffness between the CWP and the platform is a critical parameter that has been shown in numerical simulations to impact the platform motions and the strain in the pipe. The pipe will be attached to the semisubmersible with a calibrated flexible joint. Extensive calibrations of the pipe stiffness and the flexible connection will be performed as part of the test setup.

The Bidder may propose other approaches for obtaining the stiffness properties required for the cold water pipe.

Figure 0-1 Cold Water Pipe Modeling Technique

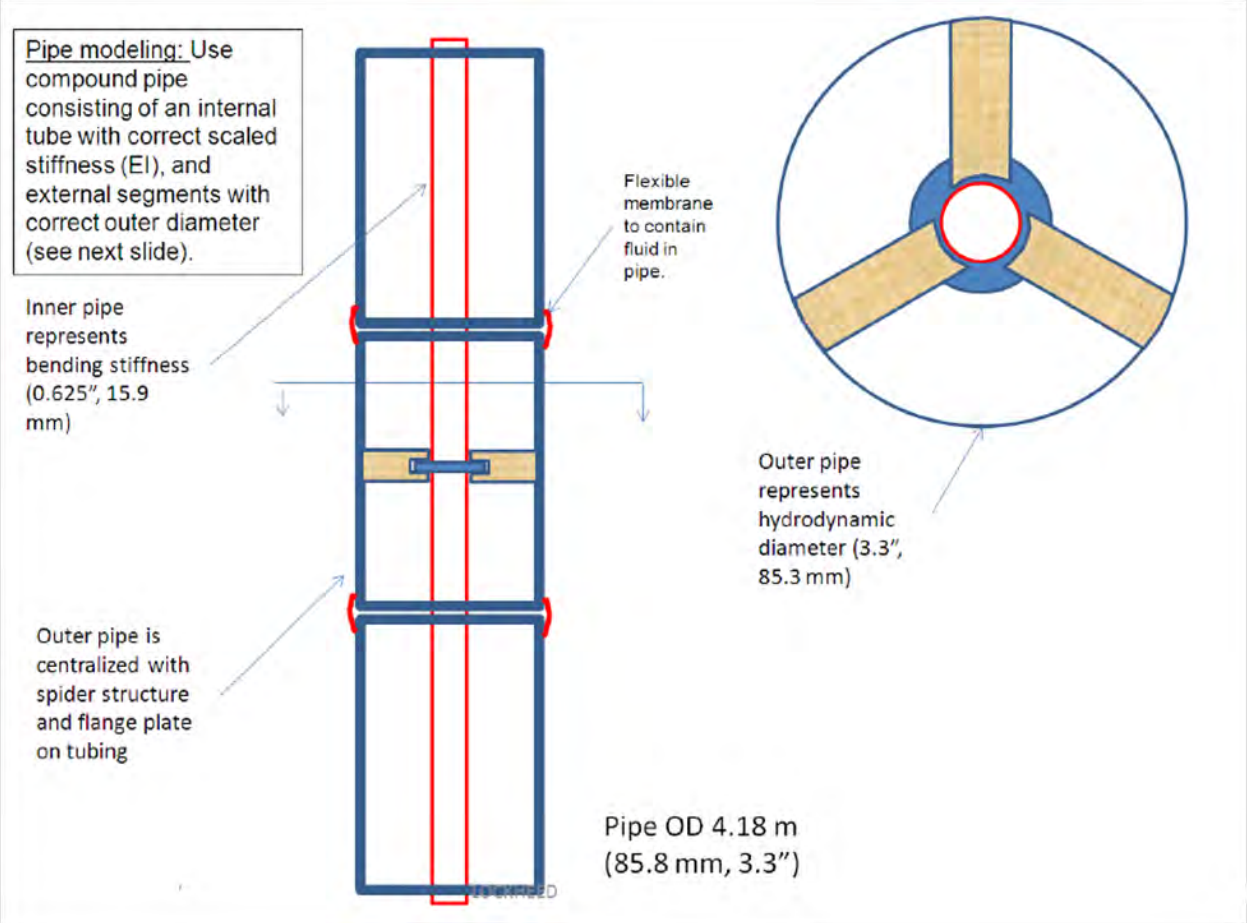

Figure 0-2 Example of Previous Cold Water Pipe Model

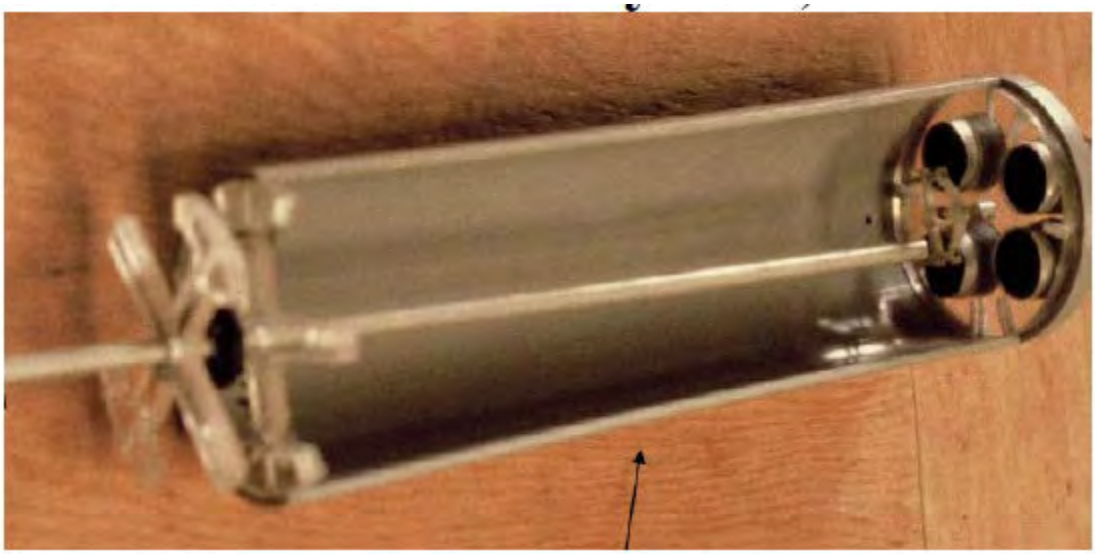

C. BMT DRY MODEL TESTS PROGRESS REPORT

This page intentionally left blank.

A part of BMT in Energy and Environment

BMT Scientific Marine Services

OTEC Model Test Consulting and Supervision for Lockheed Martin - Dry Model Tests Progress Report

SMS-E-19-MCG-2694C-0001
Revision 03
Date: October 10, 2013

Notice Statement

Data analyses and results interpretations are based on the measured data and on the information provided in already existing design documentation or from the surveys after the system is installed. All data processing is warranted to be at the highest professional level by BMT Scientific Marine Services (BMT), but BMT is not responsible for consequential damages due to errors in the data or misinterpretation of the report.

Escondido Office

955 Borra Place, Suite 100
Escondido, CA 92029
(P) 760.737.3505
(F) 760.737.0232

Houston Office

11505 West Little York
Houston, Texas 77041
(P) 281.858.8090
(F) 281.858.8898

Rio de Janeiro Office

Ed. Manhattan Tower
Avenida Rio Branco 89, 26 andar
20040-004 Rio de Janeiro, RJ

Brazil
(P) +55.21.2516.5923

info@scimar.com
www.scimar.com

Rev. No.	Rev. Date	Rev. Description	Issued By	Checked By	Engineer Approval	BMT Approval
01	3/10/13	Draft issued for review.	RS	JKN	JKN	RPJ
02	7/10/13	Approved	RS	JKN	JKN	RPJ
03	10/10/13	Minor changes following comments from client. Approved	RS	JKN	JKN	RPJ

Table of Contents

List of Figures

List of Tables

1 Executive Summary

This is a progress report on the dry model tests supervised by BMT from September 9 to 13, 2013 by John Halkyard and by Rizwan Sheikh from September 30th onwards.

Below are updates for the key dry test activities. These updates were accurate at the time of writing.

- The semi-submersible and remoras are assembled. Although some tests have been performed; mass, CoG and gyradii properties are yet to be reported.
- The Cold Water Pipe (CWP) has been fabricated and instrumented with 20 strain gauges; 18 in in the x axis and 2 in the y axis. Gaps between outer pipe sections have been covered using a 0.5mm natural rubber sleeve in order to mitigate flow in and out of the CWP.
- The span wise CWP mass and stiffness properties have been provided.
- The CWP impulse tests have been completed and data analyzed.
- The CWP static offset tests have been completed and data from the tests has been provided.
- The CWP rigidity test using a simply supported bean configuration have been conducted and CWP bending stiffness computed using simply supported beam deflection relationships indictate the bending stiffness, EI, to be with ± 10% of the specified value. However, numerical analysis of the data is required to validate the rigidity tests.
- Gimbal assembly is complete for operational (0 Nm/rad & $1x10^9$ Nm/rad angular stiffness) and installation configurations ($4.93x10^{10}$ Nm/rad). At present gimbal angular and horizontal stiffness tests for the installation configuration have been conducted. However, measured gimbal stiffness and mass properties are yet to be provided. Testing is currently in progress and due to be completed on October 4th.
- Static gimbal friction test for the operational configuration with zero gimbal stiffness has been conducted. Remaining static and dynamic friction tests for all other gimbal configurations are in progress and due to be completed by October 4th except for the installation condition which has been removed from the test programme given the rigidity of the configuration.
- Gimbal dynamometer design has been changed from a single 6DOF load cell to an arrangement using four 6DOF load cells mounted on gimbal plates. The new design is yet to be evaluated for cross-talk between measured channels. This check is currently scheduled for after completion of the gimbal stiffness tests.

This page intentionally blank

2 Introduction

This is the progress report of the OTEC dry model tests conducted in LabOceano. In summary the OTEC dry tests comprise of the following key activities:

- Cold water pipe (CWP) dry weight measurements,
- CWP dry impulse tests,
- CWP stiffness tests
- CWP mass properties
- Gimbal horizontal and angular stiffnesses,
- Gimbal static and dynamic friction tests for three configurations,
- Gimbal mass properties
- Mass, center of gravity and gyradii properties of the semi and remoras models .

The following terms have been used to described each of the gimbal stiffness configurations: “Pinned” configuration refers to a gimbal with zero angular stiffness. “Operational” configuration refers to a gimbal with $1x10^9$ Nm/rad angular stiffness, and lastly “Installation” configuration refers to a gimbal with high angular stiffness of $4.93x10^{10}$ Nm/rad.

The axial stiffness test proposed in the original LabOceano dry test procedures document [1] have been omitted from the final dry test programme after discussions with the project team. In addition, the static and dynamic friction tests of the gimbal in an installation configuration that were proposed initially in the dry test procedure have also been deemed to be unnecessary given the rigidity of the installation configuration.

Some of the contents of this report, such as photographs and plots have been extracted from status update reports submitted by LabOceano (Reference [3] to [7]) and the OTEC Model Dry-Tests Preliminary Report [8].

2.1 BMT Visit September 9 to 13, 2013

The first phase of dry testing was supervised by BMT’s appointed consultant, John E Halkyard, from September 9 to 13, 2013. Reference [2] provides a log of the observations and test results from this visit, which are summarized as follows:

- The semi and remora model fabrication incomplete.
- Instrumentation of the CWP with strain gauges complete. Gaps were observed between outer pipe sections. It was recommended that these be covered by a sleeve to mitigate water flow into the pipe.
- Gimbal dynamometer design had been changed from 1 6DOF load cell to four 6DOF load cells mounted on a plate. It was recommended that this design be evaluated for cross-talk between measured channels.

- The CWP impulse tests were performed and estimates of the natural periods for the first three modes were derived.
- The CWP static offset tests were performed.
- The CWP rigidity test had not been carried out.
- The mass check for ½ length CWP was complete.
- Static and dynamic gimbal friction test for pinned condition have been carried out. Friction tests for operational and installation configurations had not been carried out.

3 Status of OTEC Model Fabrication

The status of the OTEC model fabrication as of the date of issue of this progress report is as follows:

- Semi model, hang-off structure and remora fabrication is complete. Photographs of the semi model and gimbal hang-off frame are presented in Figure 3-1 and Figure 3-2, respectively. Photographs of the column weights and the remora model are presented in Figure 3-3 and Figure 3-4, respectively.
- CWP fabrication is complete and strain gauges have been installed on the CWP and tested to be functioning correctly. Gaps in the outer pipe have been sealed using 0.5mm natural rubber sleeves. Figure 3-5 provides photographs showing the assembled CWP and rubber sleeve together with a photograph showing the CWP core end connector.
- Gimbal fabrication is complete. Figure 3-6, Figure 3-7 and Figure 3-9 show the gimbal model with zero stiffness, springs and brackets for the operational gimbal stiffness, and the hang-off structure model, respectively. The design of the dynamometer measuring the gimbal forces had been changed from a single 6DOF load cell design to a four 6DOF load cell design. This dynamometer configuration is shown in Figure 3-10.

3.1 Semi and Remoras Mass Properties

Semi and remora mass properties are yet to be reported, although mass and center of gravity measurements of the remoras have been known to be measured. The semi model mass will be measured once gimbal stiffness and friction tests, which are currently in progress, are complete. This is so that the semi with gimbal installed can be measured.

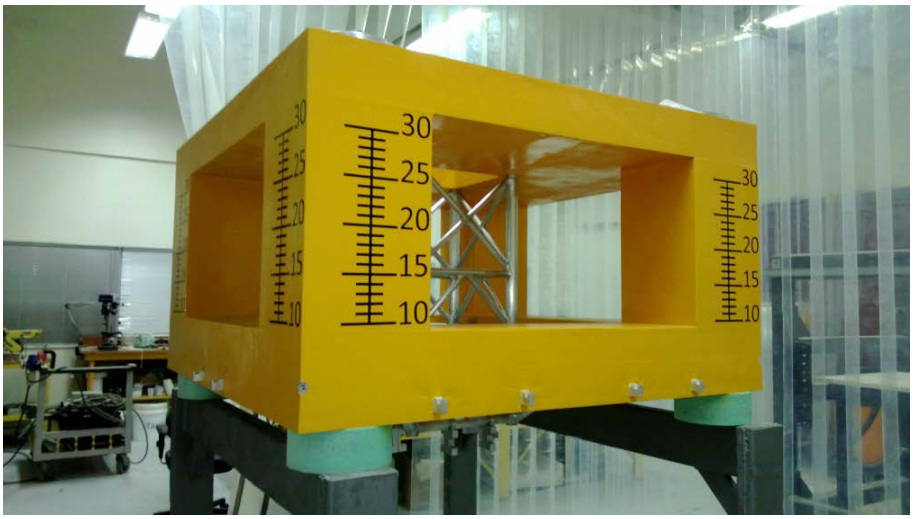

Figure 3-1. Photograph of fabricated semi model.

Figure 3-2. Hang-off structure installed in semi

Figure 3-3. Column weights for semi model.

Figure 3-4. Photograph of one remora model on load plate.

Figure 3-5. Photographs showing assembled CWP section with rubber sleeve and core connection.

Figure 3-6. Gimbal model with zero stiffness

Figure 3-7. Spring and bracket componenets for gimbal with operational stiffness.

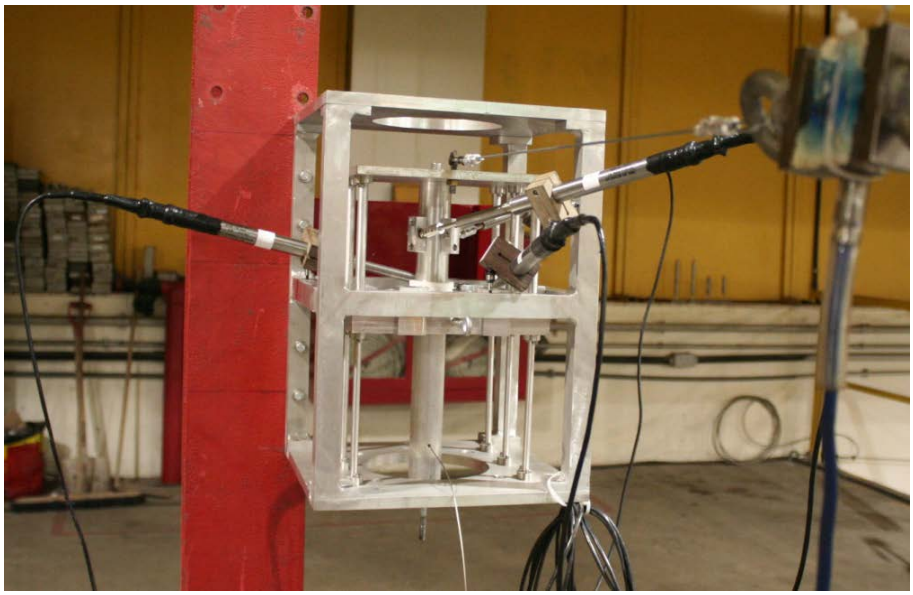

Figure 3-8. Gimbal mounted for stiffness test of installation configuration.

Figure 3-9. Truss and gimbal support showing the four load cell dynamometer design.

Figure 3-10. Load cells and Gimbal bottom plate.

4 CWP Tests

The composition of the CWP is described in greater detail in Reference [8]. This sections provides a progress update of dry tests of the CWP.

4.1 CWP Mass Properties

LabOceano have provided the span wise variation in mass and bending stiffness along the CWP that are presented in Table 4-1. This span wise variation is useful to faithfully 'model the model' in numerical simulations. In addition Table 4-2 provides the locations of the strain gauges along the CWP relative to the top of the core pipe. Here, 18 strain gauges have been installed in the x-axis and another 2 in the y-axis.

The computed model mass of the CWP are 22479.20g and 45166.93g for the ½ and full length CWP. The measured model mass of the ½ length of CWP from the impulse tests was recorded to be between 22478.7g and 22480.8g.

Table 4-1. Mass and stiffness spanwise variation along CWP.

Section	Start [mm]	End [mm]	Mass per Length [g/mm]	EI [N.mm²]	Core Tube	Conne-ctor	Outer Sheet 1	Outer Sheet 20	Outer Sheet 2 - 19
1	0	20	6.07	7.14E+09	*	*			
2	20	51.1	3.14	7.14E+09	*	*			
3	51.1	263.6	0.83	2.95E+09	*				
4	263.6	328.6	3.14	7.14E+09	*	*			
5	328.6	1010.32	2.47	2.95E+09	*		*		
6	1010.32	1020.32	0.83	2.95E+09	*				
7	1020.32	2000.62	2.37	2.95E+09	*				*
8	2000.62	2010.62	0.83	2.95E+09	*				
9	2010.62	2990.92	2.22	2.95E+09	*				*
10	2990.92	3000.92	0.83	2.95E+09	*				
11	3000.92	3981.22	2.30	2.95E+09	*				*
12	3981.22	3991.22	0.83	2.95E+09	*				
13	3991.22	4971.52	2.20	2.95E+09	*				*
14	4971.52	5036.52	3.14	7.14E+09	*	*			
15	5036.52	6016.82	2.21	2.95E+09	*				*
16	6016.82	6026.82	0.83	2.95E+09	*				
17	6026.82	7007.12	2.26	2.95E+09	*				*
18	7007.12	7017.12	0.83	2.95E+09	*				
19	7017.12	7997.42	2.16	2.95E+09	*				*
20	7997.42	8007.42	0.83	2.95E+09	*				
21	8007.42	8987.72	2.23	2.95E+09	*				*
22	8987.72	8997.72	0.83	2.95E+09	*				
23	8997.72	9978.02	2.40	2.95E+09	*				*
24	9978.02	10008.02	3.14	7.14E+09	*	*			
25	10008.02	10043.02	3.14	7.14E+09	*	*			
26	10043.02	11023.32	2.23	2.95E+09	*				*
27	11023.32	11033.32	0.83	2.95E+09	*				
28	11033.32	12013.62	2.21	2.95E+09	*				*
29	12013.62	12023.62	0.83	2.95E+09	*				
30	12023.62	13003.92	2.23	2.95E+09	*				*
31	13003.92	13013.92	0.83	2.95E+09	*				
32	13013.92	13994.22	2.22	2.95E+09	*				*
33	13994.22	14004.22	0.83	2.95E+09	*				
34	14004.22	14984.52	2.28	2.95E+09	*				*
35	14984.52	15049.52	3.14	7.14E+09	*	*			
36	15049.52	16029.82	2.24	2.95E+09	*				*
37	16029.82	16039.82	0.83	2.95E+09	*				
38	16039.82	17020.12	2.34	2.95E+09	*				*
39	17020.12	17030.12	0.83	2.95E+09	*				
40	17030.12	18010.42	2.33	2.95E+09	*				*
41	18010.42	18020.42	0.83	2.95E+09	*				
42	18020.42	19000.72	2.25	2.95E+09	*				*
43	19000.72	19010.72	0.83	2.95E+09	*				
44	19010.72	19980.72	2.29	2.95E+09	*			*	
45	19980.72	20016.02	0.83	2.95E+09	*				

Table 4-2. Strain gauge locations along core pipe relative to top.

Strain Gauge	Position [mm]	Direction
1	1120	x
2	2200	x
3	3300	x
4	4400	x
5	5500	x
6	6600	x
7	7700	x
8	8800	x
9	9880	x
10	10780	x
11	12120	x
12	13200	x
13	14300	x
14	15400	x
15	16500	x
16	17600	x
17	18700	x
18	19600	x
19	6670	y
20	13330	y

4.2 CWP Impulse Tests

Impulse tests have been conducted previously prior to the installation of the rubber sleeves. The results of these previous impulse tests are detailed in Reference [2]. Once the gaps in the CWP were sealed using a 0.5mm natural rubber sleeve impulse tests of the CWP were repeated. This report summarizes the results corresponding to these most recent CWP impulse tests, which are also detailed in Reference [8].

Impulse tests on the CWP were conducted by tapping the bottom section of the vertically suspended CWP rigidly connected at the top end while taking synchronized measurements of the pipe displacements and strains at 10 locations along the ½ length of the CWP as well as the vertical force at the top of the CWP. Figure 4-1 shows the picture of the suspended ½ length CWP. Displacements were measured using a Qualisys optical tracking system, of which Figure 4-2 shows a picture of the camera.

In total four impulse tests were performed: The bottom of the CWP model was hit in the x direction (Run #1,#2 and #3) and the y direction (Run #4) by a small hammer to excite the ½ length of CWP.

Predicted modal periods from a Felxcom3D analysis performed by Houston Offshore Engineering are presented in Table 4-3 and modal periods from spectral analysis of measured vertical loads are presented in Table 4-4. The latter results have been extracted from the LabOceano preliminary results [8], wherein the load cell data was deemed most reliable for derivation of CWP natural periods. In addition, Table 4-5 provides a modal periods computed by BMT based on the same analysis of the measured vertical loads and Figure 4-3 provides an example of the spectral analysis results for Run 1.

An inspection of the measured dry weights of the CWP in Table 4-4 show marked difference for Run 4, which should not be the case. Also, the mode 1 and 2 periods in the y axis are shorter than those from Runs 1 to 3 suggesting a greater stiffness for this direction. Therefore, Run 4 may not be a reliable test. The remaining results for Runs 1 to 3 show a longer natural periods for Mode 1 and Mode 2, but agree well with the predicted natural periods for Mode 3.

Also, the modal periods for the repeated impulse tests differ from those derived from previous tests performed prior to the installation of the rubber sleeves. The natural periods from those tests were 3.85s, 0.84s and 0.3s for Modes 1 to 3, respectively. Although, results from the previous tests showed greater agreement between the measured and predicted natural periods an inspection of data from the initial impulse tests revealed a long wave component present in the strains prior to the excitation by the hammer as well as a ‘drift’ in the strains that manifests as a longer period in the spectral analysis. Lastly, in some of the measured strains the mode 3 period was more prominent than the 2nd. In short, although the modal periods from the first impulse tests are closer to those of the numerical prediction there are some anomalies in the data.

It is not possible that the addition of the rubber sleeves could have reduced the bending stiffness of the CWP and therefore it is believed that a reduced stiffness of the top connection is most likely the reason for the longer natural periods observed in the repeated tests. A photograph of the top connection is provided in Figure 4-4.

In light of the above results it is recommended that the numerical model top stiffness be adjusted in order to match the measured natural periods. It is believed that if the periods can be matched this may provide an explanation for the difference in the measured and predicted natural periods of the CWP.

Table 4-3. Predicted Modal periods for CWP.

Mode	Predicted Modal Periods (s)		
	Pinned Configuration	Operation Configuration	Installation Configuration
1	5.20	3.88	3.72
2	1.07	0.86	0.81
3	0.37	0.32	0.30

Table 4-4. Measured Modal periods for CWP as per LabOceano spectral analysis of vertical load for the installation configuration.

Run	Dry Weight (g)	Mode 1 (s)	Mode 2 (s)	Mode 3 (s)
1	22478.7	4.71	0.91	0.30
2	22478.1	4.71	0.89	0.30
3	22480.8	4.88	1.00	0.30
4	22338.9	4.40	0.92	0.30

Table 4-5. Measured Modal periods for CWP as per BMT spectral analysis of vertical load for the installation configuration.

Run	Mode 1 (s)	Mode 2 (s)	Mode 3 (s)
1	4.87	0.90	0.30
2	4.87	0.87	0.30
3	4.87	0.92	0.30
4	4.26	0.92	0.30

Figure 4-1 Vertically suspended ½ length CWP pipe

Figure 4-2 Optical tracking camera measuring displacement of vibrating CWP

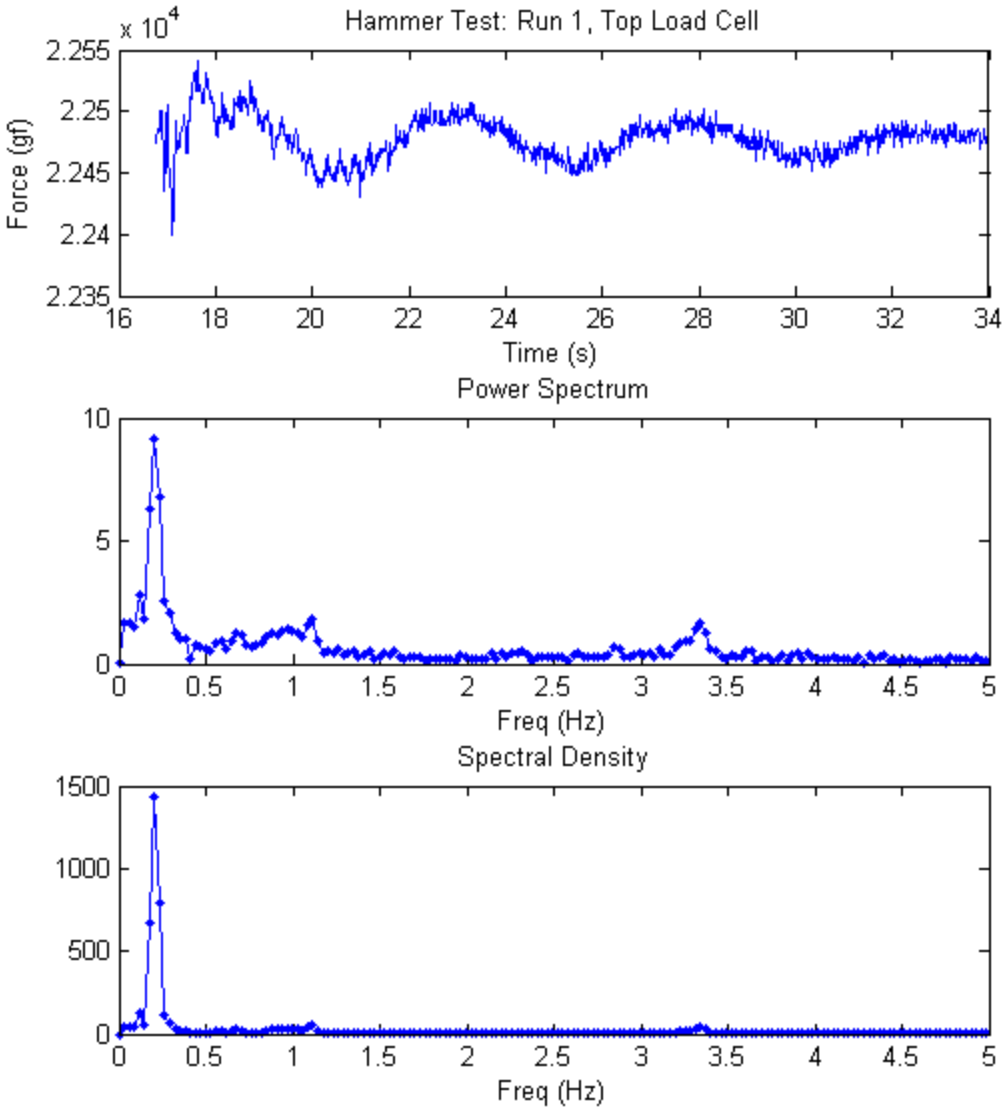

Figure 4-3. Spectral analysis (BMT) of vertical load from Run 1 of CWP impulse tests.

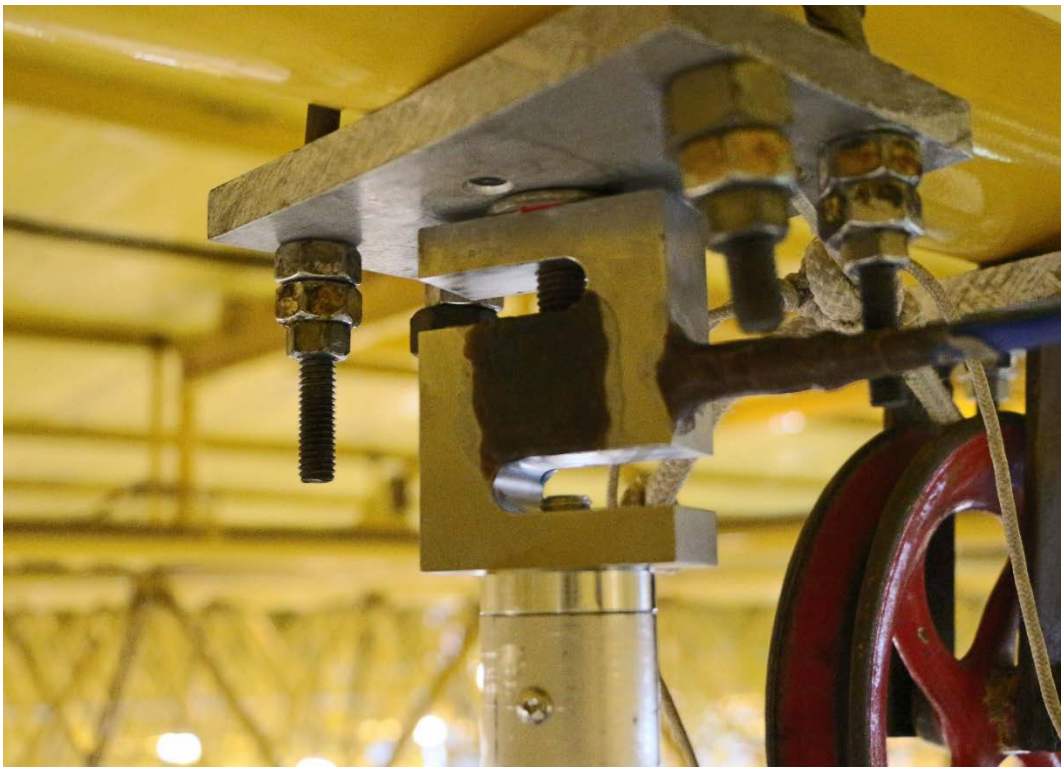

Figure 4-4. Top connection of CWP for impulse tests.

4.3 CWP Stiffness Properties

The CWP stiffness properties are evaluated using results from the CWP static offset tests and rigidity tests.

4.3.1 CWP Static Offset Test

Following the visit from John E. Halkyard a CWP static offset test was added to the dry test programme to verify the rigidity of the ½ length CWP. Using the CWP set up in the impulse test, the bottom of the pipe is displaced incrementally and measuring the strains and pipe deflection.

The static offset test set up and the load cell - pulling line arrangement is depicted in Figure 4-5. Results from this test are available on the project FTP server and have been presented by LabOceano in their Dry Test Preliminary report [8]. A plot showing the horizontal displacement along the CWP is provided in Figure 4-6.

At the time of writing no bending stiffness values for the CWP had been derived from the CWP static offset tests.

Figure 4-5. Pulling line and load cell for static offset test

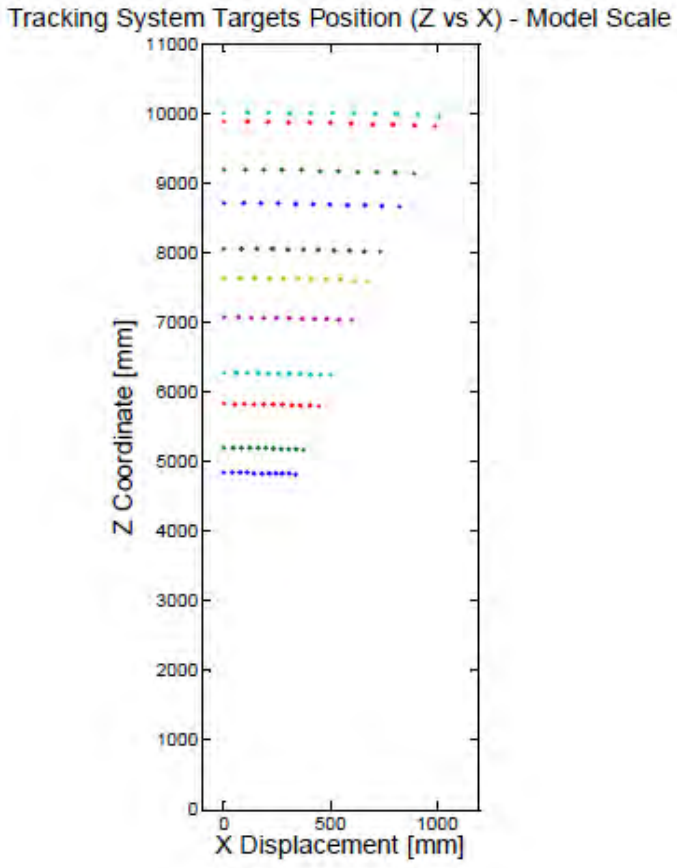

Figure 4-6. CWP displacement for static offset tests.

4.3.2 CWP Rigidity Test

The original procedure to measure the rigidity (or bending stiffness) of the CWP (EI value) using rigid supports has been replaced with another that uses a horizontally placed, simply supported CWP section 5m in length upon which a point load is applied. This arrangement is depicted in Figure 4-7. Loads are applied at a known location incrementally and the resulting deflections and stresses are measured and used to derive the rigidity of the CWP.

Results from this test are available on the project FTP server. A summary of the results are provided in Table 4-6. Here, the initial deflection of the CWP of 35.09mm below horizontal is due to the self weight of the CWP of 10.875kg. Based on the gradient of the load-deflection data provided in Table 4-6 the CWP bending stiffness, EI, at modal scale has been estimated to be 3.065kNm^2 using theoretical simply supported beam deflection relationship. This bending stiffness is withing ± 10% of the specified CWP stiffness, which is 2.95 kNm^2 at model scale. However, numerical analysis of the data is required for validation purposes.

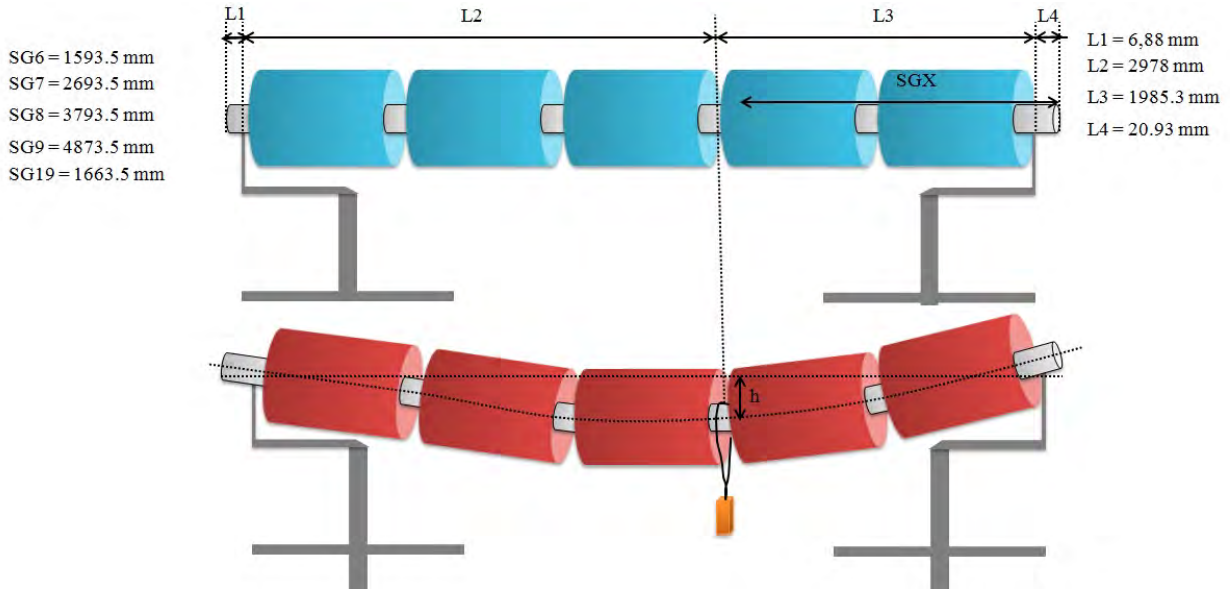

Figure 4-7. CWP simply supported test set-up and key dimensions.

Table 4-6. Applied load and resulting vertical displacement from simply supported CWP tests.

Dead Load, Weight (kg)	Vertical Displacement (mm) at point of loading
10.875	35.09
12.656	47.79
13.738	56.02
14.779	65.08
13.738	57.66
12.656	49.82
10.875	36.01

5 Gimbal Tests

Three different model test configurations are considered in the model tests, namely: Pinned, operational and installation. For each of these tests, the gimbal is designed with specific horizontal and angular stiffnesses.

5.1 Gimbal Mass

Gimbal mass properties are yet to be reported. At present mass measurements are scheduled for after Gimbal stiffness tests are completed.

5.2 Gimbal Stiffness

At the time of writing gimbal stiffness tests were underway. Table 5-1 provides a summary of the progress of these tests.

Table 5-1. Gimbal stiffness tests.

Test Description	Condition	Status
Gimbal angular and horizontal stiffness	Operation condition (x direction)	Scheduled 04 Oct
Gimbal angular and horizontal stiffness	Operation condition (y direction)	Scheduled 04 Oct
Gimbal angular stiffness	Installation condition (x direction)	Completed
Gimbal angular stiffness	Installation condition (y direction)	Scheduled 03 Oct
Gimbal horizontal stiffness	Installation condition (x direction)	Completed
Gimbal horizontal stiffness	Installation condition (y direction)	Scheduled 03 Oct

5.3 Gimbal Static Friction Tests

The static friction of the gimbal shall be determined by applying a slowly increasing horizontal force to a fixed point along the gimbal until the gimbal reaches limiting friction (starts to move). This test is performed for three different weights attached to the bottom of the gimbal: 8kg, 12kg and 18kg.

At the time of writing gimbal stactic friction tests were only partially complete. Table 5-2 provides a summary of the progress of these tests. It should be noted that given the rigid nature of the gimbal installation configuration the static friction tests for this configuration have been removed from the test programme.

Table 5-2. Gimbal static friction tests.

Test Description	Condition	Status
Gimbal static friction (3 weights)	Pinned	Completed
Gimbal static friction (3 weights)	Operational	Scheduled 04 Oct
Gimbal static friction	Installation	Not required

5.3.1 Pinned Configuration

Figure 5-1 shows a schematic of location of the gimbal center of rotation, applied pulling force, and center of gravity of ballast weight. It should be noted that the dimensions provided in Figure 5-1 will need to be verified after once the test is complete. Figure 5-2 shows a photograph of the actual experiment setup.

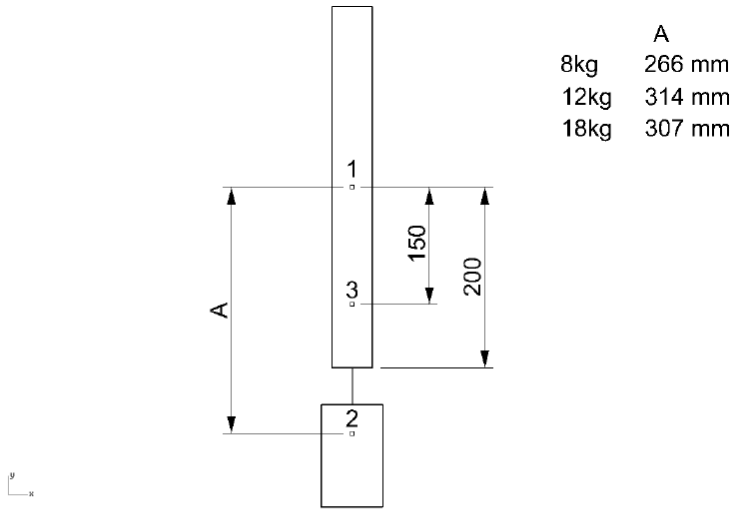

Point 1 - Center of Rotation

Point 2 - Set Center of Gravity (for ballast weight)

Point 3 - Pulling Position

Figure 5-1 Schematic of location of gimbal centre of rotation, applied pulling force and ballast weight

Repetitions of the tests show that the readings at limiting friction were repeatable and consistent. Plots of the tests for 8kg, 12kg and 18kg ballast weights are presented in Figures 5-3 to 5-5 respectively.

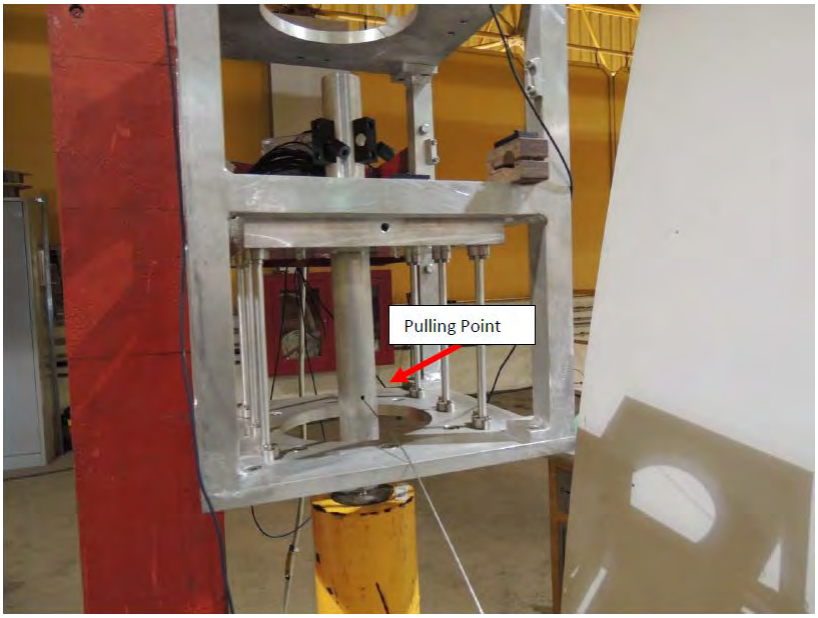

Figure 5-2 Pinned Gimbal Experiment Set Up with location of Pulling Point

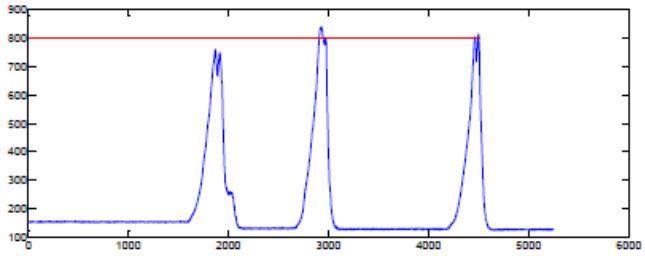

Figure 5-3 Plot of limiting friction force for 8kg ballast attached to gimbal

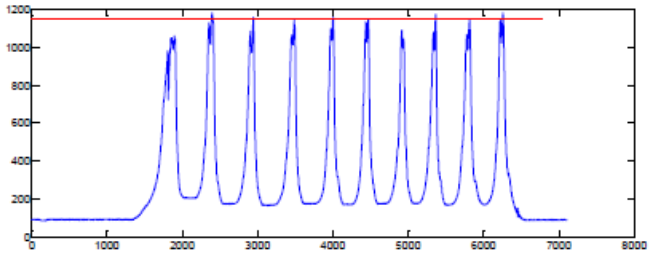

Figure 5-4 Plot of limiting friction force for 12kg ballast attached to gimbal

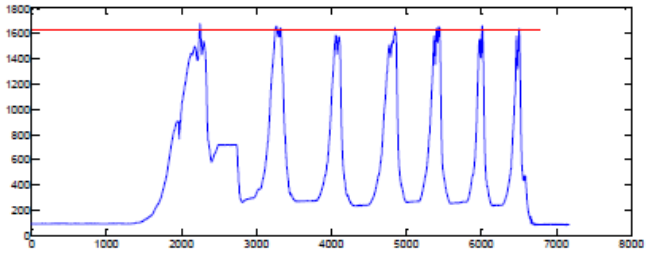

Figure 5-5 Plot of limiting friction force for 18kg ballast attached to gimbal

5.3.2 Operation Configuration

At present testing is underway and scheduled to be completed as stated in Table 5-2.

5.3.3 Installation Configuration

Static friction tests of the gimbal in its installation configuration shall not be conducted. This is due to rigidity of this configuration.

5.4 Gimbal Dynamic Friction Tests

The arrangement of the gimbal for the dynamic friction tests is similar to that of the static friction tests. In these tests, the ballast weight is offset horizontally and released. The resultant pendulum motions and the decay time to rest is recorded.

At the time of writing gimbal dynamic friction tests were only partially complete. Table 5-3 provides a summary of the progress of these tests. It should be noted that given the rigid nature of the gimbal installation configuration the dynamic friction tests for this configuration have been removed from the test programme.

Table 5-3. Gimbal dynamic friction tests.

Test Description	Condition	Status
Gimbal dynamic friction (3 weights)	Pinned	Scheduled 03 Oct
Gimbal dynamic friction (3 weights)	Operational	Scheduled 04 Oct
Gimbal dynamic friction	Installation	Not required

5.4.1 Pinned Configuration

At the time of writing no test results from the gimbal pinned configuration dynamic friction tests were available. However, this configuration had been tested preliminarily during the visit of John E Halkyard. This preliminary test was performed as a demonstration of the test set-up. At that time the LVDTs instruments were not installed. Therefore videos of the pendulum motions were recorded. From these it was estimated that the pendulum motion decays in about 7 cycles, which was estimated to correspond to a damping coefficient of approximately 7%. Figure 5-6 shows a snapshot of the pinned pendulum test.

Figure 5-6 Snapshot of Gimbal pinned configuration dynamic friction test.

5.4.2 Operation Configuration

At present testing is underway and scheduled to be completed as stated in Table 5-3.

5.4.3 Installation Configuration

Dynamic friction tests of the gimbal in its installation configuration shall not be conducted. This is due to rigidity of this configuration.

5.5 Gimbal Dynamometer Setup

During the visit of John E. Halkyard it was observed that the gimbal dynamometer setup was different to the original design. A single 6 degrees of freedom (6DOF) load cell was originally intended to be attached to the gimbal so that the forces and moments in all directions can be measured. However, the present dynamometer setup has been changed to feature four 6DOF load cells. A schematic of the 6DOF load cells and gimbal plates is shown in Figure 6-1. This design is statically indeterminate, and it is probable that there will be cross-talk (cross-coupling) of force and moment readings between the load cells. To determine the total loads on the gimbal accurately, it is necessary to evaluate the complete matrix solution of the installed load cells including cross-talk.

It is possible that the measured forces will include inertial effects from the gimbal frame and support structure. LabOceano shall provide the weight and geometry of these components for checks on inertial effects as well as a procedure for evaluating the dynamometer readings and demonstrate through testing that the there is no cross-talk between the load cells. A procedure involving applying loads at eccentric locations on the dynomomter has been discussed with the LabOceano. However, a procedure outlining the dynamometer tests is yet to be presented by LabOceano.

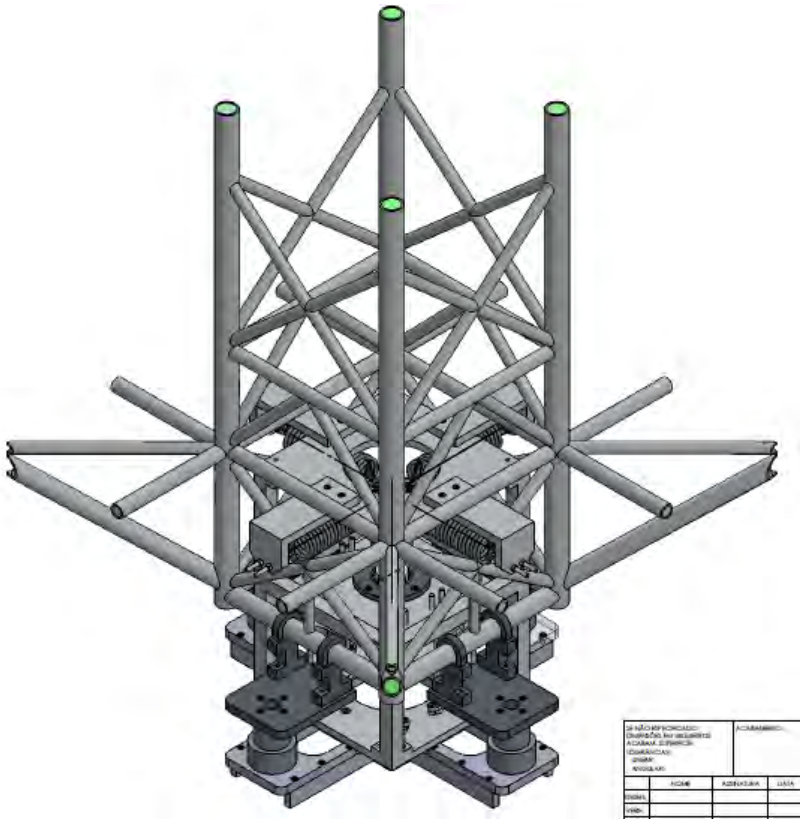

Figure 5-7. Iso view of the present dynamometer showing two of the four installed loadcells

6 Conclusions and Recommendations

In conclusion the status of the dry tests is summarized as follows:.

- Mass, CoG and gyradii properties of the semi-submersible and remoras are yet to be reported.
- The CWP impulse tests have been completed and data analyzed. Differences in measured and predicted modal periods are believed to be a result of uncertainty in the stiffness of the top connection. Therefore it is recommended that the top stiffness be adjusted in the numerical precitions to match the measured natural periods.
- The CWP static offset tests have been completed and data from the tests has been provided.
- The CWP rigidity test using a simply supported bean configuration have been conducted and CWP bending stiffness estimated using a theoretical relationship for a simply supported beam to be with ± 10% of the model test specification. However, it is recommend that these results be reproduced numerically for validation purposes.
- At present gimbal angular and horizontal stiffness tests have been conducted. Testing is currently in progress and due to be completed on October 4th. Gimbal stiffness and mass properties shall be submitted following the completion of the tests.
- Static gimbal friction test for the pinned configuration has been conducted. Remaining static and dynamic friction tests for all configurations are in progress and due to be completed by October 4th except for the installation condition which has been removed from the test programme given the rigidity of the configuration.
- Gimbal dynamometer design has been changed from a single 6DOF load cell to an arrangement using four 6DOF load cells mounted on gimbal plates. The new design is yet to be evaluated for cross-talk between measured channels. This check is currently scheduled for after completion of the gimbal stiffness tests.

LabOceano is to continue with the dry testing and provide BMT with constant updates of progress together with measured data as soon as possible following the completion of each test.

7 References

[1]. Lockheed Martin OTEC Wave Basin Test at LabOceano, Dry Test Planning. Thiago Marinho, LabOceano. August 21st, 2013

[2]. LabOceano Visit Log. John Halkyard & Associates. September 12th, 2013.

[3]. OTEC Wave Basin Test at LabOceano Daily Progress Report. Joel Sales Jr. September 20th, 2013. [008_12_LOCKHEED_OTEC_SITREP_2013_09_20.pdf]

[4]. OTEC Wave Basin Test at LabOceano Progress Report. Joel Sales Jr. September 23rd, 2013. [008_12_LOCKHEED_OTEC_SITREP_2013_09_23.pdf]

[5]. OTEC Wave Basin Test at LabOceano Progress Report. Joel Sales Jr. September 25th, 2013. [008_12_LOCKHEED_OTEC_SITREP_2013_09_25.pdf]

[6]. OTEC Wave Basin Test at LabOceano Progress Report. Joel Sales Jr. September 27th, 2013. [008_12_LOCKHEED_OTEC_SITREP_2013_09_27.pdf]

[7]. OTEC Wave Basin Test at LabOceano Progress Report. Joel Sales Jr. September 30th, 2013. [008_12_LOCKHEED_OTEC_SITREP_2013_09_30.pdf]

[8]. OTEC Model Dry-Tests Preliminary Report. Thiago Marinho, LabOceano. September 27th, 2013.

This page intentionally left blank.

D. LABOCEANO OTEC FINAL REPORT

This page intentionally left blank.

Project Number	008_12
Project Abbreviation	LOCKHEED_OTEC
Document No.	OTEC Final Report
Client	LOCKHEED MARTIN / PETROBRAS
Distribution	CLIENT

C	27/01/2014	Revision C	TMV 27/01/2014		
B	27/12/2013	Draft Report	TMV 27/12/2013	JSS 02/01/2014	PTT 02/01/2014
A	09/12/2013	Table of Content Draft	TMV 09/12/2013	-	-
Rev.	Date	Description	Prepared by	Checked by	Approved by

REFERENCES

The following documents were used as reference for the model test:

1. Lockheed OTEC Model Basin Test Specification Rev02 (072512) - Model test specification from Lockheed Martin

2. Proposal_OTEC_LOCKHEED_REV4 - Technical and commercial proposal from Laboceano

Revisions and additional specifications were documented on email exchange and over the ftp server of Lockheed Martin.

EXECUTIVE SUMMARY

This document reports the model tests conducted at LabOcean ocean basin from October 22nd, 2013 to December 06th, 2013, with an OTEC model at 1:50 scale.

The main objective of the tests was to provide data on the dynamic behavior of the cold water pipe ("CWP") under specific metocean conditions.

The measurements included platform and CWP motions, CWP strains, line tensions, gimbal angle and forces. Those values will be used to calibrate numerical design tools.

Six different test series were performed, with different model configurations, gimbal stiffness and CWP length.

Twelve environmental conditions were simulated, including waves and wind.

DELIVERED ITEMS

The following material is delivered:

1. Digital documents:
    - Main report
    - Annex A: CrossTalkingVerification
    - Annex B: Static System ID Tests Statistics
    - Annex C: Decay Tests Files Index
    - Annex D: Regular Wave Test Files Index
    - Annex E: Irregular Wave Test Files Index
    - Annex F: Instrumentation Calibration
    - Annex G: Gimbal Stiffness Design
    - Annex H: Gimbal Angle Measurement Algorithm
    - Annex I: CWP Weight 2014-01-21.xlsx
    - Annex J: Model Ballasting Plan
    - Annex K: Water Absorption Report 2013-06-05
    - Annex L: Semi_MassProperties_Measurements
    - Annex M: Remora_MassProperties_Measurements_2013_11_06

2. Data Files:
    - Recorded data (model scale) in Matlab® binary format.
    - Concatenated data (model scale) in Matlab® binary format.
    - Post-processed data (full scale) in Matlab® binary format.
    - Post-processed data (full scale) in txt ASCII format.

3. Digital Videos of the tests

Contents

1 INTRODUCTION

The experimental program included a series of about 130 wave tests, dry calibration and system identification tests. Tests were performed on different configurations of the model, with and without the Cold Water Pipe.

The main objectives of the tests were:

To obtain motion and tension response characteristics of this platform in every configuration for installation, operational and extreme environments;

To obtain response data of the Cold Water Pipe for use in calibrating and validating numerical design tools.

2 OCEAN BASIN DESCRIPTION

• Main dimensions: length of 40m, width of 30m and depth of 15m. Also, the basin has a central pit with 5m of diameter and 10m of additional depth;

• Windows at the basin walls (1.2m x 2.0m) at 5m depth level;

• Multi flap wave generator with 75 wet-back hinged flaps, capable of generating directional waves of different types: Regular waves with periods from 0.5s to 5.0s with a maximum height of 0.52m; Irregular long- and short-crested waves with a peak period of 3.0s and maximum significant height of 0.3m; all values in model scale.

• Front and lateral parabolic beaches for waves absorption with lengths of 8.0m (longitudinal beach) and 5.0m (transversal beach).

• Movable floors on the basin and on the central pit hole: operated by electric winches, can have their depth adjusted from 2.4m to 14.85m, in the basin; and from 15m to 24.85m, in the central pit.

A drawing with the basin main dimensions is shown below on figures 2-1 and 2-2:

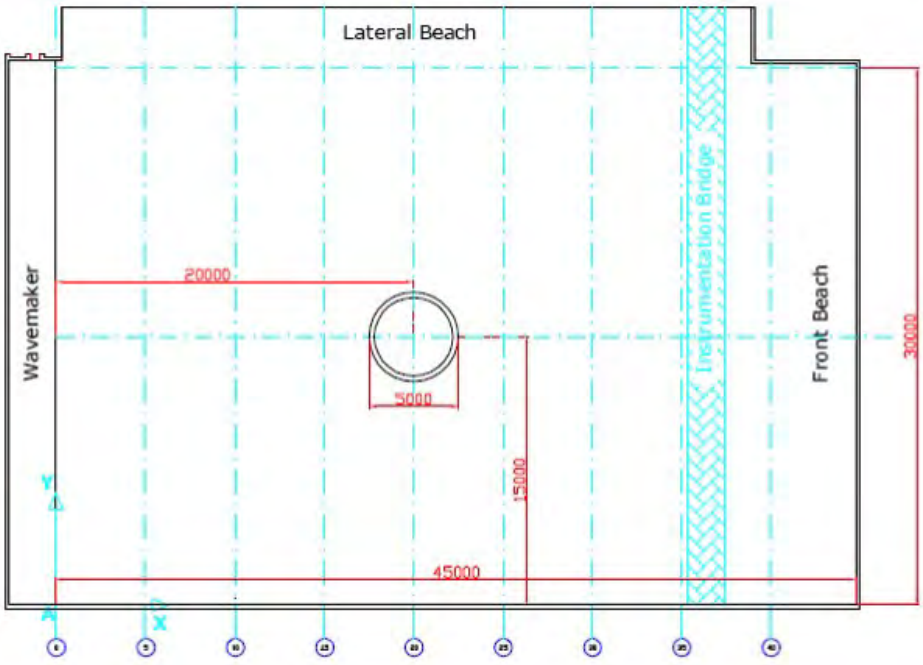

Figure 2-1 - Plan view of ocean basin

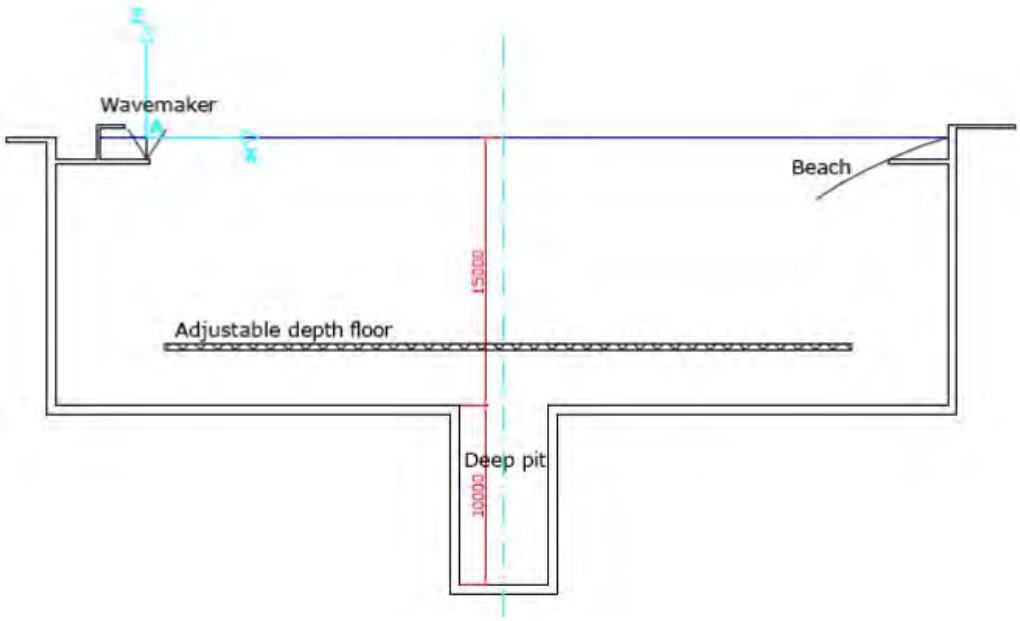

Figure 2-2 - Side view of basin layout

3 SYSTEM MODELLING

3.1 UNITS AND COORDINATE SYSTEM

The system of units adopted in the tests for both model and prototype scale quantities is described on the Table below:

Table 3-1 - Units System (model - prototype)

Quantity	Units (Model - Prototype)
Length	millimeter (mm) / meter(m)
Mass	grams (g) / kilograms(kg)
Force	gram-force (gf) / kilo-Newtons(KN)
Time	seconds(s) / seconds(s)
Angle	degrees (deg) / degrees (deg)
Strain	strain (-) / strain (-)

For the tests, the following reference coordinate systems were adopted:

• An inertial reference frame AXYZ, fixed to the basin. Plane XY of this frame coincides with the water free surface and AZ - axis points upwards. AX - axis coincides with the lateral wall of the basin and points to its front beach, AY - axis passes through the line of the flaps of the wave generator in its neutral position and points towards the lateral beach (see figure 3.1).

• An inertial reference frame oxyz, fixed to the basin. Plane xy of this frame coincides with the water free surface and oz - axis points upwards. ox - axis is parallel to the lateral wall of the basin and points to end beach, oy - axis is parallel to the line of the flaps of the wave generator in its neutral position and points towards the lateral beach of the basin (see figure 3.1). The origin point o position is (20000,15000,0)mm relative to the inertial reference frame AXYZ.

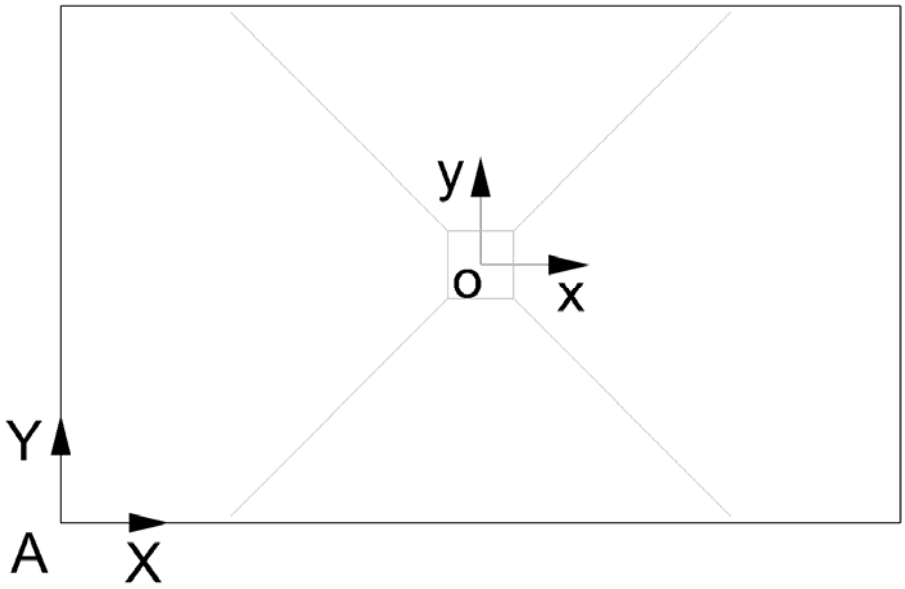

Figure 3-1 - Inertial Reference Frames

• A local reference system o'x'y'z' is fixed to the hull model. Its origin is placed in the intersection of the design waterline plane (20 meters above the keel) the centerline and the midline of the model. o'x' - axis points toward bow, o'y'-axis point towards port side, and o'z'-axis points vertically upwards in the model's upright position.

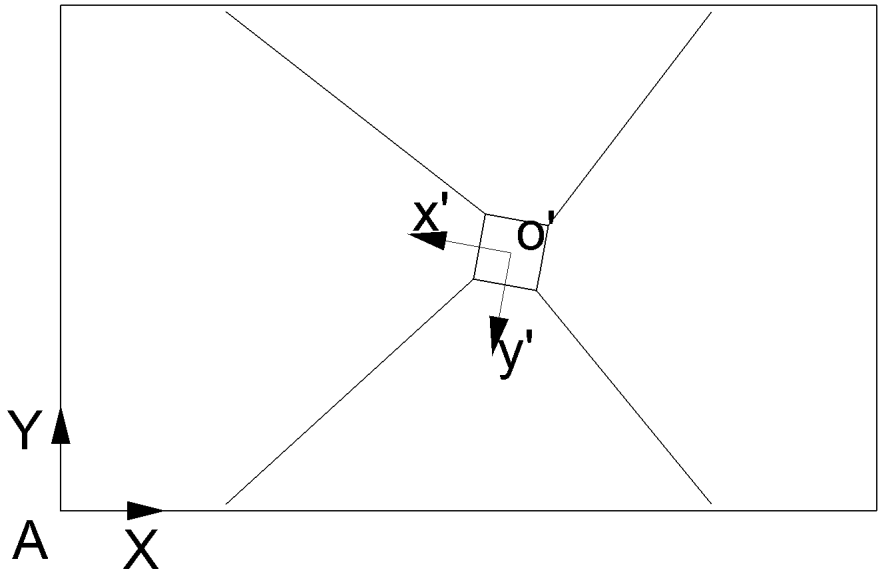

Figure 3-2 Local Reference Frame

Gimbal angle and CWP motion data use the local reference frame o'x'y'z' as reference while the Semi motion data use the inertial reference frame AXYZ as reference.

The heading angles definition for the model is illustrated in figure 3-3.

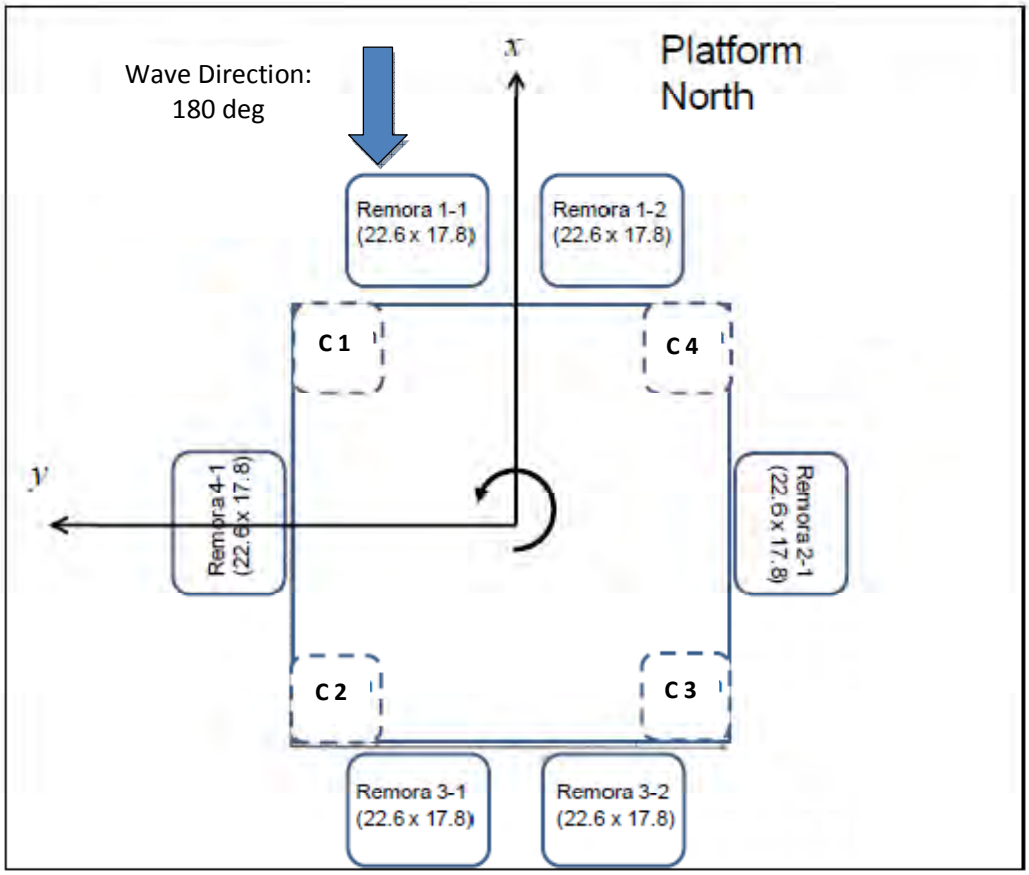

Figure 3-3 Heading and metocean incidence definitions

3.2 MODEL TEST SCALE

The scale factor (λ) was 1:50. This factor was taken considering model dimensions, basin dimensions, practical limitations of model construction and wave generation capability. The extrapolation factors for the test scale are shown on the table below.

Table 3-2 - Scale factors

Parameter	Factor
Length	λ
Area	λ^2
Volume	λ^3
Mass	$r.\lambda^3$
Time	$\lambda^{1/2}$
Force	$r.\lambda^3$
Angle	1
Acceleration	1
Velocity	$\lambda^{½}$
Angular velocity	$\lambda^{-½}$
r (correction factor for water density)	$\rho_{prototype}/\rho_{model}$

The gravity acceleration used during the entire project was 'g' = 9.80665 m/s².

During the project several readings of the basin water specific mass were taken, for this reason different values of 'r' were used during design, calibration and wave tests. The water specific mass for prototype scale was always assumed to be 1025 kg/m³. The basin water specific mass was considered as bellow:

- ρ_model = 994 kg/m³ - for design and model parameters verification reports (Remora mass properties, gimbal stiffness, gimbal mass, mooring design, etc...) - Section 3.3 through 3.7
- ρ_model = 992.2 kg/m³ - for model mass properties and systems identification tests - Section 3.8 and 7.12
- ρ_model = 993 kg/m³ - wave tests analysis and data products - Section 7.13 and 7.14

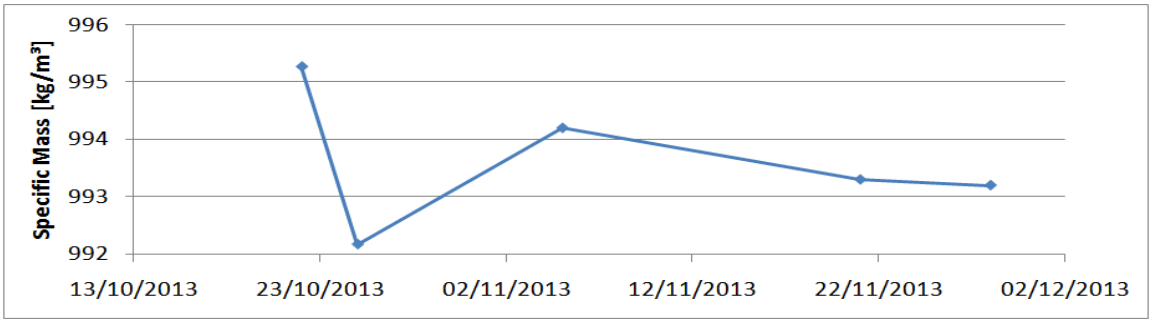

Figure 3-4 - Basin Water Specific Mass Readings

The maximum deviation from average basin water specific mass is 0.14%.

3.3 SEMI-SUBMERSIBLE

The Semi-Submersible geometry was manufactured with the following design dimensions.

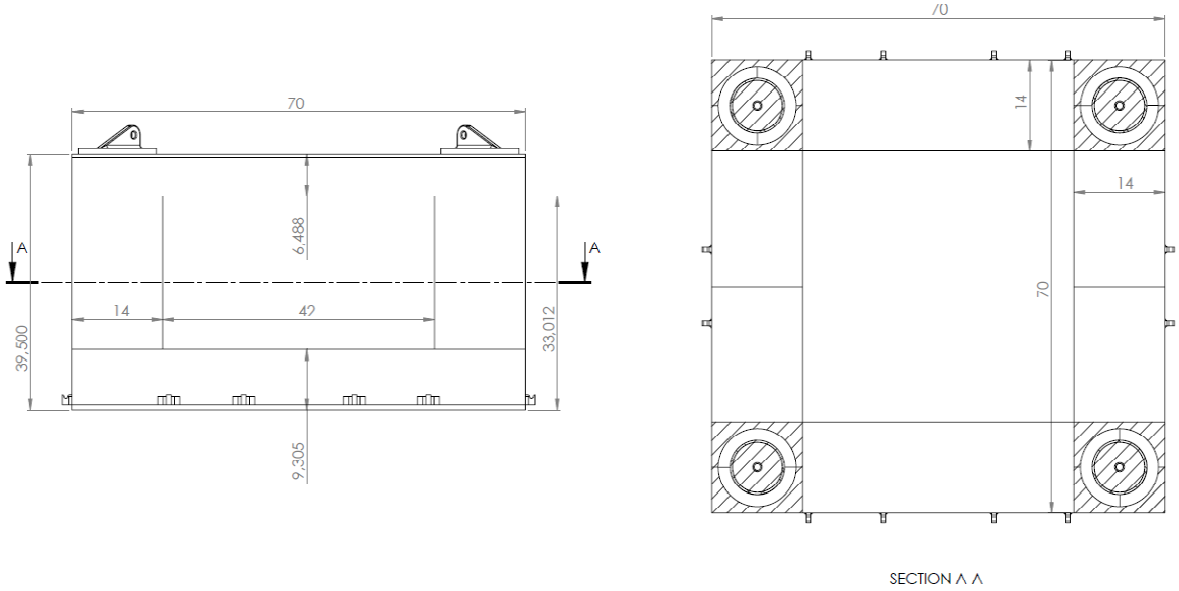

Figure 3-5 - Semi-Submersible Hull Design Dimensions

After construction the dimensional verification provided the actual model dimensions that were input on the numerical hydrostatic model in prototype scale.

Table 3-3 - Model As-built Dimensions

Item	units	Design	As-Built
Column height	m	33.01	33.02
Column depth	m	14	14.1
Column width	m	14	14.1
Column center to center spacing	m	56	56
Pontoon length	m	42	41.86
Pontoon height	m	8.5	9.4
Pontoon width	m	14	14.1
Deck length	m	70	70.05
Deck width	m	70	70.05
Upper deck elevation	m	39.5	39.49
Lower deck elevation	m	33.01	33.02
Installed draft	m	20	-

This model is composed of an aluminum core structure and PVC foam filling with a thin layer of fiberglass mat laminated with epoxy resin. The PVC foam was submitted to a water absorption test with results indicating a 1% loss of displaced volume as indicated on annex K 'Water Absorption Report 2013-06-05'.

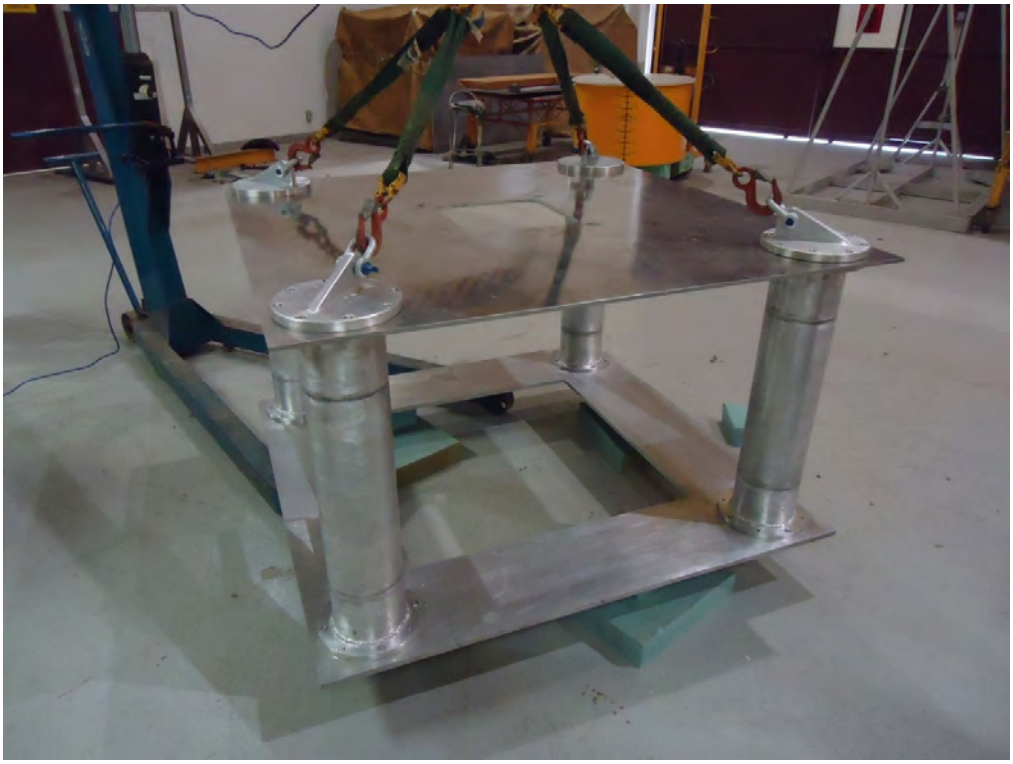

Figure 3-6 - Semi-Submersible Aluminum Structure

Figure 3-7 - Semi-Submersible PVC Foam Filling

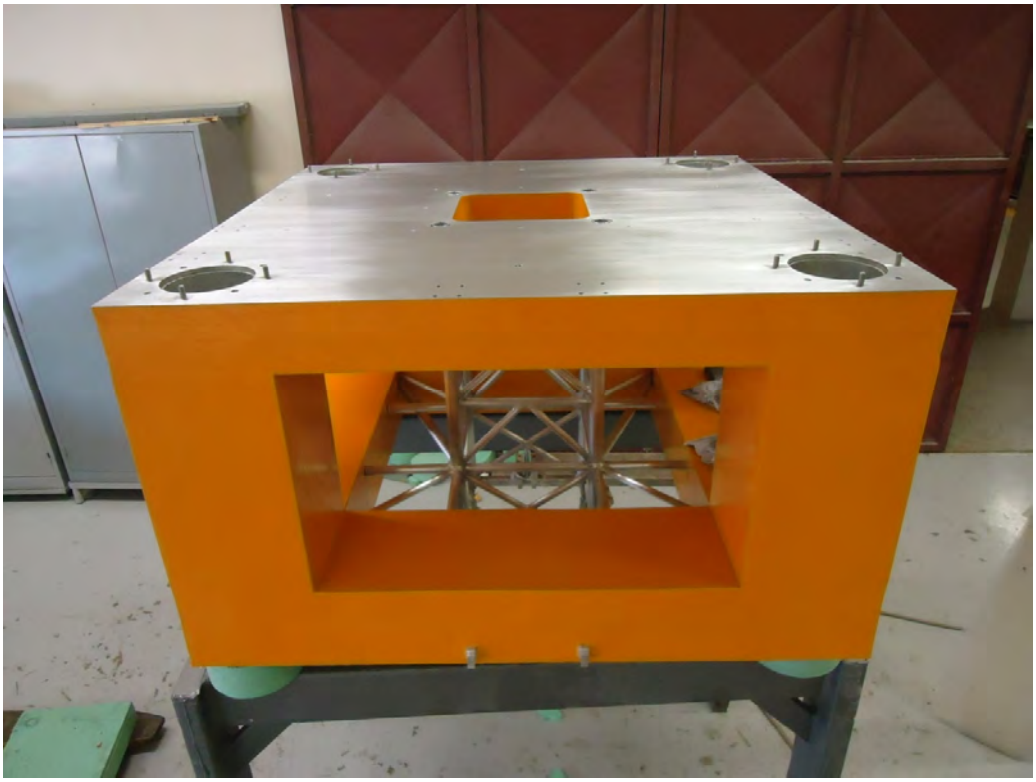

Figure 3-8 - Semi-Submersible Finishing

The CWP Hang-Off Frame was manufactured with commercial diameter aluminum tubes.

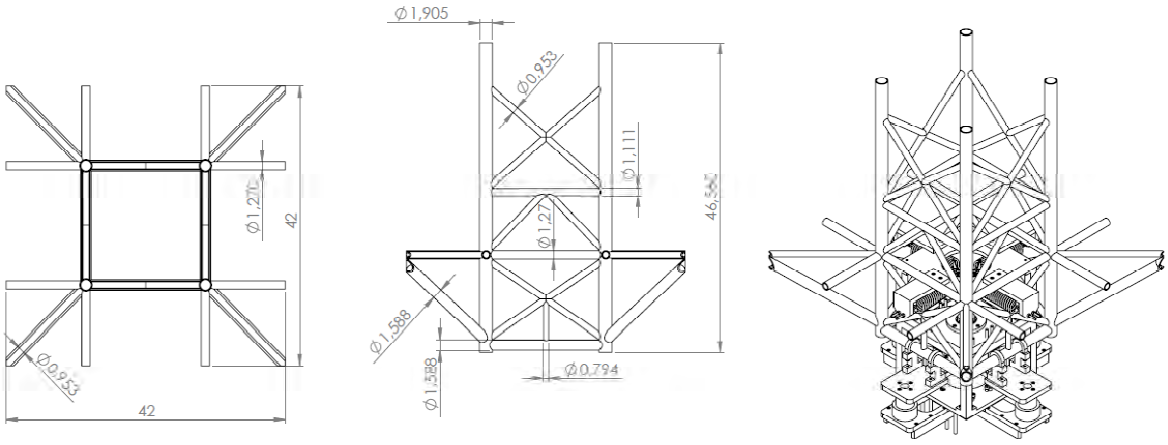

Figure 3-9 - CWP Hang-Off Frame Dimensions - Model Scale

The Hang-off frame was welded to the Semi-Submersible deck and the horizontal bracing laminated to the pontoon.

Figure 3-10 - CWP Hang-Off Frame Manufactured

Figure 3-11 - CWP Hang-Off Frame Installed

The Semi-Submersible was ballasted with two (2) sets of fixed AISI 1020 steel ballasts on the deck and keel aluminum plates and 4 sets of AISI 1020 ballasts inside the columns.

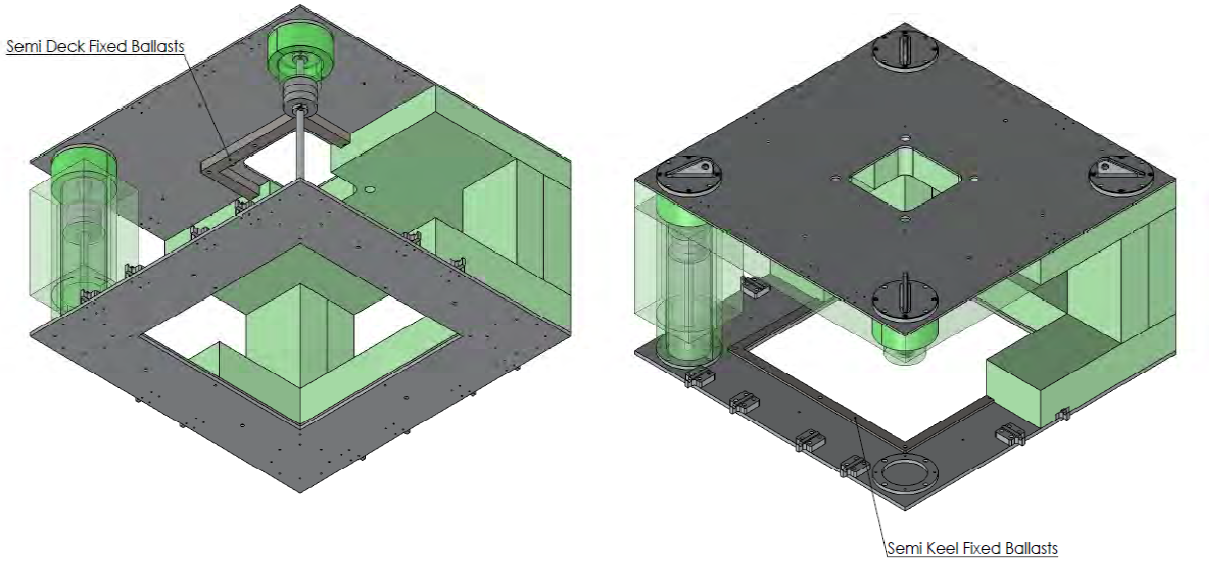

Figure 3-12 - Semi-Submersible Fixed Ballasts

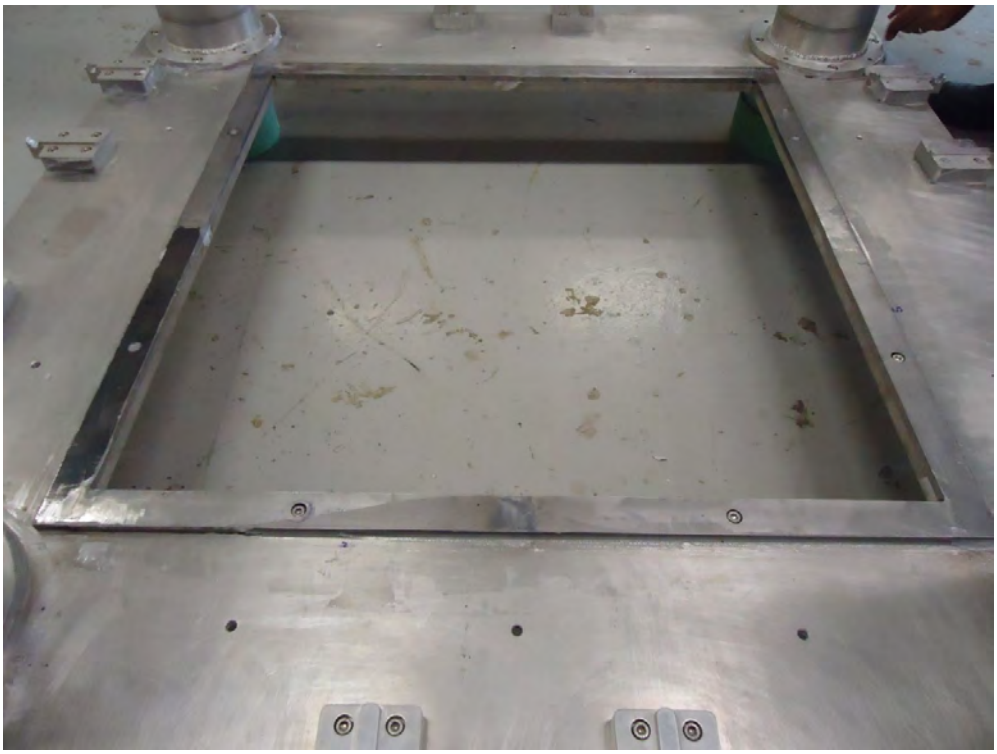

Figure 3-13 - Semi Pontoon Fixed Ballast

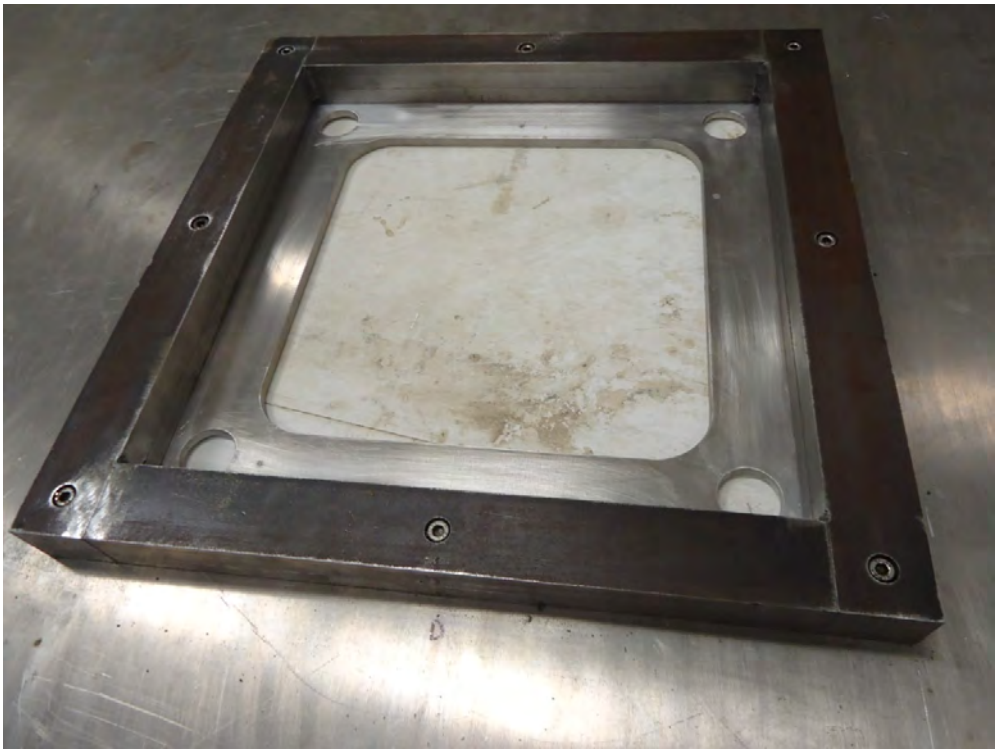

Figure 3-14 - Semi Deck Fixed Ballast

Figure 3-15 - Semi Column Removable Ballasts

3.3.1 Semi Configuration for Measurements

The semi model had its mass, center of gravity and radii of gyration measured for an intermediate configuration.

On this intermediate configuration the missing items were:

- LVDTs(4) set;
- Qualisys Tracking Targets(4);
- Instrumentation Cables;
- Column #1 to #4 packs;
- Column #1 to #4 ballasts;
- Draft adjustment ballast;
- Airgap;
- Gimbal parts operation configuration;
- Vectornav sensor;

Raw measurements are presented on annex L 'Semi_MassProperties_Measurements'.

3.3.2 Mass Measurement

The semi mass was measured hanging the model by a load cell (Alfa 100 kgf load cell).

The remaining parts were also measured, their masses are summarized on table 3-4.

Table 3-4. Instrumentation Mass - Model Scale

Item	Measured Mass [g] - Model Scale
LVDTs (4)	1296
Qualisys Tracking Targets (4)	1126
Airgap Probe	500
Column #1 Pack	1938
Column #2 Pack	1933
Column #3 Pack	1936
Column #4 Pack	1931
Column #1 Ballasts	4572
Column #2 Ballasts	4572
Column #3 Ballasts	4574
Column #4 Ballasts	4594
Instrumentation Cabling	Included in sensor
Draft Adjust Ballast	2490
Gimbal parts - operational	3775
VectorNav	242

3.3.3 Center of Gravity Measurement

The semi center of gravity was measured by placing the model on top of 4 load cells (Alfa 100 kgf load cell) on known positions. The center of gravity was calculated using the rate between the measured moment and force.

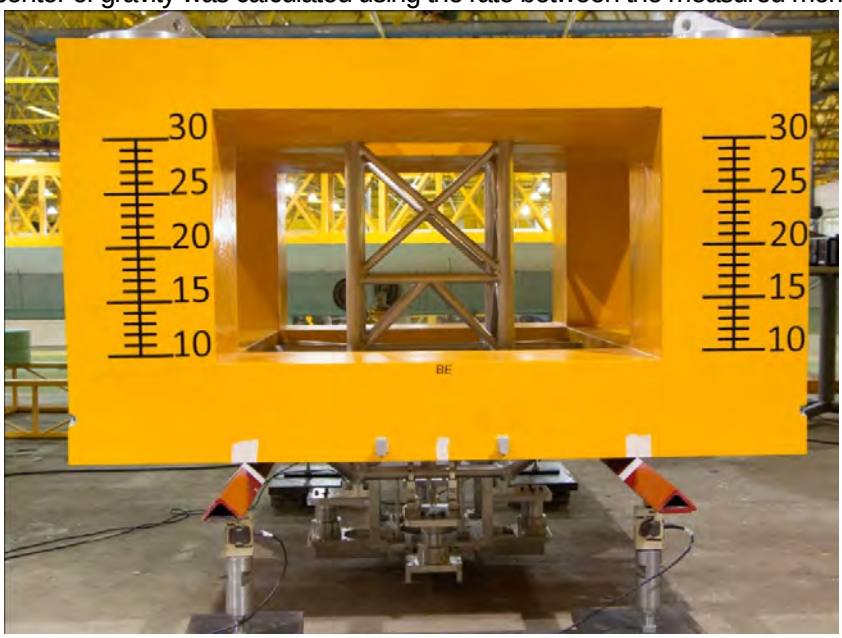

Figure 3-16. Semi Cog Measurement

3.3.4 Moment of Inertia Measurement

The semi moment of inertia was measured by the bifilar torsional pendulum method, analogue to the remora moment of inertia in the Z axis process.

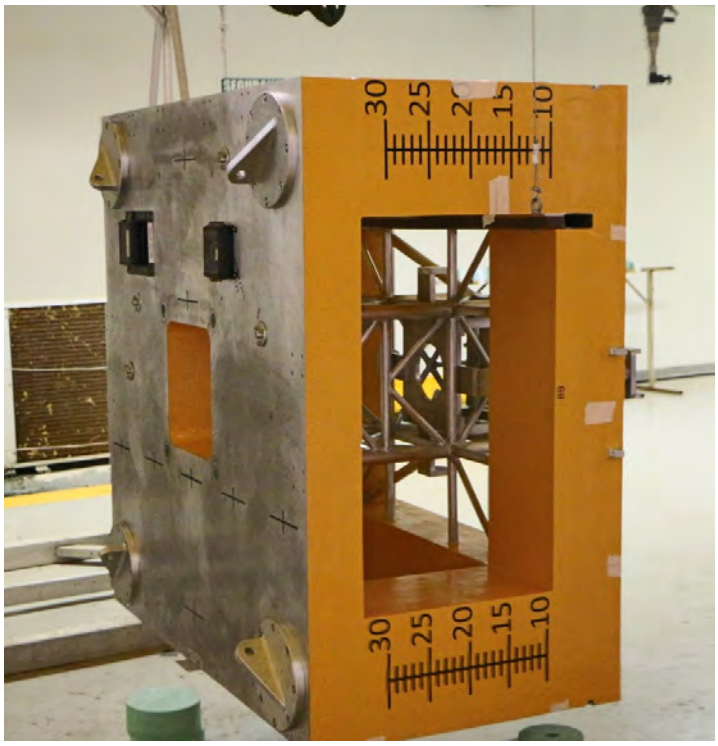

Figure 3-17. Semi Moment of Inertia - Bifilar Method

3.3.5 Additional Items Center of Gravity and Moment of Inertia Estimate

The instrumentation and its cabling and their mass distribution were modeled as solids on Solidworks. The center of gravity and moment of inertia of each component were obtained from this model.

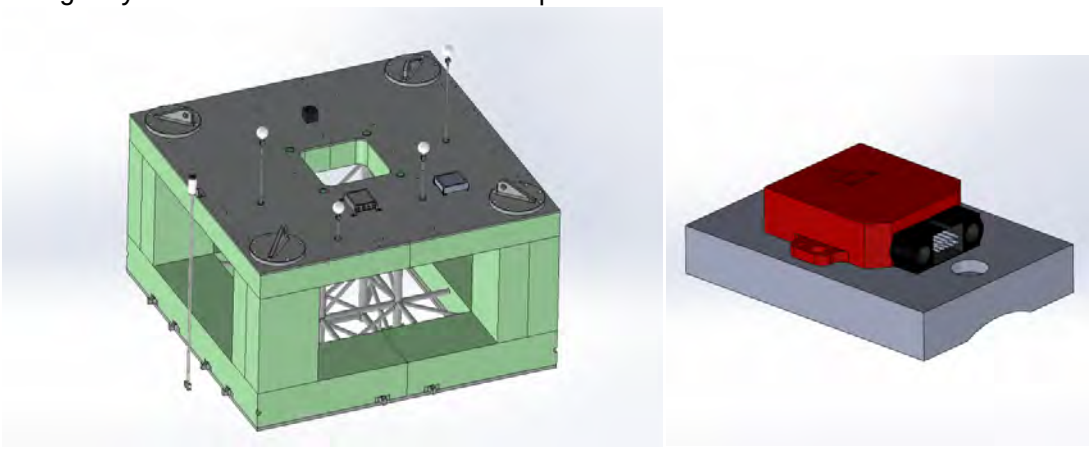

Figure 3-18. Instrumentation Solid Models

The estimates of the instrumentation cables mass properties will be reviewed after they are installed on its final arrangement.

3.3.6 Hydrostatic Model

The required value of mass was updated according to the as-built hydrostatic properties. The required CG and radii of gyration remained the same.

Table 3-5. Semi As-built Dimensions Hydrostatics Model Properties

Semi Hydrostatics	units	Specified	As-Built
Draft	m	20	20
KB	m	6.81	6.47
KMt	m	23.88	22.08
BMt	m	17.07	15.61
KMl	m	23.88	22.08
BMl	m	17.07	15.61
LCB	m	0	0.00
TCB	m	0	0.00
TPC	t/cm	-	8.36
Displacement	t	37672.64	41769.06

3.3.7 Semi-Only (T100) Equilibrium Verification

The fully ballasted semi for the T100 test group was placed on the static tank for draft verification. The Semi draft was uniform at the required value, 20m.

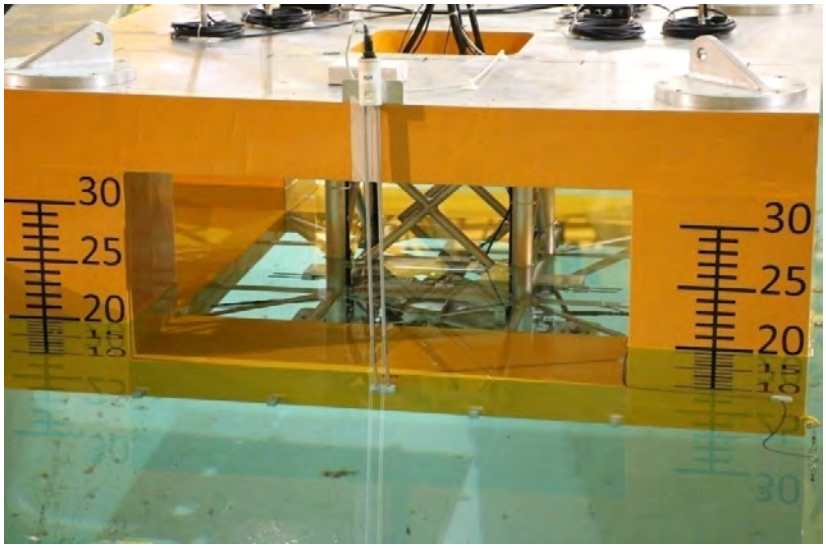

Figure 3-19. Semi Equilibrium and Draft Verification

3.4 REMORAS

The Remora model geometry was modeled according to the reference drawings supplied by the client on a 1:50 scale.

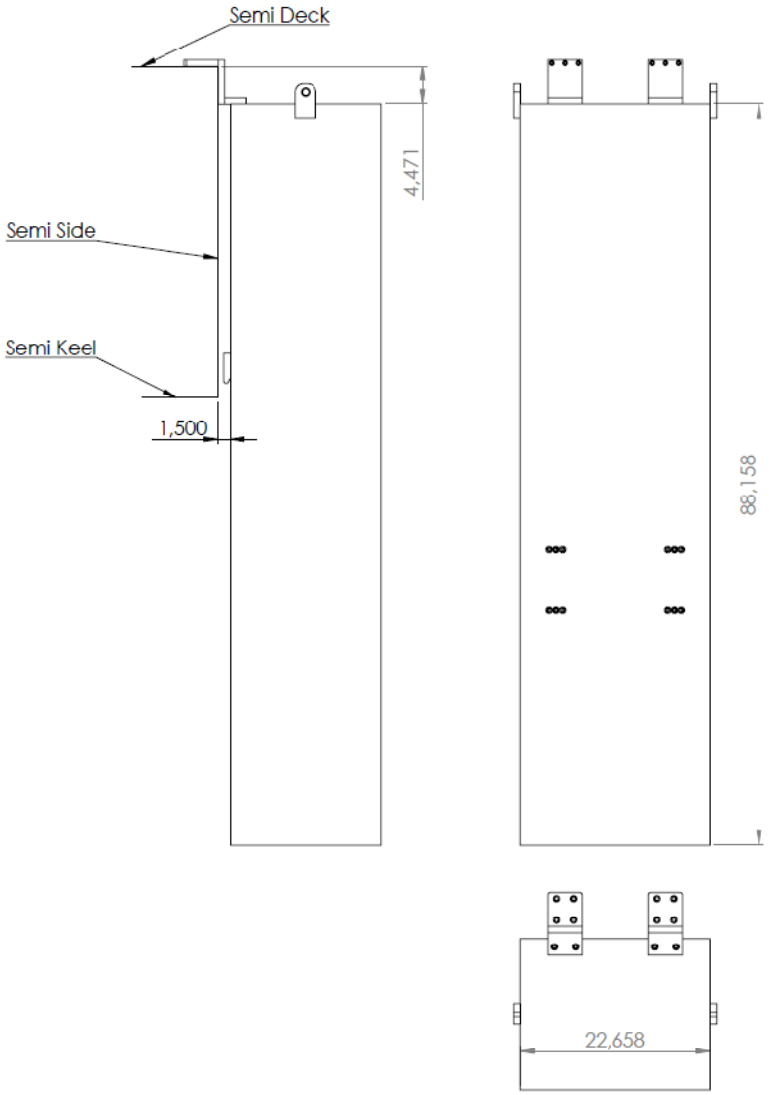

Figure 3-20 - Remora Dimensions

The 6 units are composed of aluminum tubes welded and PVC foam filling and a thin layer of fiberglass mat laminated with epoxy resin and polyester paint finishing.

Figure 3-21 - Remora Aluminum Structure

Figure 3-22 - Remora PVC Foam Filling

Figure 3-23 - Remora Finishing

The connection to the Semi is provided by two aluminum brackets on the deck and two supports on the Semi pontoon.

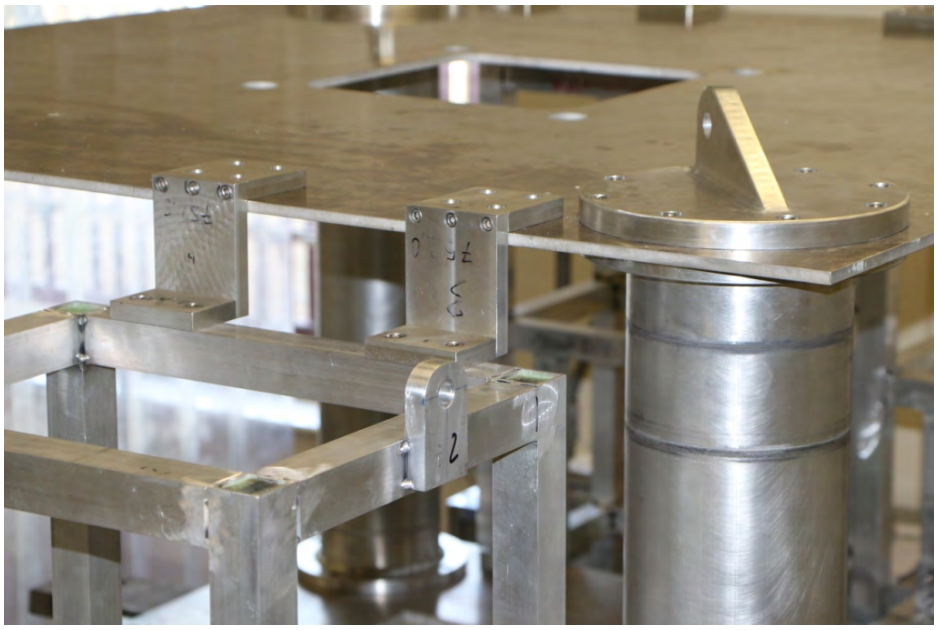

Figure 3-24 - Remora and Semi Deck Fixture

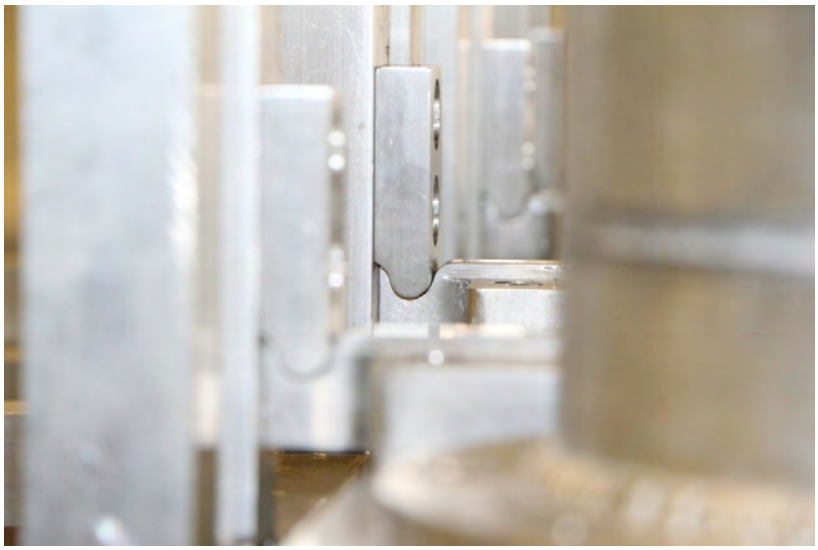

Figure 3-25 - Remora and Semi Pontoon Fixture

The Remora was ballasted by two sets of AISI 1020 steel ballasts fixed on the aluminum structure.

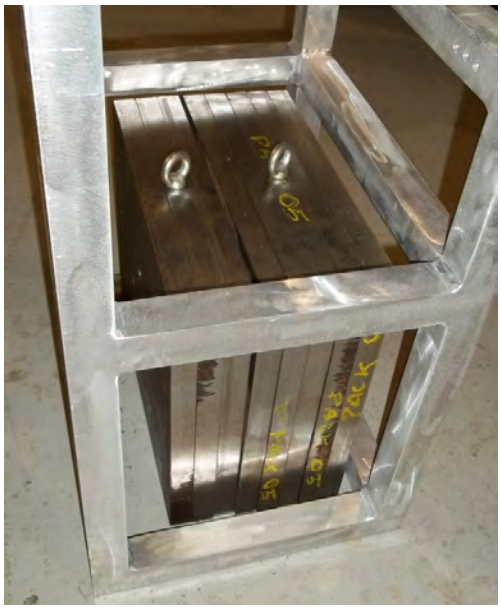

Figure 3-26 - Remora Ballast Packs

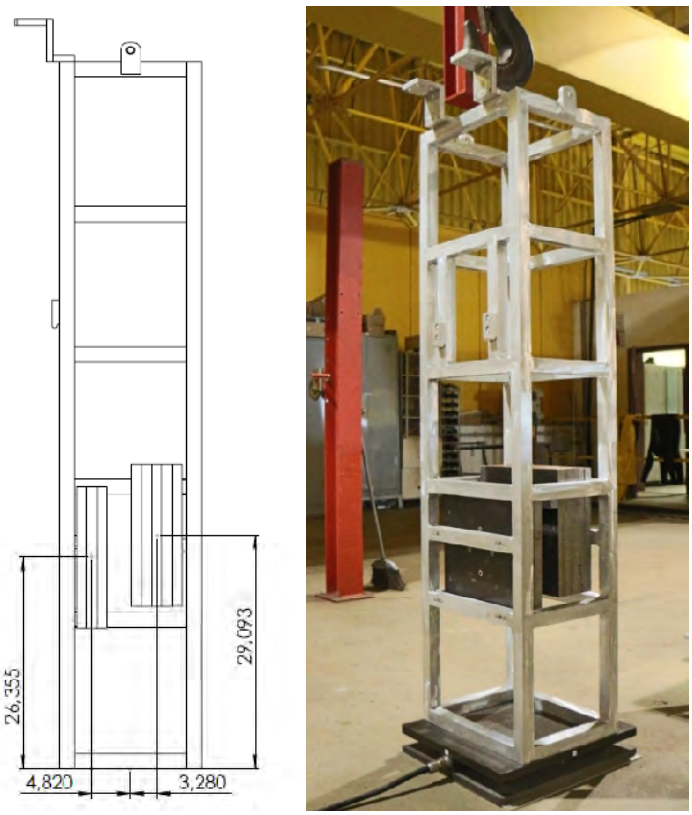

Figure 3-27 - Remora Ballast Packs Position

3.4.1 Mass Measurement

The model mass was measured zeroing the load cell with accessories and subsequently lifting the model as shown on figure 3-28.

Figure 3-28. Remora Mass Measurement

3.4.2 Center of Gravity Measurement

The model center of gravity position (Xg, Yg and Zg) was measured placing it on top of a 6 degree of freedom force plate (AMTI-OR6_WP_1000)

Figure 3-29. Remora X and Z CG Measurement

3.4.3 Radii of Gyration Rxx and Ryy

The model radius of gyration in X and Y direction (Rxx and Ryy respectively) were calculated by measuring the natural period of a trifilar torsional pendulum.

Figure 3-30. Remora Ixx Moment of Inertia Trifilar Measurement

The mass moment of inertia for a trifilar torsional pendulum is calculated with the equation:

$$I_{zz} = \frac{R^2 m g \tau^2}{4\pi^2 L}$$

$Where,$
$Izz = Moment\ of\ Inertia\ about\ rotation\ axis\ (z);$
$R = Radius\ of\ the\ trifilar\ cables;$
$\tau = Natural\ period\ and$
$L = Average\ cable\ length.$

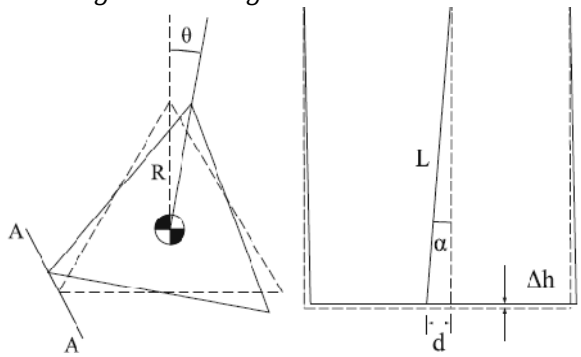

Figure 3-31. Trifilar Method Formulation

The moment of inertia for the support table alone was also measured so it could be the deducted from the compound system inertia.

3.4.4 Radius of Gyration Rzz

The model radius of gyration in Z direction (Rzz) was calculated by measuring the natural period of a bifilar torsional pendulum.

Figure 3-32. Remora Izz Moment of Inertia Bifilar Measurement

The mass moment of inertia for a bifilar torsional pendulum is calculated with the equation:

$$Jcg = \left(\frac{T}{2\pi}\right)^2 \times \frac{a^2 Mg(h_1 + h_2)}{2h_1 h_2}$$

$Where$:
$Jcg = Moment\ of\ Inertia\ about\ center\ of\ gravity$;
$T = Natural\ Period$;
$a = Half\ distance\ between\ cables$;
$M = Mass$;
$h1\ and\ h2 = Cable\ lengths\ and$
$rcg = Radius\ of\ Gyration\ about\ CG$

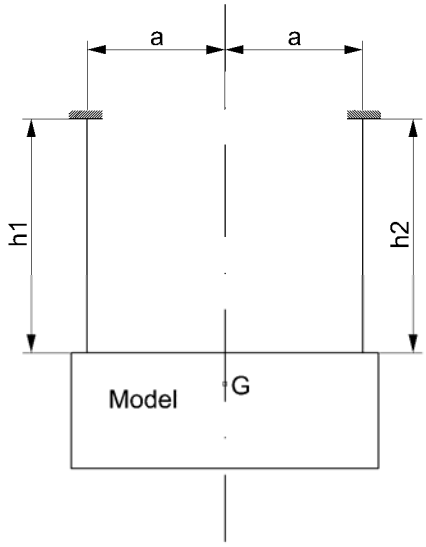

Figure 3-33. Bifilar Method Formulation

3.4.5 Draft and Natural Period Check

The model was deployed on the static tank for a draft and natural period check.

Figure 3-34. Remora Draft and Natural Period Check

The measured draft is 73m. The Remoras natural periods were measure on the static tank and the results on prototype scale are presented on table 3-6.

Table 3-6. Remora Natural Periods - Prototype Scale

Natural Periods	Heave (s)	Pitch (s)	Roll (s)
Remora 1-1	18.74	23.96	21.98
Remora 1-2	19.07	24.35	21.49
Remora 2-1	18.77	24.20	22.09
Remora 3-1	18.84	24.07	21.33
Remora 3-2	19.16	24.17	20.99
Remora 4-1	18.83	24.33	21.20

3.4.6 Mass Properties Summary

Raw measurements of the Remora models mass properties at their final configuration are presented on annex M 'Remora_MassProperties_Measurements_2013_11_06'.

The summary of the measured mass properties of the Remora models are presented on table 3-7.

Table 3-7. Remora Mass Properties Summary

	Remora 1-1	Remora 1-2	Remora 2-1	Remora 3-1	Remora 3-2	Remora 4-1
Model Scale						
Mass [kg]	233.92	233.83	233.10	234.35	234.34	233.29
XG [mm]	-1.51	-0.20	-0.01	-1.55	-0.06	0.26
YG [mm]	1.31	-0.45	0.48	-1.16	-1.17	-0.54
ZG [mm]	635.91	632.57	633.41	634.59	633.93	634.13
Rxx [mm]	314.9	317.3	315.1	316.6	316.6	315.4
Ryy [mm]	318.8	318.5	319.5	320.4	321.0	319.5
Rzz [mm]	150.2	149.1	149.7	149.4	149.0	149.8
Prototype Scale						
Mass [ton]	30151.9	30140.3	30046.2	30207.3	30206.0	30070.7
XG [m]	-0.08	-0.01	0.00	-0.08	0.00	0.01
YG [m]	0.07	-0.02	0.02	-0.06	-0.06	-0.03
ZG [m]	31.80	31.63	31.67	31.73	31.70	31.71
Rxx [m]	15.75	15.87	15.76	15.83	15.83	15.77
Ryy [m]	15.94	15.93	15.98	16.02	16.05	15.98
Rzz [m]	7.51	7.46	7.49	7.47	7.45	7.49
Reference Document	Annex M: Remora_MassProperties_Measurements_2013_11_06.pdf					

3.5 GIMBAL

The Gimbal model was manufactured for three (3) different configurations. The design was made in a way that the change of configuration would imply on the exchange of few parts.

The gimbal is connected to the hang-off frame through four (4) 6DOF load cells.

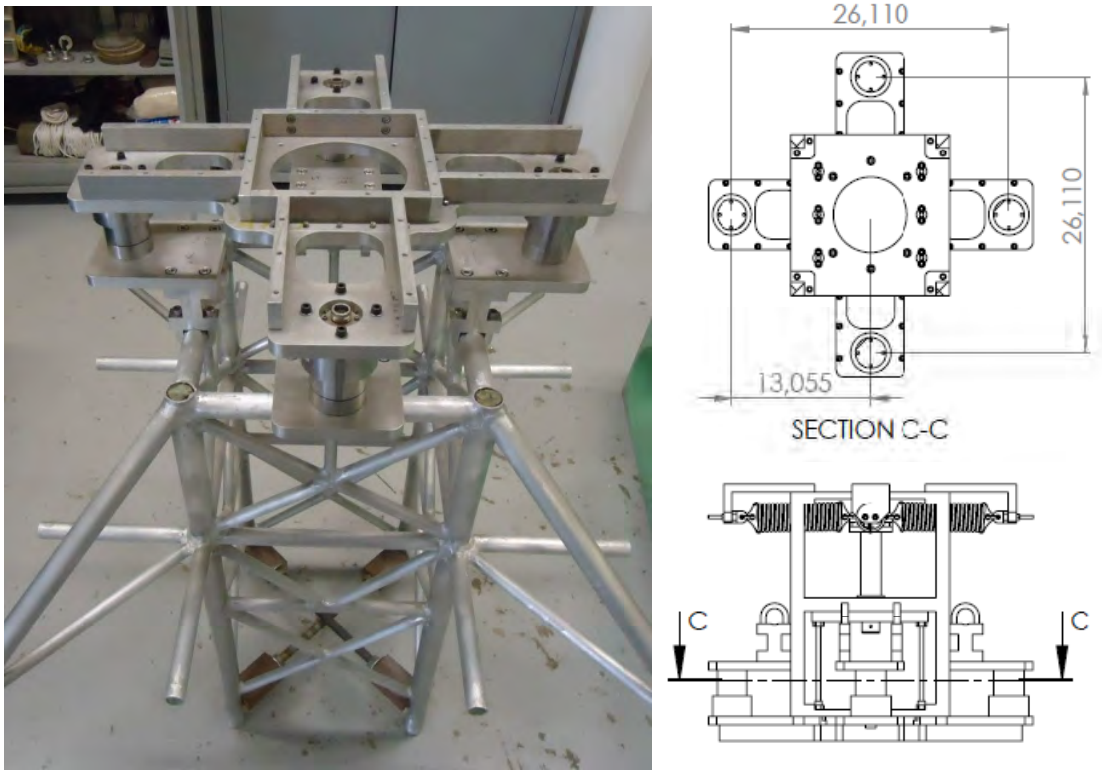

Figure 3-35 - Gimbal and Hang-Off Frame Interface

The CWP model is supported by a Teflon semi sphere ball on a aluminum cup with its pivot point located 5m below the keel. It is connected to the gimbal by a solid aluminum circular rod that extend 6.95m above the support pivot point.

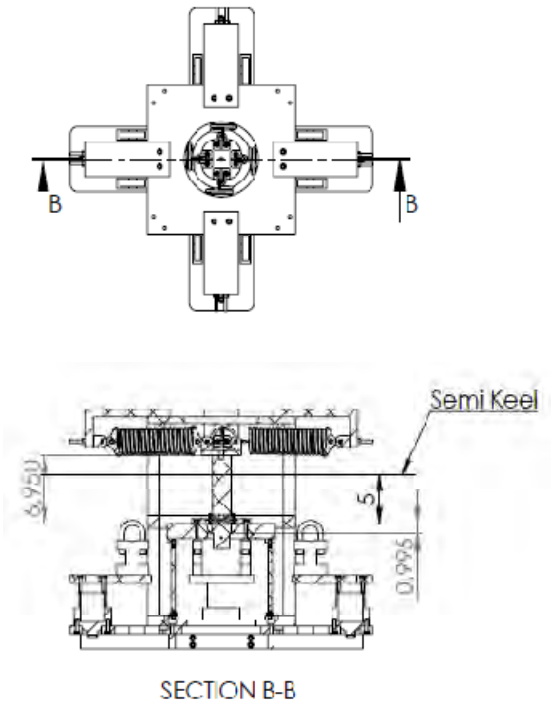

Figure 3-36 - Gimbal General Configuration

The CWP support is connected to the outer structure by a set of six (6) thin circular aluminum rods dimensioned to produce the required lateral stiffness.

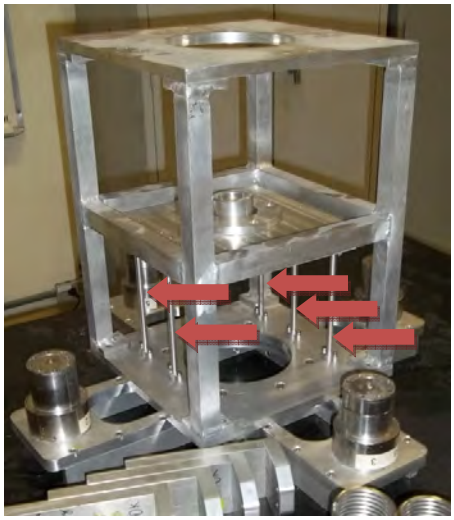

Figure 3-37 - CWP Support Table Fixture

3.5.1 Gimbal Angle Measurement

The angle of the CWP connection to the gimbal is derived from the measured distances by a set of four (4) LVDT sensors manufactured by Macro sensors, model GHSE- 750-2000. The algorithm used to derive the gimbal angles from the sensors measurements is presented and validated on 'Annex H: Gimbal Angle Measurement Algorithm'.

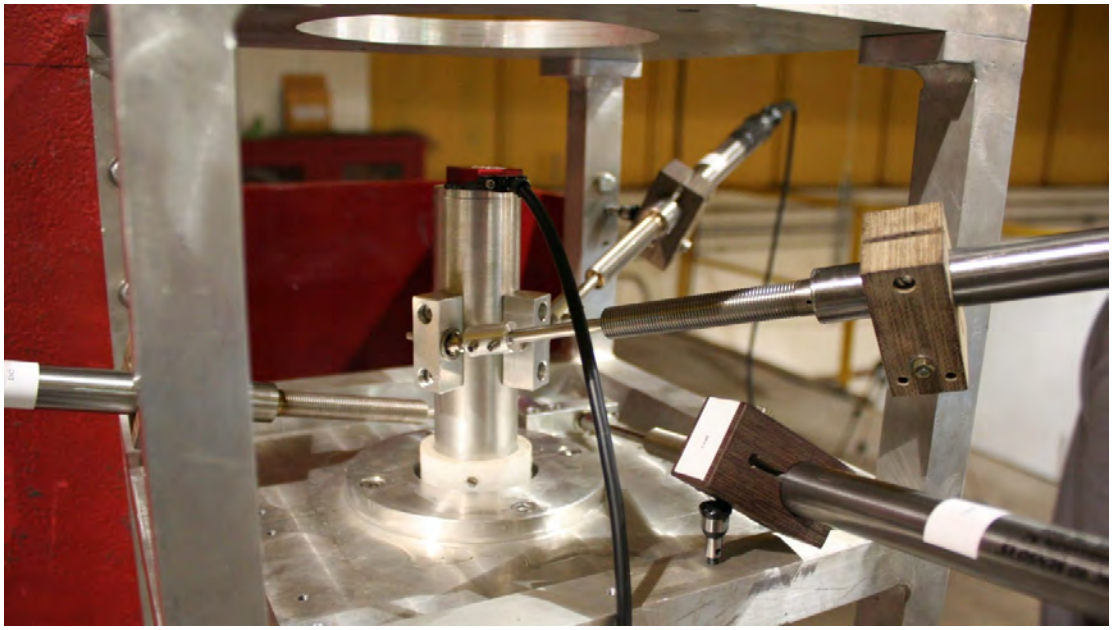

Figure 3-38. Instrumentation Setup

The arrangement of the LVDT sensors are illustrated on figure 3-39.

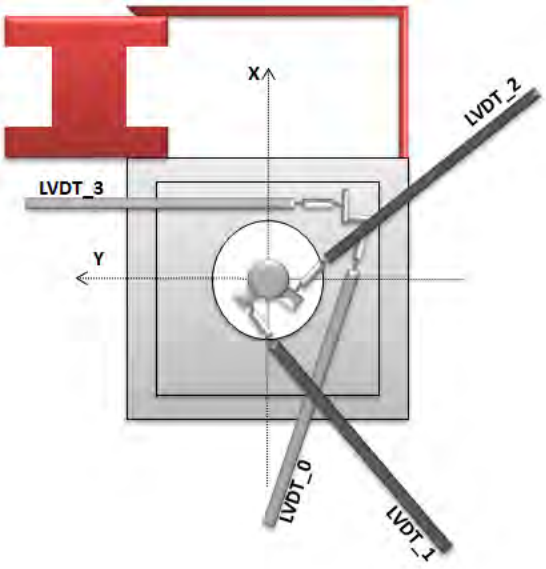

Figure 3-39. LVDT Arrangement

Two tests were done to compare the LVDT derived results to a precision attitude angle measurement instrument, VectorNav VN-100 Rugged. More information on the sensor over:

http://www.vectornav.com/products/vn100-rug

On the first test the CWP dummy was moved predominantly on a pitch direction, the comparison between the VectorNav measurements and the LVDT derived channels are plotted on figure 3-40.

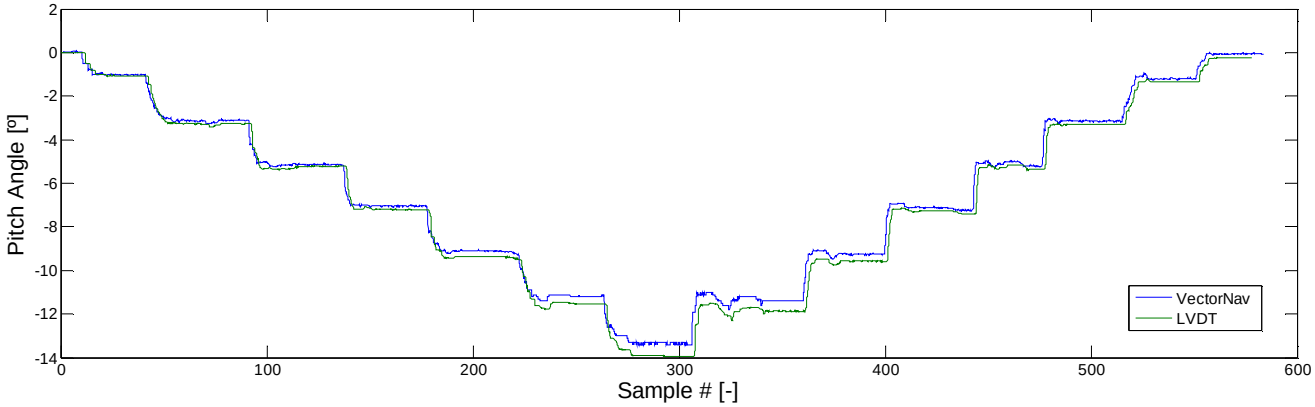

Figure 3-40. Pitch Angle Measurement Script Verification (X dir.)

On the second test the CWP dummy was moved on a combined pitch and roll direction, the comparison between the VectorNav measurements and the LVDT derived channels are plotted on figure 3-41 and 3-42.

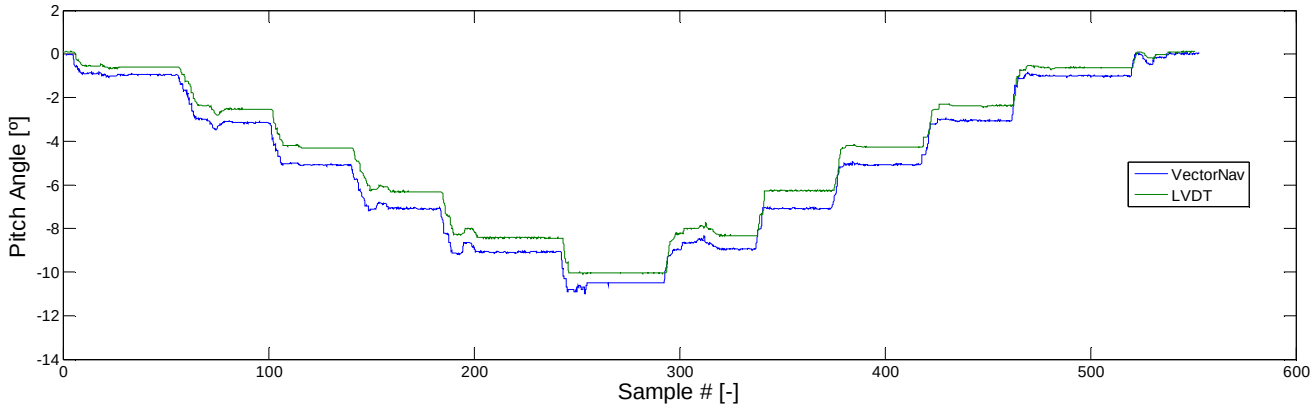

Figure 3-41. Pitch Angle Measurement Script Verification (XY dir.)

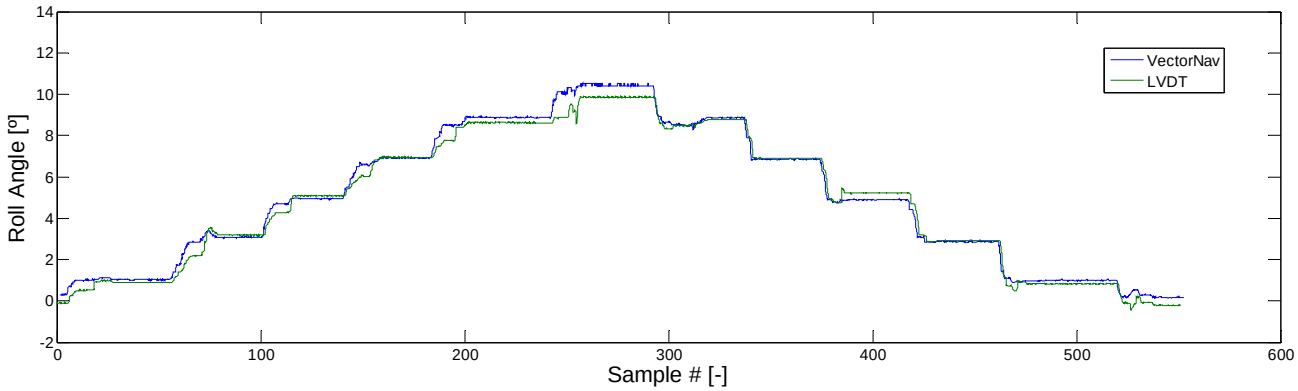

Figure 3-42. Roll Angle Measurement Script Verification (XY dir.)

Those tests results indicate a maximum deviation of 0.6º and a mean ratio of 96.5% between measured and reference gimbal angle.

3.5.2 Gimbal - Pinned Configuration Setup

For the pinned configuration the Gimbal model remains exactly as described in section 3.5.

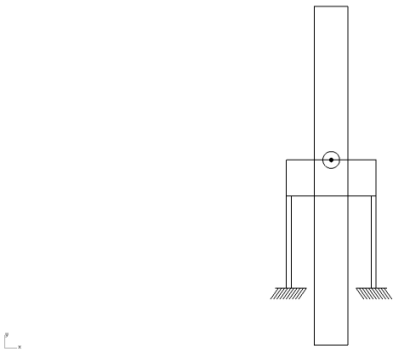

Figure 3-43 - Gimbal Pinned Configuration Setup

3.5.3 Gimbal - Installation Configuration Setup

For the installation configuration the top of the CWP connector was fixed to a top plate that was in turn connected to the CWP support plate by a set of six (6) aluminum rods dimensioned to produce the required angular stiffness.

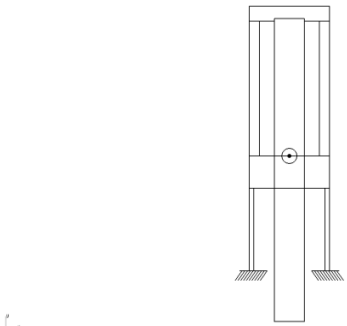

Figure 3-44 - Gimbal Installation Configuration Setup

3.5.4 Gimbal - Operational Configuration Setup

For the operational configuration the top of the CWP connector was fixed to a top plate that was in turn connected to the gimbal outer structure by a set of four (4) springs.

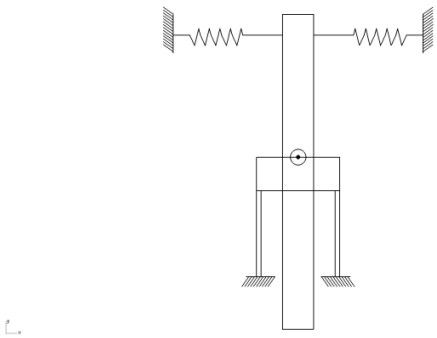

Figure 3-45 - Gimbal Operation Configuration Setup

3.5.5 Gimbal Stiffness Tests

Several tests were performed to estimate the gimbal lateral and angular stiffness for each configuration. Gimbal design parameters and procedures are detailed on 'Annex G: Gimbal Stiffness Design'.

3.5.5.1 Gimbal Horizontal Stiffness - Installation Configuration

The gimbal was assembled with both its bottom and top set of rods. With the bottom set of rods the sole responsible for the horizontal stiffness. A load was applied in the X direction and the displacement of the CWP lower support was measured by the LVDT sensors.

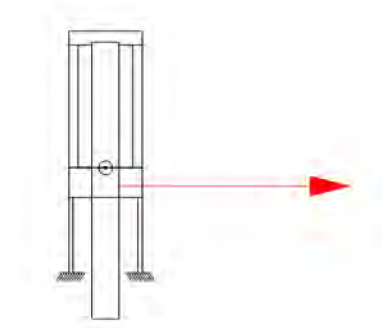

Figure 3-46. Gimbal Horizontal Stiffness - Installation Configuration

A steel cable was attached to the bottom CWP support by an eye bolt, the opposite end connected to a load cell (Alfa 250 kgf load cell) to measure the magnitude of the applied load. The other end of the load cell was connected to a winch with another steel cable.

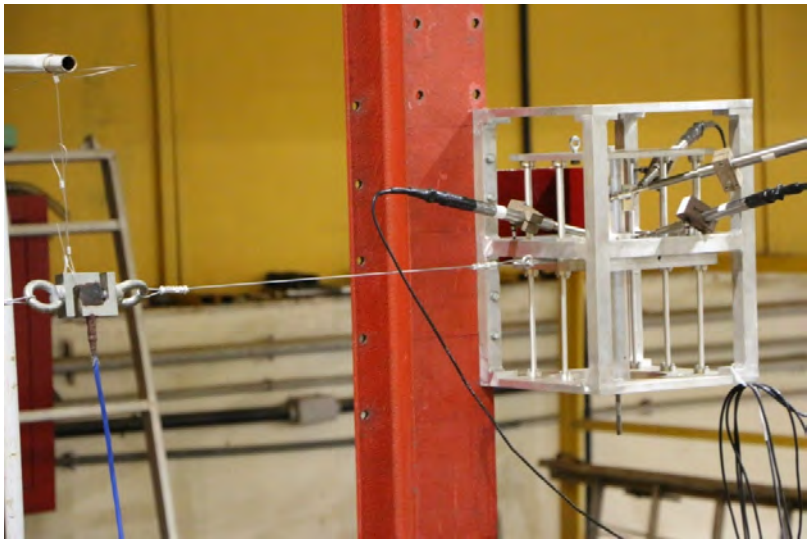

Figure 3-47. Test Setup

The data obtained from this test is plotted on figure 3-48.

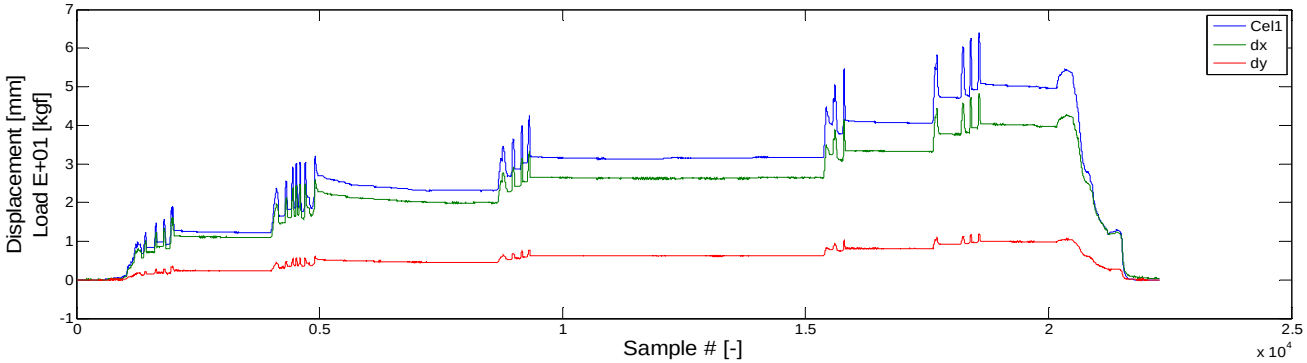

Figure 3-48. Load and Displacements Plot - Model Scale

Six (6) windows were chosen to average the values of the "dx" and "Cel1" variables in order to get a discrete plot of loads versus displacements.

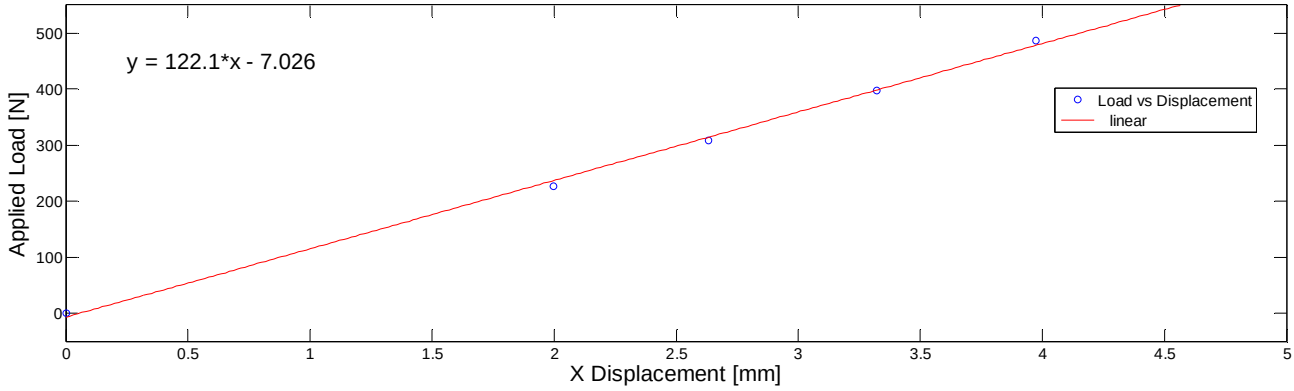

Figure 3-49. Averaged Load vs. X Displacement Plot - Model Scale

A linear equation was fitted to the selected windows averaged values. The angular coefficient of this equation, 122.1 [N/mm] is the gimbal horizontal stiffness for the installation configuration on model scale.

3.5.5.2 *Gimbal Angular Stiffness - Installation Configuration*

The gimbal configuration remained the same from the previous test, except for the lower table, that was locked into position. For this test the load was applied on the top CWP support on the X direction and the gimbal angle measured by the LVDT sensors.

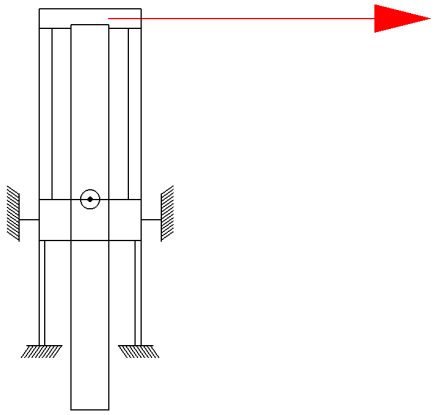

Figure 3-50. Gimbal Angular Stiffness - Installation Configuration

A steel cable was attached to the top CWP support by an eye bolt, the opposite end connected to a load cell to measure the magnitude of the applied load. The other end of the load cell (Alfa 250 kgf load cell) was connected to a winch with another steel cable.

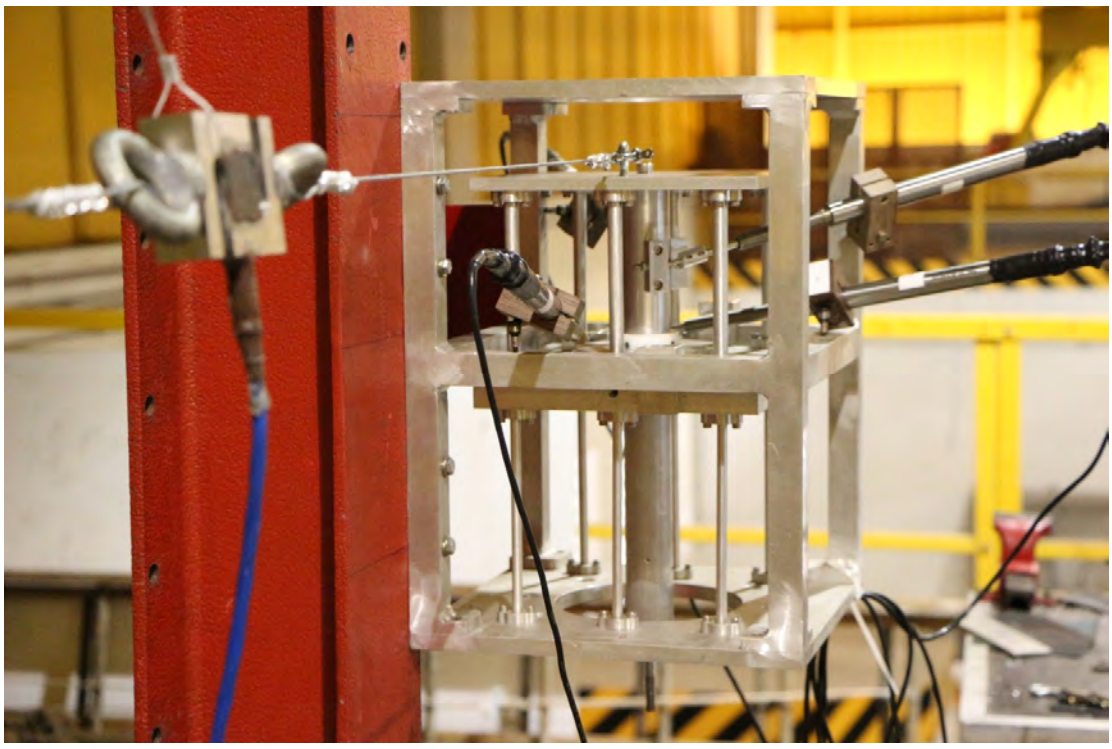

Figure 3-51. Test Setup

The data obtained from this test is plotted on figure 3-52.

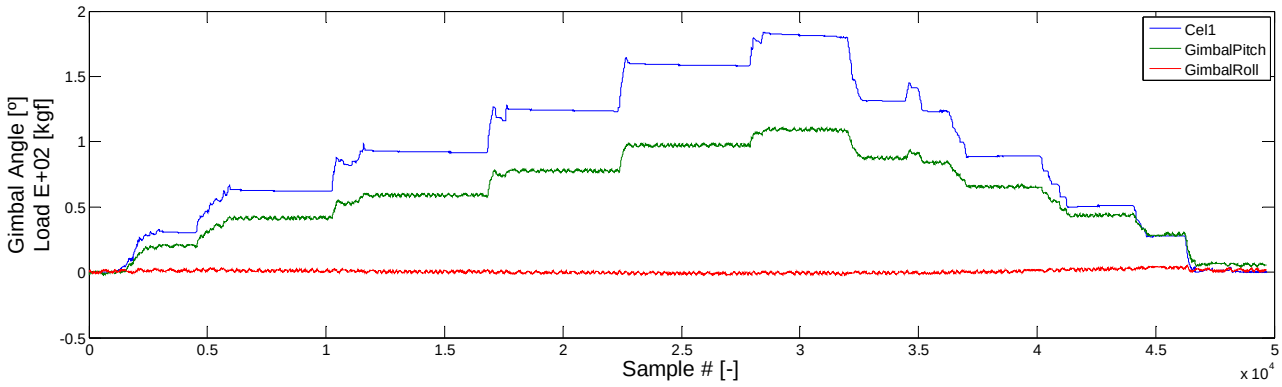

Figure 3-52. Load and Gimbal Angles Plot (model scale)

Thirteen (13) windows were chosen to average the values of the "GimbalPitch" and "Cel1" variables in order to get a few discrete values of loads and angular displacements. The applied moment was calculated assuming that the load was completely aligned in the x direction and a constant lever since the angles were quite small (0.01% difference for 1º). The lever used to calculate this moment is 163.4mm in model scale.

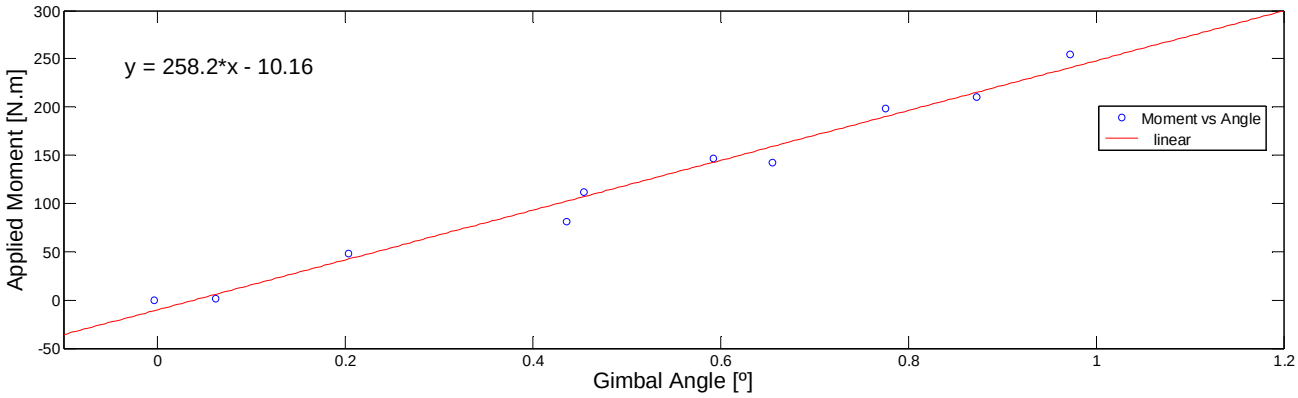

Figure 3-53. Moment versus Gimbal Angle Plot - Model Scale

A linear equation was fitted to the selected windows averaged values, the angular coefficient of this equation, 258.2 [N.m/degree] is the gimbal angular stiffness for the installation configuration on model scale.

3.5.5.3 Gimbal Angular and Horizontal Stiffness - Operation Configuration

On this configuration the top set of rods was replaced by a set of four (4) springs and the horizontal and angular stiffness are provided by a combination of the stiffness for the top springs and the bottom set of rods.

In order to evaluate the angular and horizontal stiffness it is first necessary to identify the stiffness of the individual components. Since the bottom set of rods had not changed from the installation configuration, only the top set of springs stiffness remain to be measured.

3.5.5.3.1 Spring Set Stiffness

For this test the bottom CWP support was locked in position and an aluminum part, designed to pull the CWP dummy, was attached to the spring set fixture at the same level as the springs.

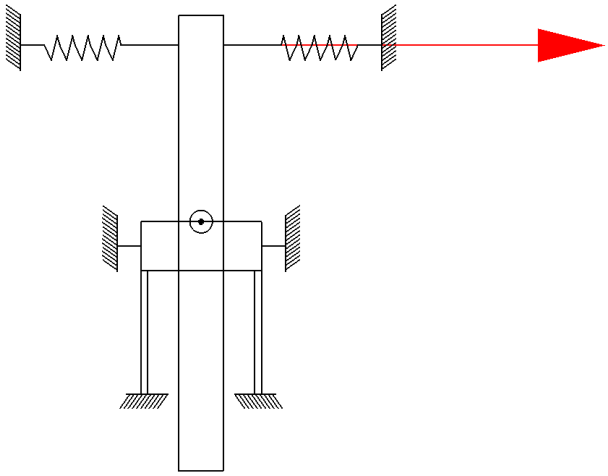

Figure 3-54. Spring Set Stiffness - Operation Configuration

A steel cable was attached to the top springs fixture, the opposite end connected to a load cell (Futek 22.5 kgf load cell) to measure the magnitude of the applied load. The other end of the load cell was connected to a winch with another steel cable.

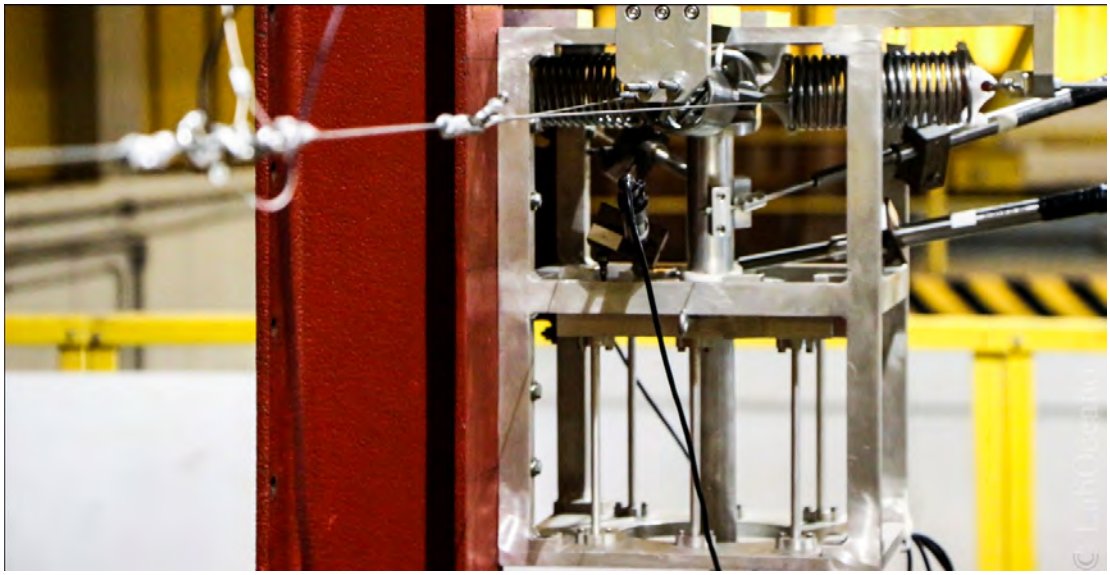

Figure 3-55. Spring set Stiffness Test Setup

The data obtained from this test in the Y direction is plotted on figure 3-56.

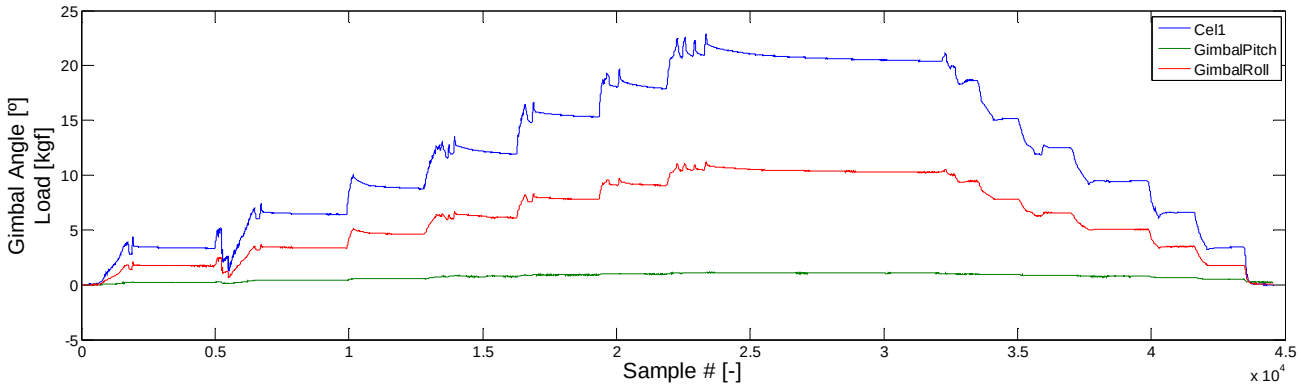

Figure 3-56. Load and Gimbal Angles Plot - dir. Y (model scale)

The data obtained from this test in the X direction is plotted on figure 3-57.

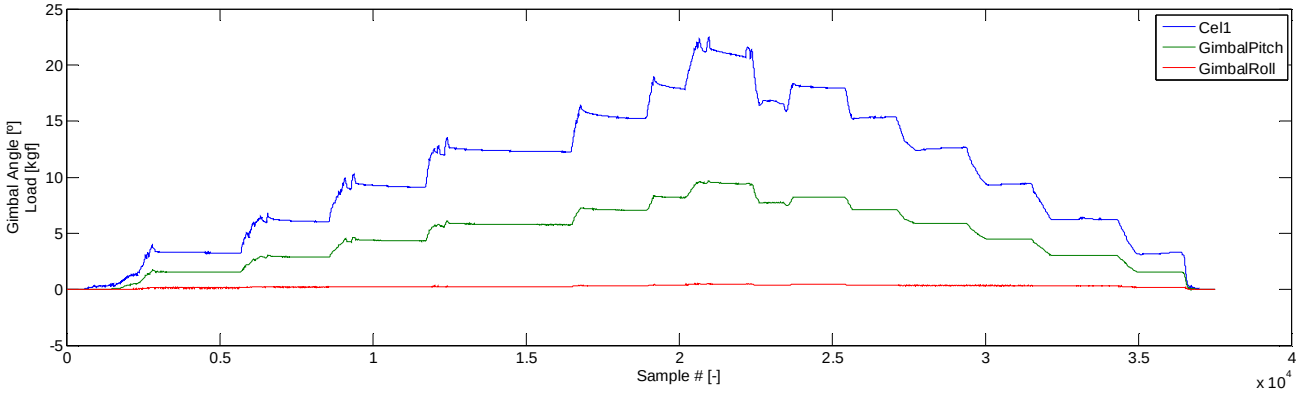

Figure 3-57. Load and Gimbal Angles Plot - dir. X (model scale)

In order to proceed with this analysis it was chosen to transform the CWP dummy angle into displacements at the springs level.

The average values of several data windows were analyzed. The applied load is obtained directly from the variable 'Cel1'. The horizontal displacement is obtained by the following equation:

$$Displacement = Sin('Gimbal\ Angle').h$$

The value of 'h' is equal to the distance from the springs to the CWP dummy center of rotation for a fixed bottom set of rods setup, 167mm.

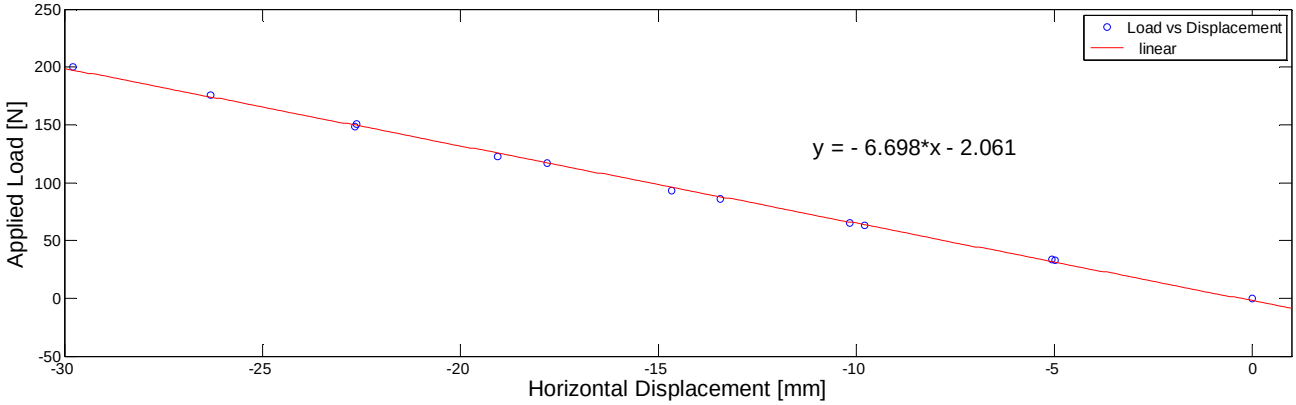

Figure 3-58. Averaged Load versus Displacement dir. Y - Model Scale

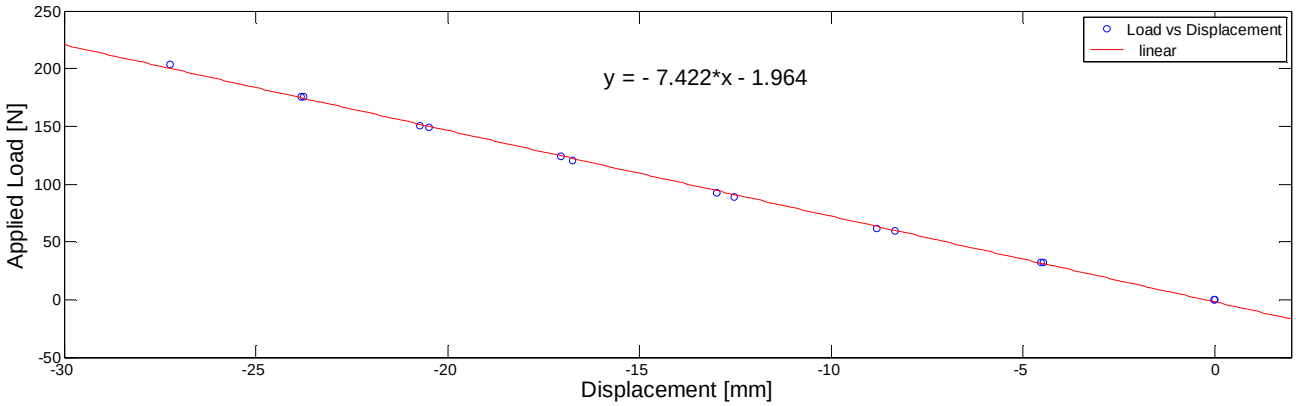

Figure 3-59. Averaged Load versus Displacement dir. X - Model Scale

A linear equation was fitted to the selected windows averaged values, the angular coefficient, 6.698 [N/mm] for the Y direction and 7.422 [N/mm] for the X direction, are the springs set stiffness values in model scale.

3.5.5.3.2 Angular Stiffness Analysis

The angular and horizontal stiffness for the operation configuration are dependent on the stiffness of the bottom set of rods, the spring set and the model geometry only. All those have been measured and were input on "Ftool", a 2D beam design software with elastic supports capability.

The gimbal support was modeled as a very stiff beam with elastic supports at the same distance as the top set of springs and the bottom set of rods.

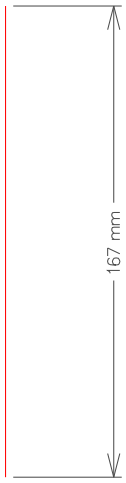

Figure 3-60. Distance between Supports - Model Scale

The beam section was defined as steel with a Young modulus of 205 GPa, and a 50mm circular rod.

The top support was defined as an elastic support, with stiffness in X equal to the top set of spring stiffness for the X direction, free to move in Z direction and free to rotate around Y.

The bottom support was defined as an elastic support, with a stiffness in X equal to the bottom set of rods stiffness, fixed in Z and free to rotate around Y.

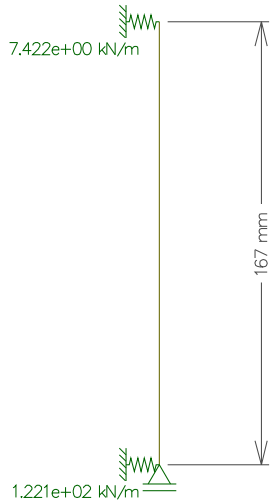

Figure 3-61. Supports Stiffness - Model Scale

To evaluate the angular stiffness a pure moment of 50 Nm was applied to the beam at the bottom support position. The resulting angular displacement was measured to determine the angular stiffness for this configuration. The point of null horizontal displacement was also identified as the pivot axis for the CWP support.

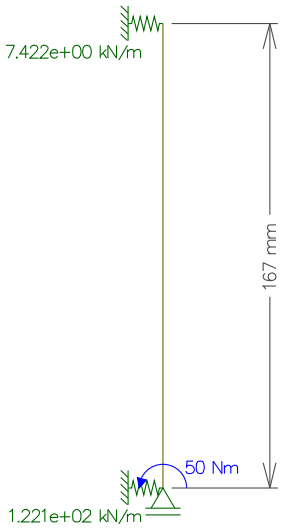

Figure 3-62. Applied Binary - Model Scale

The rotation around Z is 14.7 degrees and the position of the pivot point is 10mm above the bottom support.

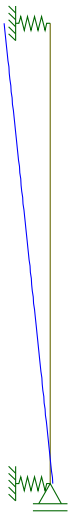

Figure 3-63. Resulting Angular Displacement - Model Scale

The analyzed angular stiffness is 3.402 [N.m/º] or 194.9 [N.m/rad] in model scale.

$$\frac{Moment}{Angular\ Offset} = \frac{50}{14.7} = 3.402\ \left[{}^{N.m}/_{º}\right]$$

3.5.5.3.3 Horizontal Stiffness Analysis

For the horizontal stiffness the same model was used with a different loading condition. A 1000 [N] force was applied at the bottom support location.

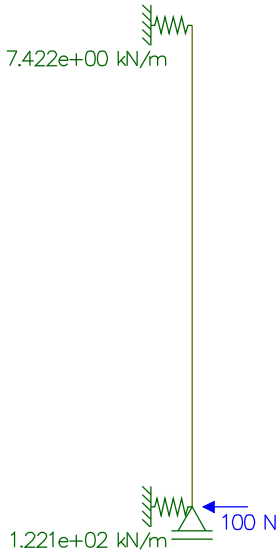

Figure 3-64. Applied Force - Model Scale

The displacement at the pivot point is the horizontal displacement that will be used to analyze the horizontal stiffness.

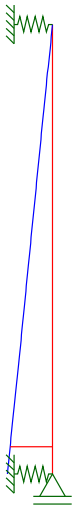

Figure 3-65. Resulting Horizontal Offset - Model Scale

The analyzed horizontal stiffness is 130 [N/mm] in model scale.

$$\frac{Applied\ Load}{Horizontal\ Displacement} = \frac{1000}{7.69} = 130.0\ \left[{}^{N}/_{mm}\right]$$

3.5.6 Gimbal Friction Tests

The static and dynamic friction for the angular movement of the gimbal was measured for the pinned and operation configuration.

3.5.6.1 Static Friction - Pinned Configuration

The gimbal was assembled on the pinned configuration, without springs or rods connected to the top and three different ballasts fixed to the top of the CWP dummy.

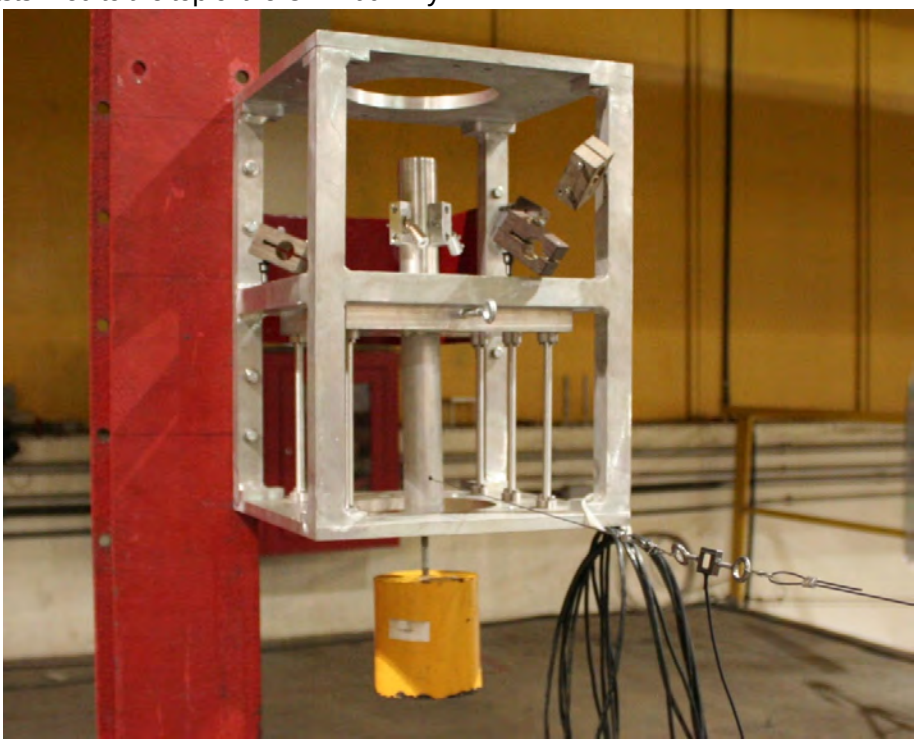

Figure 3-66. Static Friction - Pinned Configuration Setup

The center of gravity and point of rotation are described on the figure 3-67.

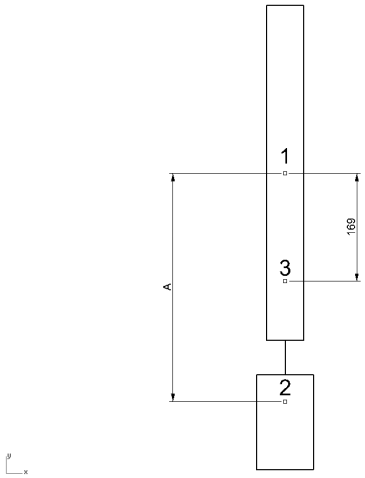

	A
8.263 kg	266.0 mm
12.388 kg	311.4 mm
16.516 kg	303.0 mm

Figure 3-67. Static Friction - Pinned Configuration CG (model scale)

Point 1 - Center of Rotation
Point 2 - Set Center of Gravity (for ballast weight)
Point 3 - Pulling Position

The gimbal support Teflon ball and cup was wet using a bottle of water. The pulling line was slowly tensioned

until the rod began to rotate. When this was observed the line was slacked. The process was repeated several times for each case.

The critical force values were obtained from the Matlab data files for weight 1, 2 and 3. Results are summarized on table 3-8.

Table 3-8. Static Friction - Pinned Configuration Results (model scale)

	Weight 1	Weight 2	Weight 3
Critical Force [gf]	709.3	839.3	1314.5
Lever [mm]	169		
Ballast Mass [kg]	8.236	12.388	16.516
Vertical Cog [mm]	266.0	311.4	303.0

The average critical moment versus the weight in model scale is plotted on figure 3-68.

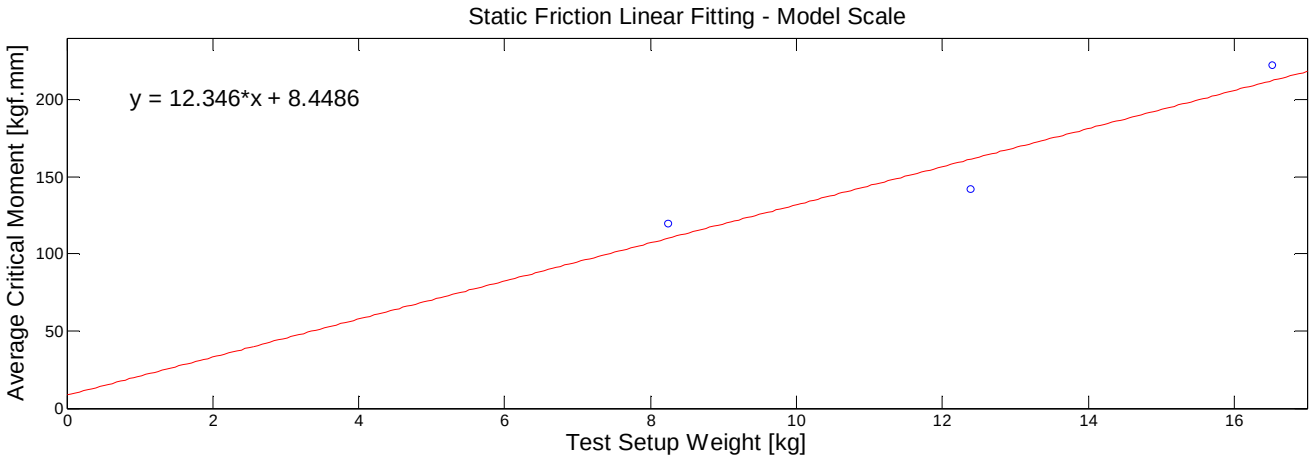

Figure 3-68. Static Friction Test Critical Force Linear Fit (Model Scale) - Pinned Configuration

3.5.6.2 Static Friction - Operation Configuration

The test setup and procedure was exactly the same except for the gimbal assembly that had its set of springs fixed to the top of the CWP dummy.

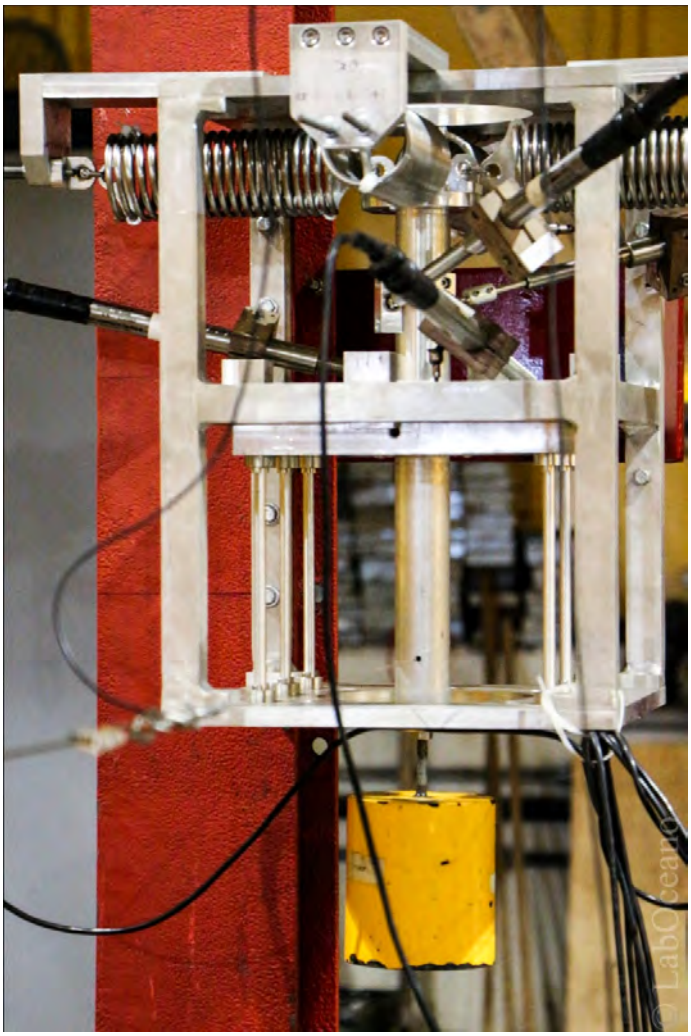

Figure 3-69. Static Friction - Operation Configuration Setup

The center of gravity and point of rotation are described on figure 3-70.

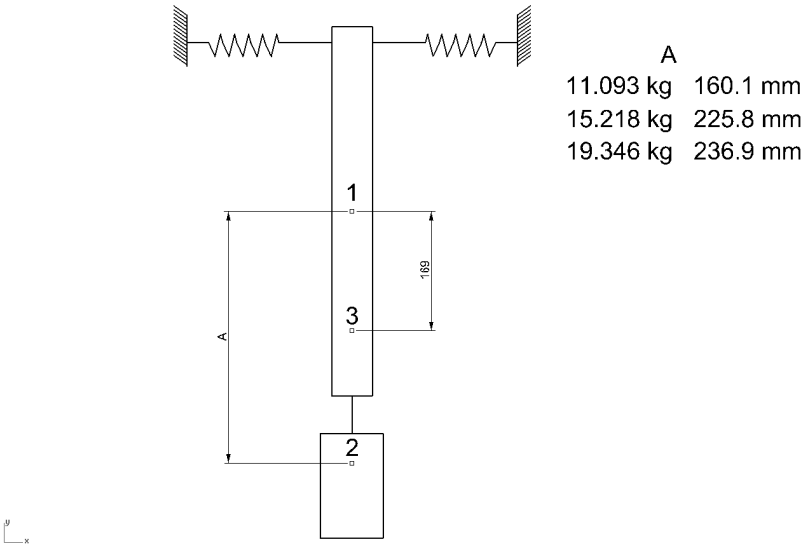

Figure 3-70. Static Friction - Operation Configuration CG (model scale)

The critical force values were obtained from the Matlab data files for weight 1, 2 and 3. Results are summarized on table 3-9.

Table 3-9. Static Friction - Operation Configuration Results (Model Scale)

	Weight 1	Weight 2	Weight 3
Critical Force [gf]	2469.9	2197.1	2887.3
Lever [mm]	169		
Weight [kg]	11.093	15.218	19.346
Vertical Cog [mm]	160.1	255.8	236.9

The average critical moment versus the weight in model scale is plotted on figure 3-71.

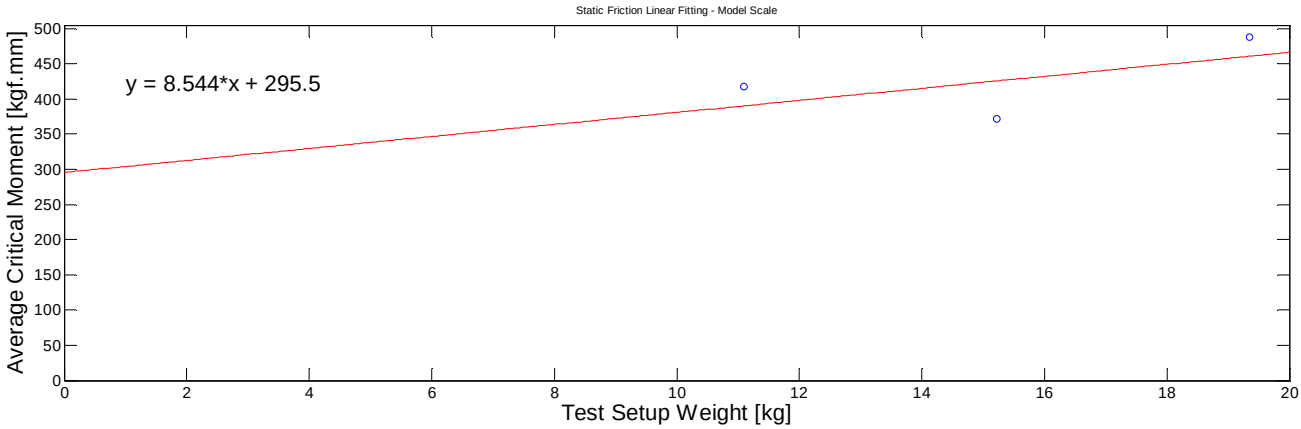

Figure 3-71. Static Friction Test Critical Force Linear Fit (Model Scale) - Operation Configuration

3.5.6.3 Dynamic Friction - Pinned Configuration

The gimbal was assembled on the pinned configuration, without springs or rods connected to the top and different ballasts fixed to the top of the CWP dummy.

Figure 3-72. Dynamic Friction - Pinned Configuration Setup

The gimbal support Teflon ball and cup was wet using a bottle of water. An initial offset was given and released. The motion and its decay were recorded on video, file names: "PT030_00400.raw.f4v", "PT030_00410.raw.f4v" and "PT030_00420.raw.f4v".

3.5.6.4 *Dynamic Friction - Operation Configuration*

For this test the gimbal was setup on the operation configuration, with the set of springs attached to the top and three different ballasts fixed to the bottom of the CWP dummy. The set of LVDT sensors were installed to record the CWP dummy movement.

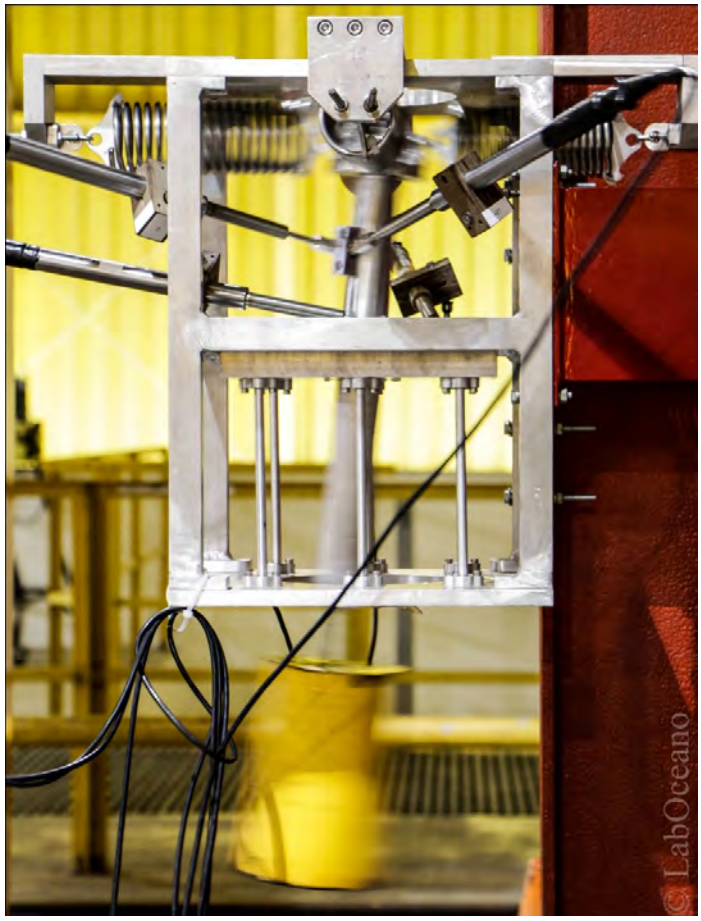

Figure 3-73. Dynamic Friction - Operation Configuration Setup

The free decay movement of the CWP dummy in the form of roll and pitch are plotted on figure 45 and in Matlab format on files: "PT031_00400.pro.mat", "PT031_00410.pro.mat", "PT031_00420.pro.mat".

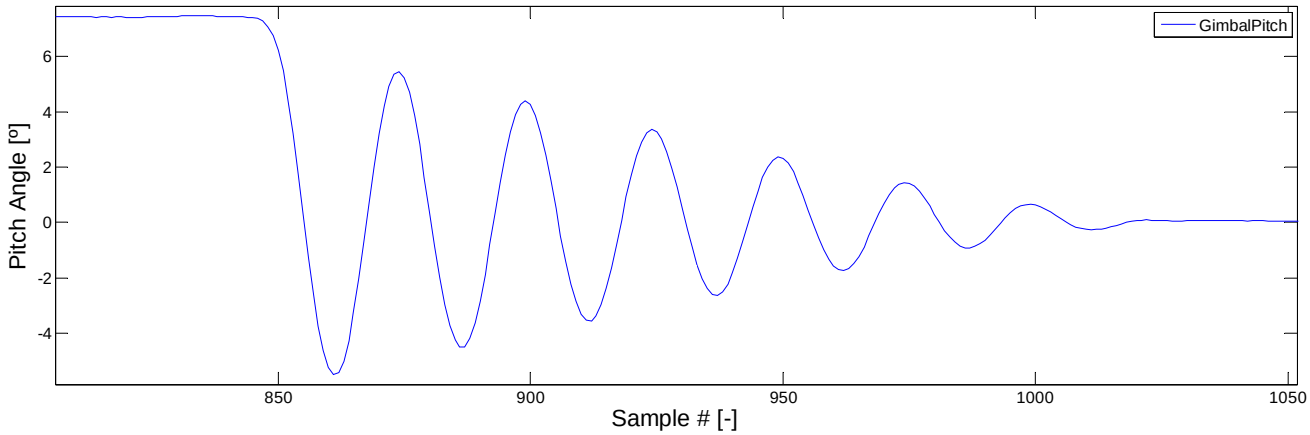

Figure 3-74. Gimbal Pitch Decay - Dynamic Friction Test

3.5.7 Data products

The tests were identified following the nomenclature:
PT03X_YYYYY.ZZZ.extension

where:
X=0 for pinned configuration,
X=1 for operation configuration and
X=2 for installation configuration

Y is the test configuration, refer to section 3.5

ZZZ=lvd for raw LVDT displacement data in [mm],
ZZZ=vec for Vectornav attitude angles raw data in [º x 10^6],
ZZZ=cel for load cell raw data in [gf],
ZZZ=raw for generic raw data and
ZZZ=pro for prototype scale derived channels.

extension=mat for Matlab files,
extension=f4v for video files and
extension=txt for ASCII files.

Table 3-10 lists the measured and derived variables with a brief description and units of measurement in model scale. The order that the parameters are listed is the same as the column order on the ASCII file.

Table 3-10. Variables Description

Variable Name	Description
GimbalPitch	Gimbal Pitch Angle derived from LVDT
GimbalRoll	Gimbal Roll Angle derived from LVDT
dx	Lower Support X displacement
dy	Lower Support Y displacement
Pitch	VectorNav Pitch angle
Roll	VectorNav Roll angle
Cel1 or FUTEK	Load Cell - Only for stiffness tests
tempo	Time record
canais	List of channels (for ASCII file header)
unidades	List of channels units (for ASCII file header)

3.5.8 Gimbal Dry-Tests Results Summary

The summary of the stiffness tests are presented on table 3-11.

Table 3-11. Gimbal Tests Summary

1 - Angle Measurement Script Verification (X dir.)			
ID: GIMBAL LVDT SCRIPT X			
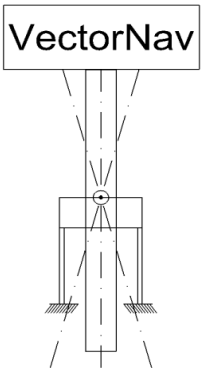	Pictures:	TEST ID:	
	IMG_PRJ_008_12_04_001_A.JPG IMG_PRJ_008_12_04_003_A.JPG	PT030_00100	

2 - Angle Measurement Script Verification (XY dir.)			
ID: GIMBAL LVDT SCRIPT XY			
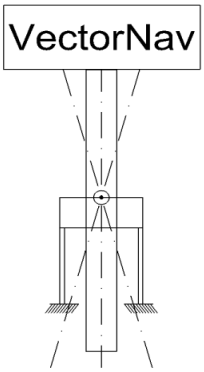	Pictures:	Data Files:	
	IMG_PRJ_008_12_05_0062_A.JPG	PT030_00200	

Table 3-11. Gimbal Tests Summary

3 - Gimbal Horizontal Stiffness - Installation Configuration (X dir.)			
ID: GIMBAL INST HOR STIF X			
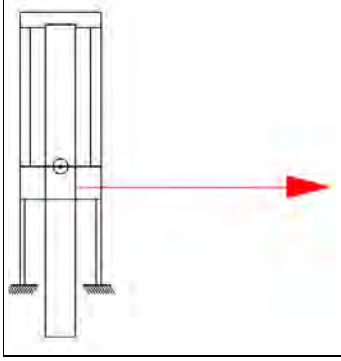	Pictures:	Data Files:	Results (Model / Full): [N/m]
	IMG_PRJ_008_12_05_00110_A.JPG IMG_PRJ_008_12_05_00111_A.JPG	PT032_00100	1.22E+05 / 3.15E+08 *

4 - Gimbal Angular Stiffness - Installation Configuration (X dir.)			
ID: GIMBAL INST ANG STIF X			
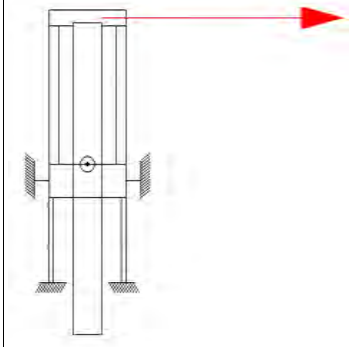	Pictures:	Data Files:	Results (Model / Full): [N.m/rad]
	IMG_PRJ_008_12_05_00106_A.JPG IMG_PRJ_008_12_05_00107_A.JPG	PT032_00300	1.48E+04 / 9.53E+10

* Gimbal lateral stiffness for the pinned configuration is the same as the lateral stiffness for the installation configuration presented on this table.

Table 3-11. Gimbal Tests Summary

5 - Gimbal Springs Stiffness - Operation Configuration (X dir.)			
ID: GIMBAL OPER SPR STIF X			
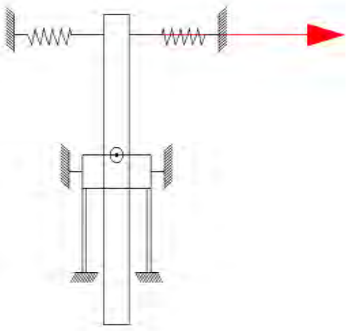	Pictures:	Data Files:	Results (Model / Full): [N/m]
	IMG_PRJ_008_12_05_00128_A.JPG IMG_PRJ_008_12_05_00135_A.JPG	PT031_00100	7.42E+03 / 1.91E+07

6 - Gimbal Ang. and Hor. Stiffness - Operation Configuration (X dir.)		
ID: Not Applicable		
Derived from Numerical Analysis	Angular Results (Model / Full):	Horizontal Results (Model / Full):
	1.95E+02 / 1.26E+09 [N.m/rad]	1.30E+05 / 3.35E+08 [N/m]

Table 3-11. Gimbal Tests Summary

7 - Gimbal Static Friction - Pinned Configuration		
ID: GIMBAL STAT FRICTION		
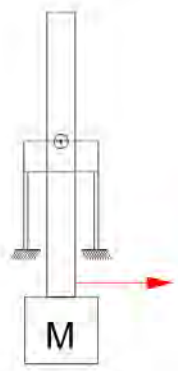	Pictures: IMG_PRJ_008_12_05_00115_A.JPG IMG_PRJ_008_12_05_00117_A.JPG	Data Files: PT030_00300 PT030_00310 PT030_00320

8 - Gimbal Static Friction - Operation Configuration		
ID: GIMBAL OPER STAT FRICTION		
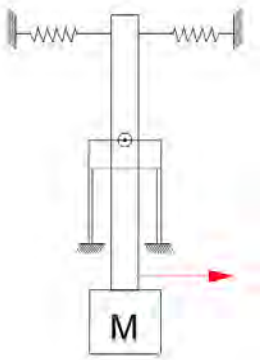	Pictures: IMG_PRJ_008_12_05_00136_A.JPG	Data Files: PT031_00300 PT031_00310 PT031_00320

Table 3-11. Gimbal Tests Summary

9 - Gimbal Dynamic Friction - Pinned Configuration		
ID: GIMBAL DYN FRICTION		
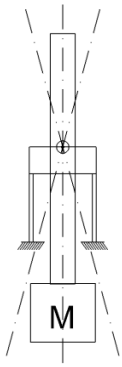	Pictures: IMG_PRJ_008_12_05_00138_A.JPG	Data Files: PT030_00400 PT030_00410 PT030_00420

10 - Gimbal Dynamic Friction - Operation Configuration		
ID: GIMBAL OPER DYN FRICTION		
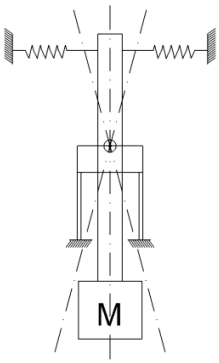	Pictures: IMG_PRJ_008_12_05_00119_A.JPG	Data Files: PT031_00400 PT031_00410 PT031_00420

3.6 COLD WATER PIPE

The CWP model was manufactured as a compound model with an internal aluminum tube core (6351-T6 alloy) dimensioned to the proper scaled flexural rigidity and segmented outer sheet sections to provide the correct outer diameter.

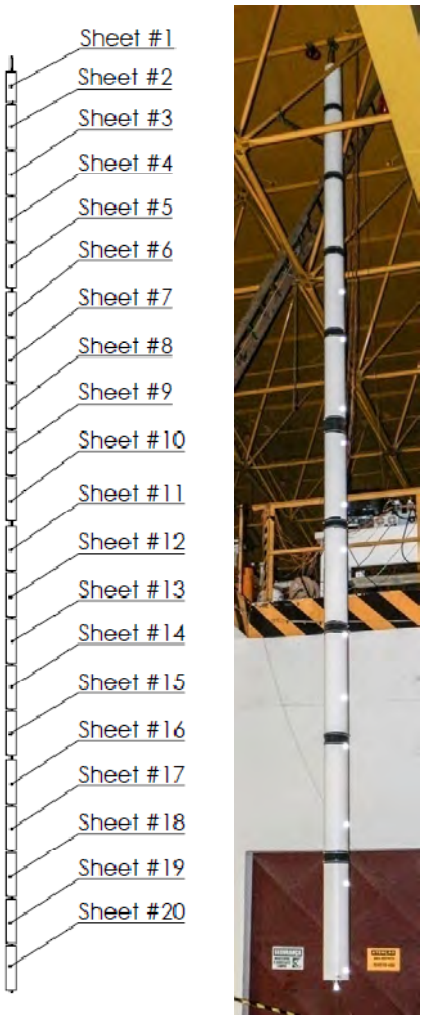

Figure 3-75 - CWP Model Assembly

The CWP core was divided into 5 parts connected to each other by a solid aluminum connector with angularly distributed threaded holes for bolts to connect the tubes and a longitudinal hole.

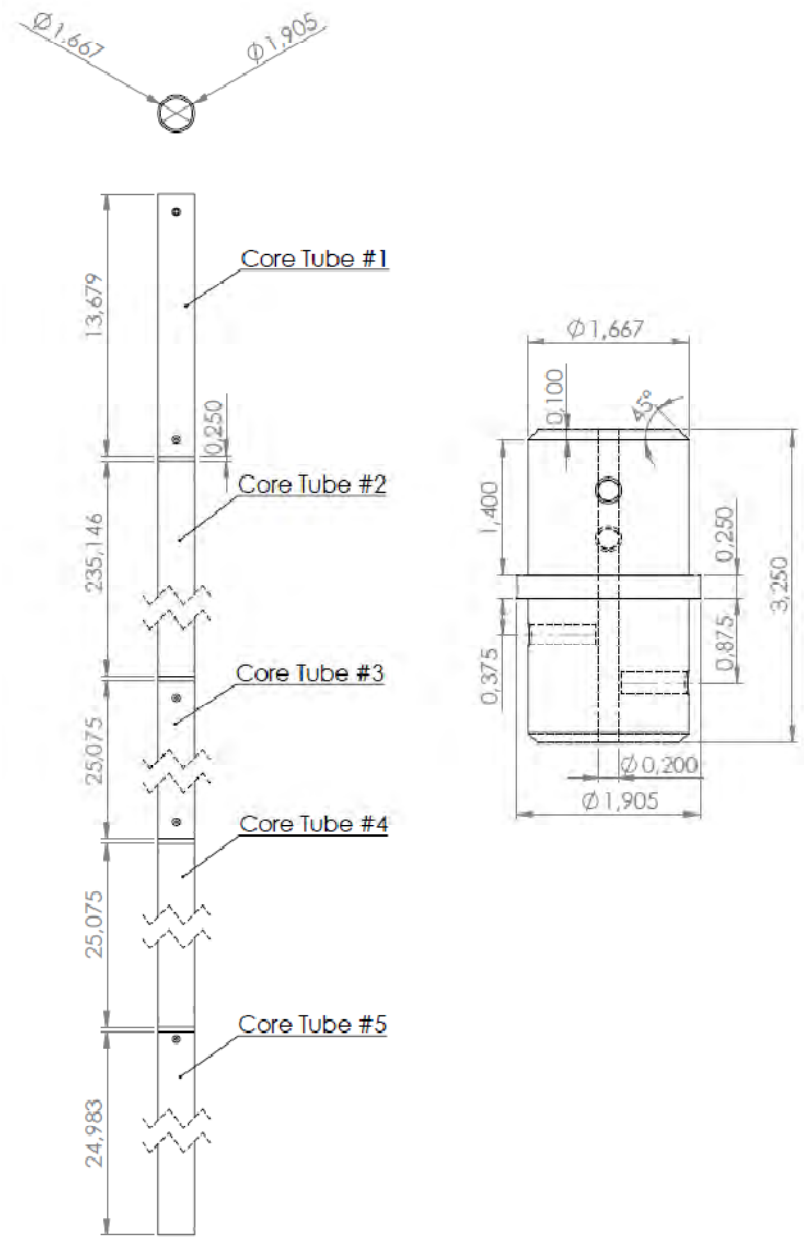

Figure 3-76 - CWP Model Core Tube and Connector

The CWP outer sheet is segmented into 20 parts, roughly 50m long, manufactured on a composite fiberglass woven roven, mat and polyester resin structure with polyester gelcoat finishing. The connection to the CWP core was made by end plates manufactured as a sandwich composite structure with fiberglass mat, PVC foam and polyester resin and a center nylon glove with hose clamps to attach it to the core tube. The end plates rested on internal PVC foam with polyester resin finishing preventing water absorption.

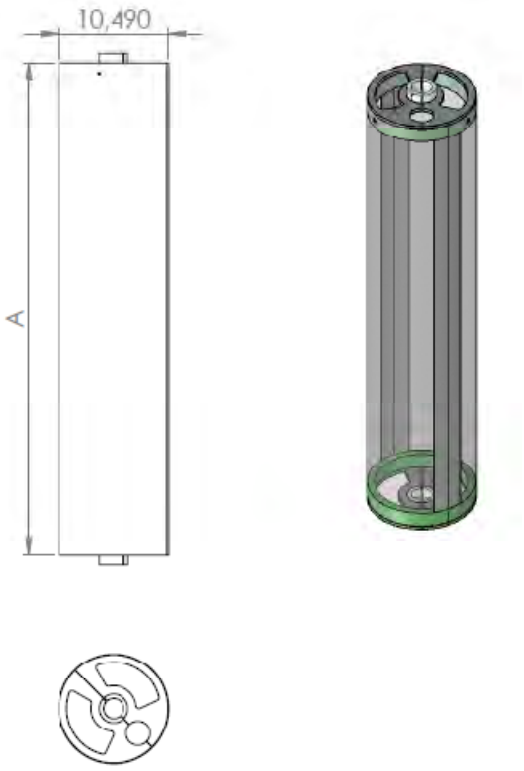

Figure 3-77 - CWP Model Outer Sheet Dimensions

Table 3-12 - CWP Outer Sheets Length

	Dimension A [m]
Sheet #1	34.086
Sheet #2 - #19	49.015
Sheet #20	48.5

There is a 0.5m spacing between the outer sheets, except where there is a core tube connector, in which case the spacing is 3.25m. A thin rubber film was attached to each outer sheet end to prevent entrapped water to flow out of the CWP model through those gaps.

Figure 3-78 - CWP Model Outer Sheets Gap Closure

3.6.1 CWP Impulse and Dry Weight Test

3.6.1.1 Instrumentation

- 1 unidirectional load cell ALPHA 250 kgf
- 1 unidirectional load cell FUTEK 22.65 kgf
- 10 Tracking System Targets
- 1 Qualisys Tracking System
- 10 Strain Gages model: kfg-2-120-c1-11-1m2r

3.6.1.2 Test Assembly and Procedure

Core tube #1, #2 and #3 and their respective fiberglass outer sheets were assembled fully instrumented.

The lower half was instrumented with the tracking system targets.

The top of core tube #1 was attached through a solid connector to the ALPHA 250kgf load cell. It is important to note that for the fully assembled CWP model for the wet test there will be a 20mm solid aluminum section on top of the core tube #1 for its interface with the gimbal.

The load cell was fixed to the ceiling frame structure.

The bottom of the CWP model was hit in the X direction (Run #1,#2 and #3) and the Y direction (Run #4) by a small hammer to excite the model.

The data obtained from the sensors was acquired prior to the model excitation up to a few minutes after it was hit.

3.6.1.3 Dry weight Analysis Procedure

The dry weight for 3/5 of the CWP was obtained by calculating the average value of the load cell reading before the pipe was hit.

The mass distribution of the CWP model and strain gages positions are detailed on 'Annex I: CWP Weight 2014-01-21.xlsx' in model scale. The individual components measured mass was input on this spreadsheet and the core tube mass was adjusted to match the upper half of the CWP measured mass in order to take in account the mass of instrumentation and rubber sleeves. This adjusted value was used to estimate the full model dry weight.

3.6.1.4 Data Products

The tests were identified following the nomenclature:
PT020_00XYY.ZZZ.extension

where:
X=1 for X direction and
X=2 for Y direction

Y =00 for Run #1
Y=10 for Run #2 and so forth for each type of test

ZZZ=qtm for raw Qualisys tracking data in [mm],
ZZZ=sgs for strain gages raw data in nondimensional pure strain,

ZZZ=cel for load cell raw data in [gf] and
ZZZ=pro for prototype scale derived channels.

extension=mat for Matlab files and
extension=txt for ASCII files.

Table 3-13 lists the derived variables with a brief description and units of measurement in model scale.

Table 3-13. Impulse Test Variables Description

Variable Name	Description
ALFA	CWP Top Support Vertical Load Cell
SG1-9 and SG19	Strain gages corrected to outside diameter
X01-10	Tracking targets X coordinate displacements
Y01-Y10	Tracking targets Y coordinate displacements
Z01-Z10	Tracking targets Z coordinate displacements
DW	CWP Model Dry-Weight
ED	Energy Density - Spectral Analysis
Freq	Frequency Domain - Spectral Analysis
tempoCEL	Time record for load cell variables
tempoQTM	Time record for Qualisys tracking variables
tempoSGS	Time record for strain gages variables
canais	List of channels (for ASCII file header)
unidades	List of channels units (for ASCII file header)

3.6.1.5 Results Summary

The spectral analysis plot of this test is presented on figure 3-79.

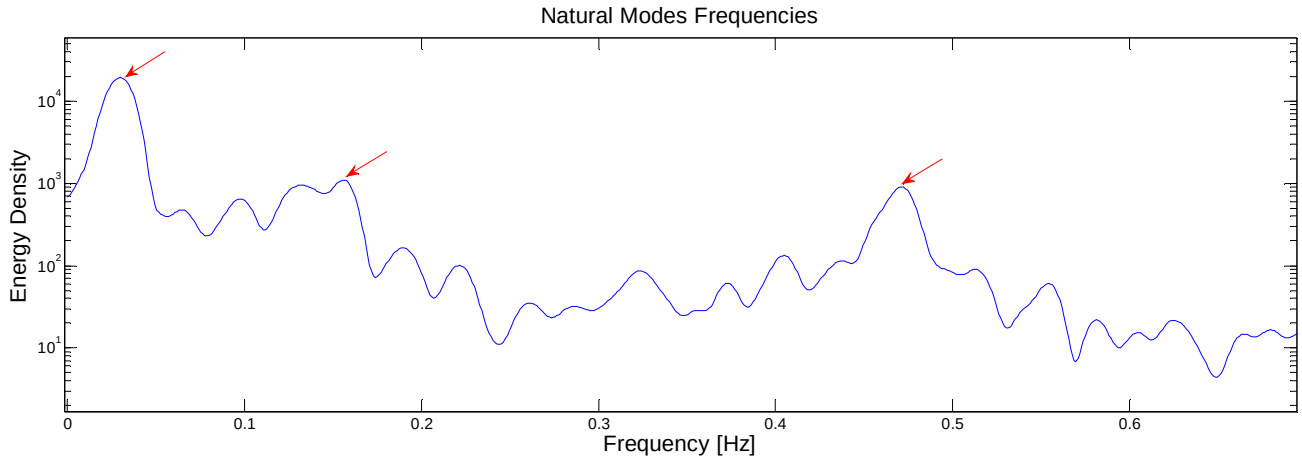

Figure 3-79 - CWP Impulse Test Modal Frequencies [Hz] - Model Scale

The test results are summarized on the table 3-14 and 3-15.

Table 3-14. CWP Natural Modes Tests Summary - Model Scale

	Natural Frequency - Mode 1 [Hz]	Natural Frequency - Mode 2 [Hz]	Natural Frequency - Mode 3 [Hz]	Dry-Weight 3/5 CWP [kgf]	Data Files
Run #1	0.030	0.156	0.471	28.413	PT020_00100
Run #2	0.030	0.157	0.472	28.412	PT020_00110
Run #3	0.029	0.141	0.469	28.415	PT020_00120
Run #4	0.032	0.153	0.467	28.236	PT020_00200

Table 3-15. CWP Natural Modes Tests Summary - Prototype Scale

	Natural Frequency - Mode 1 [Hz]	Natural Frequency - Mode 2 [Hz]	Natural Frequency - Mode 3 [Hz]	Dry-Weight 3/5 CWP [tonf]	Data Files
Run #1	0.0042	0.0221	0.0666	3669.0	PT020_00100
Run #2	0.0042	0.0222	0.0668	3668.9	PT020_00110
Run #3	0.0041	0.0199	0.0663	3669.3	PT020_00120
Run #4	0.0045	0.0216	0.0660	3646.2	PT020_00200

The dry weight for the full CWP model is 45166.93gf and 5832.496tonf in model and full scale respectively.

3.6.2 CWP - Static Offset Test

3.6.2.1 Instrumentation

Please refer to section 3.6.1.1.

3.6.2.2 Test Assembly and Procedure

A load cell installed in line with a steel wire was connected to the bottom of the CWP pipe at 20010 mm vertical distance from the model origin in model scale.

A tracking target was attached to the bottom of the CWP pipe, with its center 11mm (model scale) below the bottom of core tube #3.

Figure 3-80 - CWP Static Offset Setup

For this test the Qualisys tracking system coordinate system was realigned with the X, Y and Z axis aligned with the model X, Y and Z axis respectively.

The other end of the load cell was connected to another steel wire that was pulled in the X direction and data from the horizontal load, strains and target positions were acquired at every 100mm in horizontal displacement.

3.6.2.3 *Analysis Procedure*

The position at the end of the test was considered as the reference value (Xref and Zref) for the X and Z coordinates of the targets for the pipe at rest on the vertical position.

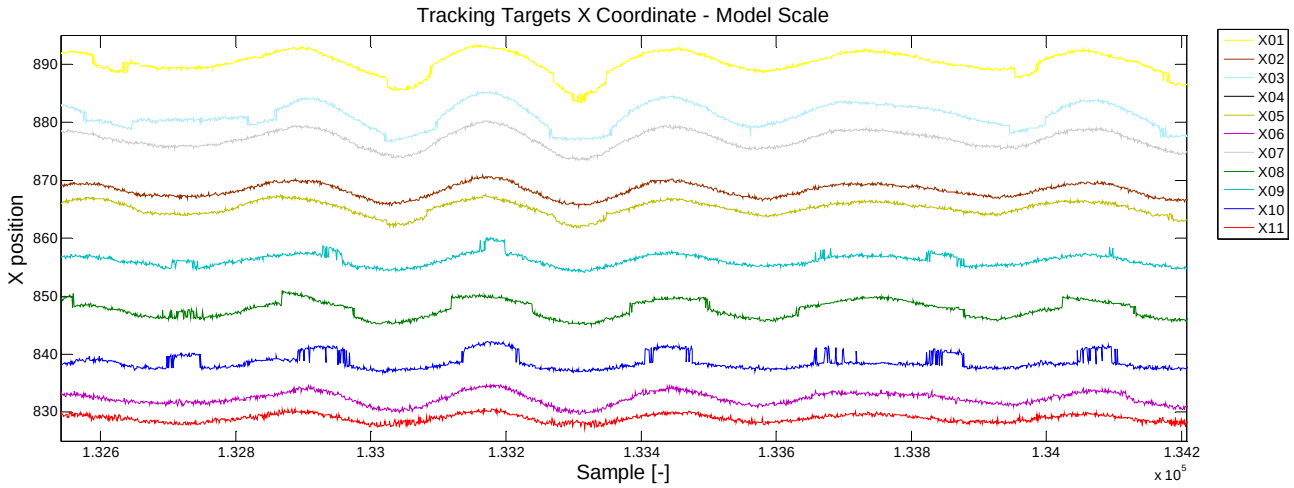

Figure 3-81 - Reference X Position [mm] Interval - Model Scale

The Z coordinate of the targets were offset to obtain the target coordinates relative to the CWP model coordinate system. The order of the targets were also reorganized sorting them crescent from top down.

$$
\begin{aligned}
Z01\_CWP &= Z11 + Offset\ Z \\
Z02\_CWP &= Z06 + Offset\ Z \\
Z03\_CWP &= Z10 + Offset\ Z \\
Z04\_CWP &= Z08 + Offset\ Z \\
Z05\_CWP &= Z09 + Offset\ Z \\
Z06\_CWP &= Z05 + Offset\ Z \\
Z07\_CWP &= Z02 + Offset\ Z \\
Z08\_CWP &= Z07 + Offset\ Z \\
Z09\_CWP &= Z03 + Offset\ Z \\
Z10\_CWP &= Z01 + Offset\ Z \\
Z11\_CWP &= Z04 + Offset\ Z
\end{aligned}
$$

The same target order was used for the horizontal displacements, with the targets X coordinates calculated relative to their average position at rest.

$$
\begin{aligned}
dX01 &= X11 - X11ref \\
dX02 &= X06 - X06ref \\
dX03 &= X10 - X10ref \\
dX04 &= X08 - X08ref \\
dX05 &= X09 - X09ref \\
dX06 &= X05 - X05ref \\
dX07 &= X02 - X02ref \\
dX08 &= X07 - X07ref \\
dX09 &= X03 - X03ref \\
dX10 &= X01 - X01ref \\
dX11 &= X04 - X04ref
\end{aligned}
$$

The time series of the horizontal position of the bottom target was analyzed to identify the intervals where the model was at rest. Those intervals will be used to calculate the average value for each offset step. The time series of the load cell, strain and other coordinates were checked to adjust the size of the intervals not to introduce any additional noise on the average values calculated.

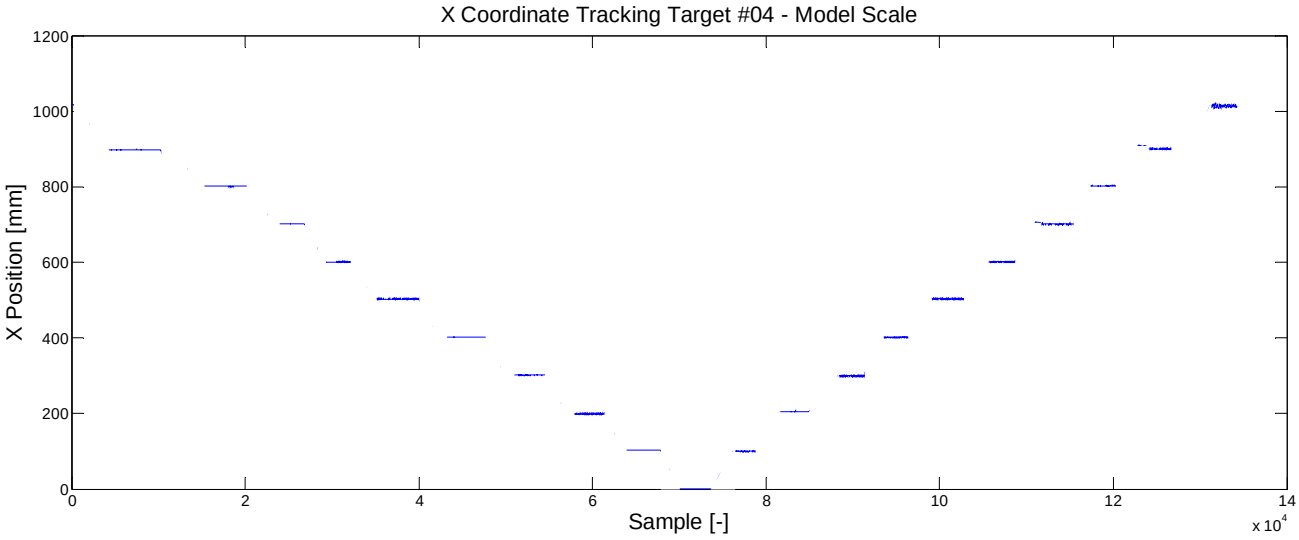

Figure 3-82 - Offset Steps Intervals - Model Scale

The average values for the horizontal load, X and Z target coordinates and strains were calculated for those intervals.

The shape of the CWP model for each step was plotted using the targets X and Z coordinates.

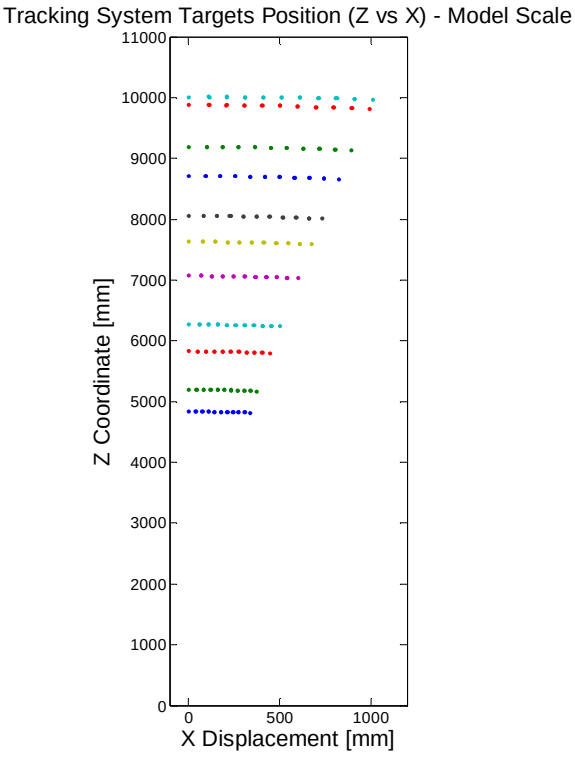

Figure 3-83 - Static Offset CWP Model Shape - Model Scale

3.6.2.4 Data Products

The tests were identified following the nomenclature:
PT020_00300.ZZZ.extension

where:
ZZZ=qtm for raw Qualisys tracking data in [mm],
ZZZ=sgs for strain gages raw data in nondimensional pure strain,
ZZZ=cel for load cell raw data in [gf] and
ZZZ=pro for prototype scale derived channels.

extension=mat for Matlab files and
extension=txt for ASCII files.

For the raw data files the measurement units are in model scale. The displacements are in mm, the loads in gf and the strains in the nondimensional form.

Table 3-16 lists the derived variables with a brief description and units of measurement in model scale.

Table 3-16. Static Offset Test Variables Description

Variable Name	Description
ALFA	CWP Top Support Vertical Load Cell
FUTEK	CWP Pulling Line Load Cell
SG1-9 and SG19	Strain gages corrected to outside diameter
X01-10	Tracking targets X coordinate displacements
Z01-Z10	Tracking targets Z coordinate displacements
tempoCEL	Time record for load cell variables
tempoQTM	Time record for Qualisys tracking variables
tempoSGS	Time record for strain gages variables
canais	List of channels (for ASCII file header)
unidades	List of channels units (for ASCII file header)

3.6.3 CWP Stiffness Test

3.6.3.1 Test Assembly and Procedure

The CWP core tube #3, a 5m long section, in model scale, was setup fully instrumented on top of two supports. Three (3) known weights were hanged on the model at a specific location and the beam deflection was measured at the same location. Before the beginning of the test the strain values were zeroed with the model fully supported on a leveled structure.

Figure 3-84. CWP Stiffness Test Setup

The test setup, with support distances, beam length and strain gages positions are summarized on figure 3-84.

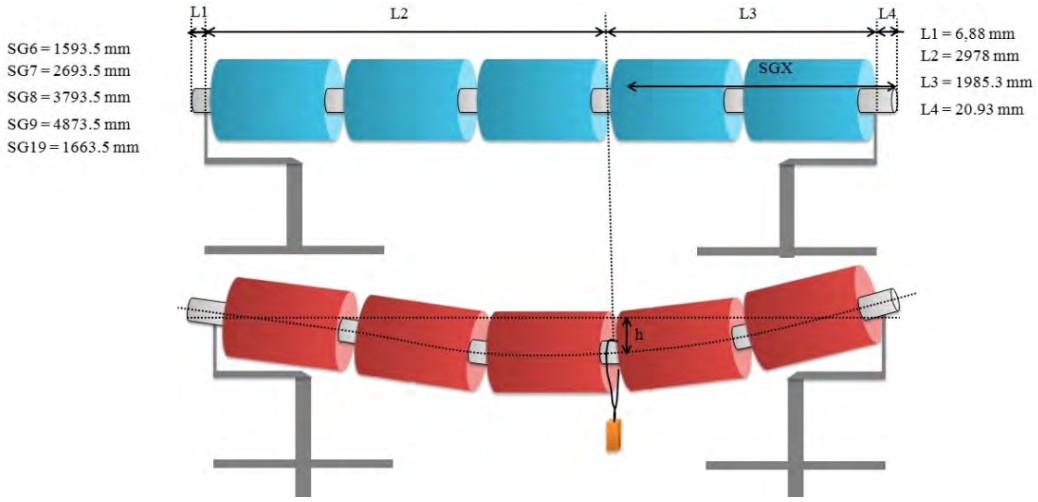

Figure 3-85. CWP Stiffness Test Setup Dimensions - Model Scale

3.6.3.2 Analysis Procedure

The applied loads and vertical displacements were input on the deflection equation for a simply supported beam for a similar setup in prototype scale. The output value is the flexural rigidity value "EI".

$$h = -\frac{P.b.x}{6.L.EI}.(L^2 - b^2 - x^2)$$

$$re - arranging:$$
$$EI = -\frac{P.b.x}{6.L.h}.(L^2 - b^2 - x^2)$$

3.6.3.3 Data Products

The tests were identified following the nomenclature:
PT020_00400.ZZZ.extension

where:
ZZZ=sgs for strain gages raw data in nondimensional pure strain,
ZZZ=pro for prototype scale derived channels.

extension=mat for Matlab files and
extension=txt for ASCII files.

For the raw data files the measurement units are in model scale. The strains are in the nondimensional form.

Table 3-17 lists the derived variables with a brief description and units of measurement in model scale.

Table 3-17. Stiffness Test Variables Description

Variable Name	**Description**
Displacement	CWP Top Support Load Cell
Weight	Mass of known weight
SG6-9 and SG19	Strain gages corrected to outside diameter
canais	List of channels (for ASCII file header)
unidades	List of channels units (for ASCII file header)

3.6.3.4 Results Summary

The resulting EI value is presented on table 3-18 in prototype scale.

Table 3-18. CWP Stiffness Test Result

Average Displacements [m]	Applied Loads [KN]	Adjusted EI [KN.m²]
0.023	0	-
0.68575	2251.4	9.63E+08
1.0875	3619.1	9.77E+08
1.4995	4934.1	9.66E+08
Mean EI [KN.m²]		9.69E+08

3.7 MOORING

3.7.1 Specification

Horizontal mooring, linear stiffness, horizontal stiffness obtained from test specification, section 2.7, pag. 21: "Taut Mooring stiffness: 650 kN/m (estimated maximum offset 27 m)"

3.7.2 Schematic

Four (4) mooring lines were installed horizontally at positive and negative 45º from the X axis.

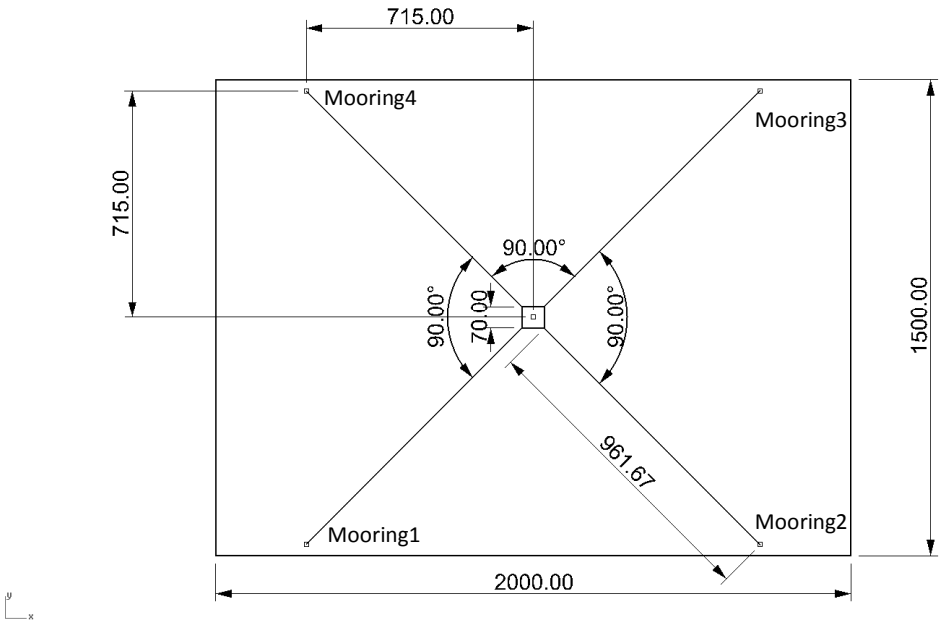

Figure 3-86. Mooring Schematic

After 961 meters the lines passes through a pulley to a vertical direction and is fixed at the ceiling. The pulleys position are listed on table 3-19 according to reference frame oxyz.

Table 3-19. Mooring Pulley Positions

	Prototype Scale [m]			Model Scale [m]		
	X position	Y position	Z position	X position	Y position	Z position
Pulley #1	715	715	-15.75	14.3	14.3	-0.315
Pulley #2	-715	715	-15.75	-14.3	14.3	-0.315
Pulley #3	-715	-715	-15.75	-14.3	-14.3	-0.315
Pulley #4	715	-715	-15.75	14.3	-14.3	-0.315

A spring and a pre-tension adjustment are connected on the vertical portion of the line.

3.7.3 Mooring Design

For the purpose of modeling the mooring the steel cable was modeled up until the pulley position, and connected to a small spring segment with the actual springs stiffness and pre-tension. A clump weight was added to represent the load cell weight on the line.

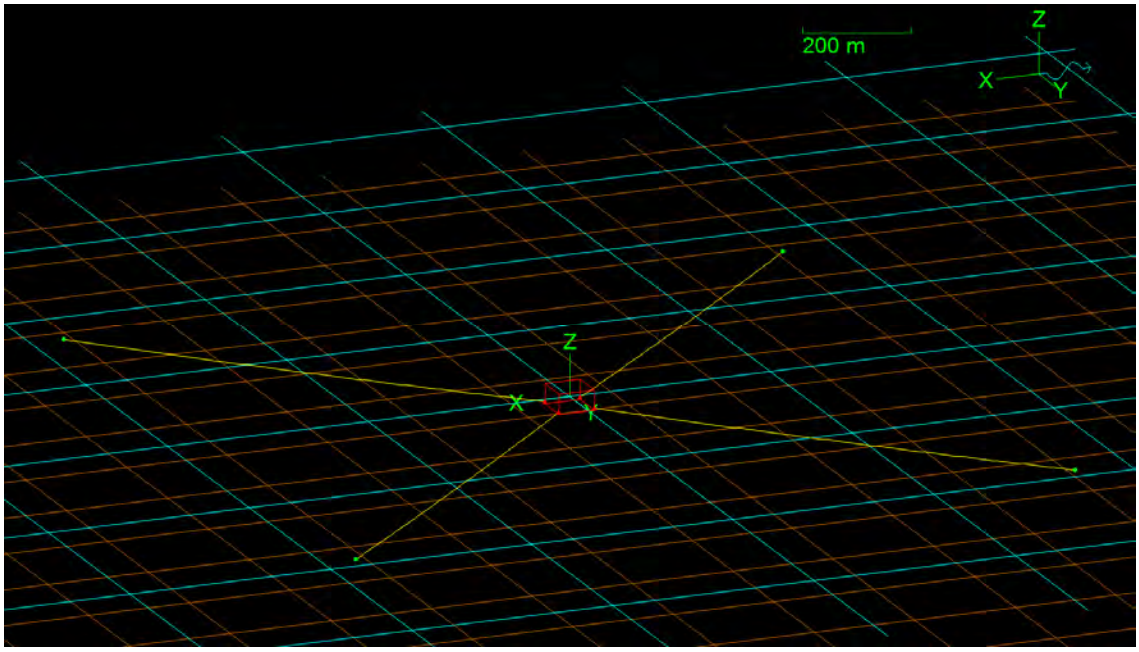

Figure 3-87. Mooring Orcaflex Model

This model was offset in X and Y direction to produce a restoring force vs. offset plot.

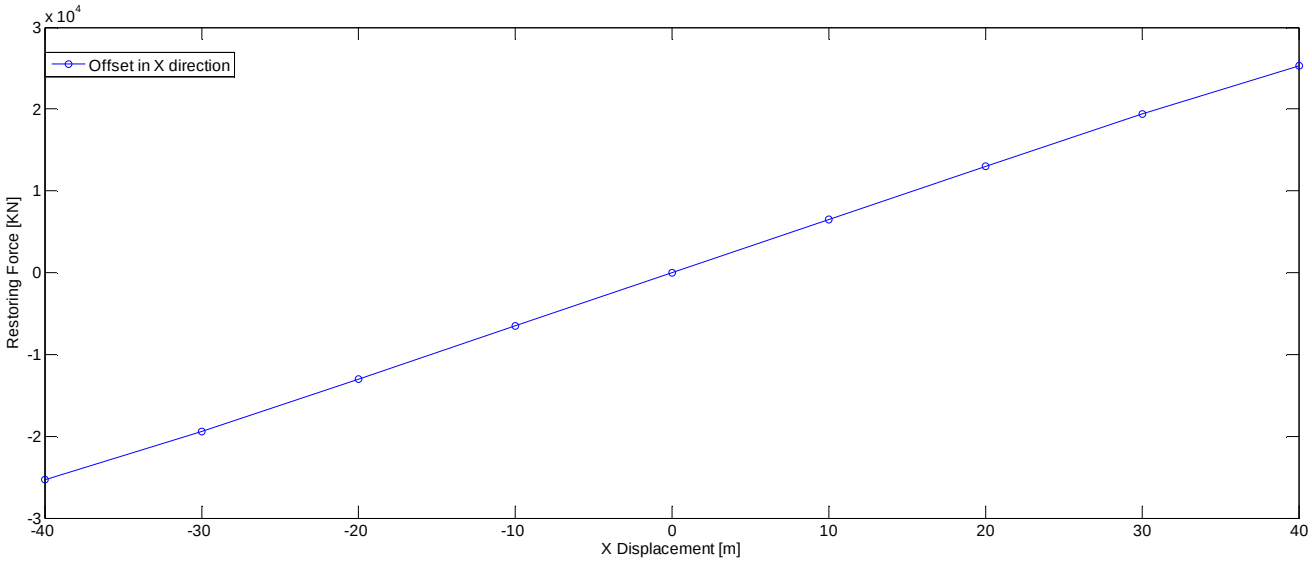

Figure 3-88. Static Offset Design Curve

The plot for the Y direction is identical since the mooring is completely symmetrical. The design mooring stiffness is 647 [KN/m] for surge and sway directions. The as-built mooring stiffness is provided in sections 7.12.2.1 through 7.12.2.3 for surge, sway and yaw directions.

The springs design stiffness is 320 KN/m, 126.5 gf/cm, the pre-tension on the line is 13735 KN and 10862 gf in prototype and model scale respectively.

The maximum expected tension for the line is 26719 KN and 19549 gf in prototype and model scale respectively.

3.7.4 Mooring Elements Descriptions

The mooring system elements are listed on the figure 3-88.

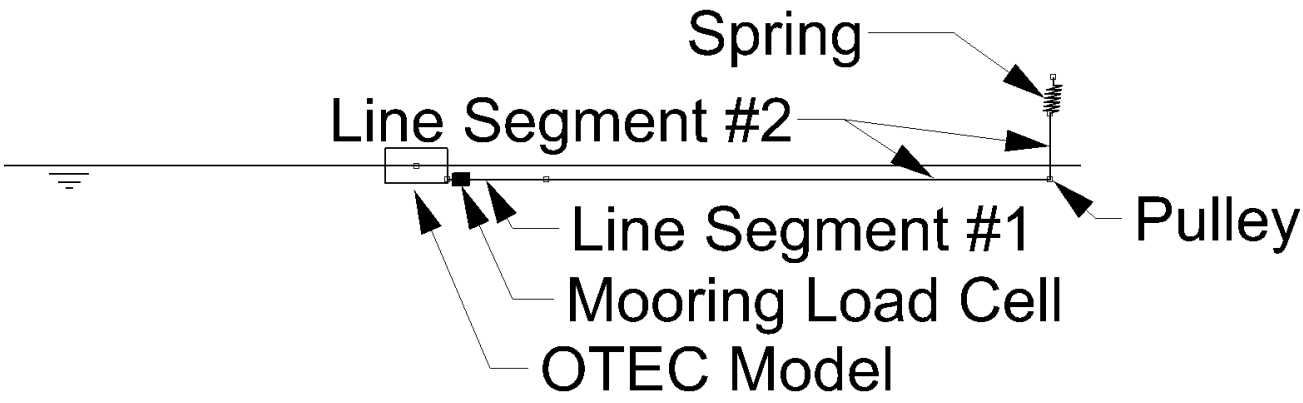

Figure 3-89. Model Mooring Elements

The mooring springs as-built stiffness are summarized on table 3-20.

Table 3-20. Mooring Springs As-Built Stiffness

	As-Built Stiffness - Prototype Scale [KN/m]	*As-Built Stiffness - Model Scale [gf/cm]*
Mooring #1	*313.363*	*123.731*
Mooring #2	*309.954*	*122.385*
Mooring #3	*315.020*	*124.385*
Mooring #4	*308.721*	*121.898*

The mooring elements properties are described on table 3-21.

Table 3-21. Model Elements Description

Item	**Description (Model - Full)**	**Length [m] (Prototype)**	**Weight (Prototype)**	**Length [mm] (Model)**	**Weight (Model)**
Semi Fairleads	Eye bolt on model	See figure 3-89			
Fairlead Fixture	Shackle	See figure 3-89			
Mooring Load Cell	FUTEK 50lb	-	2.3 ton	-	18g
Line Segment #1	Adjustable length chain	51.5	dry: 211kg/m	1030	dry: 82g/m
Line Segment #2	1.5 - 75mm Steel cable	1125	dry: 26 kg/m wet:21 kg/m	22,500	dry: 10 g/m wet: 8 g/m
Spring	ref. Table 17	51	dry: 5852 kg	1020	dry: 2266 g
Line Fixture	Shackle on vertical strut	See figure 3-89			

The eye bolts and fixture shackles are shown in detail on figure 3-89.

Figure 3-90. Mooring Fairleads and Shackle

The pulley and spring setup is shown on figure 3-90.

Figure 3-91 - Mooring Pulley and Spring Setup

3.8 Model Configuration and Mass Properties

The complete ballast plans for the models on each configuration are detailed on the 'Annex J: Model Ballasting Plan' document.

3.8.1 Mass properties Summary - Gimbal

The gimbal mass for each configuration is listed on table 3-22.

Table 3-22 - Gimbal Mass

Gimbal Configuration	Gimbal Mass [kg]
OPERATIONAL A (1.26E+9N.m/rad)	3.33E+6
OPERATIONAL B (0 N.m/rad)	2.97E+6
INSTALLATION 1 & 2	3.17E+6

3.8.2 Mass properties Summary - T100

For this configuration the Semi-submersible model is installed on the basin connected to the horizontal mooring.

The semi is ballasted to compensate the absence of vertical load from the hanging CWP pipe.

The gimbal is setup for the operation configuration angular stiffness (1.26E+09 N.m/rad) with a short section of the CWP installed, core tube #1 (12 m).

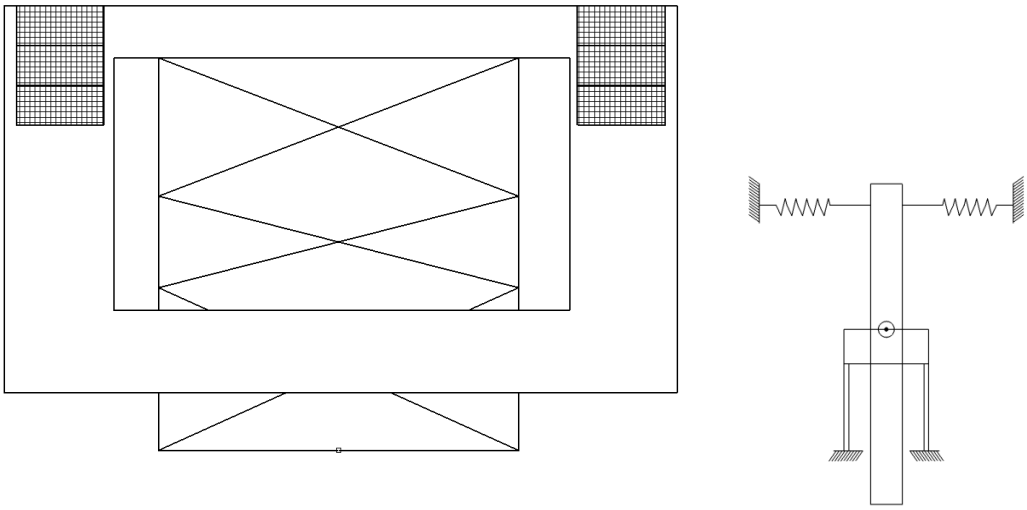

Figure 3-92 - T100 Test Group Model Setup

The summary of the model mass properties are presented on table 3-23.

Table 3-23 - T100 Mass Properties Summary

	Model Scale		Prototype Scale	
rho_{agua}	992.2	kg/m³	1025	kg/m³
m	321.15	kg	41472.117	ton
Ixx	1.05E+08	kg.mm²	3.38E+07	ton.m²
Iyy	1.06E+08	kg.mm²	3.43E+07	ton.m²
Izz	1.17E+08	kg.mm²	3.78E+07	ton.m²
Xcg	1.05	mm-SM	0.053	m-SM
Ycg	-4.21	mm-LC	-0.211	m-LC
Zcg	360.16	mm-LB	18.008	m-LB

3.8.3 Mass properties Summary - T200

For this test group the only change in the model configuration is the addition of the six (6) Remora models.

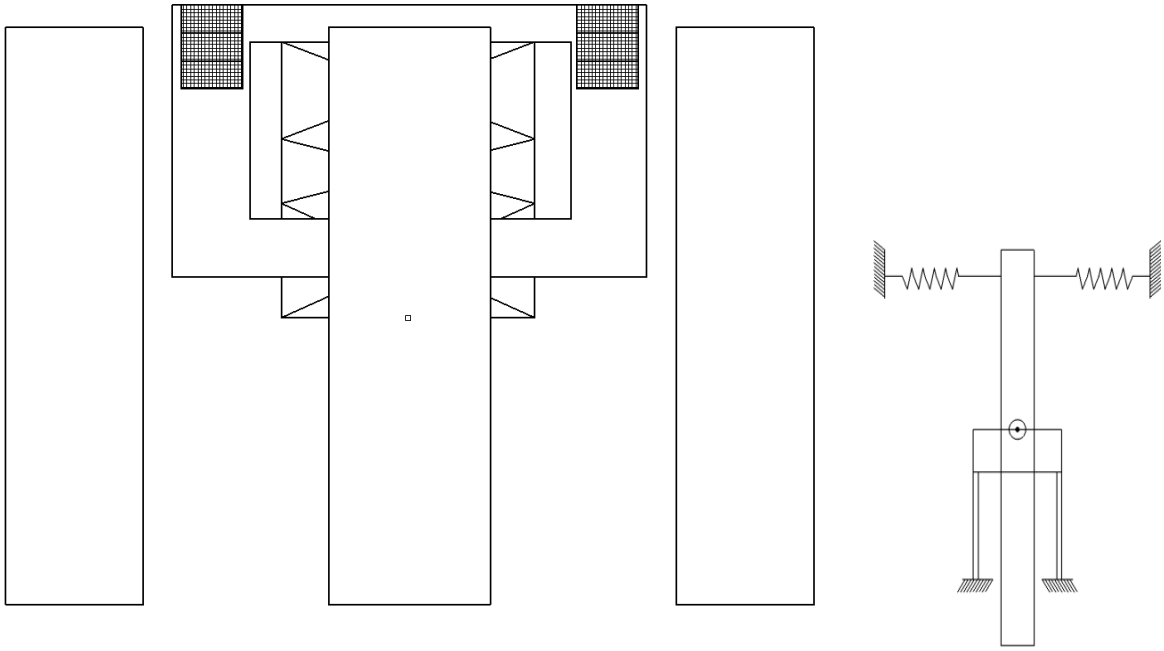

Figure 3-93 - T200 Test Group Model Setup

The summary of the model mass properties are presented on table 3-24.

Table 3-24 - T200 Mass Properties Summary

	Model Scale		Prototype Scale	
rho_{agua}	992.2	kg/m³	1025	kg/m³
m	1725.55	kg	222831.242	ton
Ixx	8.72E+08	kg.mm²	2.81E+08	ton.m²
Iyy	1.19E+09	kg.mm²	3.83E+08	ton.m²
Izz	1.38E+09	kg.mm²	4.46E+08	ton.m²
Xcg	-0.81	mm-SM	-0.040	m-SM
Ycg	-0.65	mm-LC	-0.033	m-LC
Zcg	-279.98	mm-LB	-13.999	m-LB

3.8.4 Mass properties Summary - T400

For this configuration the full length of the CWP model is installed. The semi is de-ballasted now that the CWP model is installed with its full wet weight.

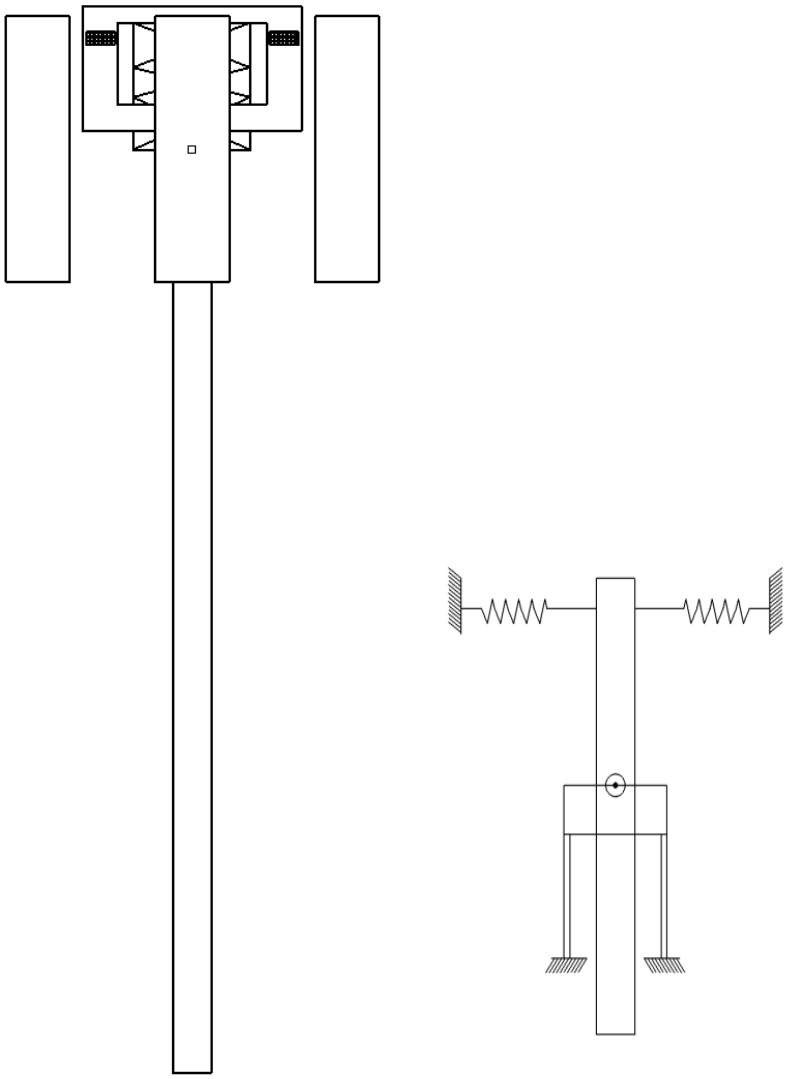

Figure 3-94 - T400 Test Group Model Setup

The summary of the model mass properties are presented on table 3-25.

Table 3-25 - T400 Mass Properties Summary

	Model Scale		Prototype Scale	
rho_{agua}	992.2	kg/m³	1025	kg/m³
m	1709.40	kg	220745.436	ton
Ixx	8.50E+08	kg.mm²	2.75E+08	ton.m²
Iyy	1.16E+09	kg.mm²	3.76E+08	ton.m²
Izz	1.37E+09	kg.mm²	4.43E+08	ton.m²
Xcg	-0.80	mm-SM	-0.040	m-SM
Ycg	-0.65	mm-LC	-0.033	m-LC
Zcg	-289.36	mm-LB	-14.468	m-LB

3.8.5 Mass properties Summary - T300

For this configuration the top set of springs are removed and the gimbal provides zero angular stiffness.

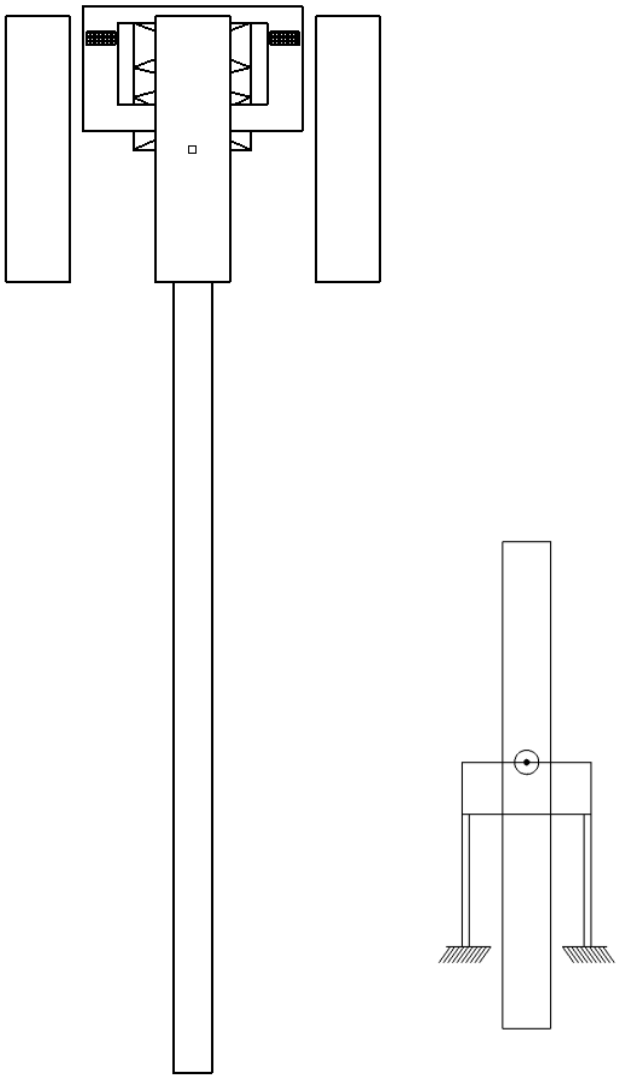

Figure 3-95 - T300 Test Group Model Setup

The summary of the model mass properties are presented on table 3-26.

Table 3-26 - T300 Mass Properties Summary

	Model Scale		Prototype Scale	
rho_{agua}	992.2	kg/m³	1025	kg/m³
m	1705.63	kg	220373.335	ton
Ixx	8.50E+08	kg.mm²	2.74E+08	ton.m²
Iyy	1.16E+09	kg.mm²	3.76E+08	ton.m²
Izz	1.37E+09	kg.mm²	4.43E+08	ton.m²
Xcg	-0.80	mm-SM	-0.040	m-SM
Ycg	-0.65	mm-LC	-0.033	m-LC
Zcg	-290.06	mm-LB	-14.495	m-LB

3.8.6 Mass properties Summary - T600

For this configuration the top set of rods are installed to provide the installation angular stiffness and the Remoras were removed.

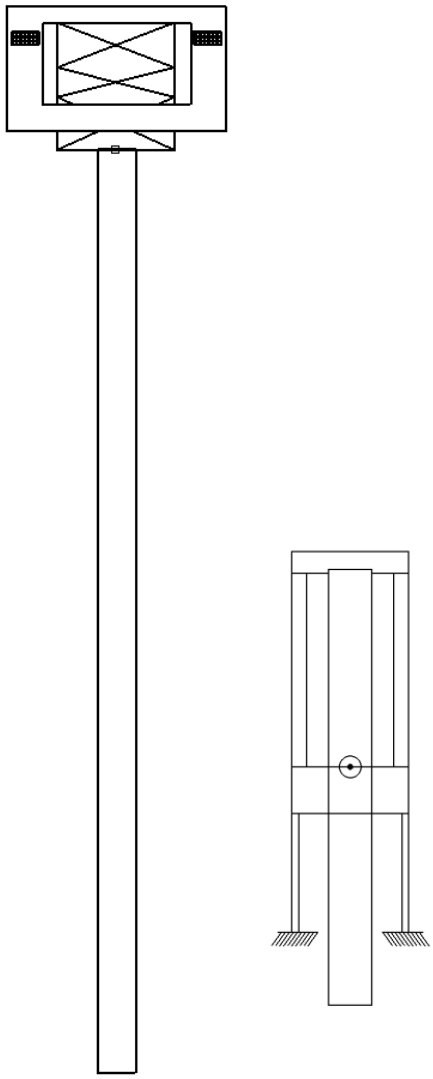

Figure 3-96 - T600 Test Group Model Setup

The summary of the model mass properties are presented on table 3-27.

Table 3-27 - T600 Mass Properties Summary

	Model Scale		Prototype Scale	
rho_{agua}	992.2	kg/m³	1025	kg/m³
m	314.12	kg	40563.748	ton
Ixx	1.00E+08	kg.mm²	3.23E+07	ton.m²
Iyy	1.05E+08	kg.mm²	3.38E+07	ton.m²
Izz	1.11E+08	kg.mm²	3.58E+07	ton.m²
Xcg	-0.20	mm-SM	-0.010	m-SM
Ycg	-4.22	mm-LC	-0.211	m-LC
Zcg	357.59	mm-LB	17.879	m-LB

3.8.7 Mass properties Summary - T500

For this configuration half of the CWP length is removed and the pipe is tested with 500.4 meters. All of the movable ballasts in the columns were installed to achieve the required draft.

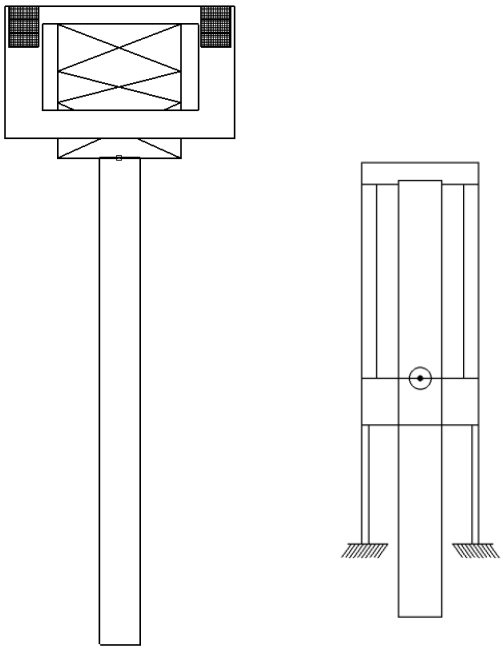

Figure 3-97 - T500 Test Group Model Setup

The summary of the model mass properties are presented on table 3-28.

Table 3-28 - T500 Mass Properties Summary

	Model Scale		Prototype Scale	
rho_{agua}	992.2	kg/m³	1025	kg/m³
m	318.79	kg	41167.847	ton
Ixx	1.04E+08	kg.mm²	3.37E+07	ton.m²
Iyy	1.06E+08	kg.mm²	3.42E+07	ton.m²
Izz	1.17E+08	kg.mm²	3.78E+07	ton.m²
Xcg	0.10	mm-SM	0.005	m-SM
Ycg	-4.57	mm-LC	-0.229	m-LC
Zcg	358.58	mm-LB	17.929	m-LB

4 TEST SET-UP AND PROCEDURES

4.1 MOORING OFFSET TESTS

For all pullout tests the model was installed on the basin, the mooring lines pre-tension equalized and adjusted to design values.

For the Surge and Sway pullout tests a pair of steel cables were attached on the fairleads, connected together to a single cable that was connected to a load cell and the end of the cables passed through a pulley to a winch in order to pull the model and mooring at specific positions.

For the Mooring Yaw Pullout, two separate steel cables, load cells, pulleys and winches were used, each pulling in one direction, positive and negative Y axis on the vessel coordinate system.

The position of each of the steel cables on the model and of the pulley-winch system on the basin are detailed on figure 4-1.

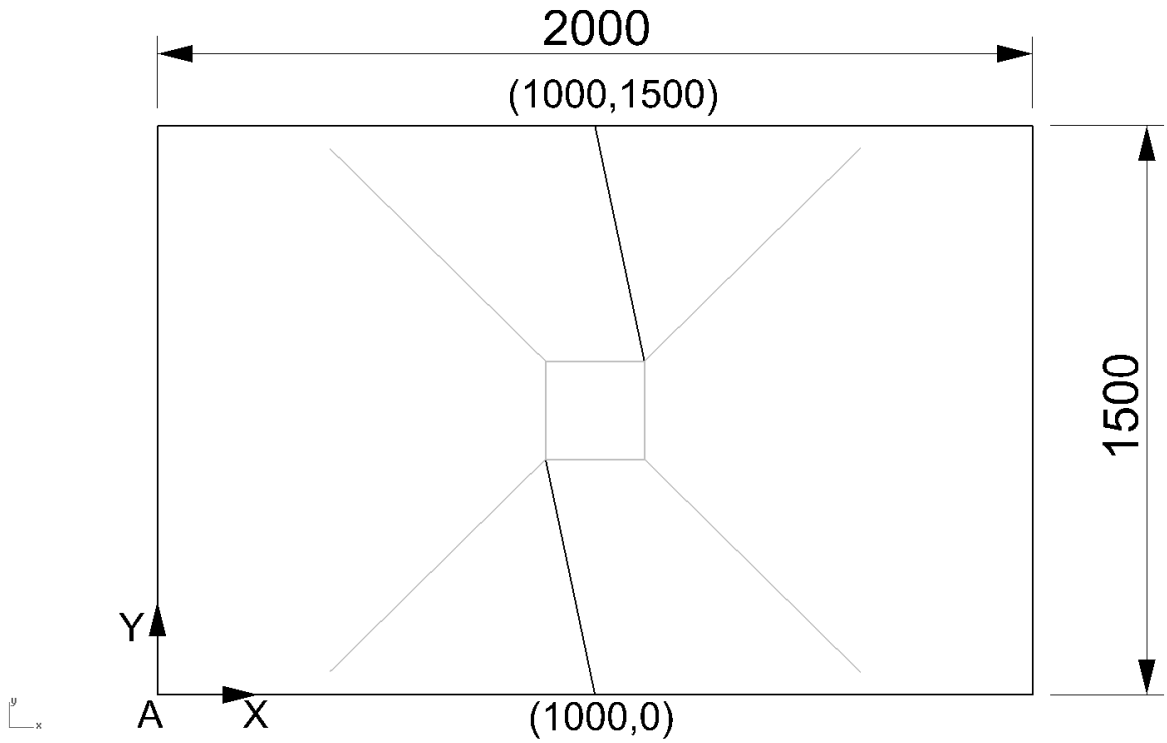

Figure 4-1 - Yaw Pullout Test Setup

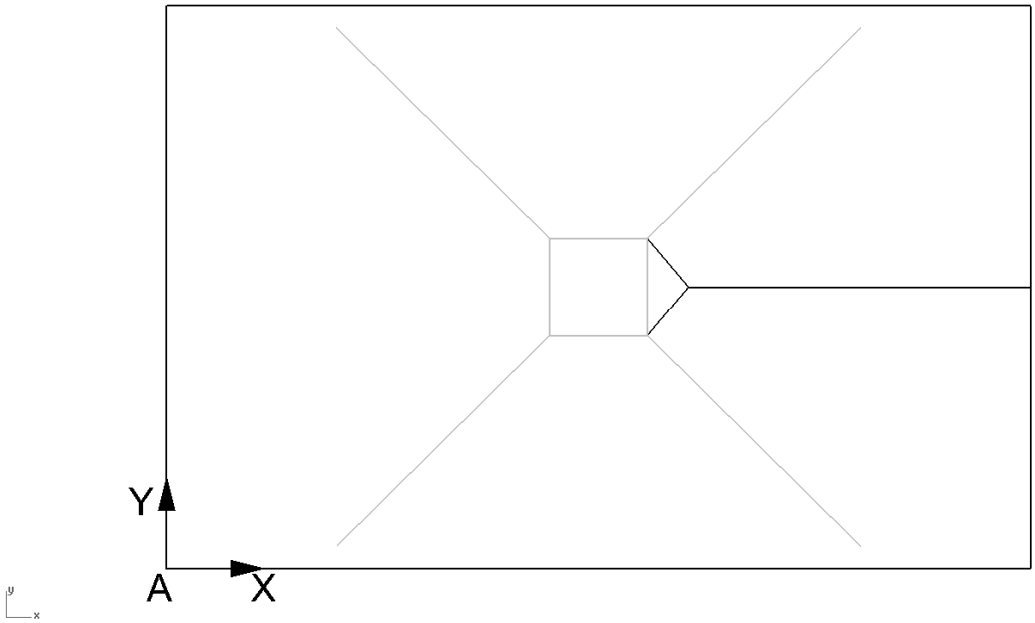

Figure 4-2 - Surge Pullout Test Setup

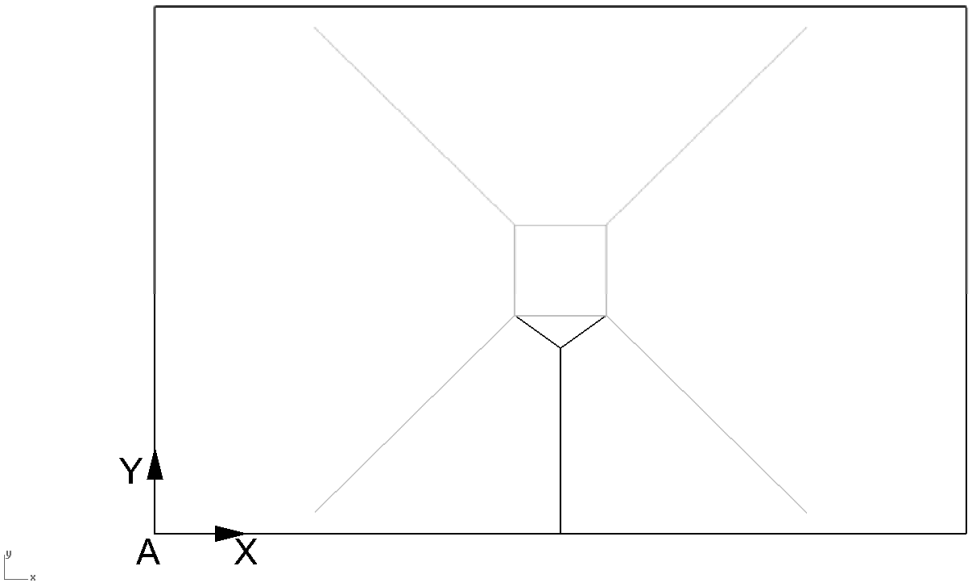

Figure 4-3 - Sway Pullout Test Setup

4.2 STATIC INCLINING TESTS

For static inclining tests, a set of markers were installed at model deck (Figure 5-3), in a way that a known weight could be positioned precisely at each required position. After the positioning of the weight at each point, the system was let free to equilibrium and the mean position was then registered.

4.3 CWP STATIC OFFSET TEST

For this test a steel cable was attached to the CWP at a -1025.5m elevation on a horizontal direction aligned with the vessel positive X axis. Close to the CWP a FUTEK load cell was attached to measure the pullout load. After the load cell the steel cable passed through a pulley upward above water level to a winch in order to produce the pipe offset. The pulley position is (125,0,-1025.5)m relative to reference frame oxyz.

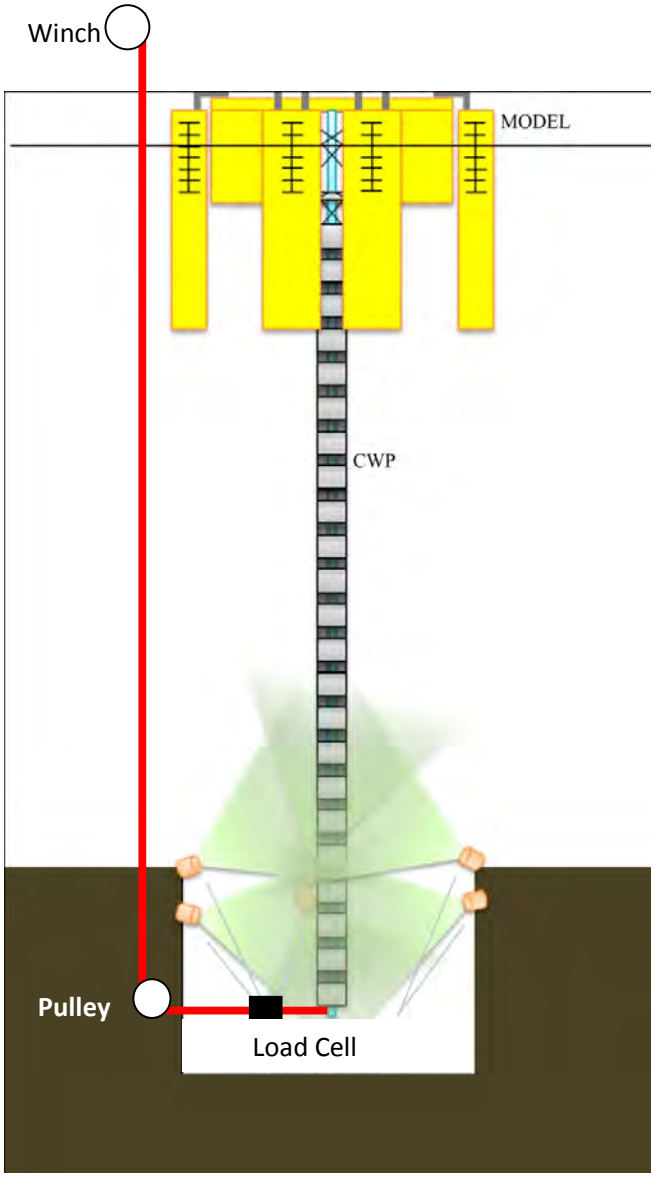

Figure 4-4 - CWP Static Offset Test Setup

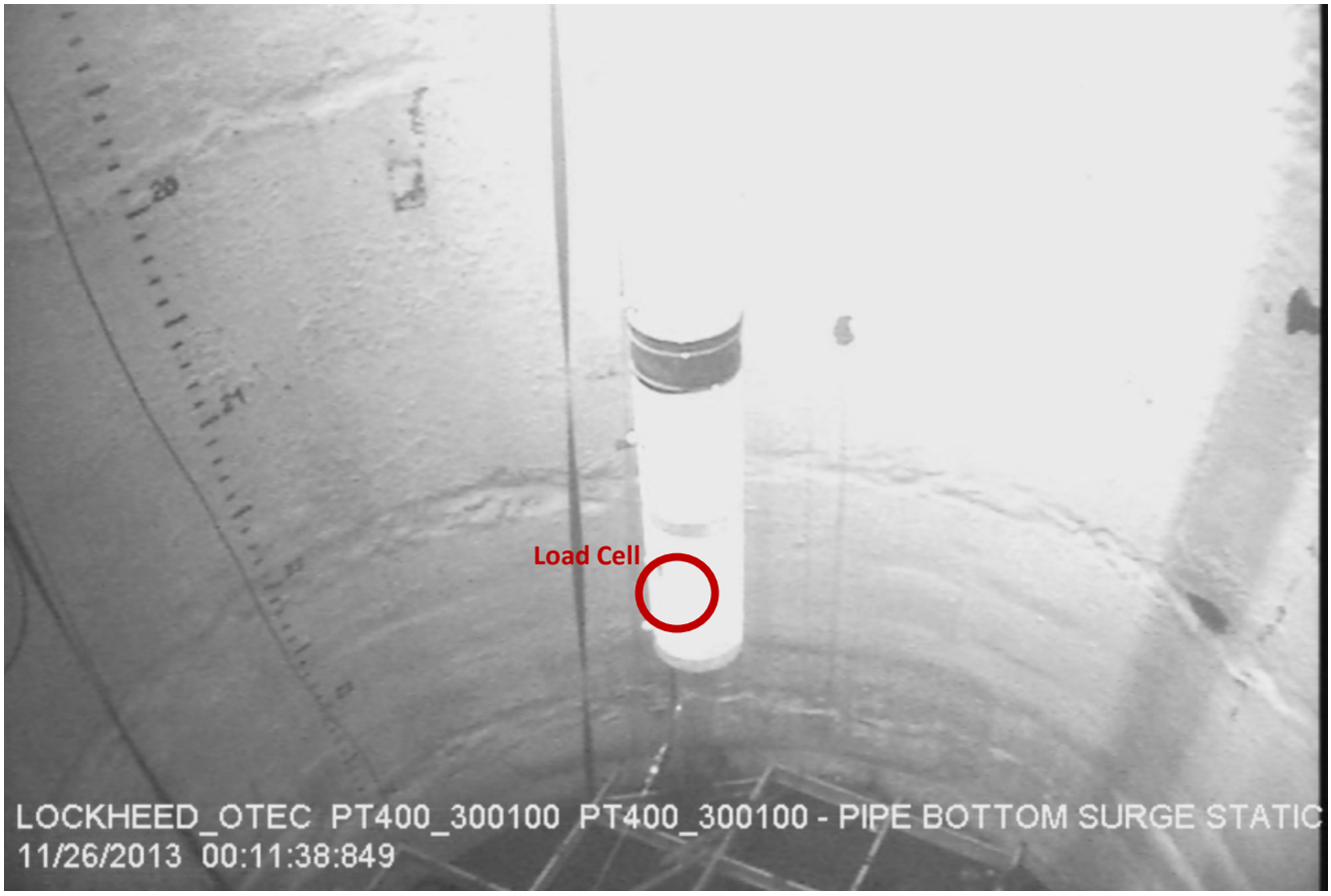

Figure 4-5 - CWP Static Offset Load Cell Fixture

The model was fixed in position by its mooring system only with the stiffness measured on the system identification tests.

4.4 CWP IMPULSE TEST

The CWP model was hit on the bottom in the x direction by a diver with a hammer to provide the necessary excitation. All instrumentation readings were recorded from before the pipe was hit until its movement had decayed.

4.5 INCLINING LVDT CHECK TESTS

Similar procedure to the regular inclining test, but with bigger inclining weights.

4.6 FREE-DECAY TESTS

Two different setups were used for the free-decay test.

For the Surge, Sway and Yaw tests, the procedure was similar to the mooring pullout tests, but after the model stabilized at the maximum offset the cable was released at the pulley end.

For the Heave, Roll and Pitch tests the initial offset was imposed by a stick pushing the deck downward on the center, bow and portside respectively.

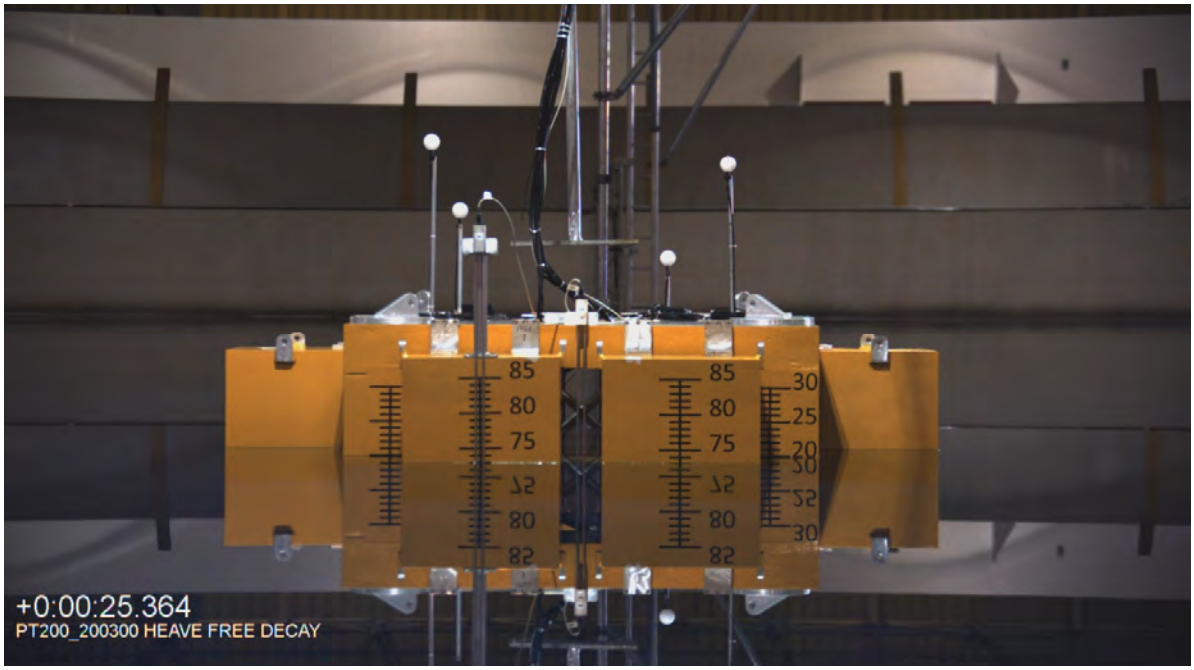

Figure 4-6 - Heave Free Decay with Stick

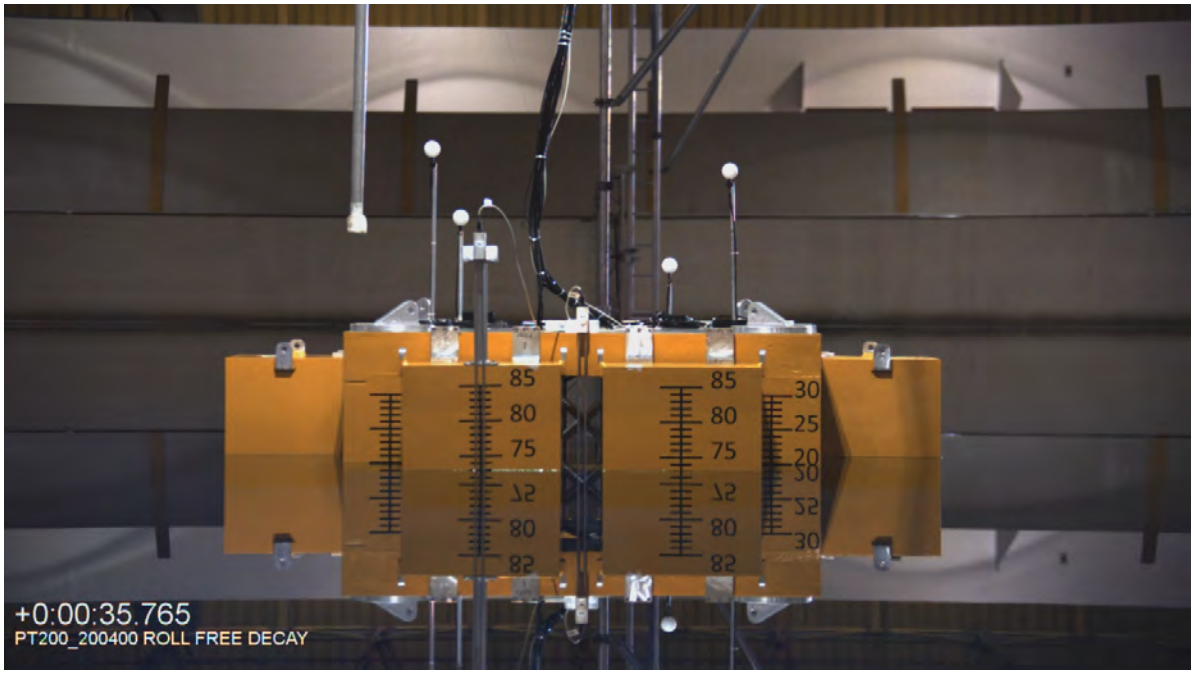

Figure 4-7 - Roll Free Decay with Stick

4.7 WAVE TESTS

The free surface elevation (wave elevation) is measured by conductive wave probes. The positions of these sensors are referred to the inertial reference frame *AXYZ*. The wave elevation reference (zero elevation) is the calm water free surface of the basin (Z=0), positive wave up.

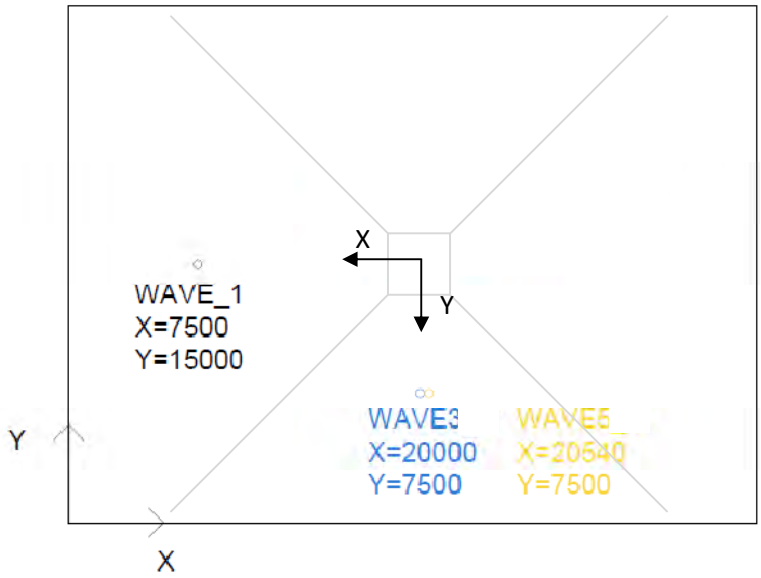

Figure 4-8 - Wave probes set-up

The model is installed fully instrumented and with mooring in place and equalized on the beginning of each day.

5 INSTRUMENTATION AND DATA ACQUISITION

Following is the list of transducers used in the tests:

- Wave height meter from LabOceano and DHI;
- Load cell 6 component (forces and moments) model UDW3-1000 from AMTI;
- VectorNav multisensor VN-100;
- Linear Variable Differential Transformer (LVDT GHS-720-2000);
- Load cell model LSB210, 10 lb and 50 lb from Futek;
- KYOWA strain gages KFG-2-120-C1;
- Qualisys motion capture system;
- Underwater Qualisys motion capture system;
- FULL-HD camera system;
- Underwater Hydratec Camera MCH-3000;
- ICEL manual regulated power supply PS-5000 and PS-6000;

5.1 MEASURED CHANNELS

The measured channels on the tests and its units are listed on table 5-1. The conversion factor used on the tests data products are also listed.

Table 5-1 - Channel List

Sensor	Channel	Units Model	Units Prototype	Conversion Factor
6-DOF Load Cells	AMTI1_Fx	gf	KN	1.26507957
	AMTI1_Fy	gf	KN	1.26507957
	AMTI1_Fz	gf	KN	1.26507957
	AMTI1_Mx	gf.m	gf.m	1
	AMTI1_My	gf.m	gf.m	1
	AMTI1_Mz	gf.m	gf.m	1
	AMTI2_Fx	gf	KN	1.26507957
	AMTI2_Fy	gf	KN	1.26507957
	AMTI2_Fz	gf	KN	1.26507957
	AMTI2_Mx	gf.m	gf.m	1
	AMTI2_My	gf.m	gf.m	1
	AMTI2_Mz	gf.m	gf.m	1
	AMTI3_Fx	gf	KN	1.26507957
	AMTI3_Fy	gf	KN	1.26507957
	AMTI3_Fz	gf	KN	1.26507957
	AMTI3_Mx	gf.m	gf.m	1
	AMTI3_My	gf.m	gf.m	1
	AMTI3_Mz	gf.m	gf.m	1
	AMTI4_Fx	gf	KN	1.26507957
	AMTI4_Fy	gf	KN	1.26507957
	AMTI4_Fz	gf	KN	1.26507957
	AMTI4_Mx	gf.m	gf.m	1
	AMTI4_My	gf.m	gf.m	1
	AMTI4_Mz	gf.m	gf.m	1
Derived from 6-DOF Load Cells	Gimbal_Fx	gf	KN	1.26507957
	Gimbal_Fy	gf	KN	1.26507957
	Gimbal_Fz	gf	KN	1.26507957
Linear Variable Differential Transformers	LVDT0	mm	m	0.05
	LVDT1	mm	m	0.05
	LVDT2	mm	m	0.05
	LVDT3	mm	m	0.05
Derived from LVDTs	Gimbal_Pitch	Degrees	Degrees	1
	Gimbal_Roll	Degrees	Degrees	1

Uni-Axial Load Cells	Mooring1	gf	KN	1.26507957
	Mooring2	gf	KN	1.26507957
	Mooring3	gf	KN	1.26507957
	Mooring4	gf	KN	1.26507957
	Pullout_Semi	gf	KN	1.26507957
	Pullout_CWP	gf	KN	1.26507957
	Pullout_YAW	gf	KN	0
	Wind	gf	KN	1.26507957
Wave Probes	Airgap	mm	m	0.05
	Runup	mm	m	0.05
	WAVE1	mm	m	0.05
	WAVE3	mm	m	0.05
	WAVE5	mm	m	0.05
	WAVE1_C	mm	m	0.05
	WAVE2_C	mm	m	0.05
	WAVE3_C	mm	m	0.05
	WAVE4_C	mm	m	0.05
	WAVE5_C	mm	m	0.05
Strain Gages	SG1	-	-	5.49070924
	SG10	-	-	5.49070924
	SG11	-	-	5.49070924
	SG12	-	-	5.49070924
	SG13	-	-	5.49070924
	SG14	-	-	5.49070924
	SG15	-	-	5.49070924
	SG16	-	-	5.49070924
	SG17	-	-	5.49070924
	SG18	-	-	5.49070924
	SG19	-	-	5.49070924
	SG2	-	-	5.49070924
	SG20	-	-	5.49070924
	SG3	-	-	5.49070924
	SG4	-	-	5.49070924
	SG5	-	-	5.49070924
	SG6	-	-	5.49070924
	SG7	-	-	5.49070924
	SG8	-	-	5.49070924
	SG9	-	-	5.49070924
Underwater Qualisys Measurement System	CWP1_X	mm	m	0.05
	CWP1_Y	mm	m	0.05
	CWP1_Z	mm	m	0.05
	CWP2_X	mm	m	0.05
	CWP2_Y	mm	m	0.05
	CWP2_Z	mm	m	0.05
	CWP3_X	mm	m	0.05
	CWP3_Y	mm	m	0.05
	CWP3_Z	mm	m	0.05
	CWP4_X	mm	m	0.05
	CWP4_Y	mm	m	0.05
	CWP4_Z	mm	m	0.05
	CWP5_X	mm	m	0.05
	CWP5_Y	mm	m	0.05
	CWP5_Z	mm	m	0.05
	CWP6_X	mm	m	0.05
	CWP6_Y	mm	m	0.05
	CWP6_Z	mm	m	0.05
Qualisys Measurement System	Semi_X	mm	m	0.05
	Semi_Y	mm	m	0.05
	Semi_Z	mm	m	0.05
	Semi_Pitch	Degrees	Degrees	1
	Semi_Roll	Degrees	Degrees	1
	Semi_Yaw	Degrees	Degrees	1
DAQ	Time	s	s	7.07106781

5.1.1 Semi-Submersible 6-DOF Motions

The instantaneous position of the model was measured using the Motion Capture System (MCS - QUALISYS®) which consists on tracking a set of active markers installed on the model through a set of infrared cameras installed onshore the basin.

The recognition of the rigid body is part of the calibration process. In this process a reference position on the rigid body is determined as the center around which the attitude angles are applied. The selected reference position is positioned in the intersection between the deck plane, centerline plane and amidships plane, (x',y',z') = (0,0,19.5)m.

The rotational motions (roll, pitch and yaw) are expressed as Euler angles based on successive rotations of the local system. The yaw angle direction follows the heading angle definition.

5.1.2 WIND TENSION, PULLOUTS AND MOORING LINES TENSION LOAD CELLS

The load cell used to measure the simulated wind, Pullouts and mooring lines tension (fig. 5-1) is the LSB210, 10 lb and 50 lb model (fig. 5-2), this load cell is a submersible version with IP68 protection, and measures tension and compression.

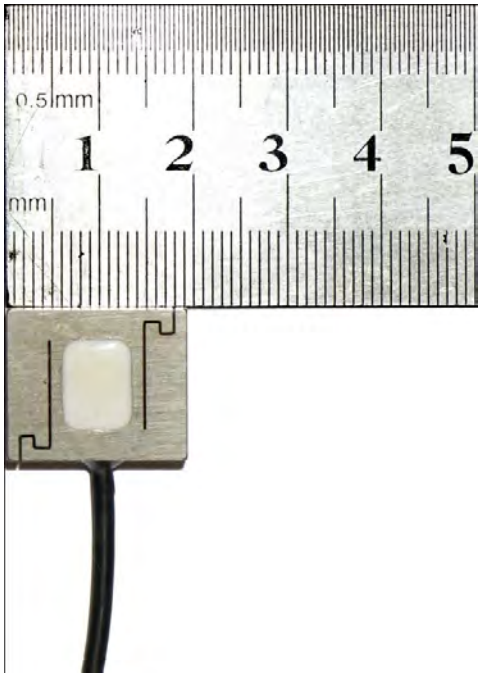

Figure 5-1 - Mooring Load Cell Detail

Figure 5-2 - Mooring Load Cell Installed

5.1.3 Wave Elevations, Air Gap and Run-up

Wave elevations at the basin were measured using inductive wave probes. Relative wave elevation was taken parallel to the O'z'-axis. Initial zero elevation corresponded to Still water.

Part of the wave meters (air gap and run-up) used, as shown in figure 5-3, were made in LabOceano. Its manufacturing followed the patterns of wave probes of the DHI Company. The other part (wave height) is from DHI Company (fig. 5-4)

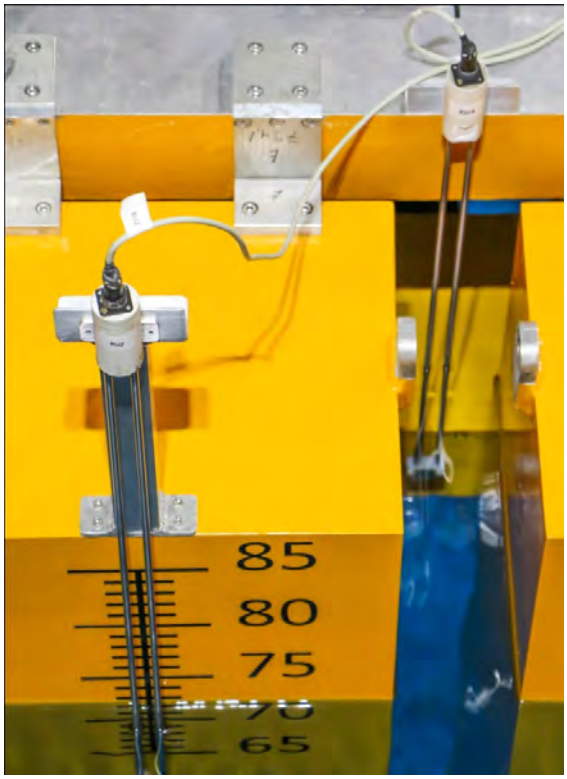

Figure 5-3 Airgap and Runup Installed

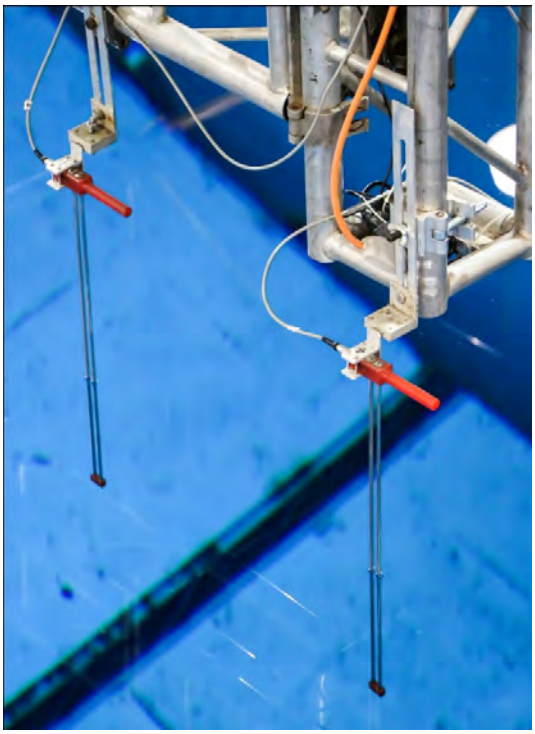

Figure 5-4 - Wave Probes Installed

The wave meters were fed by the DHI conditioner type 102E. Below follows the technical specification.

Wave Amplifier Modules Type 102E & 108

Supply voltage/current	±15 VDC/±16mA
Output voltage	Maximum ±10V (RI>2 kohm)
Output impedance	<1 ohm
Linearity	Better than: 0.1% F.S. (Type 108) / 0.2% F.S. (Type 102E)
Output offset vs temperature	<10 µV/°C RTI
Frequency response	0-100 Hz, -3 dB
Gain ranges	1/1, 1/2, 1/5
Gain adjustment	2.5 times with 10 turn dial
Step response	5 ms
Zero suppression	**Coarse**: ±45% of gauge length **Fine**: ±0.9% of gauge length
Carrier frequency	2,800 Hz
Water conductivity	0.1-1.2 mS/cm at 15°C
Noise on output	<1mV pp
Ambient conditions	10°C to 40°C, <95% non-condensing RH
Connector, gauge	6-pole LEMO
Connector, signal out	BNC on front (or multiconnector on rear side of Type 101E cabinet)
Dimensions and weight	50.6 x 129 x 160 mm; 560 g

Figure 5-5 - DHI Wave Probe Conditioner Specifications

5.1.4 Gimbal Forces

To measure the resultant forces (Fx, Fy, Fz) acting on the Gimbal (fig. 8), was used the force meter type UDW3 - 1000 from AMTI company (fig. 5-6). We use an external power supply PS-6000 to excite all four transducers with 10 V. This transducer was designed for accurate underwater force measurement. It has a fully waterproof design, complete with an internal pressure compensation bladder for accurate underwater measurements. Below follows the UDW3 specifications:

Units: Metric Capacity: 1000

Dimensions(LxDia.)	88.9 x 75.44 mm		
Weight	2.05 Kg.	**Sensing elements**	Strain gage bridge
Channels	Fx, Fy, Fz, Mx, My, Mz	**Amplifier**	Required
Top plate material	Stainess Steel	**Analog outputs**	6 Channels
Temperature range	-17.78 to 51.67°C	**Digital outputs**	None

Channel	Fx	Fy	Fz	Units	Mx	My	Mz	Units
Capacity	2224	2224	4448	N	113	113	56	N-m
Sensitivity	0.674	0.674	0.169	µv/v-lb	33.21	33.21	26.57	µv/v-in-lb
Natural frequency	-	-	-	Hz	-	-	-	Hz
Stiffness (X 105)	210	210	2981	N/m	-	-	0.181	N-m/rad

Figure 5-6 - AMTI UDW3-1000 Load Cell Specifications

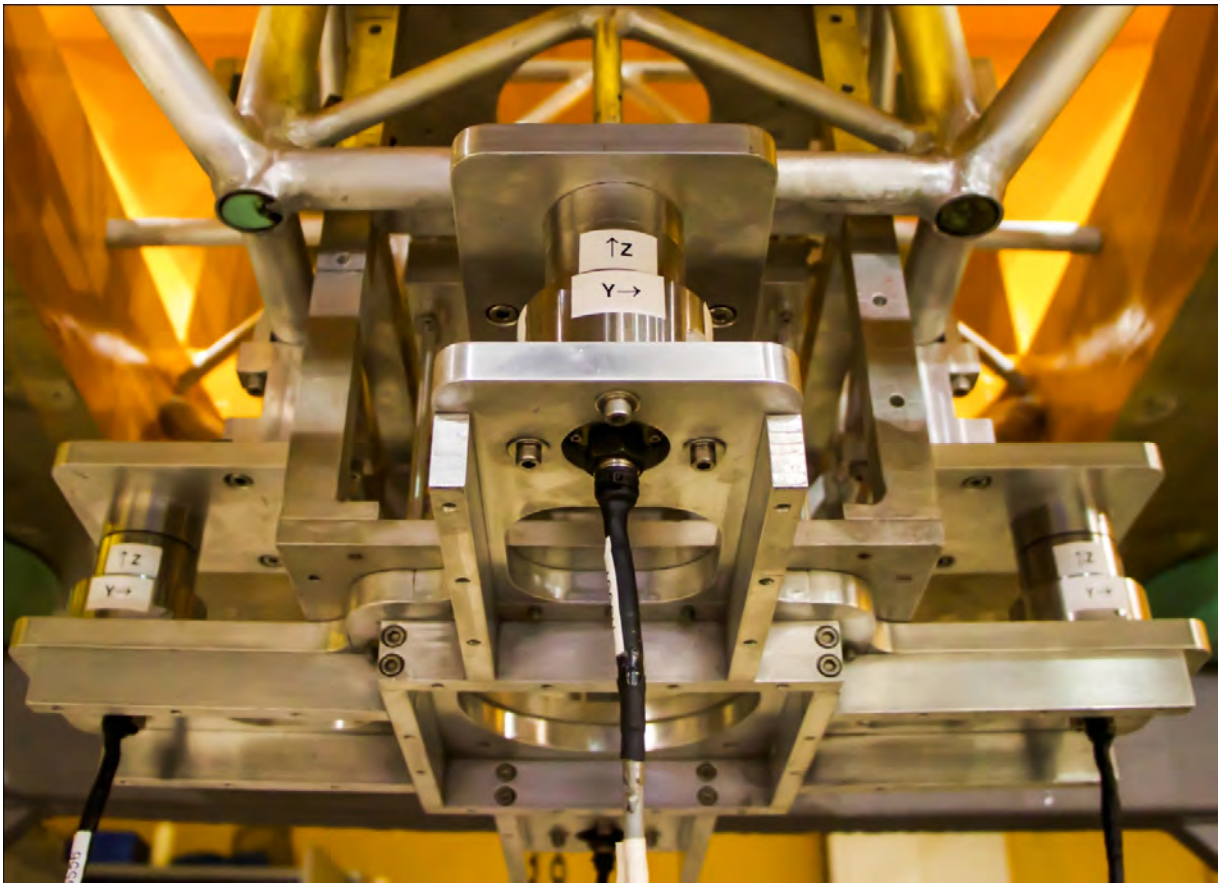

Figure 5-7 - Load Cells Assembly on Gimbal

5.1.5 Gimbal Angle

The LVDT GHS 750 model 2000 (fig. 5-8) provides an extremely reliable solution for a precise linear displacement (position) and gaging measurement. This rugged, hermetically sealed sensor is constructed entirely of stainless steel and has 50 mm range with a maximum linearity error ±0.10% of full range output.

Figure 5-8 - LVDT GHS 750 sensor

With an arrangement of four LVDT´s (fig. 5-9) installed in CWP, we derived through the measured distances, the inclination angles of the CWP.

Figure 5-9 - LVDT sensors Arrangement

5.1.6 Cold Water Pipe Strain

Strain gages are designed to electrically detect “strain”, small mechanical changes occurring in response to applied force. Strain Gages enable detection of imperceptible elongations or shrinkages occurring in structures. For the CWP measurements we used the uniaxial strain gage (fig. 5-10 and 5-11) model **KFG-2-120-C1** from KYOWA a general-purpose foil Strain Gage. The KFG gages use polyimide resin for the base approximately 13 µm thick, ensuring excellent flexibility. Was used the LOCTITE 496 instant adhesive (fig.5-13) for strain gage bonding. For damp proofing was used a protective coating liquid from Quimatic-Tapmatic (fig.5-12).

Below follows the strain gages specifications:

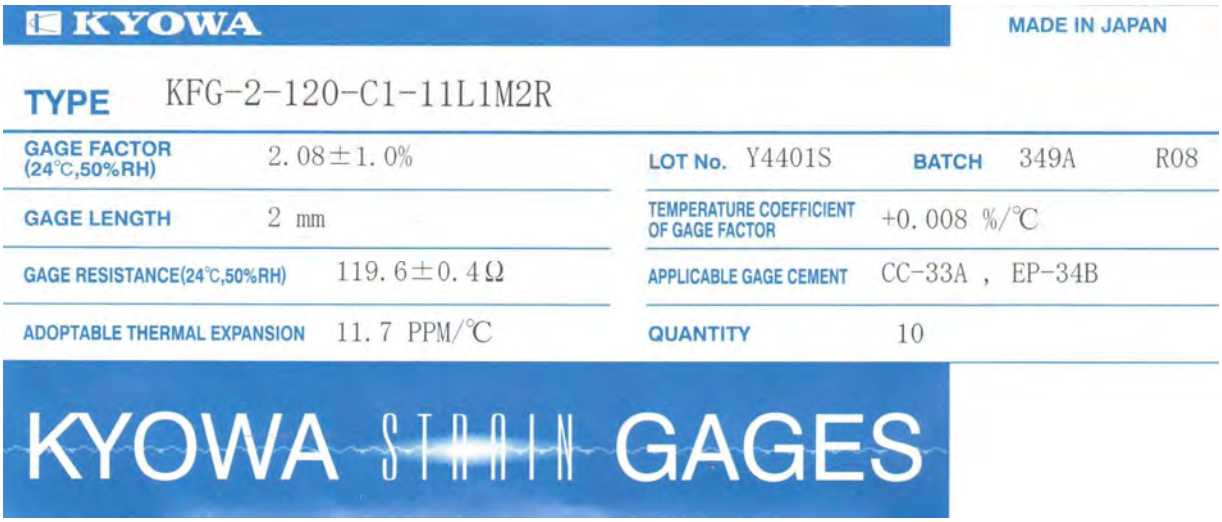

Figure 5-10 - Strain Gages Specification

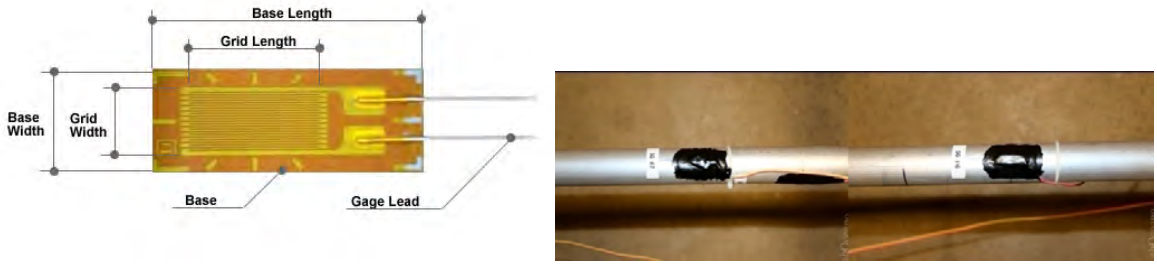

Figure 5-11 - Strain Gage Installation

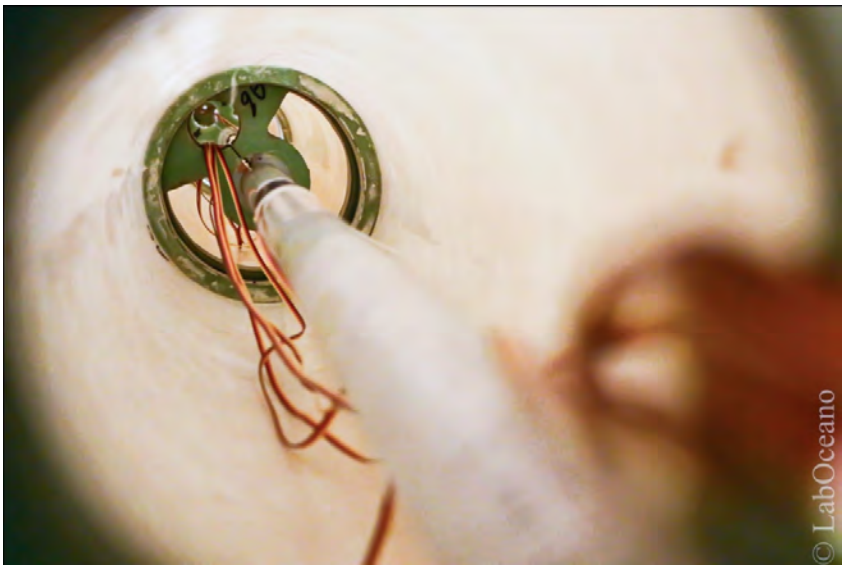

Figure 5-12 - Strain Gages Waterproofing

Figure 5-13 - Strain Gage Adhesive

5.1.7 Cold Water Pipe Motions

For measuring the relative movements of the CWP was used the underwater Qualisys motion capture system. With this system, 6 cameras (fig. 5-14 and 5-15) and 7 passive underwater markers around the tube, we guarantee a highly accurate positioning of the tube.

Figure 5-14 - Underwater Qualisys Cameras

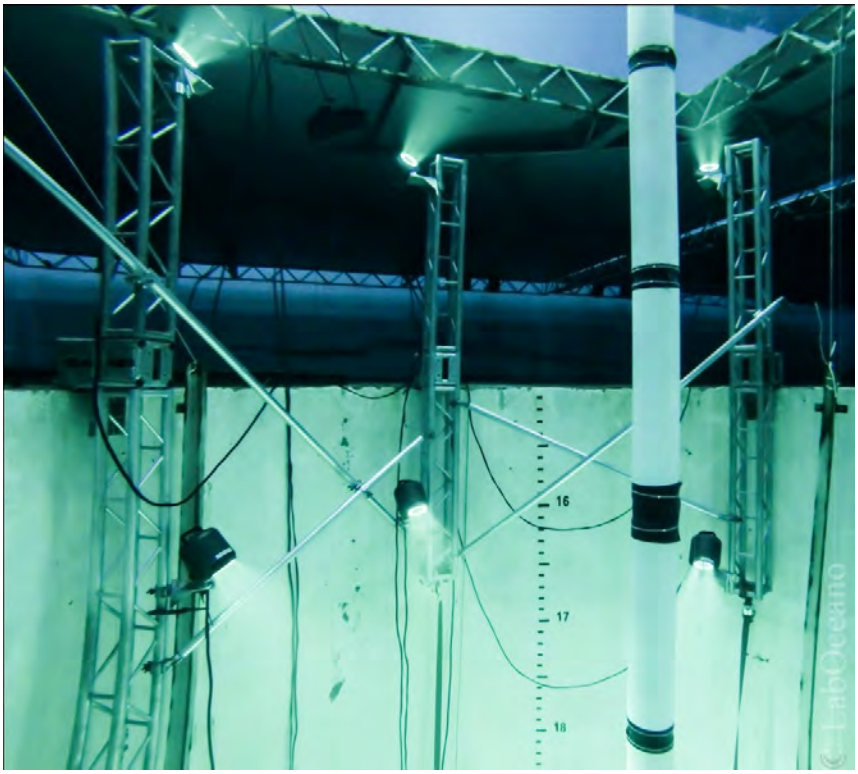

Figure 5-15 - Underwater Qualisys Cameras Setup

5.1.8 INSTRUMENTS LOCATIONS

Below are the positions of the transducers.

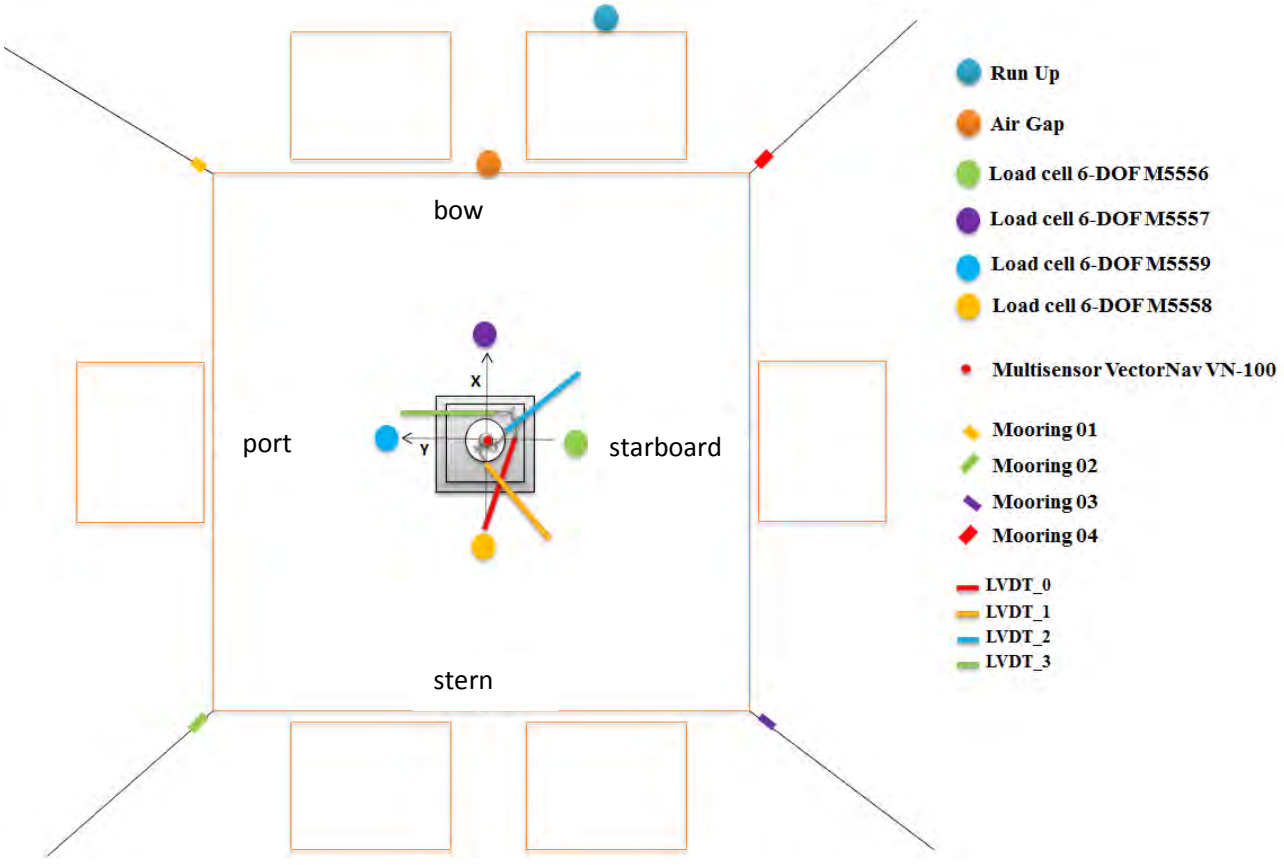

Figure 5-16 - Semi Instrumentation Location

Below are the positions of the strain gages.

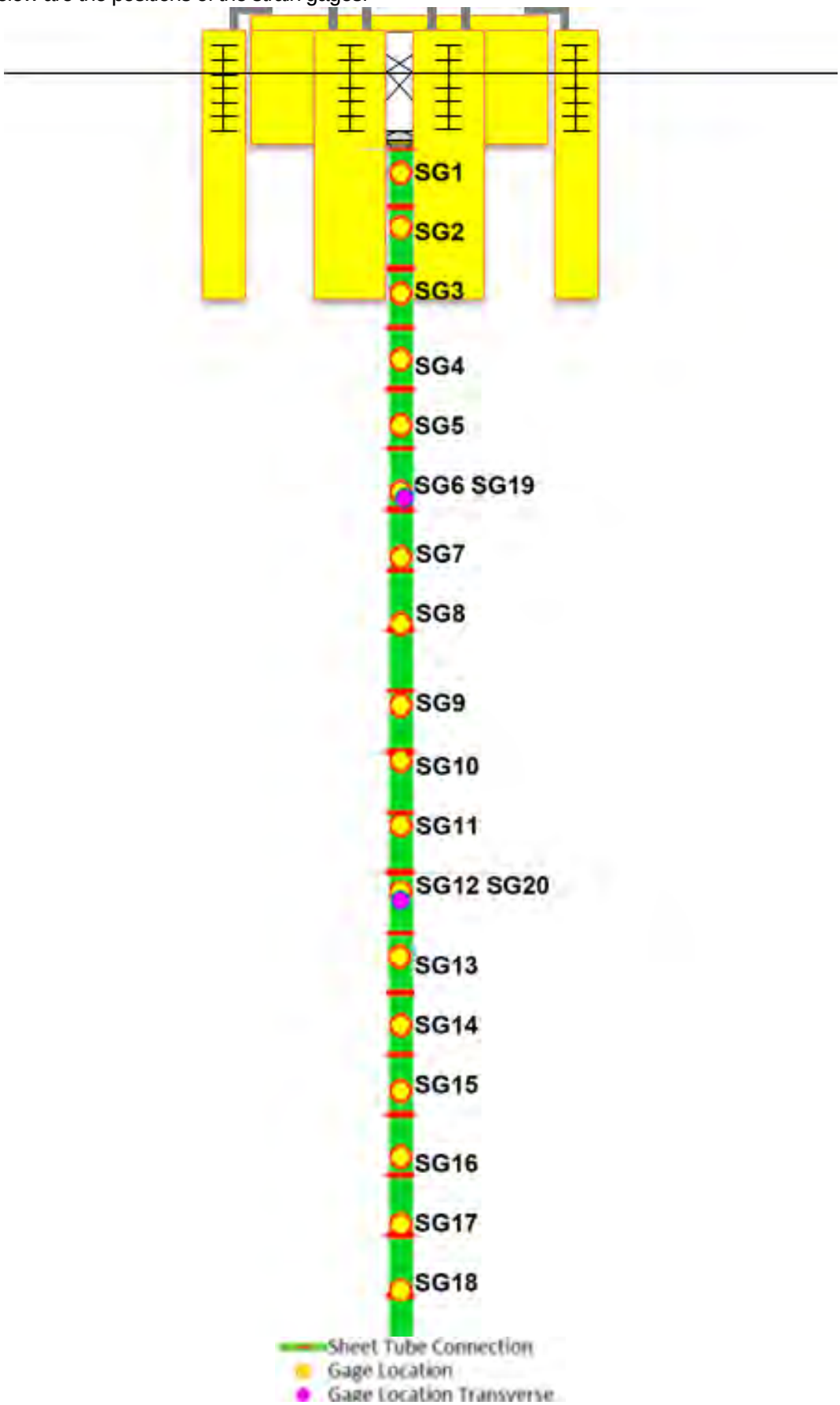

Figure 5-17 - CWP Instrumentation Location

The strain gages position relative to the model reference frame are listed on table 5-2.

Table 5-2 - Strain Gages Location

SG Nº	Proposal #3	Semi Reference Frame o'x'y'z'		
	Model Scale [mm]	Model Scale [mm]	Prototype Scale [m]	
1	19600	-916	-45.8	
2	18700	-1816	-90.8	
3	17600	-2916	-145.8	
4	16500	-4016	-200.8	
5	15400	-5116	-255.8	
6	14300	-6216	-310.8	
7	13200	-7316	-365.8	
8	12120	-8396	-419.8	
9	10780	-9736	-486.8	
10	9880	-10636	-531.8	
11	8800	-11716	-585.8	
12	7700	-12816	-640.8	
13	6600	-13916	-695.8	
14	5500	-15016	-750.8	
15	4400	-16116	-805.8	
16	3300	-17216	-860.8	
17	2200	-18316	-915.8	
18	1120	-19396	-969.8	
19	13330	-7186	-359.3	* in Y dir.
20	6670	-13846	-692.3	* in Y dir.

5.2 INSTRUMENTS CALIBRATION

Each transducer was individually calibrated according the ITTC recommended procedures and guidelines calibration standards, at the LabOceano laboratory to determine each sensor's unique calibration coefficients. During the calibration stage, each of the transducers were digitally compensated to eliminate the known systematic errors due to scale factor and axis-misalignment. The data collected from these tests are used at the laboratory to calculate these coefficients for each individual sensor, and these calibration coefficients are permanently stored in PDF files.

The calibrations sheets are present in 'Annex F: Instrumentation Calibration' in .pdf files, with their accuracy and file names detailed on table 5-3.

Table 5-3 - Instruments Accuracy and Calibration Sheets Index

Channel name / Instrument	Accuracy (model scale)	Reference
Mooring1	7.476 gf	Annex F: Instrumentation Calibration, page 50
Mooring2	4.868 gf	Annex F: Instrumentation Calibration, page 58
Mooring3	4.565 gf	Annex F: Instrumentation Calibration, page 38
Mooring4	2.157 gf	Annex F: Instrumentation Calibration, page 54
Pullout_Semi	3.786 gf	Annex F: Instrumentation Calibration, page 46
Pullout_Semi_reserva	5.291 gf	Annex F: Instrumentation Calibration, page 42
Pullout_CWP	2.094 gf	Annex F: Instrumentation Calibration, page 66
Pullout_CWP_reserva*	3.110 gf	Annex F: Instrumentation Calibration, page 78
Wind	2.026 gf	Annex F: Instrumentation Calibration, page 62
Runup	1.344 mm	Annex F: Instrumentation Calibration, page 32
Runup_reserva	1.604 mm	Annex F: Instrumentation Calibration, page 35
Airgap	0.627 mm	Annex F: Instrumentation Calibration, page 74
Airgap_reserva	1.002 mm	Annex F: Instrumentation Calibration, page 70
WAVE1_C	1.453 mm	Annex F: Instrumentation Calibration, page 20
WAVE2_C	1.048 mm	Annex F: Instrumentation Calibration, page 26
WAVE3_C	0.834 mm	Annex F: Instrumentation Calibration, page 23
WAVE4_C	1.197 mm	Annex F: Instrumentation Calibration, page 17
WAVE5_C	0.931 mm	Annex F: Instrumentation Calibration, page 94
WAVE6_C	1.319 mm	Annex F: Instrumentation Calibration, page 29
LVDT0	0.117 mm	Annex F: Instrumentation Calibration, page 9
LVDT1	0.032 mm	Annex F: Instrumentation Calibration, page 1
LVDT2	0.055 mm	Annex F: Instrumentation Calibration, page 5
LVDT3	0.077 mm	Annex F: Instrumentation Calibration, page 13
Gimbal Forces	~ 5%	Main Report, section 5.3
Gimbal Angles	0.6 º	Main Report, section 3.5.1

(*) Used for the Pullout_YAW channel on the mooring pullout test.

Transducers calibrated in LabOceano:

- Wave meters
- Tension and compression load cells
- LVDT´s

Transducers with factory calibration:

- 6 component (forces and moments) meter
- Vectornav VN-100 multisensor

5.2.1 WAVE HEIGHT, AIR GAP AND RUN-UP METERS

The wave meters calibration was made using a millimetric ruler as shown in figure 5-18. The gauge length of the height meters was 640 mm, and for the air gap and run-up was 900 mm.

The maximum tolerance on calibration was 2 mm of accuracy for all the wave meters.

Figure 5-18 - Wave Meter Calibration

5.2.2 MOORING LINES TENSION LOAD CELLS, PULLOUT AND WIND LOAD CELL

Calibration of the load cells as shown in figure 5-19 was made using calibrated weights.

Figure 5-19 - Load Cell Calibration

5.2.3 LINEAR VARIABLE DIFFERENTIAL TRANSFORMERS (LVDT)

The calibration of the LVDT´S as shown in figure 5-20, was made using Standard Tempered Carbon Steel block, shifting the cursor for each height of the set blocks. The dimensions of these blocks have high accuracy, providing accurate displacement of the cursor. We use an external power supply PS-5000 to excite all four transducers with 20 V.

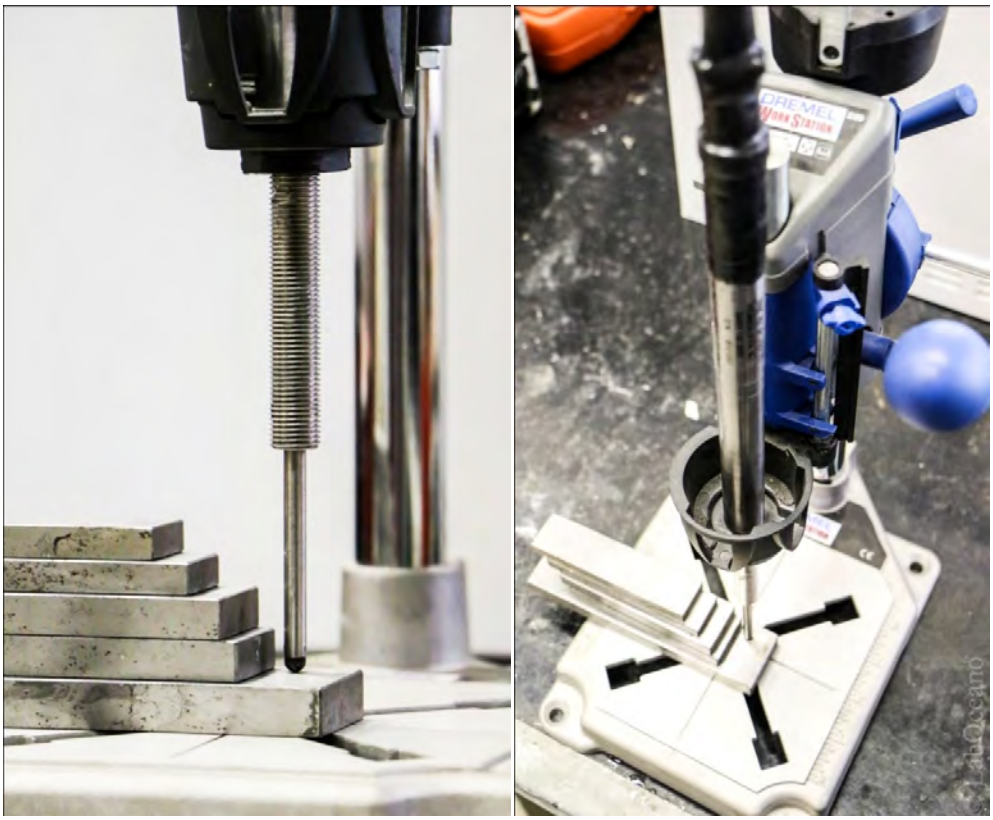

Figure 5-20 - LVDT Sensor Calibration

5.2.4 6 DOF MOTIONS MEASUREMENT

The calibration of the motion capture system uses 16 reference markers fixed on the tank walls, the system knows the position of all the sixteen markers and the nine cameras, with this information it creates a calibrated volume as show in figure 5-21.

Each camera is mounted to see at least 3 reference markers. Example camera 1 view reference markers 1, 2 and 3

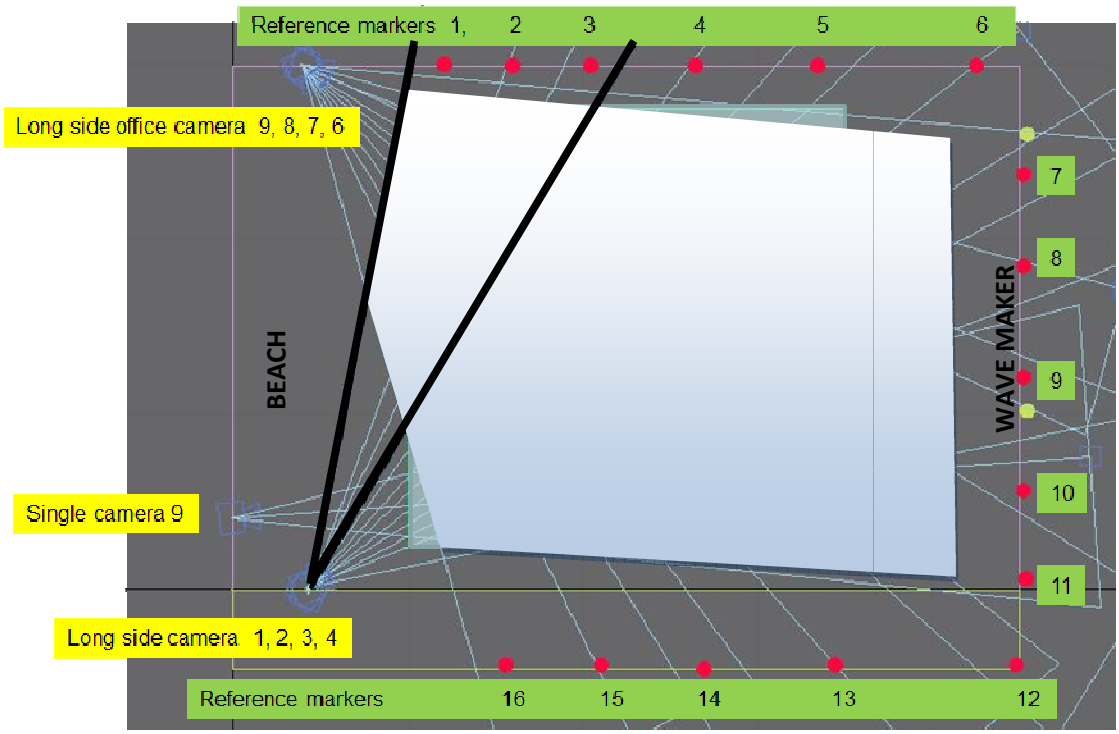

Figure 5-21 - Semi Qualisys System Setup

The calibration was performed successfully on 31 May 2013, as shown in figure 5-22.

Current Calibration

Calibration file:
20130531_150343.qca

Calibration results

Calibration passed

Camera results

Camera	X (mm)	Y (mm)	Z (mm)	Points	Average residual (mm)
01	42323.07	30129.15	1088.59	3	0.51584
02	41951.57	30138.65	1088.35	3	1.16069
03	41582.20	30150.44	1088.02	3	1.58908
04	41214.81	30165.40	1087.95	3	1.69998
05	44952.55	26092.90	1100.51	3	0.85108
06	41163.03	-115.20	1104.86	3	0.27463
07	41529.22	-103.81	1104.28	4	1.80029
08	41899.04	-93.18	1104.09	3	0.49483
09	42269.32	-85.50	1102.21	3	1.85740

Calibration carried out: 2013-05-31 15:03:43

Figure 5-22 - Semi Qualisys System Calibration

5.2.5 UNDERWATER 6 DOF MOTIONS MEASUREMENT

The calibration of the underwater motion capture system uses 7 reference markers fixed on the CWP tube and two groups of 3 cameras, totaling 6 cameras, a higher group and a lower group. The system knows the position of all markers and the cameras, with this information it creates a calibrated volume.

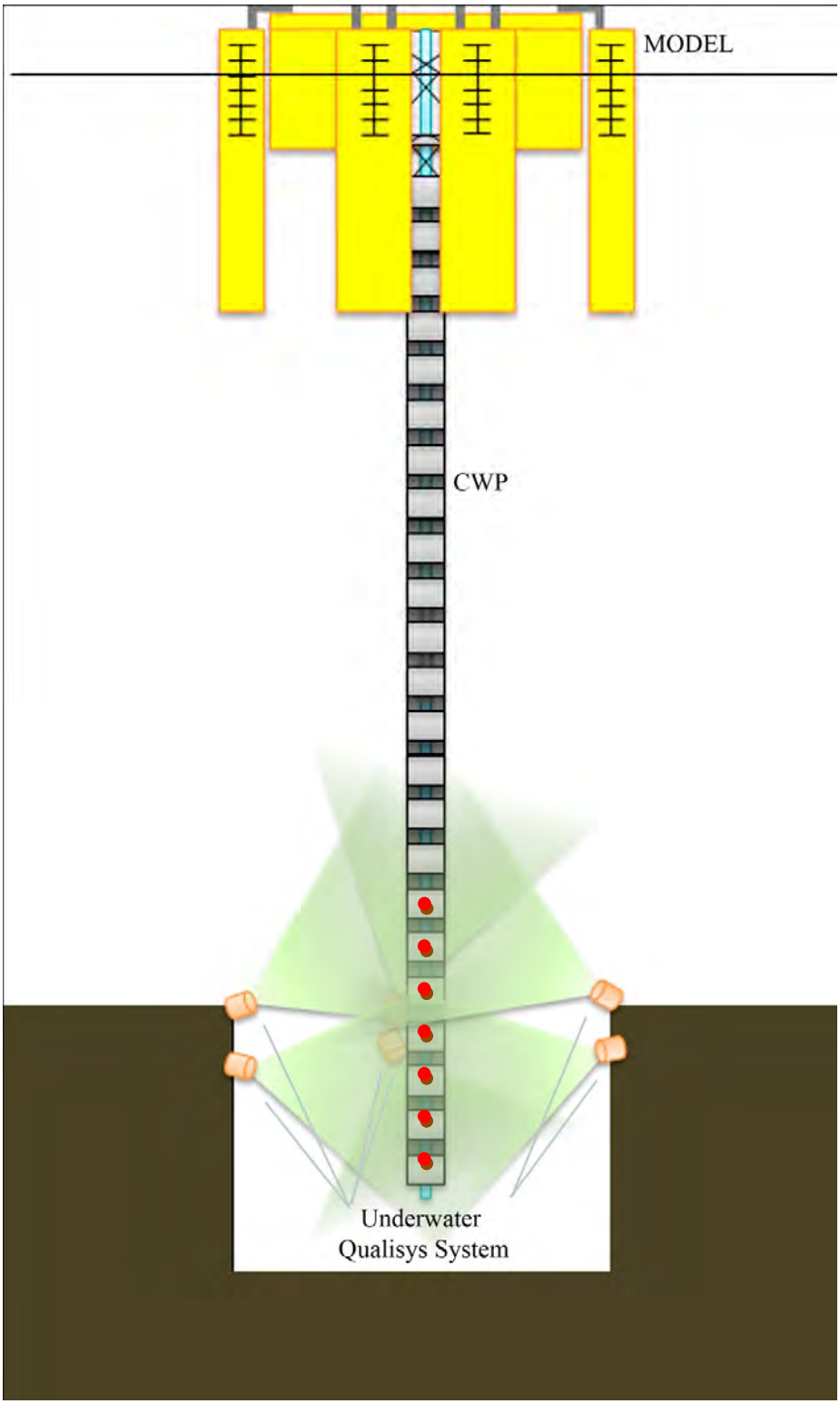

Figure 5-23 - CWP Tracking Targets Setup

For the higher position of the underwater cameras, the calibration was not performed even being installed, because the need of this measurement was discarded, thus, was not used for the tests. For the lower position of the underwater cameras, the calibration was performed successfully on 13 November 2013, as shown in figure 5-24.

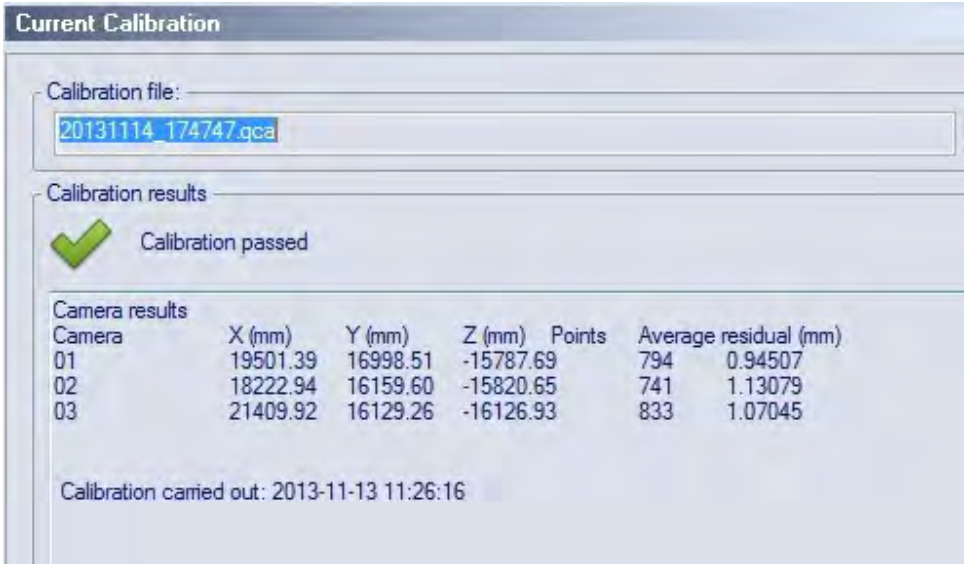

Figure 5-24 - CWP Qualisys System Calibration

5.3 GIMBAL DYNAMOMETER

The assembly of four (4) 6dof load cells into a single force plate structure to measure the gimbal loads was verified by a cross-talk check procedure. Known forces were applied in each pure direction (X,Y,Z) at specific points on the aluminum structure to verify that there is no readings on the other directions.

To perform this test, three (3) points were selected to apply the known forces in each direction and (02) two levels of force will be applied in each direction: Maximum expected force and ½ of the Maximum expected force. The known forces will be applied on the structure using a cable connected to a pulley and weight.

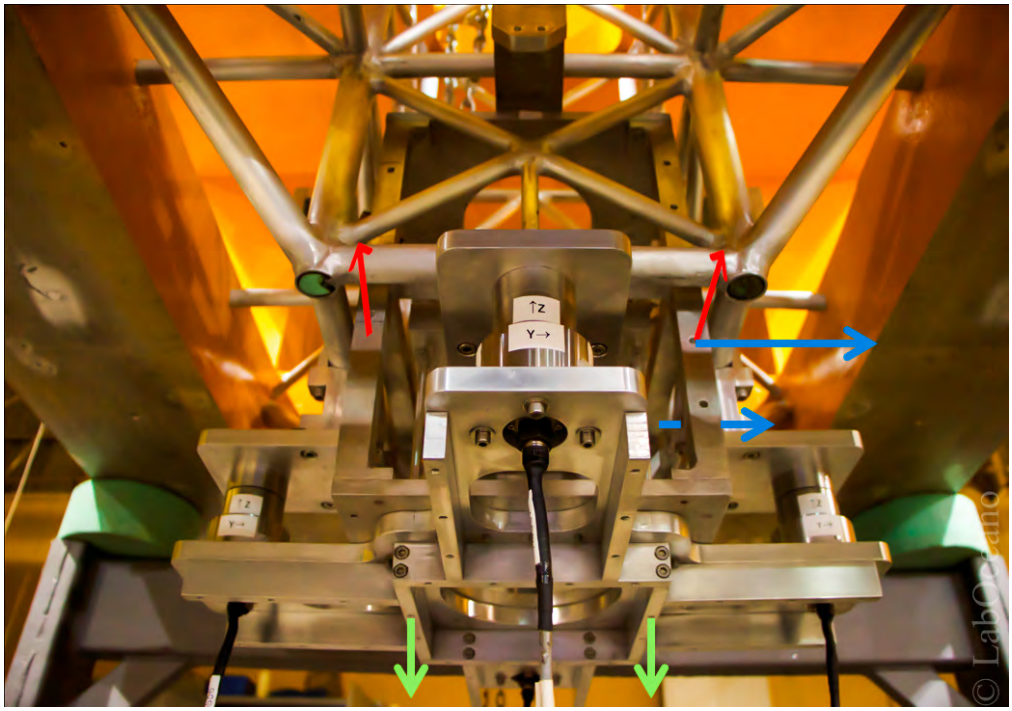

Figure 5-25 - Cross Talking Test Procedure

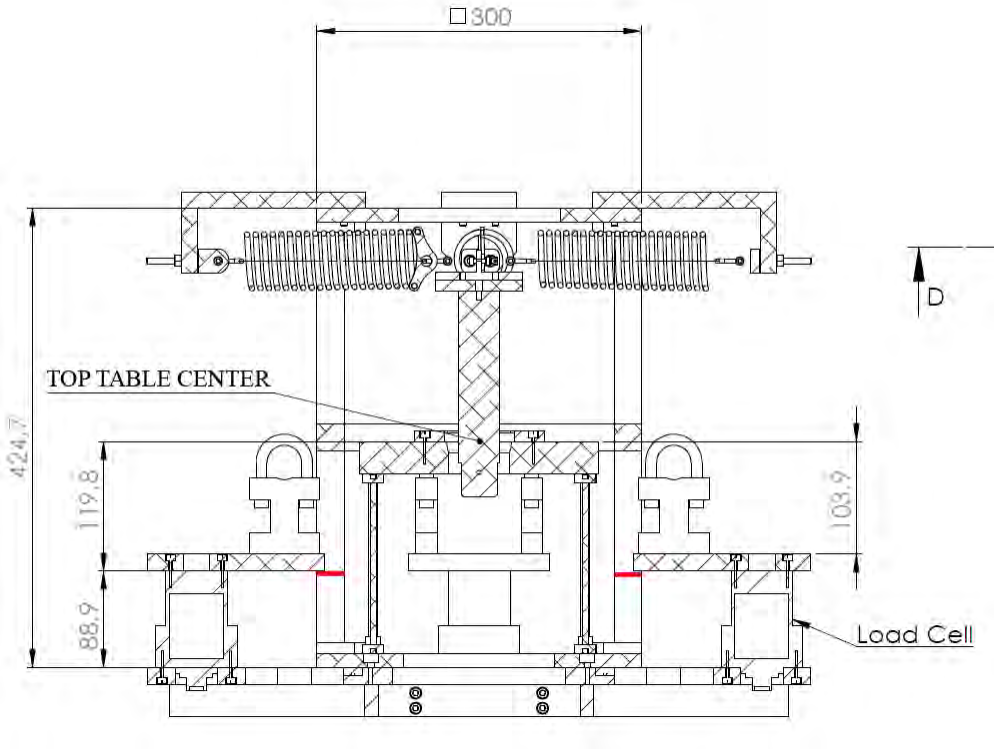

Figure 5-26 - Force application positions

Table 5-4 - Cross Talking Test Setup

	Max Force [kgf]	½ Max Force [kgf]	X [mm]*	Y [mm]*	Z [mm]*
Force in X direction	10	5	150	0	120
Force in Y direction	10	5	0	150	120
Force in Z direction	25	12.5	0	0	209

- Reference: Top table center

The summary of the results are presented on table 5-5.

Table 5-5 - Cross Talking Test Results Summary

	Direction of applied load		
Applied Force (zero offset) - Stage 1	x	y	z
Measured Fx / Applied Load (%)	**95.98**	4.46	-1.20
Measured Fz / Applied Load (%)	-3.40	**95.40**	-0.66
Measured Fz / Applied Load (%)	7.70	3.64	**95.92**
Applied Force (zero offset) - Stage 2	x	y	z
Measured Fx / Applied Load (%)	**97.07**	5.13	-1.49
Measured Fz / Applied Load (%)	-3.84	**97.13**	-0.99
Measured Fz / Applied Load (%)	9.47	3.61	**95.37**
Applied Force (y & z offset) - Stage 1	x	y	z
Measured Fx / Applied Load (%)	**-**	7.65	-1.50
Measured Fz / Applied Load (%)	-	**94.75**	-2.31
Measured Fz / Applied Load (%)	-	3.04	**95.85**
Applied Force (y & z offset) - Stage 2	x	y	z
Measured Fx / Applied Load (%)	**-**	8.45	-1.86
Measured Fz / Applied Load (%)	-	**95.71**	-2.04
Measured Fz / Applied Load (%)	-	4.56	**94.74**

The full report on the cross talk check is presented on 'Annex A: CrossTalkingVerification' document.

After the tests an additional check of the gimbal dynamometer was performed. The gimbal measured forces displayed a mean offset on most tests, for this test the measured force was offset in order to have a starting point of 0 [KN]. Loads were applied in several steps and measured by a pullout load cell. The ratio between the gimbal measured force and the pullout force was then calculated and plotted for part of the test on figure 5-7.

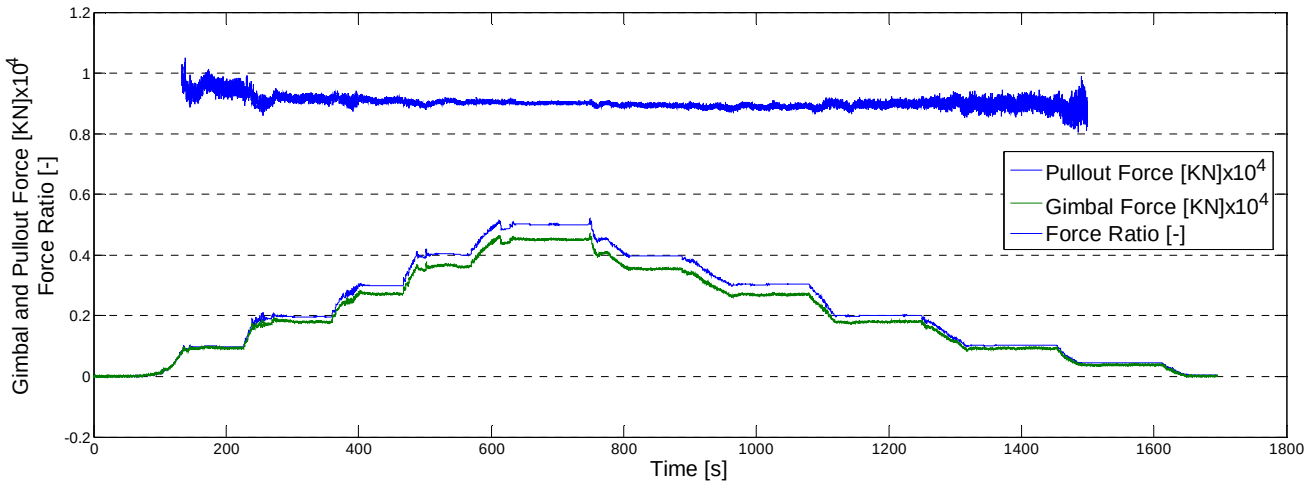

Figure 5-27 - Cross Talking Post-Test Verification

The mean value of the ratio between the gimbal measured force and pullout force was around 90%.

5.4 DATA ACQUISITION

The acquisition system used is manufactured by the National Instruments Company. This system has an acquisition board model PXI-6289, with analog to digital converter of 18 bits, and signal conditioners model SCXI – 1520 with adjustable gain from 1 up to 1000 per channel, and tunable filters of 10 Hz, 100Hz, 1 KHz and 10 KHz per channel, this conditioner was used on all transducers unless the Run up probe and air gap probe, for them were used the signal conditioners model SCXI – 1125 with adjustable gain (1 up to 2000) and filter (4 Hz or 10 KHz). For the tests we used three systems, one in the rack and other two in the instrumentation bridge (closer to the model) as show in figure 5-28. In the figure 5-29, you can see all the cables of the transducers going out from the model.

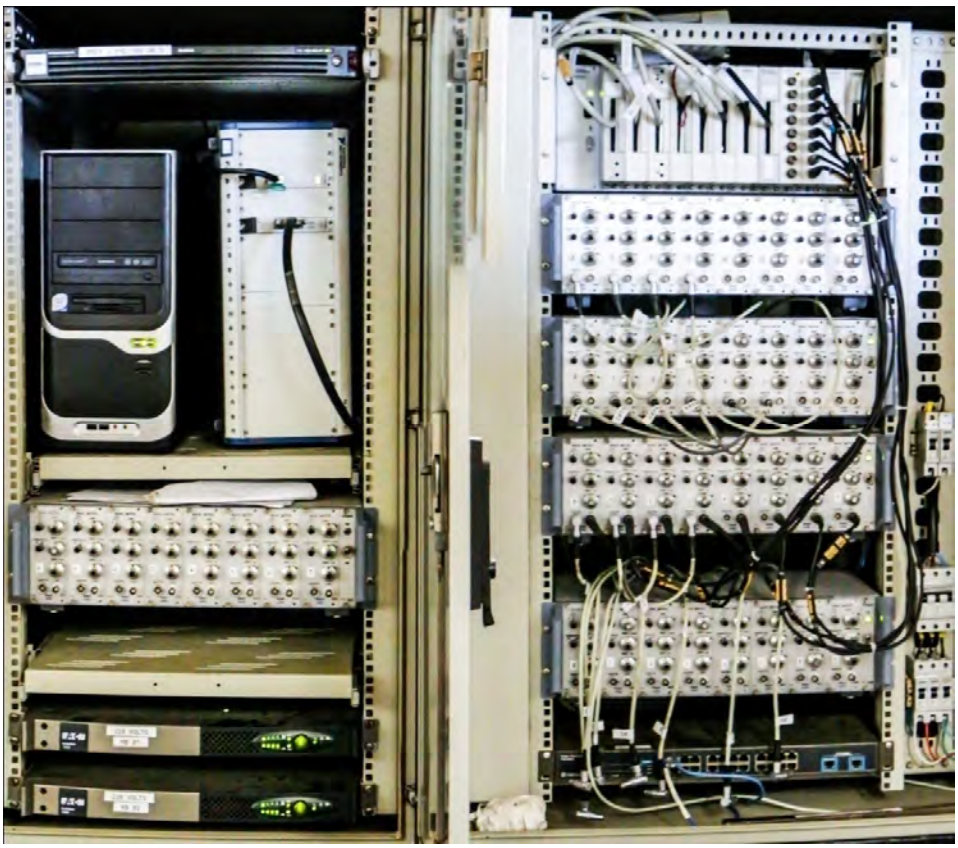

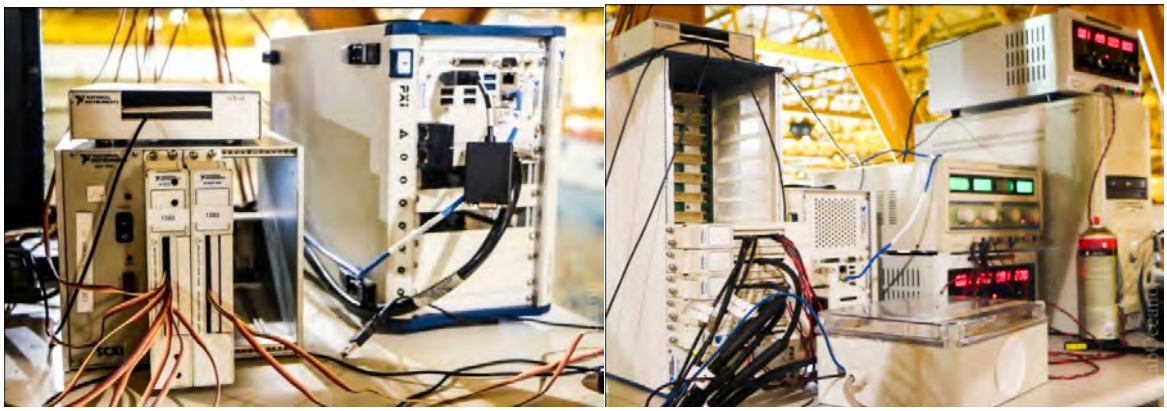

Figure 5-28 - Data Acquisition System

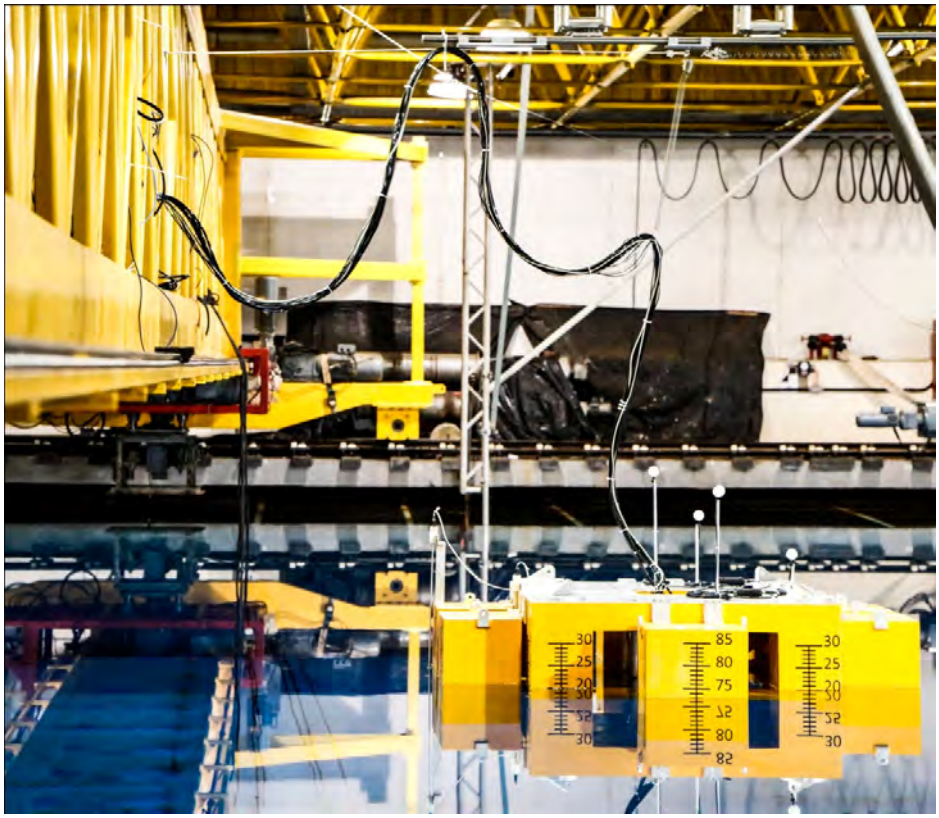

Figure 5-29 - Instrumentation Cables Rigging

For the tests were used four different sampling rates:

- 60 Hz for all transducers;
- 40 Hz VectorNav VN-100;
- 30 Hz Full-HD camera system;
- 29.97 Hz for the underwater SD video recordings.

5.5 FILTERING

For the tests was used only one analog filtering:

- 10 Hz low pass filter for all transducers.

5.6 Video

To film the tests we used a combination of a HD camera with a HD lens (fig. 5-30).

The Prosilica GX1910 is a high-resolution CCD camera with a Gigabit Ethernet interface. The GX1910 incorporates the new True sense KAI-02150 CCD sensor providing excellent image quality in High Definition resolution (1080p). The GX1910 has two screw-captivated Gigabit Ethernet ports configured as a Link Aggregation Group (LAG) to provide a sustained maximum data rate of 240 MBytes per second. The Prosilica GX1910 can also work at half the bandwidth (120 MB/s) using a single cable. We used a HD-Multi-Megapixel lens XD glass with extra low dispersion and motorized iris control, focus and zoom. To acquire a synchronized signal from the cameras, we used the StreamPix 5 (fig. 5-31) from NORPIX. With this software is possible to view, control and acquire from multiple camera simultaneously, all in the same user interface. StreamPix 5 provides a complete management console for cameras, simplifying the setup, control and acquisition from any number and type of camera. The number of digital video camera supported is only limited by a condition wherein the combined

data rate of the cameras exceeds the internal bus bandwidth or processor capabilities of the computer.

Figure 5-30 - HD Camera

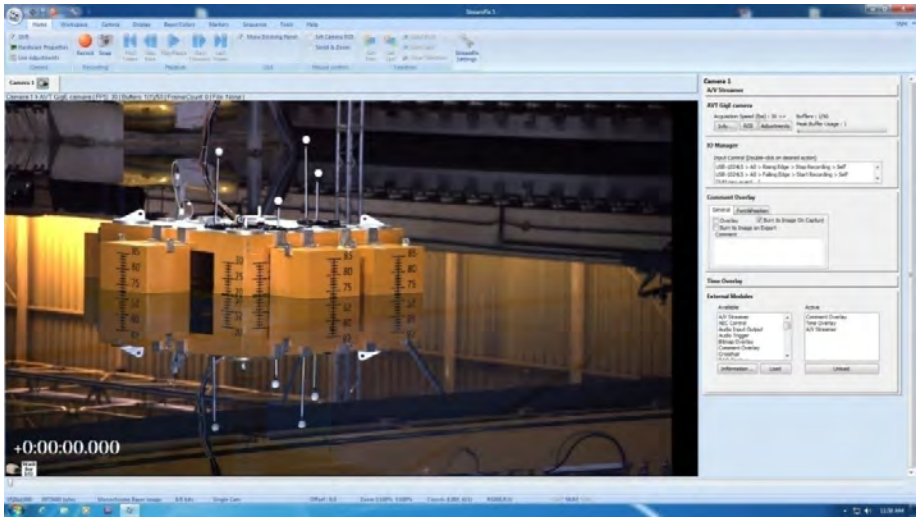

Figure 5-31 - Streampix Video Acquisition Software

5.7 Underwater Video

The MCH-3000 (fig. 5-32) is a CCD Sony Exview HAD ultra-high Sensibility camera with a 530 lines of resolution. The MCH-3000 incorporates underwater connectors and microlens with 6.6 mm, f2.00/ underwater optimized focus 10 cm to 5 m distance. Its operational maximum depth is 100 m. The image signal and the electric supply are transmitted by a single coaxial cable. Dimensions: 110mm X 32 mm and underwater weight of 110 gf.

Figure 5-32 - Underwater Camera

5.8 CONTROL AND CHECK ROUTINES

With the instrumented model on the test site in the basin, function tests were performed to check the complete instrumentation chain, the channel identity, sign convention and the measuring level. Immediately after each test, inspection of control signals and time series for all channels was, in general, performed on a data screen (fig. 5-33). From left to right respectively: first screen (mooring lines, wave probes, pullouts load cells), second screen (6 DOF load cells, LVDT´s), third screen (all strain gages), fourth screen (wave generator control), fifth screen (Qualisys system), sixth screen (VectorNav VN-100), seventh screen (underwater Qualisys system), eighth, ninth and tenth screen (Videos), eleventh (underwater video).

Before each sequence of tests, all procedures check were repeated. Due to possible damage on damp proofing treatment or on the excitation cables, some transducers presented suspect behavior, not measuring correctly values during the verifications but only after some mounting procedures. Thus, these were replaced by their respective replacements before sequence tests.

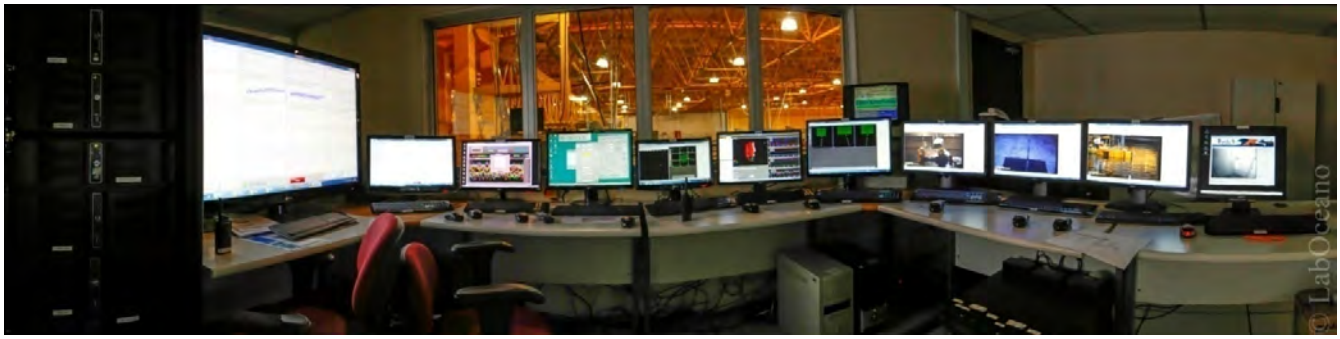

Figure 5-33 - Data Monitoring Screen

Note: During the gimbal assembly for the T600 test group the LVDT sensors were removed and reinstalled, so the standard gimbal angle calibration may not apply for the T600 and T500 test groups.

5.9 ENVIRONMENTAL CALIBRATION

5.9.1 WAVE CALIBRATION

During wave calibration tests, wave elevations are measured at three basin locations (X, Y) – see Figure 5-34. The time record of each of these points are stored in its respective data channel– see list on table 5-6.

The free surface elevation (wave elevation) is measured by conductive wave probes. The positions of these sensors are referred to the inertial reference frame *AXYZ*. The wave elevation reference (zero elevation) is the calm water free surface of the basin (Z=0), positive wave up.

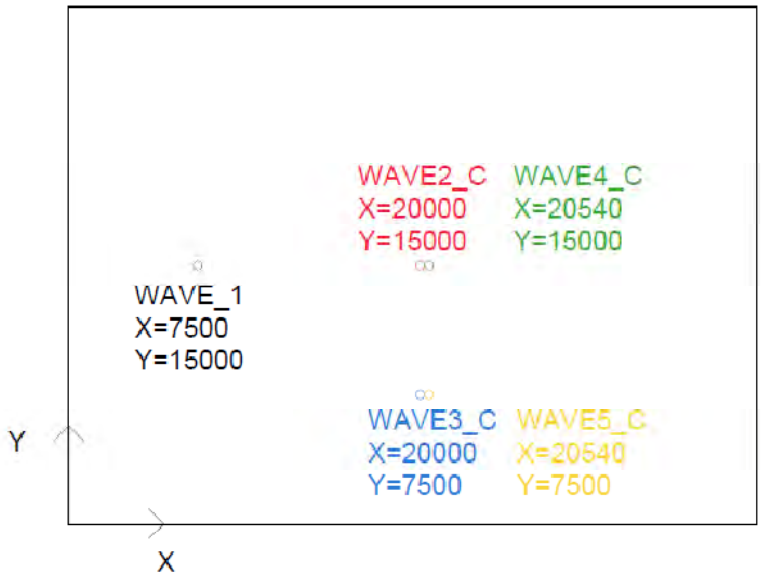

Figure 5-34 - Wave probes set-up

Table 5-6 - Wave Probes Location

Channel name	Units	Measured parameter	Measured point	Description
WAVE1_C	mm	Instantaneous wave elevation (free surface of the basin)	X1 = 7500mm Y1 = 15000 mm	Synchronism channel for the waves
WAVE2_C	mm	Instantaneous wave elevation (free surface of the basin)	X2 = 20000 mm Y2 = 15000 mm	Incident wave channel at model LCG position.
WAVE3_C	mm	Instantaneous wave elevation (free surface of the basin)	X3= 20000 mm Y3= 7500 mm	Phase wave channel for 180° wave incidence
WAVE4_C	mm	Instantaneous wave elevation (free surface of the basin)	X4 = 20540 mm Y4 = 7500 mm	Incident wave channel at model estimated equilibrium
WAVE5_C	mm	Instantaneous wave elevation (free surface of the basin)	X5 = 20540 mm Y5 = 7500 mm	Phase wave channel for model estimated equilibrium

5.9.2 WIND

The wind forces will be simulated by weights, so there will be no acquisition channels during calibration

5.9.3 METOCEAN BATTERIES NOMENCLATURE

The three (03) initial characters of the name of each metocean condition correspond to the battery identification, and the following five (05) characters to each individual condition. The nomenclature for the name of a metocean condition obeys the following logic:

For Wave Files:

XYY_abbjj

Where:

XYY : battery identification

a : wave incidence angle identifier, referred to wave maker reference (1 = 180°) for irregular waves

bb : number of the metocean condition (01, 02, 03, ...)

jj : repetition number of the metocean condition (00, 01, 02, ...)

For Wind Files:

XYY_aabbb

Where:

XYY: battery identification

aa: wind load identification (10 – without remoras, 20 – with remoras)

bbb: number of metocean condition (100 – 100yr cyclone, 200 – 10yr sea, 300 – 10yr swell, 400 – fatigue, 500 – white noise).

The metocean batteries nomenclatures are described in table 5-7:

Table 5-7 - Batteries Nomenclature

CODE	DESCRIPTION
X = type W	WAVE
X = type V	WIND
YY = subtype W01	REGULAR WAVES
YY = subtype W02	IRREGULAR WAVE WITH STANDARD SPECTRUM
YY = subtype W05	WHITE NOISE
YY = subtype V01	CONSTANT WIND

5.9.4 METOCEAN BATTERIES

The batteries names for the metocean conditions are described in table 5-8:

Table 5-8 - Metocean Batteries

BATTERY	DESCRIPTION
W02	IRREGULAR WAVES
W05	WHITE NOISE
W01	REGULAR WAVES
V01	CONSTANT WIND

5.9.5 SPECIFIED TEST WAVES

Table 5-9 - Wave program – Irregular and white noise – PROTOTYPE SCALE

WAVES								
GROUP	FILE	IDENTIFICATION	SPECTRUM	HEIGTH (m)	PERIOD (s)	GAMA	DIR	DURATION* (s)
W02	W02_20100	100 YR CYCLONE	JS	10.2	12.8	2	180	12781
W02	W02_20200	10 YR SEA	JS	4.2	8.3	1	180	12781
W02	W02_20300	10 YR SWELL	JS	3.8	15.7	6	180	12781
W02	W02_20400	FATIGUE WAVE	JS	2.5	16.6	6	180	12781
W05	W05_50100	WHITE NOISE	WN	2.0	2-26	-	180	4300

(*) Acquisition time – 3,0h sea state + 0,5h transient motions + 181sec first wave hitting time, Time series realization – 3,0h

Table 5-10 – Wave program – Irregular and white noise – MODEL SCALE

WAVES									
GROUP	FILE	IDENTIFICATION	SPECTRUM	HEIGTH (m)	PERIOD (s)	GAMA	DIR	DURATION Time series (s)	DURATION Wave calibration (s)
W02	W02_20100	100 YR CYCLONE	JS	0.204	1.810	2	180	1527	1808
W02	W02_20200	10 YR SEA	JS	0.084	1.174	1	180	1527	1808
W02	W02_20300	10 YR SWELL	JS	0.076	2.220	6	180	1527	1808
W02	W02_20400	FATIGUE WAVE	JS	0.050	2.348	6	180	1527	1808
W05	W05_50100	WHITE NOISE	WN	0.040		-	180	509	509

Table 5-11 - Wave program – Regular waves – PROTOTYPE SCALE

WAVES								
GROUP	FILE	IDENTIFICATION	SPECTRUM	HEIGTH (m)	PERIOD (s)	GAMA	DIR	DURATION (s)
W01	W01_10100	Regular Wave 1	-	1.5	5.5	-	180	2121
W01	W01_10200	Regular Wave 2	-	2.5	7	-	180	2121
W01	W01_10300	Regular Wave 3	-	3.6	8.5	-	180	2121
W01	W01_10400	Regular Wave 4	-	5.0	10	-	180	2121
W01	W01_10500	Regular Wave 5	-	6.6	11.5	-	180	2121
W01	W01_10600	Regular Wave 6	-	8.5	13	-	180	2121
W01	W01_10700	Regular Wave 7	-	11.3	15	-	180	2121

Table 5-12 - Wave program – Regular waves – MODEL SCALE

WAVES								
GROUP	FILE	IDENTIFICATION	SPECTRUM	HEIGTH (m)	PERIOD (s)	GAMA	DIR	DURATION (s)
W01	W01_10100	Regular Wave 1	-	0.030	0.778	-	180	300
W01	W01_10200	Regular Wave 2	-	0.049	0.990	-	180	300
W01	W01_10300	Regular Wave 3	-	0.072	1.202	-	180	300
W01	W01_10400	Regular Wave 4	-	0.100	1.414	-	180	300
W01	W01_10500	Regular Wave 5	-	0.132	1.626	-	180	300
W01	W01_10600	Regular Wave 6	-	0.169	1.838	-	180	300
W01	W01_10700	Regular Wave 7	-	0.225	2.121	-	180	300

5.9.6 CALIBRATED TEST WAVES

The calibrated regular waves parameters are described on table 5-13.

Table 5-13 - Regular Waves Calibration Parameters

	Wave Height (m)	Wave Period (s)	Analysis Start Period (s)	Analysis End Period (s)	Number of Waves *	Analysis Products File
Regular Wave #1	1.8920	6.3857	349.6643	1768.7098	> 220	W01_10109.pdf
Regular Wave #2	2.5593	7.0009	293.0958	2093.0361	> 250	W01_10201.pdf
Regular Wave #3	3.4584	8.4935	233.5809	2072.1764	> 210	W01_10303.pdf
Regular Wave #4	4.7139	9.9864	227.6884	2089.9719	> 180	W01_10401.pdf
Regular Wave #5	6.1213	11.4862	200.9362	2095.9824	> 160	W01_10501.pdf
Regular Wave #6	8.2489	13.0693	194.9258	2093.0361	> 140	W01_10603.pdf
Regular Wave #7	11.1342	15.0060	269.2898	2110.0066	> 120	W01_10703.pdf
Regular Wave #7*	6.3955	14.9649	162.1632	2121.2025	> 130	W01_10703b.pdf

* Regular Wave #7 was post calibrated with a smaller gain for the test groups with the cold water pipe

The calibrated irregular waves parameters are listed on table 5-14. The analysis window used for all irregular waves were the last 3(three) hours, except for the white noise wave where 1(one) hour was used as the analysis window.

Table 5-14 - Irregular Waves Calibration Parameters

	Wave Height - Hs (m)	Wave Period - Tp (s)	Hmax (m)	m0 (m²)	Data Products File
100 YR CYCLONE	10.4024	12.7031	17.6912	6.7631	W02_20104.pdf
10 YR CYCLONE	4.1582	8.4687	7.5095	1.0806	W02_20206.pdf
10 YR SWELL	3.7829	15.5716	6.7446	0.89438	W02_20304.pdf
FATIGUE WAVE	2.5435	16.6455	4.3342	0.40435	W02_20404.pdf
WHITE NOISE	2.5407	-	-	-	W05_00501.pdf

The calibrated irregular waves spectral density are presented on figure 5-35 through 5-39.

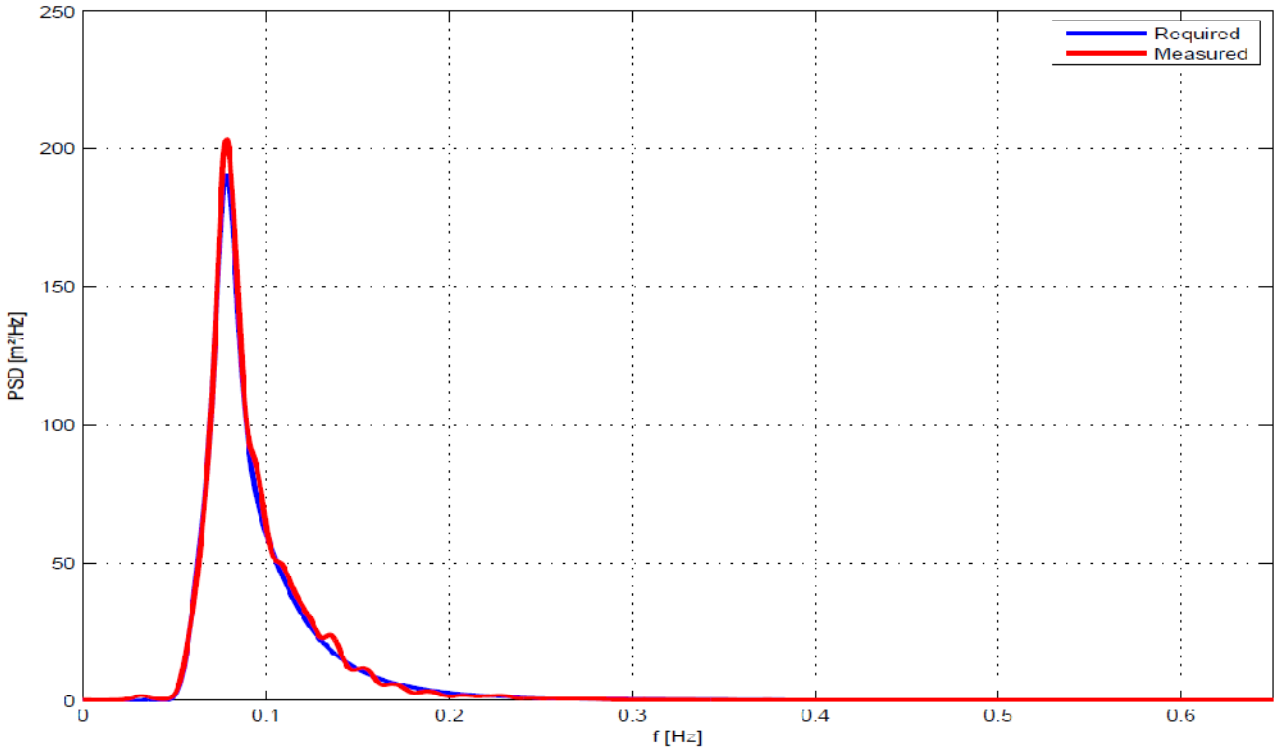

Figure 5-35 - Calibrated 100 year Cyclone Spectral Comparison

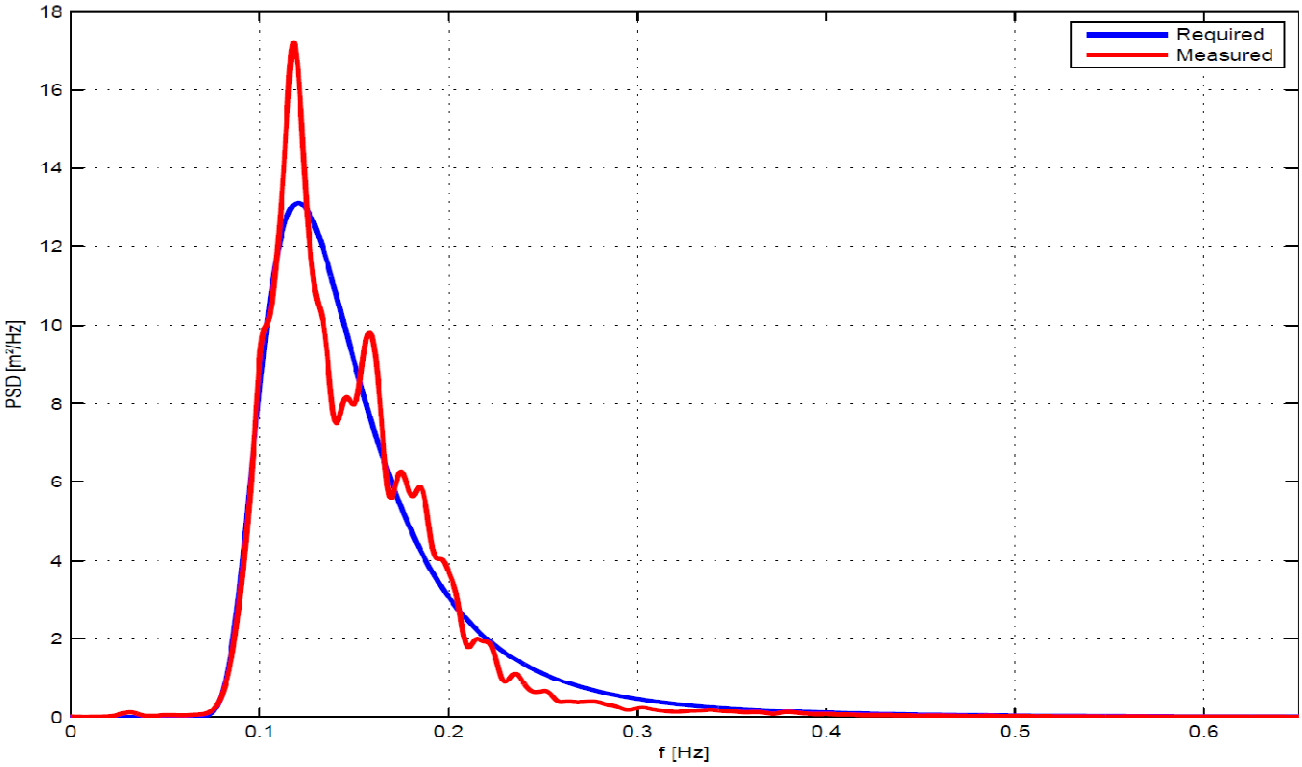

Figure 5-36 - Calibrated 10 year Sea Spectral Comparison

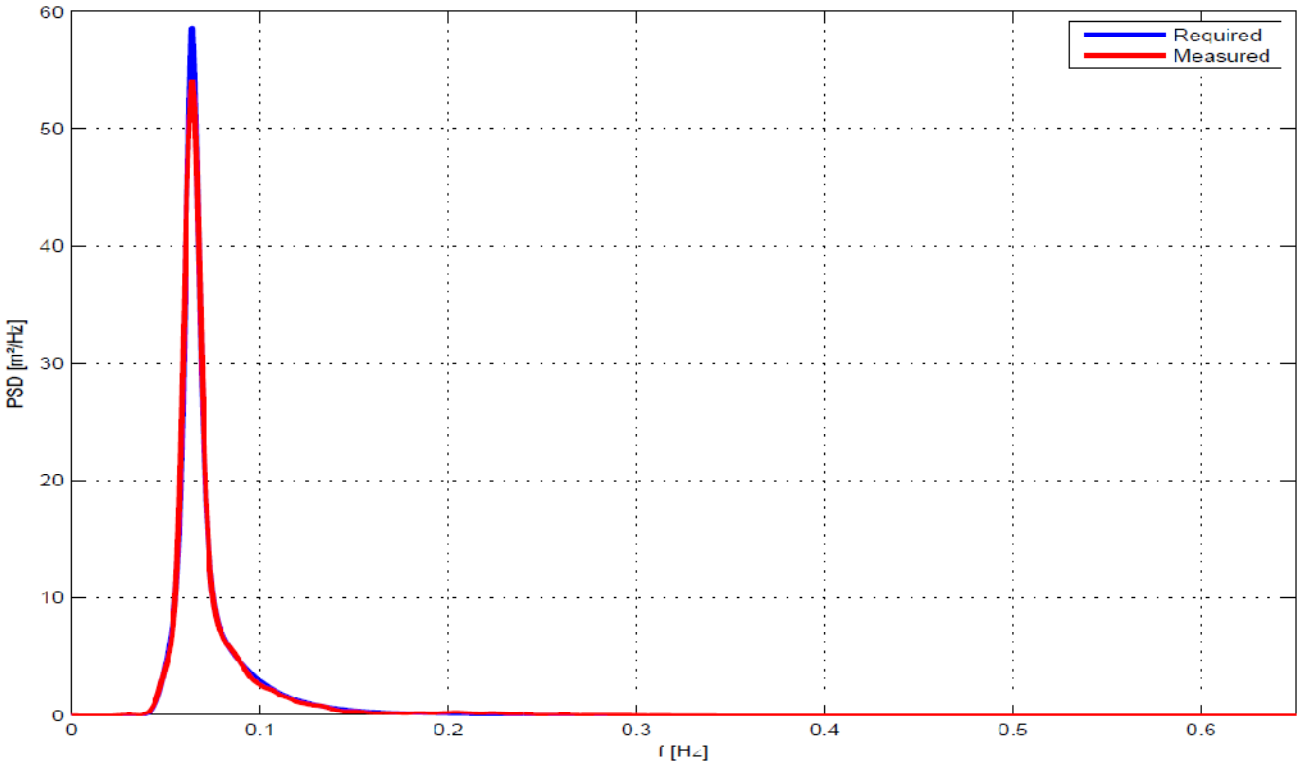

Figure 5-37 - Calibrated 10 year Swell Spectral Comparison

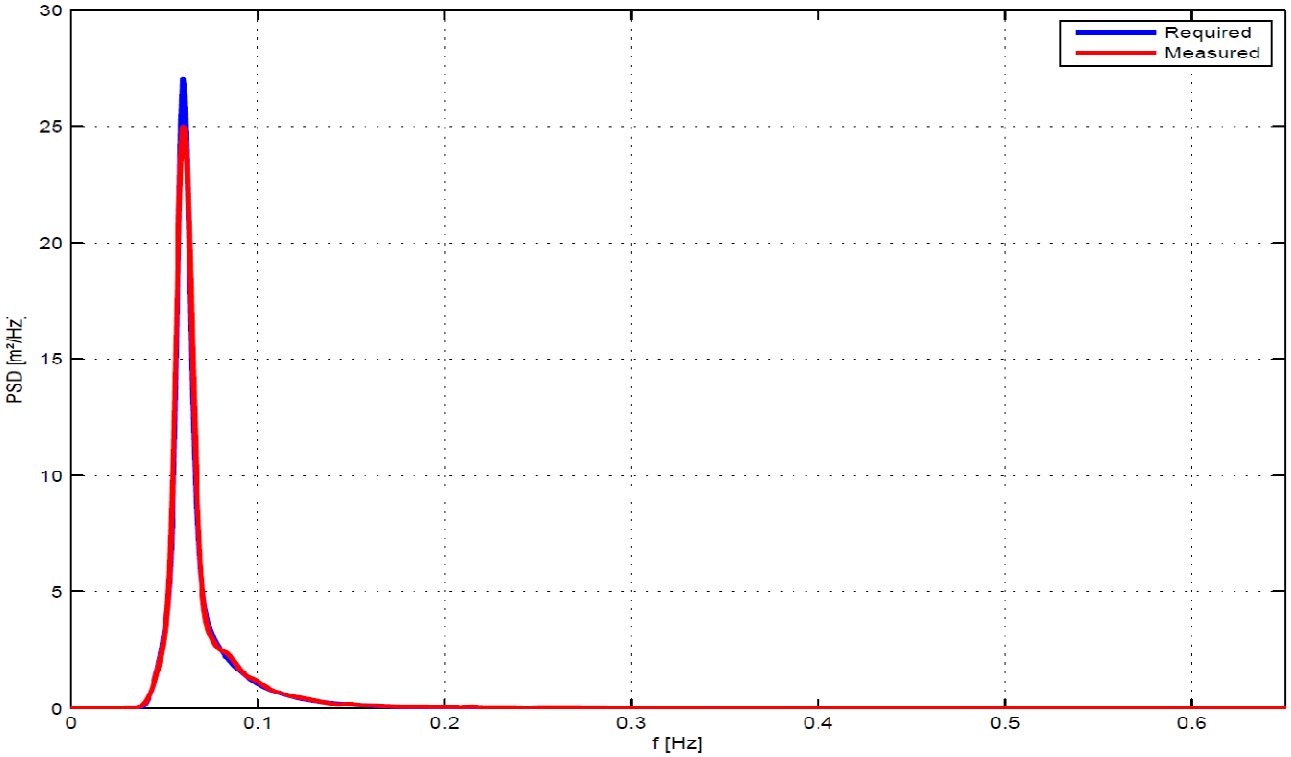

Figure 5-38 - Calibrated Fatigue Wave Spectral Comparison

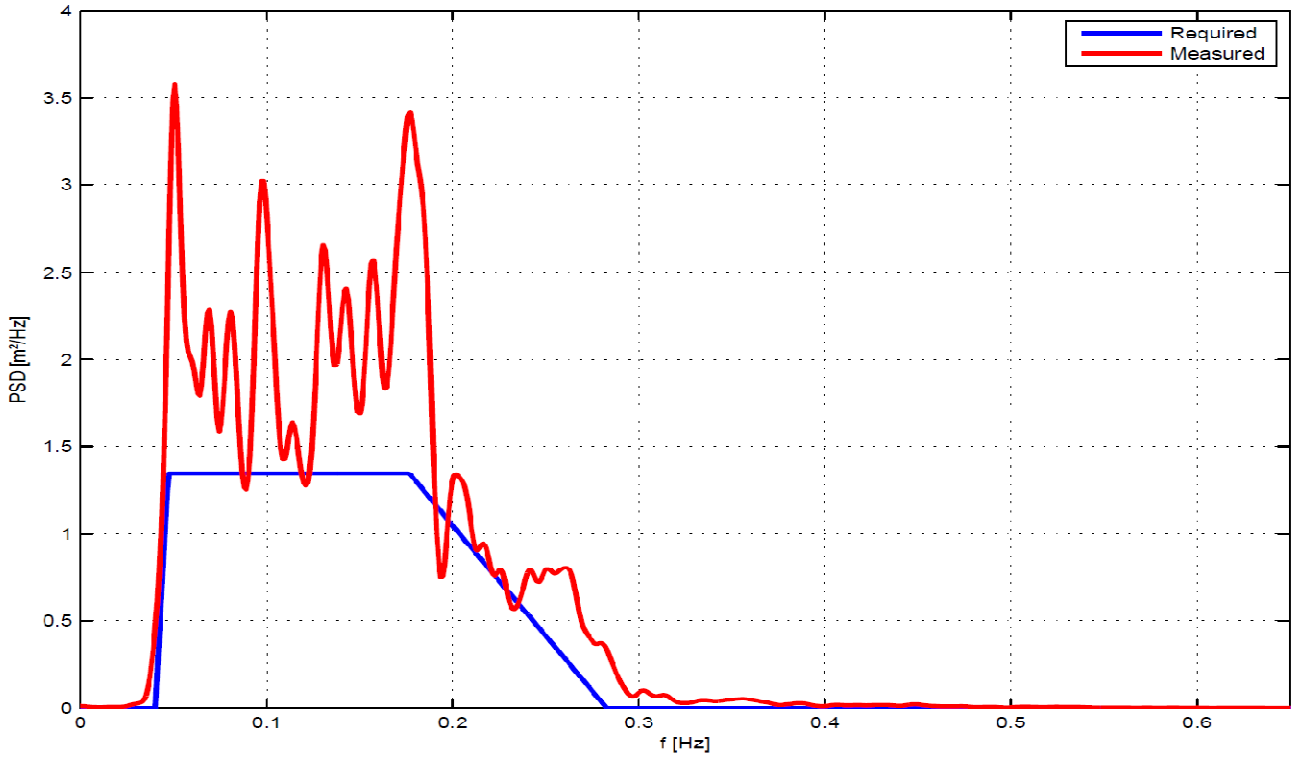

Figure 5-39 - Calibrated White Noise Wave Spectral Comparison

The 10 year sea irregular wave 'W02_20206' has presented a resonant behavior near the paddle generating transverse waves.

Figure 5-40 - Transverse Waves Generated on the 10 year Sea Wave

A null gain on frequencies higher than 0.25Hz was applied to reduce the resonance at the wave paddle, acting as a low pass filter for the input wave. The resonant effect diminished this wave repeatability as may be noticed from wave comparison of WAVE1 and WAVE1_C wave probes channels from different tests for this particular metocean condition shown on figure 5-41.

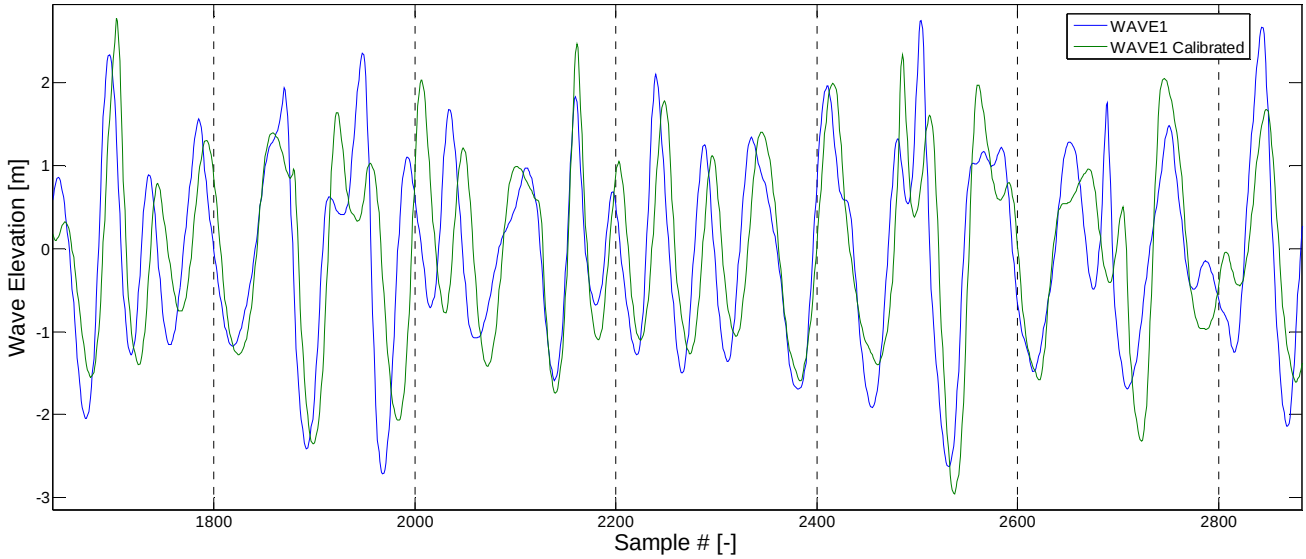

Figure 5-41 - T200 Test Group, 10 year cyclone Wave Probe #1 clipped data comparison plot

5.9.7 SPECIFIED TEST WIND

Table 5-15 - WIND program – Constant winds – PROTOTYPE SCALE

WINDS								
GROUP	FILE	IDENTIFICATION	SPECTRUM	Velocity (m/s)	Center of Application height (m)	Load (KN)	DIR	DURATION (s)
V01	V01_10100	Uw 33.8 F1547.2 H16.6	-	33.8	16.6	1547.2	180	-
V01	V01_10200	Uw 15.7 F333.8 H16.6	-	15.7	16.6	333.8	180	-
V01	V01_10300	Uw 14.6 F288.7 H16.6	-	14.6	16.6	288.7	180	-
V01	V01_10400	Uw 8.0 F86.7 H16.6	-	8	16.6	86.7	180	-
V01	V01_20100	Uw 33.8 F2002.2 H14.3	-	33.8	14.3	2002.2	180	-
V01	V01_20200	Uw 15.7 F432.0 H14.3	-	15.7	14.3	432	180	-
V01	V01_20300	Uw 14.6 F373.6 H14.3	-	14.6	14.3	373.6	180	-
V01	V01_20400	Uw 8.0 F112.2 H14.3	-	8	14.3	112.2	180	-

Table 5-16 – WIND program – Constant winds – MODEL SCALE

WINDS								
GROUP	FILE	IDENTIFICATION	SPECTRUM	Velocity (m/s)	Center of Application height (mm)	Load (gf)	DIR	DURATION (s)
V01	V01_10100	Uw 33.8 F1547.2 H16.6	-	-	332	1224.1	180	-
V01	V01_10200	Uw 15.7 F333.8 H16.6	-	-	332	264.1	180	-
V01	V01_10300	Uw 14.6 F288.7 H16.6	-	-	332	228.4	180	-
V01	V01_10400	Uw 8.0 F86.7 H16.6	-	-	332	68.6	180	-
V01	V01_20100	Uw 33.8 F2002.2 H14.3	-	-	286	1582.5	180	-
V01	V01_20200	Uw 15.7 F432.0 H14.3	-	-	286	341.8	180	-
V01	V01_20300	Uw 14.6 F373.6 H14.3	-	-	286	295.6	180	-
V01	V01_20400	Uw 8.0 F112.2 H14.3	-	-	286	88.8	180	-

5.9.8 CALIBRATED TEST WIND

The actual values of the calibrated masses used as wind forces are listed on table 5-17 and 5-18, in prototype and full scale respectively.

Table 5-17 - Measured Wind Masses - Prototype Scale

Wind File	Center of Application Height (m)	Load (KN)
V01_10100	16.6	1549.6
V01_10200	16.6	334.2
V01_10300	16.6	288.7
V01_10400	16.6	83.6
V01_20100	14.3	2004.1
V01_20200	14.3	433.0
V01_20300	14.3	373.5
V01_20400	14.3	11.4

Table 5-18 - Measured Wind Masses - Model Scale

Wind File	Center of Application Height (mm)	Load (gf)
V01_10100	332	1224
V01_10200	332	264
V01_10300	332	228
V01_10400	332	66
V01_20100	286	1583
V01_20200	286	342
V01_20300	286	295
V01_20400	286	88

6 TEST MATRIX

6.1 TEST GROUPS

The test matrix is divided in six test groups, T100, T200, T300, T400, T500 and T600.

Table 6-1 - Test Groups

Test Group	Client Ref.	Remoras	Gimbal Angular Stiffness	CWP Length
T100 - INSTALLATION SEMI ALONE	GROUP 3	None	1.26E+09 [N.m/rad]	None
T200 - OPERATIONAL SEMI & REMORAS	GROUP 1	Six (6)	1.26E+09 [N.m/rad]	None
T300 - OPERATIONAL A	GROUP 1	Six (6)	1.26E+09 [N.m/rad]	Full
T400 - OPERATIONAL B	GROUP 2	Six (6)	0 [N.m/rad]	Full
T500 - CWP INSTALLATION 1	GROUP 3	None	9.53E+10 [N.m/rad]	Full
T600 - CWP INSTALLATION 2	GROUP 4	None	9.53E+10 [N.m/rad]	Half

6.2 TEST PROGRAM

The tables below show the full test program for each test Group.

Table 6-2 - Test Group T100 Tests List

GROUP	NUMBER	CLIENTS REF	ID	WAVE FILE	WIND FILE
PT100_	00100	GM l	INCLINING PITCH		
PT100_	00200	GM t	INCLINING ROLL		
PT100_	100100	Surge Static Offset	OFFSET SURGE		
PT100_	100200	Sway Static Offset	OFFSET SWAY		
PT100_	100600	Yaw Static Offset	OFFSET YAW		
PT100_	200102	Surge Free Decay	DECAY SURGE		
PT100_	200202	Sway Free Decay	DECAY SWAY		
PT100_	200302	Heave Free Decay	DECAY HEAVE		
PT100_	200401	Roll Free Decay	DECAY ROLL		
PT100_	200501	Pitch Free Decay	DECAY PITCH		
PT100_	200602	Yaw Free Decay	DECAY YAW		
T100_	100100	Regular Wave 1	REG H2.0 T6.36	W01_10109	-
T100_	100200	Regular Wave 2	REG H2.5 T7.0	W01_10201	-
T100_	100300	Regular Wave 3	REG H3.6 T8.5	W01_10303	-
T100_	100400	Regular Wave 4	REG H5.0 T10.0	W01_10401	-
T100_	100500	Regular Wave 5	REG H6.6 T11.5	W01_10501	-
T100_	100600	Regular Wave 6	REG H8.5 T13.0	W01_10603	-
T100_	100700	Regular Wave 7	REG H11.3 T15.0	W01_10701	-
T100_	200100	100 Year Cyclone	IRR JS H10.2 T12.8 G2.0 Uw 33.8	W02_20104	V01_10100
T100_	200200	10-yr Sea	IRR JS H4.2 T8.3 G1.0 Uw 15.7	W02_20206	V01_10200
T100_	200300	10-yr Swell	IRR JS H3.8 T15.7 G6.0 Uw 14.6	W02_20304	V01_10300
T100_	500100	White Noise	WN H2.5 DT 3.5 25.0 Uw 8.0	W05_00101	V01_10400

Table 6-3 - Test Group T200 Tests List

GROUP	NUMBER	CLIENTS REF	ID	WAVE FILE	WIND FILE
PT200_	00100	GM l	INCLINING PITCH	-	-
PT200_	00200	GM t	INCLINING ROLL	-	-
PT200_	200102	Surge Free Decay	DECAY SURGE	-	-
PT200_	200202	Sway Free Decay	DECAY SWAY	-	-
PT200_	200302	Heave Free Decay	DECAY HEAVE	-	-
PT200_	200400	Roll Free Decay	DECAY ROLL	-	-
PT200_	200501	Pitch Free Decay	DECAY PITCH	-	-
PT200_	200600	Yaw Free Decay	DECAY YAW	-	-
T200_	100100	Regular Wave 1	REG H2.0 T6.36	W01_10109	-
T200_	100300	Regular Wave 3	REG H3.6 T8.5	W01_10303	-
T200_	100500	Regular Wave 5	REG H6.6 T11.5	W01_10501	-
T200_	100700	Regular Wave 7	REG H11.3 T15.0	W01_10701	-
T200_	200100	100 Year Cyclone	IRR JS H10.2 T12.8 G2.0 Uw 33.8	W02_20104	V01_20100
T200_	200200	10-yr Sea	IRR JS H4.2 T8.3 G1.0 Uw 15.7	W02_20206	V01_20200
T200_	200300	10-yr Swell	IRR JS H3.8 T15.7 G6.0 Uw 14.6	W02_20304	V01_20300
T200_	500100	White Noise	WN H2.5 DT 3.5 25.0 Uw 8.0	W05_00101	V01_20400

Table 6-4 - Test Group T300 Tests List

GROUP	NUMBER	CLIENTS REF	ID	WAVE FILE	WIND FILE
PT300_	00100	GM l	INCLINING PITCH	-	-
PT300_	00200	GM t	INCLINING ROLL	-	-
~~PT300_~~	~~300100~~	~~Pipe bottom Surge Static offset~~	~~OFFSET TEST CWP~~ *	-	-
~~PT300_~~	~~400100~~	~~Pipe impulse~~	~~IMPULSE TEST CWP~~ *	-	-
PT300_	200501	Pitch Free Decay	DECAY PITCH	-	-
PT300_	500100	-	INCLINING LVDT CHECK	-	-
T300_	100100	Regular Wave 1	REG H2.0 T6.36	W01_10109	-
T300_	100200	Regular Wave 2	REG H2.5 T7.0	W01_10201	-
T300_	100300	Regular Wave 3	REG H3.6 T8.5	W01_10303	-
T300_	100401	Regular Wave 4	REG H5.0 T10.0	W01_10401	-
T300_	100500	Regular Wave 5	REG H6.6 T11.5	W01_10501	-
T300_	100600	Regular Wave 6	REG H8.5 T13.0	W01_10603	-
T300_	100700	Regular Wave 7	REG H11.3 T15.0	W01_10703b	-
T300_	200100	100 Year Cyclone	IRR JS H10.2 T12.8 G2.0 Uw 33.8	W02_20104	V01_20100
T300_	200200	10-yr Sea	IRR JS H4.2 T8.3 G1.0 Uw 15.7	W02_20206	V01_20200
T300_	200300	10-yr Swell	IRR JS H3.8 T15.7 G6.0 Uw 14.6	W02_20304	V01_20300
T300_	200400	Fatigue Wave	IRR JS H2.5 T16.6 G6.0 Uw 8.0	W02_20404	V01_20400
T300_	500100	White Noise	WN H2.5 DT 3.5 25.0 Uw 8.0	W05_00101	V01_20400

(*) Canceled to meet schedule

Table 6-5 - Test Group T400 Tests List

GROUP	NUMBER	CLIENTS REF	ID	WAVE FILE	WIND FILE
PT400_	00100	GM l	INCLINING PITCH	-	-
PT400_	00200	GM t	INCLINING ROLL	-	-
PT400_	200101	Surge Free Decay	DECAY SURGE	-	-
PT400_	200201	Sway Free Decay	DECAY SWAY	-	-
PT400_	200300	Heave Free Decay	DECAY HEAVE	-	-
PT400_	200400	Roll Free Decay	DECAY ROLL	-	-
PT400_	200502	Pitch Free Decay	DECAY PITCH	-	-
PT400_	200600	Yaw Free Decay	DECAY YAW	-	-
PT400_	300100	Pipe bottom Surge Static offset	OFFSET TEST CWP	-	-
PT400_	400100	Pipe impulse	IMPULSE TEST CWP	-	-
PT400_	500100	-	INCLINING LVDT CHECK	-	-
T400_	100100	Regular Wave 1	REG H2.0 T6.36	W01_10109	-
T400_	100200	Regular Wave 2	REG H2.5 T7.0	W01_10201	-
T400_	100300	Regular Wave 3	REG H3.6 T8.5	W01_10303	-
T400_	100400	Regular Wave 4	REG H5.0 T10.0	W01_10401	-
T400_	100500	Regular Wave 5	REG H6.6 T11.5	W01_10501	-
T400_	100600	Regular Wave 6	REG H8.5 T13.0	W01_10603	-
T400_	100700	Regular Wave 7	REG H11.3 T15.0	W01_10703b	-
T400_	200100	100 Year Cyclone	IRR JS H10.2 T12.8 G2.0 Uw 33.8	W02_20104	V01_20100
T400_	200200	10-yr Sea	IRR JS H4.2 T8.3 G1.0 Uw 15.7	W02_20206	V01_20200
T400_	200300	10-yr Swell	IRR JS H3.8 T15.7 G6.0 Uw 14.6	W02_20304	V01_20300
T400_	200400	Fatigue Wave	IRR JS H2.5 T16.6 G6.0 Uw 8.0	W02_20404	V01_20400
T400_	500101	White Noise	WN H2.5 DT 3.5 25.0 Uw 8.0	W05_00101	V01_20400

Table 6-6 - Test Group T500 Tests List

GROUP	NUMBER	CLIENTS REF	ID	WAVE FILE	WIND FILE
PT500_	00100	GM l	INCLINING PITCH	-	-
PT500_	00200	GM t	INCLINING ROLL	-	-
PT500_	200501	Pitch Free Decay	DECAY PITCH	-	-
~~PT500_~~	~~300100~~	~~Pipe bottom Surge Static offset~~	~~OFFSET TEST CWP~~ *	-	-
~~PT500_~~	~~400100~~	~~Pipe impulse~~	~~IMPULSE TEST CWP~~ *	-	-
T500_	100100	Regular Wave 1	REG H2.0 T6.36	W01_10109	-
T500_	100200	Regular Wave 2	REG H2.5 T7.0	W01_10201	-
T500_	100300	Regular Wave 3	REG H3.6 T8.5	W01_10303	-
T500_	100400	Regular Wave 4	REG H5.0 T10.0	W01_10401	-
T500_	100500	Regular Wave 5	REG H6.6 T11.5	W01_10501	-
T500_	100600	Regular Wave 6	REG H8.5 T13.0	W01_10603	-
T500_	100700	Regular Wave 7	REG H11.3 T15.0	W01_10703b	-
T500_	200200	10-yr Sea	IRR JS H4.2 T8.3 G1.0 Uw 15.7	W02_20206	V01_10200
T500_	200300	10-yr Swell	IRR JS H3.8 T15.7 G6.0 Uw 14.6	W02_20304	V01_10300
T500_	500100	White Noise	WN H2.5 DT 3.5 25.0 Uw 8.0	W05_00101	V01_10400

(*) Canceled to meet schedule

Table 6-7 - Test Group T600 Tests List

GROUP	NUMBER	CLIENTS REF	ID	WAVE FILE	WIND FILE
PT600_	00100	GM l	INCLINING PITCH	-	-
PT600_	00200	GM t	INCLINING ROLL	-	-
~~PT600_~~	~~200100~~	~~Surge Free Decay~~	~~DECAY SURGE~~ *	-	-
~~PT600_~~	~~200200~~	~~Sway Free Decay~~	~~DECAY SWAY~~ *	-	-
PT600_	200302	Heave Free Decay	DECAY HEAVE	-	-
PT600_	200400	Roll Free Decay	DECAY ROLL	-	-
PT600_	200500	Pitch Free Decay	DECAY PITCH	-	-
~~PT600_~~	~~200600~~	~~Yaw Free Decay~~	~~DECAY YAW~~	-	-
~~PT600_~~	~~300100~~	~~Pipe bottom Surge Static offset~~	~~OFFSET TEST CWP~~ *	-	-
~~PT600_~~	~~400100~~	~~Pipe impulse~~	~~IMPULSE TEST CWP~~ *	-	-
T600_	100100	Regular Wave 1	REG H2.0 T6.36	W01_10109	-
T600_	100200	Regular Wave 2	REG H2.5 T7.0	W01_10201	-
T600_	100300	Regular Wave 3	REG H3.6 T8.5	W01_10303	-
T600_	100400	Regular Wave 4	REG H5.0 T10.0	W01_10401	-
T600_	100500	Regular Wave 5	REG H6.6 T11.5	W01_10501	-
T600_	100600	Regular Wave 6	REG H8.5 T13.0	W01_10603	-
T600_	100700	Regular Wave 7	REG H11.3 T15.0	W01_10703b	-
T600_	200200	10-yr Sea	IRR JS H4.2 T8.3 G1.0 Uw 15.7	W02_20206	V01_10200
T600_	200300	10-yr Swell	IRR JS H3.8 T15.7 G6.0 Uw 14.6	W02_20304	V01_10300
T600_	500100	White Noise	WN H2.5 DT 3.5 25.0 Uw 8.0	W05_00101	V01_10400

(*) Canceled to meet schedule

7 ANALYSIS PROCEDURES AND RESULTS

7.1 SPECTRAL ANALYSIS

7.1.1 Power Spectrum

The power spectra are obtained directly from the time series. For a series with N points $(\{x_0, x_1, x_2, ..., x_n\})$, with rate Δt and a sampling period of $T = N\Delta t$, the associated spectrum is given by:

$$S(f) = \frac{2}{N\Delta t}\left|\sum_{m=1}^{N} x_m e^{\frac{i2\pi mf}{N}} \Delta t\right|^2$$

The power spectra are calculated using the Welch method and smoothed by a Hanning type window with 50% of overlap. A Gaussian frequency window is also used to obtain consistent estimative.

Where the spectral plots are presented on the time domain, the relation between frequency and period is given by:

$$t = \frac{1}{f}$$

In order to maintain the same statistical properties the spectral density is corrected according to the following relationship:

$$S(t) = \frac{S(f)}{T^2}$$

7.1.2 Parameters derived from power spectra

The spectral moments are calculated by:

$$m_n = \int_0^\infty f^n S(f) df$$

where *n* = moment order.

Those moments are used to estimate the following parameters:

- m_0 = RMS of the process, also representing the variance (σ_n^2) of the random signal given by:

$$\eta = \sum_{n=0}^{\infty} a_n \cos(n\omega_0 t) + b_n \sin(n\omega_0 t)$$

where, ω_0 is the fundamental frequency and,

a_n and b_n are the Fourier coefficients.

The variance is given by:

$$\sigma_n^2 = \sum_{i=1}^{\infty} \frac{a_i^2}{2} = m_0$$

- m_2 = mean square velocity
- m_4 = mean square acceleration

- Significant wave height (H_s): $H_s = 4\sqrt{m_0}$
- Mean Period ($\overline{T}$): $\overline{T} = \frac{m_0}{m_1}$
- Zero-ascendant mean period: $\overline{T}_z = \sqrt{\frac{m_0}{m_2}}$
- Crest mean period ($\overline{T}_c$): $\overline{T}_c = \sqrt{\frac{m_2}{m_4}}$
- Spectral width ($_\varepsilon$): $\varepsilon = 1 - \left(\frac{m_2^2}{m_0 \cdot m_4} \right)$ Cartwright & Longuet-Higgins (1956)
- Spectral peakness (Q_p): $Q_p = \frac{2}{m_0^2} \int_0^\infty f \cdot S^2(f) df$ Goda (1970)
- Spectral peak period (T_p): Obtained from the spectral density curve.

7.2 STATISTICAL ANALYSIS

The wave elevation is assumed to be formed by:

$$z(t) = \sum_{n=1}^{N \to \infty} z_n(t) = \sum_{n=1}^{N \to \infty} z_{0n} \cos(\omega_n t - \varphi_n)$$

where, $z(t)$ is considered to be the sum of *n* random variables:

$$z(t) = z_1 + z_2 + \ldots + z_n + \ldots$$

being:

$z_n = z_{0n} \cos(\omega_n t - \varphi_n)$

ω_n frequencies on the interval (0, ∞)

φ_n phases, assumed to be uniformly distributed between [0, 2π], and

z_{0n} harmonic components amplitudes.

7.2.1 Statistical Parameters

- Mean value ($\overline{X}$): $\overline{X} = \frac{1}{N} \sum_{i=1}^{N} X_i$
- Maximum value ($X_{\max}$): Taken from the time signal.
- Minimum ($X_{\min}$): The same as the maximum.
- Standard deviation ($_\sigma$): $\sigma = \sqrt{\frac{1}{N-1} \sum_{i=1}^{N} (X_i - \overline{X})^2}$

  where,

N total number of samples

X_i sample of the time series.

- Asymmetry or skewness (γ_1): $\gamma_1 = \frac{m_3}{\sigma^3}$
- Kurtosis(γ_2): $\gamma_2 = \frac{m_4}{\sigma^4} - 3$

7.2.2 Analysis of peak values

- Number of maximum values (N^+): obtained from the local maxima (crests).
- Number of minimum values (N^-): obtained from the local minima (troughs).
- Number of zero crossing ($N^{(u)}$): obtained from the number of ascendant zeros.
- Maximum height ($H_{\max}$): obtained from the maximum value between ascendant zeros.
- Significant height ($H_{1/3}$): mean of the one third highest values for the wave heights between ascendant zeros.
- Crest to trough significant height ($H_{1/3\,Cc}$): same as above, but obtained from the crest to trough method
- $H_{1/10}$ value: mean of the one tenth highest values for the wave heights between ascendant zeros.
- Significant Maximum ($X^+_{1/3}$): mean of the one third highest amplitudes taken between ascendant zeroes (crests).
- Significant Minimum ($X^-_{1/3}$): mean of the one third highest amplitudes taken between ascendant zeroes (troughs).

7.3 WEIBULL ANALYSIS

7.3.1 Probability of peak values

The probabilities of heights are assumed to have Weibull distribution, according to the expression below.

$$P[A] = 1 - \exp\left[-\frac{1}{G}\left(\frac{A-\overline{X}}{\sigma}\right)^{G}\right]$$

where,

$\overline{X}$ = mean value of the signal

σ = standard deviation of A

G = declivity parameter, being 2 for Raleigh distribution of peaks and 1 for exponential distribution

7.3.2 Extreme values estimate

The extreme values are estimated through adjusts on the Weibull probability plot. The adjustments are done for a probability level above 0.87, which is the significant response level taken from experience. However, for some special cases, this analysis may not represent a correct fitting of the Weibull plot.

7.3.3 Most probable maximums

The most probable maximum heights are taken from Weibull adjustments of the time series, for a value in which:

$$P(A>Hmpm) = 1 - 1/e = 0.63;$$

7.4 RAO ANALYSIS

7.4.1 Transfer Functions

Linear transfer functions or R.A.O curves and relative phases when required are estimated from cross-spectral analysis (see subsection below), according to the formula:

$$H(f) = \frac{S_{xy}(f)}{S_{xx}(f)}$$

where *H*(*f*) is the complex transfer function, such that:
RAO = modulus of *H*
Phase= phase angle of *H*

Here *S*xy is the cross spectrum between the response *y* and the reference *x*, and *S*xx is the reference spectrum (alternatively the RAO may be defined as the square root of the ratio between the power spectrum of the response divided by the power spectrum of the reference wave).

The RAO curves will be with the following unit:

$$\left[\frac{\text{basic unit of response}}{\text{meter}}\right]$$

The function is normally plotted in the range where the coherence (see the sub-section below) is larger than 40%, and where reference spectrum is larger than 1% of its peak value. In seakeeping tests the reference wave is normally corrected to the actual frequency of encounter.

The reference wave is used in the calculation of the transfer functions is normally the wave at the location of the model (middle of the Ocean Basin) without the model present.

7.4.2 Coherence function and cross spectra

The coherence function between two signals *x(t)* (reference) e *y(t)* (response) is defined by:

$$y_{xy}(f) = \frac{S_{xy}(f)}{\sqrt{S_x(f)S_y(f)}} = \left|y_{xy}(f)\right| \cdot \exp(k^{[j\phi_{xy}(f)]})$$

where,

$S_{xy}(f) = \frac{1}{T} < X_T^*(f)Y_T(f) >$ is the cross spectrum between x and y

where,

$X_T^*(f) \cdot Y_T(f) = \left|X_T(f)\right| \cdot \left|Y_T(f)\right| \cdot e^{j(\phi_y - \phi_x)}$

$S_x(f) = \frac{1}{T} < \left|X_T(f)\right|^2 >$ = autocorrelation spectrum of x

$S_y(f) = \frac{1}{T} < \left|Y_T(f)\right|^2 >$ = autocorrelation spectrum of y

$X_T(f) = \left|X_T(f)\right| \cdot e^{j\phi_x(f)} = \int_{-\infty}^{\infty} dt x_T(t) \exp^{(-j2\pi ft)}$ = Fourier transform for a sample of length T, taken from the signal x(t)

$X_T^*(f) = \left|X_T(f)\right| \cdot e^{j\phi_x(f)}$

$Y_T(f) = |Y_T(f)| \cdot e^{j\phi_y(f)} = \int_{-\infty}^{\infty} dt y_T(t) \exp^{(-j2\pi ft)}$ = Fourier transform for a sample of length T, taken from the signal y(t)

For $Y_T(f) = H(f) \cdot X_T(f), \gamma_{xy}(f) \equiv 1$ (linear relation between x and y)

Notation:

* = conjugate complex

j = imaginary unit

$\phi_x(f)$ = reference phase

$\phi_y(f)$ = response phase

$\phi_{xy}(f)$ = relative phase

$| \, |$ = absolute value

<> = statistic expected value

7.5 CWP STRAINS

This analysis is performed in the concatenation of the raw files into the ".tra.mat" files.

The strains are measured in the outer surface of the core tube on the CWP model. They will be corrected to the correct diameter of the actual CWP.

SGx(outer) = SGx(core) x 209.8 / 38.21

7.6 SEMI-SUBMERSIBLE 6DOF MOTION

This analysis is performed in the concatenation of the raw files into the ".tra.mat" files.

The calibrated reference point for the semi attitude angles is placed on the deck. In order to obtain the correct values of translations this reference point must be moved to the origin of the local reference frame o'x'y'z'.

The inertial frame for calculation of the 6DOF motions of the semi is by default AXYZ, this will also be moved to oxyz the inertial reference frame in the model initial position so the model has a small initial offset during testing.

Initially the measured position values are translated to the inertial reference frame oxyz

Semi_X(oxyz) = Semi_X(measured) - 20000 [mm];
Semi_Y(oxyz) = Semi_Y(measured) - 15000 [mm];
Semi_Z(oxyz) = Semi_Z(measured) + 34 [mm]; (Correction for the waterline level in the basin)

Afterwards the translation values are corrected using the origin of the local reference frame o'x'y'z', fixed to the semi, as the reference point for the rotation angles. For this analysis the Euler rotation matrix will be used. The rotation order is Yaw, Pitch and Roll. The distance vector is opposite position vector of the Qualisys reference point on the (o'x'y'z') reference frame.

Vector = (0,0,-19.5) x 1000 / 50 [mm];
3DOF Semi Position (o'x'y'z') = 3DOF Semi Position (oxyz) + Euler Rotation Matrix x Vector;

The Semi attitude angles do not need to be corrected, they are provided in Euler angles order Yaw, Pitch and Roll.

7.7 CWP MOTION ANALYSIS

This analysis is performed in the concatenation of the raw files into the ".tra.mat" files.

The CWP motion is measured on the inertial global reference frame AXYZ. The targets position is first subtracted from the model position. This is equivalent to translating the global reference frame to the model position.

$$CWP\_X = CWP\_X - (dx + 20000)$$
$$CWP\_Y = CWP\_Z - (dy + 15000)$$
$$CWP\_Z = CWP\_Z - (dz)$$

$where,$
$CWP\_X, CWP\_Y\ and\ CWP\_Z\ = CWP\ targets\ position$
$dx, dy\ and\ dz = Semi\ position\ after\ initial\ offset$

Afterwards the targets positions are transferred to local reference frame fixed at the model on the waterline height by application of the rotation matrix where the angles are the Semi attitude angles measured by Qualisys.

Since the tracking targets are fixed on the outer sheet their position will be translated to the center of the CWP core tube. For this it is necessary to know their initial X and Y position (Z offset due to this translation will be neglected due to the high aspect ratio of the model).

Calm Water data file:"CALM_50_6.mat" was used for calibrating the initial position of the CWP position tracking targets. Mean Semi position from Calm Water data file: "CALM_50_4.mat" was added to Semi tracking reference, X=20000, Y=15000, Z=0 and was considered as the Semi reference frame initial position.

Table 7-1 - CWP Targets Position - Inertial Reference Frame AXYZ

	X position [mm]	Y position [mm]	Z position [mm]
CWP_1	0	0	0
CWP_2	0	0	0
CWP_3	0	0	0
CWP_4	19697.3	15056.0	-18674.8
CWP_5	19959.9	15049.7	-19358.6
CWP_6	19969.0	15061.7	-20333.5
Semi	20047.3	14962.8	7.7

In order to obtain the CWP targets initial position for a null offset of the Semi the CWP target position is subtracted of the Semi initial position coordinates.

This operation yields the following initial positions for the CWP targets on the global reference frame.

Table 7-2 - CWP Targets Position - Inertial Reference Frame oxyz

	X position [mm]	Y position [mm]	Z position [mm]
CWP'_1	0	0	0
CWP'_2	0	0	0
CWP'_3	0	0	0
CWP'_4	-77.6	93.2	-18682.5
CWP'_5	-87.4	86.9	-19366.3
CWP'_6	-78.3	98.9	-20341.2
Semi'	0	0	0

For this operation the Semi mean attitude, obtained from the same calm water data file, will be input on the rotation matrix to transform the position values to the local reference frame.

Table 7-3 - CWP Targets Position - Local Reference Frame o'x'y'z'

	Yaw [º]	Pitch[º]	Roll[º]
Semi	180.1197	-0.1013	0.0492

	X position [mm]	Y position [mm]	Z position [mm]
CWP''_1	0	0	0
CWP''_2	0	0	0
CWP''_3	0	0	0
CWP''_4	44.8	-109.2	-18682.5
CWP''_5	53.4	-103.4	-19366.3
CWP''_6	42.6	-116.0	-20341.2

7.8 CWP IMPULSE TEST

Data from the support load, strain from the first strain gages and X displacement from the bottom target were compared and the support load reading was chosen for this analysis because it was the sensor that better captured higher modal periods.

The support load time series was analyzed to identify the moment when the model was hit. This time was used on spectral analysis. A small period smaller than 3 cycles of the first modal was chosen in order not to attenuate the energy of the 2nd and 3rd modal periods that are present for a very short time on the dry test.

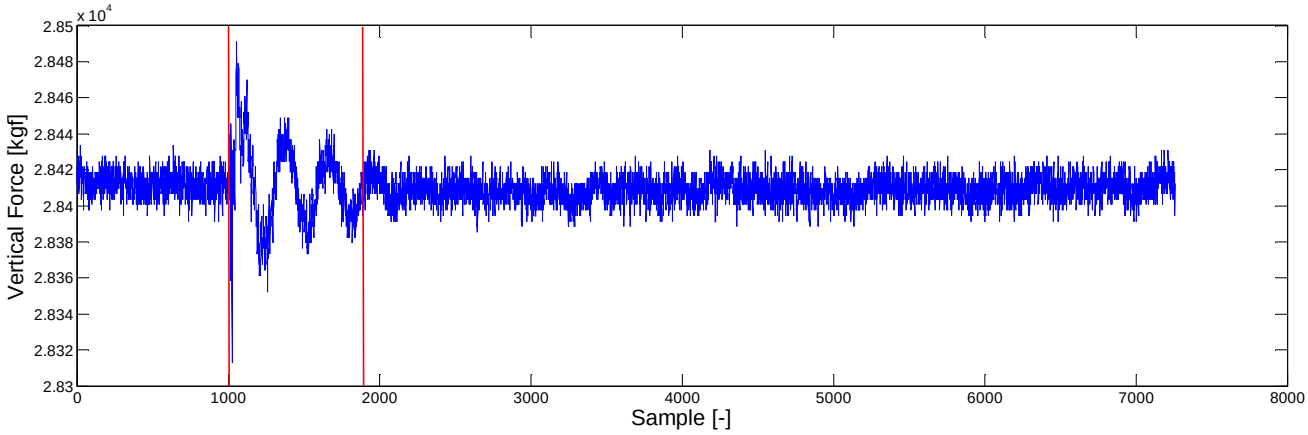

Figure 7-1 - Support load [kgf] Time Series - Model Scale (red vertical lines showing the time window used)

The time series data were converted to frequency domain and plotted in the format of Energy Density versus

Frequencies to allow us to identify the modal frequencies.

The spectral analysis plot is checked to identify the peak response frequencies.

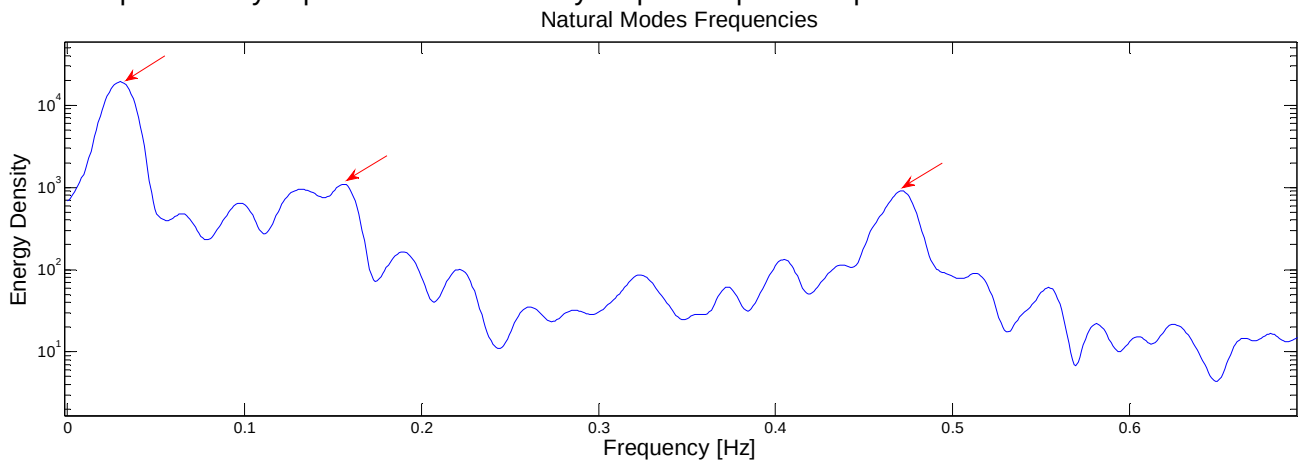

Figure 7-2 - CWP Impulse Test Natural Modes Frequencies Identification

7.9 GIMBAL ANGLE ANALYSIS

This analysis is performed in the concatenation of the raw files into the ".tra.mat" files.

The gimbal angle script calculates the pipe attitude from four (4) distances measured from the LVDT sensors. The sensors base positions are known from measurement and the initial position of the probe is calibrated according to the procedure described in this section.

The sensor probe initial position is calibrated by the mean readings from the LVDT sensors that were obtained from the Calm Water data file: "CALM_50_2.gin.mat".

LVDT0 = -0.0597 mm
LVDT1 = -2.6972 mm
LVDT2 = -0.5265 mm
LVDT3 = -0.1189 mm

Those values were used as input for a calibration script together with a known CWP attitude which is assumed to be null pitch and roll. The output from the calibration script are 4 parameters that are used for the LVDT reading to gimbal attitude script, equivalent to the probe initial position.

b0 = 188.3701 mm
b1 = 194.4512 mm
b2 = 181.8720 mm
b3 = 195.7378 mm

7.10 GIMBAL LOADS

This analysis is performed in the concatenation of the raw files into the ".tra.mat" files.

The gimbal forces are equal to the sum of each individual load cell force on each direction. The load on each cell is offset by an initial value measured as initial condition, already including the gimbal mass.

7.11 INCLINING TESTS

Using equi-volumetric inclining theory the initial restoring moment for a floating body can be described as:

$$Mr = \Delta . GM . Sin(\theta)$$

$$where,$$

$$Mr = Restoring\ Momen,$$

$$\Delta = Vessel\ displacement\ and$$

$$\theta = Roll\ or\ Pitch\ angle$$

When the vessel is in equilibrium the restoring moment is equal to the inclining moment, known from ballasts mass and position on the model. The inclining angle is measured by Qualisys tracking system and the displacement of the vessel is known from the ballast plan updated to the test condition when ballasts are added to provide inclining moment.

In order to obtain the estimate of the vessel center of gravity height the following relationship is used:

$$GM = KM - KG$$

The KM value is obtained from the hydrostatic model updated to the as-built dimensions and draft during the inclining test.

During the inclining tests the model will be connected to a mooring system, so there will be both a hydrostatic and mooring restoration. The mooring restoration moment versus inclining moment was identified comparing the inclining tests for the semi only configuration with and without the mooring.

A linear fit was performed for both cases Moments vs. Pitch Angle and the coefficients were subtracted to obtain the mooring stiffness linear fit equation as demonstrated on table 7-4.

Table 7-4 - Mooring Longitudinal Moments Coefficients

Longitudinal Moment vs. Pitch Angle [kgf.mm] vs. [º]		
	a1	a0
Semi Free Float	410	141
Semi with Mooring	784	-51
Mooring Only	374	-192

$$Ml_{mooring} = 374 . Pitch - 192$$

$$where,$$

$$Ml_{mooring} = Longitudinal\ Moment\ from\ Mooring\ [kgf.mm]$$

$$Roll = Semi\ Roll\ Angle$$

A linear fit was performed for both cases Moments vs. Roll Angles and the coefficients were subtracted to obtain the mooring stiffness linear fit equation as demonstrated on table 7-5.

Table 7-5 - Mooring Transversal Moments Coefficients

Transversal Moment vs. Roll Angle [kgf.mm] vs. [º]		
	a1	a0
Semi Free Float	403	-223
Semi With Mooring	770	-8
Mooring Only	367	215

$$Mt_{mooring} = 367.Roll + 215$$

$$where,$$
$$Mt_{mooring} = Transversal\ Moment\ from\ Mooring\ [kgf.mm]$$
$$Roll = Semi\ Roll\ Angle$$

The moment versus inclining angle curve was subtracted from the inclining moment for each of the configurations inclining tests prior to analysis.

7.12 TEST RESULTS

All results are delivered in prototype values. The Froude law of scaling was applied and numerical scaling factors and units used are listed in table below. Basic statistics for the static system identification tests are presented on 'Annex B: Static System ID Tests Statistics'.

7.12.1 Scaling

The scale factors used for the systems id tests are listed on table 7-6.

Table 7-6 - Scaling factors

Parameter	Scaling	Model Unit	Prot. Unit	Num. Factor
Length	λ	mm	m	0.05
Time	$\lambda^{1/2}$	s	s	7.071
Angle	1	deg	deg	1
Mass	$r.\lambda^3$	g	Kg	129.132
Force	$g.r.\lambda^3$	gf	KN	1.266
Strain	1	-	-	5.491 *
r (correction factor)	-	-	-	1.033

(*) This scale factor was already applied on the raw data in order to transfer the strain from the core tube to the outer diameter of the cold water pipe.

7.12.2 Mooring Offset Tests

7.12.2.1 Surge Static Offset - PT100_100100

The mooring stiffness on the surge direction was identified by a Pullout test, with the measurements recorded on the data file PT100_100100.

The measurements time series were separated in static data windows.

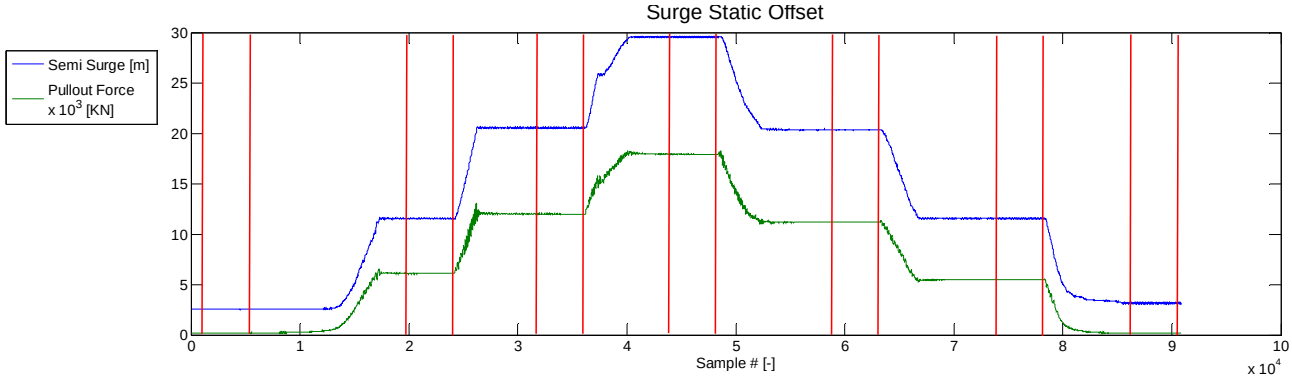

Figure 7-3 - Mooring Surge Pullout Time Series Data Windows

The mean values of pullout force and surge positions were calculated for each window marked by the vertical red lines. The data windows used for this analysis are listed on table 7-7.

Table 7-7 - Mooring Surge Pullout Time Series Data Windows

Data Window	Start Time [s]	End Time [s]	Pullout Force [KN]	Semi Surge Displacement [m]
#1	8.485E+01	6.327E+02	2.15E+02	2.566
#2	2.326E+03	2.833E+03	6.11E+03	11.525
#3	3.731E+03	4.234E+03	1.20E+04	20.528
#4	5.160E+03	5.687E+03	1.79E+04	29.541
#5	6.943E+03	7.426E+03	1.12E+04	20.354
#6	8.710E+03	9.219E+03	5.48E+03	11.540
#7	1.015E+04	1.066E+04	2.10E+02	3.158

A linear equation was fitted to the mean values data, where the angular coefficient is the mooring stiffness. The results from this analysis are plotted on figure 7-4.

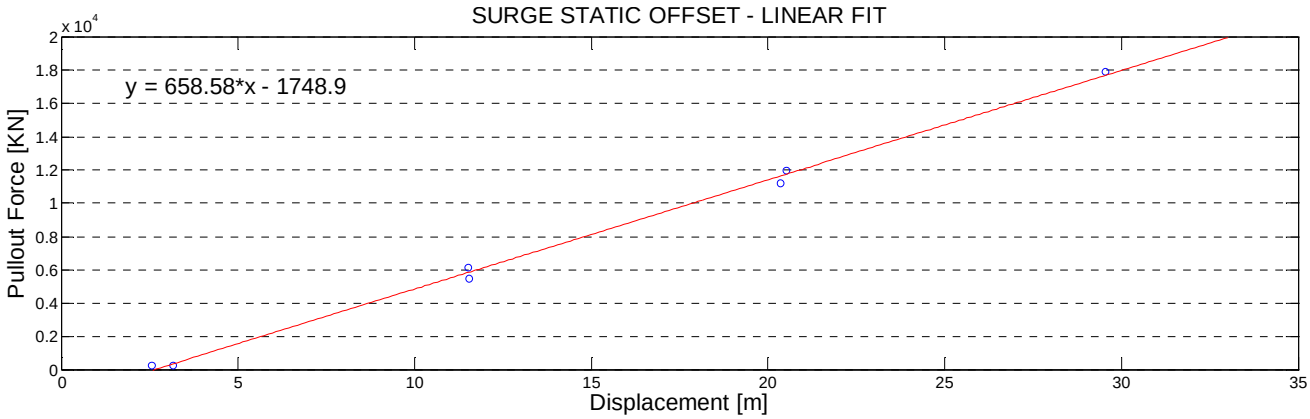

Figure 7-4 - Mooring Surge Pullout Stiffness Linear Fit

The measured mooring stiffness on the surge direction is **658.58 KN/m**.

7.12.2.2 Sway Static Offset - PT100_100200

The mooring stiffness on the sway direction was identified by a Pullout test, with the measurements recorded on the data file PT100_100200.

An analysis procedure similar to the one used for the surge static offset was used. The data windows used for calculating the mean values are listed on table 7-8.

Table 7-8 - Mooring Sway Pullout Time Series Data Windows

Data Window	Start Time [s]	End Time [s]	Pullout Force [KN]	Semi Sway Displacement [m]
#1	1.179E-01	3.771E+01	1.80E+02	-1.980
#2	1.213E+03	1.473E+03	6.09E+03	-11.102
#3	2.370E+03	2.563E+03	1.21E+04	-20.265
#4	3.583E+03	3.801E+03	1.78E+04	-28.989
#5	4.673E+03	4.940E+03	1.15E+04	-19.963
#6	6.224E+03	6.688E+03	5.61E+03	-11.082
#7	7.725E+03	8.193E+03	1.57E+02	-2.596

The mean values of the pullout force versus the Semi sway displacements are plotted on figure 7-5.

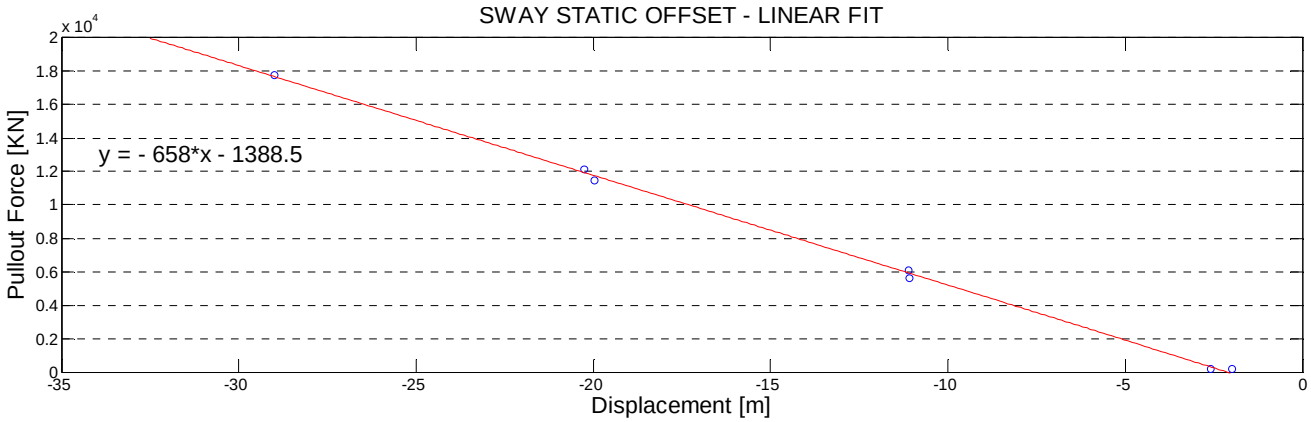

Figure 7-5 - Mooring Sway Pullout Stiffness Linear Fit

The measured mooring stiffness on the sway direction is **658 KN/m**.

7.12.2.3 Yaw Static Offset - PT100_100600

The mooring stiffness on the yaw direction was identified by a Pullout test, with the measurements recorded on the data file PT100_100600.

The lever between the two lines was calculated on a geometric model for 180º and 170º Yaw as presented on figure X.

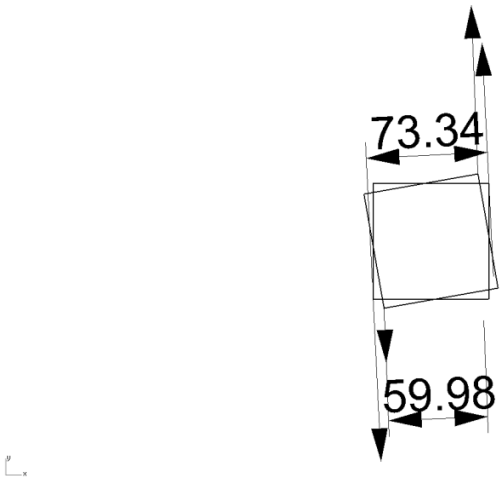

Figure 7-6 - Mooring Yaw Pullout Cables Setup

A linear fit was made to model the relationship between the model yaw and the lever between the pullout lines.

$$lever = -1.336 \times Yaw - 167.14$$

The measurements time series were separated in static data windows.

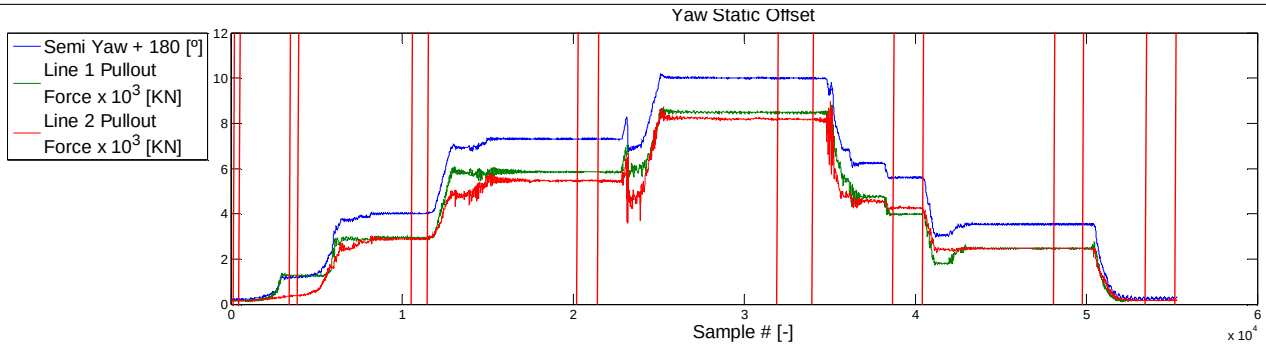

Figure 7-7 - Mooring Yaw Pullout Time Series Data Windows

The mean pullout forces value for each time window, illustrated by the vertical red lines, was multiplied by the estimated lever to obtain the Yaw Moment.

Table 7-9 - Mooring Yaw Pullout Time Series Data Window

Data Window	Start Time [s]	End Time [s]	Line 1 Force [KN]	Line 2 Force [KN]	Semi Yaw [º]	Lever [m]	Yaw Moment [KN.m]
#1	1.650E+01	5.893E+01	1.58E+02	1.37E+02	-179.787	73.055	10797
#2	4.007E+02	4.690E+02	3.70E+02	1.29E+03	-178.798	71.734	59424
#3	1.241E+03	1.355E+04	2.89E+03	2.93E+03	-175.990	67.982	197991
#4	2.381E+03	2.528E+03	5.47E+03	5.86E+03	-172.695	63.580	360092
#5	3.771E+03	4.015E+03	8.18E+03	8.47E+03	-170.005	59.987	499424
#6	4.563E+03	4.764E+03	4.27E+03	3.98E+03	-174.393	65.850	271531
#7	5.669E+03	5.873E+03	2.48E+03	2.47E+03	-176.468	68.621	169817
#8	6.304E+03	6.507E+03	1.81E+02	1.61E+02	-179.742	72.995	12486

A linear equation was fitted to the post processed moment and yaw angle data. The results from this analysis are plotted on figure 7-8.

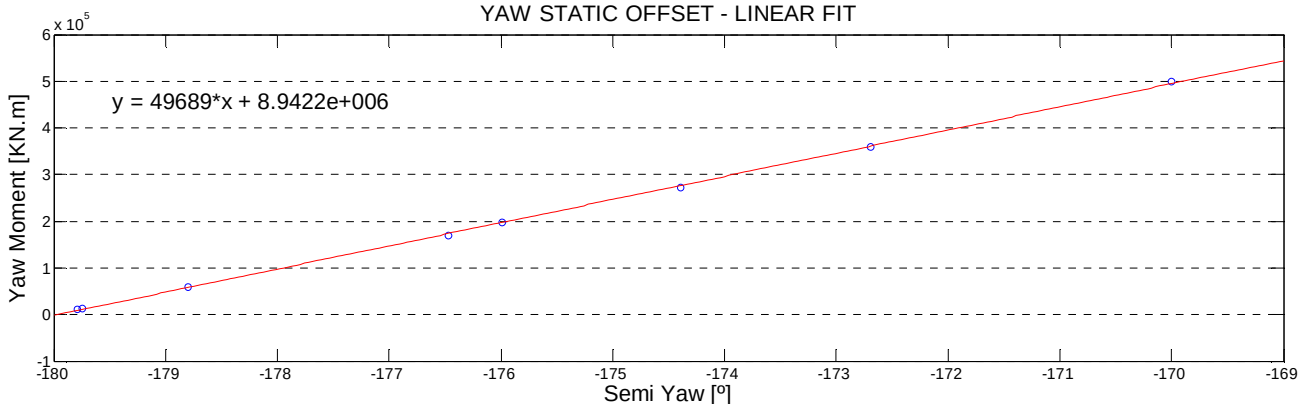

Figure 7-8 - Mooring Yaw Pullout Stiffness Linear Fit

The mooring yaw stiffness is **49689 KN.m/degrees**.

7.12.3 Inclining Tests

7.12.3.1 GM I - PT100_00100

The inclining tests are performed to measure the model hydrostatic restoration to roll and pitch movements.

Ballasts with known weights were added to the semi deck at known positions and the resulting model attitude was registered by a precision inclinometer (Mitutoyo S/Nº 12110039) and the Qualisys tracking system for the test without and with the mooring installed respectively.

The ballasts positions, measured pitch and calculations for the test without the mooring are listed on table 7-10

Table 7-10 - T100 Longitudinal Inclining Test Results

Item	Description	Weight [kgf]	Ballasts position		
			x [mm-SM]	y [mm-CL]	z [mm-BL]
01	Peso 1 - BB (P1)	2.588	220	0	832
02	Peso 2 - BE (P2)	2.548	-220	0	832
03	Accessories	0.320	570	0	816
	Total =	5.456	35	0	831

Movim. No.	Ballasts P1 and P2 position		Inclin.* [ϕ] [deg]	tan ϕ	Mom. [kgf-mm]	GM_ens [mm]
	pos_P1 [mm]	pos_P2 [mm]				
0 (Initial)	220	-220	0.09	0.002	191.040	372.375
01	562	-220	2.32	0.041	1074.842	81.297
02	562	220	5.00	0.087	2197.256	77.190
03	220	-562	-2.03	-0.035	-679.102	58.699
04	-220	-562	-4.75	-0.083	-1819.096	67.260

The inclining moment versus the tangent of the pitch angle is plotted on figure 7-9.

	Model Scale	Full Scale
R6.1 Displacement, Δ [kgf; t]:	321.15	41472
R6.2 Target VCG, KG_{req} [mm; m]:	368	18.400
R6.3 Estimated Metacentric Height, GM_{req} [mm, m]	78	3.920
R6.4 Calculated VCG, KG_{obt} [mm; m]:	379	18.967
R6.5 Measured Metacentric Height, GM_{obt} [mm, m]	78	3.913
R6.6 VCG deviation [mm, %]:	11	3.1%
R6.7 GM deviation [mm, %]:	0	-0.2%

Moment vs. tan ϕ (Model Scale)

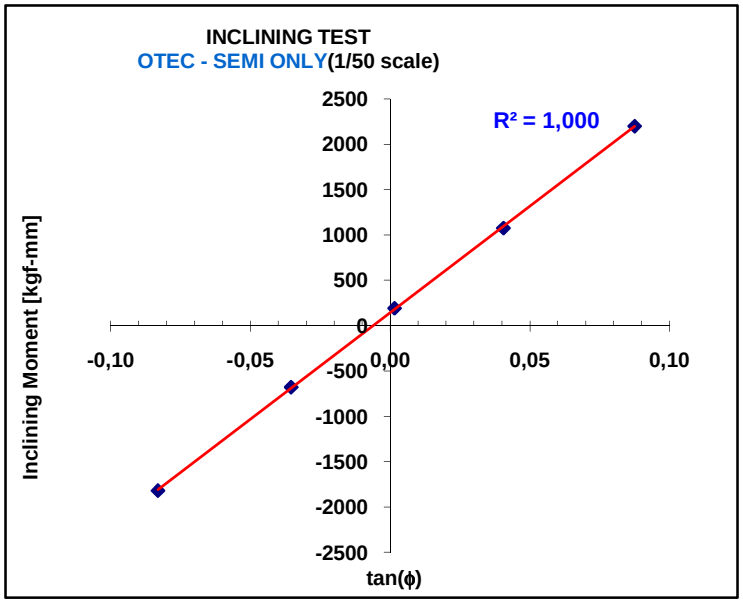

Figure 7-9 - T100 Longitudinal Inclining Moment Linear Fit

7.12.3.2 GM t - PT100_00200

Same setup and analysis procedure as described for the GM l test.

The ballasts positions, measured roll and calculations for the test without the mooring are listed on table 7-11.

Table 7-11 - T100 Transversal Inclining Test Results

Item	Description	Weight [kgf]	Ballasts position		
			x [mm-SM]	y [mm-CL]	z [mm-BL]
01	Peso 1 - BB (P1)	2.588	220	0	832
02	Peso 2 - BE (P2)	2.548	-220	0	832
03	Accessories	0.320	0	-685	816
	Total =	5.456	2	-40	831

Movim. No.	Ballasts P1 and P2 position		Inclin.* [ϕ] [deg]	tan ϕ	Mom. [kgf-mm]	GM_ens [mm]
	pos_P1 [mm]	pos_P2 [mm]				
0 (Initial)	0	0	0.03	0.001	-219.197	-1281.778
01	-288	0	-1.87	-0.033	-963.250	90.380
02	-575	0	-3.67	-0.064	-1707.300	81.666
03	288	0	1.86	0.032	526.144	49.633
04	575	0	3.70	0.065	1268.900	60.204

The inclining moment versus the tangent of the roll angle is plotted on figure 7-10.

	Model Scale	Full Scale
R6.1 Displacement, Δ [kgf; t]:	321.15	41472
R6.2 Target VCG, KG_{req} [mm; m]:	368	18.400
R6.3 Estimated Metacentric Height, GM_{req} [mm, m]	78	3.920
R6.4 Calculated VCG, KG_{obt} [mm; m]:	380	19.000
R6.5 Measured Metacentric Height, GM_{obt} [mm, m]	78	3.880
R6.6 VCG deviation [mm, %]:	12	3.3%
R6.7 GM deviation [mm, %]:	-1	-1.0%

Moment vs. tan ϕ (Model Scale)

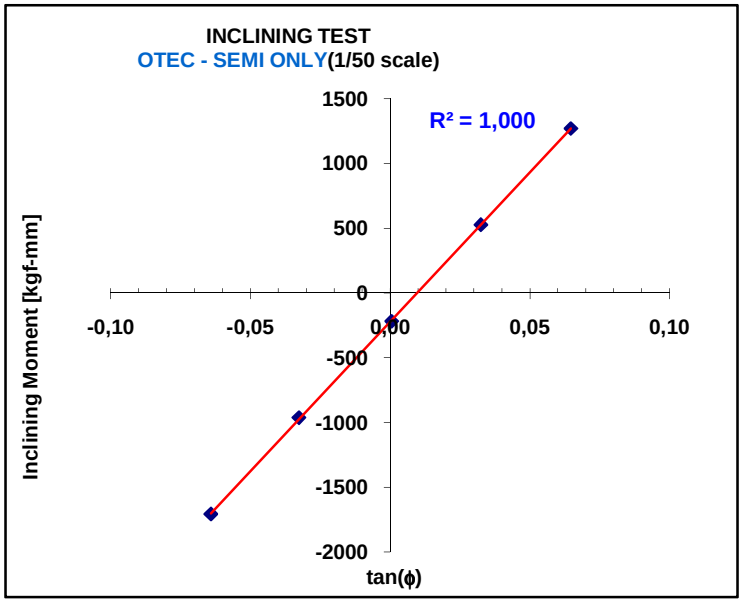

Figure 7-10 - T100 Transversal Inclining Moments Linear Fit

7.12.3.3 GM I - PT200_0010X

The ballasts positions, measured roll and calculations for the test are listed on table 7-12.

Table 7-12 - T200 Longitudinal Inclining Test Results

Item	Description	Weight [kgf]	Ballasts position		
			x [mm-SM]	y [mm-CL]	z [mm-BL]
01	Peso 1 - BB (P1)	9.750	210	0	770
02	Peso 2 - BE (P2)	9.730	-210	0	770
03	Accessories	0.000	0	0	0
	Total =	19.480	0	0	770

Movim. No.	Ballasts P1 and P2 position		Inclin.* [ϕ] [deg]	tan ϕ	Mom. [kgf-mm]	GM_ens [mm]
	pos_P1 [mm]	pos_P2 [mm]				
0 (Initial)	210	-210	0.04	0.001	182.811	167.664
01	1005	210	1.00	0.018	11658.217	380.935
02	1005	1005	1.64	0.029	19156.190	383.663
03	-210	-1005	-0.92	-0.016	-11289.397	402.136
04	-1005	-1005	-1.52	-0.027	-18816.770	406.404

The inclining moment versus the tangent of the pitch angle is plotted on figure 7-11.

	Model Scale	Full Scale
R6.1 Displacement, Δ [kgf; t]:	1725.6	222830859
R6.2 Target VCG, KG_{req} [mm; m]:	-292	-14.610
R6.3 Estimated Metacentric Height, GM_{req} [mm, m]	413	20.640
R6.4 Calculated VCG, KG_{obt} [mm; m]:	-280	-13.990
R6.5 Measured Metacentric Height, GM_{obt} [mm, m]	400	20.020
R6.6 VCG deviation [mm, %]:	12	-4.2%
R6.7 GM deviation [mm, %]:	-12	-3.0%

Moment vs. tan ϕ (Model Scale)

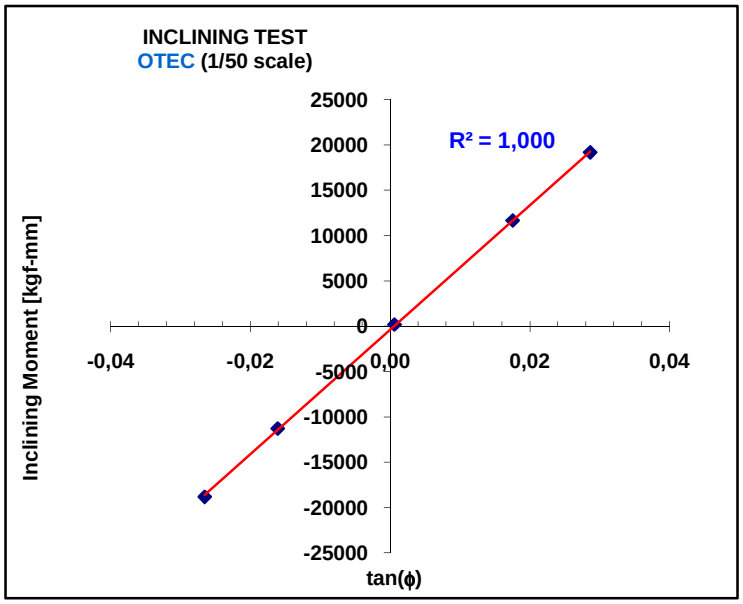

Figure 7-11 - T200 Longitudinal Inclining Moments Linear Fit

7.12.3.4 GM t - PT200_0020X

The ballasts positions, measured roll and calculations for the test are listed on table 7-13.

Table 7-13 - T200 Transversal Inclining Test Results

Item	Description	Weight [kgf]	Ballasts position		
			x [mm-SM]	y [mm-CL]	z [mm-BL]
01	Peso 1 - BB (P1)	9.750	289	0	770
02	Peso 2 - BE (P2)	9.730	-289	0	770
03	Accessories	0.000	0	0	0
	Total =	19.480	0	0	770

Movim. No.	Ballasts P1 and P2 position		Inclin.* [ϕ] [deg]	tan ϕ	Mom. [kgf-mm]	GM_ens [mm]
	pos_P1 [mm]	pos_P2 [mm]				
0 (Initial)	289	-289	0.03	0.001	-219.900	-248.114
01	932	289	1.33	0.023	11196.154	276.590
02	932	932	2.07	0.036	17181.477	272.876
03	-289	-932	-1.40	-0.024	-11586.209	271.173
04	-932	-932	-2.13	-0.037	-17590.302	271.789

The inclining moment versus the tangent of the roll angle is plotted on figure 7-12.

	Model Scale	Full Scale
R6.1 Displacement, Δ [kgf; t]:	1725.6	222830859
R6.2 Target VCG, KG_{req} [mm; m]:	-292	-14.610
R6.3 Estimated Metacentric Height, GM_{req} [mm, m]	295	14.759
R6.4 Calculated VCG, KG_{obt} [mm; m]:	-275	-13.739
R6.5 Measured Metacentric Height, GM_{obt} [mm, m]	278	13.889
R6.6 VCG deviation [mm, %]:	17	-6.0%
R6.7 GM deviation [mm, %]:	-17	-5.9%

Moment vs. tan ϕ (Model Scale)

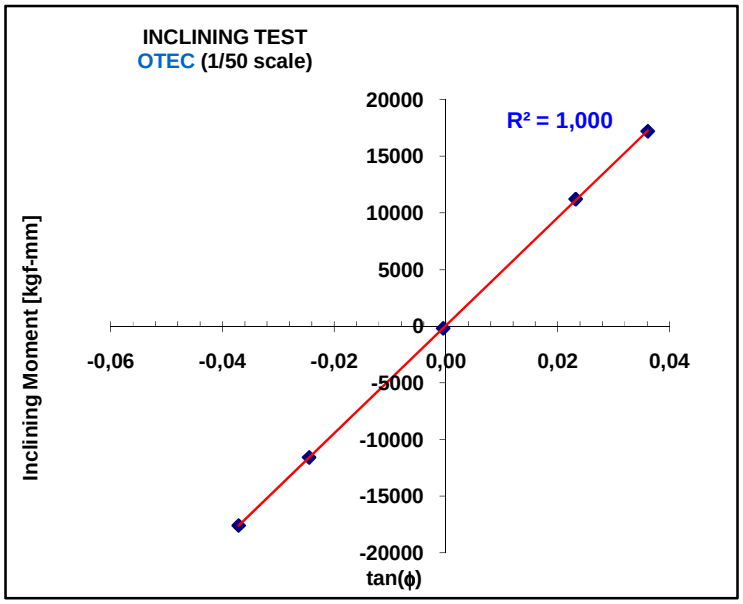

Figure 7-12 - T200 Transversal Inclining Moments Linear Fit

7.12.3.5 GM I - PT400_0010X

The ballasts positions, measured roll and calculations for the test are listed on table 7-14.

Table 7-14 - T400 Longitudinal Inclining Test Results

Item	Description	Weight [kgf]	Ballasts position		
			x [mm-SM]	y [mm-CL]	z [mm-BL]
01	Peso 1 - BB (P1)	9.750	210	0	770
02	Peso 2 - BE (P2)	9.730	-210	0	770
03	Accessories	0.000	0	0	0
	Total =	19.480	0	0	770

Movim. No.	Ballasts P1 and P2 position		Inclin.* [ϕ] [deg]	tan ϕ	Mom. [kgf-mm]	GM_ens [mm]
	pos_P1 [mm]	pos_P2 [mm]				
0 (Initial)	210	-210	-0.09	-0.002	231.431	-81.419
01	1005	210	0.87	0.015	11707.885	444.925
02	1005	1005	1.49	0.026	19210.457	426.038
03	-210	-1005	-1.06	-0.018	-11238.682	352.256
04	-1005	-1005	-1.66	-0.029	-18765.345	375.160

The inclining moment versus the tangent of the pitch angle is plotted on figure 7-13.

	Model Scale	Full Scale
R6.1 Displacement, Δ [kgf; t]:	1709.4	220745311
R6.2 Target VCG, KG_{req} [mm; m]:	-296	-14.790
R6.3 Estimated Metacentric Height, GM_{req} [mm, m]	413	20.640
R6.4 Calculated VCG, KG_{obt} [mm; m]:	-289	-14.446
R6.5 Measured Metacentric Height, GM_{obt} [mm, m]	410	20.476
R6.6 VCG deviation [mm, %]:	7	-2.3%
R6.7 GM deviation [mm, %]:	-3	-0.8%

Moment vs. tan ϕ (Model Scale)

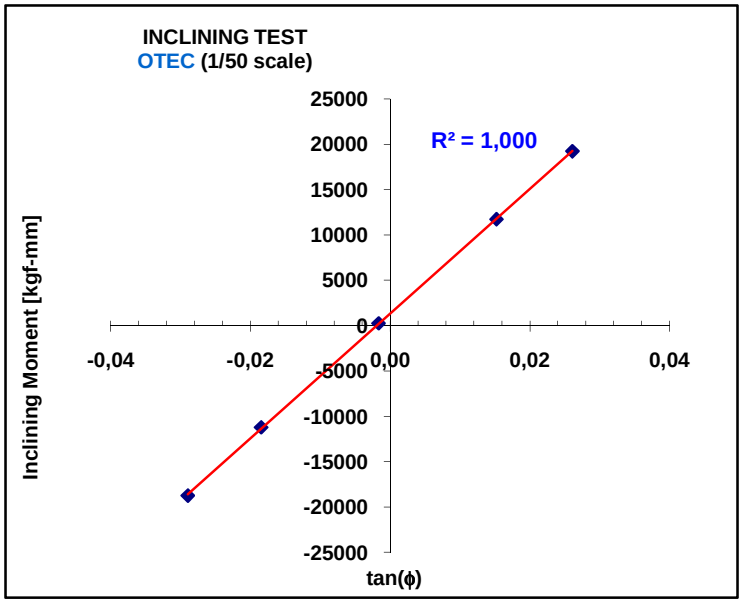

Figure 7-13 - T400 Longitudinal Inclining Moment Linear Fit

7.12.3.6 GM t - PT400_0020X

The ballasts positions, measured roll and calculations for the test are listed on table 7-15.

Table 7-15 - T400 Transversal Inclining Test Results

Item	Description	Weight [kgf]	Ballasts position		
			x [mm-SM]	y [mm-CL]	z [mm-BL]
01	Peso 1 - BB (P1)	9.750	289	0	770
02	Peso 2 - BE (P2)	9.730	-289	0	770
03	Accessories	0.000	0	0	0
	Total =	19.480	0	0	770

Movim. No.	Ballasts P1 and P2 position		Inclin.* [ϕ] [deg]	tan ϕ	Mom. [kgf-mm]	GM_ens [mm]
	pos_P1 [mm]	pos_P2 [mm]				
0 (Initial)	289	-289	-0.05	-0.001	-189.072	114.133
01	932	289	1.26	0.022	11221.734	295.294
02	932	932	1.97	0.034	17218.765	290.280
03	-289	-932	-1.39	-0.024	-11592.815	277.421
04	-932	-932	-2.08	-0.036	-17608.358	281.113

The inclining moment versus the tangent of the roll angle is plotted on figure 7-14.

	Model Scale	Full Scale
R6.1 Displacement, Δ [kgf; t]:	1709.4	220745311
R6.2 Target VCG, KG_{req} [mm; m]:	-296	-14.790
R6.3 Estimated Metacentric Height, GM_{req} [mm, m]	295	14.759
R6.4 Calculated VCG, KG_{obt} [mm; m]:	-292	-14.579
R6.5 Measured Metacentric Height, GM_{obt} [mm, m]	295	14.729
R6.6 VCG deviation [mm, %]:	4	-1.4%
R6.7 GM deviation [mm, %]:	-1	-0.2%

Moment vs. tan ϕ (Model Scale)

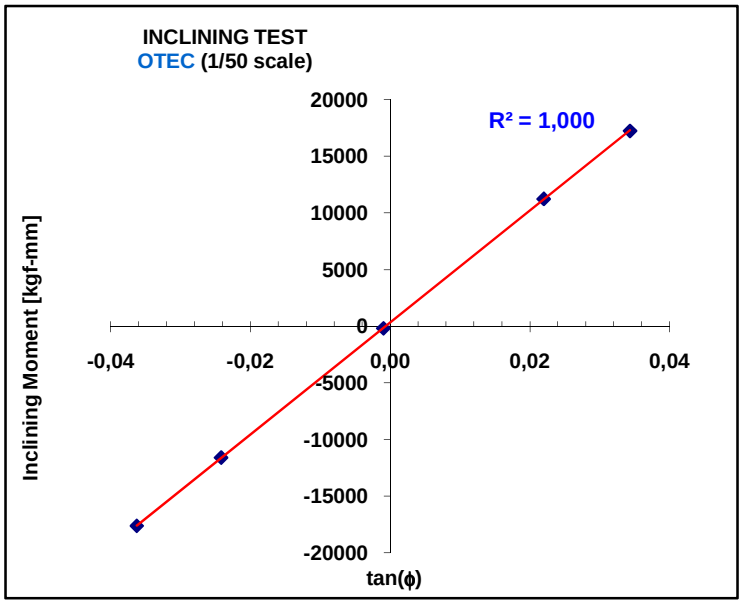

Figure 7-14 - T400 Transversal Inclining Moments Linear Fit

7.12.3.7 GM I - PT300_0010X

The ballasts positions, measured roll and calculations for the test are listed on table 7-16.

Table 7-16 - T300 Longitudinal Inclining Test Results

Item	Description	Weight [kgf]	Ballasts position		
			x [mm-SM]	y [mm-CL]	z [mm-BL]
01	Peso 1 - BB (P1)	9.750	210	0	770
02	Peso 2 - BE (P2)	9.730	-210	0	770
03	Accessories	0.000	0	0	0
	Total =	19.480	0	0	770

Movim. No.	Ballasts P1 and P2 position		Inclin.* [ϕ] [deg]	tan ϕ	Mom. [kgf-mm]	GM_ens [mm]
	pos_P1 [mm]	pos_P2 [mm]				
0 (Initial)	210	-210	-0.11	-0.002	235.507	-74.423
01	1005	210	0.56	0.010	11823.525	697.635
02	1005	1005	1.47	0.026	19218.947	433.745
03	-210	-1005	-1.07	-0.019	-11233.671	348.453
04	-1005	-1005	-1.52	-0.027	-18816.770	411.097

The inclining moment versus the tangent of the pitch angle is plotted on figure 7-15.

	Model Scale	Full Scale
R6.1 Displacement, Δ [kgf; t]:	1705.6	220258468
R6.2 Target VCG, KG_{req} [mm; m]:	-296	-14.790
R6.3 Estimated Metacentric Height, GM_{req} [mm, m]	413	20.640
R6.4 Calculated VCG, KG_{obt} [mm; m]:	-364	-18.177
R6.5 Measured Metacentric Height, GM_{obt} [mm, m]	484	24.207
R6.6 VCG deviation [mm, %]:	-68	22.9%
R6.7 GM deviation [mm, %]:	71	17.3%

Moment vs. tan ϕ (Model Scale)

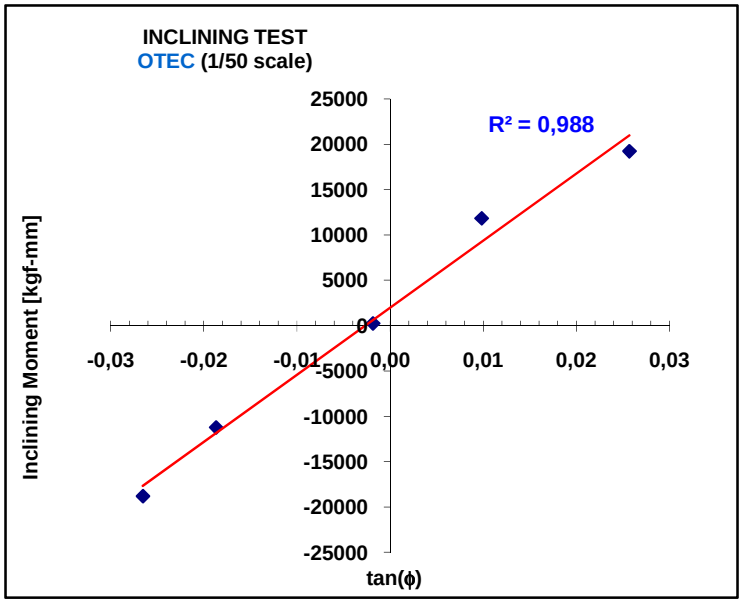

Figure 7-15 - T300 Longitudinal Inclining Moments Linear Fit

7.12.3.8 GM t - PT300_0020X

The ballasts positions, measured roll and calculations for the test are listed on table 7-17.

Table 7-17 - T300 Transversal Inclining Test Results

Item	Description	Weight [kgf]	Ballasts position		
			x [mm-SM]	y [mm-CL]	z [mm-BL]
01	Peso 1 - BB (P1)	9.750	289	0	770
02	Peso 2 - BE (P2)	9.730	-289	0	770
03	Accessories	0.000	0	0	0
	Total =	19.480	0	0	770

Movim. No.	Ballasts P1 and P2 position		Inclin.* [ϕ] [deg]	tan ϕ	Mom. [kgf-mm]	GM_ens [mm]
	pos_P1 [mm]	pos_P2 [mm]				
0 (Initial)	289	-289	0.02	0.000	-216.120	-381.805
01	932	289	0.73	0.013	11415.620	518.538
02	932	932	2.08	0.036	17176.523	274.159
03	-289	-932	-0.72	-0.013	-11836.173	544.567
04	-932	-932	-2.05	-0.036	-17617.716	285.381

The inclining moment versus the tangent of the roll angle is plotted on figure 7-16.

	Model Scale	Full Scale
R6.1 Displacement, Δ [kgf; t]:	1705.6	220258468
R6.2 Target VCG, KG_{req} [mm; m]:	-296	-14.790
R6.3 Estimated Metacentric Height, GM_{req} [mm, m]	295	14.759
R6.4 Calculated VCG, KG_{obt} [mm; m]:	-414	-20.681
R6.5 Measured Metacentric Height, GM_{obt} [mm, m]	417	20.831
R6.6 VCG deviation [mm, %]:	-118	39.8%
R6.7 GM deviation [mm, %]:	121	41.1%

Moment vs. tan ϕ (Model Scale)

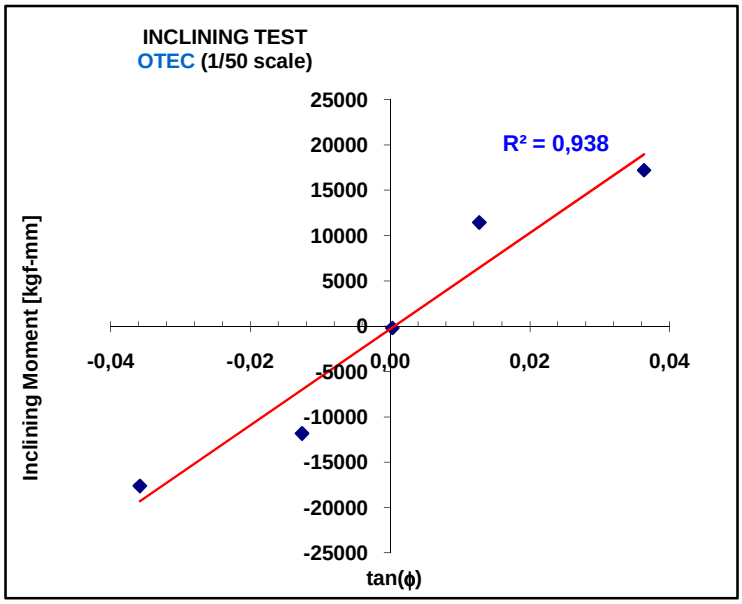

Figure 7-16 - T300 Transversal Inclining Moments Linear Fit

7.12.3.9 GM I - PT600_0010X

The ballasts positions, measured roll and calculations for the test are listed on table 7-18.

Table 7-18 - T600 Longitudinal Inclining Test Results

Item	Description	Weight [kgf]	Ballasts position		
			x [mm-SM]	y [mm-CL]	z [mm-BL]
01	Peso 1 - BB (P1)	4.938	220	0	841
02	Peso 2 - BE (P2)	5.170	-220	0	841
03	Accessories	0.000	0	0	0
	Total =	10.108	-5	0	841

Movim. No.	Ballasts P1 and P2 position		Inclin.* [ϕ] [deg]	tan ϕ	Mom. [kgf-mm]	GM_ens [mm]
	pos_P1 [mm]	pos_P2 [mm]				
0 (Initial)	220	-220	-0.27	-0.005	240.220	-159.949
01	562	-220	1.71	0.030	1186.139	122.288
02	562	220	3.43	0.060	2821.736	145.463
03	220	-562	-1.68	-0.029	-995.116	104.496
04	-220	-562	-3.27	-0.057	-2576.920	139.335

The inclining moment versus the tangent of the pitch angle is plotted on figure 7-17.

	Model Scale	Full Scale
R6.1 Displacement, Δ [kgf; t]:	314.1	40564243
R6.2 Target VCG, KG_{req} [mm; m]:	358	17.890
R6.3 Estimated Metacentric Height, GM_{req} [mm, m]	78	3.920
R6.4 Calculated VCG, KG_{obt} [mm; m]:	296	14.796
R6.5 Measured Metacentric Height, GM_{obt} [mm, m]	145	7.274
R6.6 VCG deviation [mm, %]:	-62	-17.3%
R6.7 GM deviation [mm, %]:	67	85.6%

Moment vs. tan ϕ (Model Scale)

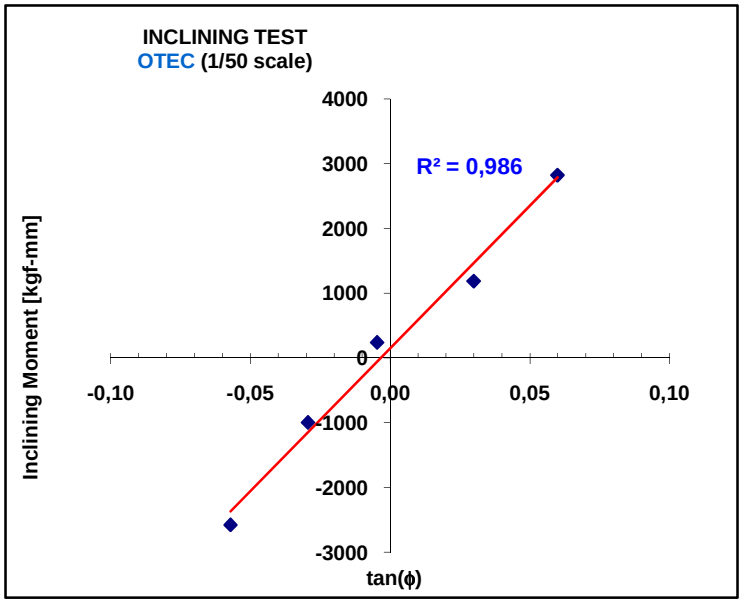

Figure 7-17 - T600 Longitudinal Inclining Moments Linear Fit

7.12.3.10 GM t - PT600_0020X

The ballasts positions, measured roll and calculations for the test are listed on table 7-19.

Table 7-19 - T600 Transversal Inclining Test Results

Item	Description	Weight [kgf]	Ballasts position		
			x [mm-SM]	y [mm-CL]	z [mm-BL]
01	Peso 1 - BB (P1)	4.938	220	0	841
02	Peso 2 - BE (P2)	5.170	-220	0	841
03	Accessories	0.000	0	0	0
	Total =	10.108	-5	0	841

Movim. No.	Ballasts P1 and P2 position		Inclin.* [ϕ] [deg]	tan ϕ	Mom. [kgf-mm]	GM_ens [mm]
	pos_P1 [mm]	pos_P2 [mm]				
0 (Initial)	0	0	0.02	0.000	-224.023	-1609.275
01	-288	0	-1.53	-0.027	-1073.422	124.051
02	-575	0	-2.65	-0.046	-2083.341	139.197
03	288	0	1.31	0.023	727.732	98.455
04	575	0	2.37	0.041	1756.138	131.218

The inclining moment versus the tangent of the roll angle is plotted on figure 7-18.

	Model Scale	Full Scale
R6.1 Displacement, Δ [kgf; t]:	314.1	40564243
R6.2 Target VCG, KG_{req} [mm; m]:	358	17.890
R6.3 Estimated Metacentric Height, GM_{req} [mm, m]	78	3.920
R6.4 Calculated VCG, KG_{obt} [mm; m]:	301	15.036
R6.5 Measured Metacentric Height, GM_{obt} [mm, m]	141	7.034
R6.6 VCG deviation [mm, %]:	-57	-16.0%
R6.7 GM deviation [mm, %]:	62	79.4%

Moment vs. tan ϕ (Model Scale)

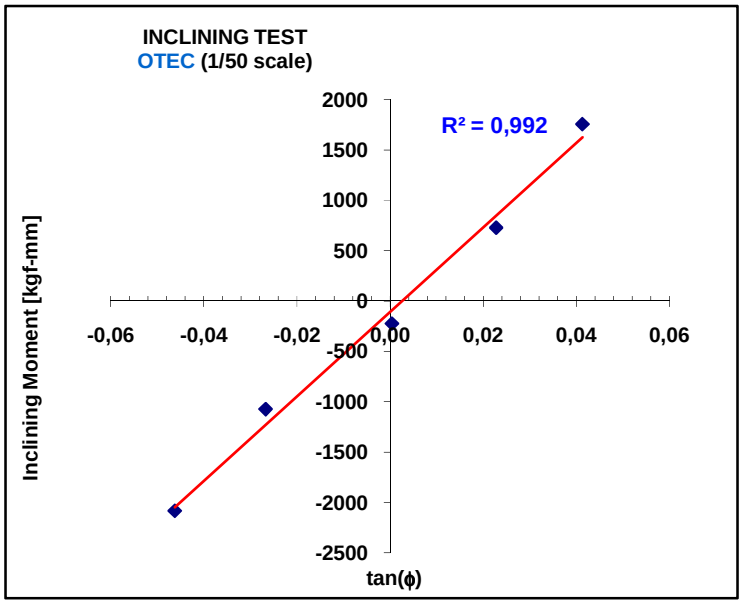

Figure 7-18 - T600 Transversal Inclining Moments Linear Fit

7.12.3.11 GM I - PT500_0010X

The ballasts positions, measured roll and calculations for the test are listed on table 7-20.

Table 7-20 - T500 Longitudinal Inclining Test Results

Item	Description	Weight [kgf]	Ballasts position		
			x [mm-SM]	y [mm-CL]	z [mm-BL]
01	Peso 1 - BB (P1)	4.938	220	0	841
02	Peso 2 - BE (P2)	5.170	-220	0	841
03	Accessories	0.000	0	0	0
	Total =	10.108	-5	0	841

Movim. No.	Ballasts P1 and P2 position		Inclin.* [ϕ] [deg]	tan ϕ	Mom. [kgf-mm]	GM_ens [mm]
	pos_P1 [mm]	pos_P2 [mm]				
0 (Initial)	220	-220	-0.08	-0.001	170.431	-376.777
01	562	-220	2.00	0.035	1079.287	94.028
02	562	220	4.00	0.070	2608.593	113.703
03	220	-562	-1.85	-0.032	-932.284	87.752
04	-220	-562	-3.85	-0.067	-2359.850	106.848

The inclining moment versus the tangent of the pitch angle is plotted on figure 7-19.

	Model Scale	Full Scale
R6.1 Displacement, Δ [kgf; t]:	318.8	41167309
R6.2 Target VCG, KG_{req} [mm; m]:	363	18.140
R6.3 Estimated Metacentric Height, GM_{req} [mm, m]	78	3.920
R6.4 Calculated VCG, KG_{obt} [mm; m]:	325	16.227
R6.5 Measured Metacentric Height, GM_{obt} [mm, m]	117	5.843
R6.6 VCG deviation [mm, %]:	-38	-10.5%
R6.7 GM deviation [mm, %]:	38	49.0%

Moment vs. tan ϕ (Model Scale)

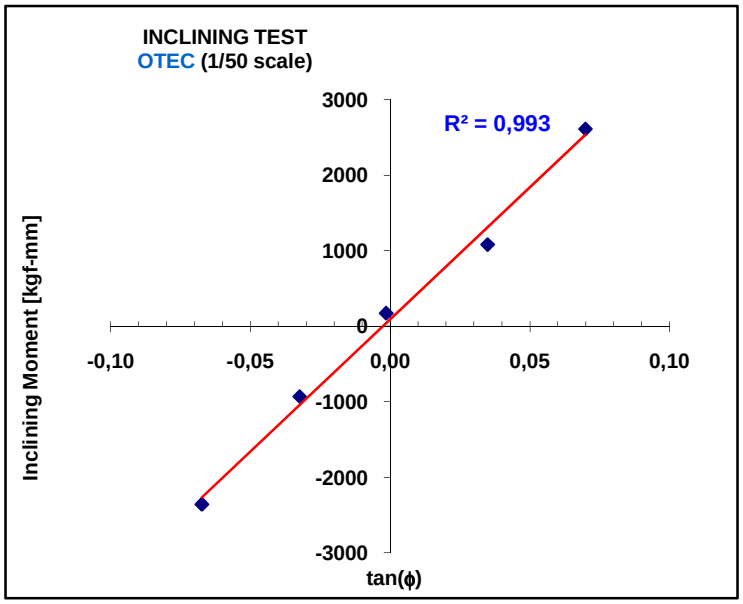

Figure 7-19 - T500 Longitudinal Inclining Moments Linear Fit

7.12.3.12 GM t - PT500_0020X

Similar setup and analysis procedure as described for the longitudinal inclining test.

The ballasts positions, measured roll and calculations for the test are listed on table 7-21.

Table 7-21 - T500 Transversal Inclining Test Results

Item	Description	Weight [kgf]	Ballasts position		
			x [mm-SM]	y [mm-CL]	z [mm-BL]
01	Peso 1 - BB (P1)	4.938	220	0	841
02	Peso 2 - BE (P2)	5.170	-220	0	841
03	Accessories	0.000	0	0	0
	Total =	10.108	-5	0	841

Movim. No.	Ballasts P1 and P2 position		Inclin.* [ϕ] [deg]	tan ϕ	Mom. [kgf-mm]	GM_ens [mm]
	pos_P1 [mm]	pos_P2 [mm]				
0 (Initial)	0	0	0.03	0.000	-224.850	-1450.744
01	-288	0	-1.57	-0.027	-1060.092	117.327
02	-575	0	-2.98	-0.052	-1967.964	115.235
03	288	0	1.51	0.026	654.753	75.376
04	575	0	2.94	0.051	1552.856	92.190

The inclining moment versus the tangent of the roll angle is plotted on figure 7-20.

	Model Scale	Full Scale
R6.1 Displacement, Δ [kgf; t]:	318.8	41167309
R6.2 Target VCG, KG_{req} [mm; m]:	363	18.140
R6.3 Estimated Metacentric Height, GM_{req} [mm, m]	78	3.920
R6.4 Calculated VCG, KG_{obt} [mm; m]:	325	16.256
R6.5 Measured Metacentric Height, GM_{obt} [mm, m]	116	5.814
R6.6 VCG deviation [mm, %]:	-38	-10.4%
R6.7 GM deviation [mm, %]:	38	48.3%

Moment vs. tan ϕ (Model Scale)

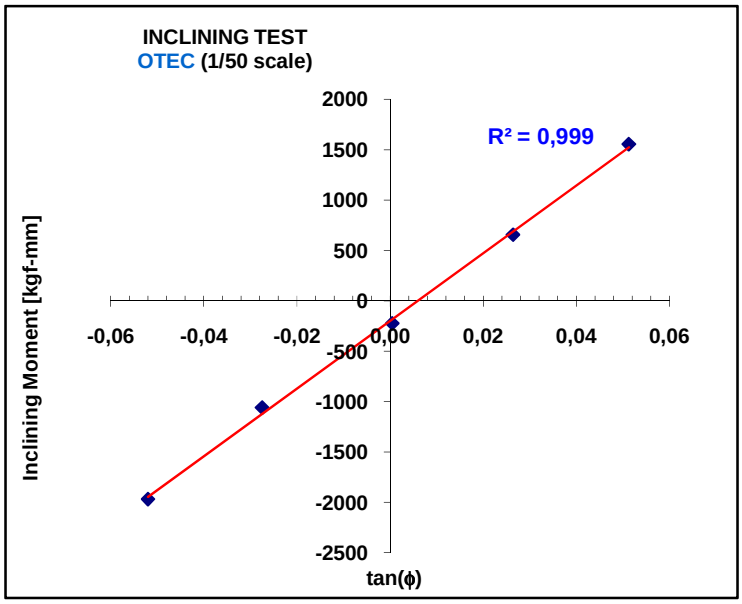

Figure 7-20 - T500 Transversal Inclining Moments Linear Fit

7.12.4 CWP Static Offset Test

During the test the CWP Motion relative to the Semi was measured, six (6) windows of data were selected and the mean value for the pullout force and targets position were calculated and are presented on table 7-22.

Table 7-22 - CWP Static Offset Test Results

CWP STATIC OFFSET - MODEL SCALE										
Step	Force [gf]	CWP4_X [mm]	CWP4_Y [mm]	CWP4_Z [mm]	CWP5_X [mm]	CWP5_Y [mm]	CWP5_Z [mm]	CWP6_X [mm]	CWP6_Y [mm]	CWP6_Z [mm]
#0	20.3	40.4	1.4	-18682.9	43.1	2.5	-19366.4	47.3	3.7	-20341.9
#1	209.4	961.3	21.7	-18640.7	1010.1	22.9	-19316.0	-	-	-
#2	187.9	875.9	27.9	-18651.0	918.7	27.1	-19323.1	-	-	-
#3	126.6	605.7	30.6	-18673.3	638.4	25.0	-19342.6	-	-	-
#4	63.1	306.2	17.3	-18676.5	323.9	18.6	-19358.2	350.2	25.6	-20339.5
#5	19.0	36.7	14.5	-18682.8	38.9	17.1	-19366.4	42.4	21.1	-20342.2

CWP STATIC OFFSET - PROTOTYPE SCALE										
Step	Force [KN]	CWP4_X [m]	CWP4_Y [m]	CWP4_Z [m]	CWP5_X [m]	CWP5_Y [m]	CWP5_Z [m]	CWP6_X [m]	CWP6_Y [m]	CWP6_Z [m]
#0	1.988E-04	2.02	0.07	-934.14	2.16	0.13	-968.32	2.37	0.18	-1017.09
#1	2.053E-03	48.06	1.08	-932.04	50.50	1.15	-965.80	-	-	-
#2	1.842E-03	43.79	1.39	-932.55	45.93	1.35	-966.15	-	-	-
#3	1.242E-03	30.29	1.53	-933.66	31.92	1.25	-967.13	-	-	-
#4	6.185E-04	15.31	0.87	-933.83	16.20	0.93	-967.91	17.51	1.28	-1016.97
#5	1.863E-04	1.83	0.73	-934.14	1.94	0.85	-968.32	2.12	1.06	-1017.11

7.12.5 CWP Impulse Test

A spectral analysis of the gimbal load in the X direction provided a plot, shown on figure 7-21, that was use to identify the natural modes frequencies of the Cold Water Pipe on the T400 test group configuration.

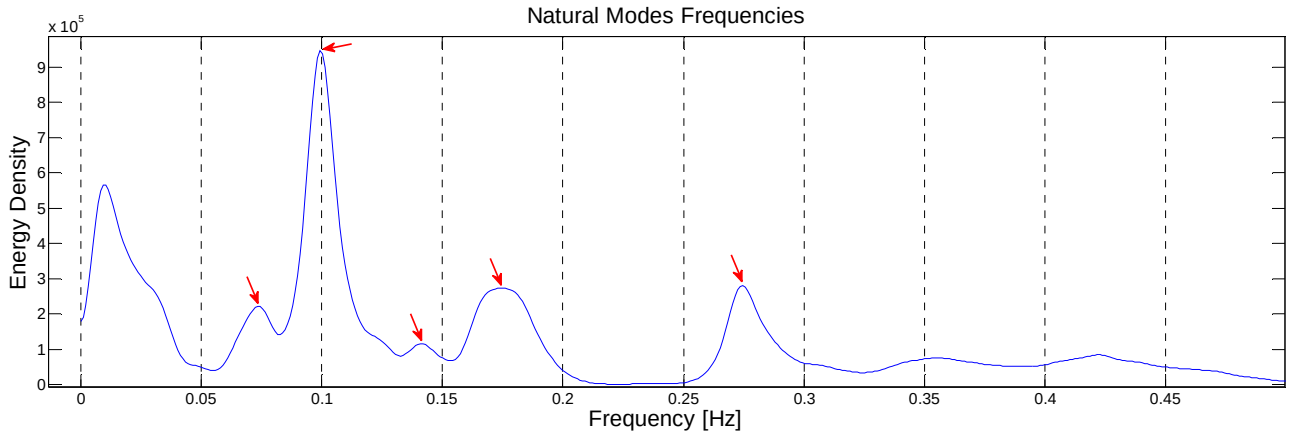

Figure 7-21 - CWP Impulse Test Natural Modes Identification

The parameters summary of the identified natural modes are presented on table 7-23.

Table 7-23 - CWP Impulse Test Natural Modes Frequencies

	Frequency [Hz]	Period [s]
Mode #1	0.07354	13.598
Mode #2	0.09944	10.0563
Mode #3	0.1409	7.0972
Mode #4	0.1751	5.7110
Mode #5	0.2745	3.6430

The first identified mode is not necessarily the first natural mode of the CWP model.

7.12.6 Free-Decay Tests

The results from the motion decay tests for heave, roll and pitch (free floating condition) and for surge, sway, heave, roll and pitch (horizontal mooring system) are presented in 'Annex C – Decay Tests Reports'. The decay tests have been analyzed to give natural periods and relative damping.

The T500 and T600 test groups with the installation stiffness gimbal pitch and roll decay tests presented strange behavior, with coupling of movements in different degrees of freedom, making impossible a meaningful analysis.

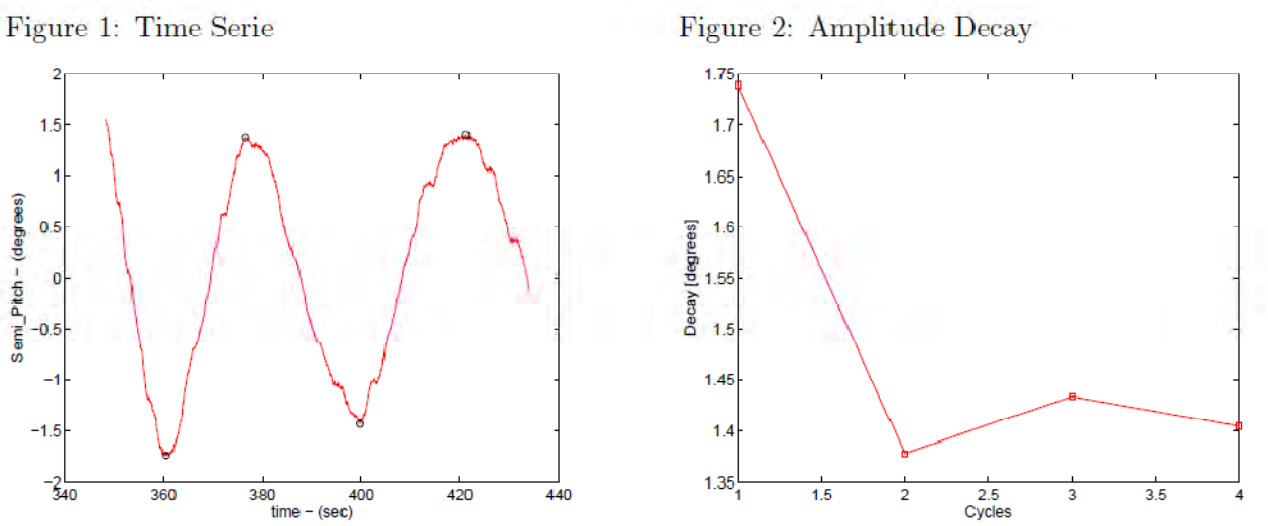

Figure 7-22 - T500 and T600 Free Decay Tests Results

7.12.7 Inclining LVDT Check

7.12.7.1 Operation Configuration - PT400_50010X

For the purpose of checking the LVDT measurement of the gimbal angle an extreme inclining test was executed with 40 kgf of load on the extreme ballast position to provide maximum pitch and roll of the model.

The measured pitch and roll angles from the Semi and Gimbal are listed on table 7-24.

Table 7-24 - T400 Inclining LVDT Check Test Results

	PT400_500100		PT400_500101		PT400_500102	
	PITCH	ROLL	PITCH	ROLL	PITCH	ROLL
SEMI	2.711	0.045	-2.967	0.049	-0.126	-4.015
GIMBAL	0.572	-2.708	3.694	-2.464	1.871	-0.329

7.12.7.2 Pinned Configuration - PT300_50010X

For the purpose of checking the LVDT measurement of the gimbal angle an extreme inclining test was executed with 40kg of load on the extreme ballast position to provide maximum pitch and roll of the model.

Since the cold water pipe was pinned at the gimbal, the measured angle from the LVDT should be the opposite pitch and roll angle of the Semi, measured by Qualisys instruments. The opposite value of the semi attitude angles were plotted against the gimbal attitude measured by the LVDT sensors on figure 7-23, for comparison.

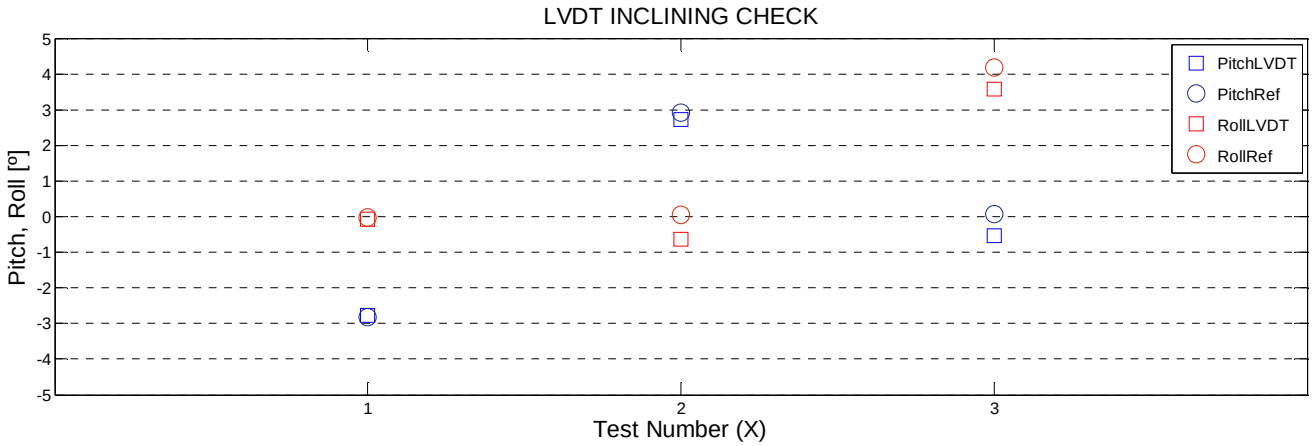

Figure 7-23 - T300 Inclining LVDT Check Test Comparison plot

The measured pitch and roll angles from the Semi and Gimbal are listed on table 7-25.

Table 7-25 - T400 Inclining LVDT Check Test Results

	PT300_500100		PT300_500101		PT300_500102	
	PITCH	ROLL	PITCH	ROLL	PITCH	ROLL
SEMI	2.811	0.013	-2.9205	-0.050	-0.0633	-4.175
GIMBAL	-2.780	-0.076	2.730	-0.628	-0.524	3.565

7.13 REGULAR WAVES TESTS

The analyzed channels for the regular waves are listed on table 7-26.

Table 7-26 - Channels on Regular Wave Tests Analysis Products

Analyzed Channels - Regular Waves			
Gimbal_Fx	WAVE2_C *	SG13	CWP3_Z
Gimbal_Fy	WAVE3_C *	SG14	CWP4_X
Gimbal_Fz	WAVE4_C *	SG15	CWP4_Y
Gimbal_Pitch	WAVE5_C *	SG16	CWP4_Z
Gimbal_Roll	SG1	SG17	CWP5_X
Mooring1	SG2	SG18	CWP5_Y
Mooring2	SG3	SG19	CWP5_Z
Mooring3	SG4	SG20	CWP6_X
Mooring4	SG5	CWP1_X	CWP6_Y
Wind	SG6	CWP1_Y	CWP6_Z
Runup	SG7	CWP1_Z	Semi_X
Airgap	SG8	CWP2_X	Semi_Y
WAVE1 *	SG9	CWP2_Y	Semi_Z
WAVE3 *	SG10	CWP2_Z	Semi_Pitch
WAVE5 *	SG11	CWP3_X	Semi_Roll
WAVE1_C *	SG12	CWP3_Y	Semi_Yaw

(*) Not included in RAO analysis

For the regular wave tests those channels were analyzed to provide:

- Time Series plots with the transient period trimmed out;
- Basic Statistics: mean, maximum, minimum, standard deviation, skewness and kurtosis;
- Linear RAOs, with amplitude, phase and coherence plots

For the full analysis products refer to annex 'D Regular Wave Test Files Index'.

The RAO of SG1, SG2, SG3, SG4 and SG5 for the T400 regular waves test group are compared to the natural periods identified by the impulse test on the plot presented on figure 7-24.

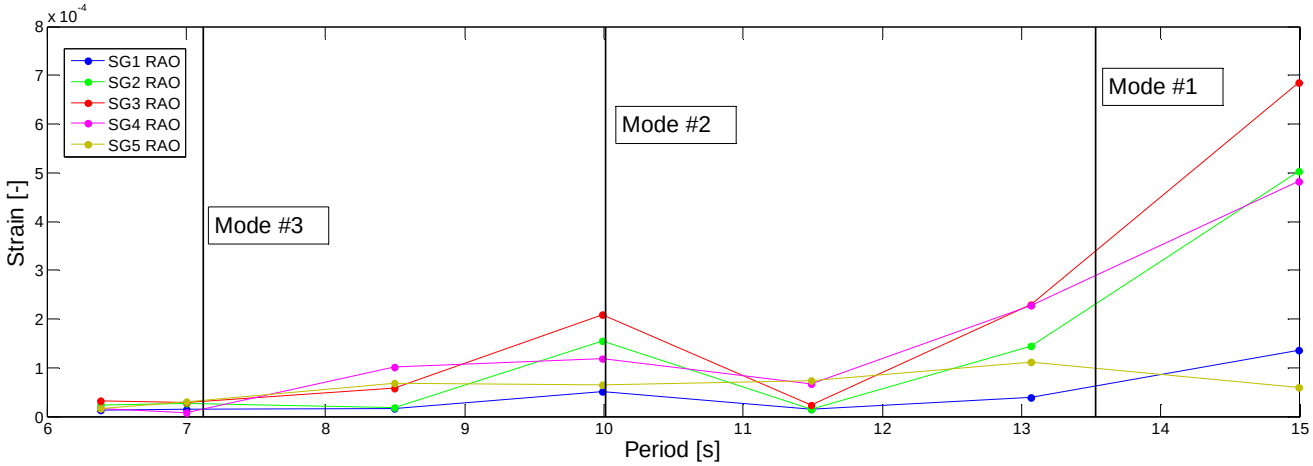

Figure 7-24 - T400 Regular Waves Strain Gages RAO Comparison

This plot demonstrates a peak in the RAO for mode #2 period very close to the period of regular wave 4.

Mode #3 does not appear to have been excited by regular wave 2. This could be either because the regular wave period is slightly different from the modal period or because the applied energy is too small to significantly excite the pipe.

Mode #1 period is between the regular wave 6 and 7 periods, but from regular wave 7 period it is clear that there are lower modes than mode #1 identified on the impulse test.

For the T400 test groups strain gage #3 had the biggest response on regular wave 1, 2, 4, 6 and 7, strain gage #4 on regular wave 3 and strain gage #5 on regular wave 5.

The RAO of SG3 is compared for all different test groups on figure 7-25.

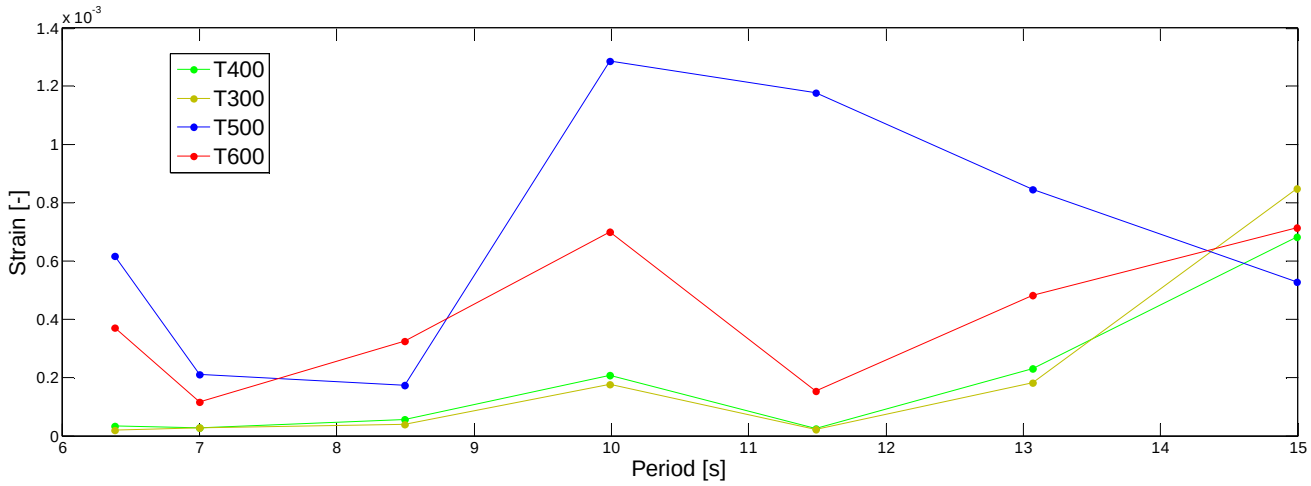

Figure 7-25 Regular Waves Strain Gage SG3 RAO Test Groups Comparison

It can be seen from this plot that the installation cases are definitely the most critical condition. Smaller periods seen to excite the pipe in higher modes, as observed on regular wave 1.

The pipe maximum response is on regular wave 4 for test group T500 with installation stiffness and half length of cold water pipe. The peak response seems to be on a period between regular wave 4 and 5. Compared to the full length of pipe, test group T600 this result could be a consequence of either or both a higher excitation from the semi or a smaller inertia from the pipe, causing natural modes to shift to smaller periods.

The gimbal operational stiffness for the T400 test group compared to zero stiffness on test group T300 does not seem to affect the pipe responses, except for extremely high periods tested on regular wave 7.

Those analyses will be further investigated on the irregular waves analysis and comparisons.

7.14 IRREGULAR WAVES TESTS

The analyzed channels for the irregular waves are listed on table 7-27.

Table 7-27- Channels on Regular Wave Tests Analysis Products

Analyzed Channels - Regular Waves			
Gimbal_Fx	WAVE2_C *	SG13	CWP3_Z
Gimbal_Fy	WAVE3_C *	SG14	CWP4_X
Gimbal_Fz	WAVE4_C *	SG15	CWP4_Y
Gimbal_Pitch	WAVE5_C *	SG16	CWP4_Z
Gimbal_Roll	SG1	SG17	CWP5_X
Mooring1	SG2	SG18	CWP5_Y
Mooring2	SG3	SG19	CWP5_Z
Mooring3	SG4	SG20	CWP6_X
Mooring4	SG5	CWP1_X	CWP6_Y
Wind	SG6	CWP1_Y	CWP6_Z
Runup	SG7	CWP1_Z	Semi_X
Airgap	SG8	CWP2_X	Semi_Y
WAVE1 *	SG9	CWP2_Y	Semi_Z
WAVE3 *	SG10	CWP2_Z	Semi_Pitch
WAVE5 *	SG11	CWP3_X	Semi_Roll
WAVE1_C *	SG12	CWP3_Y	Semi_Yaw

(*) Not included in RAO analysis

For the irregular wave tests those channels were analyzed to provide:

- Time Series plots with the transient period trimmed out;
- Basic Statistics: mean, maximum, minimum, standard deviation, skewness and kurtosis;
- Spectral Analysis plots and table with spectra area, moments, Tz and Tc parameters;
- Weibull Analysis plots and table with linear fitting coefficients, number of zero crossing and most probable maximum for a 3 hours period;
- RAO analysis plots for amplitude, phase and coherence.

For the full analysis products refer to annex E Irregular Wave Test Files Index.

The spectral analysis of the wave elevation at the model position, for the white noise tests, is presented on figure 7-26.

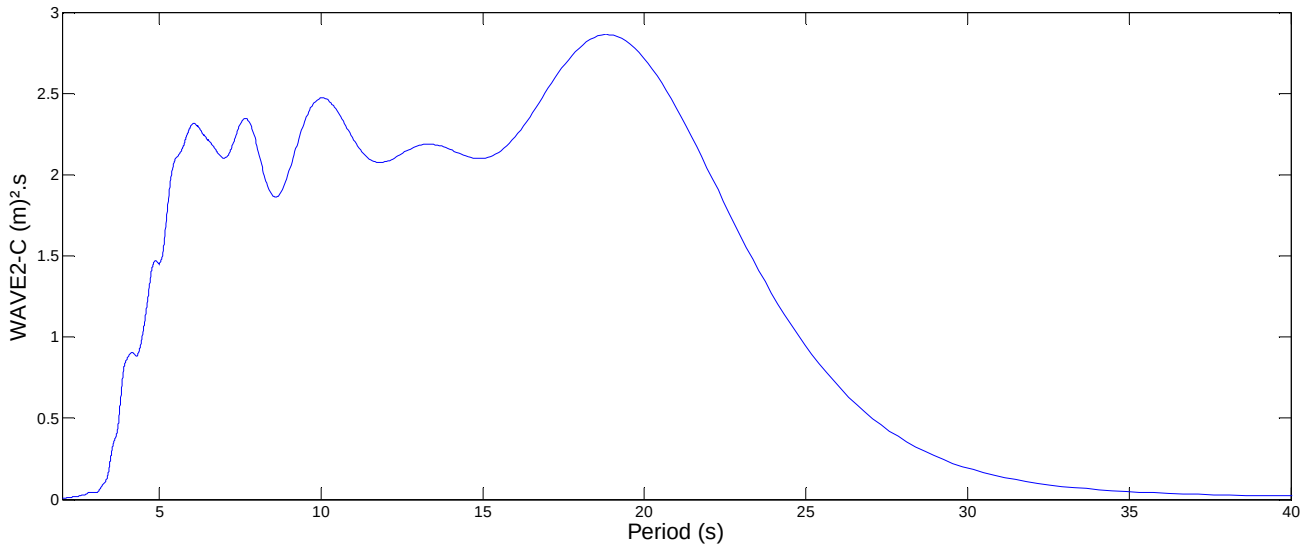

Figure 7-26 - White Noise Wave Elevation Spectral Analysis

The Semi pitch, surge and heave motions RAOs for the T200 and T400 white noise test cases were plotted for comparison on figure 7-27.

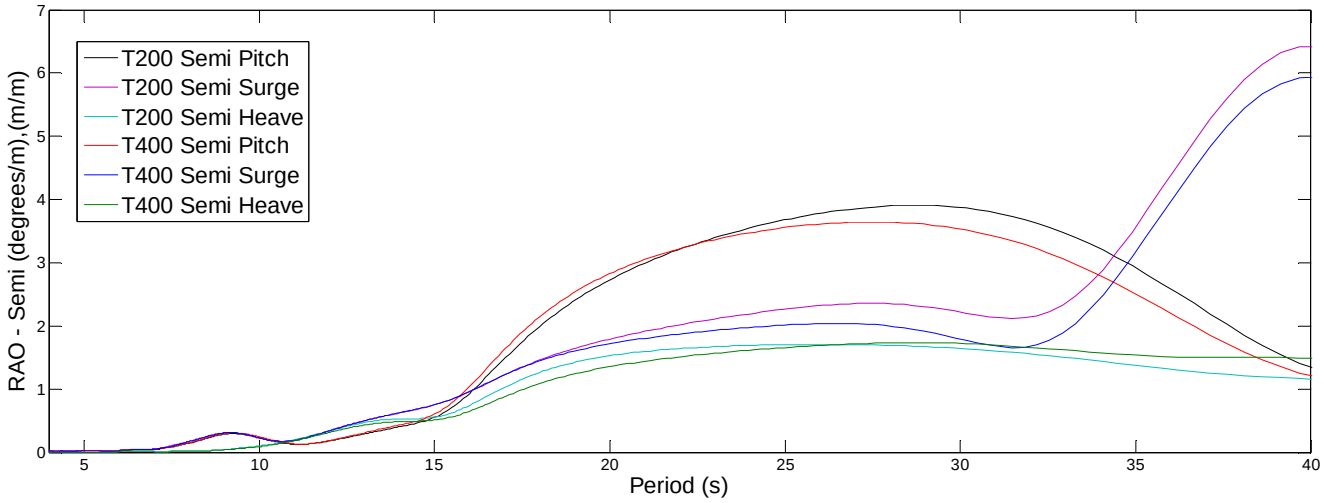

Figure 7-27 - Semi-Submersible XZ Plane Motion RAO - T200 and T400 Comparison

Comparing the Pitch and Surge response RAOs of the Semi for the T400 and T200 test cases, the presence of the pipe appears to decrease the semi motion responses. The Heave response RAO seems to be increased by the presence of the CWP pipe on periods higher than 15 seconds.

From this analysis it can be observed a peak response in the Surge and Pitch Semi motions close to 9 seconds period and on all motions on periods higher than 15 seconds.

The RAO of SG1, SG2, SG3, SG4 and SG5 for the T400 test group white noise wave were compared to the natural periods identified by the impulse test on the plot presented on figure 7-28.

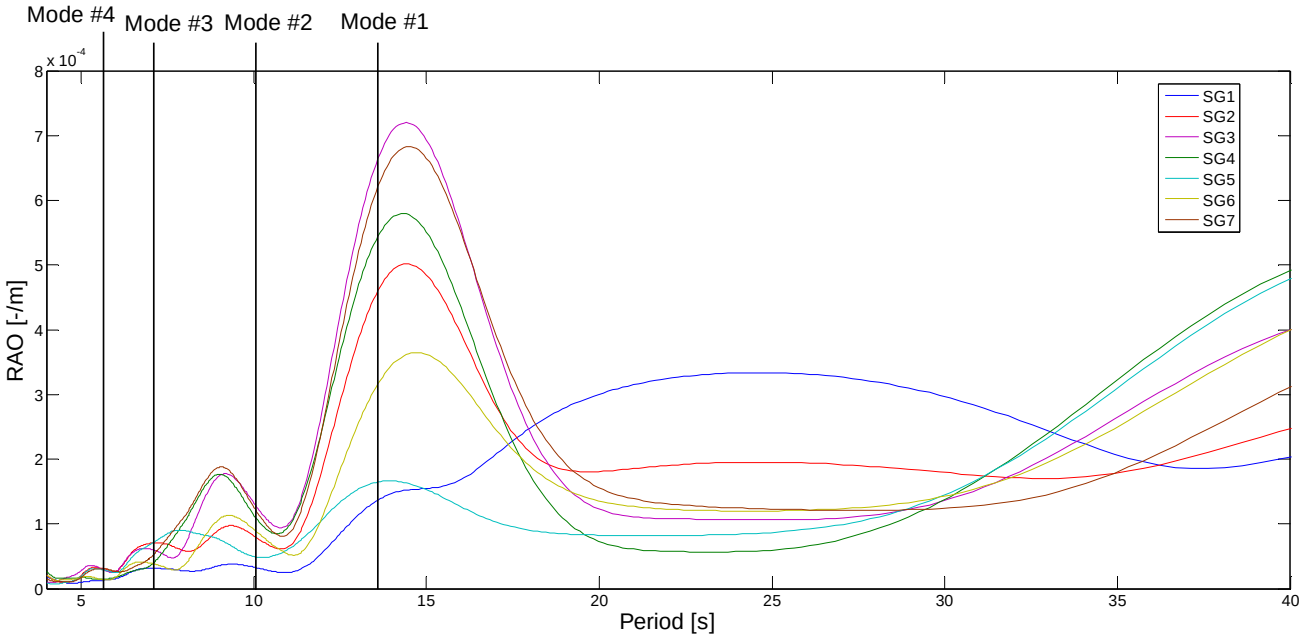

Figure 7-28 - T400 Strain Gages RAO Comparison

This analysis confirms strain gage #3 as the most responsive.

This analysis indicates a peak response on 9 seconds for most strain gages, between mode #2 and #3. This is probably due to the Semi motion exciting the pipe on this frequency as observed on the previous analysis. Strain gage #1, the closest one to the Semi also indicates a similar response RAO to the Semi's motion RAO. The peak response RAO on 15 seconds is the highest one, combining the Semi motion with the CWP natural period. This indicates that the CWP model is much more sensitive to the Semi motions than direct wave excitation.

Strain gage #3 responses RAO for the T300, T400, T500 and T600 white noise wave test cases are plotted for comparison on figure 7-29.

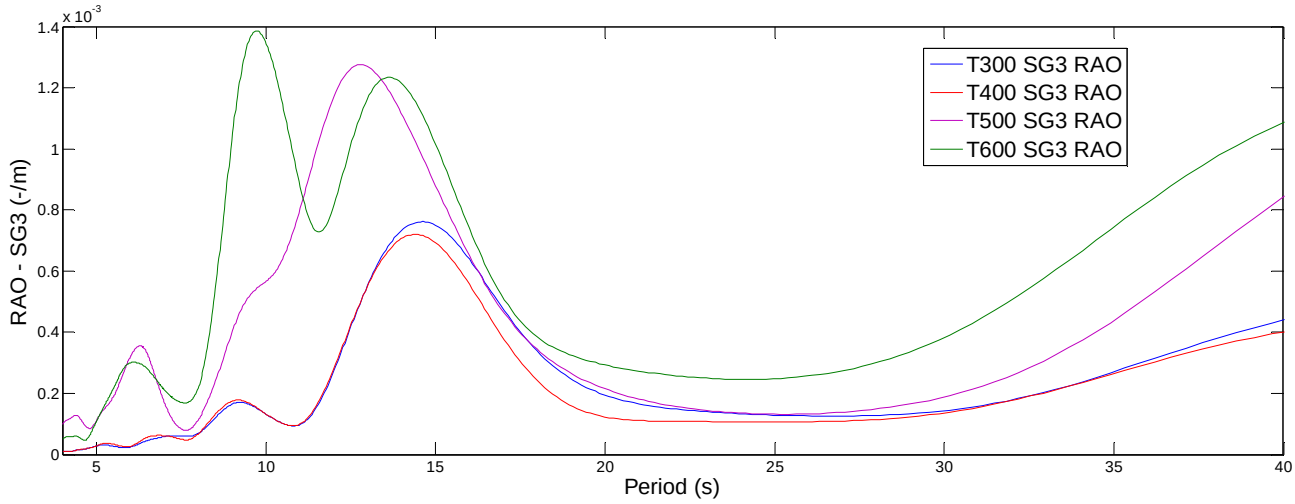

Figure 7-29 - Strain Gage SG3 RAO Test Groups Comparison

This analysis indicates that, at least for strain gage #3, the change of stiffness from test group T400 to T300 did not cause an impact on the CWP response.

The response on test groups T500 and T600 are similar, except for the peak at 9 seconds that does not occur

on the T500 test group. This could be because of a shift in the CWP natural periods or from a different excitation from the Semi.

The Semi surge response RAO for the T500 and T600 white noise test case are compared on figure 7-30.

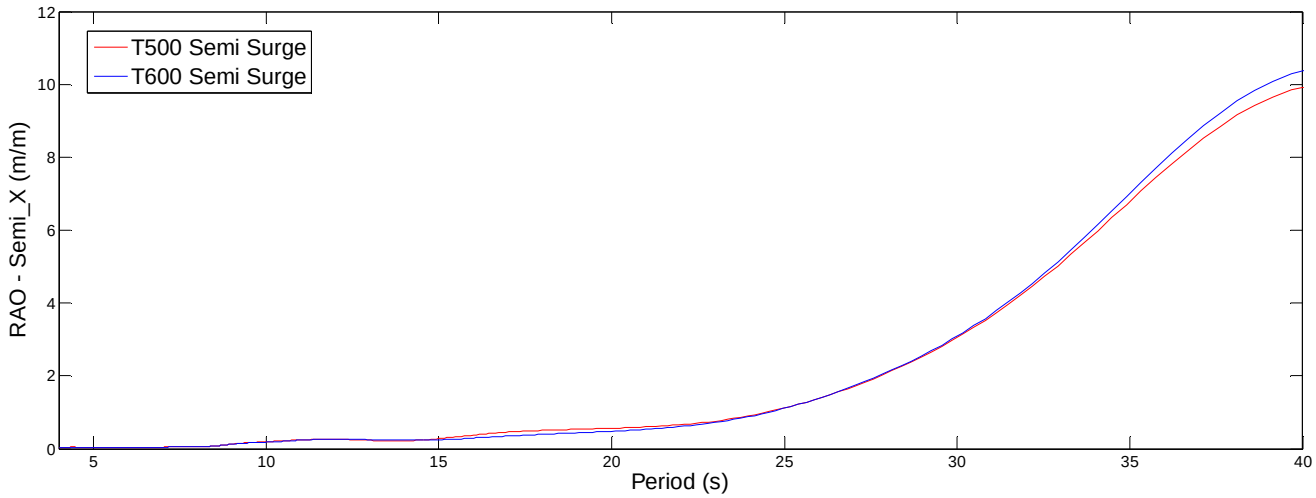

Figure 7-30 - T500 and T600 Semi Surge RAO Comparison

This analysis confirms that the change of length of the CWP did not cause a big change in the Semi response, so the different strain responses on the CWP for those test cases are most likely a consequence of the different natural modes of the CWP model.

For most wave tests the gimbal attitude had a mean offset from zero. Observing the analysis of the CWP tracking targets initial position this value does not appear to reflect the actual model attitude and it is most probably due to the uncertainties of the boundary conditions of the gimbal attitude script.

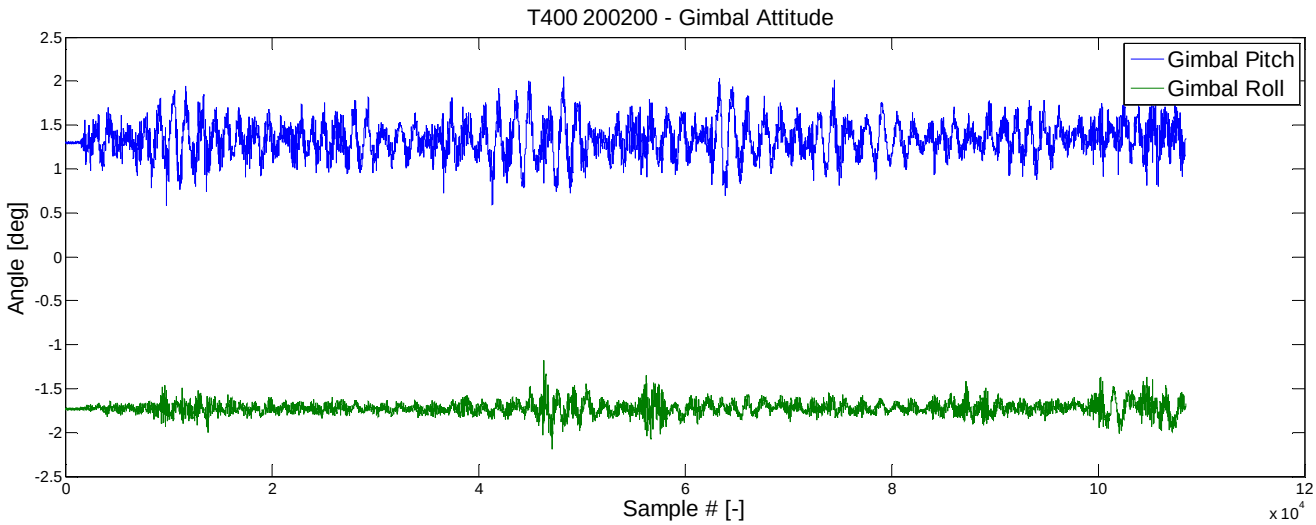

Figure 7-31 - Gimbal Attitude Mean Value Initial Offset

For the T300, pinned gimbal, 10 year sea test case the gimbal dynamometer displayed a strange response, the cause is unknown. From comparison to other tests in the same test group the initial vertical load on the gimbal for this particular case appears to be higher than usual.

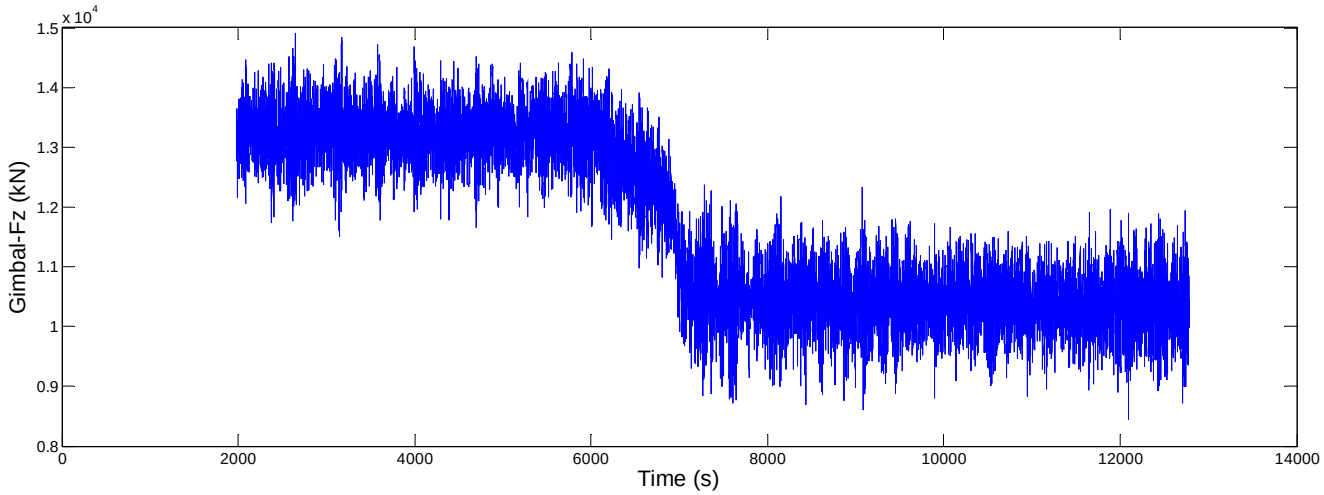

Figure 7-32 - T300_200200 Gimbal Vertical Force Offset

For the T300, pinned gimbal, 10 year swell test case the Semi sway motion displayed a strange behavior, the cause is unknown.

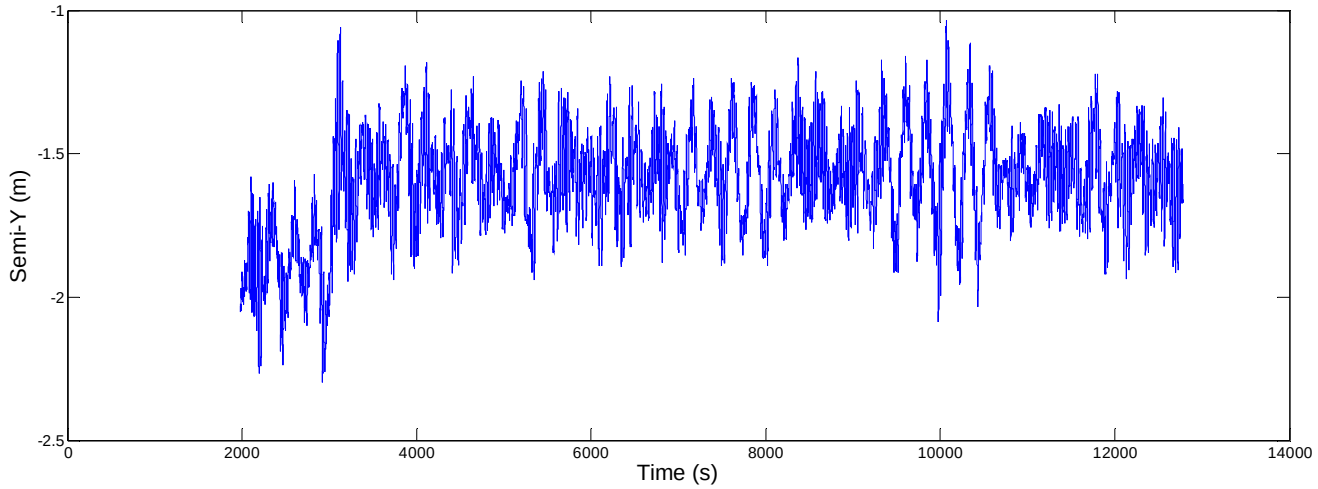

Figure 7-33 - T300_200300 Semi Sway Motion Mean Value Offset

For the T400, operational stiffness gimbal, 100 years cyclone test case, the CWP #4 tracking target was out of sight from the cameras, causing a discontinuous signal. For this reason the spectral analysis of this target was not done on this test case.

For the T600 and T500 test groups the gimbal attitude derived from the LVDTs measurements appeared to be less reliable than the other test groups. This was probably because of a different setup of the LVDTs that would require an additional calibration.

Many green water incidents were observed, even though this was not the focus of the model tests it should be noted when designing the final Semi model.

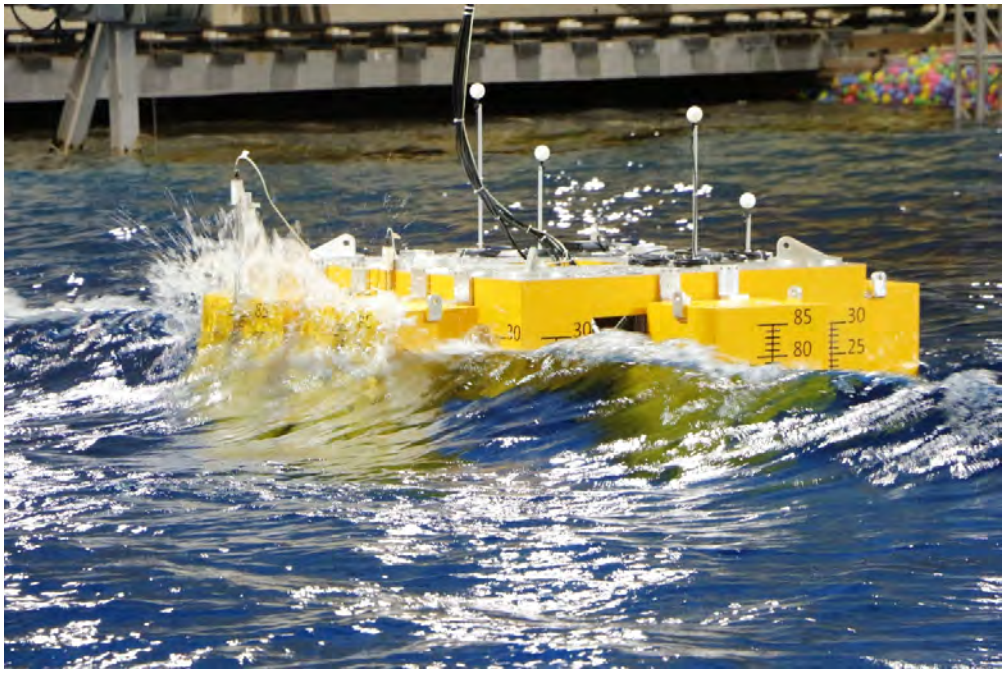

Figure 7-34 - Green Water Incident

Viscous effects like flow vortex shedding were observed on the many sharp edges of the model. Those effects will not be captured by Potential Theory numerical models and should be quantified.

8 FINAL COMMENTS

Model and CWP calibration and verification were acceptable for testing purposes.

The deviations on gimbal angle measurements through LVDT sensors were close to the measured values. This was due to the small angles measured, that lead to small values measured at LVDTs. The gimbal loads were below the expected values from numerical models.

Some dry tests measurements were out of the suggested tolerance but it was agreed that their applicability was acceptable for simulating different operation and installation configurations. All of the measured parameters were summarized on this document, raw and processed data were delivered on separate files.

The strain gages RAO analysis for the regular waves have shown a good match with the impulse test analysis results. For future tests the regular wave periods could be reviewed to match exactly the expected model natural modes. The comparison between tests configuration have shown that the higher gimbal stiffness was only an advantage on extreme conditions and confirmed the expectance of higher loads on the installation configuration.

The strain gages RAO analysis for the white noise indicated a slight shift on the natural modes compared to the impulse test analysis results, the cause may be the influence of the semi response inputting a motion on the cold water pipe. The comparison between tests configuration have confirmed the small difference in the strain gage response for the different gimbal operational stiffness.

The VectorNav sensor was installed on top of the CWP model to measure the CWP angle relative to the semi keel. The data provided by this sensor was shown unreliable when compared to the LVDT check inclining test. We suspect that the reason for the deviation observed was a drift on the magnetometer responsible for the heading. Different configurations could be tested to minimize this effect on future tests.

Future tests could take in consideration the possibility of green water and vortex shedding on current loads, since these effects are hard to model numerically and can be avoided or diminished through design solutions.

9 APPENDIX

9.1 Natural Periods

The natural periods, observed on the free decay tests are presented on table 9-1. Full report index on 'Annex C: Decay Tests Files Index'.

Table 9-1 - Free-Decay Tests Natural Periods [s]

	T100	T200	T300	T400	T500	T600
Surge [s]	54.9186	167.5843	-	191.3431	-	-
Sway [s]	58.4070	58.4070	-	180.8779	-	-
Heave [s]	22.4310	20.3441	-	20.7614	-	40.8943
Roll [s]	27.6200	22.1048	-	22.1283	-	37.9245
Pitch [s]	27.6414	21.7963	36.6864	21.2819	39.7158	35.5439
Yaw [s]	28.6331	97.7575	-	97.7154	-	-

9.2 Basic Statistics

The basic statistics for some channels for each test group are plotted in bar charts on figure 9-1 through 9-17.

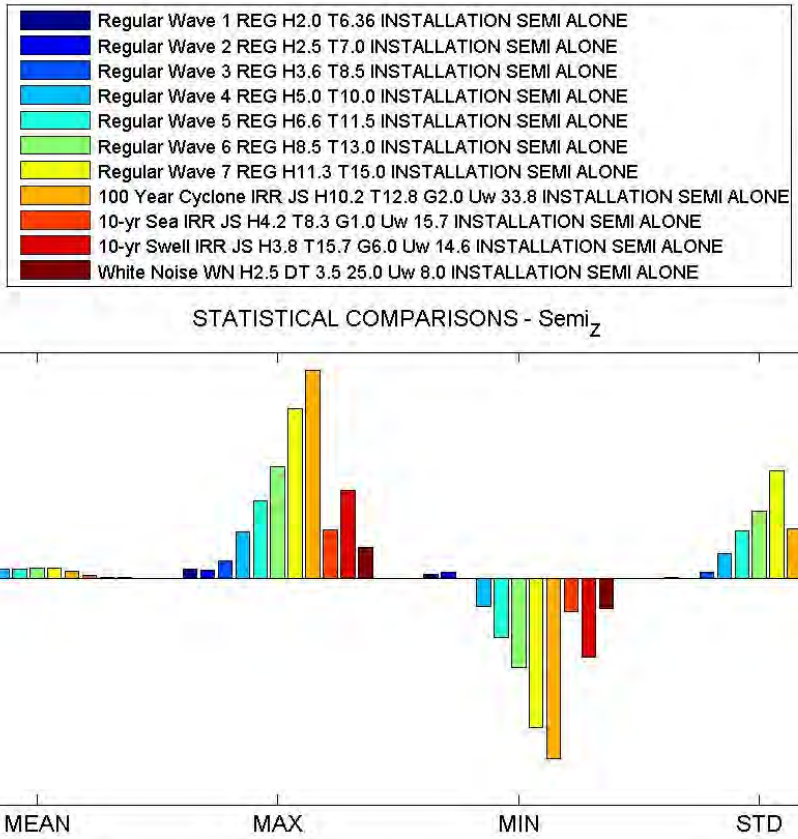

Figure 9-1. T100, Semi_Z Channel Basic Statistics

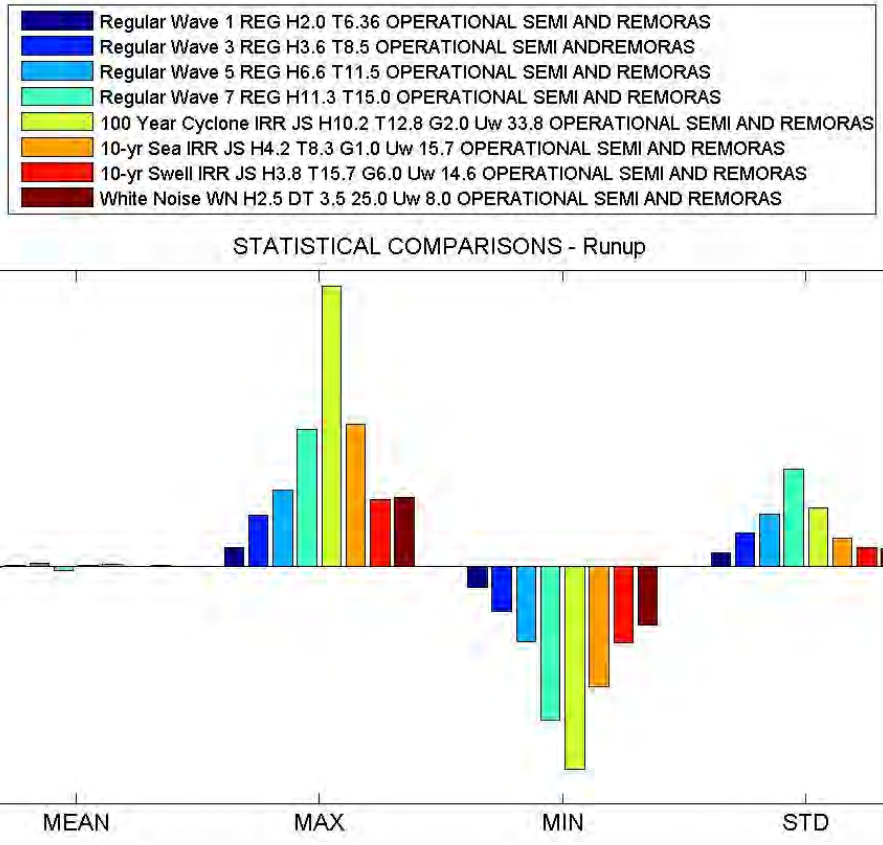

Figure 9-2. T200, Runup Channel Basic Statistics

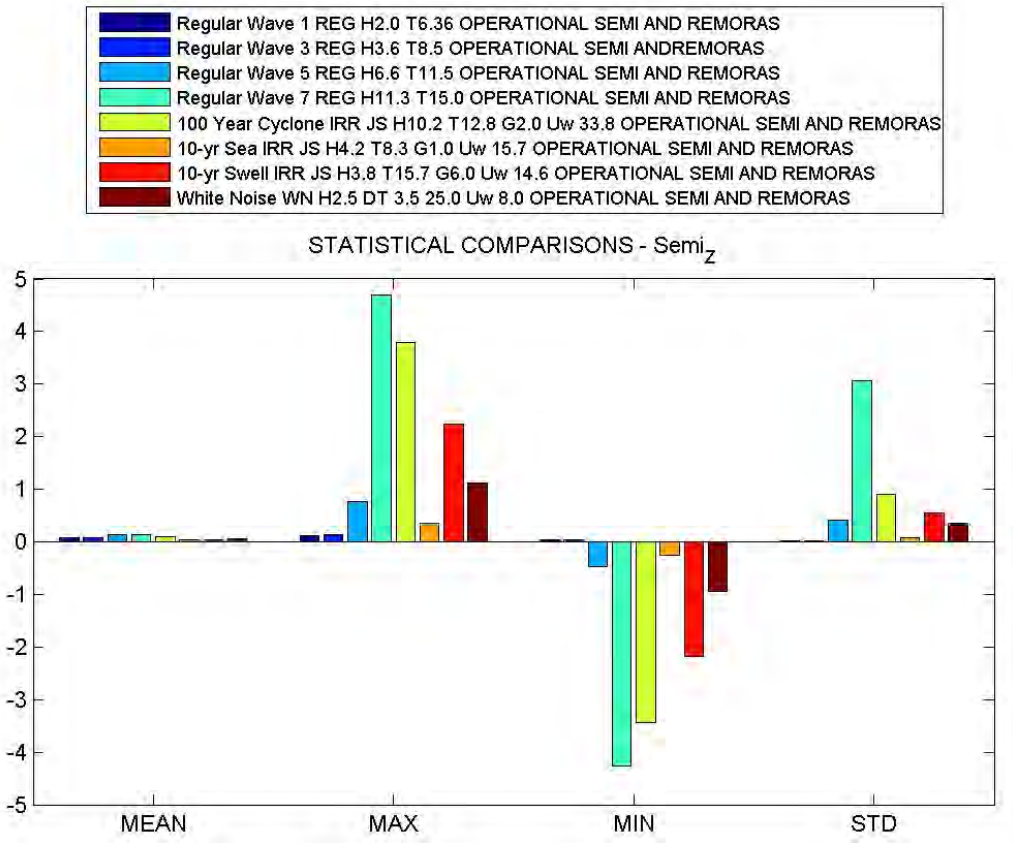

Figure 9-3. T200, Semi_Z Channel Basic Statistics

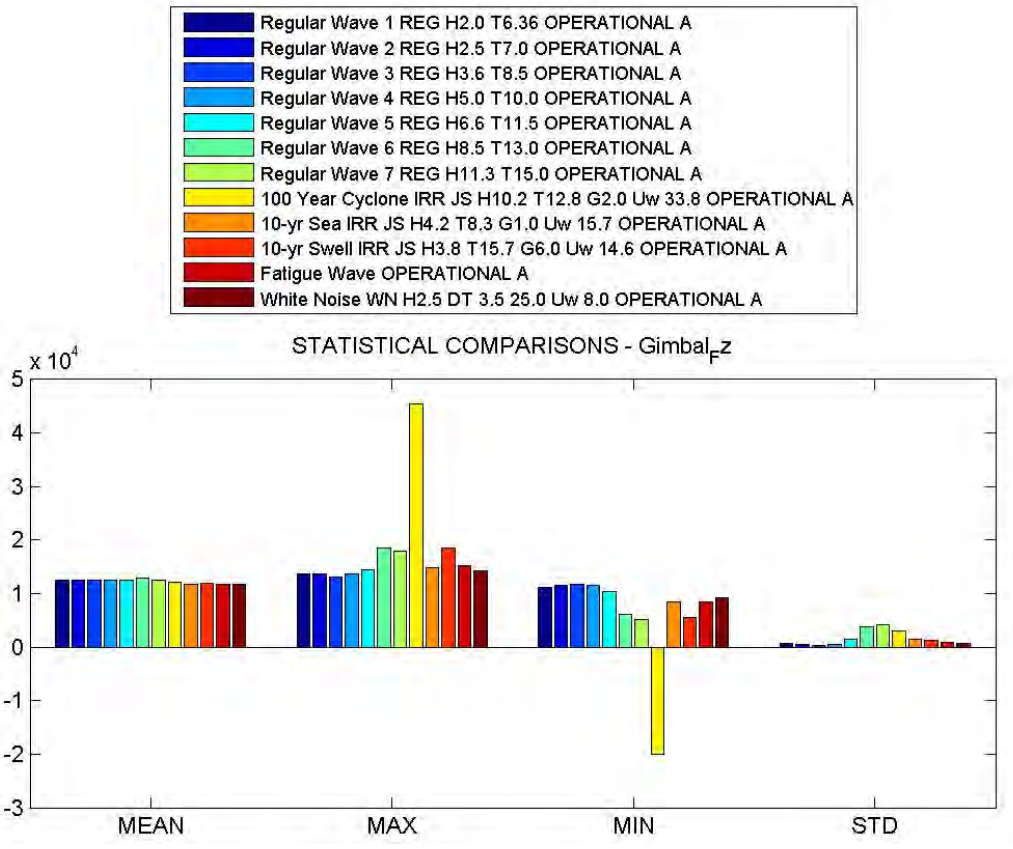

Figure 9-4 . T300, Gimbal_Fz Channel Basic Statistics

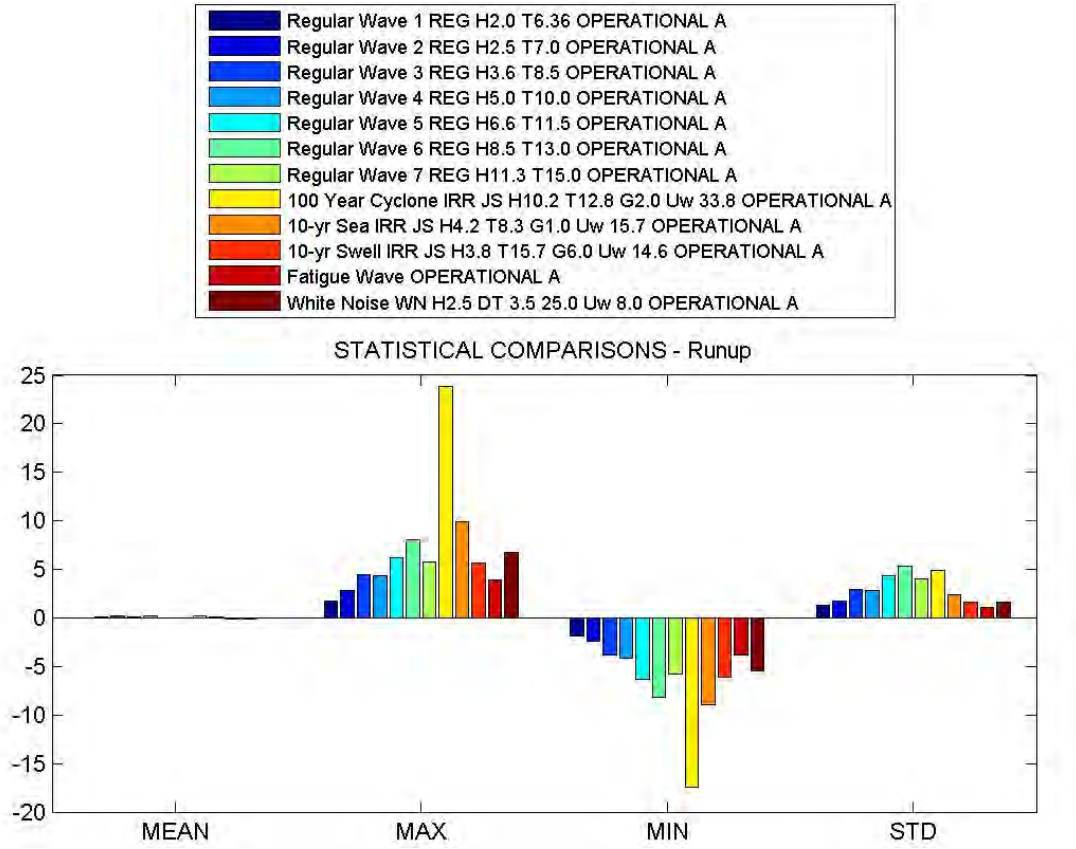

Figure 9-5. T300, Runup Channel Basic Statistics

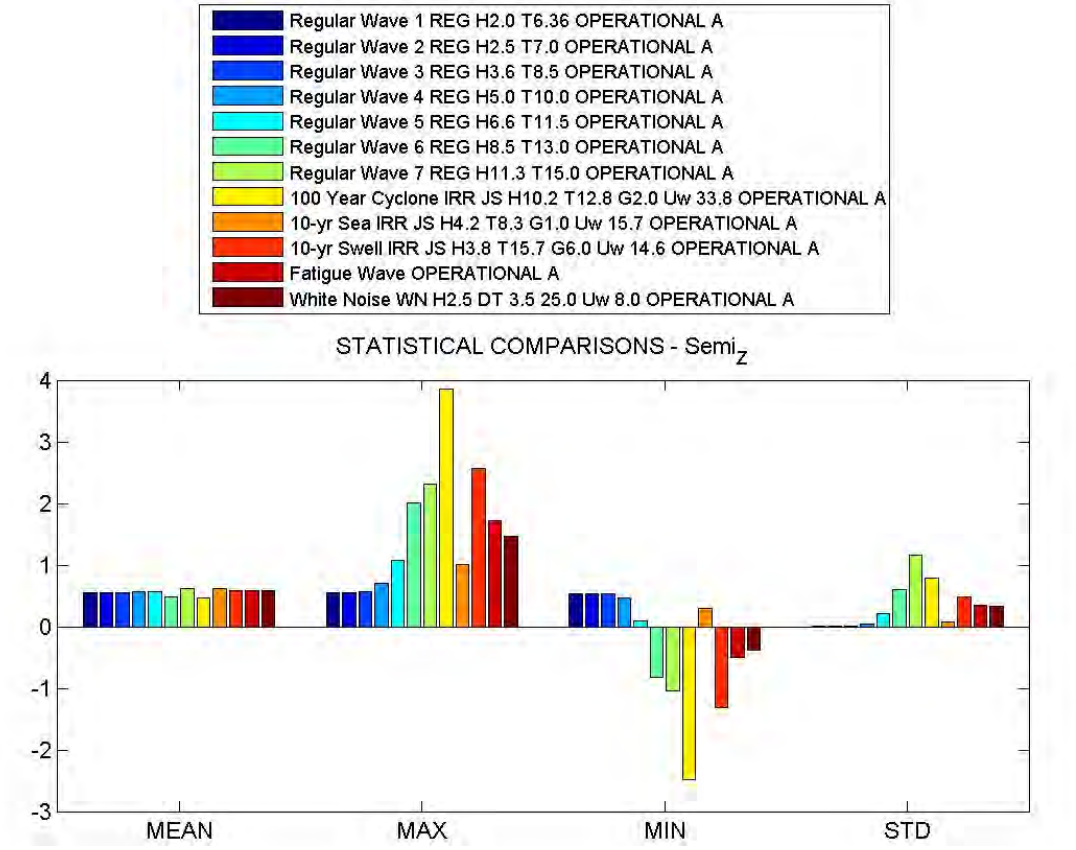

Figure 9-6. T300, Semi_Z Channel Basic Statistics

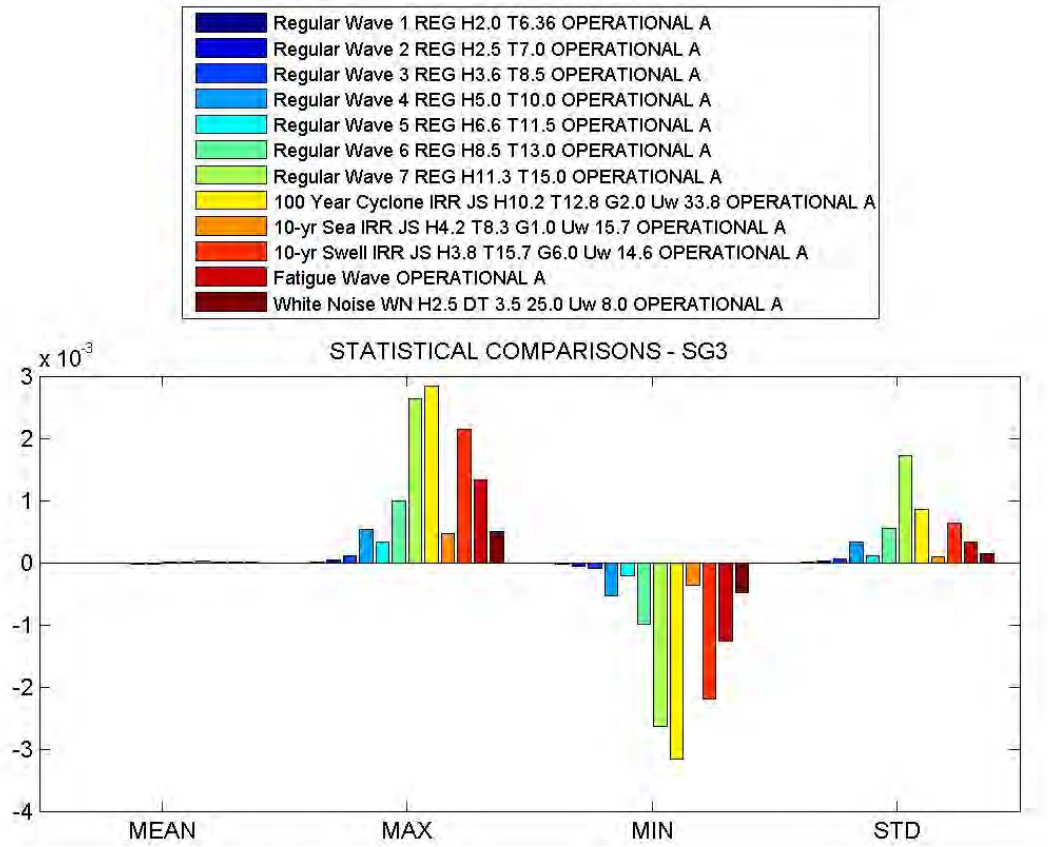

Figure 9-7. T300, SG3 Channel Basic Statistics

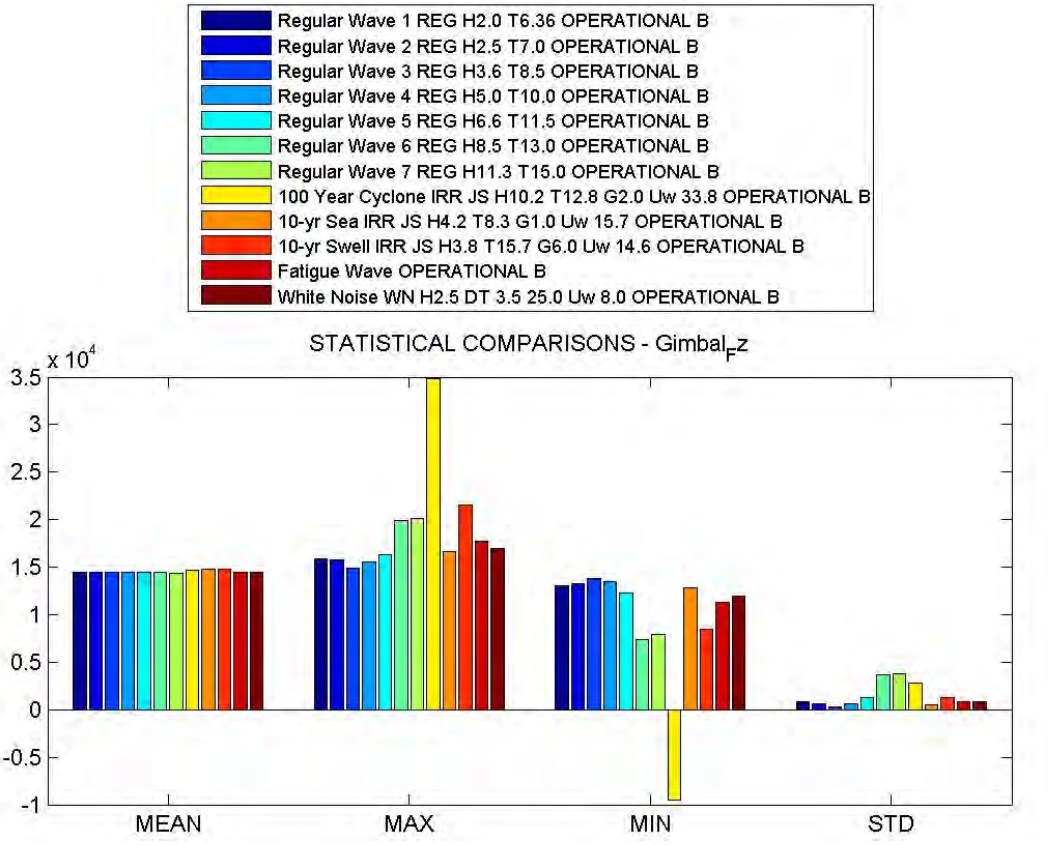

Figure 9-8. T400, Gimbal_Fz Channel Basic Statistics

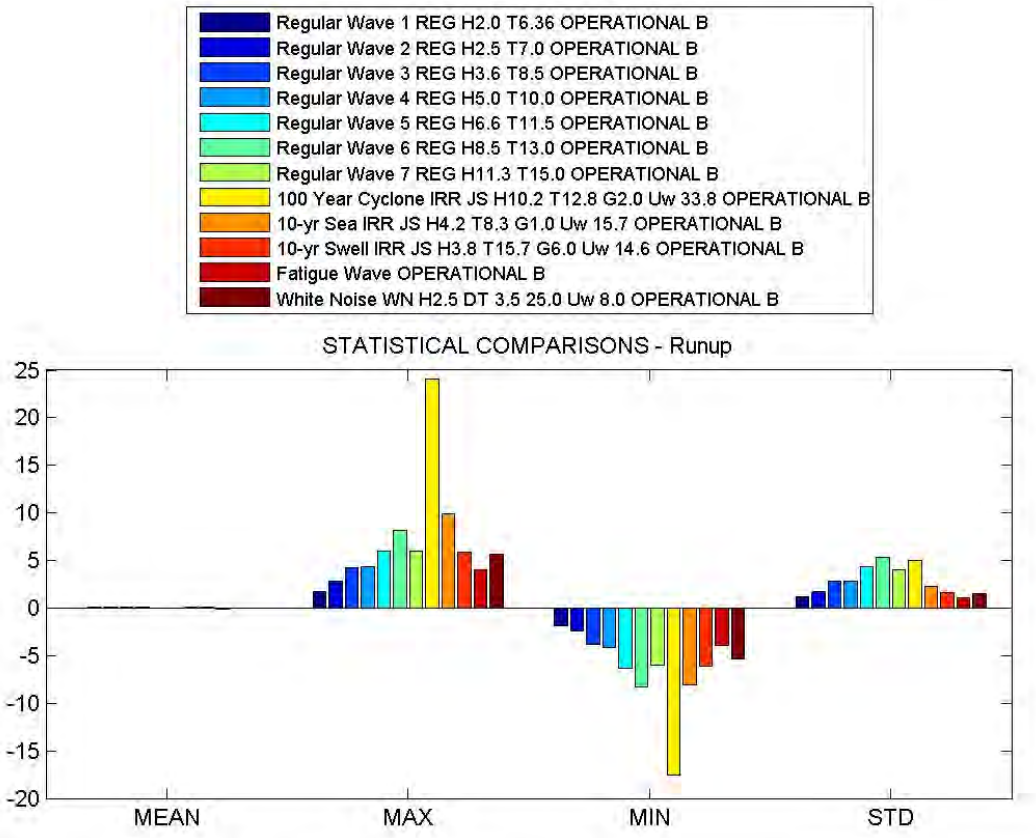

Figure 9-9. T400, Runup Channel Basic Statistics

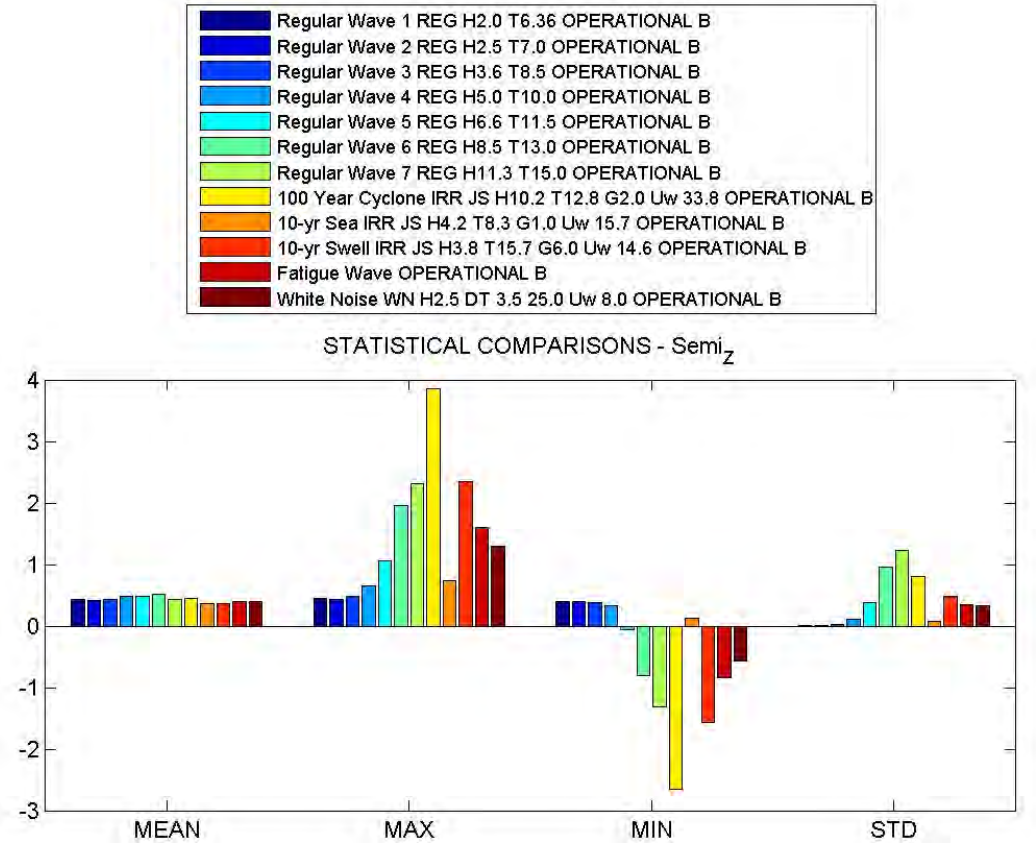

Figure 9-10. T400, Semi_Z Channel Basic Statistics

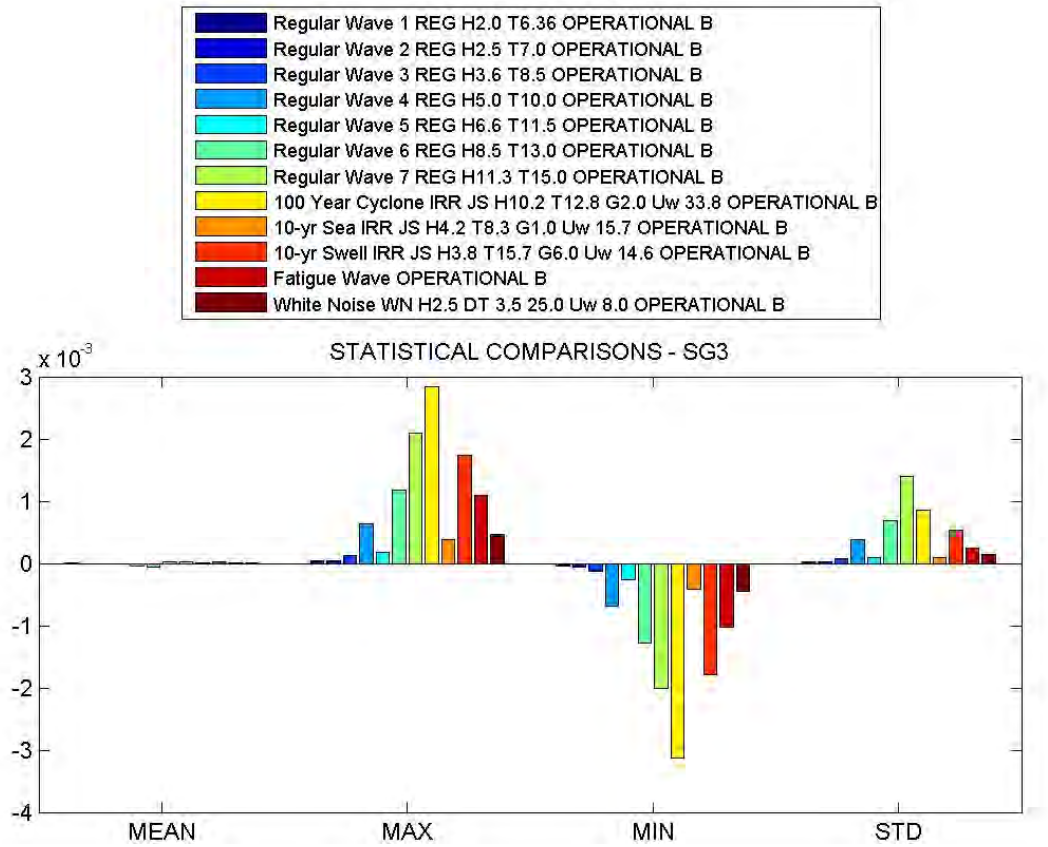

Figure 9-11. T400, SG3 Channel Basic Statistics

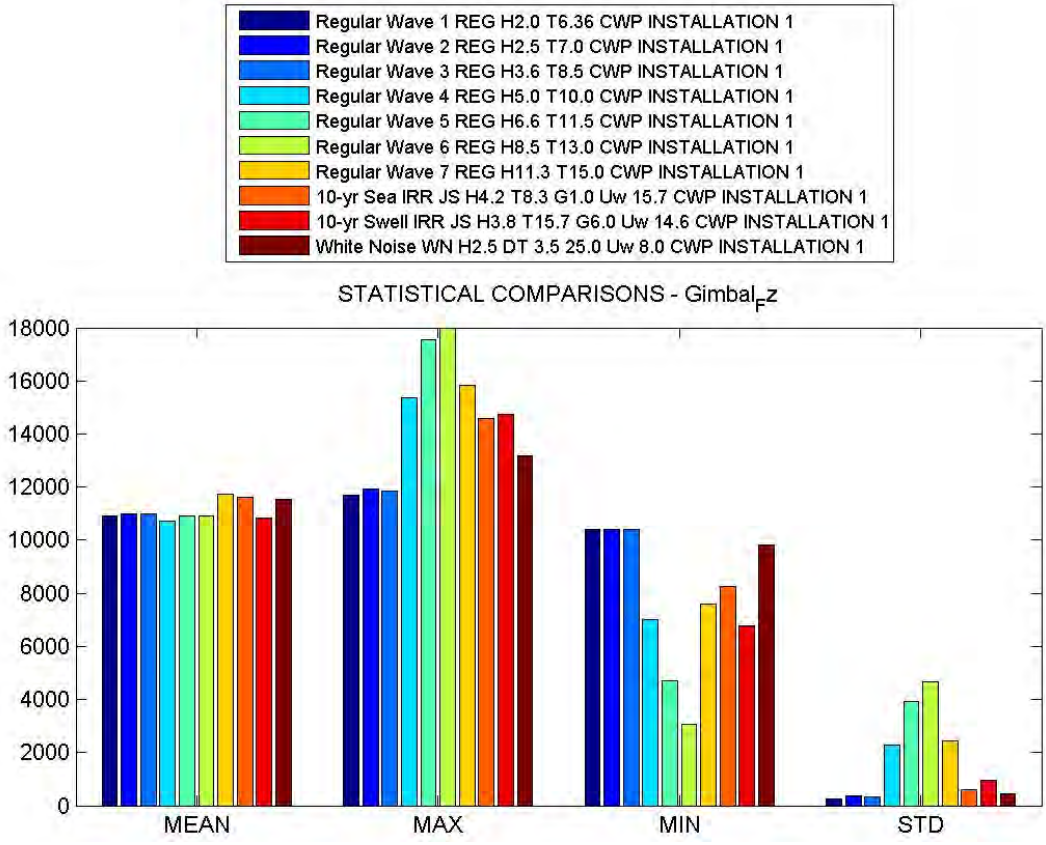

Figure 9-12. T500, Gimbal_Fz Channel Basic Statistics

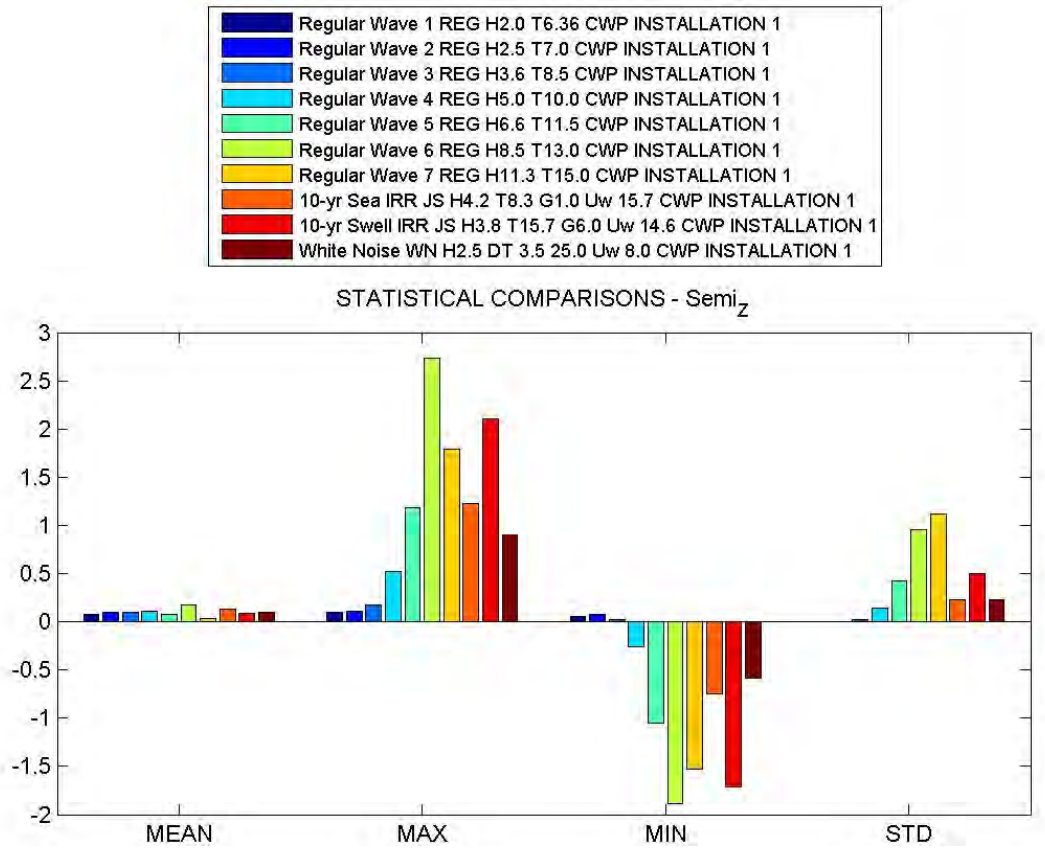

Figure 9-13. T500, Semi_Z Channel Basic Statistics

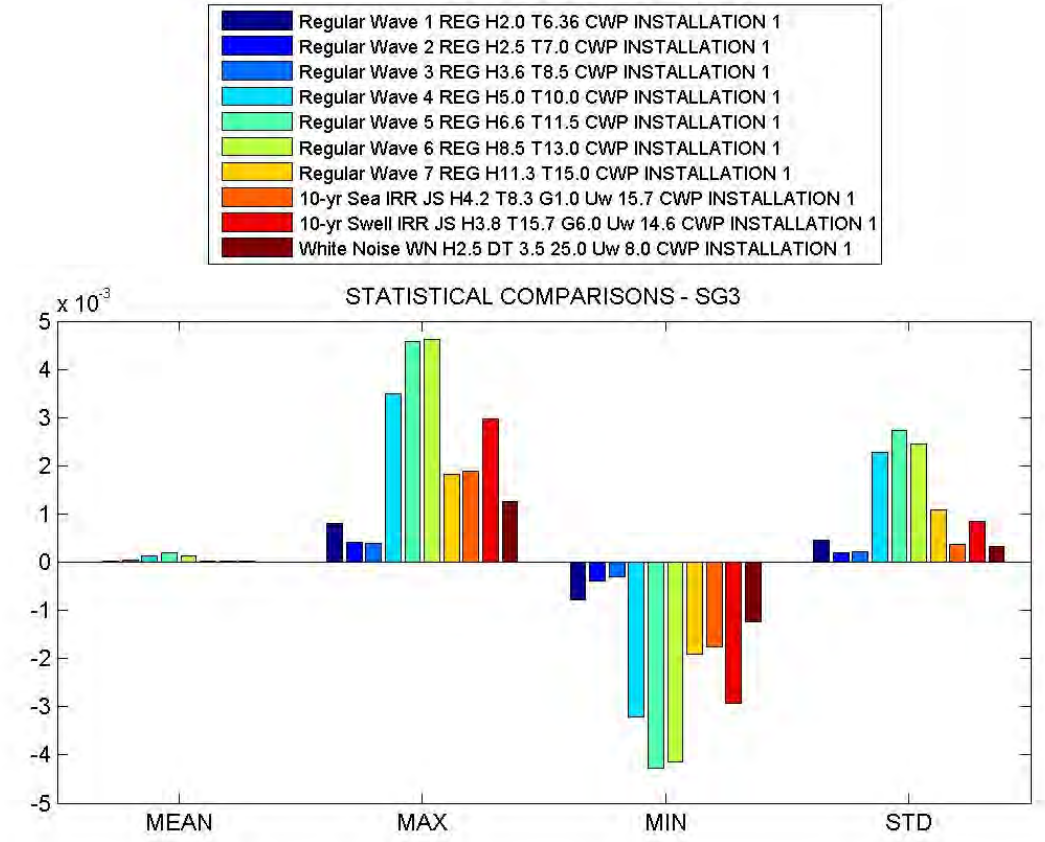

Figure 9-14. T500, SG3 Channel Basic Statistics

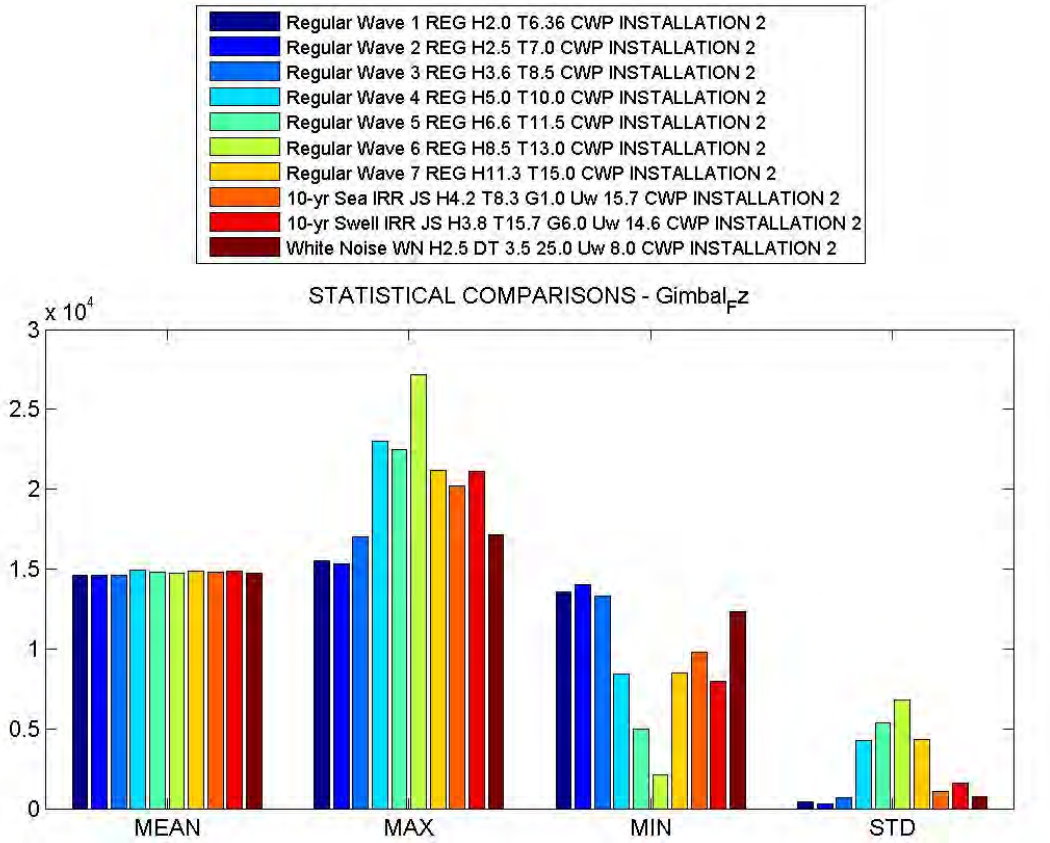

Figure 9-15. T600, Gimbal_Fz Channel Basic Statistics

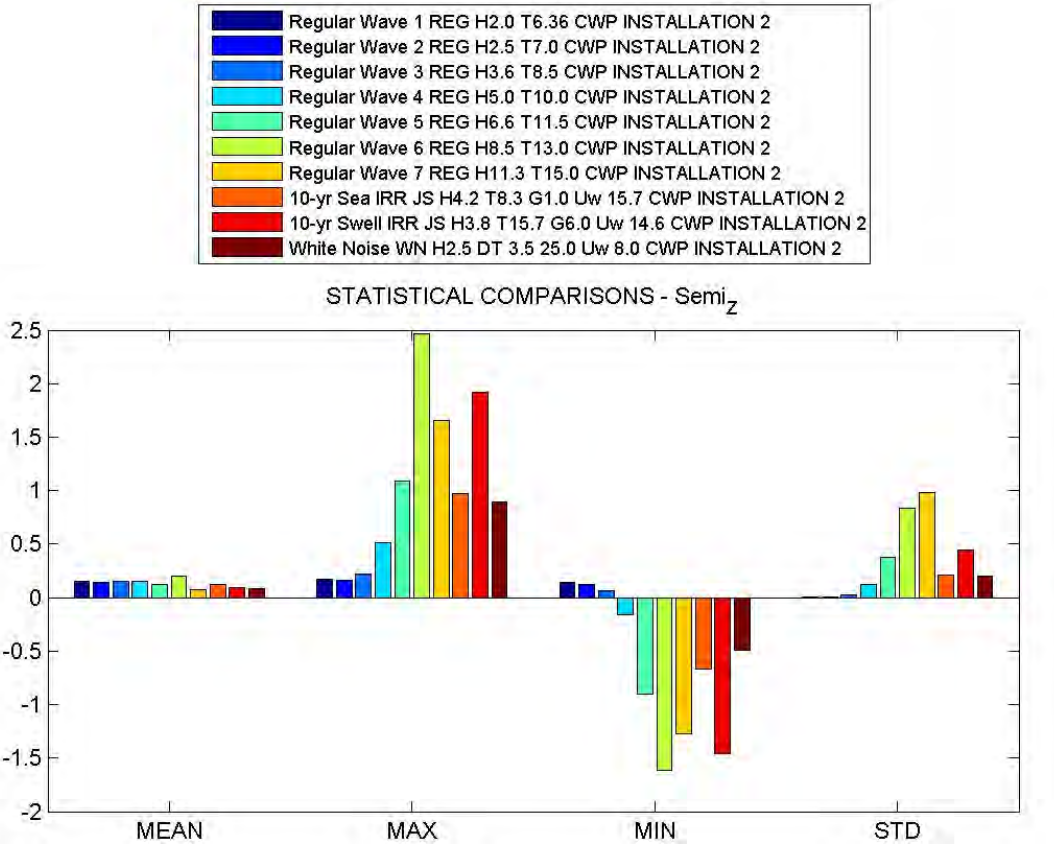

Figure 9-16. T600, Semi_Z Channel Basic Statistics

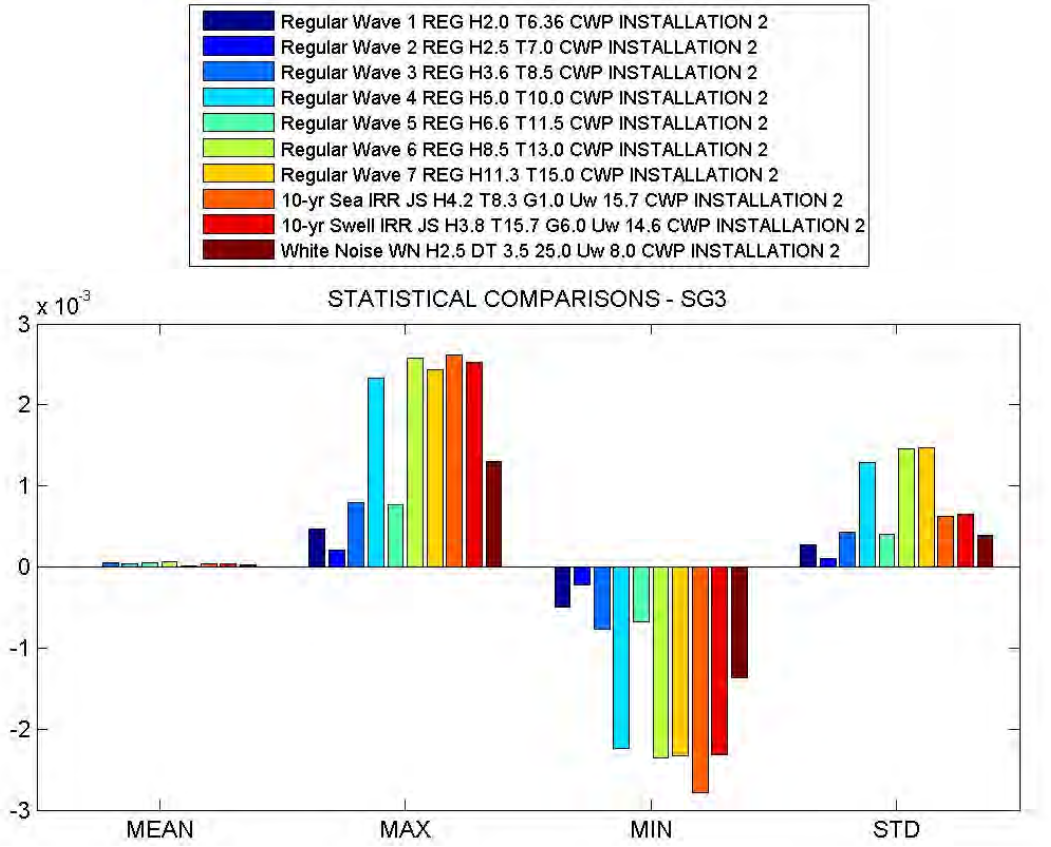

Figure 9-17. T600, SG3 Channel Basic Statistics

9.3 Strain Envelope Plots

The strain envelope plots for each test group are plotted on figure 9.18 through 9.25.

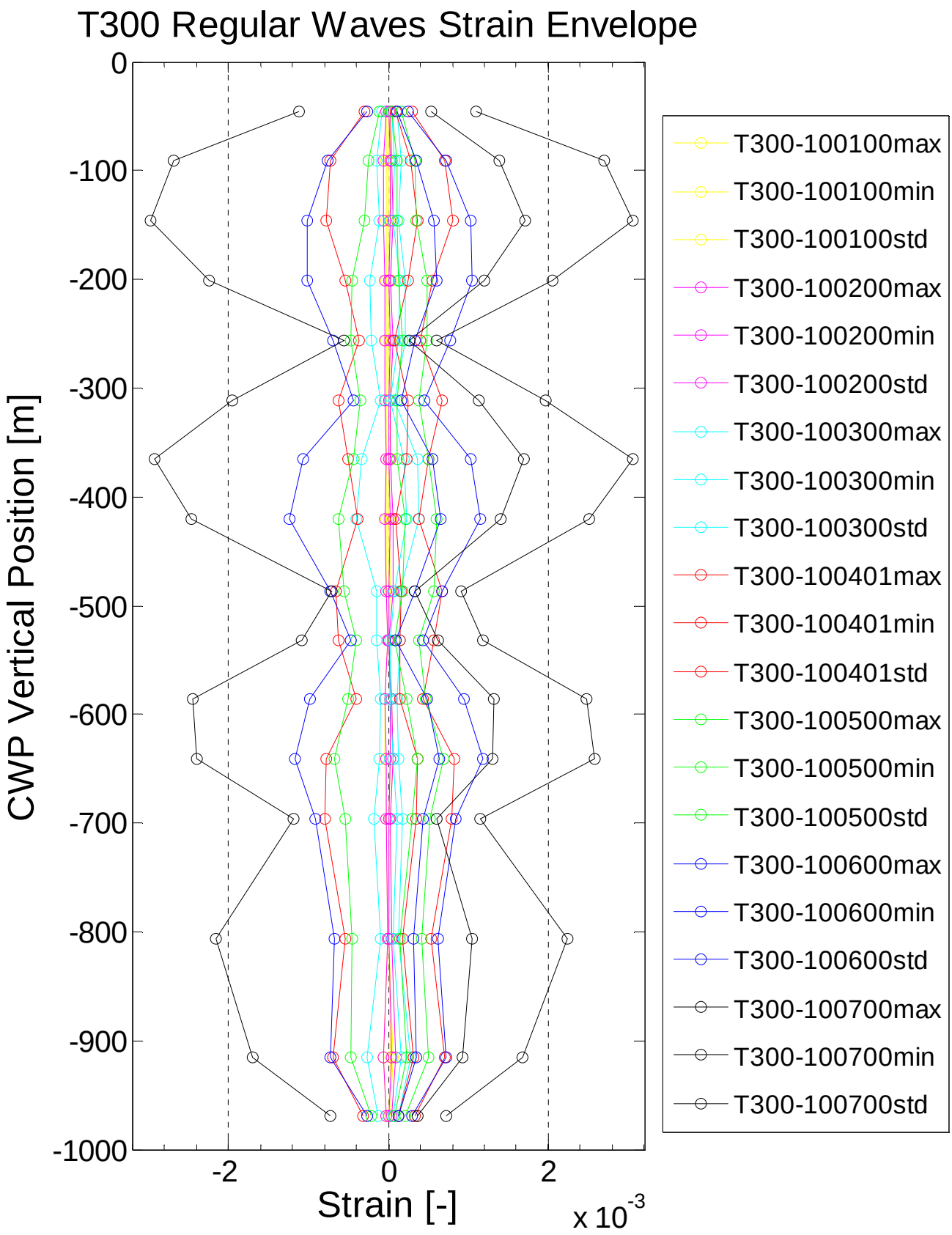

Figure 9-18. T300 Regular Waves Strain Envelope

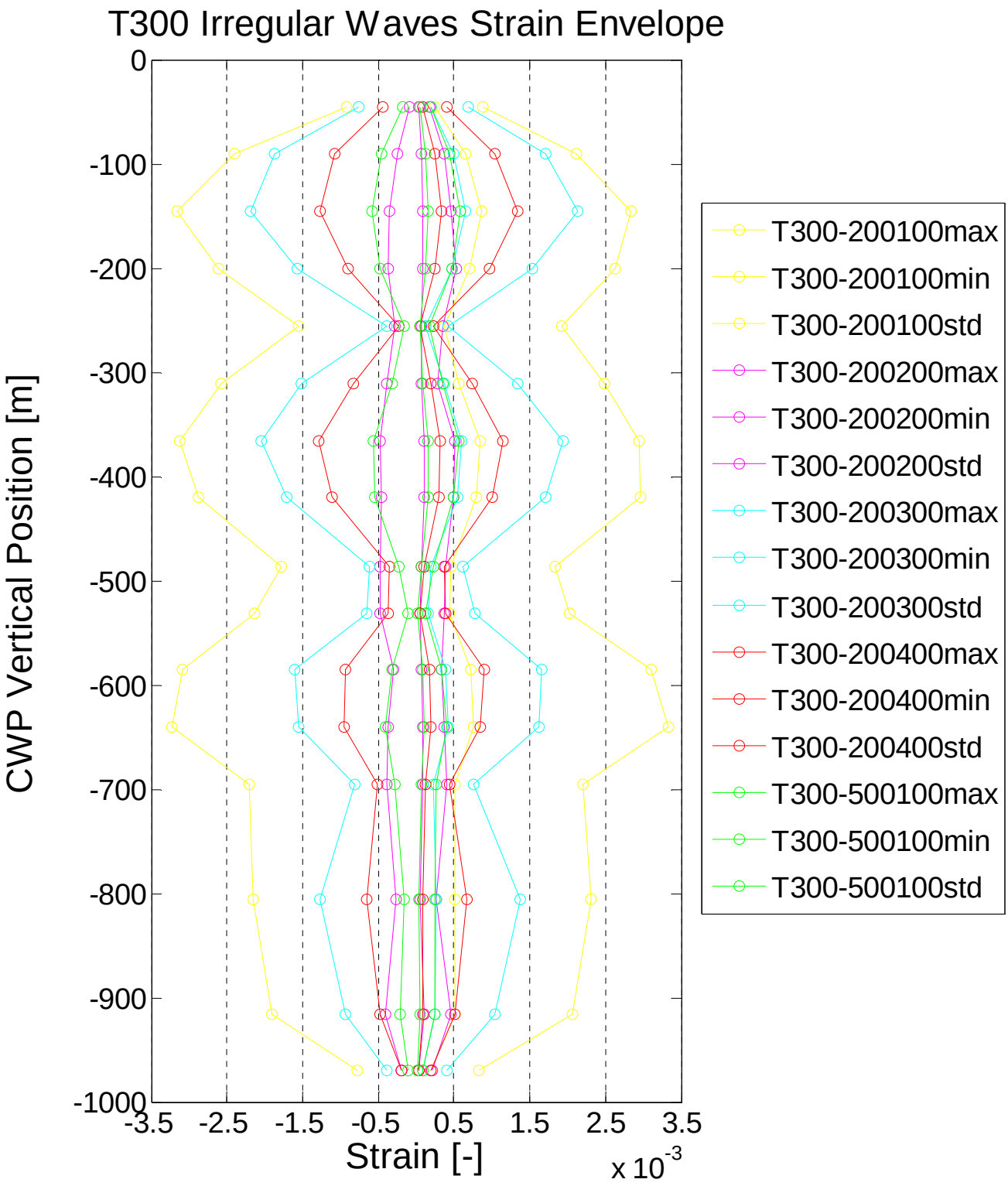

Figure 9-19. T300 Irregular Waves Strain Envelope

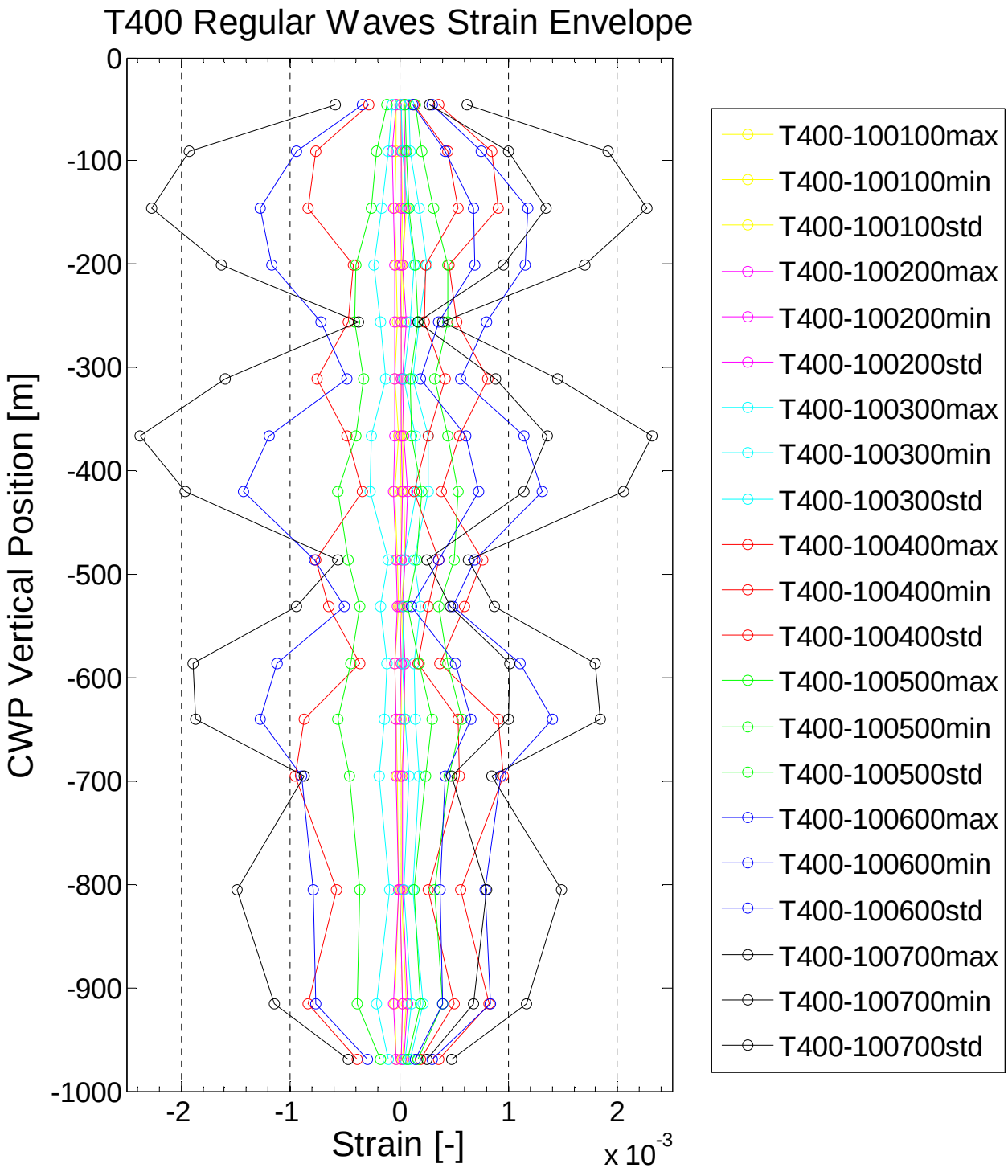

Figure 9-20. T400 Regular Waves Strain Envelope

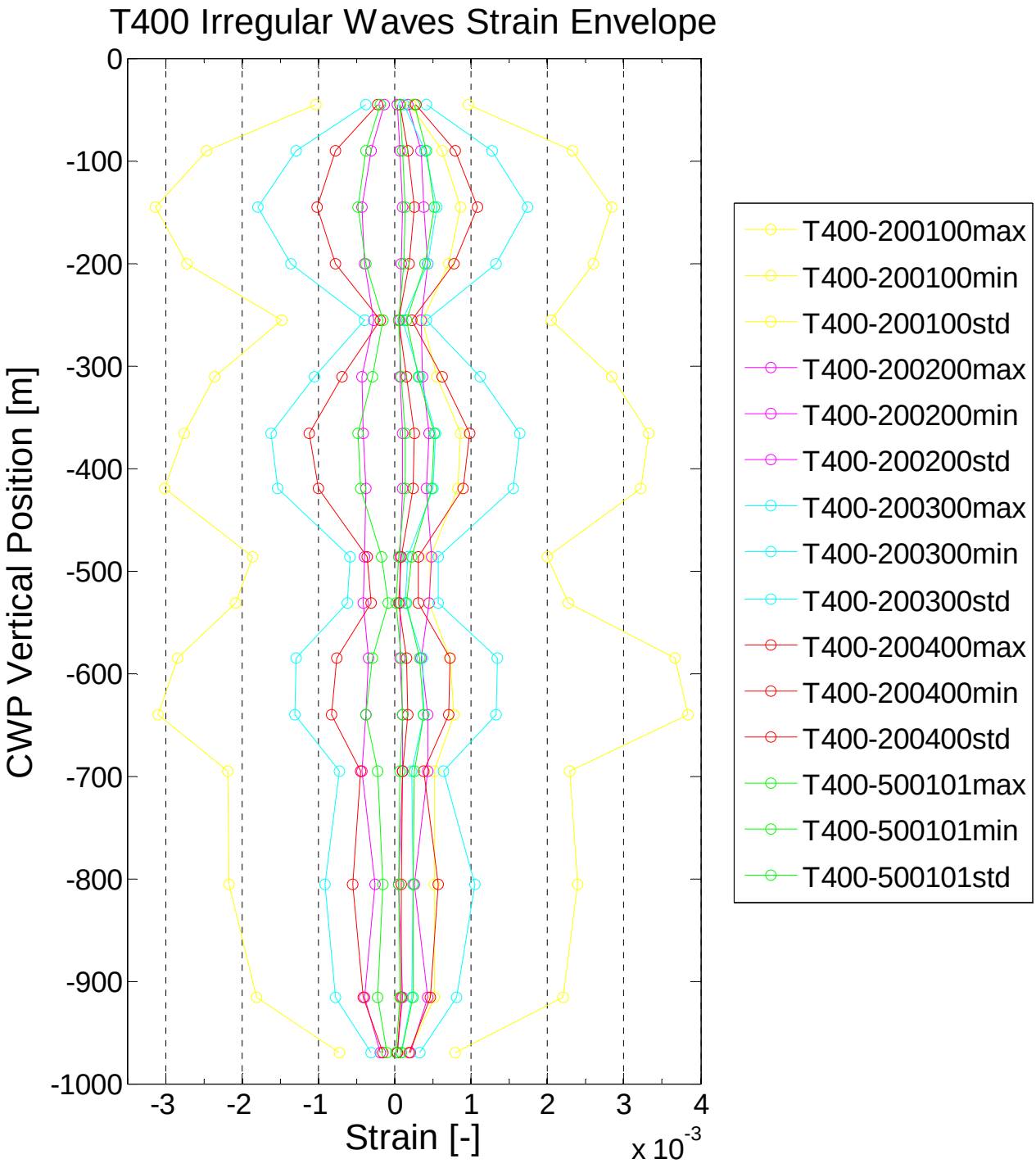

Figure 9-21. T400 Irregular Waves Strain Envelope

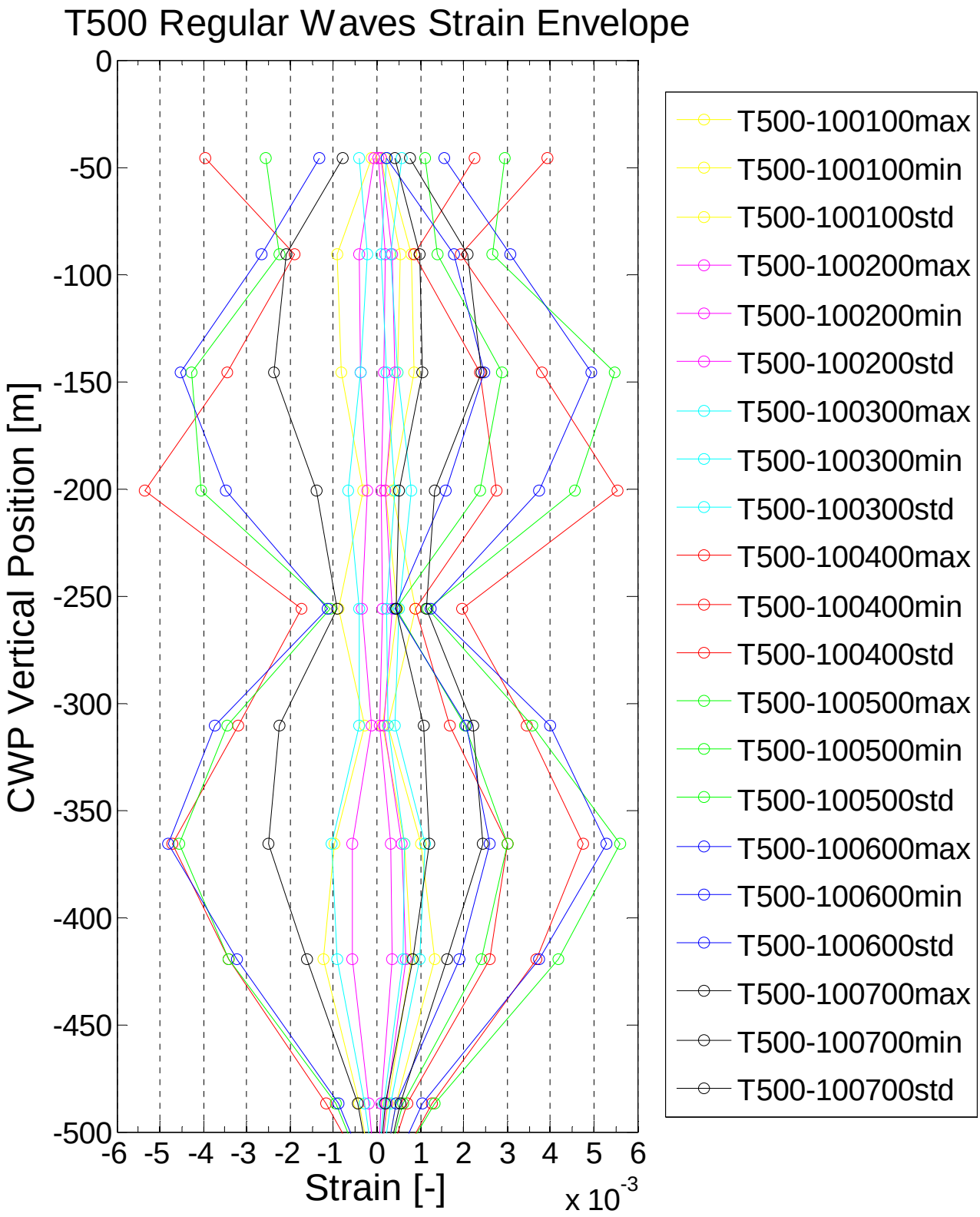

Figure 9-22. T500 Regular Waves Strain Envelope

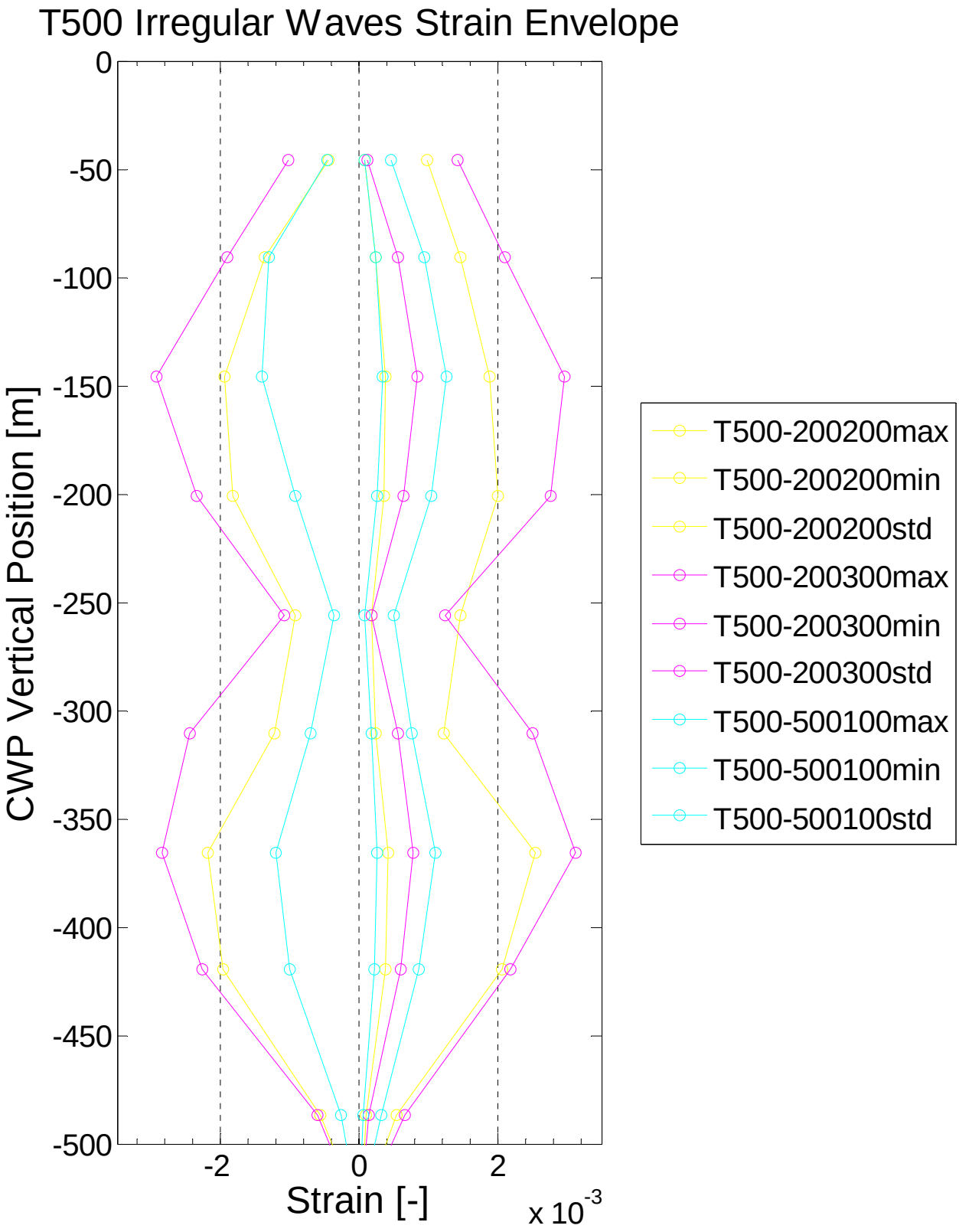

Figure 9-23. T500 Irregular Waves Strain Envelope

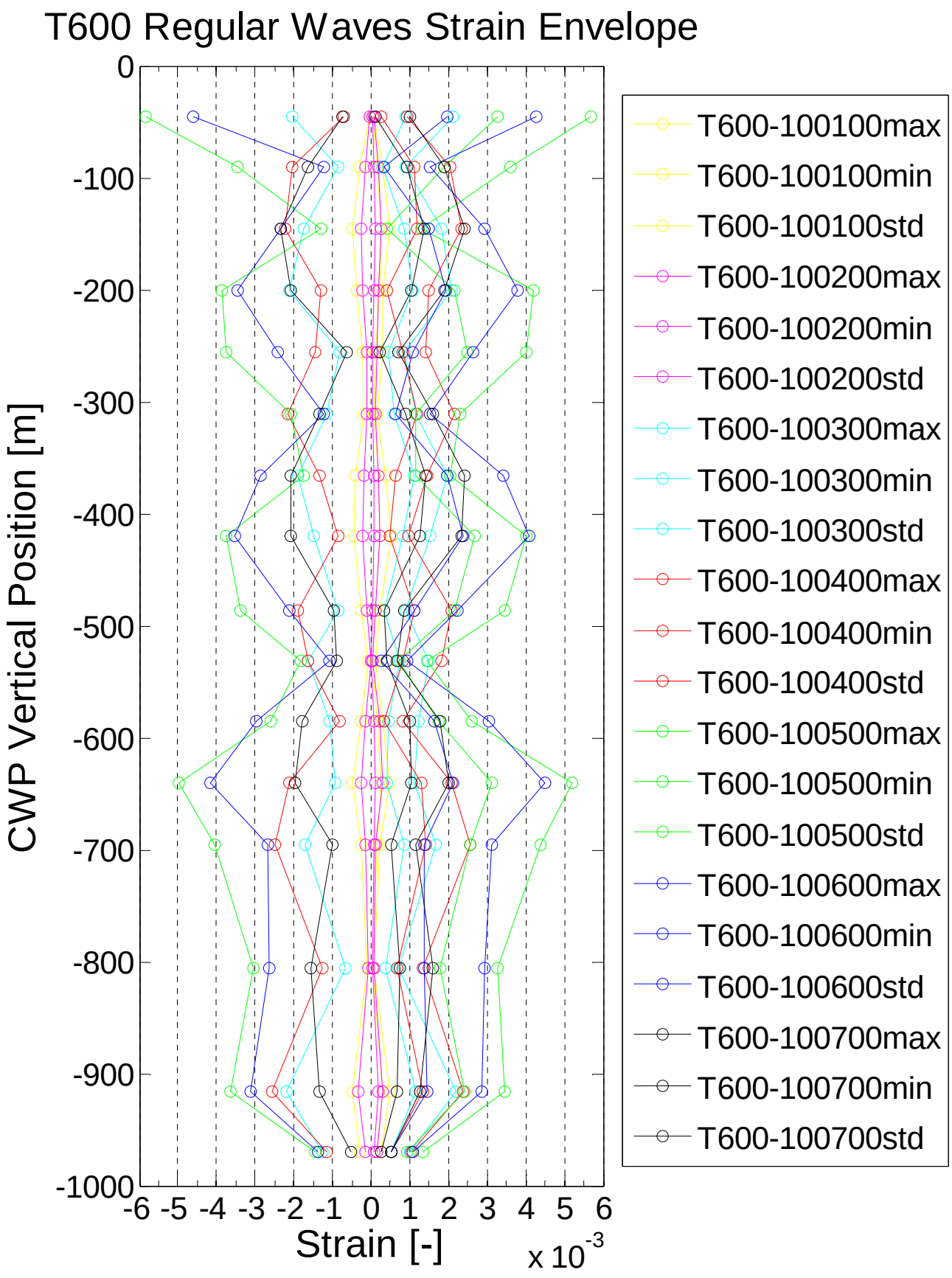

Figure 9-24. T600 Regular Waves Strain Envelope

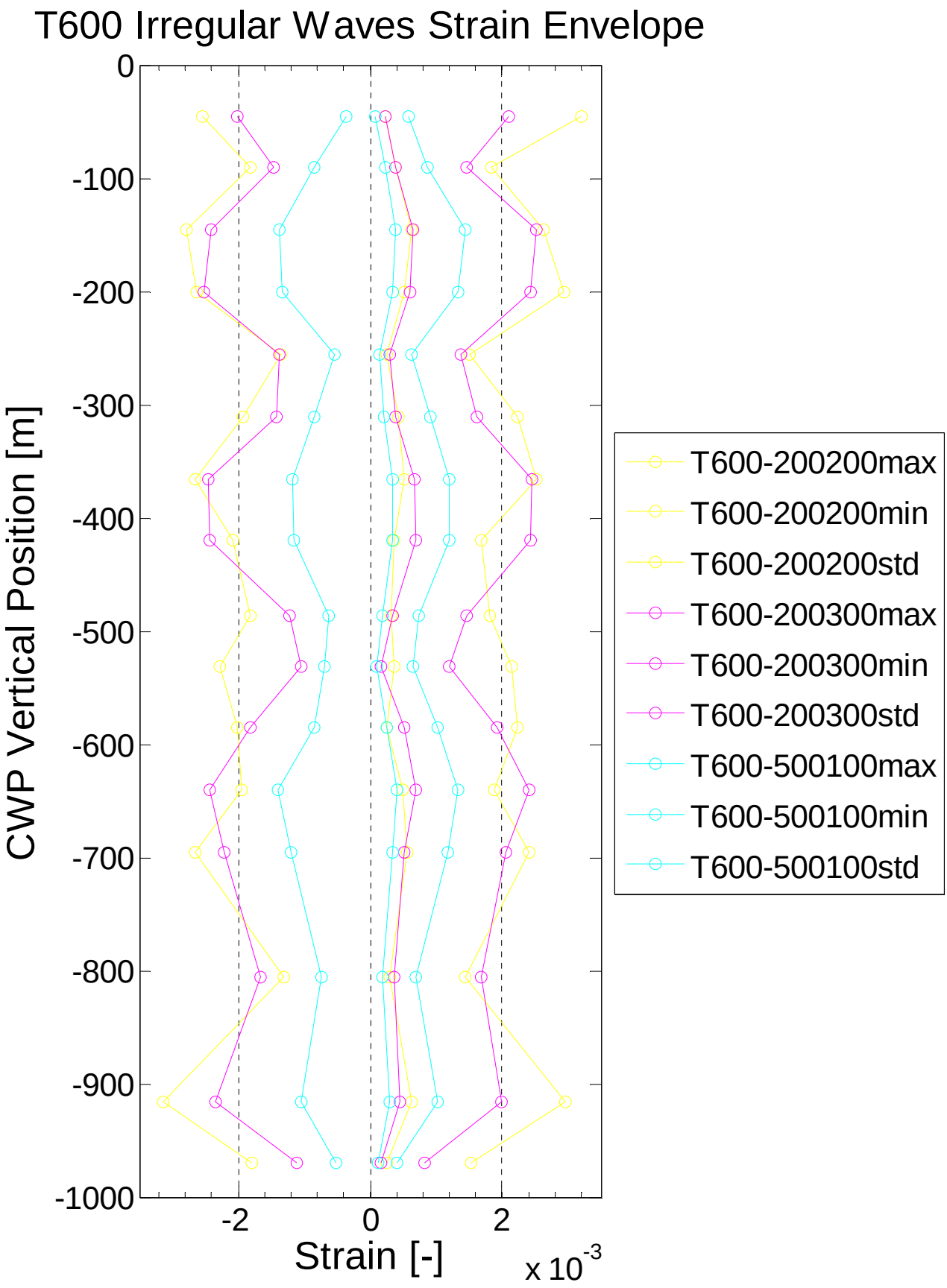

Figure 9-25. T600 Irregular Waves Strain Envelope

9.4 White-Noise RAO Plots

The white noise RAO plots for the Semi and Gimbal motion are plotted on figure 9.26 through 9.31.

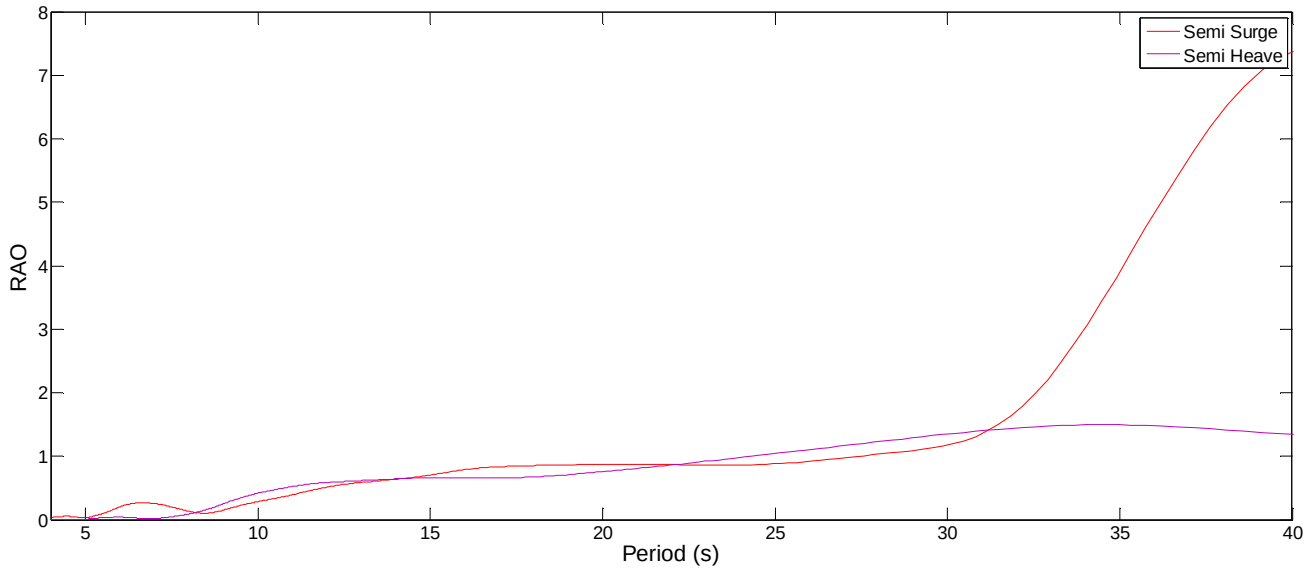

Figure 9-26. T100 White Noise wave test Semi motion RAO

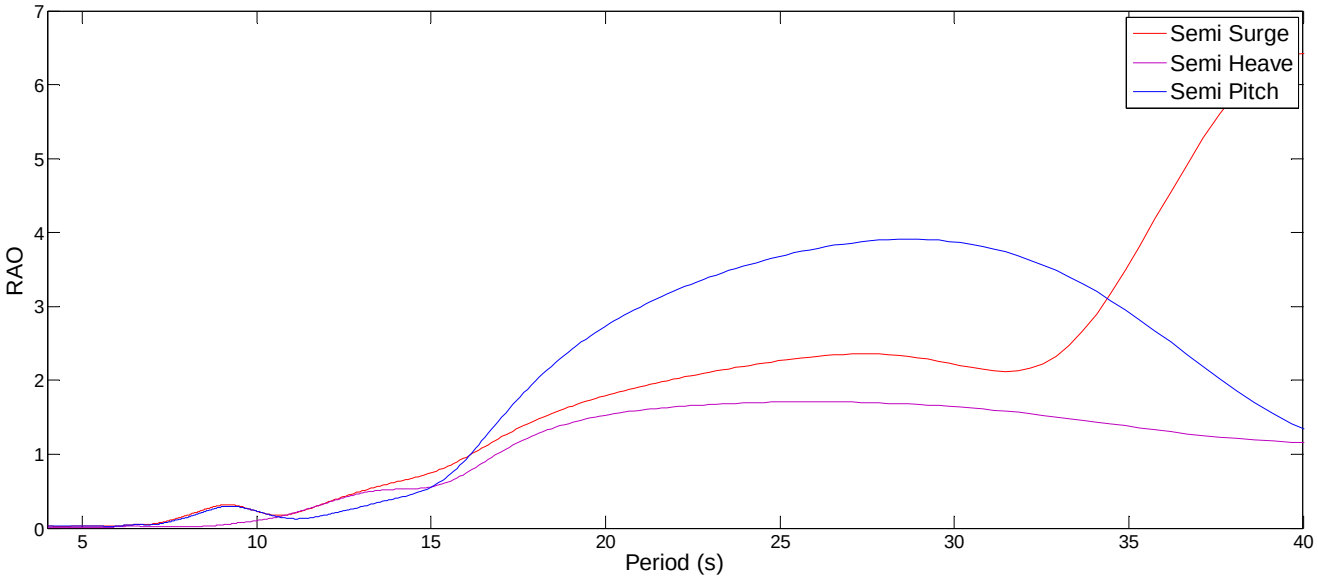

Figure 9-27. T200 White Noise wave test Semi motion RAO

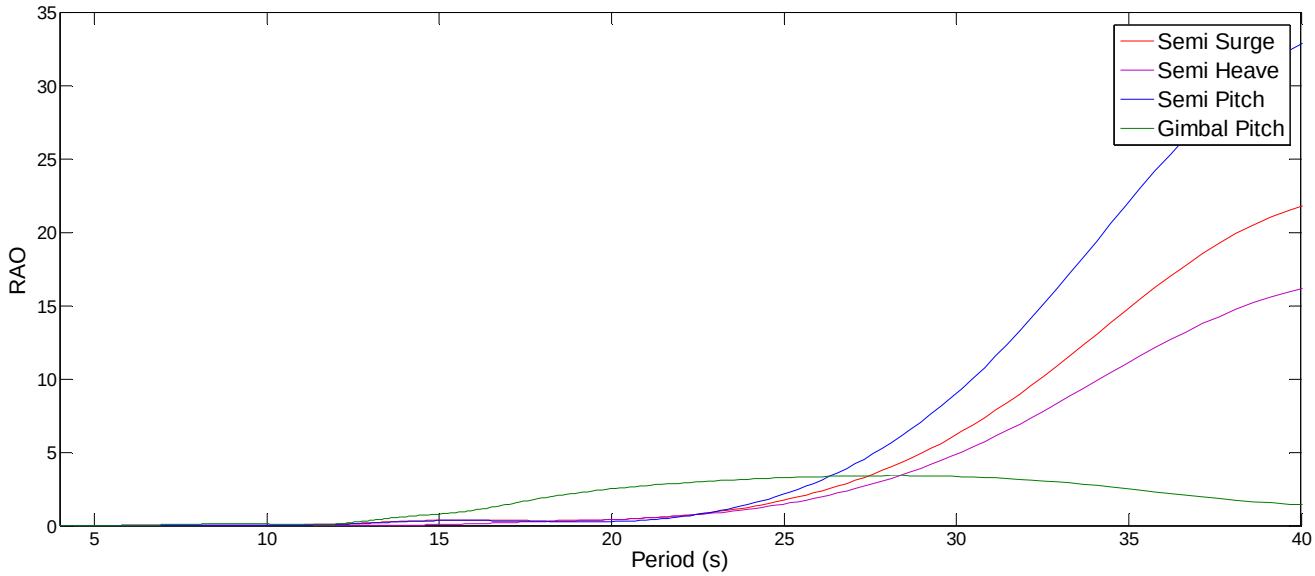

Figure 9-28. T300 White Noise wave test Semi and Gimbal motion RAO

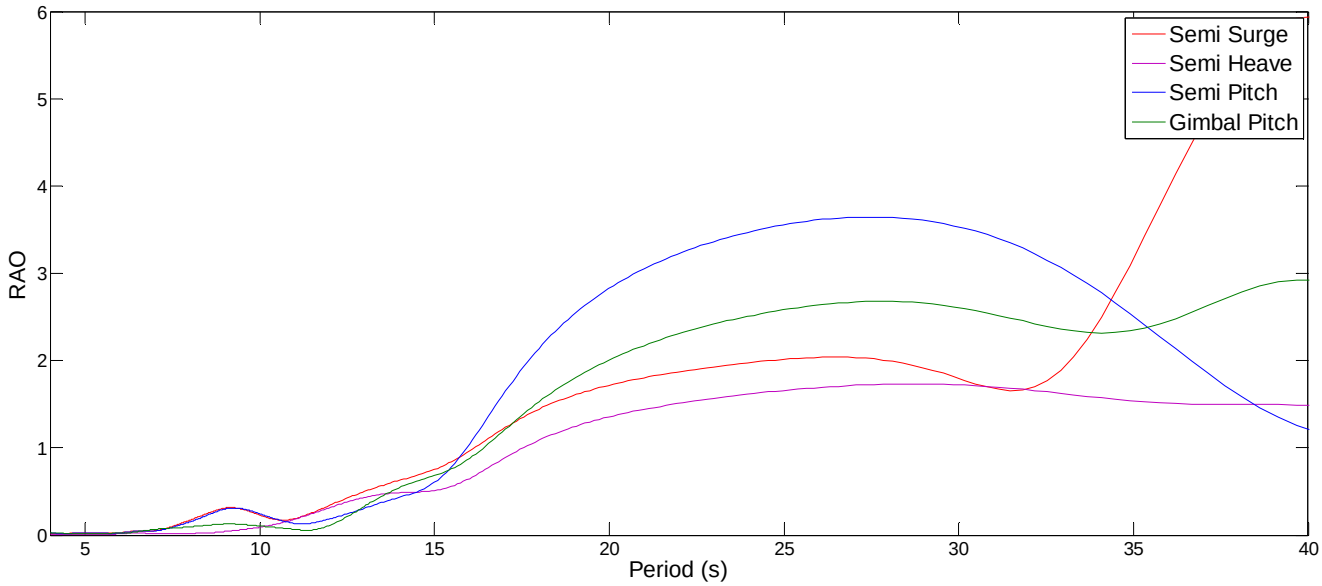

Figure 9-29. T400 White Noise wave test Semi and Gimbal motion RAO

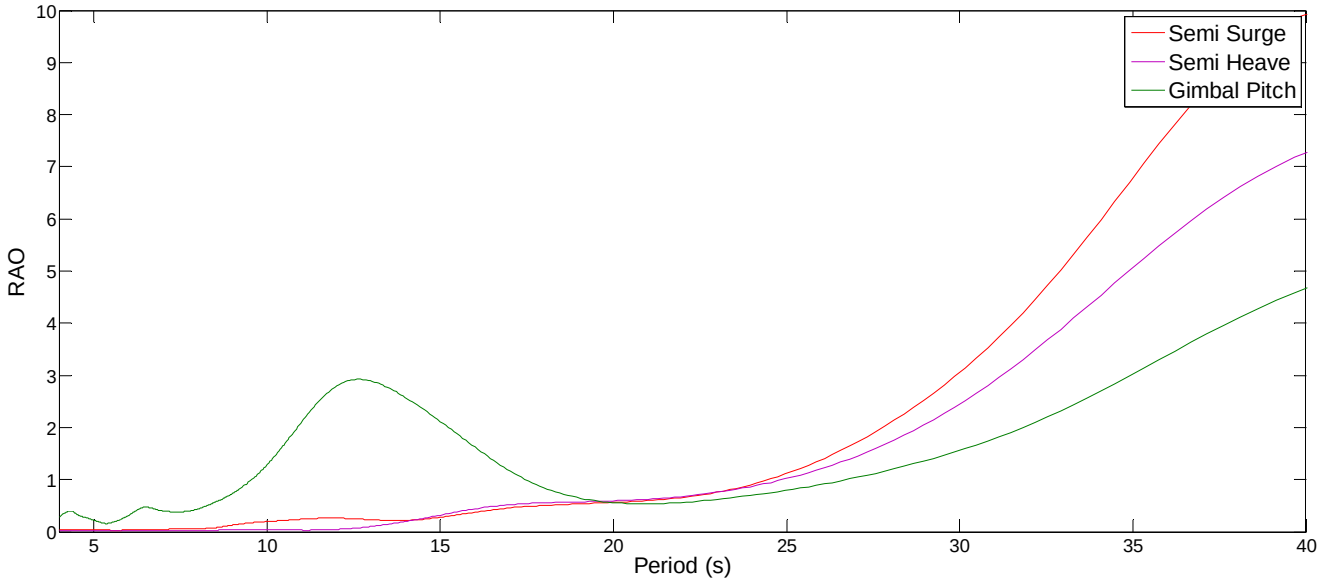

Figure 9-30. T500 White Noise wave test Semi and Gimbal motion RAO

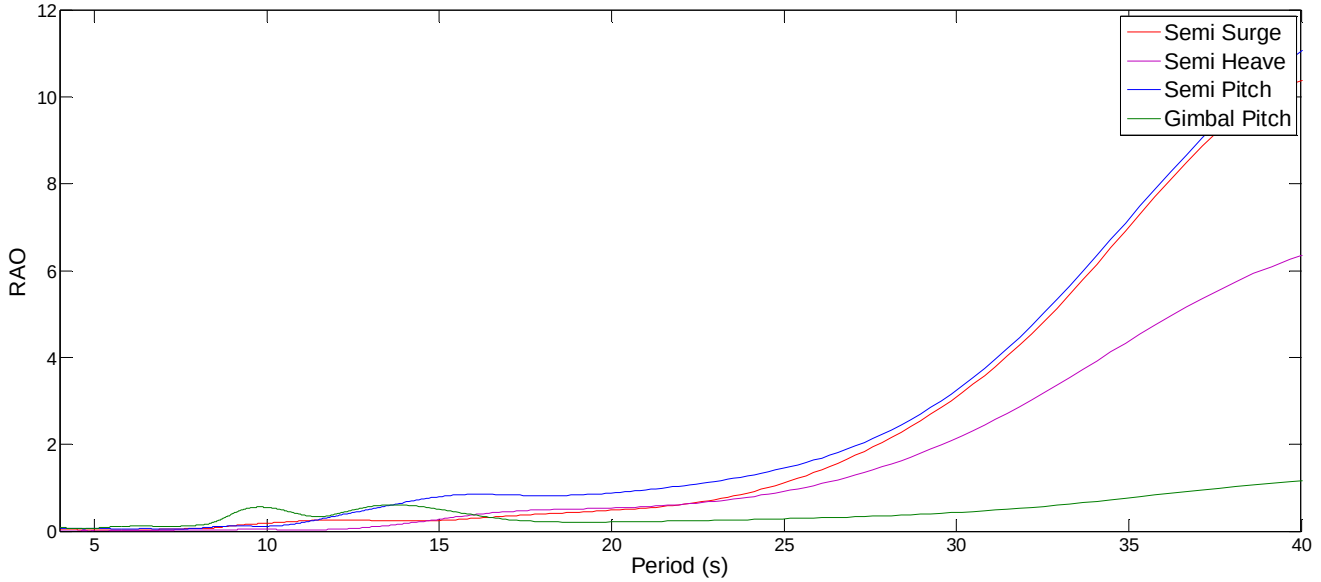

Figure 9-31. T600 White Noise wave test Semi and Gimbal motion RAO

This page intentionally left blank.

E. HOE NUMERICAL MODELING AND SIMULATION REPORT

This page intentionally left blank.

Ocean Thermal Energy Conversion (OTEC) Plant Modeling Test

Numerical Modeling and Simulation Report

H12129-G-RPT-RI-00001

Rev	Date	Document Status	Originator	Checked	Approved
A	2-26-2014	Issue for comment	SS	JHA	
0	4-30-2014	Issued for use	SS	JHA	

Table of Contents

1 Introduction

1.1 Objective

This project will validate the ability to numerically model the dynamic interaction between a large cold water-filled fiberglass pipe and a floating ocean thermal energy conversion (OTEC) platform excited by meteorological and ocean (metocean) weather conditions using measurements from a scale model tested in an ocean basin test facility.

1.2 Background

An OTEC system generates electrical power by running a Rankine thermodynamic cycle supported on a moored, floating platform subsystem. Warm surface water evaporates a working fluid. The working fluid gas is expanded through a turbo-generator, producing electricity. The discharged gas is condensed using cold deep sea water accessed through a large cold water pipe (CWP). For power plant capacities of 100 MW, the CWP may be 10 meters in diameter and up to 1,000 meters long.

The interaction of this CWP-platform subsystem from combinations of metocean conditions must be understood to design an OTEC system to survive for typical utility life cycles. The offshore industry uses software modeling tools validated by scale model tests in facilities able to replicate real at-sea metocean conditions to provide the understanding and confidence to proceed to final design and full scale fabrication. However, today's offshore platforms (similar to and usually larger than those needed for OTEC applications) incorporate risers (or pipes) with diameters well under 1 meter. In the case of the OTEC system, the mass of the cold water pipe, including entrained water, can exceed the mass of the platform supporting it. This situation is quite different than that of most marine risers. Secondly, the preferred construction method for large diameter CSPs is the use of composite materials, primarily a form of fiber-reinforced plastic. The use of this material results in relatively low pipe stiffness and large strains compared to steel construction. These factors suggest the need for further validation of the software.

The fiberglass CWP is a key component for an OTEC system. Challenges with this kind of pipe in this application are the construction and installation. Lockheed Martin is developing a method for fabricating and installing the pipe from the floating platform as a single piece, without connectors. A particular requirement of this installation process is that the pipe be "gripped" and guided below the manufacturing equipment as it is built. The grippers and guides must be able to suspend the pipe and minimize pipe deflections during curing (NAVFAC). The loads on the pipe at the lower guide from platform and pipe motions control the design of the pipe core from the standpoint of bending loads. Proving the ability of the present numerical models to predict these loads is a key objective of these tests.

Once the pipe is manufactured, it is hung off from the keel of the platform using a gimbal or other suspension mechanism of a given rotational stiffness. It is critical to be able to predict the axial and bending strains in the pipe in this condition. Tests on fiberglass fatigue in seawater indicate that the fatigue life is VERY sensitive to the dynamic strain amplitudes.

Analysis of the pipe responses is complicated by several factors, e.g.:

1. The pipe has a major influence on platform motions, e.g. the pipe itself has a suspended mass about equal to the platform mass,

2. Pipe strains are dependent upon relative stiffness between the pipe and the platform

3. Flow around the pipe may influence the hydrodynamic loads on the platform from waves and current

We have benchmarked several industry standard numerical modeling software programs against one another and have been able to show agreement to about +/- 15% on the maximum pipe strains. In order to proceed to the next level of development we need to verify the computational tools and establish “best practices” for the analysis in a comprehensive model basin test..

2 OTEC Model Test System Summary

2.1 OTEC Model Test System Configuration

The OTEC system will be supported on a four column semisubmersible, shown in Figure 2-1and Figure 2-2. A “gripper” to hold the pipe is installed at elevation 37 m. This gripper supports the weight of the pipe by friction. The top of the pipe in this configuration is at elevation 53 m and is free standing above the gripper. The motion at the pipe at the top is important to the manufacturing process and should be measured.

The other unique feature of the LMCO OTEC system compared to previous systems is the fabrication of the FRP pipe on board the vessel. This avoids the need for connectors in the large diameter pipe, and the pipe is fabricated as one single section, 1000 m long. This also eliminates the need to float out a long FRP pipe from shore and upending it. Figure 9 illustrates how the fabricated pipe is supported in the semisubmersible. Two “grippers” compress the pipe and support its weight while it is being fabricated. The upper gripper is fixed. The lower gripper travels up and down to stalk the pipe. The upper and lower grippers alternately grip and un-grip the pipe. There is always one gripper engaged.

A lower guide insures the pipe remains aligned with the grippers and the fabrication equipment.

A challenge for this method of pipe installation is the fact that during the running operation the pipe is rigidly constrained in roll and pitch. It is not possible to gimbal the pipe to relieve bending at the platform connection. Hence, the pipe is vulnerable to severe weather during this operation.

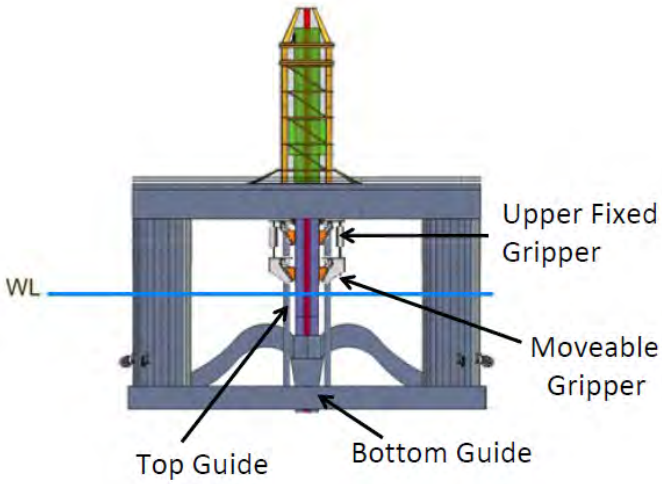

Figure 2-1 Installation Configuration with CWP in Grippers (Lockheed Martin)

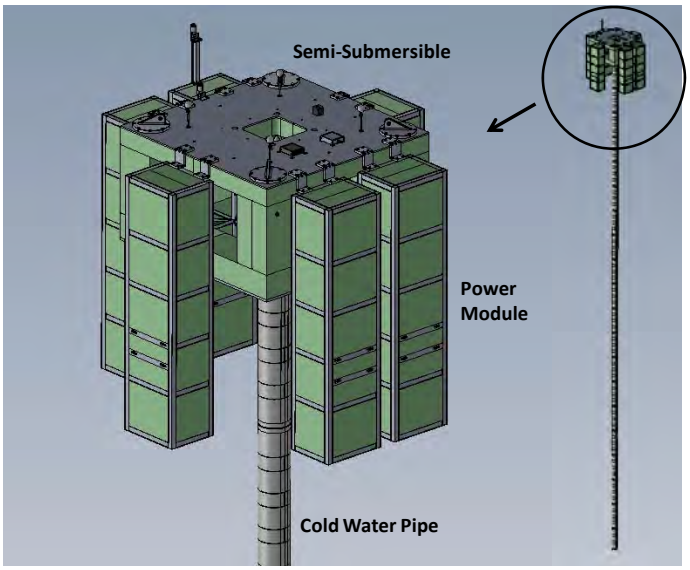

Figure 2-2 Illustration of the OTEC Model in the Operational Configuration (LabOceano)

Figure shows an illustration of the model with the power modules attached, the "operational" configuration. Figure shows a plan view of the platform at the upper guide and Table 2-1 shows the mass properties with and without the power modules (T100 and T200 references respectively).

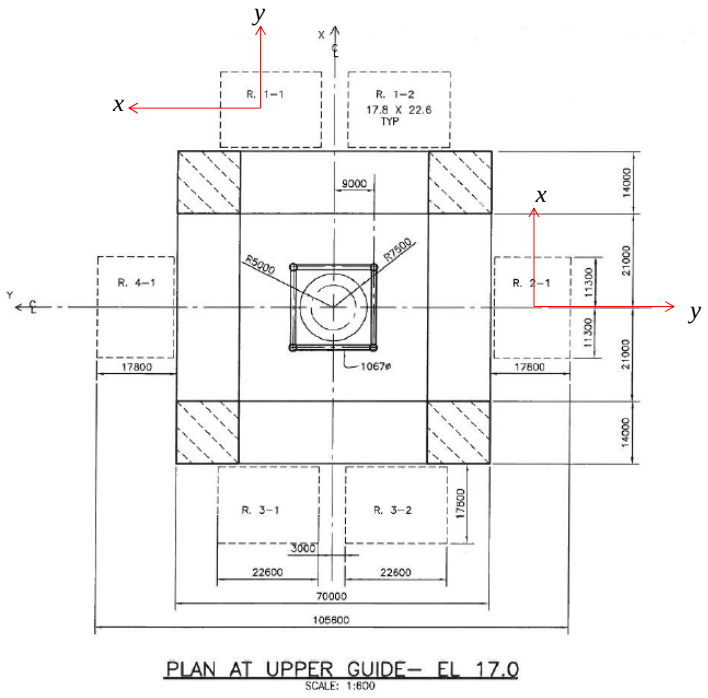

Figure 2-3 Plan View of Platform and Power Modules

Table 2-1 Mass Properties

	T100	T200
m (t)	41470.8	220738.6
Rgx (m)	28.6	35.3
Rgy (m)	28.7	41.2
Rgz (m)	30.2	44.8
XCG (m)	0.1	0.0
YCG (m)	-0.2	0.0
ZCG (m)	-1.99	-34.00
ZB (m)	-13.5	-32.2
GMx (m) (longitudinal)	3.9	20.3
GMy (m) (lateral)	3.9	14.1
Waterplane Area (m^2)	784.0	3197.7

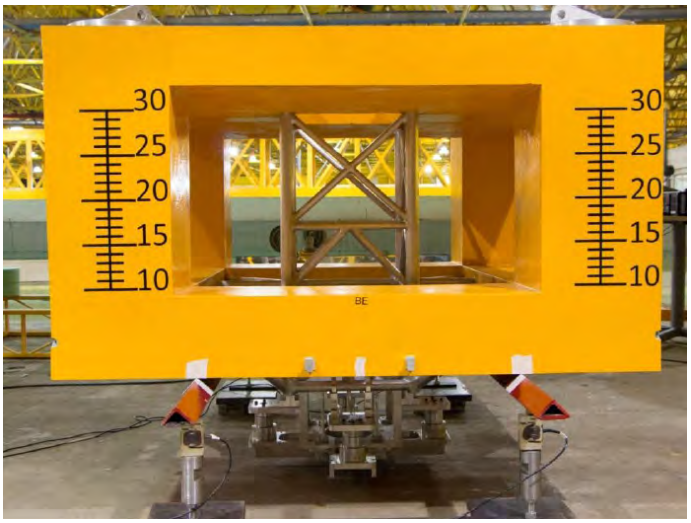

Figure 2-4 Semi Model

Figure shows the semi model with the CWP support frame attached.

During this installation phase the power modules would not be present. In this case, the lower displacement of the semi results in greater wave responses. The responses are also complicated by the fact that the mass of the pipe, including entrained water when fully deployed, exceeds the mass of the platform. The table below illustrates the relative mass of the platform and pipe for the two installation and operational configuration.

Table 2-2 Platform Mass Property

Mass (mt)	Installation	Operations
Semi-Submersuble	36627	36637
Power Modules w/ entrained water		215637
Total Platform w/ entrained water	36627	252274
CWP w/ Internal Water	135680	135680

Most of the mass in the pipe is from the internal water. Of the 136000 mt total mass, only 4800 mt is associated with the pipe structure. A good percentage of the power module mass is also entrained water within the power module structure (57% of the power module mass is entrained water). During operations the internal water in the pipe will only effect the pipe's horizontal motion. Vertical motion of the platform and pipe will induce pressure fluctuations associated with relative velocity fluctuations in the pipe and ducting, as the mass of water in the pipe is unable to accelerate with the heave motions of the platform. These pressure fluctuations present an operational challenge for the pump controller and can lead to a restricted weather window for operations.

The issues with the relative mass of the pipe compared to the platform, and the very large diameter and high elasticity of the FRP pipe makes the dynamics of the OTEC system distinctly different than typical oil & gas riser problems. Model tests are critical to confirm our ability to accurately compute the motions and loads of the platform and pipe.

2.2 COLD WATER PIPE

In order to validate the analysis of the coupled platform and pipe it was desirable to scale the mass, elasticity and hydrodynamic properties of the pipe along with the stiffness of the connection to the platform and the platform's mass and hydrodynamic properties. Froude Scaling suffices for scaling the wave forces and responses of the platform, however for geometrically similar platform and CWP models, the modal periods and shapes of the CWP will only be preserved if these values for the pipe are preserved:

$$\frac{wL^3}{EI} = \text{constant}$$

$$\frac{\rho \mathrm{A} \mathrm{U}^2 L^2}{EI} = \text{constant}$$

$$\frac{EI}{mL^4} = \text{constant}$$

Where

EI is bending stiffness

w is weight per unit length

$\rho A = m$ is mass per unit length (w/g)

L is pipe length

U is fluid velocity in pipe

Since the mass of the pipe is dominated by the entrained water, m/L2 is approximately constant, and the scaling may be satisfied if

$$\frac{EI}{L^5} = \text{constant}$$

For a uniform pipe cross section and a scale factor λ, this yields

$$(EI)_m = (EI)_p$$

"m" and "p" refer to model and prototype values respectively. For CWP of geometrically similar wall thickness or with equal model and prototype E:

$$E_m = E_p\lambda^{-1} \text{ for } t_m = t_p\lambda^{-1}$$
$$t_m = t_p\lambda^{-2} \text{ for } \mathrm{E_m} = E_p$$

This means for material of the same stiffness as the FRP pipe the model wall thickness will be on the order of 96 microns! For a geometrically scaled pipe, the material elasticity would have to be 1/50th that of the fiberglass. As pointed out by (Barr and Sheldon) this scaling is for all practical purposes impossible for scales smaller than about 1/10. For these tests we adopted the approach hybrid approach shown above (**Error! Reference source not found.**).

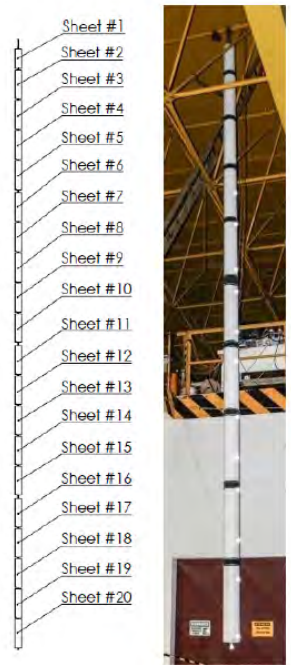

Figure 2-5 CWP Model

The CWP model was manufactured as a compound model with an internal aluminum tube core (6351-T6 alloy) dimensioned to the proper scaled flexural rigidity and segmented outer sheet sections to provide the correct outer diameter, Figure . The CWP core was divided into 5 parts connected to each other by a solid aluminum connector with angularly distributed threaded holes for bolts to connect the tubes and a longitudinal hole.

Figure 2-6 "Amazon" rubber sleeves sealing the interior between outer sheets.

The CWP outer sheet is segmented into 20 parts, roughly 50m long (prototype scale), manufactured on a composite fiberglass woven roven, mat and polyester resin structure with polyester gelcoat finishing. The connection to the CWP core was made by end plates manufactured as a sandwich composite structure with fiberglass mat, PVC foam and polyester resin and a center nylon glove with hose clamps to attach it to the core tube. The end plates rested on internal PVC foam with polyester resin finishing preventing water absorption. In order to contain entrained mass of water while not affecting the bending stiffness, the outer sheets were sealed with rubber sleeves as shown in Figure .

Figure 2-7 Setup for Pipe Bending Calibration

In order to verify the bending stiffness of the pipe an instrumented section of pipe was suspended horizontally between two pivots, Figure . Various loads were applied to a point in the middle of the pipe and the deflections and strains were recorded. Fitting this data to the beam equation gave verification of the stiffness.

Mass properties of the pipe were verified by suspending a half section of pipe from the ceiling and weighing the section. The “dry” natural periods were also measured by tapping the lower portion of the suspended pipe with a hammer and recording the strains. Wet mass properties including entrained water were estimated from the geometry. Impulse tests on the suspended pipe in water were performed to verify the modal properties including natural frequencies and damping.

2.3 GIMBAL

The attachment of the pipe to the platform was a critical and challenging part of this project. The affect of rotational stiffness of the attachment point was particularly important as the installation scenario required a high equivalent stiffness. Various gimbal designs are being considered for the operational scenario which could have varying stiffness values. For these tests three different rotational stiffnesses were tested: a free (pinned) connection; a stiff connection representing the installation equivalent stiffness, and an intermediate value.

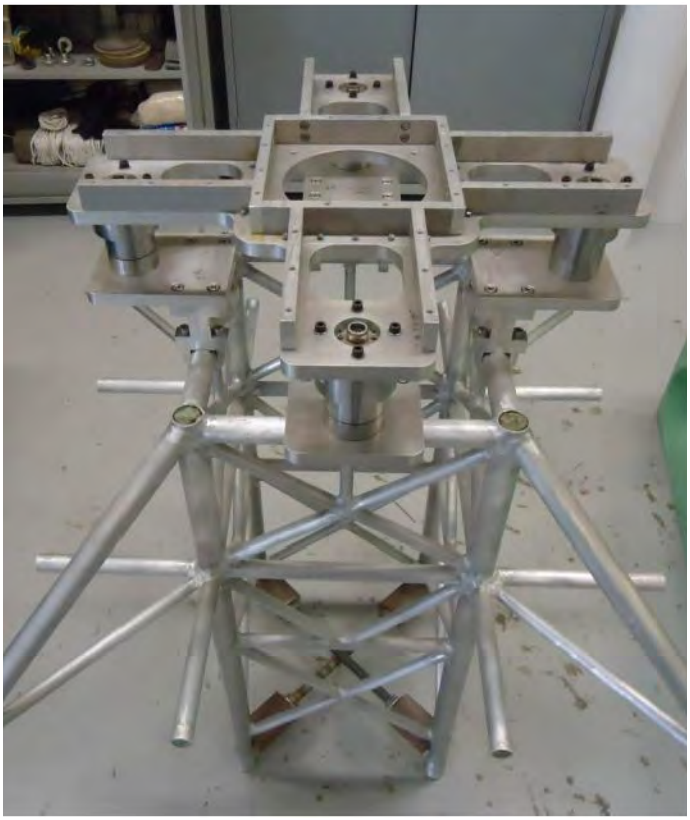

Figure 2-8 Gimbal Hangoff Frame

The gimbal was attached to a hangoff truss that was suspended below the deck and between the pontoons of the semisubmersible, Figure . The gimbal itself consisted of a Teflon semi-sphere which was supported in an aluminum cup, in effect a ball joint. The gimbal suspension system was connected to the hangoff frame through 4- 6 degree of freedom load cells in order to measure the forces and moments at the top of the gimbal.

The gimbal assembly itself is shown in Figure . It consists of a plate with the aluminum cup and ball joint suspended on six rods which represent the lateral stiffness of the gimbal assembly in the prototype frame. An aluminum tube is supported on the gimbal. The lower end of the tubing attaches to the CWP. The motion of the upper end of the tubing, and the gimbal plate is measured with four LVDTs which allow determination of the angle and lateral deflection of the gimbal. Gimbal rotational stiffness is achieved by attaching springs between the upper end of the tube to the frame. For the installation stiffness this is achieved by connecting the tube to a plate attached to cantilevered rods, see the upper left photo in Figure . The intermediate stiffness is achieved by connecting pretensioned four coil springs between the upper tube and the frame, see the upper right photo. The lower photos of Figure show the free gimbal with a suspended weight. Dynamic pendulum tests were conducted to assess the frictional damping in the gimbal.

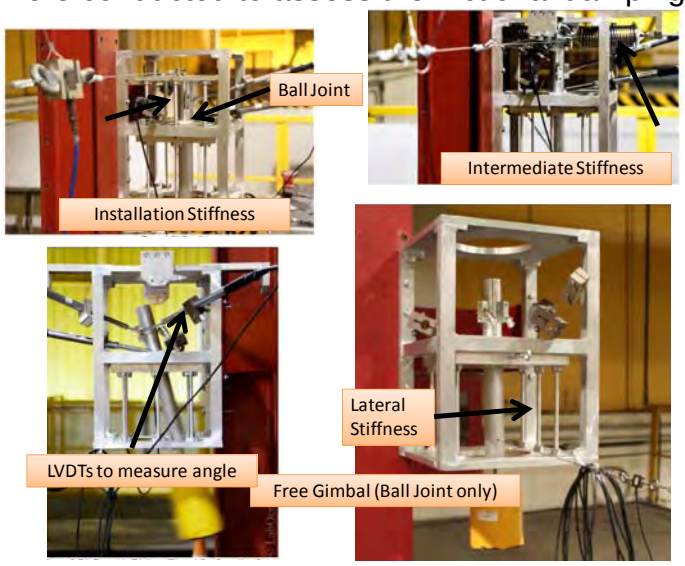

Figure 2-9 Gimbal Assembly

The gimbal angle measurements were calibrated by comparing derived angles from the LVDTs with measurements of a VECTOR-NAV VN-100 Inclinometer.

2.4 TEST ENVIRONMENTS AND CONFIGURATIONS

The tests were conducted over the 25 m deep pit of the LabOceano facility, Figure . The deep facility allowed testing at the relative large scales of these experiments.

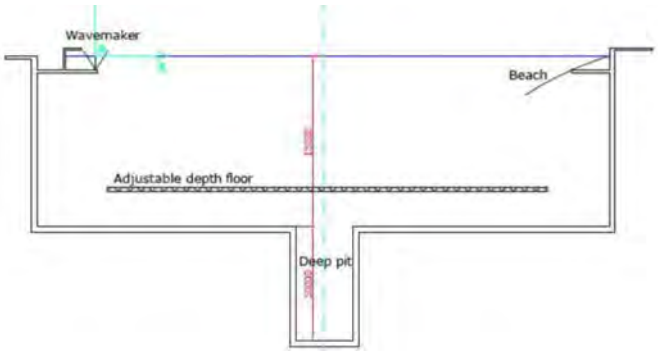

Figure 2-10 Cross Section of the LabOceano Tanks

The test environments consisted of five irregular waves and seven regular waves. The irregular wave environments are listed in Table .

Table 2-3 Test Environments

	100 Year Cyclone	10-Yr Sea	10-Yr Swell	Fatigue Wave	White Noise
Uw, m/sec	33.8	15.7	14.6	8	8
Hs, m (measure)	10.4	4.2	3.8	2.5	2
Tp, sec (measured)	12.7	8.5	15.6	16.6	2 - 26
Gamma	2	1	6	6	
Wind Force, kN (w/ PM)	2002.2	432	373.6	112.2	112.2
Center of Pressure (w/ PM)	14.3	14.3	14.3	14.3	14.3
Wind Force, kN (w/o PM)	1547.2	333.8	288.7	86.7	86.7
Center of Pressure (w/o PM)	16.6	16.6	16.6	16.6	16.6

Wind force was simulated with a steady force applied with a string and mass attached through a pulley. No current or current forces were simulated in this program. Current was initially specified but the LabOceano facility current system had not been installed at the time of these tests so it was decided to proceed with software validation without current. Future tests are planned to address current CWP interactions.

The environments represent conditions expected for an OTEC facility in Hawaii. In particular, our previous analysis has shown the semi-CWP combination to be particularly sensitive to long period swell such as that found in the Hawaiian winter as represented by the 10-yr swell and most damaging fatigue sea state. The 10-year sea and swell cases are considered survival cases for the installation scenario.

Table 2-4 Test Configurations

					Gimbal Stiffness	
CONFIGURATION	**GROUP**	**Semi**	Power Mod	Pipe Length	Rotation	Lateral
				m	N-m/rad	N/m
MODEL CALIBRATION	T000					
INSTALLATION SEMI ALONE	T100	Y	N	0		
OPERATIONAL SEMI & PMs	T200	Y	Y	0		
OPERATIONAL A	T300	Y	Y	1000	0	3.15E+08
OPERATIONAL B	T400	Y	Y	1000	1.26E+09	3.33E+08
CWP INSTALLATION 1	T500	Y	N	500	9.55E+10	3.15E+08
CWP INSTALLATION 2	T600	Y	N	1000	9.55E+10	3.15E+08

Six different configurations were tested, Table . Two configurations were tested without the CWP: The semi-alone (T100) and semi+power modules (T200). Two operational cases were performed to represent the different values of gimbal stiffness. T300 is with a free gimbal and T400 is with an intermediate stiffness. Two installation cases were run with 500m and 1000m of pipe deployed (T500 and T600 respectively).

2.5 MOORING

The mooring system consisted of four taut horizontal lines attached to the model at the corners, 15.75 m from the waterline, Figure . The lines are arranged at 45 degree angles and expend 961 m to pulleys where they turn and are each connected to a linear spring that is pretensioned. The springs design stiffness is 320 KN/m, 126.5 gf/cm, the pre-tension on the line is 13735 KN and 10862 gf in prototype and model scale respectively.

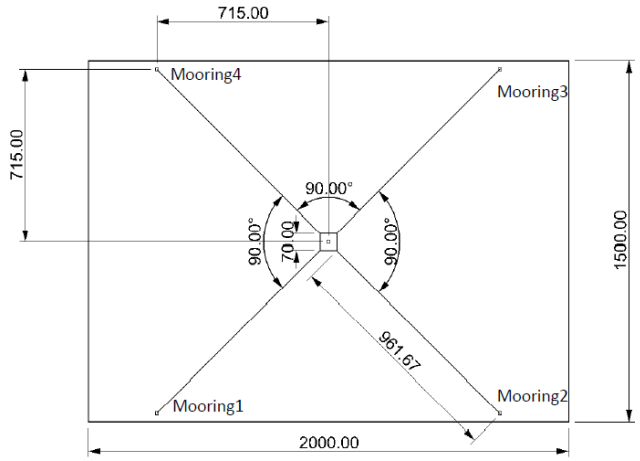

Figure 2-11 Mooring Layout

This arrangement resulted in a linear mooring system stiffness of 650 kN/m.

2.6 INSTRUMENTATION

Measurements included 90 sensors and five derived channels as shown in Table . The VECTOR-NAV inclinometer was attached to the gimbal and values recorded, but they were not time synchronized and some observations indicated the readings were unreliable.

Table 2-5 Sensors and Derived Channels

	Sensors	Derived
6-DOF Platfomr Motions (Qualisys)	6	
Underwater Qualisys (CWP XYZ @ 6 locations)	18	
CWP Strain Gages: In-line	18	
CWP Strain Gages: transverse	2	
Wave Probes	10	
Axial load: Wind	1	
Axial Load: Mooring	4	
Axial Load: Pulling forces	3	
GIMBAL (LVDTs)	4	2
Gimbal Support Load Cells	24	3
TOTAL	90	5

The sensors performed well throughout the test. The author has had bad experiences with underwater strain gages in the past, and the fact that all but two of the CWP strain gauges functioned throughout several weeks of testing was remarkable. We did not specify the measurement of the moment at the pipe attachment point so the gimbal frame was not calibrated for moments (only x, y, z forces are derived). The moment at the attachment point may be derived from the measured angles and rotational stiffness of the gimbal, and the moments could be derived from the frame load cells. As of this writing we are still evaluating these moments. A post test calibration of the frame for moments is being considered.

3 T000 - MODEL CALIBRATION

3.1 Matching Modal Period during Installation Configuration

Data from Laboceano

Measured Modal periods for CWP as per LabOceano spectral analysis of vertical load for the installation configuration.

Table 3-1 Measured Modal Period per LabOceano

Run	Dry Weight (g)	Mode 1 (s)	Mode 2 (s)	Mode 3 (s)
1	22478.7	4.71	0.91	0.30
2	22478.1	4.71	0.89	0.30
3	22480.8	4.88	1.00	0.30
4	22338.9	4.40	0.92	0.30

Measured Modal periods for CWP as per BMT spectral analysis of vertical load for the installation configuration.

Table 3-2 Measured Modal Period per BMT

Run	Mode 1 (s)	Mode 2 (s)	Mode 3 (s)
1	4.87	0.90	0.30
2	4.87	0.87	0.30
3	4.87	0.92	0.30
4	4.26	0.92	0.30

An inspection of the measured dry weights of the CWP in Table 3-1 show marked difference for Run 4, which should clearly not be the case. Therefore, it is recommended that Run 4 be ignored. The remaining results show for Runs 1 to 3 show a longer natural periods for Mode 1 and Mode 2 but agree well with the predicted natural periods for Mode 3.

FlexcomModal Analysis

The averages of the data obtained above is shown below (Run 4 is ignored)

Table 3-3 Average Modal Period

Mode	Average of LabOceano Spectral Analysis	Average of BMT Spectral Analysis	Average of All Spectral Analysis
	Time Period(s)	Time Period(s)	Time Period(s)
1	4.77	4.87	4.82
2	0.93	0.90	0.92
3	0.30	0.30	0.30

Flexcom3D Modal Analysis was performed with different top stiffness (K) to match the time period of the 1st mode obtained in the table above. The results are shown below.

Table 3-4 HOE Flexcom3D Analysis Results

Mode	K=2.35e9 Nm/rad		K=1.64e9 Nm/rad		K=1.99e9 Nm/rad	
	Time Period		Time Period		Time Period	
	FS (s)	MS (s)	FS (s)	MS (s)	FS (s)	MS (s)
1	33.73	4.77	34.44	4.87	34.07	4.82
2	7.26	1.03	7.34	1.04	7.30	1.03
3	2.55	0.36	2.56	0.36	2.56	0.36

The matching top stiffness for all three averages are shown in the Table below.

Table 3-5 Matching Top Stiffness

	Average of LabOceano Spectral Analysis	Average of BMT Spectral Analysis	Average of All Spectral Analysis
Top Stiffness matching Mode 1 (N-m/rad)	2.35E+09	1.64E+09	1.99E+09

3.2 Determine EI from Static Offset

Forces of 1799880 N , 966500 N and 299230 N are applied laterally to the bottom of the CWP and the curves compared to the experimental data. EI and K (top stiffness) are varied to fit the curve for each force value. The following Tables gives the values at each stiffness:

Table 3-6 EI and K (top stiffness)

Force Applied (N)	EI	K	
	Nm^2	Nm/deg	Nm/rad
299230	4.00E+11	1.00E+06	5.73E+07
966500	6.00E+11	2.00E+07	1.15E+09
1799880	7.00E+11	8.00E+07	4.58E+09

Table 3-7 Best fit at 1799880 N

EI	K	
Nm^2	Nm/deg	Nm/rad
7.00E+11	8.00E+07	4.58E+09

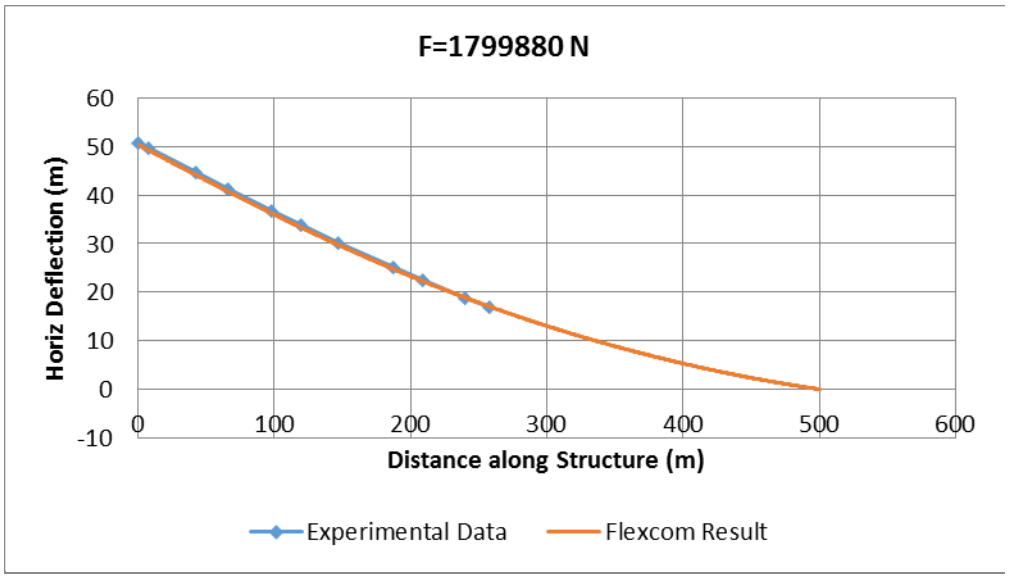

Figure 3-1 CWP Deflection for Run#1

Table 3-8 Best fit at 966500 N

EI	K	
Nm^2	Nm/deg	Nm/rad
6.00E+11	2.00E+07	1.15E+09

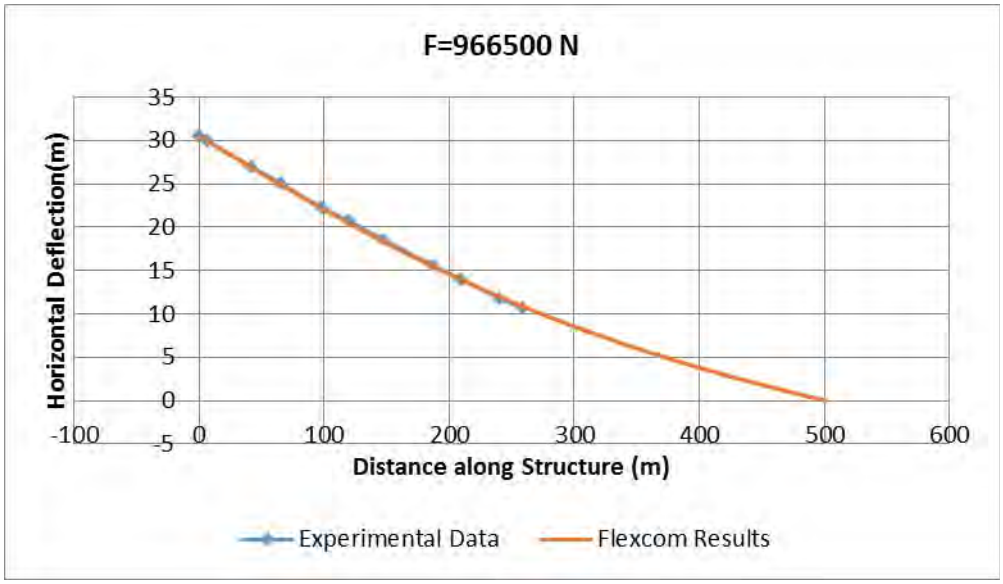

Figure 3-2 CWP Deflection for Run#2

Table 3-9 Best fit at 299230 N

EI	K	
Nm^2	Nm/deg	Nm/rad
4.00E+11	1.00E+06	5.73E+07

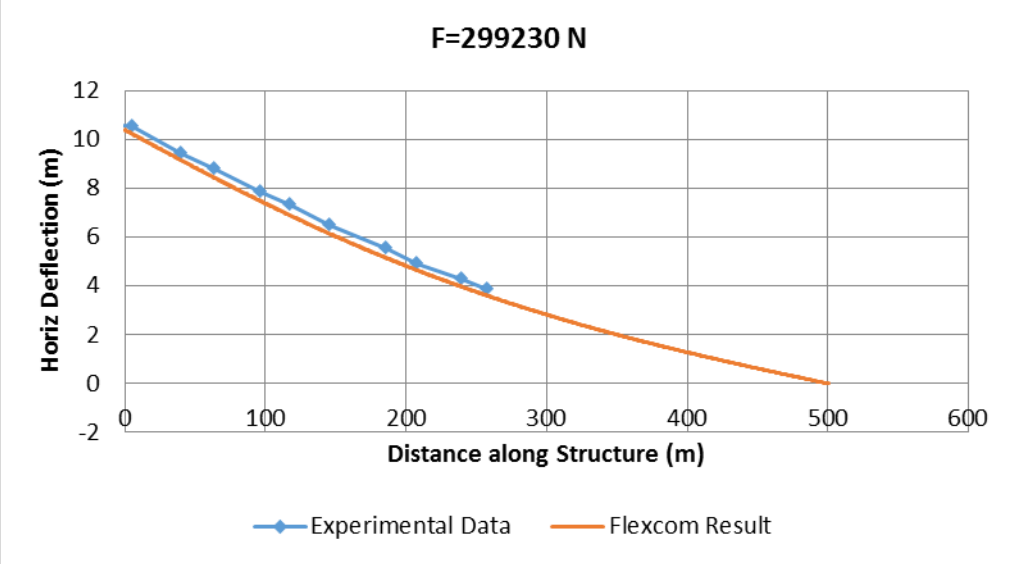

Figure 3-3 CWP Deflection for Run#3

4 T100 - INSTALLATION SEMI ALONE

4.1 T100 HARP Free Decay Results Summary

Surge free decay

HARP analysis result:
Period = 69.97 sec
Damping = 0.09157

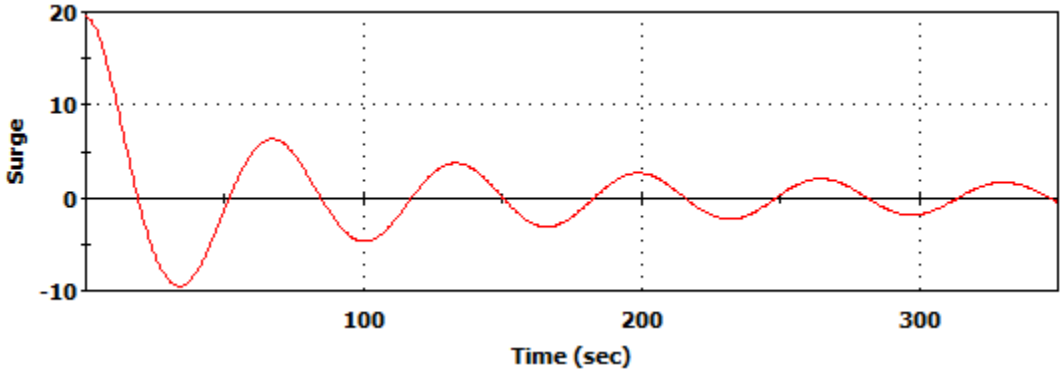

Figure 4.1-1 T100 Surge Free Decay form HARP

Model test result:

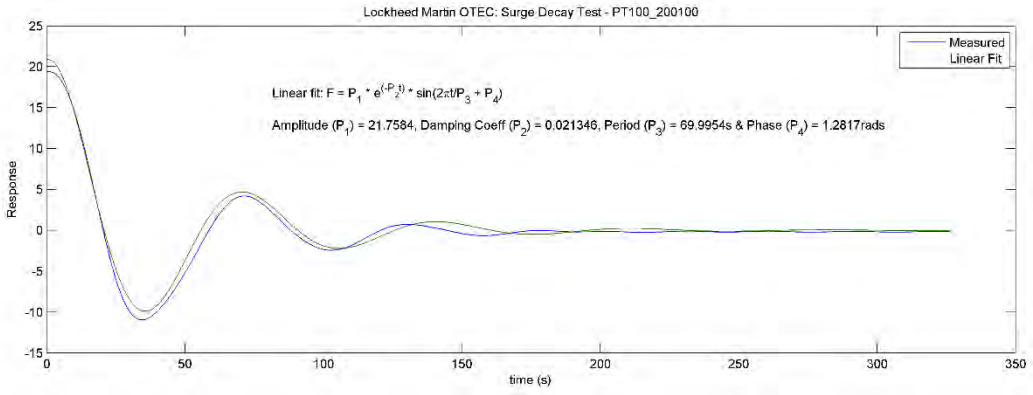

Figure 4.1-2 T100 Surge Free Decay form Test

Heave free decay

HARP analysis result:
Period = 21.78 sec
Damping = 0.04298

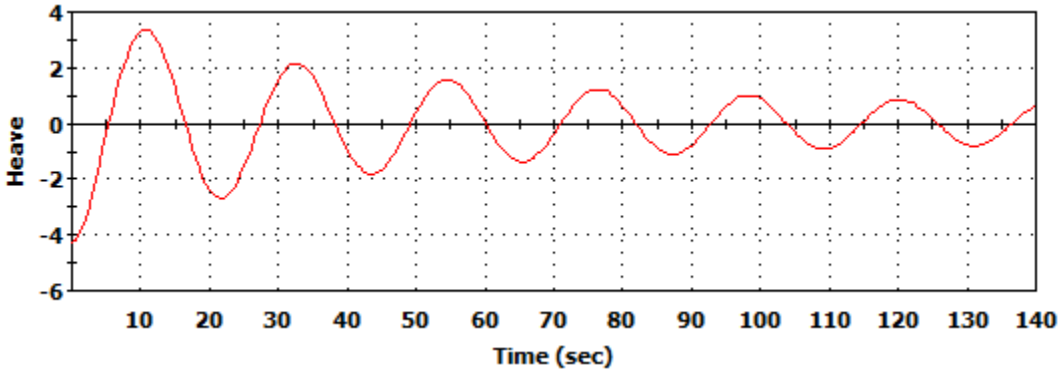

Figure 4.1-3 T100 Heave Free Decay form HARP

Model test result:

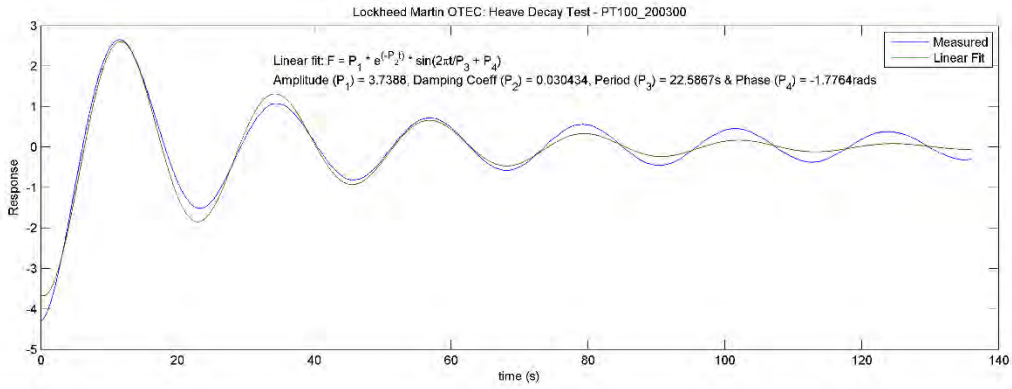

Figure 4.1-4 T100 Heave Free Decay form Test

Roll free decay

HARP analysis result:
Period = 27.68 sec
Damping = 0.06397

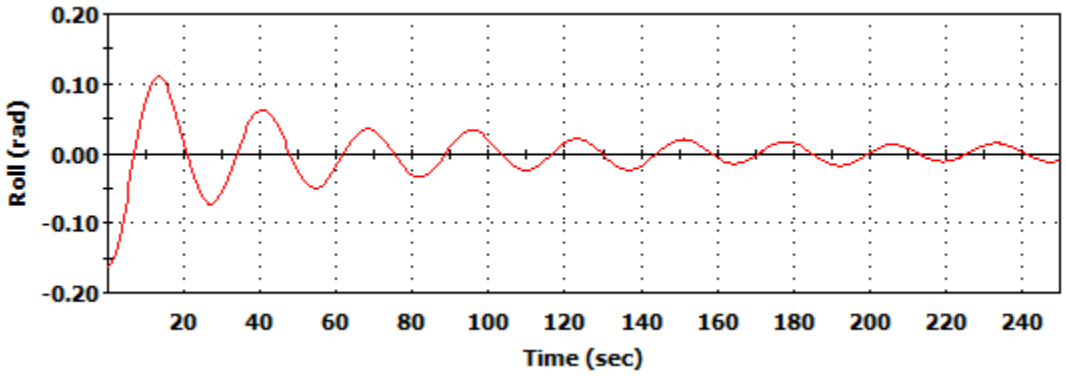

Figure 4.1-5 T100 Roll Free Decay form HARP

Model test result:

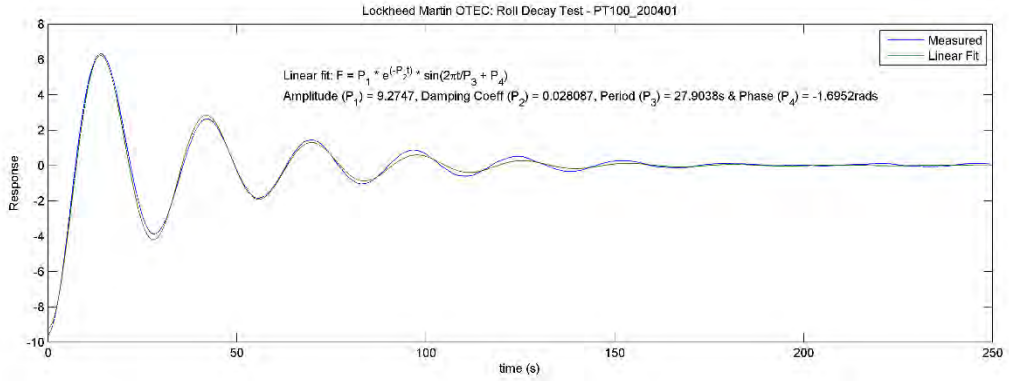

Figure 4.1-6 T100 Roll Free Decay form Test

4.2 T100 HARP Regular Wave Analysis Results Summary

Regular wave 1: H = 2.13 sec, T = 6.35 sec.

Dynamic Motion Statistics - Motion: [Unit: m, second, degree]

	Surge	Sway	Heave	Roll	Pitch	Yaw
STDV	0.17650	0.00000	0.02617	0.00000	0.05020	0.00000
MAX	-0.05144	0.00000	0.06167	0.00000	0.01129	0.00000
MIN	-0.56577	0.00000	-0.01283	0.00000	-0.13529	0.00000
MEAN	-0.31163	0.00000	0.02406	0.00000	-0.06321	0.00000

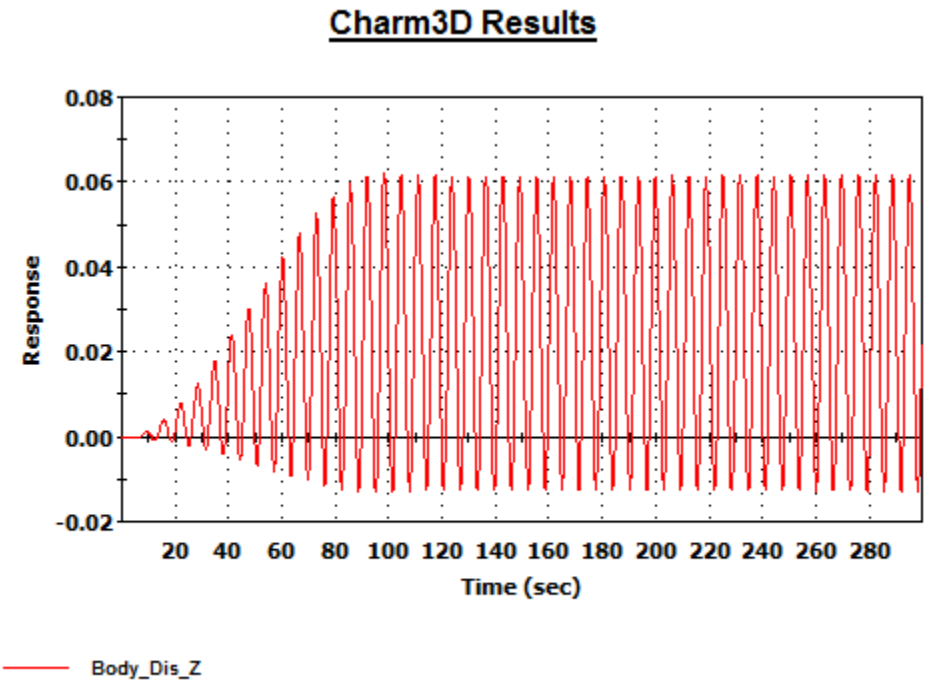

Figure 4.2-1 Heave Motion Time History

Regular wave 2: H = 2.60 sec, T = 7.00 sec.

Dynamic Motion Statistics - Motion: [Unit: m, second, degree]

	Surge	Sway	Heave	Roll	Pitch	Yaw
STDV	0.23980	0.00000	0.00488	0.00000	0.16724	0.00000
MAX	-0.01180	0.00000	0.05618	0.00000	0.15601	0.00000
MIN	-0.69807	0.00000	0.04227	0.00000	-0.31793	0.00000
MEAN	-0.36174	0.00000	0.04925	0.00000	-0.08511	0.00000

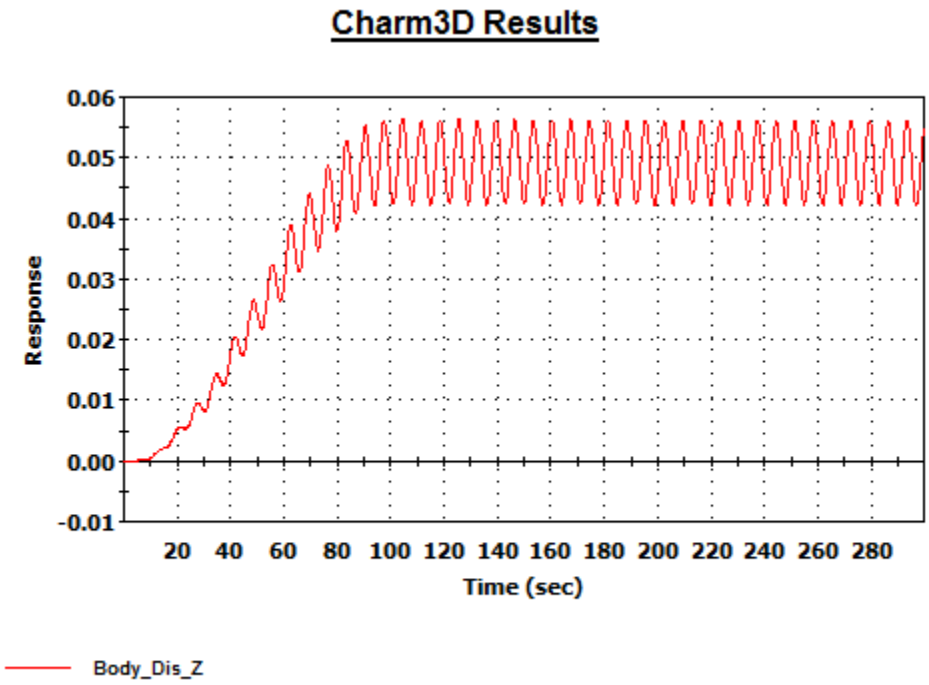

Figure 4.2-2 Heave Motion Time History

Regular wave 3: H = 3.65 sec, T = 8.50 sec.

Dynamic Motion Statistics - Motion: [Unit: m, second, degree]

	Surge	Sway	Heave	Roll	Pitch	Yaw
STDV	0.01003	0.00000	0.16624	0.00000	0.72023	0.00000
MAX	-0.74646	0.00000	0.34565	0.00000	0.82309	0.00000
MIN	-0.78022	0.00000	-0.12236	0.00000	-1.20977	0.00000
MEAN	-0.76374	0.00000	0.11360	0.00000	-0.20323	0.00000

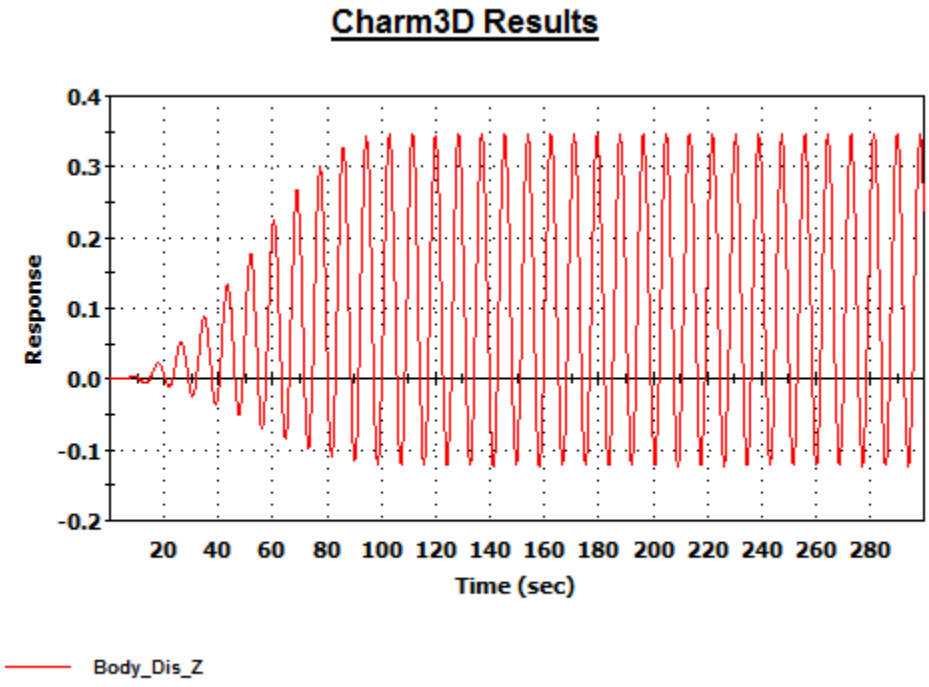

Figure 4.2-3 Heave Motion Time History

Regular wave 4: H = 5.19 sec, T = 10.0 sec.

Dynamic Motion Statistics - Motion: [Unit: m, second, degree]

	Surge	Sway	Heave	Roll	Pitch	Yaw
STDV	0.46926	0.00000	0.70423	0.00000	1.09720	0.00000
MAX	-0.23403	0.00000	1.09733	0.00000	1.38394	0.00000
MIN	-1.56649	0.00000	-0.89237	0.00000	-1.71891	0.00000
MEAN	-0.90266	0.00000	0.10715	0.00000	-0.16691	0.00000

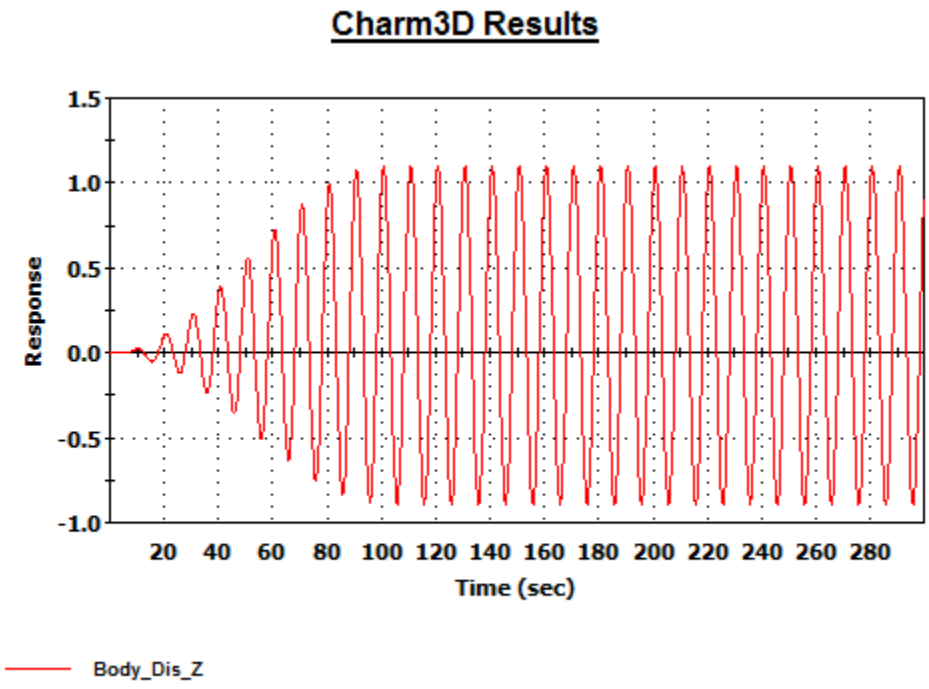

Figure 4.2-4 Heave Motion Time History

Regular wave 5: H = 6.83 sec, T = 11.49 sec.

Dynamic Motion Statistics - Motion: [Unit: m, second, degree]

	Surge	Sway	Heave	Roll	Pitch	Yaw
STDV	1.02649	0.00000	1.32465	0.00000	1.35172	0.00000
MAX	0.78024	0.00000	1.86984	0.00000	1.88418	0.00000
MIN	-2.15137	0.00000	-1.84405	0.00000	-1.97271	0.00000
MEAN	-0.64664	0.00000	0.01802	0.00000	-0.09927	0.00000

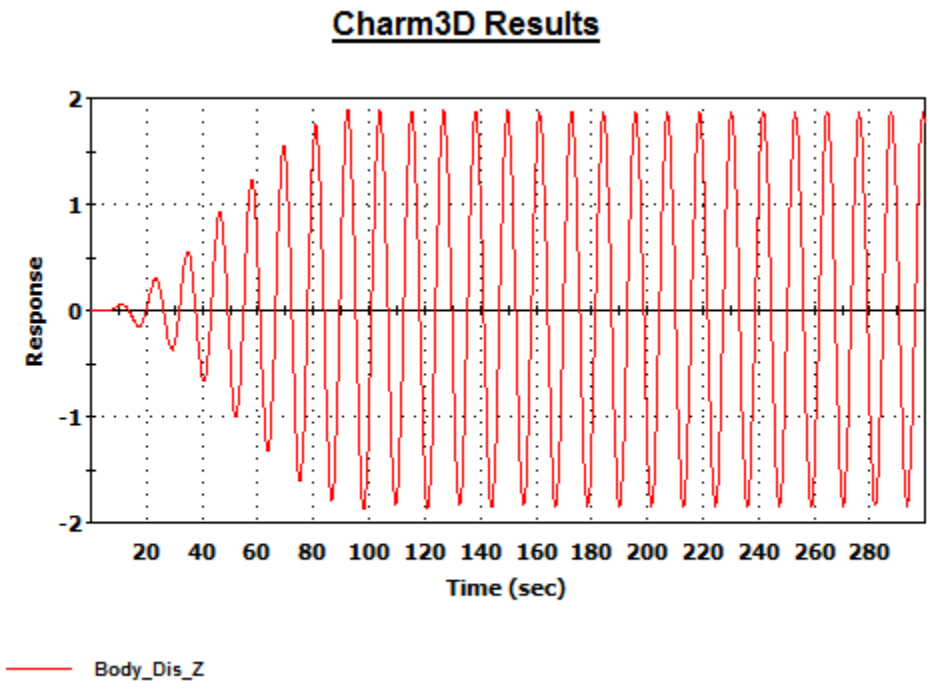

Figure 4.2-5 Heave Motion Time History

Regular wave 6: H = 8.36 sec, T = 13.02 sec.

Dynamic Motion Statistics - Motion: [Unit: m, second, degree]

	Surge	Sway	Heave	Roll	Pitch	Yaw
STDV	1.64472	0.00000	1.80524	0.00000	1.52952	0.00000
MAX	1.75367	0.00000	2.49723	0.00000	2.17766	0.00000
MIN	-2.93913	0.00000	-2.57759	0.00000	-2.19063	0.00000
MEAN	-0.51510	0.00000	-0.05263	0.00000	-0.07668	0.00000

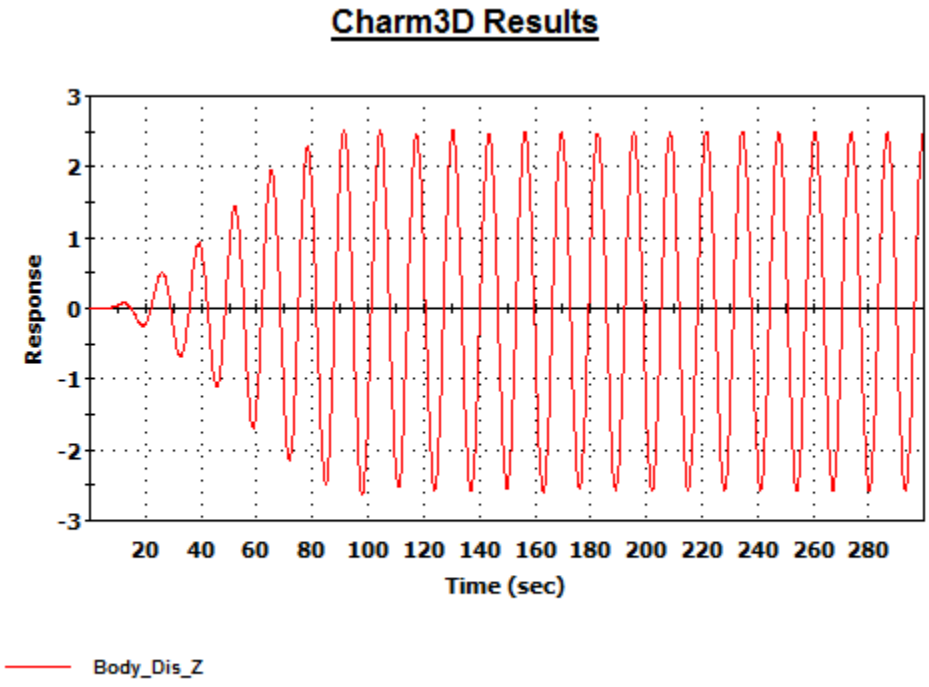

Figure 4.2-6 Heave Motion Time History

Regular wave 7: H = 11.56 sec, T = 15.0 sec.

Dynamic Motion Statistics - Motion: [Unit: m, second, degree]

	Surge	Sway	Heave	Roll	Pitch	Yaw
STDV	2.77643	0.00000	2.58415	0.00000	1.89399	0.00000
MAX	3.21489	0.00000	3.63052	0.00000	2.68435	0.00000
MIN	-4.68757	0.00000	-3.67105	0.00000	-2.71410	0.00000
MEAN	-0.59781	0.00000	-0.07043	0.00000	-0.10493	0.00000

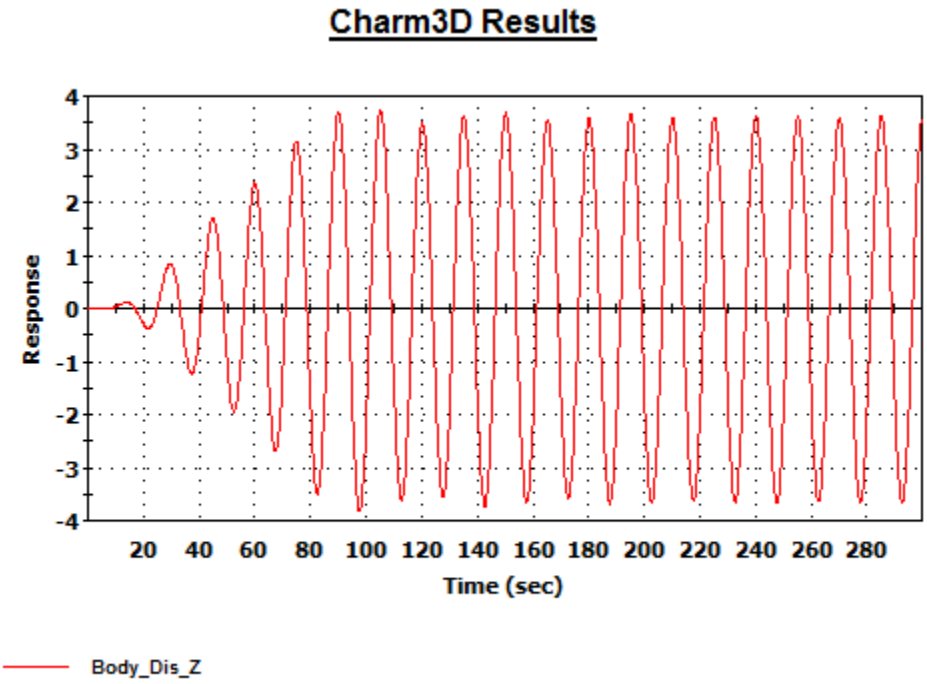

Figure 4.2-7 Heave Motion Time History

The regular wave HARP analysis results are summarized below compared with model test results.

Table 4.2-1 RAOs Comparison

	H (m)	T (s)	RAO [HARP]			RAO [Testing]		
			Surge	Heave	Pitch	Surge	Heave	Pitch
Regular Wave 1	2.13	6.35	0.24	0.03	0.07	0.29	0.03	0.03
Regular Wave 2	2.6	7	0.26	0.01	0.18	0.24	0.01	0.17
Regular Wave 3	3.65	8.5	0.01	0.13	0.56	0.01	0.12	0.54
Regular Wave 4	5.19	10	0.26	0.38	0.60	0.28	0.43	0.62
Regular Wave 5	6.83	11.49	0.43	0.54	0.56	0.50	0.54	0.63
Regular Wave 6	8.36	13.02	0.56	0.61	0.52	0.53	0.66	0.48
Regular Wave 7	11.56	15	0.68	0.63	0.47	0.94	0.70	0.65

5 T200 - OPERATIONAL SEMI & REMORAS

5.1 T200 Free Decay Results Summary

T200 Free Decay HARP simulation results compared with 3 model test runs.

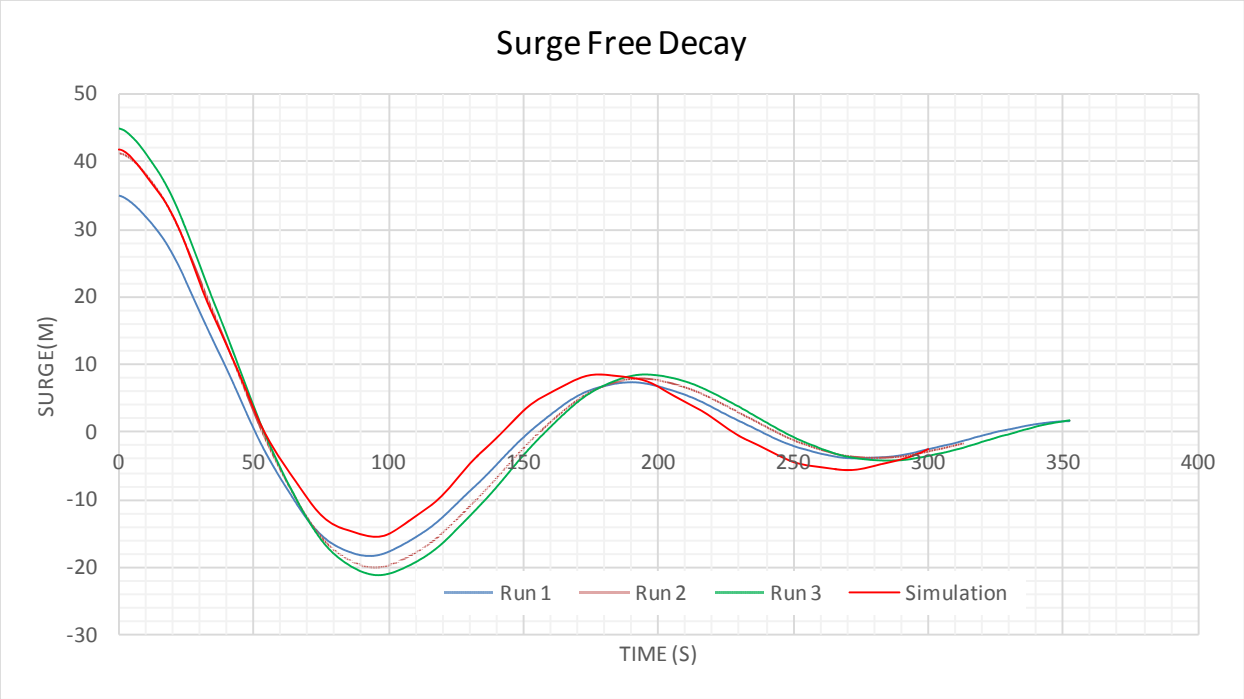

Figure 5.1-1 T200 Surge Free Decay Comparison

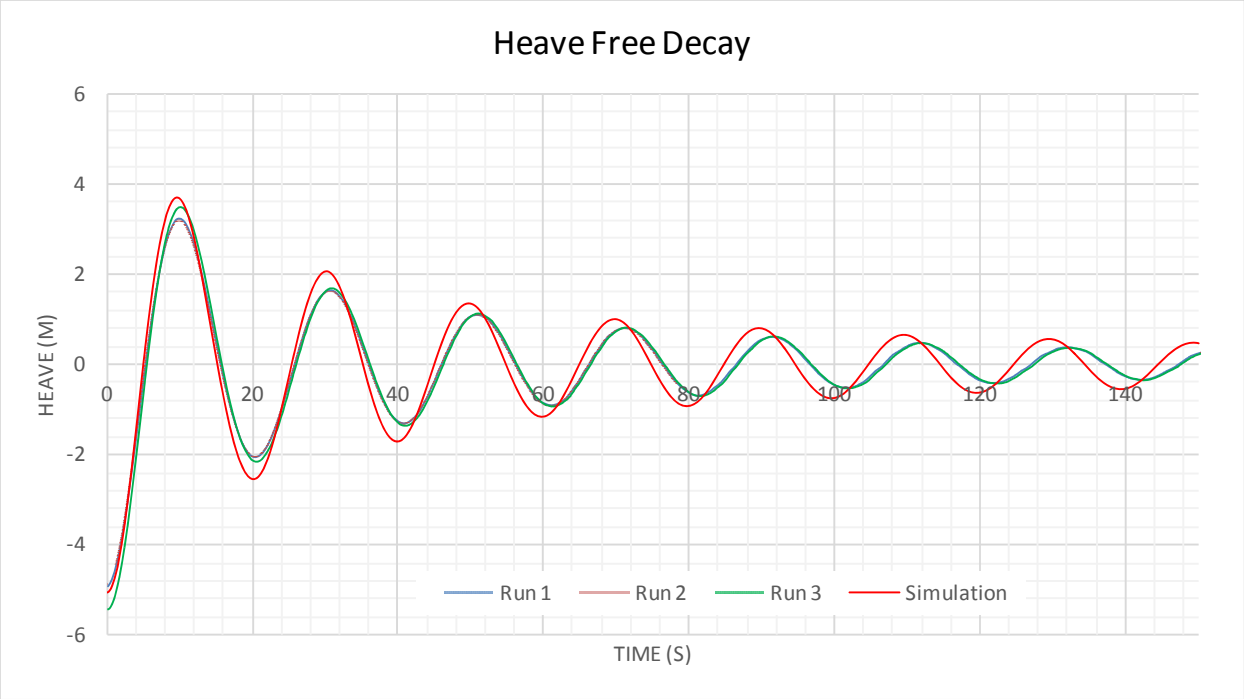

Figure 5.1-2 T200 Heave Free Decay Comparison

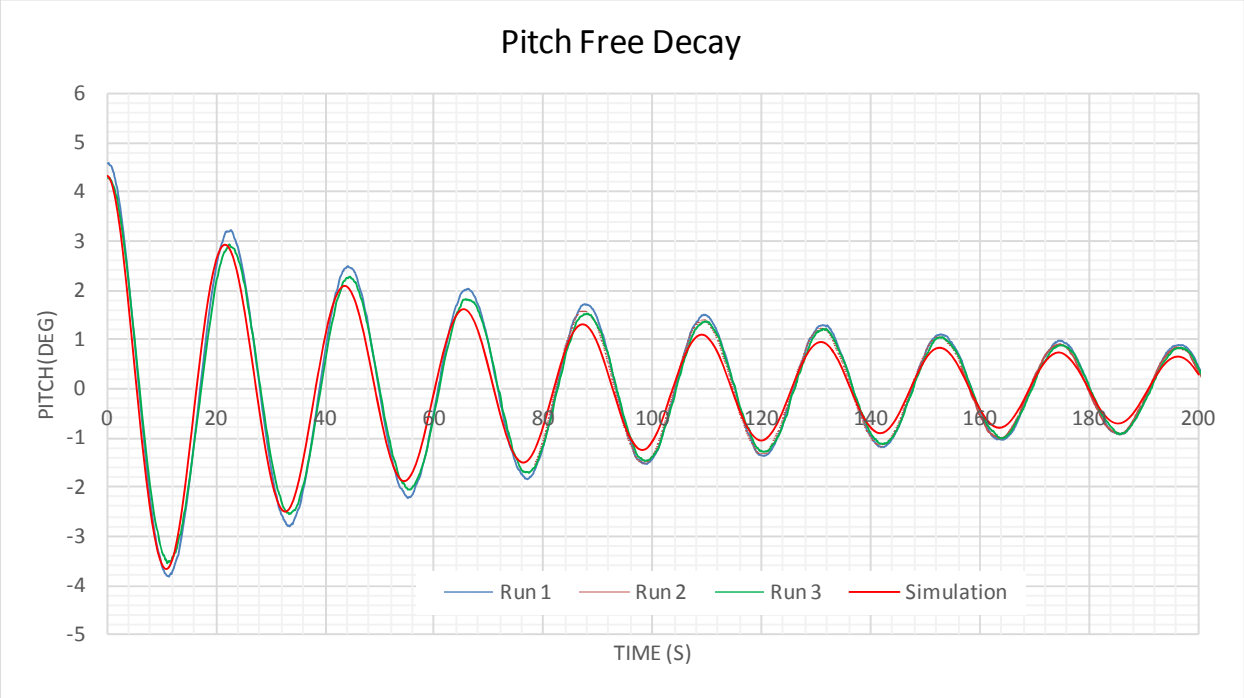

Figure 5.1-3 T200 Pitch Free Decay Comparison

5.2 T200 Random Wave Analysis

Table 5.2-1 T200 10yr Swell Calculated Motion Statistics

Summary of T200 10yr Swell Wave					
	Surge (m)			Heave (m)	Pitch (deg)
	Original	Low-Freq	High-Freq	Original	Original
Mean	-1.31	0.00	0.00	0.23	-0.09
Max	11.50	11.80	2.33	3.72	2.05
Min	-14.43	-11.49	-3.19	-2.71	-2.52
RMS	4.34	4.08	0.69	0.83	0.65
Tz (sec)	82.83	167.03	16.31	17.94	18.04

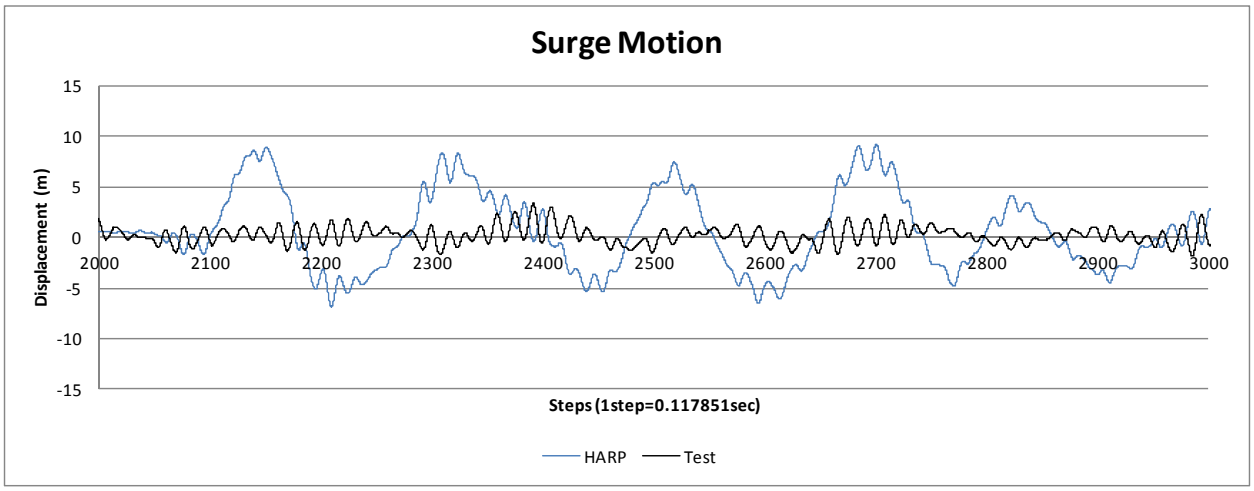

Figure 5.2-1 T200 10yr Swell – Low frequency + Wave frequency

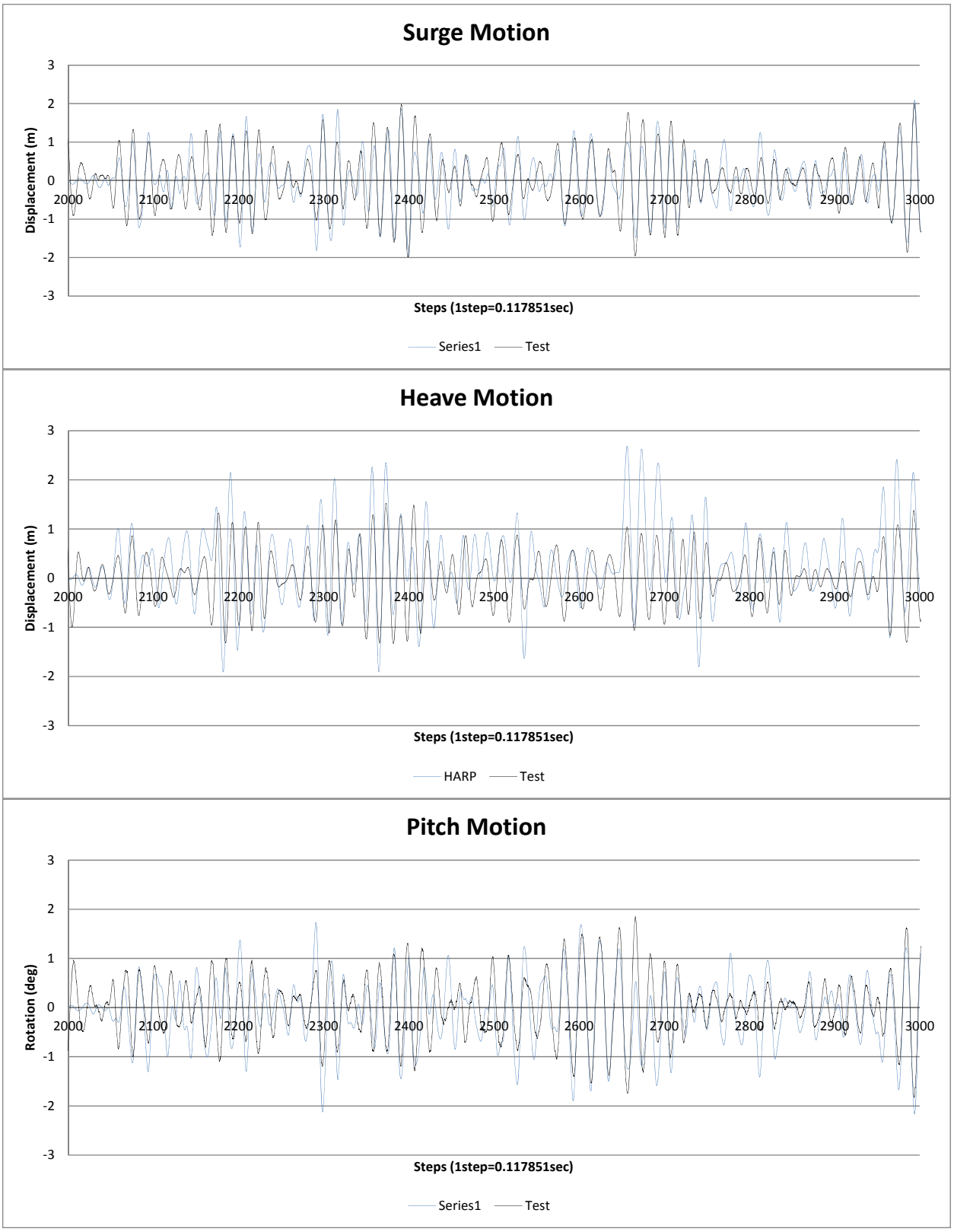

Figure 5.2-2 T200 10yr Swell Wave Motions – Wave frequency only

Table 5.2-2 T200 10yr WindSea Calculated Motion Statistics

Summary of T200 10yr WindSea Wave					
	Surge (m)			Heave (m)	Pitch (deg)
	Original	Low-Freq	High-Freq	Original	Original
Mean	0.44	0.00	0.00	-0.02	0.01
Max	10.24	9.60	1.64	0.89	2.85
Min	-9.37	-9.17	-1.96	-0.83	-2.86
RMS	2.98	2.92	0.40	0.19	0.58
Tz (sec)	81.35	162.80	13.38	18.22	16.70

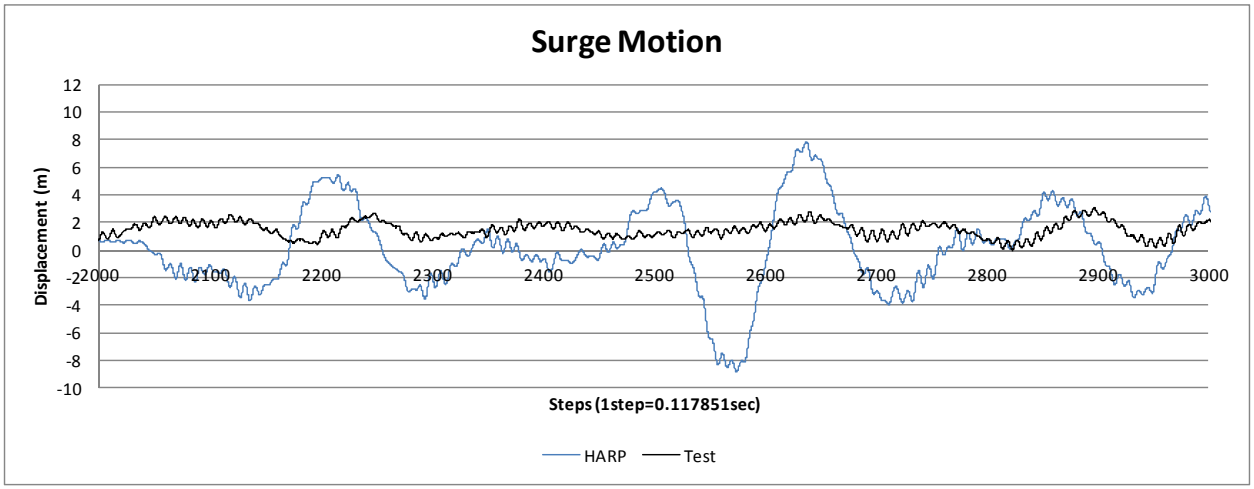

Figure 5.2-3 T200 10yr WindSea Motions – Low frequency + Wave frequency

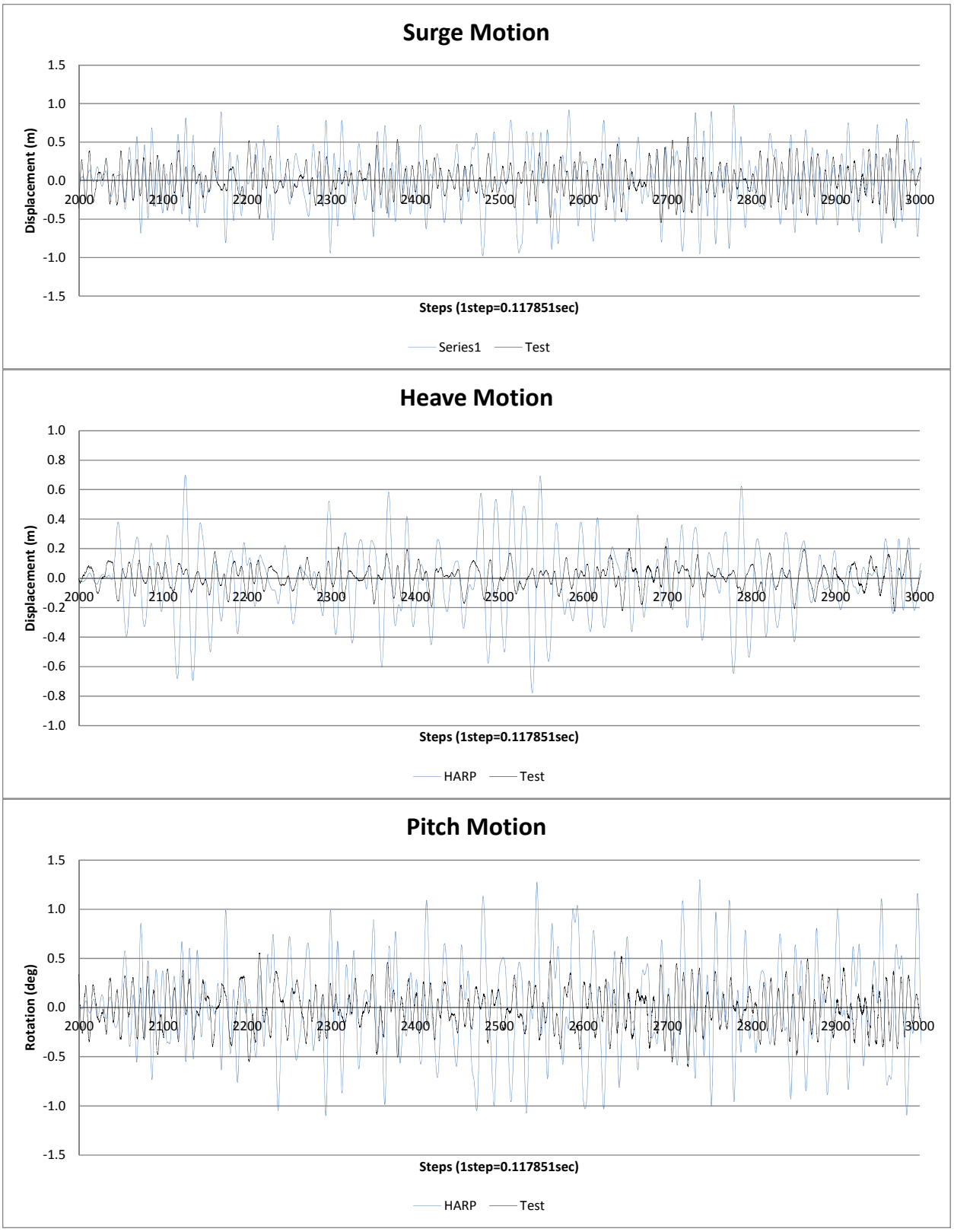

Figure 5.2-4 T200 10yr WindSea Wave Motions - Wave frequency only

Table 5.2-3 T200 100yr Cyclone Calculated Motion Statistics

Summary of T200 100yr Cyclone Wave					
	Surge (m)			Heave (m)	Pitch (deg)
	Original	Low-Freq	High-Freq	Original	Original
Mean	1.05	0.00	0.00	0.30	0.14
Max	25.78	24.19	4.72	7.30	5.45
Min	-23.48	-23.37	-4.77	-3.84	-5.94
RMS	7.91	7.73	1.25	1.36	1.22
Tz (sec)	84.04	168.07	14.41	16.50	15.26

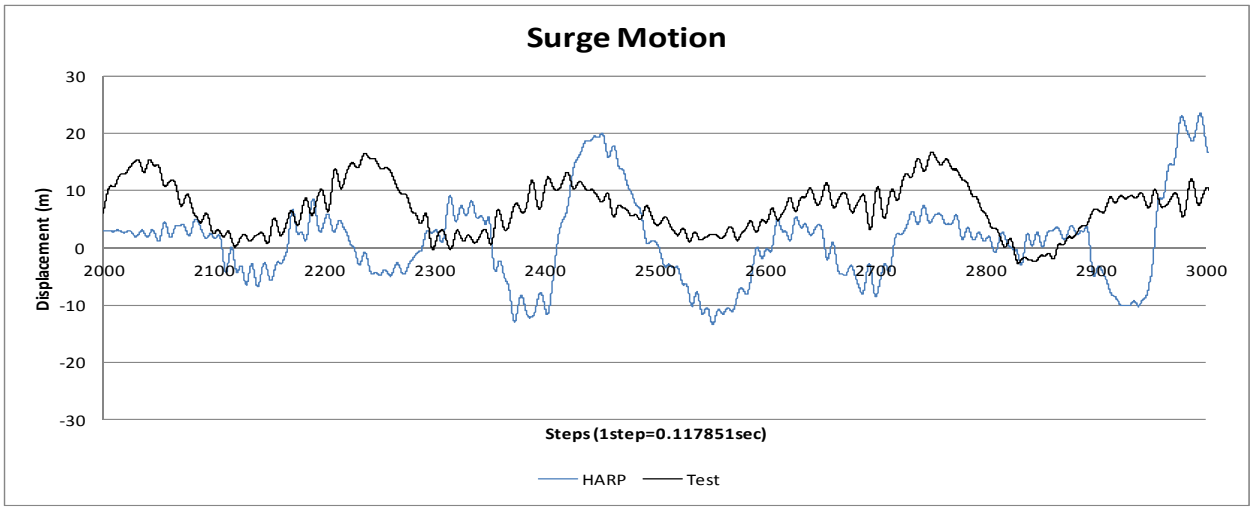

Figure 5.2-5 T200 100yr Cyclone Motions – Low frequency + Wave frequency

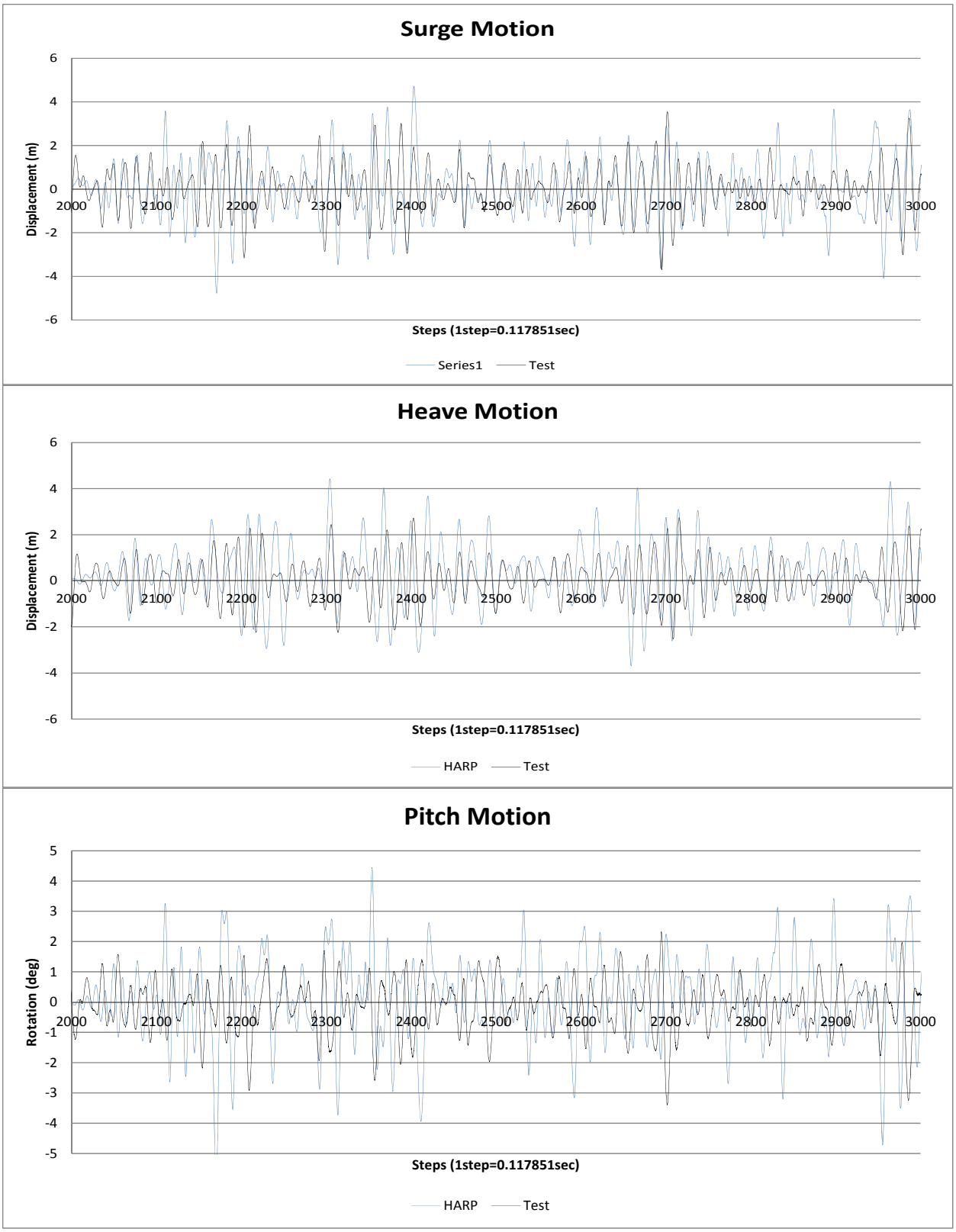

Figure 5.2-6 T200 100yr Cyclone Wave Motions - Wave frequency only

Table 5.2-4 T200 WhiteNoise Calculated Motion Statistics

Summary of T200 WhiteNoise Wave					
	Surge (m)			Heave (m)	Pitch (deg)
	Original	Low-Freq	High-Freq	Original	Original
Mean	0.27	0.00	0.00	0.03	-0.03
Max	7.88	7.00	1.26	1.51	1.68
Min	-6.68	-6.89	-1.26	-1.19	-1.89
RMS	2.60	2.55	0.42	0.39	0.59
Tz (sec)	68.81	149.32	18.38	19.59	20.00

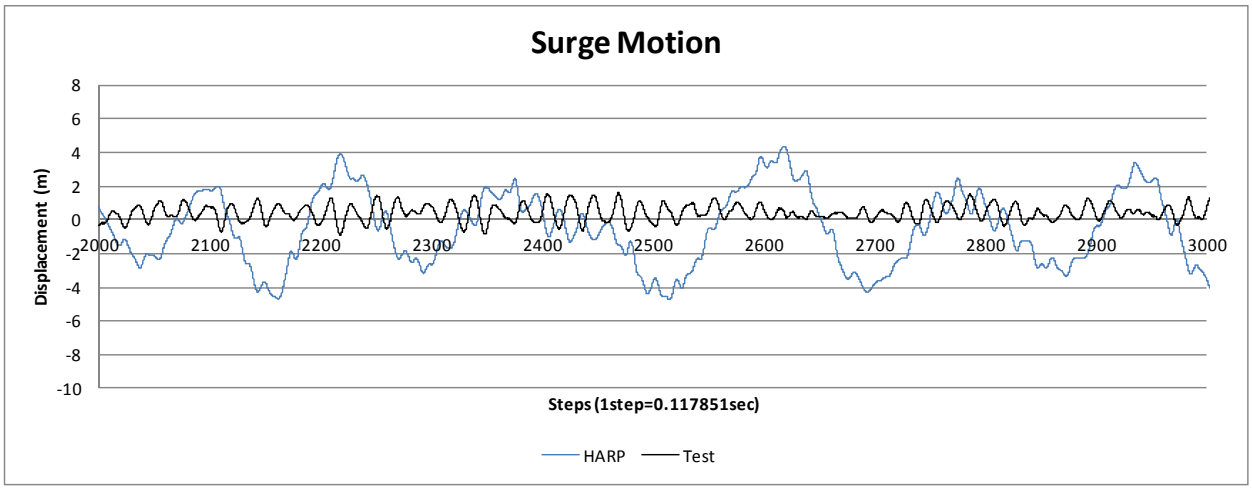

Figure 5.2-7 T200 WhiteNoise Motions – Low frequency + Wave frequency

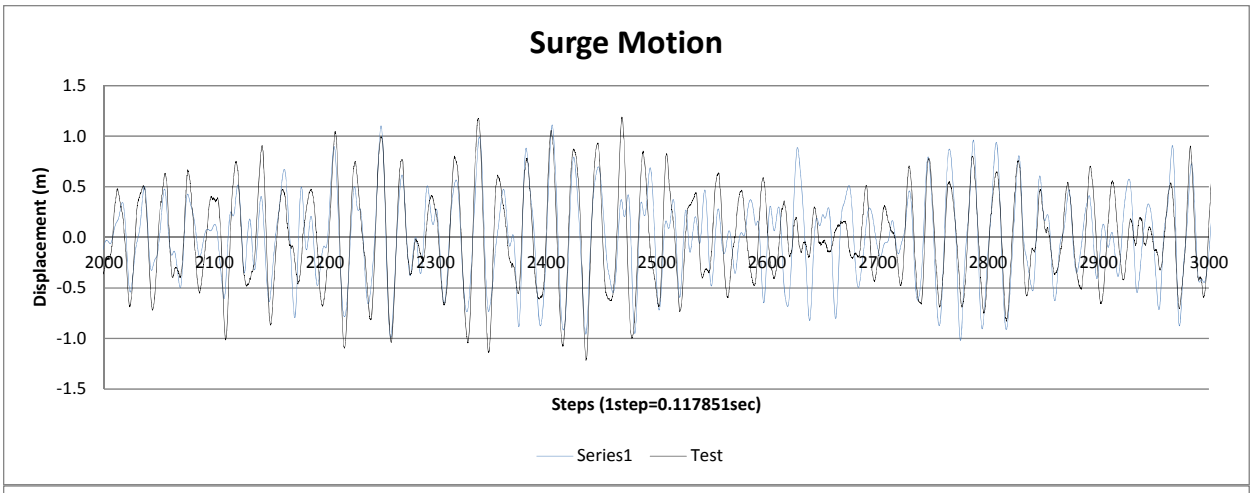

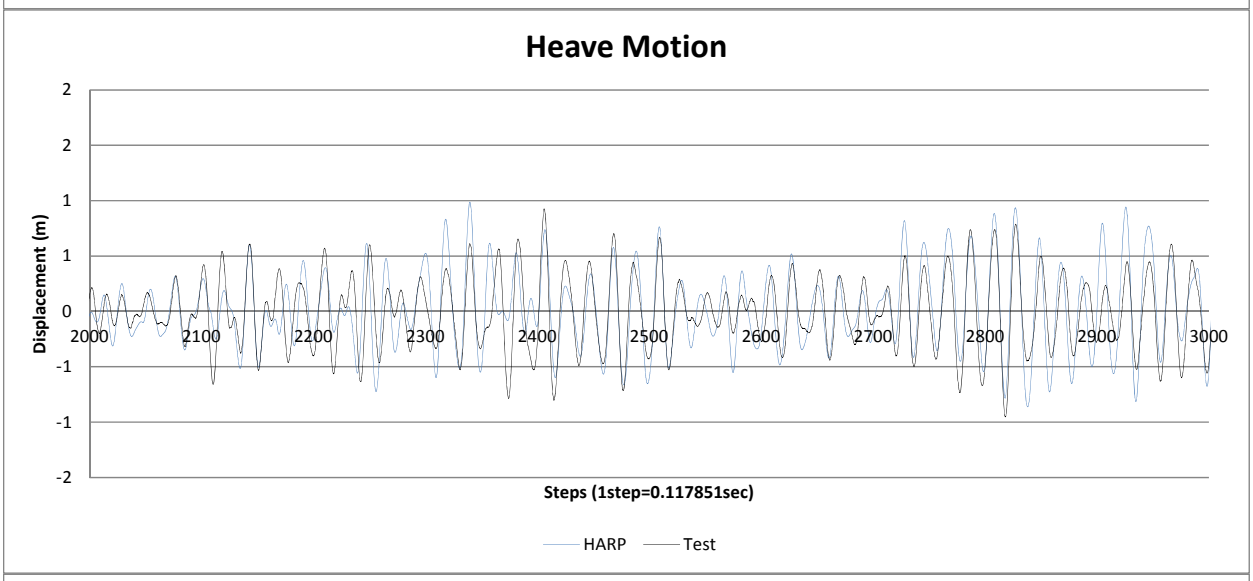

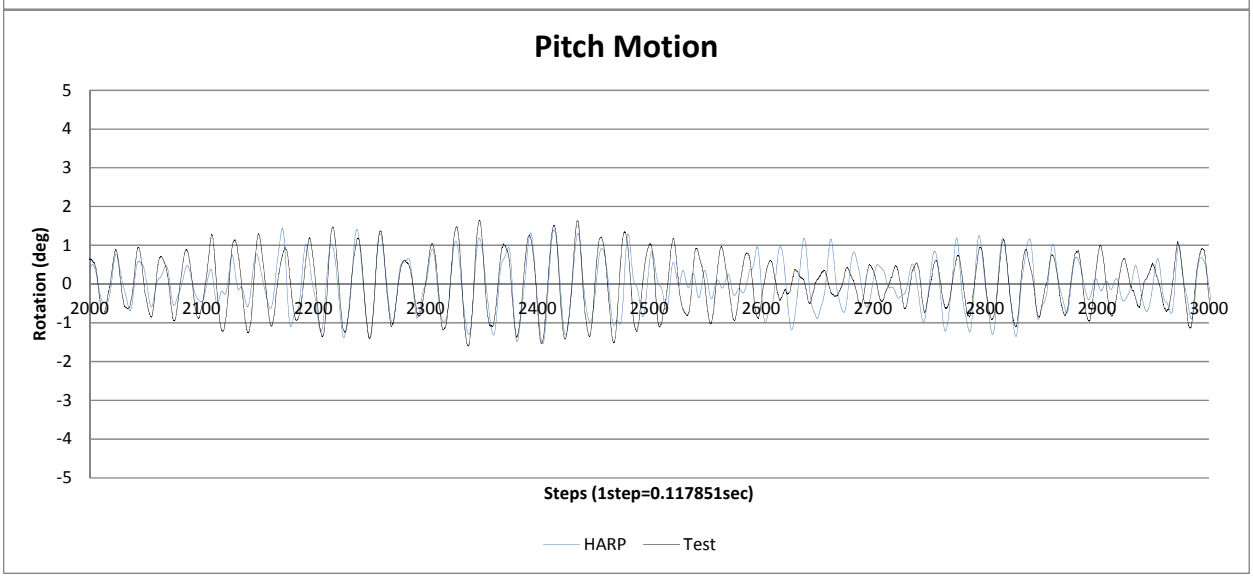

5.2-8 T200 WhiteNoise Wave Motions - Wave frequency only

6 T300 - OPERATIONAL A

6.1 T300 Free Decay Results Summary

Free decay analysis is not performed for T300

6.2 T300 Random Wave Analysis

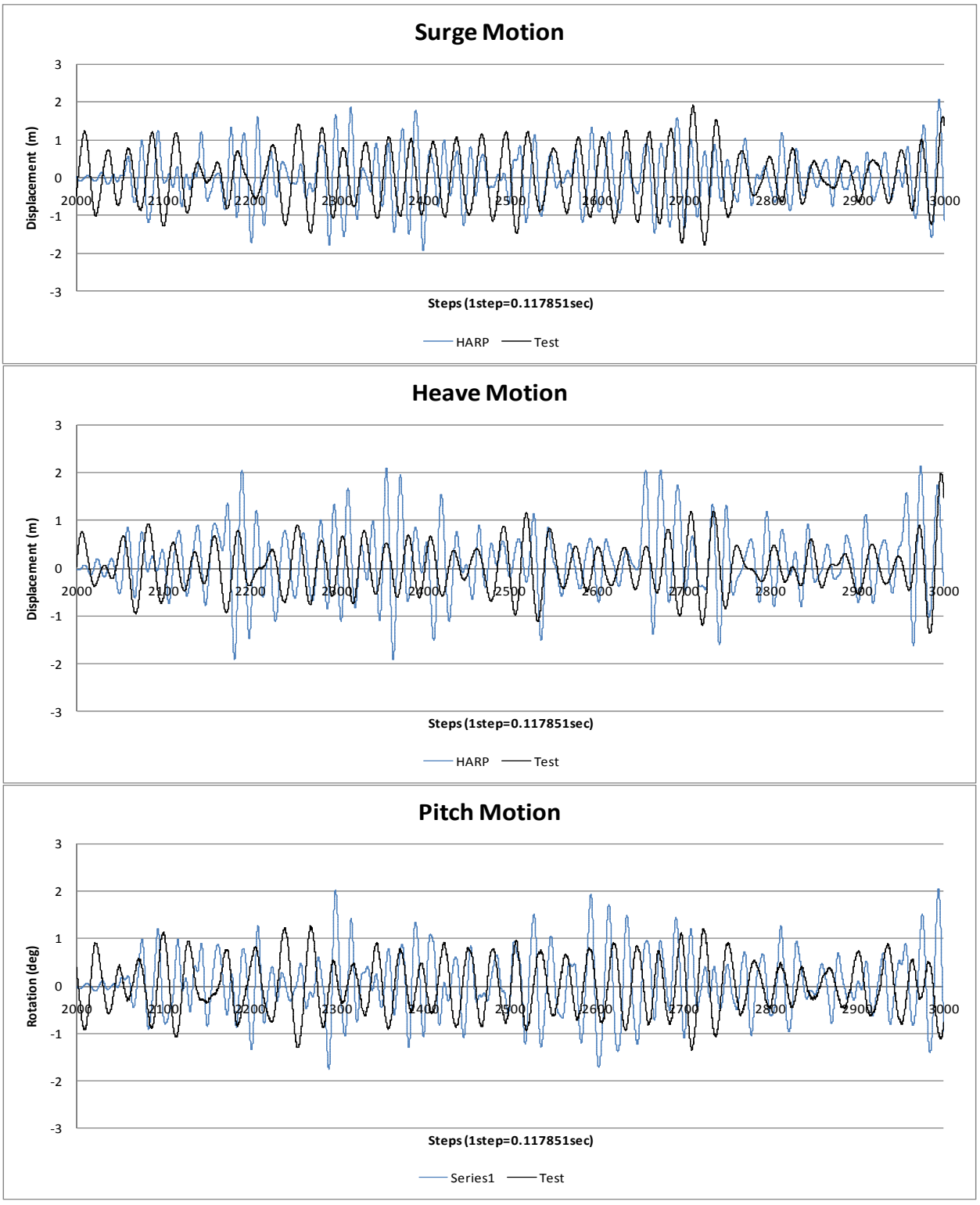

Figure 6.2-1 T300 10yr Swell Wave Motions

Table 6.2-1 T300 10yr Swell Calculated Motion Statistics

Summary of T300 10yr Swell Wave					
	Surge (m)			Heave (m)	Pitch (deg)
	Original	Low-Freq	High-Freq	Original	Original
Mean	-1.32	0.00	0.00	0.13	0.04
Max	9.33	9.72	2.21	3.44	2.42
Min	-12.74	-9.87	-2.40	-2.62	-2.05
RMS	3.78	3.48	0.67	0.76	0.64
Tz (sec)	76.60	175.70	16.47	17.76	18.09

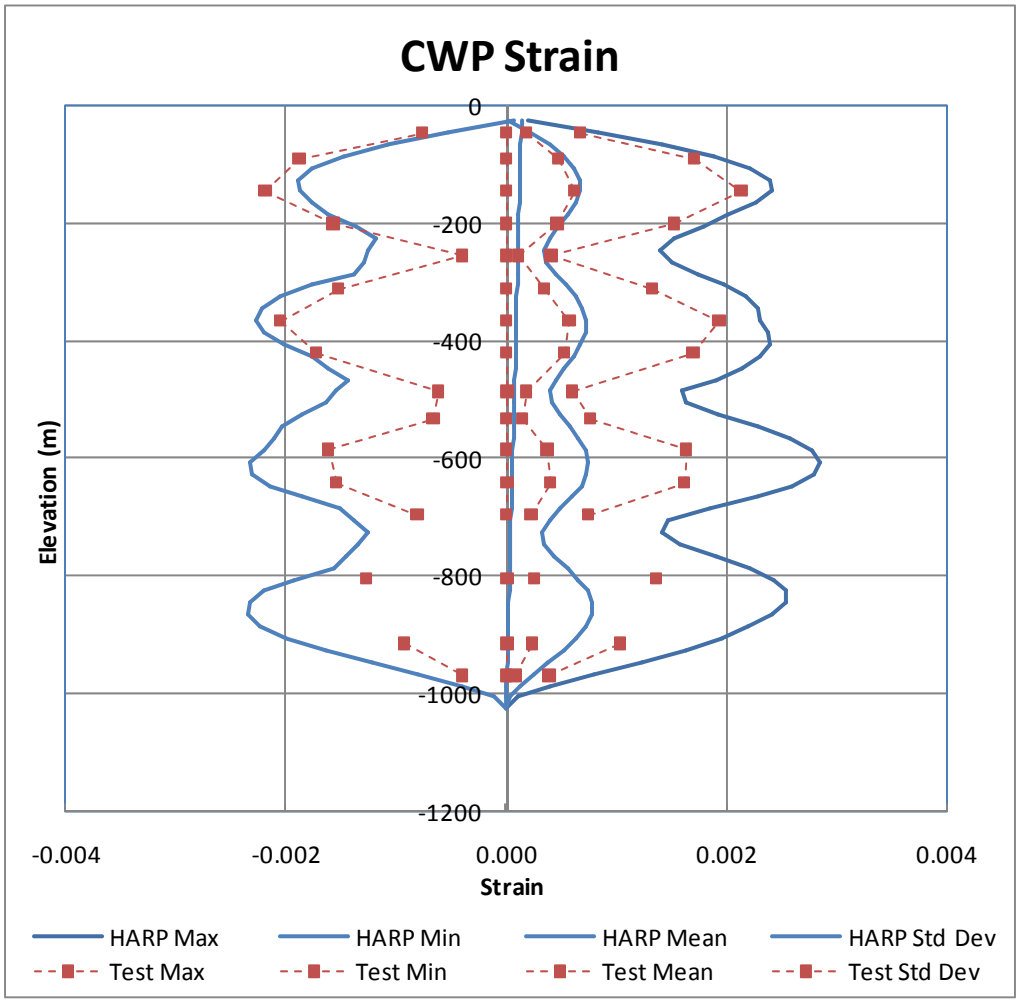

Figure 6.2-2 T300 10yr Swell CWP Strain Envelope

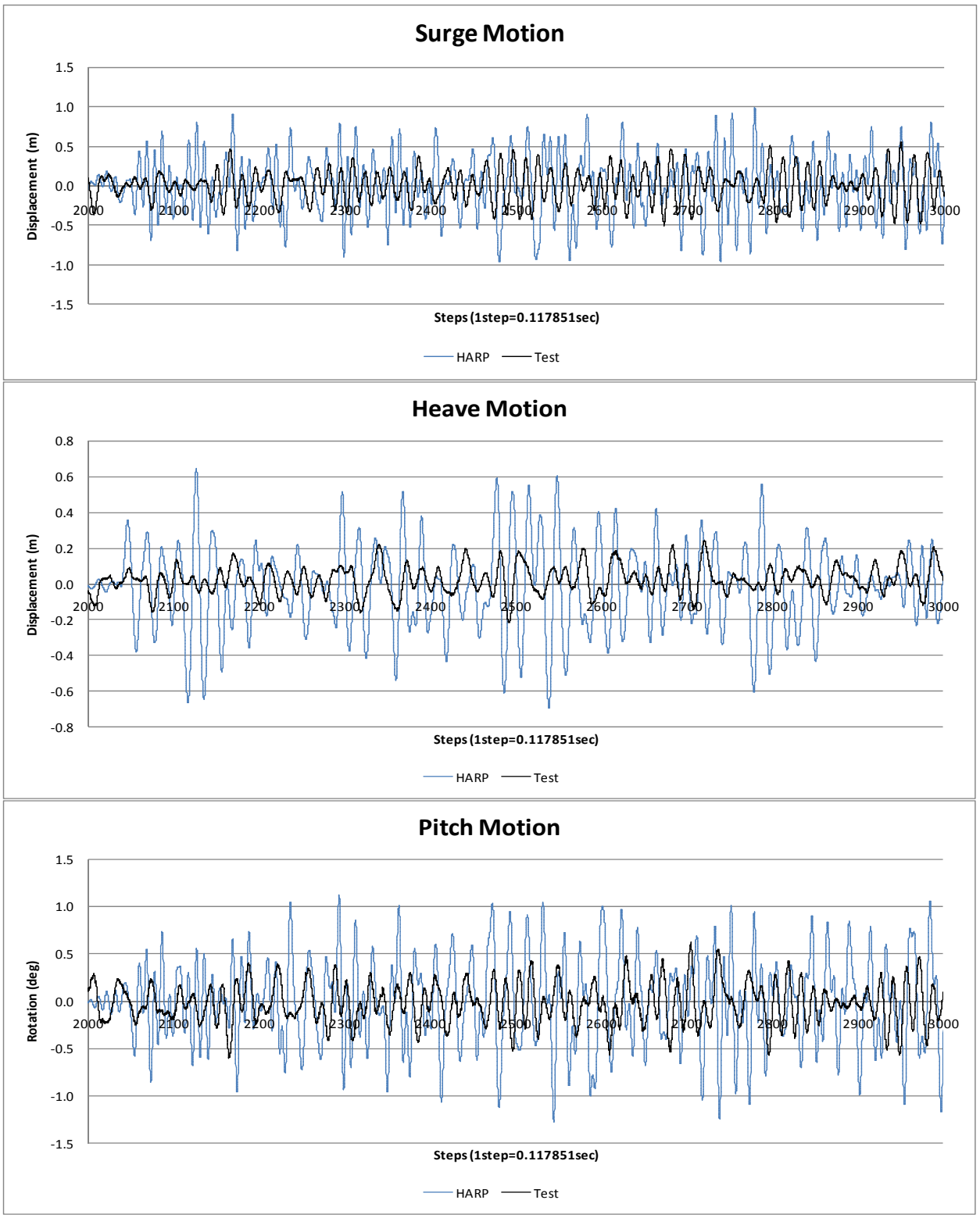

Figure 6.2-3 T300 10yr WindSea Wave Motions

Table 6.2-2 T300 10yr WindSea Calculated Motion Statistics

Summary of T300 10yr WindSea Wave					
	Surge (m)			Heave (m)	Pitch (deg)
	Original	Low-Freq	High-Freq	Original	Original
Mean	0.45	0.00	0.00	-0.02	-0.01
Max	8.36	7.71	1.63	0.82	2.84
Min	-7.77	-7.48	-1.95	-0.81	-2.81
RMS	2.44	2.36	0.39	0.18	0.57
Tz (sec)	69.85	162.74	13.41	18.85	16.61

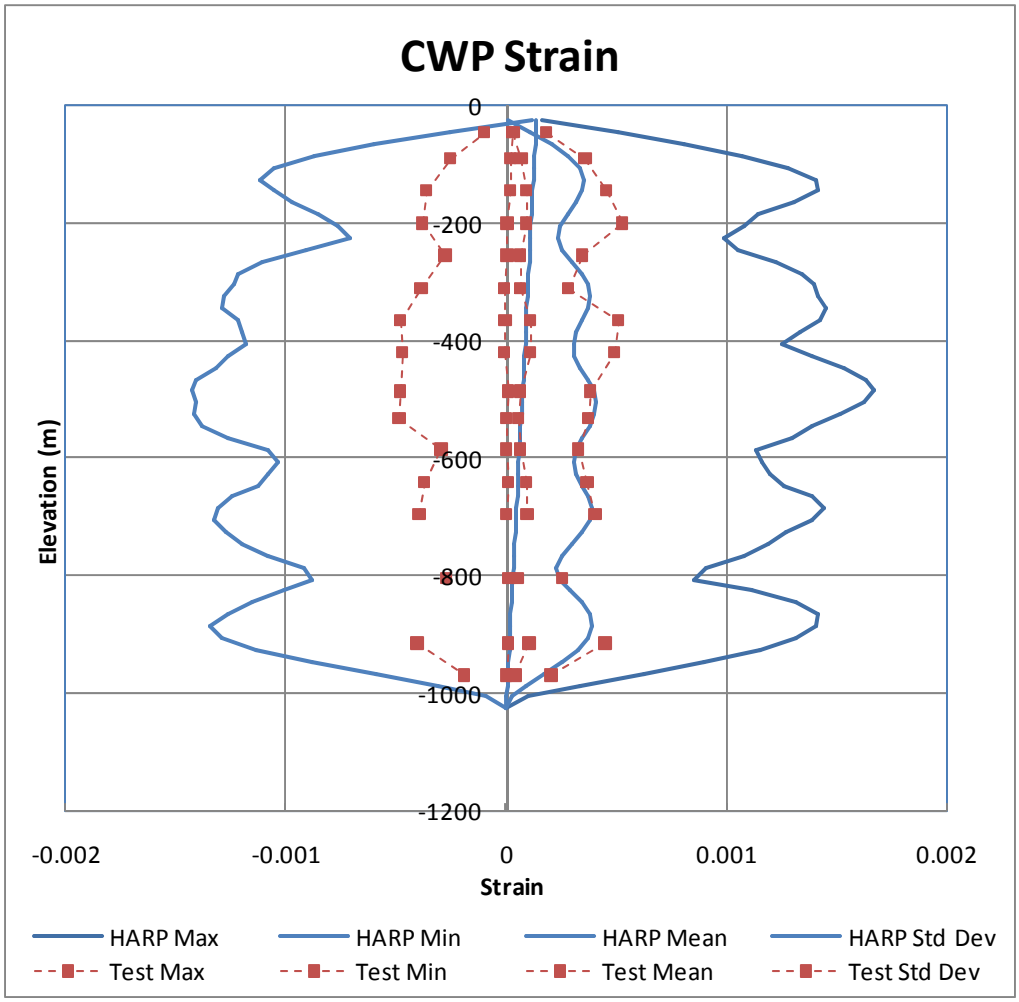

Figure 6.2-4 T300 10yr WindSea CWP Strain Envelope

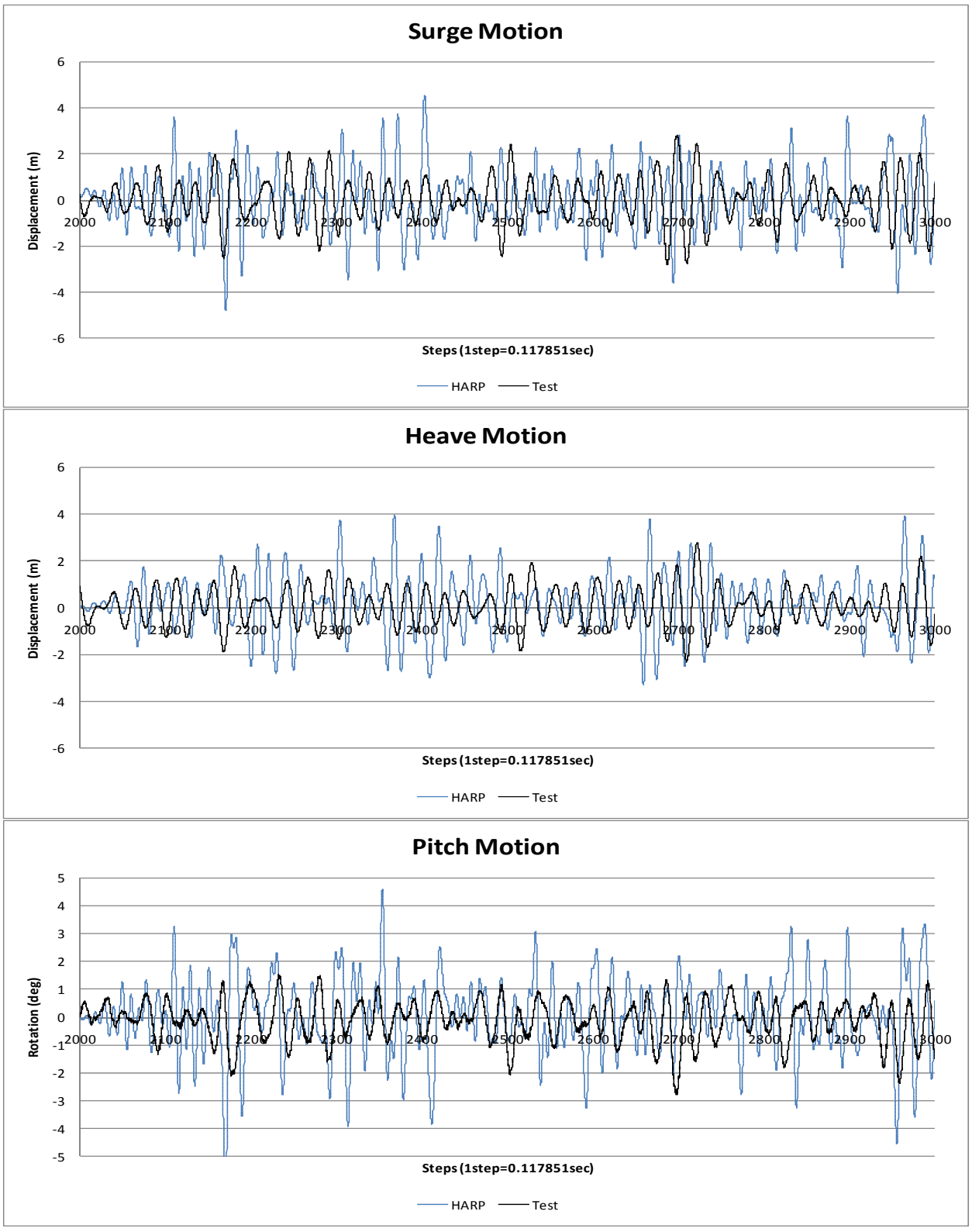

Figure 6.2-5 T300 100yr Cyclone Wave Motions

Table 6.2-3 T300 100yr Cyclone Calculated Motion Statistics

Summary of T300 100yr Cyclone Wave					
	Surge (m)			Heave (m)	Pitch (deg)
	Original	Low-Freq	High-Freq	Original	Original
Mean	1.17	0.00	0.00	0.16	0.08
Max	22.93	21.29	4.55	5.67	5.37
Min	-21.11	-21.14	-4.81	-3.77	-5.98
RMS	6.98	6.77	1.23	1.22	1.20
Tz (sec)	78.25	170.79	14.37	16.39	15.24

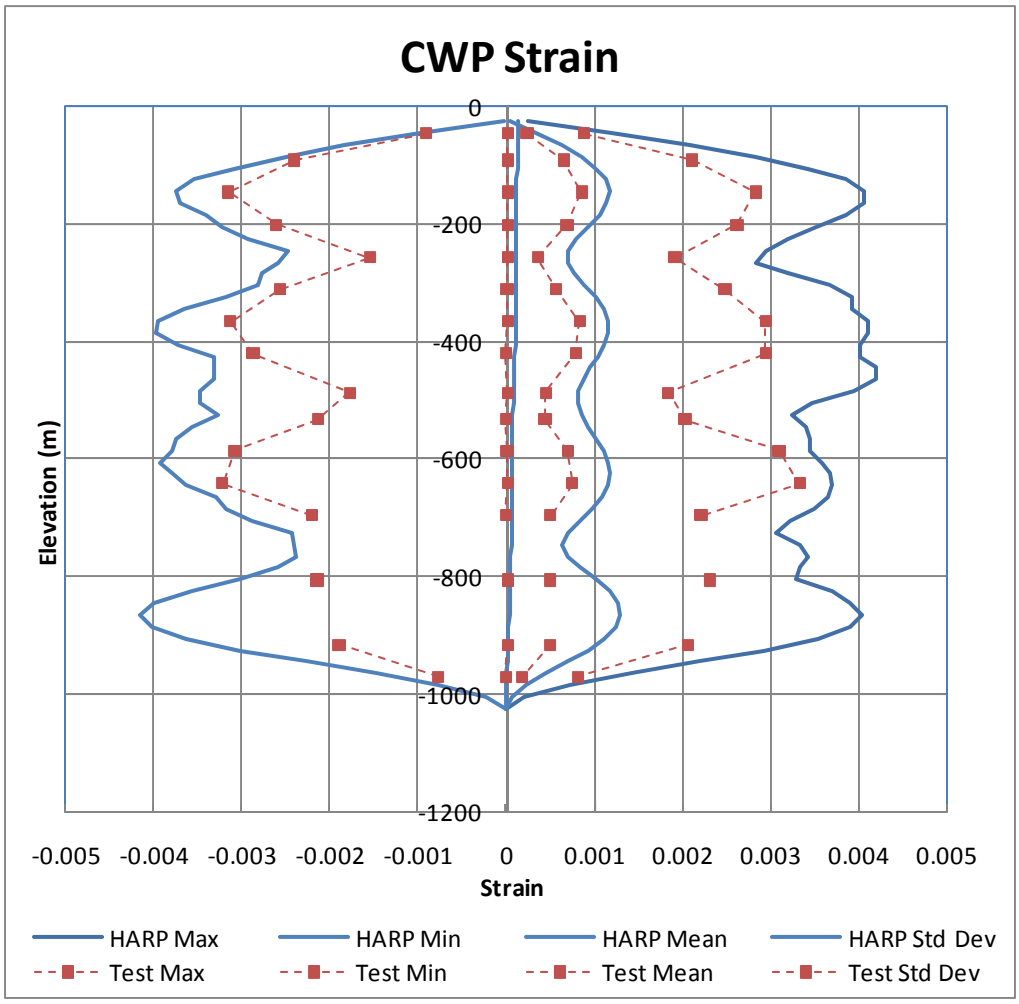

Figure 6.2-6 T300 100yr Cyclone CWP Strain Envelope

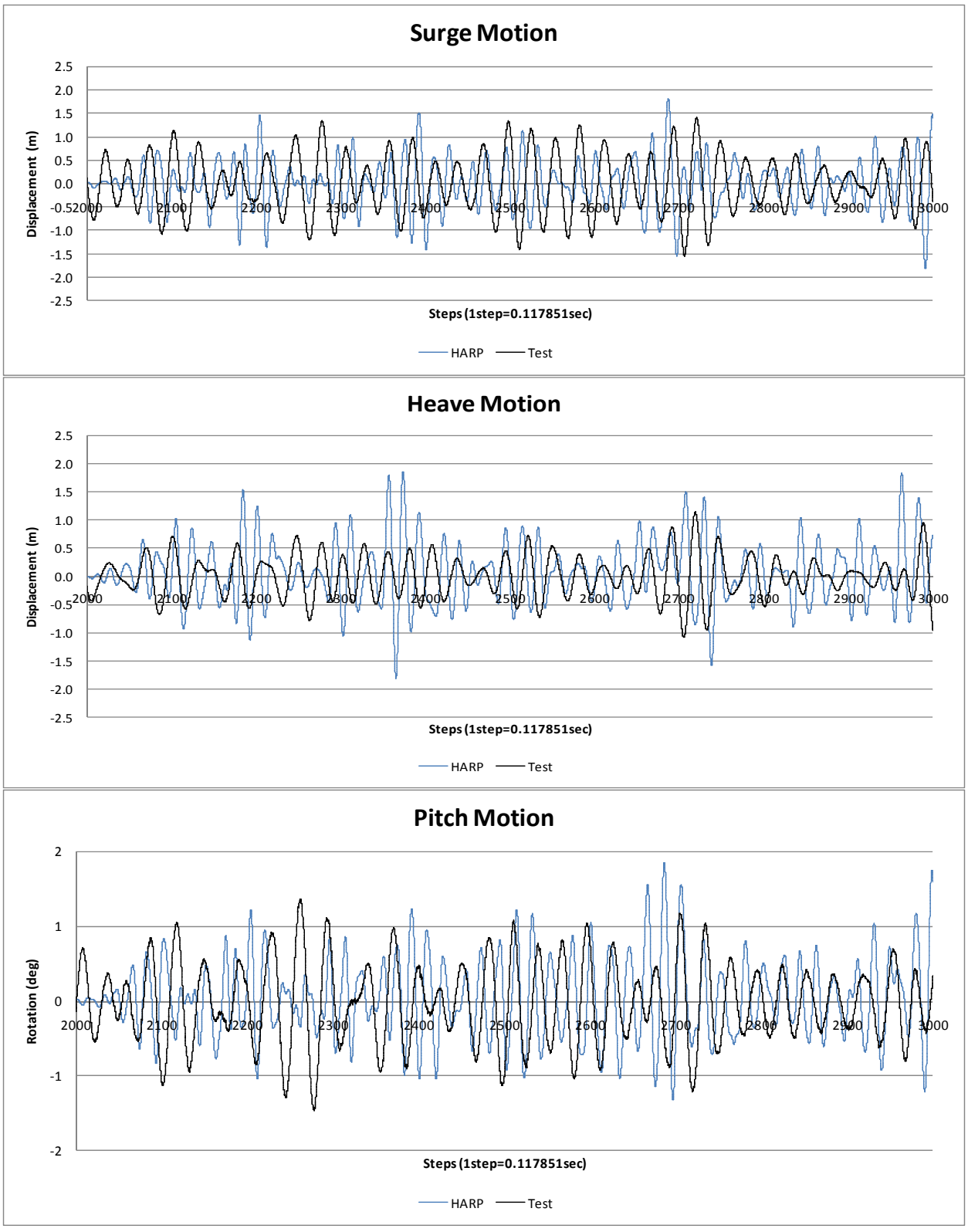

Figure 6.2-7 T300 Fatigue Wave Motions

Table 6.2-4 T300 Fatigue Calculated Motion Statistics

Summary of T300 Fatigue Wave					
	Surge (m)			Heave (m)	Pitch (deg)
	Original	Low-Freq	High-Freq	Original	Original
Mean	-0.10	0.00	0.00	0.07	0.04
Max	8.98	8.03	1.81	2.25	1.98
Min	-8.75	-8.10	-1.92	-1.92	-1.89
RMS	2.66	2.61	0.51	0.55	0.55
Tz (sec)	76.20	156.37	17.34	19.32	18.82

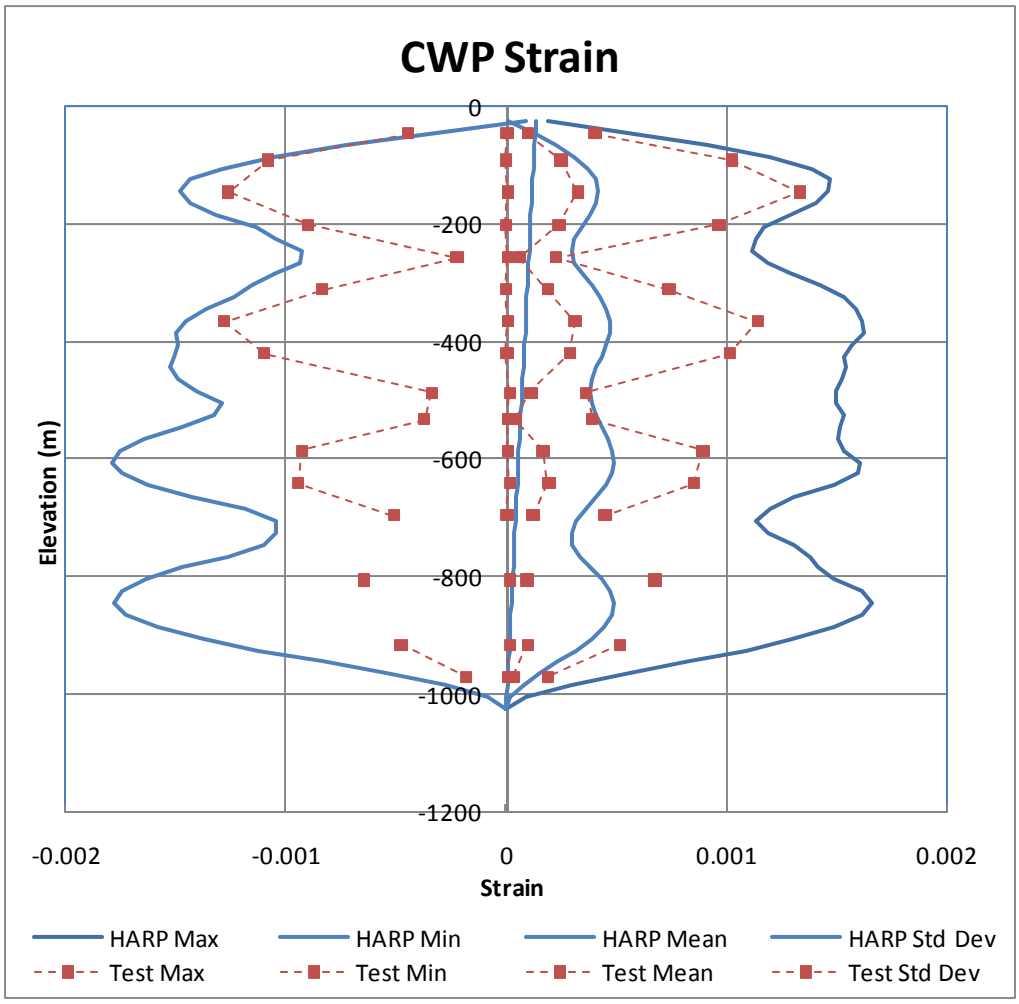

Figure 6.2-8 T300 Fatigue CWP Strain Envelope

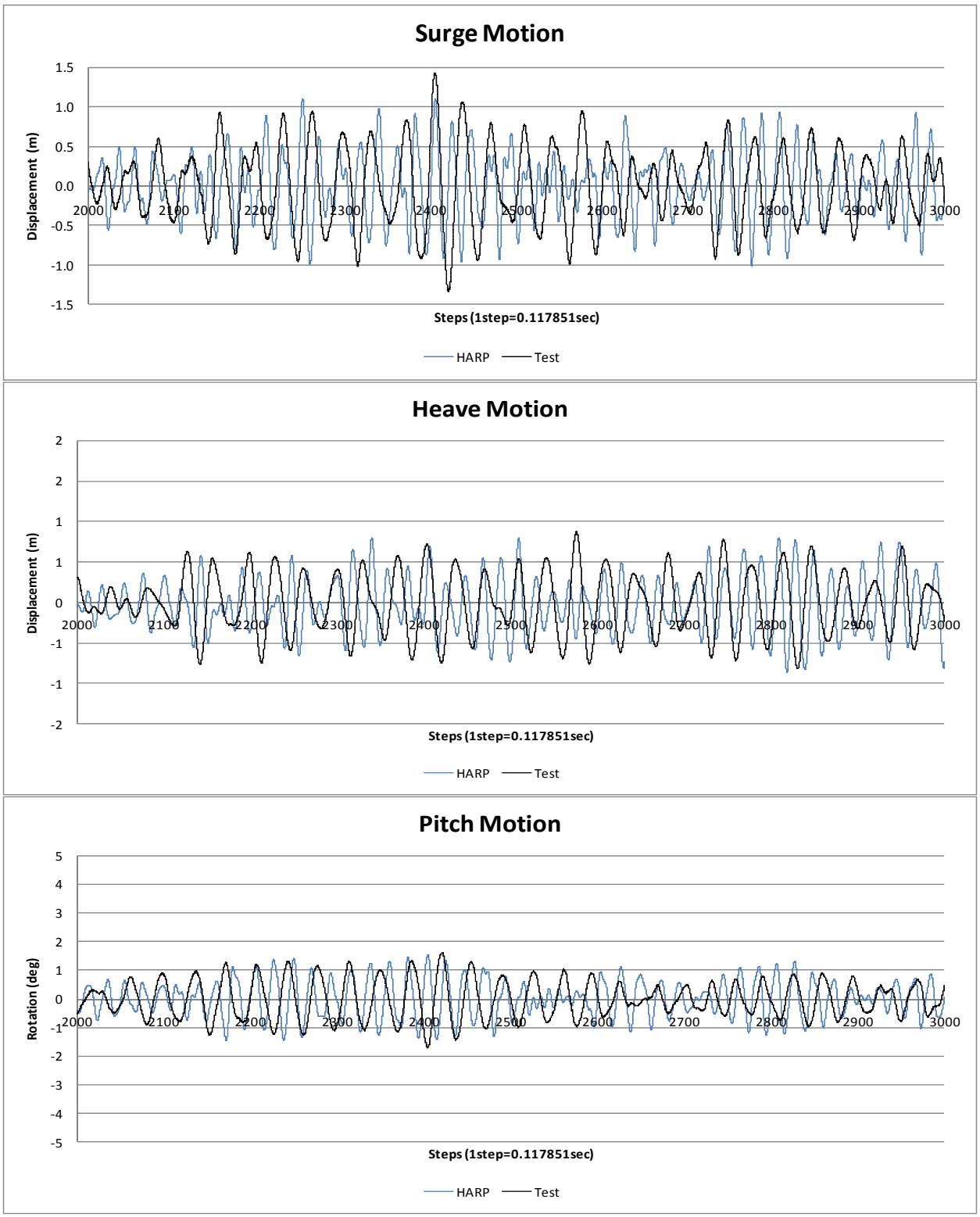

Figure 6.2-9 T300 WhiteNoise Wave Motions

Table 6.2-5 T300 WhiteNoise Calculated Motion Statistics

Summary of T300 WhiteNoise Wave					
	Surge (m)			Heave (m)	Pitch (deg)
	Original	Low-Freq	High-Freq	Original	Original
Mean	0.31	0.00	0.00	-0.02	0.02
Max	6.61	5.86	1.26	1.41	1.85
Min	-5.08	-5.26	-1.26	-1.16	-1.74
RMS	2.10	2.03	0.42	0.37	0.59
Tz (sec)	61.55	149.49	18.28	19.27	19.86

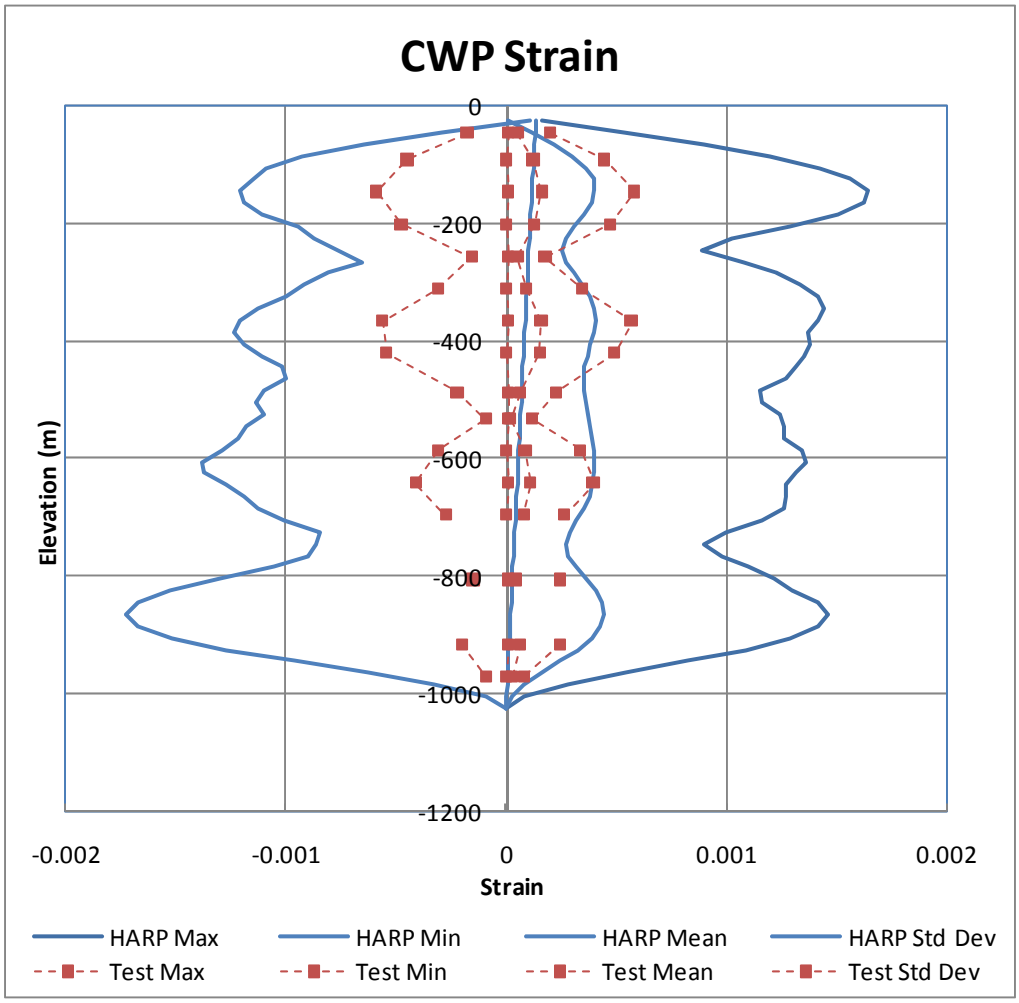

Figure 6.2-10 T300 WhiteNoise CWP Strain Envelope

7 T400 - OPERATIONAL B

7.1 T400 Free Decay Results Summary

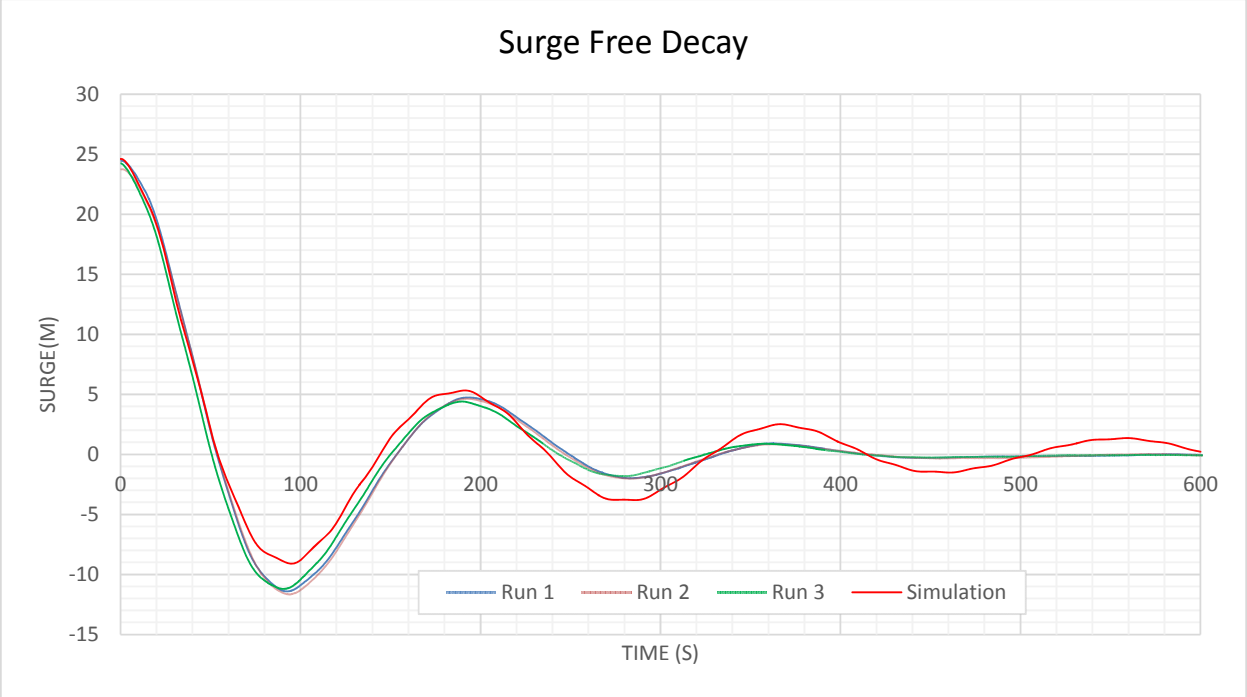

Figure 7.1-1 T400 Surge Free Decay Comparison

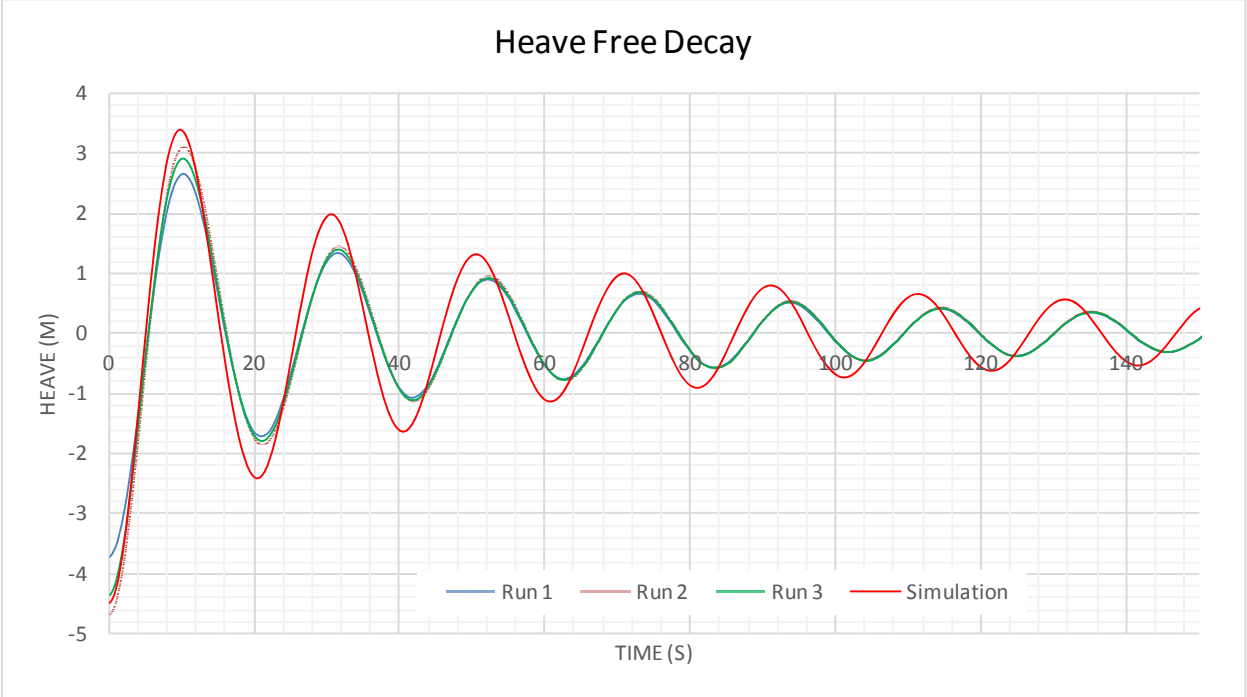

Figure 7.1-2 T400 Heave Free Decay Comparison

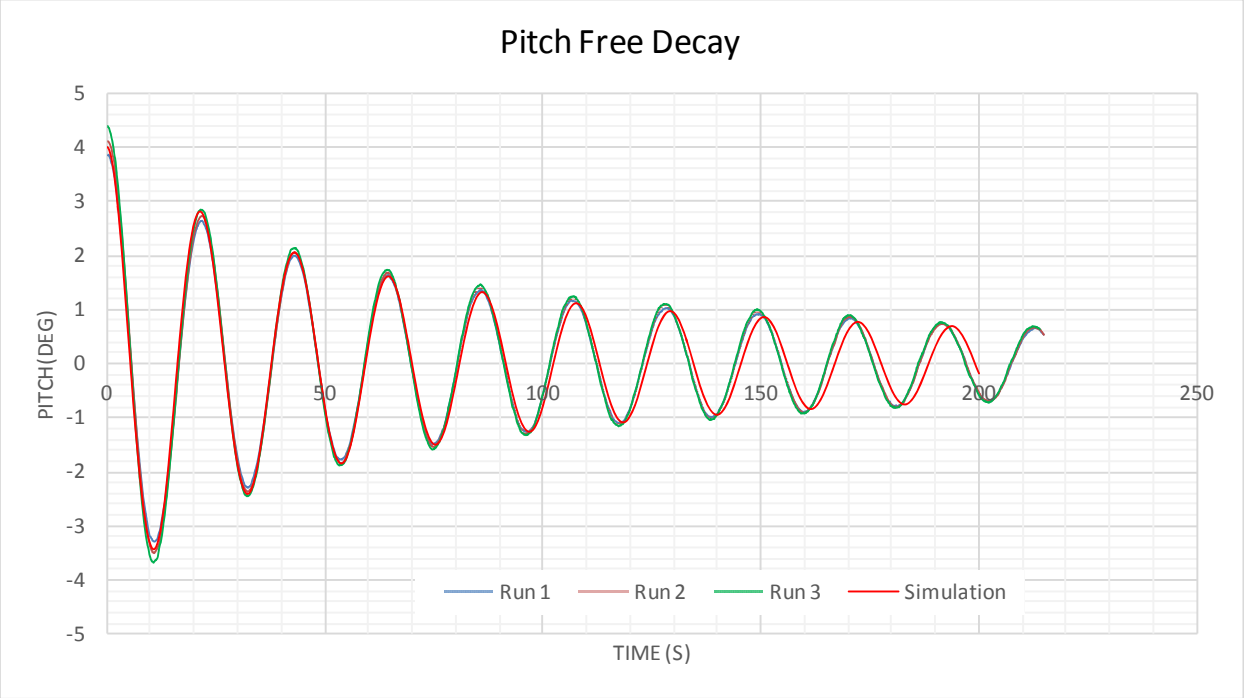

Figure 7.1-3 T400 Pitch Free Decay Comparison

7.2 T400 Random Wave Analysis

Table 7.2-1 T400 10yr Swell Calculated Motion Statistics

Summary of T400 10yr Swell Wave					
	Surge (m)			Heave (m)	Pitch (deg)
	Original	Low-Freq	High-Freq	Original	Original
Mean	-1.32	0.00	0.00	0.13	-0.04
Max	9.17	9.56	2.23	3.43	1.94
Min	-12.78	-9.80	-2.41	-2.62	-2.36
RMS	3.75	3.45	0.68	0.76	0.64
Tz (sec)	77.17	181.95	16.39	17.73	17.82

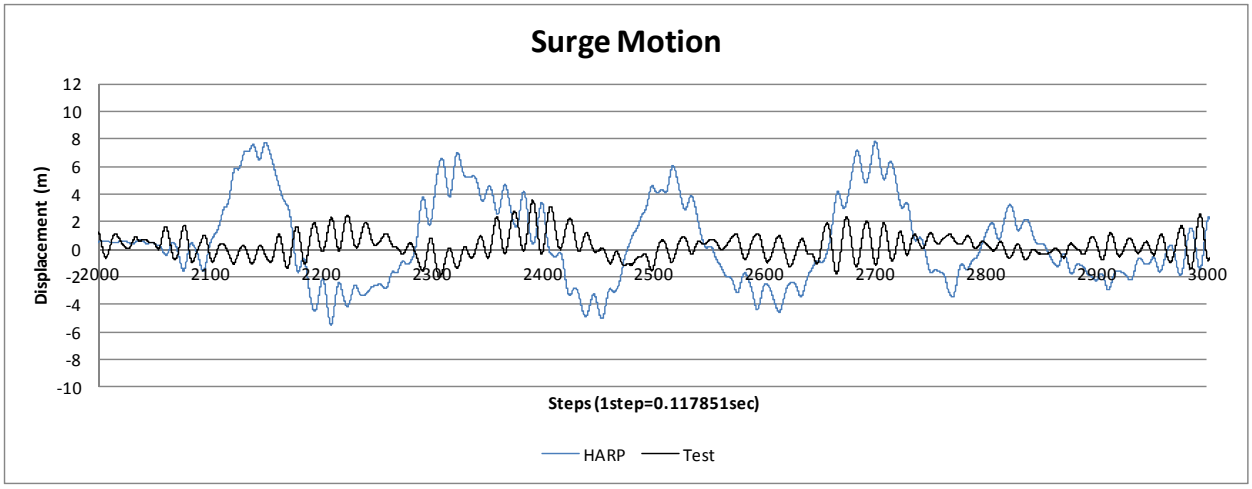

Figure 7.2-1 T400 10yr Swell Motions

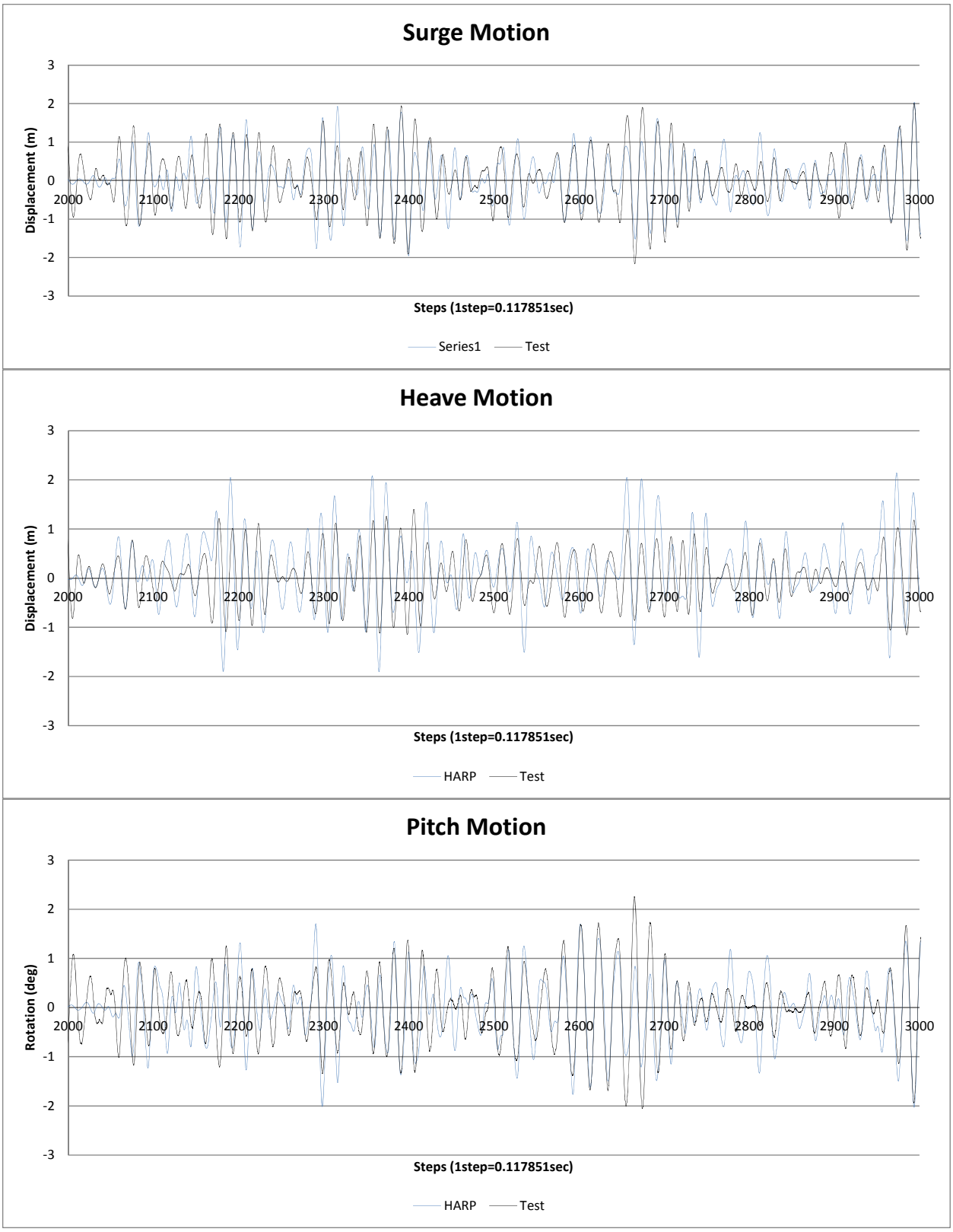

Figure 7.2-2 T400 10yr Swell Wave Motions

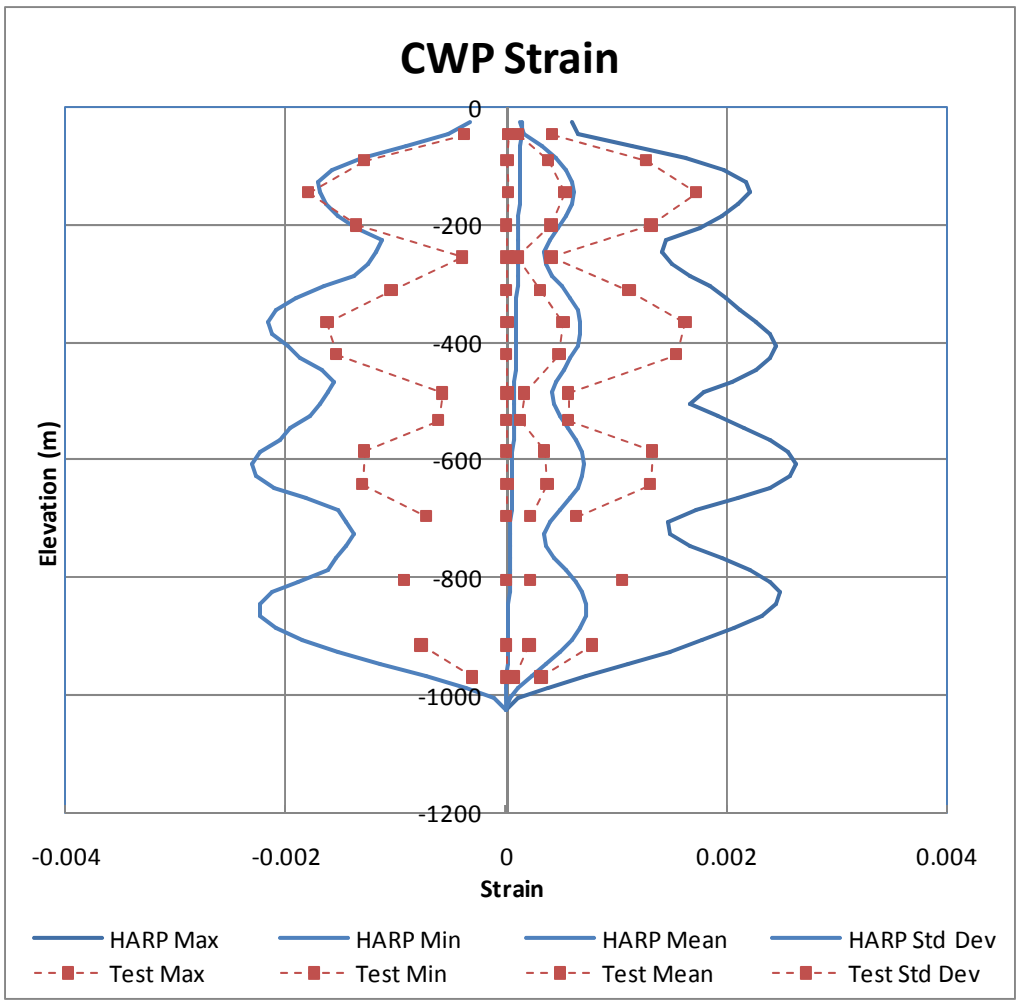

Figure 7.2-3 T400 10yr Swell CWP Strain Envelope

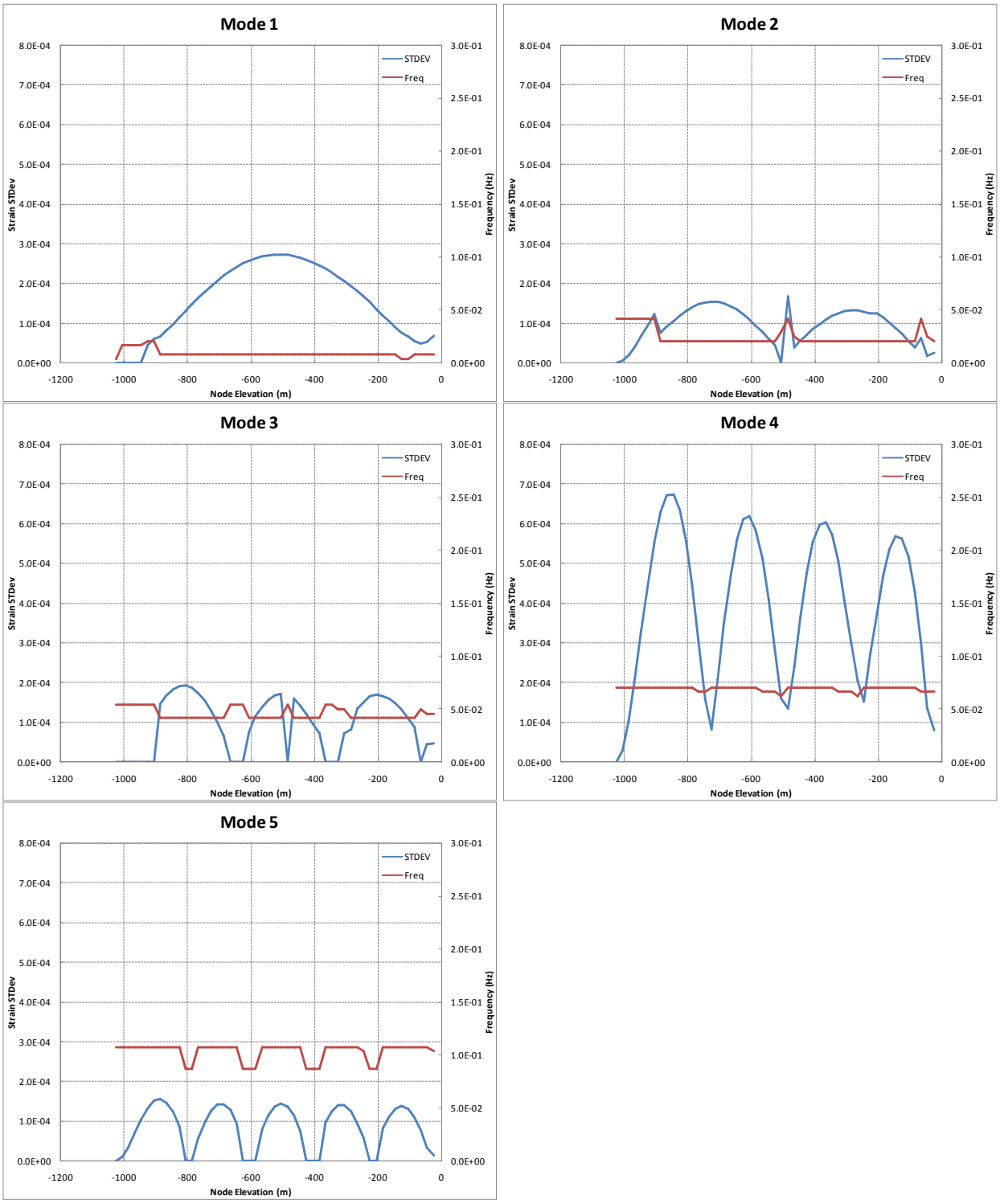

Figure 7.2-4 T400 10yr Swell Mode Shapes Using HARP

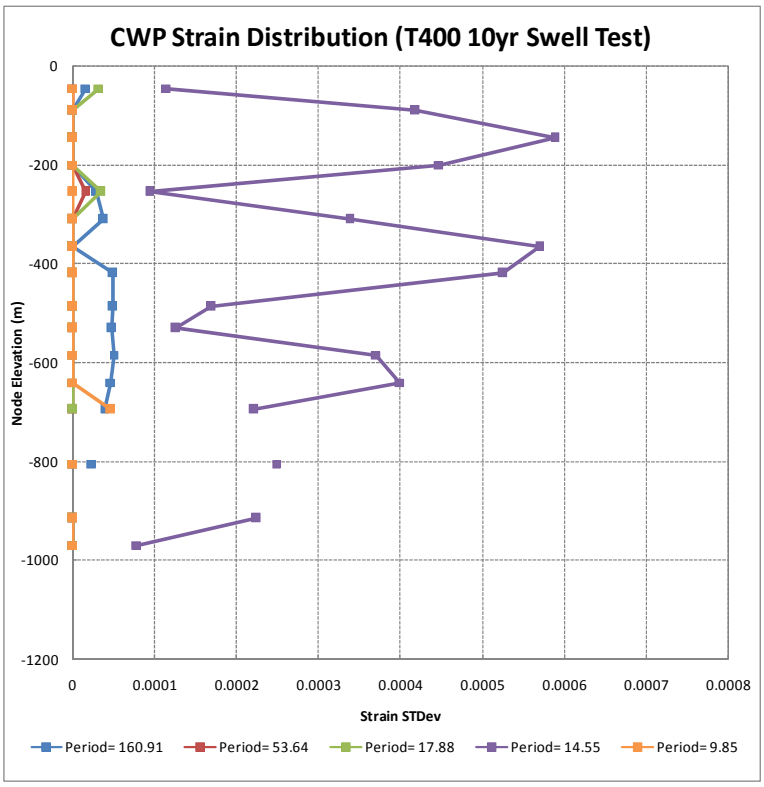

Figure 7.2-5 T400 10yr Swell Mode Shapes from TEST

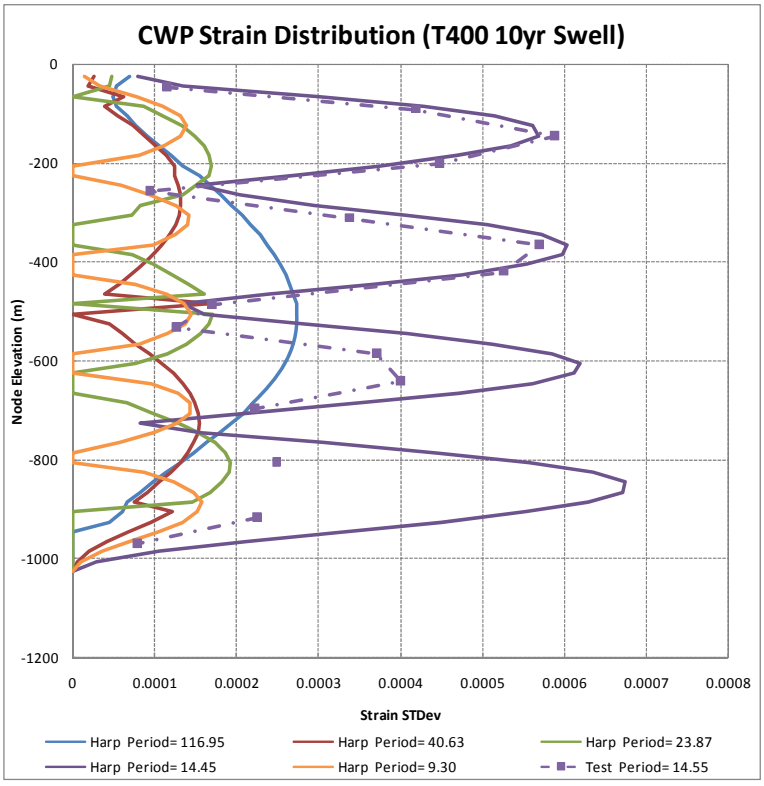

Figure 7.2-6 T400 10yr Swell Mode Shapes Comparison between HARP and TEST

Table 7.2-2 T400 10yr WindSea Calculated Motion Statistics

Summary of T400 10yr WindSea Wave					
	Surge (m)			Heave (m)	Pitch (deg)
	Original	Low-Freq	High-Freq	Original	Original
Mean	0.45	0.00	0.00	-0.02	-0.01
Max	8.34	7.72	1.59	0.82	2.82
Min	-7.72	-7.58	-1.91	-0.81	-2.74
RMS	2.43	2.36	0.39	0.18	0.55
Tz (sec)	69.88	160.23	13.19	18.92	16.37

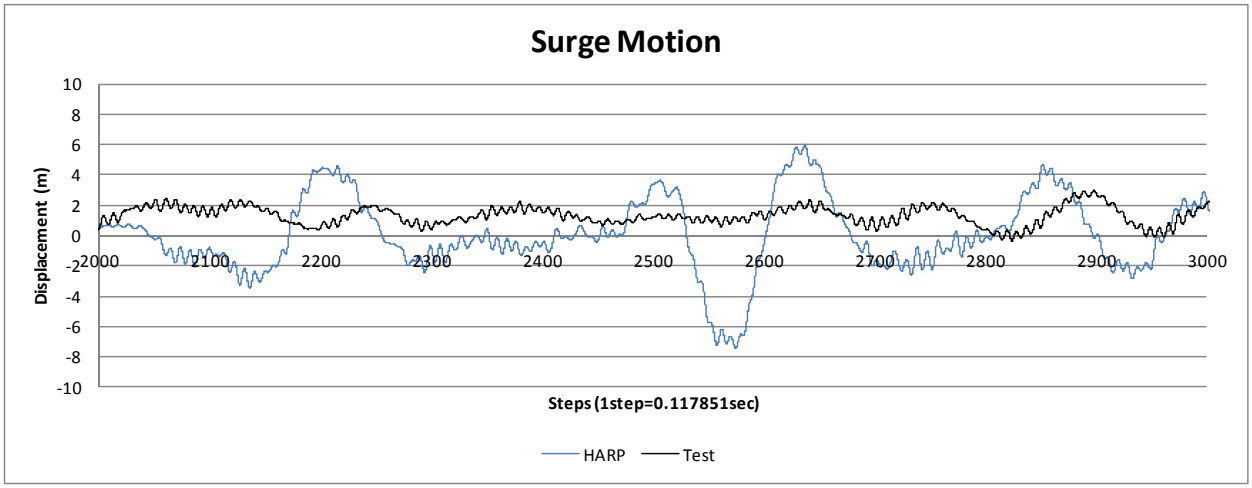

Figure 7.2-7 T400 10yr WindSea Motions

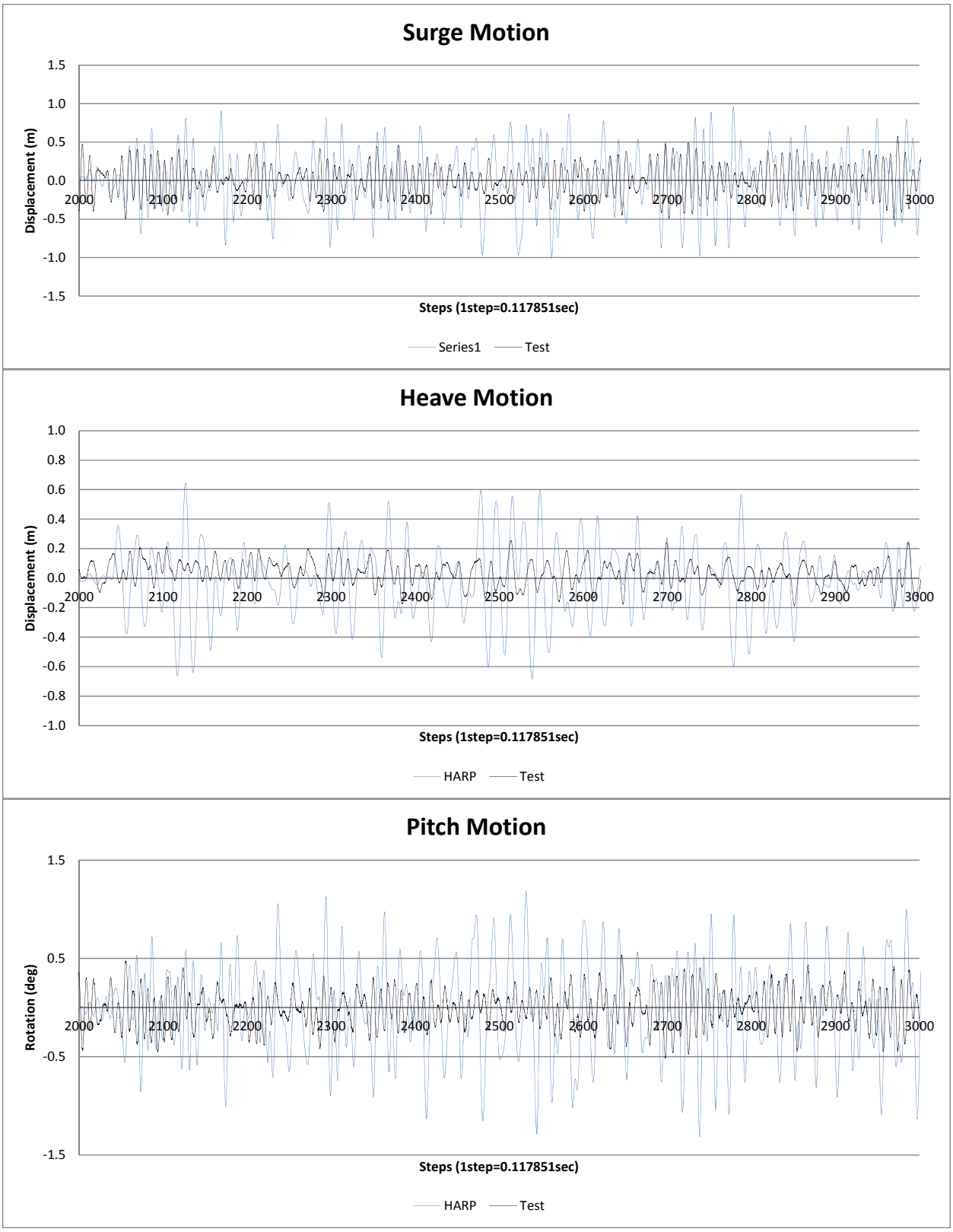

Figure 7.2-8 T400 10yr WindSea Wave Motions

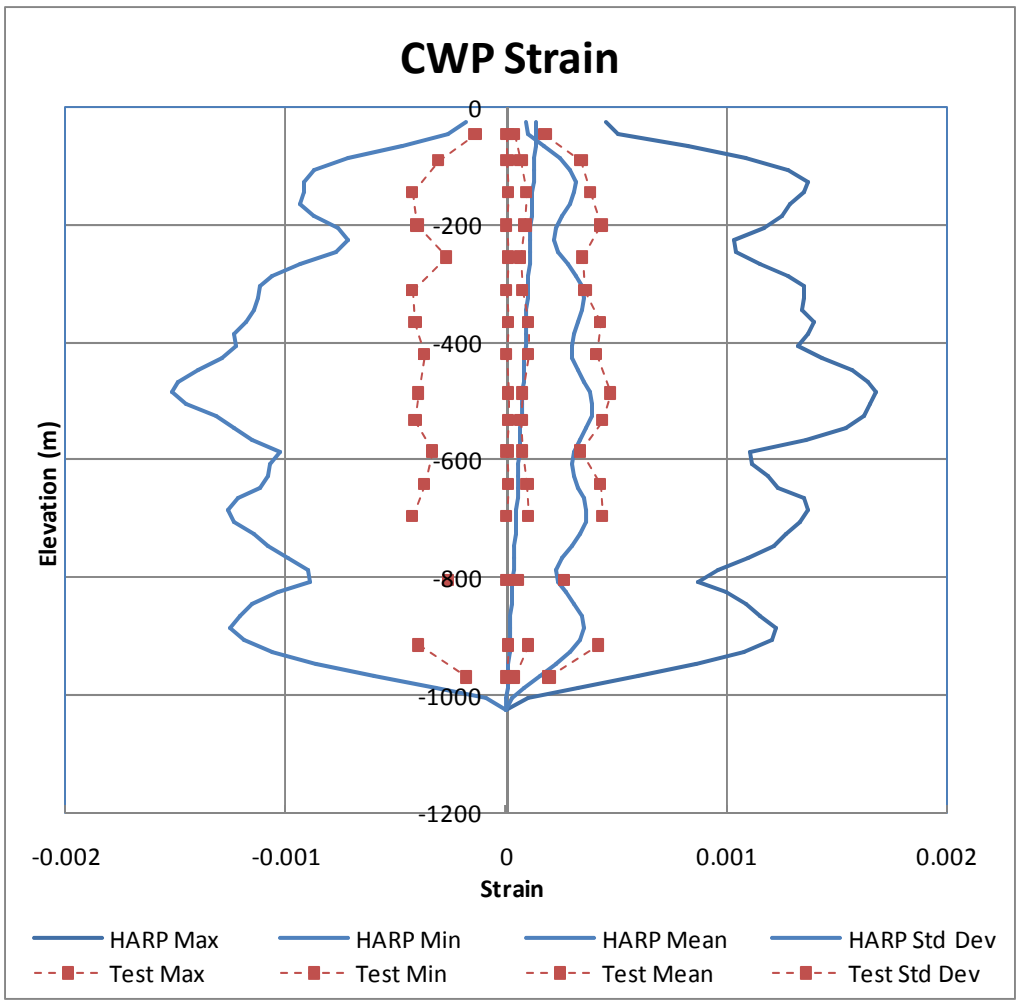

Figure 7.2-9 T400 10yr WindSea CWP Strain Envelope

Table 7.2-3 T400 100yr Cyclone Calculated Motion Statistics

Summary of T400 100yr Cyclone Wave					
	Surge (m)			Heave (m)	Pitch (deg)
	Original	Low-Freq	High-Freq	Original	Original
Mean	1.17	0.00	0.00	0.16	0.08
Max	22.81	21.18	4.62	5.64	5.43
Min	-20.84	-20.87	-4.78	-3.78	-5.95
RMS	6.94	6.73	1.23	1.22	1.19
Tz (sec)	77.08	170.77	14.43	16.34	15.20

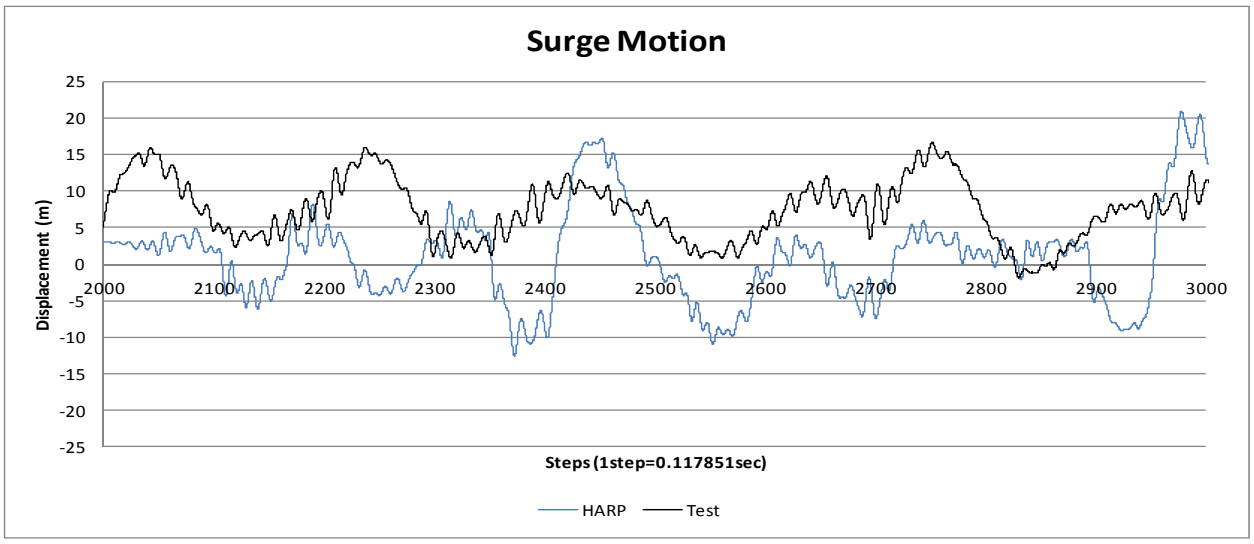

Figure 7.2-10 T400 100yr Cyclone Motions

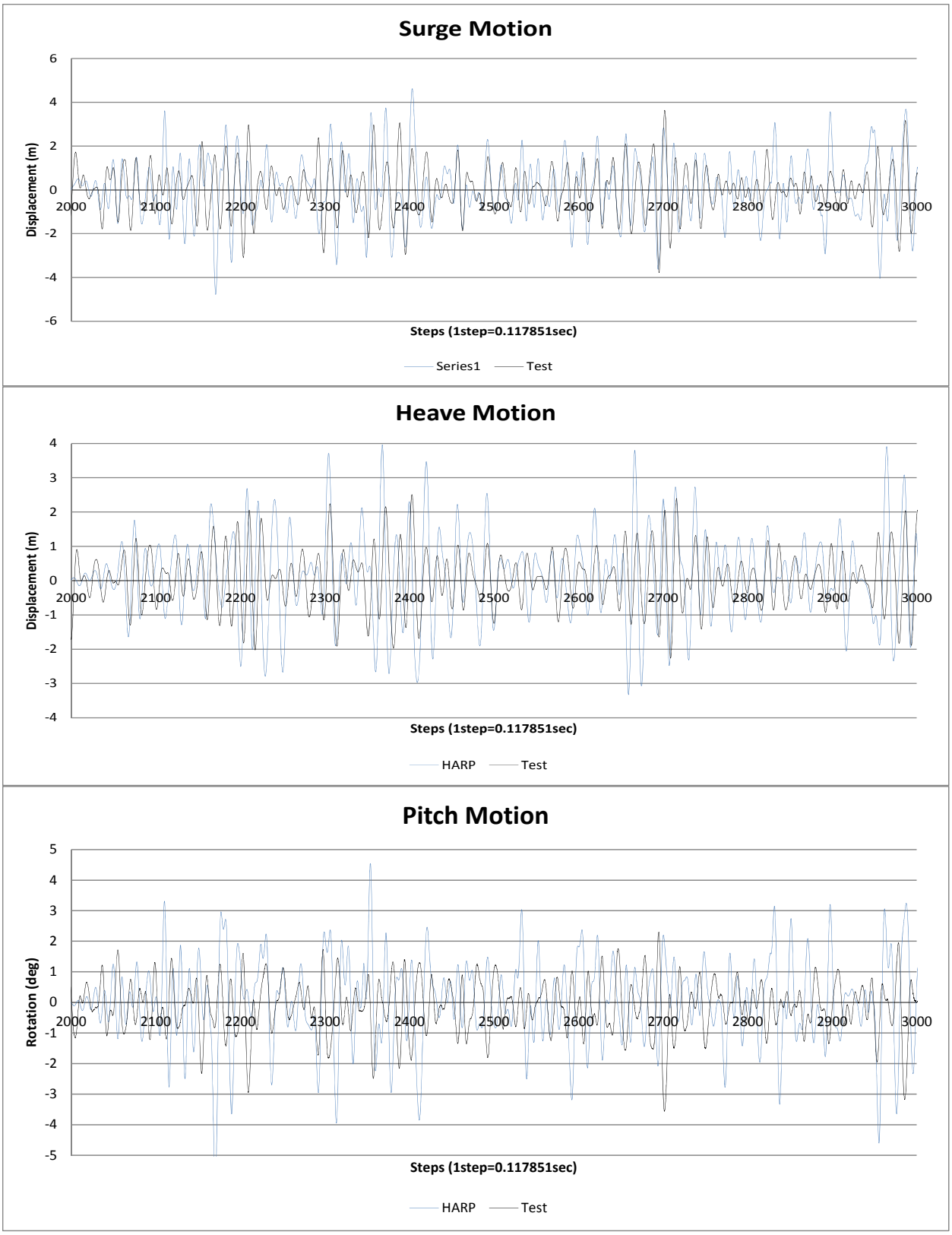

Figure 7.2-11 400 100yr Cyclone Wave Motions

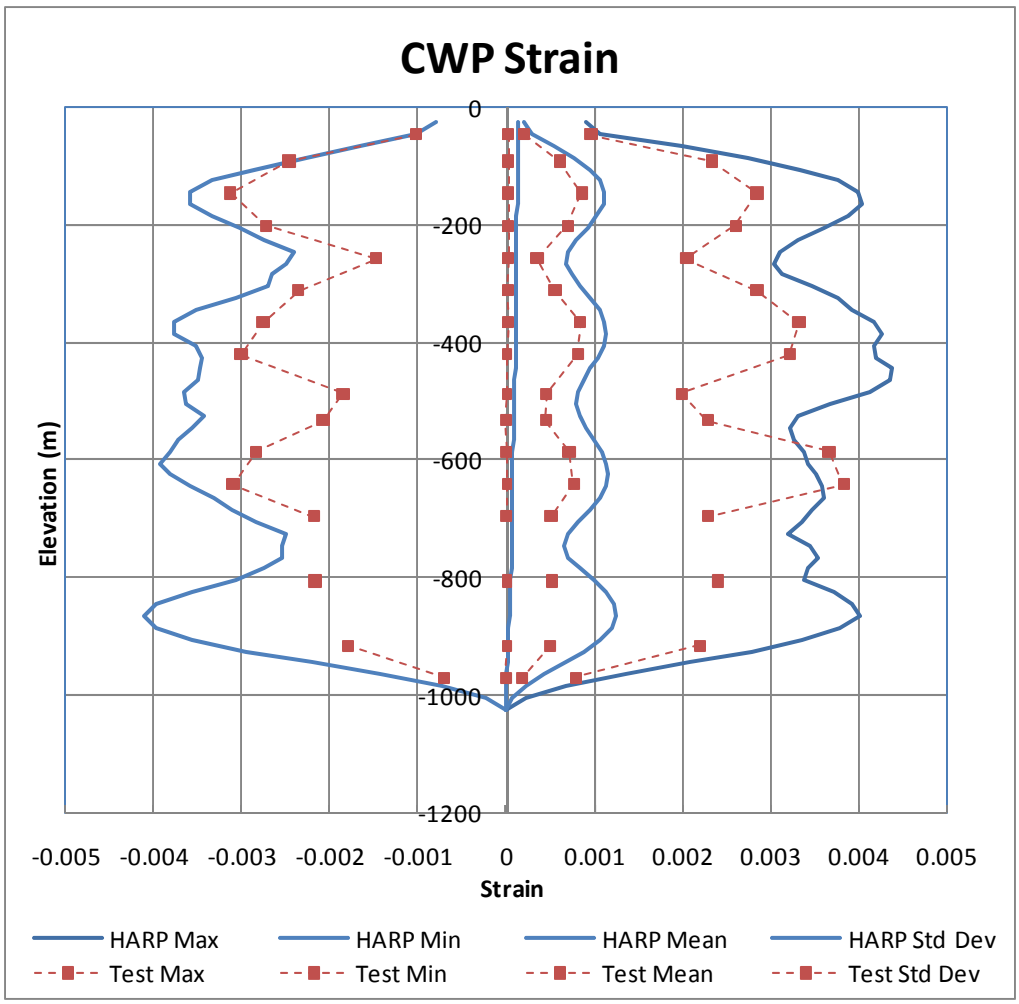

Figure 7.2-12 T400 100yr Cyclone CWP Strain Envelope

T400 100yr Cyclone

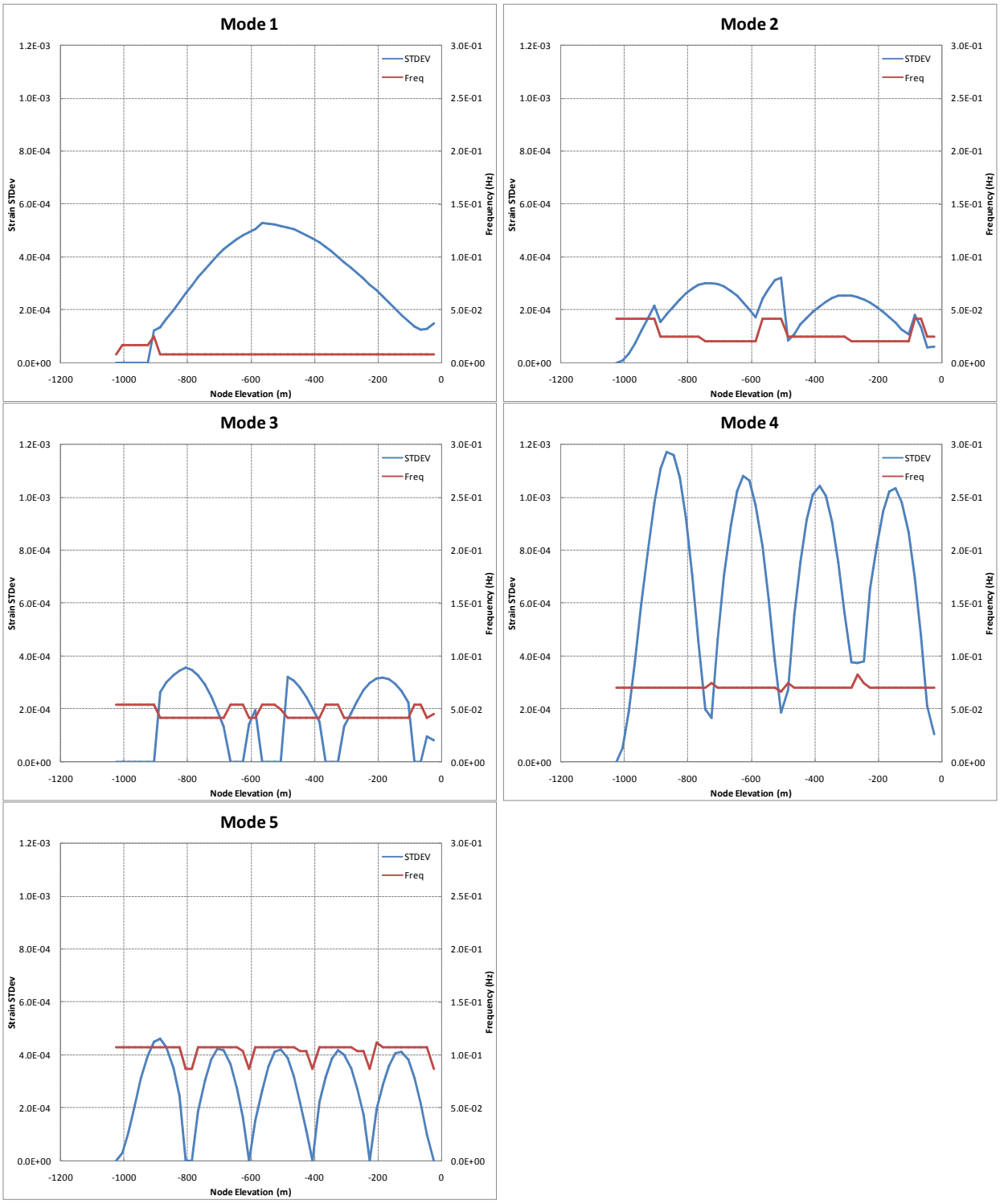

Figure 7.2-13 T400 100yr Cyclone Mode Shapes Using HARP

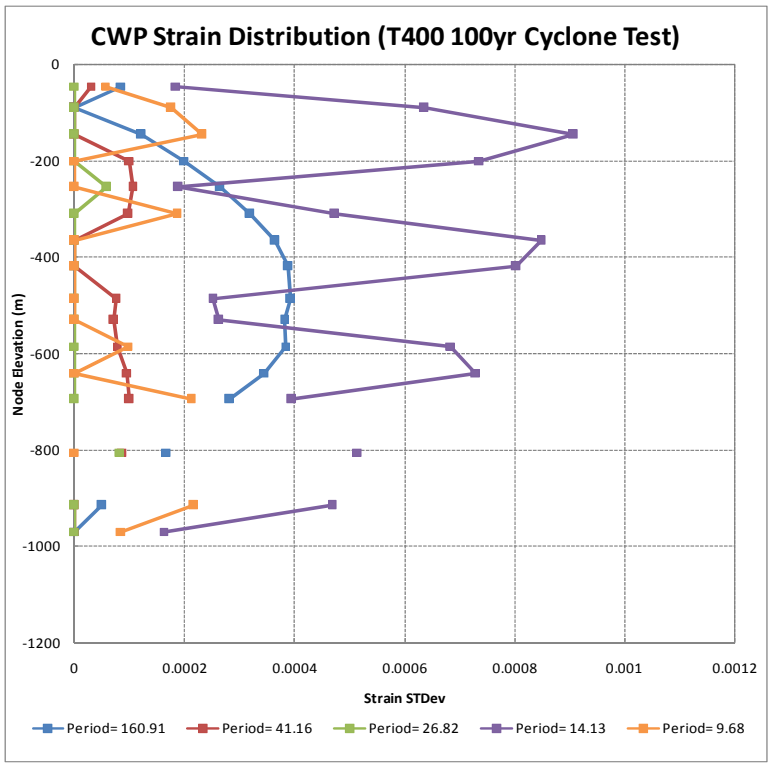

Figure 7.2-14 T400 100yr Cyclone Mode Shapes from TEST

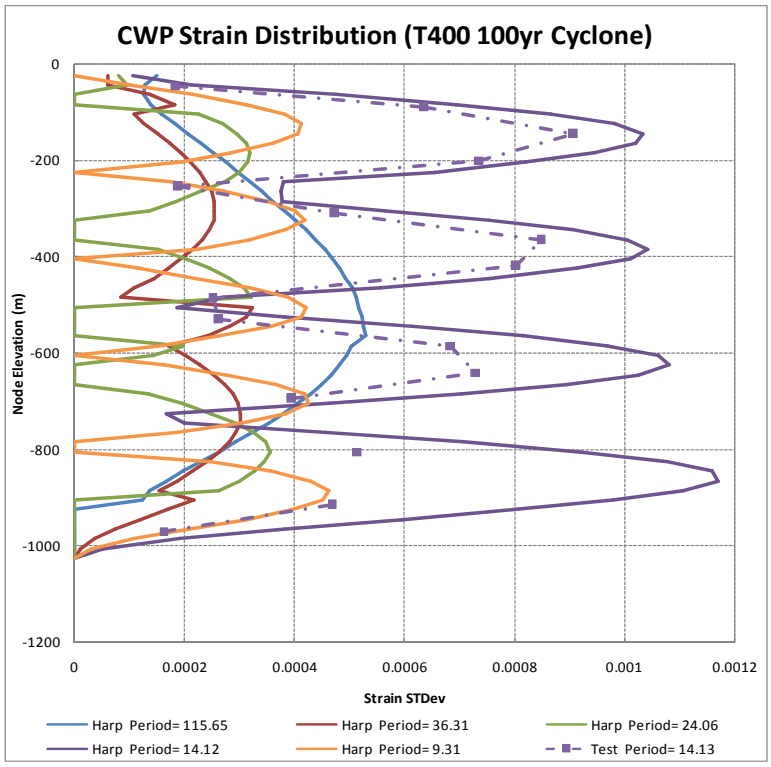

Figure 7.2-15 T400 100yr Cyclone Mode Shapes Comparison between HARP and TEST

Table 7.2-4 T400 Fatigue Calculated Motion Statistics

Summary of T400 Fatigue Wave					
	Surge (m)			Heave (m)	Pitch (deg)
	Original	Low-Freq	High-Freq	Original	Original
Mean	-0.11	0.00	0.00	0.07	-0.04
Max	8.82	7.91	1.78	2.24	1.94
Min	-8.59	-7.99	-1.92	-1.92	-1.88
RMS	2.64	2.58	0.51	0.55	0.54
Tz (sec)	75.11	156.38	17.37	19.39	18.83

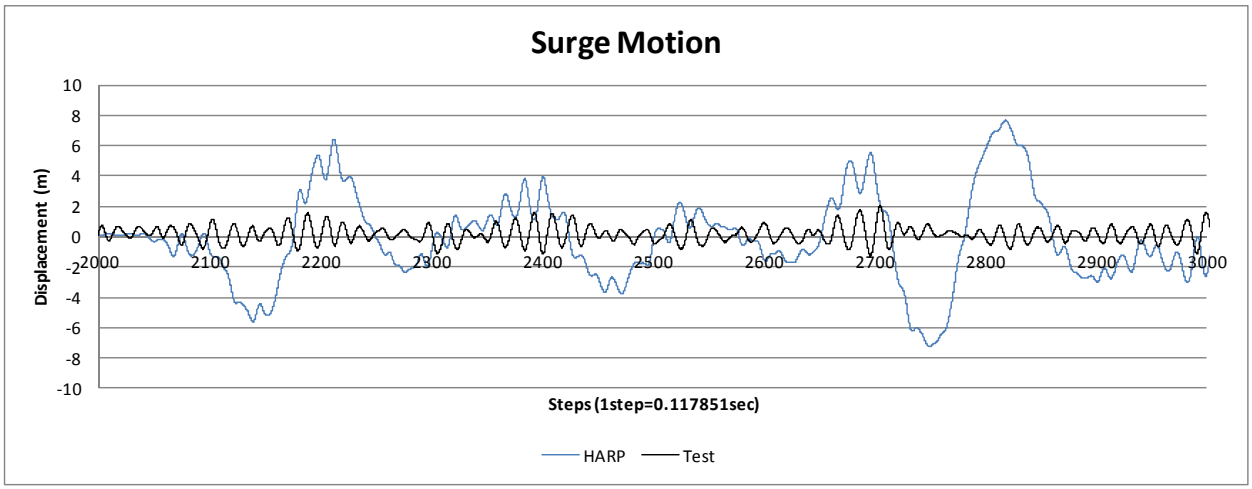

Figure 7.2-16 T400 Fatigue Motions

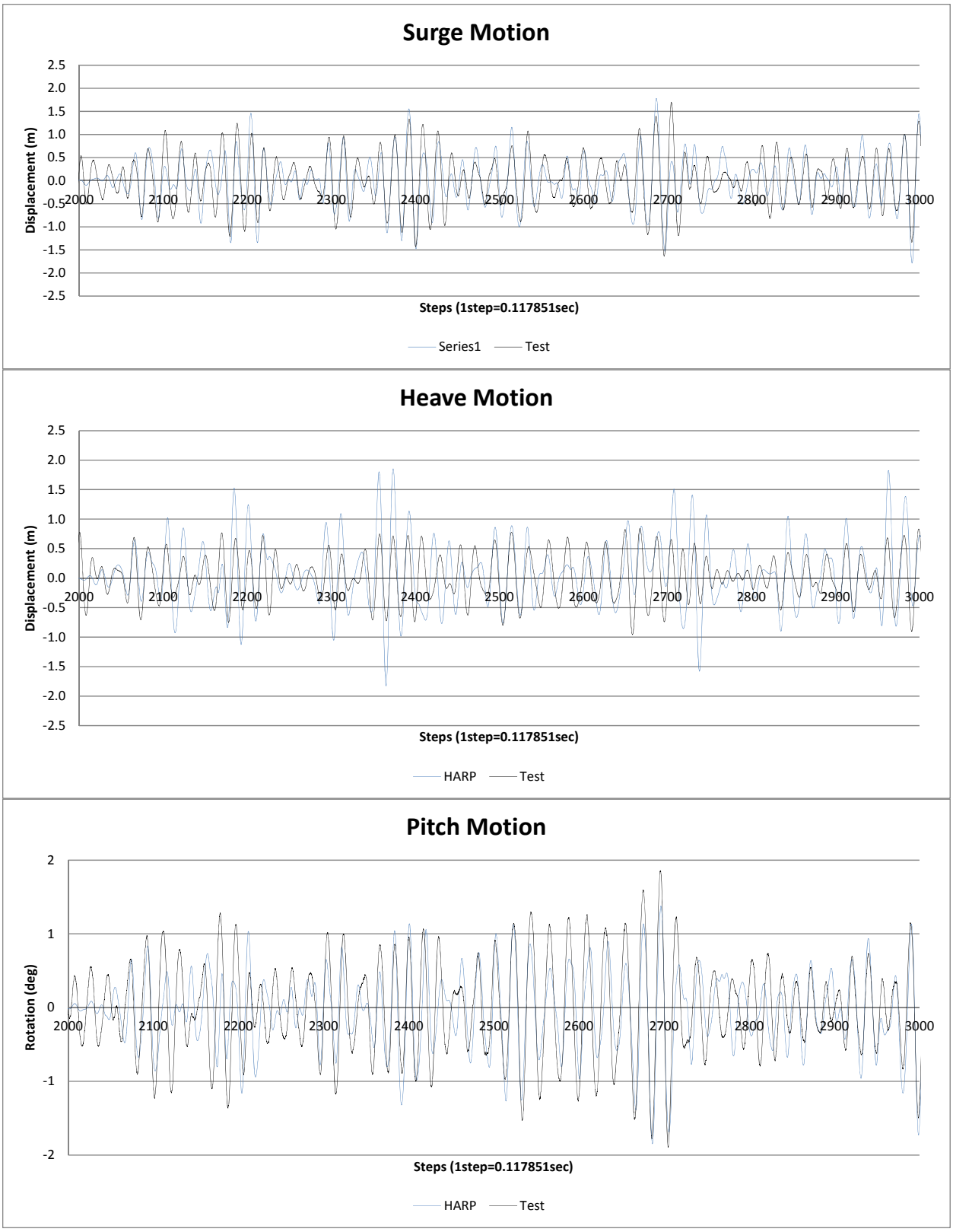

Figure 7.2-17 T400 Fatigue Wave Motions

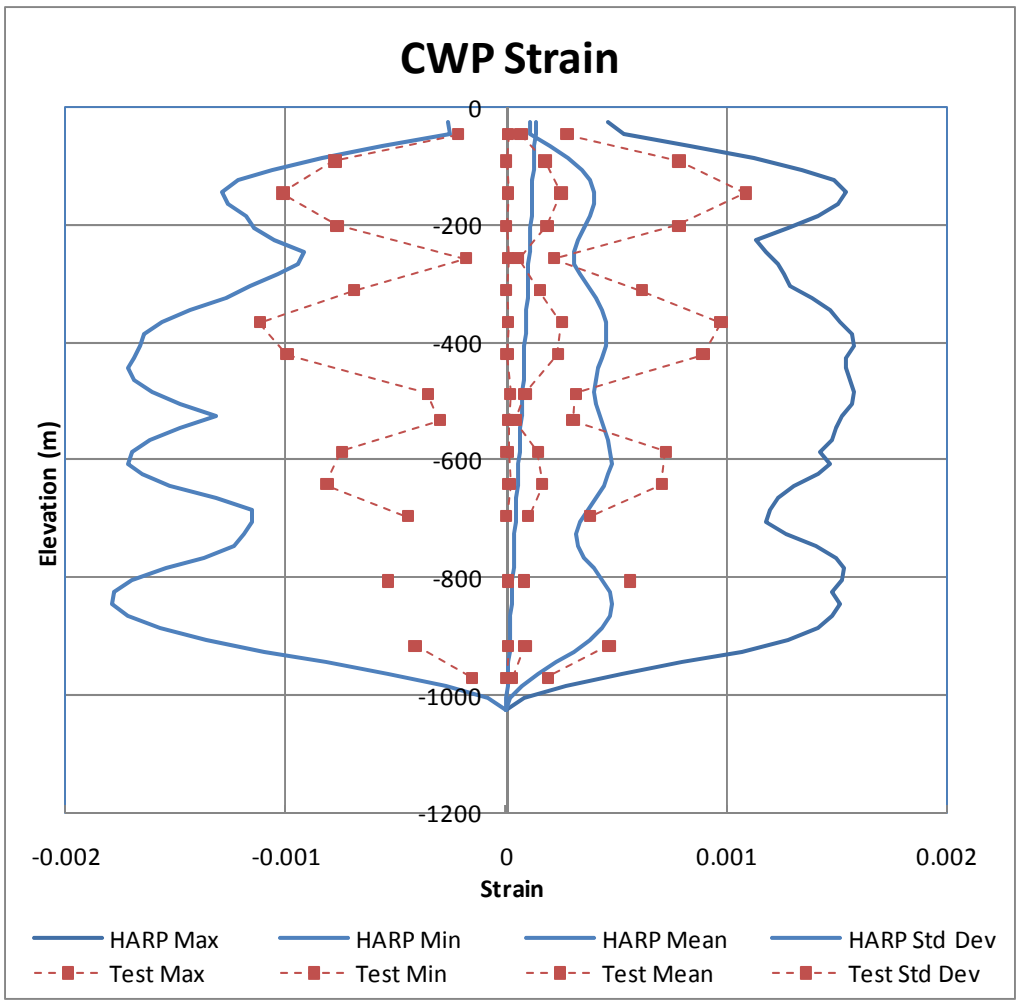

Figure 7.2-18 T400 Fatigue CWP Strain Envelope

Table 7.2-5 T400 WhiteNoise Calculated Motion Statistics

Summary of T400 WhiteNoise Wave					
	Surge (m)			Heave (m)	Pitch (deg)
	Original	Low-Freq	High-Freq	Original	Original
Mean	0.30	0.00	0.00	-0.01	-0.01
Max	6.47	5.79	1.25	3.58	45.99
Min	-54.19	-5.13	-53.65	-1.16	-1.72
RMS	2.11	2.03	0.52	0.37	0.64
Tz (sec)	66.79	165.26	18.57	19.39	19.90

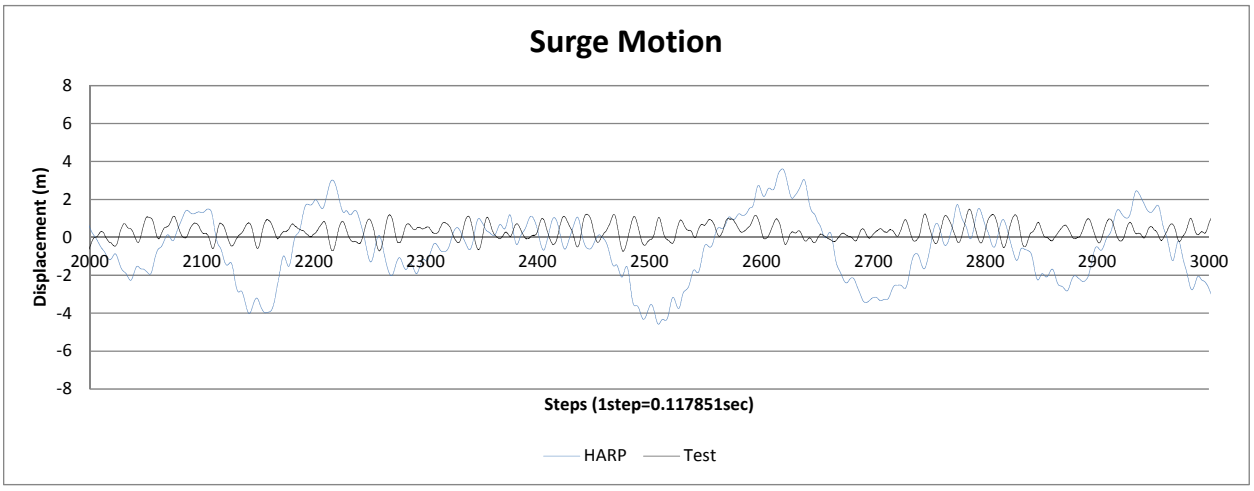

Figure 7.2-19 T400 WhiteNoise Motions

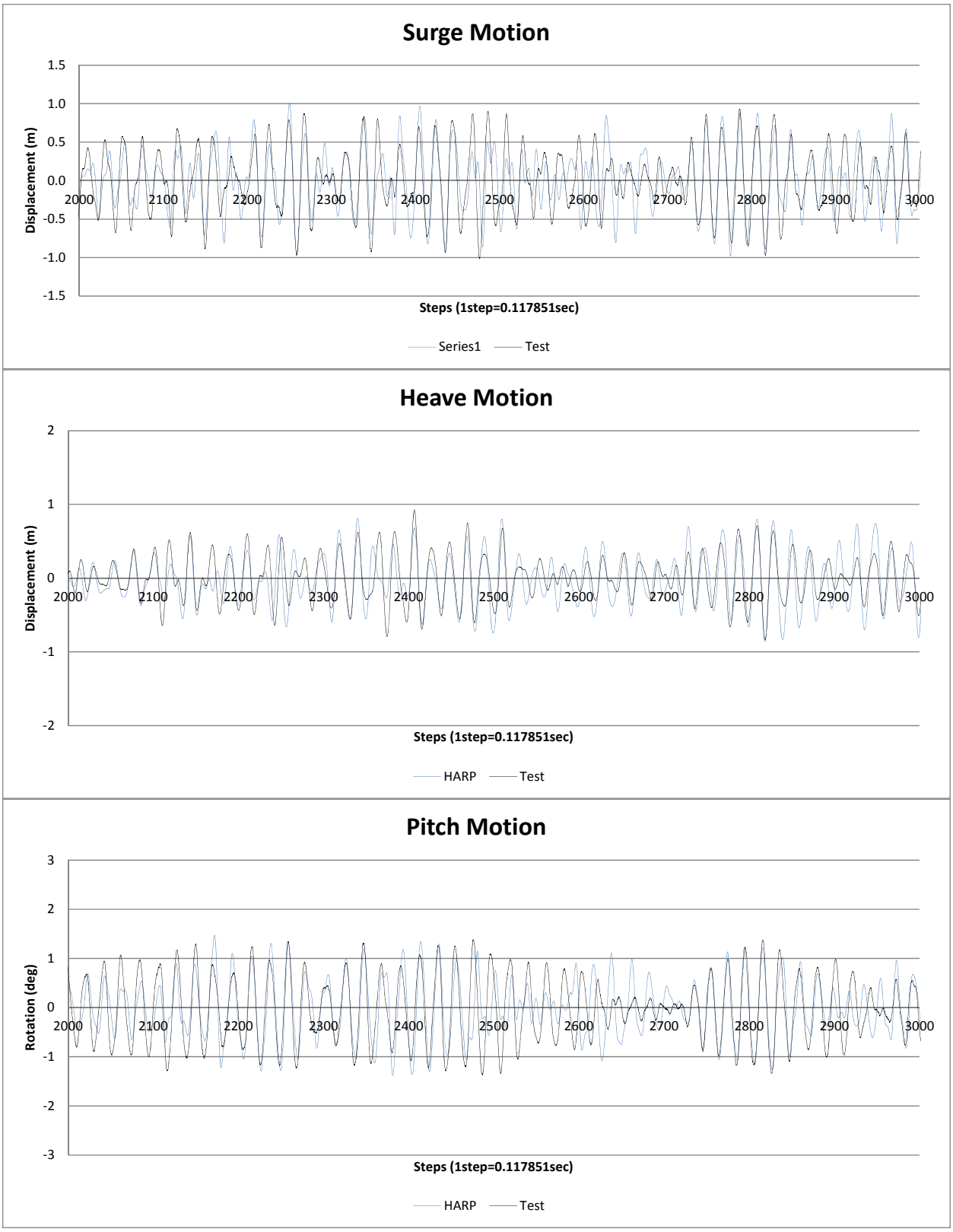

Figure 7.2-20 T400 WhiteNoise Wave Motions

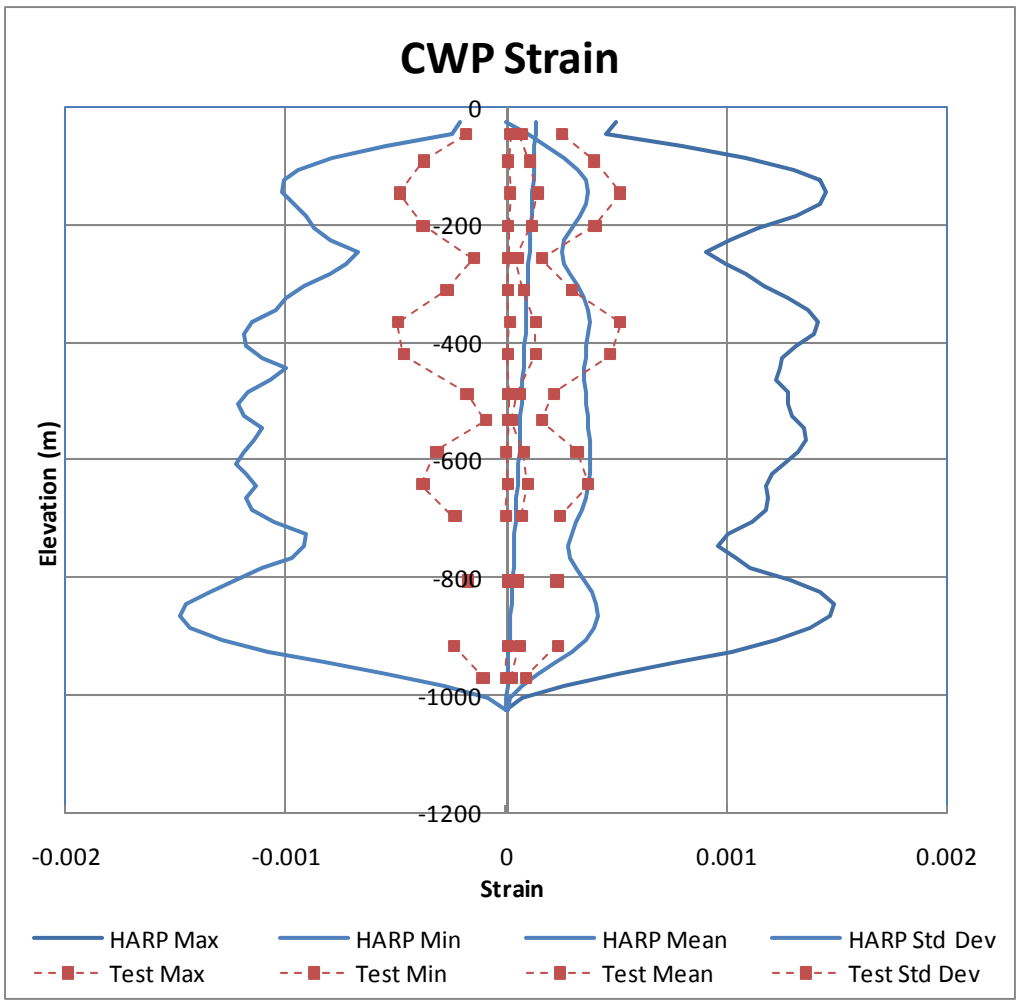

Figure 7.2-21 T400 WhiteNoise CWP Strain Envelope

8 T500 - CWP INSTALLATION 1

8.1 T500 Random Wave Analysis

Table 8.1-1 T500 10yr Swell Calculated Motion Statistics

Summary of T500 10yr Swell Wave					
	Surge (m)			Heave (m)	Pitch (deg)
	Original	Low-Freq	High-Freq	Original	Original
Mean	-1.26	0.00	0.00	0.14	0.04
Max	12.23	12.31	2.98	4.10	3.35
Min	-15.35	-12.76	-3.38	-3.64	-3.58
RMS	4.36	4.10	0.81	0.95	1.01
Tz (sec)	79.63	172.72	16.19	18.62	17.76

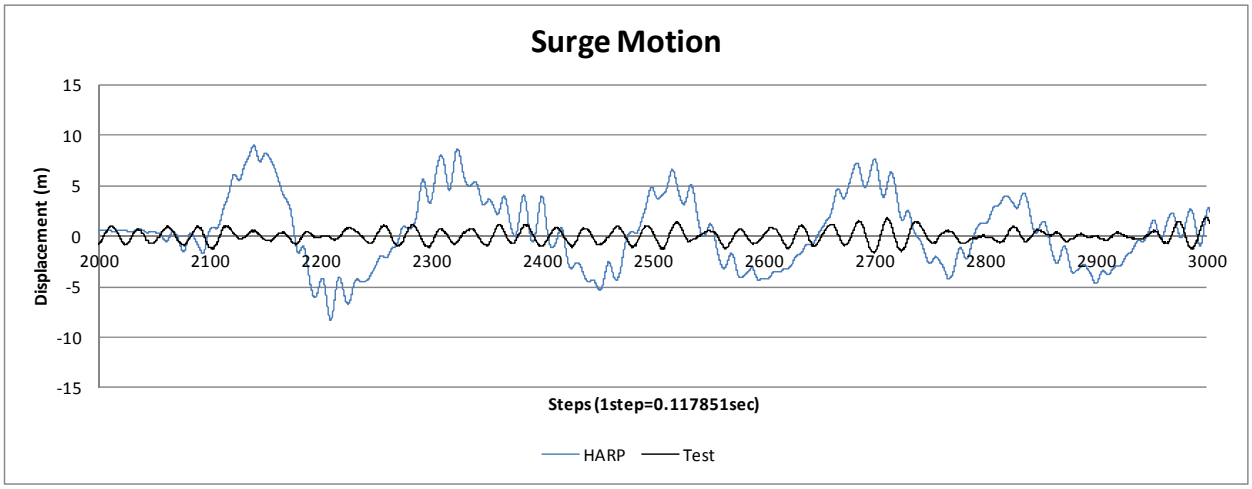

Figure 8.1-1 T500 10yr Swell Motions

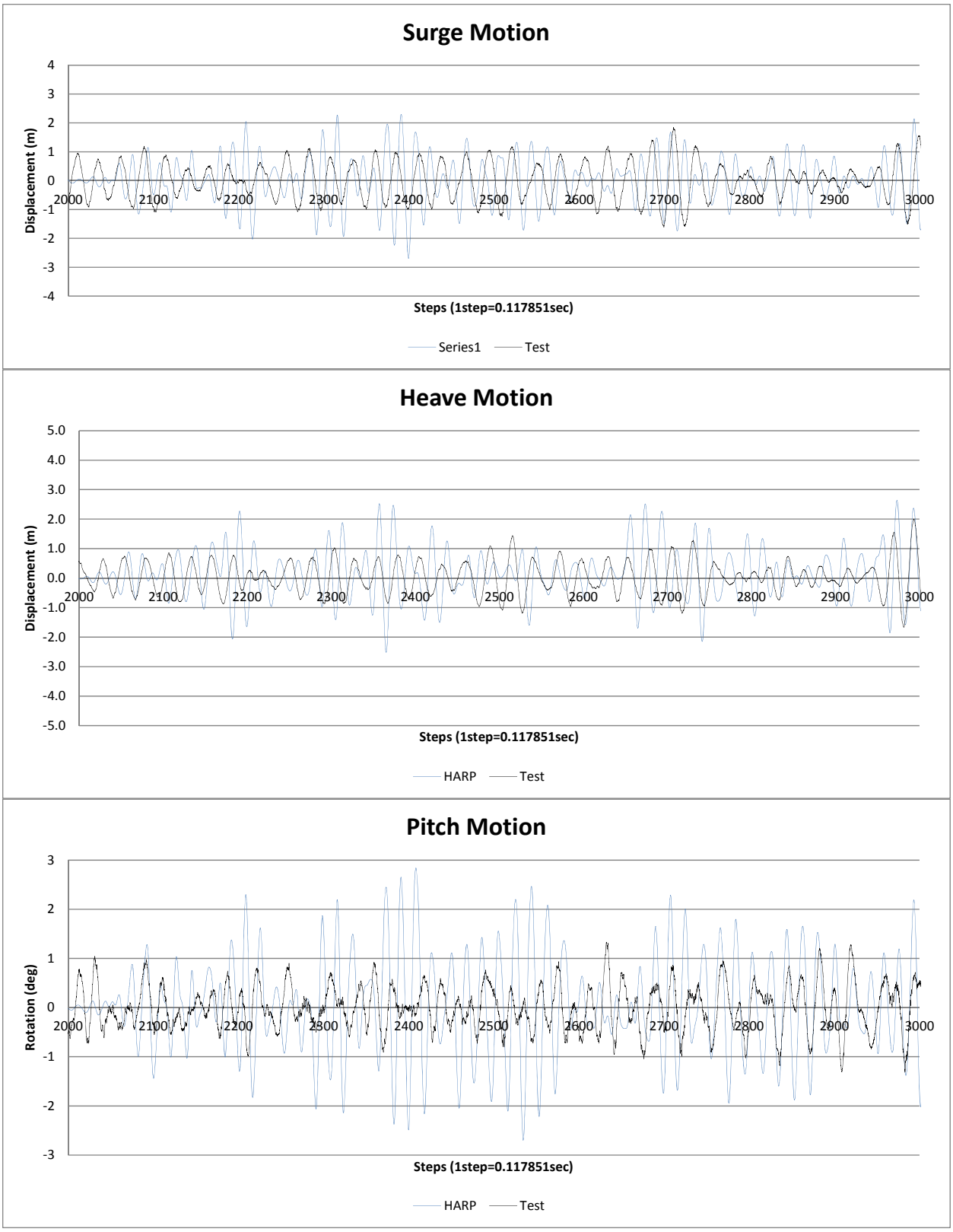

Figure 8.1-2 T500 10yr Swell Wave Motions

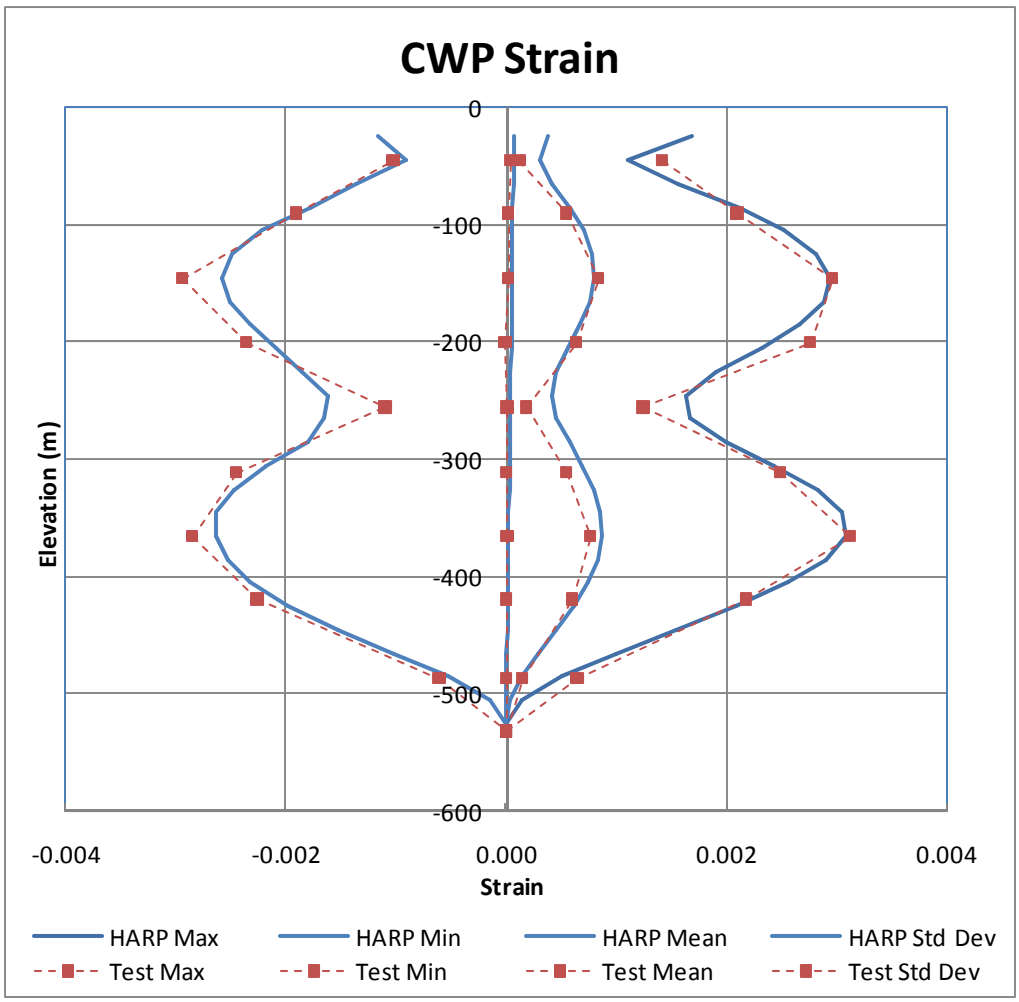

Figure 8.1-3 T500 10yr Swell CWP Strain Envelope
[Gimbal Stiffness = 3.15E+09, 3.3% Installation Stiffness, 2.5x Operation Stiffness]

T500 10yr Swell

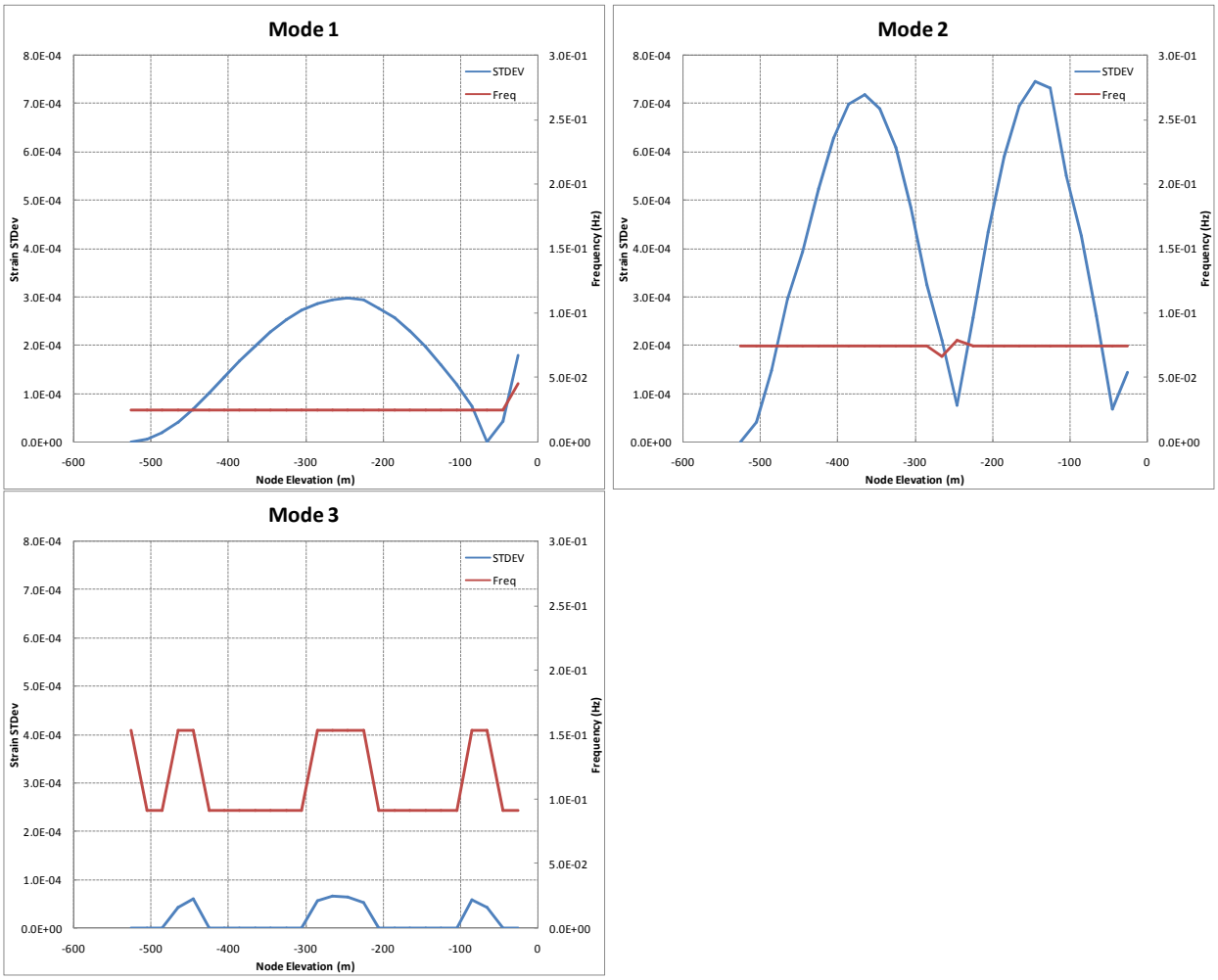

Figure 8.1-4 T500 10yr Swell Mode Shapes Using HARP

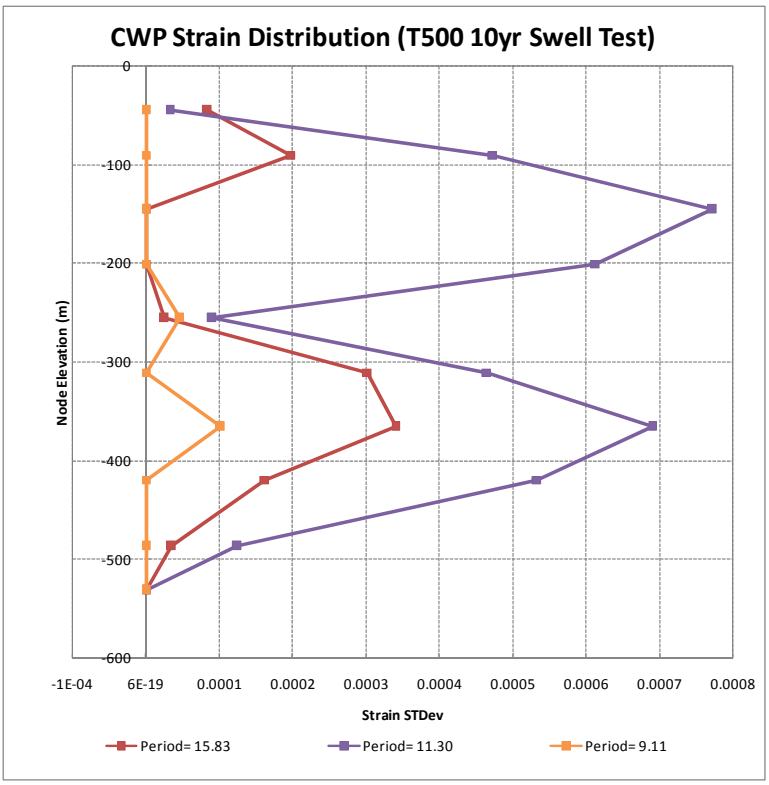

Figure 8.1-5 T500 10yr Swell Mode Shapes from TEST

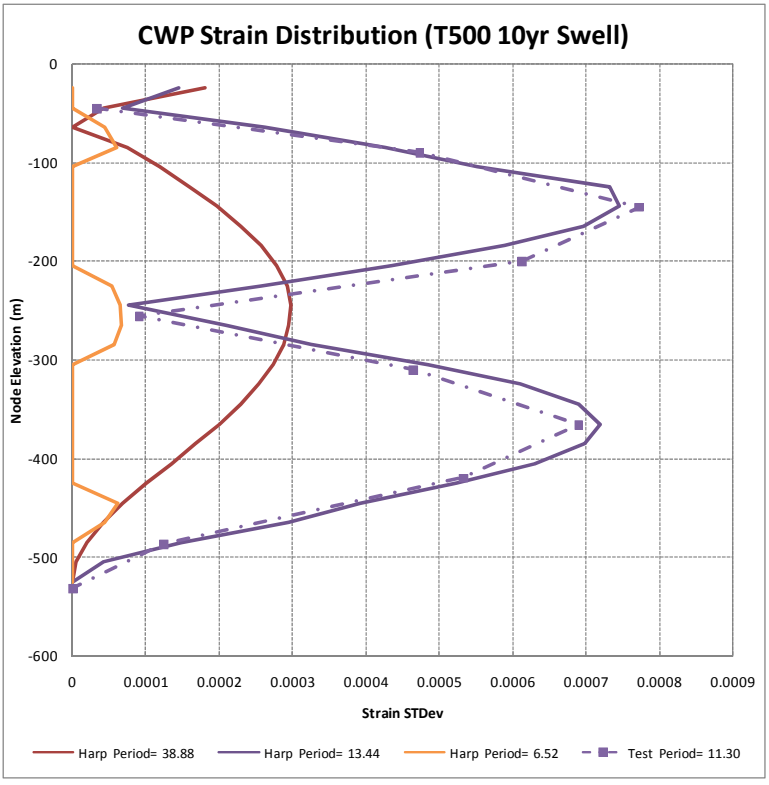

Figure 8.1-6 T500 10yr Swell Mode Shapes Comparison between HARP and TEST

Table 8.1-2 T500 10yr WindSea Calculated Motion Statistics

Summary of T500 10yr WindSea Wave					
	Surge (m)			Heave (m)	Pitch (deg)
	Original	Low-Freq	High-Freq	Original	Original
Mean	0.54	0.00	0.00	-0.02	-0.01
Max	9.74	9.16	2.34	0.91	2.43
Min	-8.45	-8.60	-2.00	-0.90	-2.84
RMS	2.80	2.72	0.41	0.21	0.61
Tz (sec)	75.41	157.66	13.08	18.75	15.44

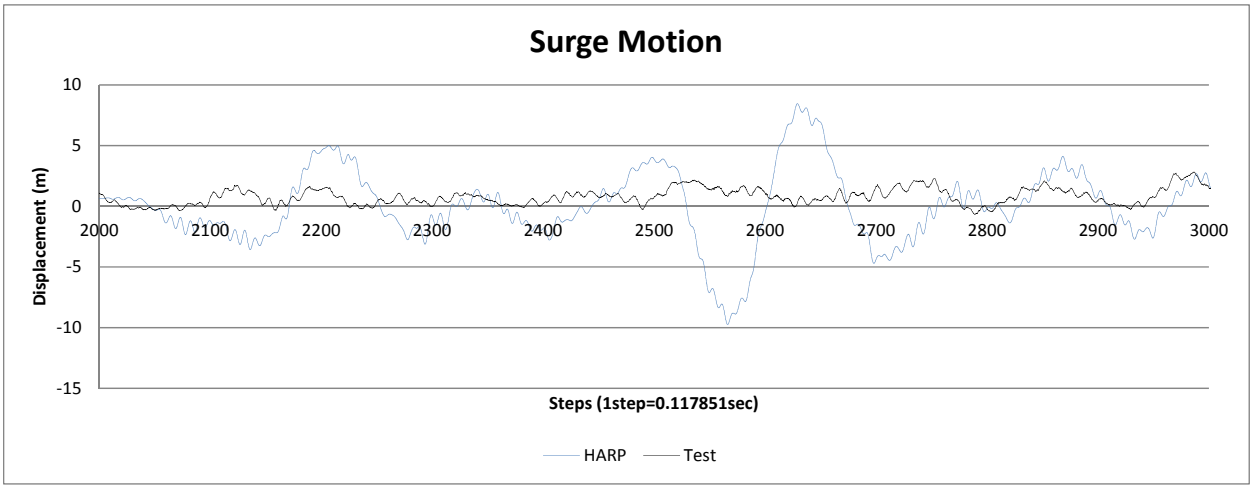

Figure 8.1-7 T500 10yr WindSea Motions

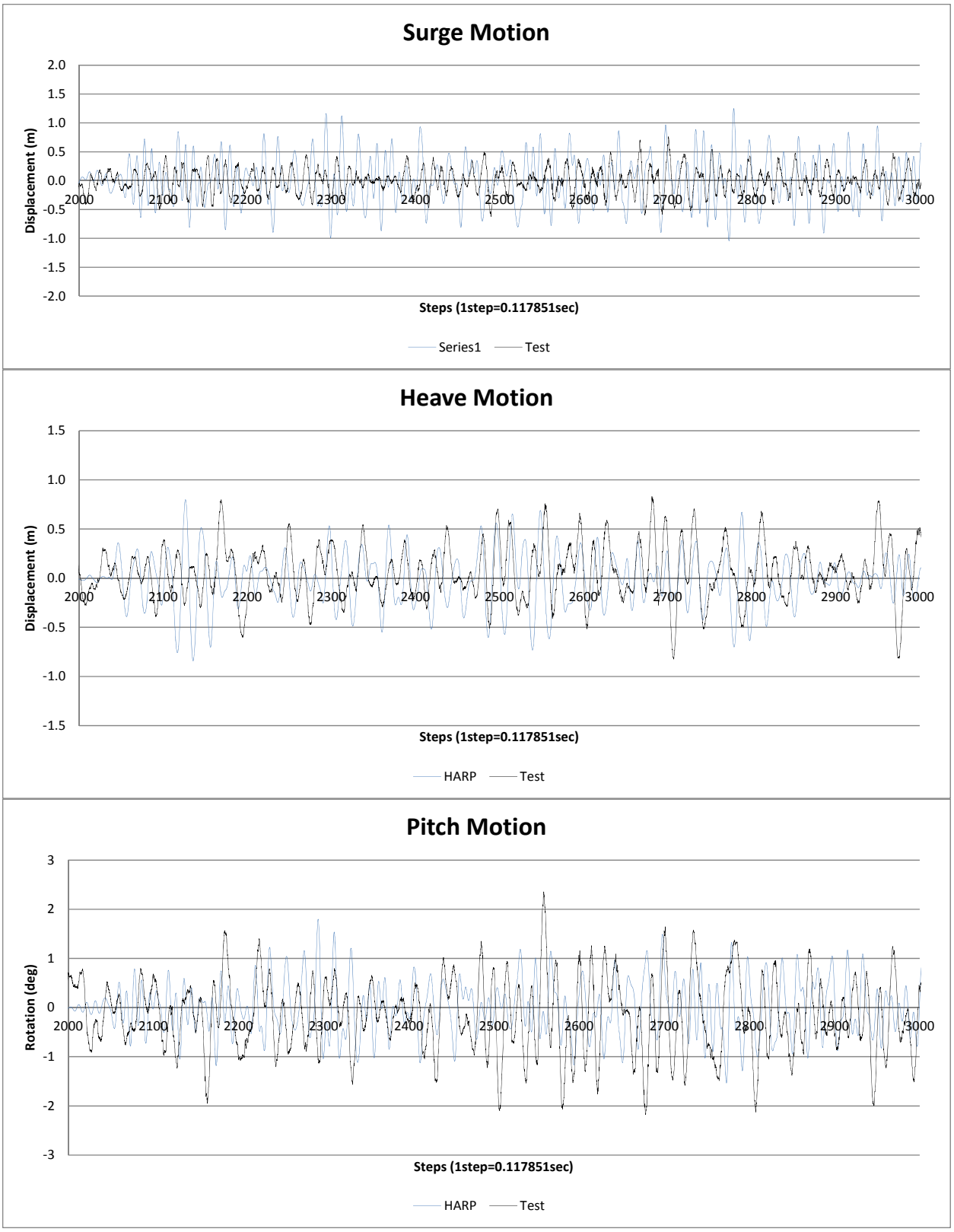

Figure 8.1-8 T500 10yr WindSea Wave Motions

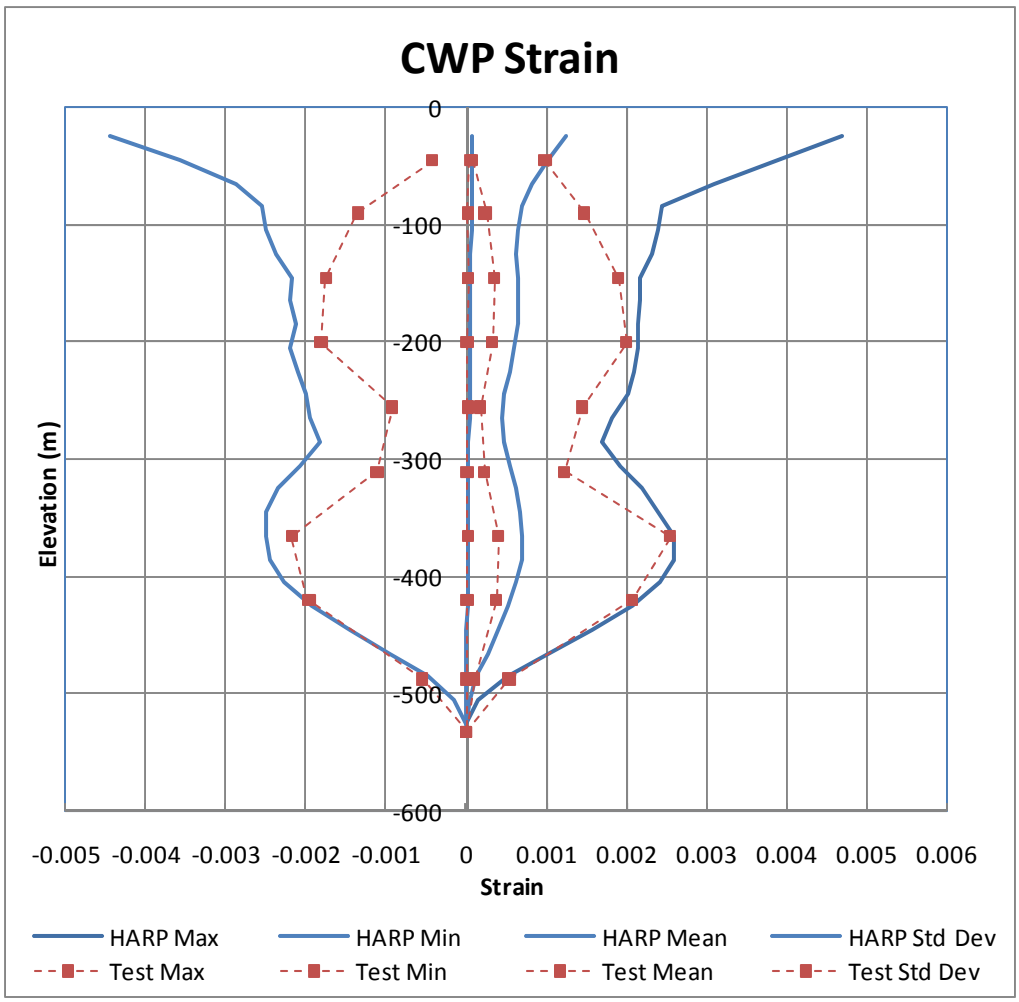

Figure 8.1-9 T500 10yr WindSea CWP Strain Envelope

Table 8.1-3 T500 WhiteNoise Calculated Motion Statistics

Summary of T500 WhiteNoise Wave					
	Surge (m)			Heave (m)	Pitch (deg)
	Original	Low-Freq	High-Freq	Original	Original
Mean	0.32	0.00	0.00	-0.01	0.01
Max	12.51	7.10	11.99	12.67	9.56
Min	-6.44	-6.38	-1.63	-1.68	-2.79
RMS	2.37	2.30	0.45	0.54	0.79
Tz (sec)	73.26	157.18	17.37	19.50	18.65

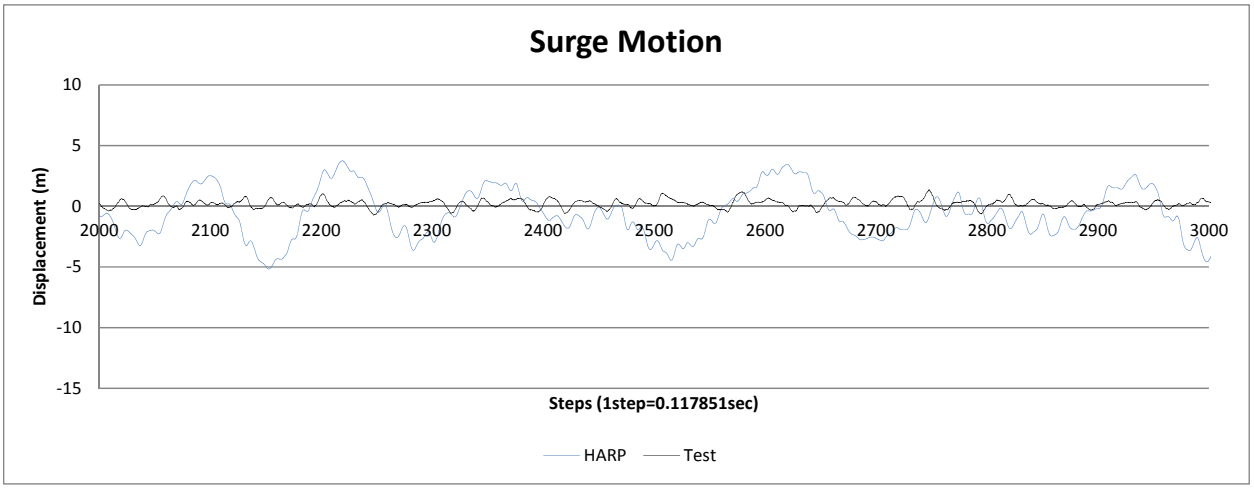

Figure 8.1-10 T500 WhiteNoise Motions

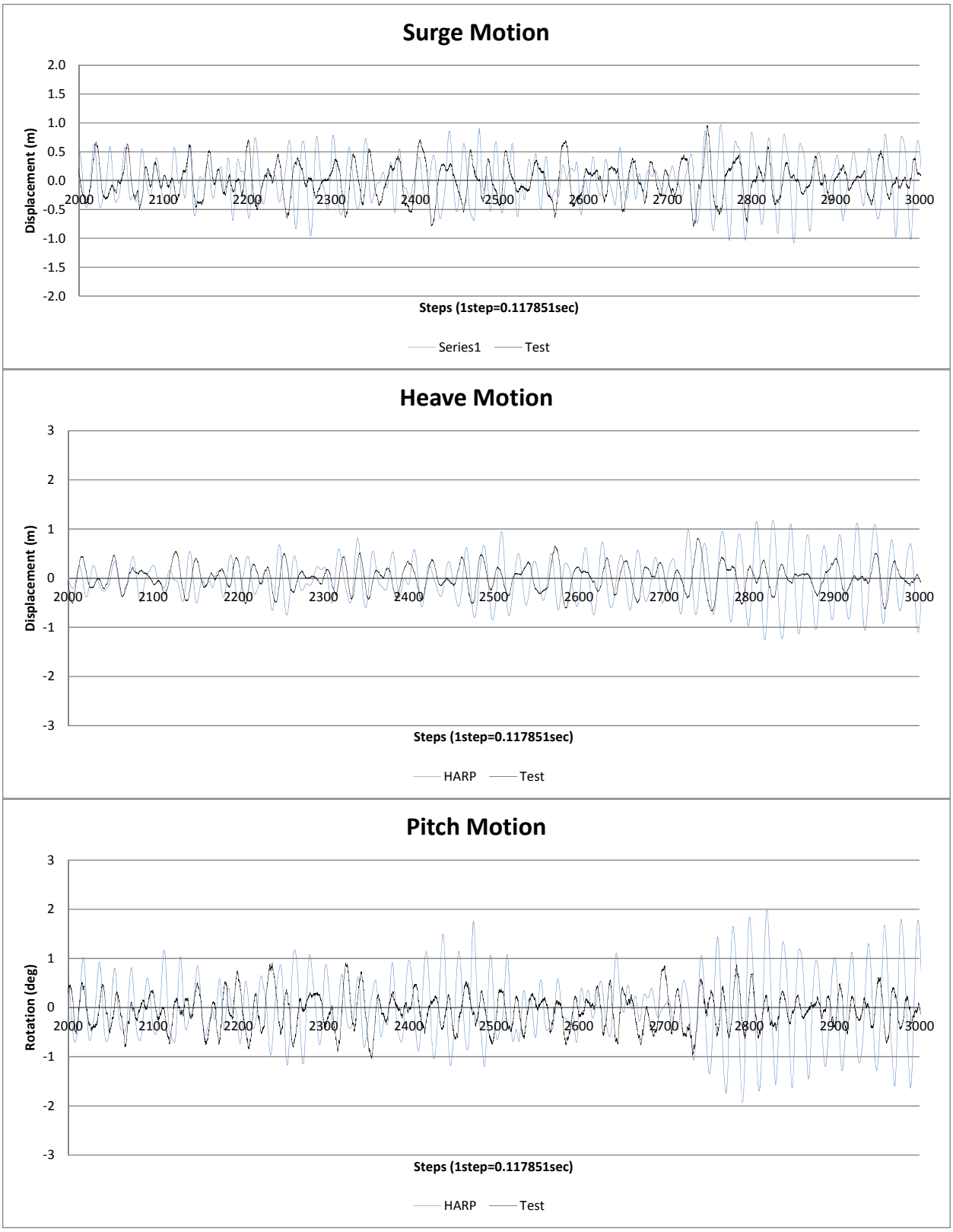

Figure 8.1-11 T500 WhiteNoise Wave Motions

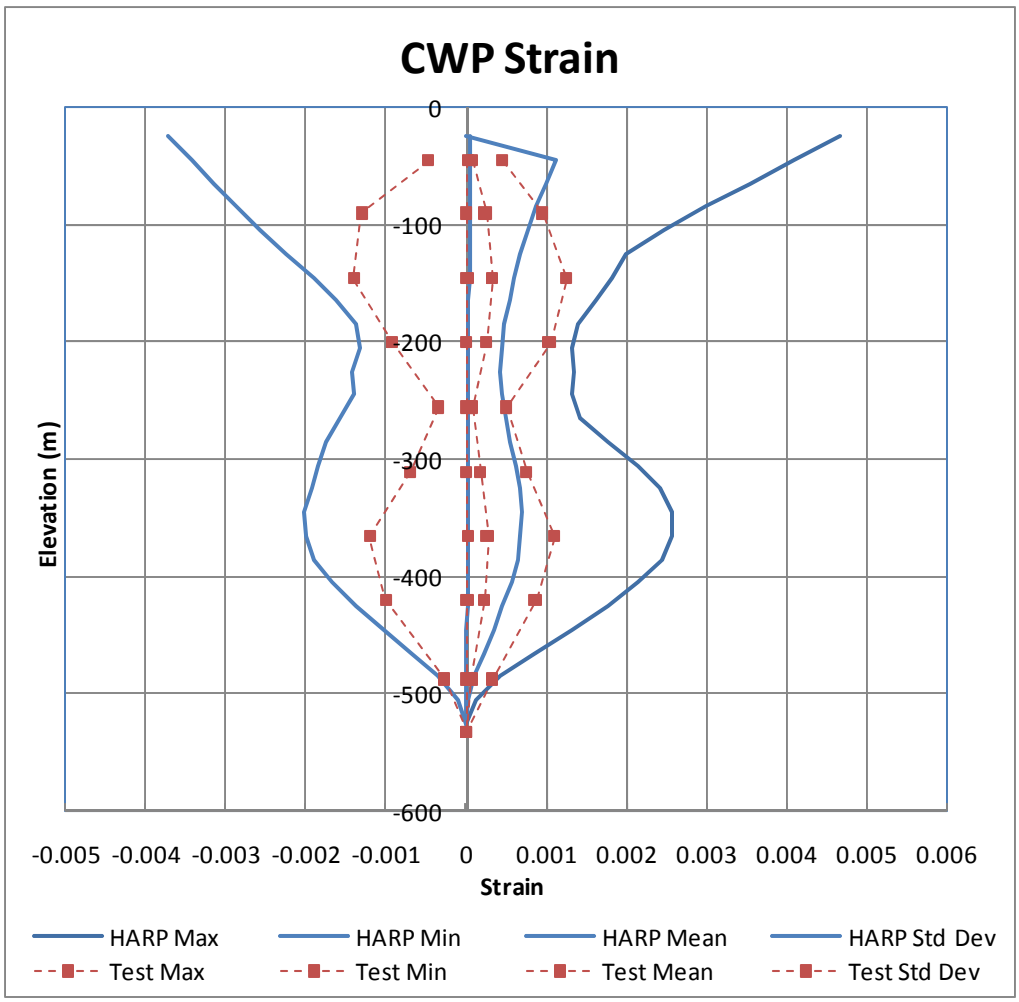

Figure 8.1-12 T500 WhiteNoise CWP Strain Envelope

9 T600 - CWP INSTALLATION 2

9.1 T600 Random Wave Analysis

Table 9.1-1 T600 10yr Swell Calculated Motion Statistics

Summary of T600 10yr Swell Wave					
	Surge (m)			Heave (m)	Pitch (deg)
	Original	Low-Freq	High-Freq	Original	Original
Mean	-1.23	0.00	0.00	0.13	-0.04
Max	13.89	14.04	2.69	4.09	2.99
Min	-17.16	-13.77	-4.62	-3.65	-3.37
RMS	4.80	4.58	0.77	0.95	0.90
Tz (sec)	84.19	167.01	17.29	18.49	20.01

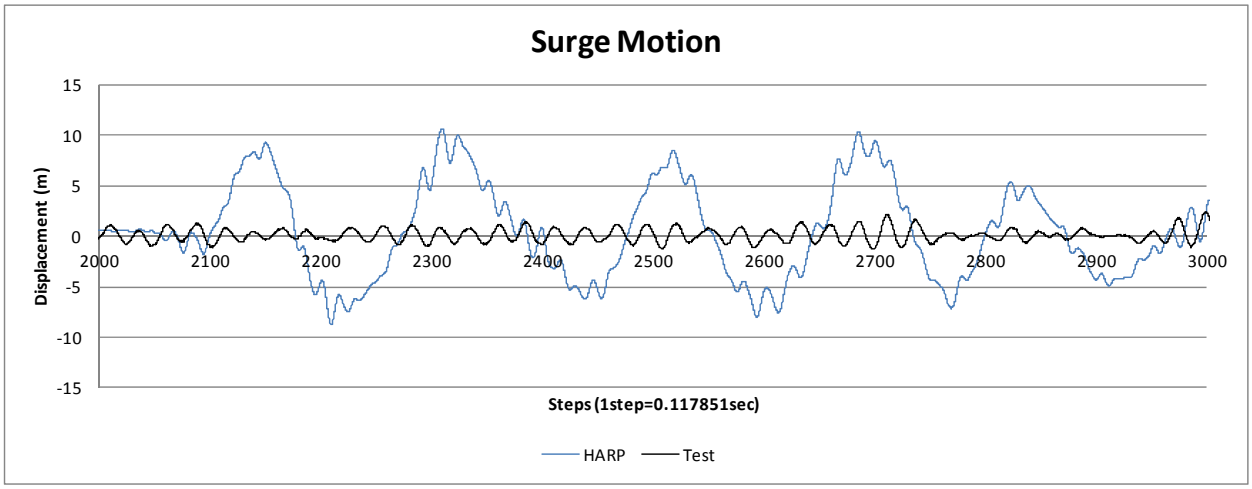

Figure 9.1-1 T600 10yr Swell Motions

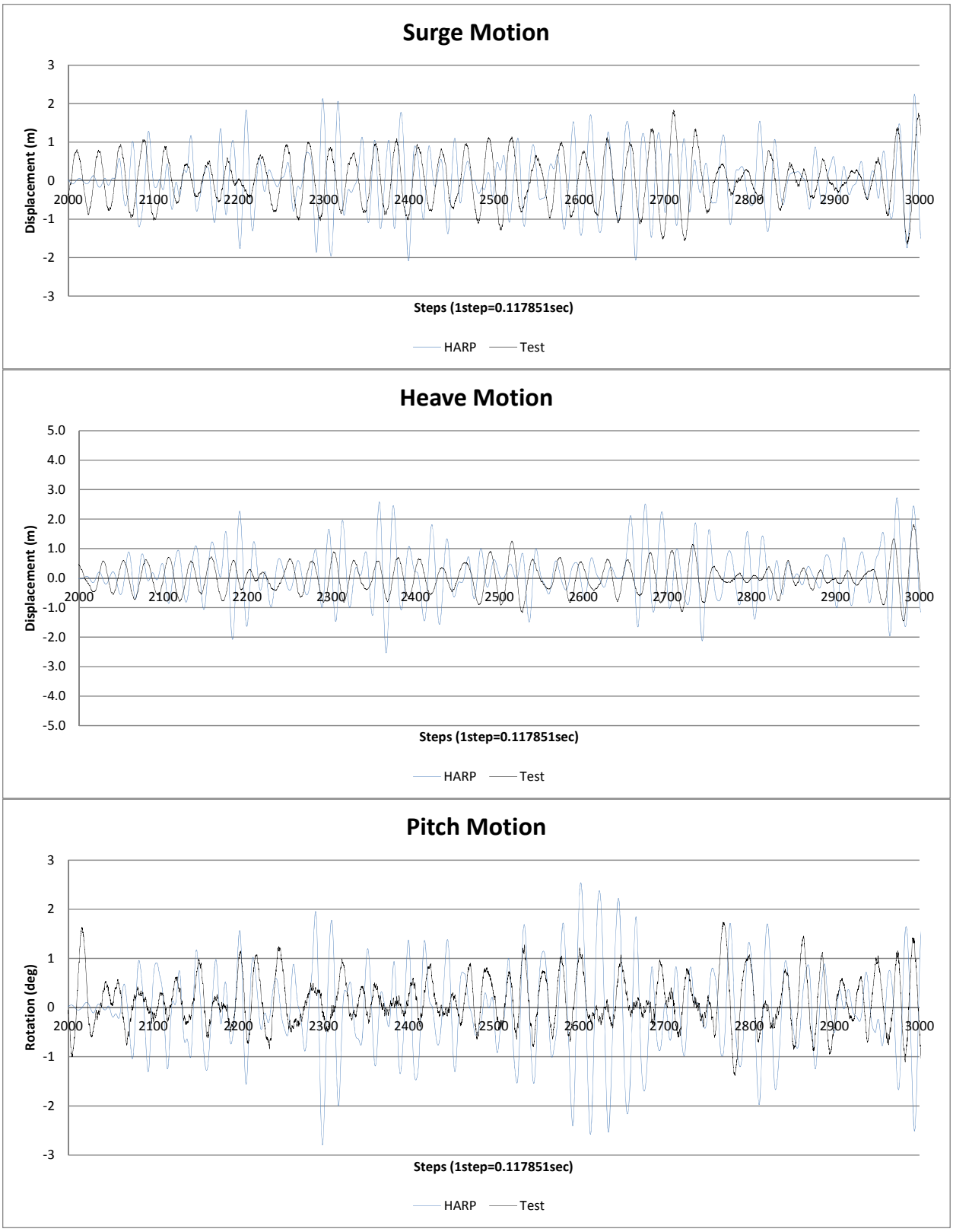

Figure 9.1-2 T600 10yr Swell Wave Motions

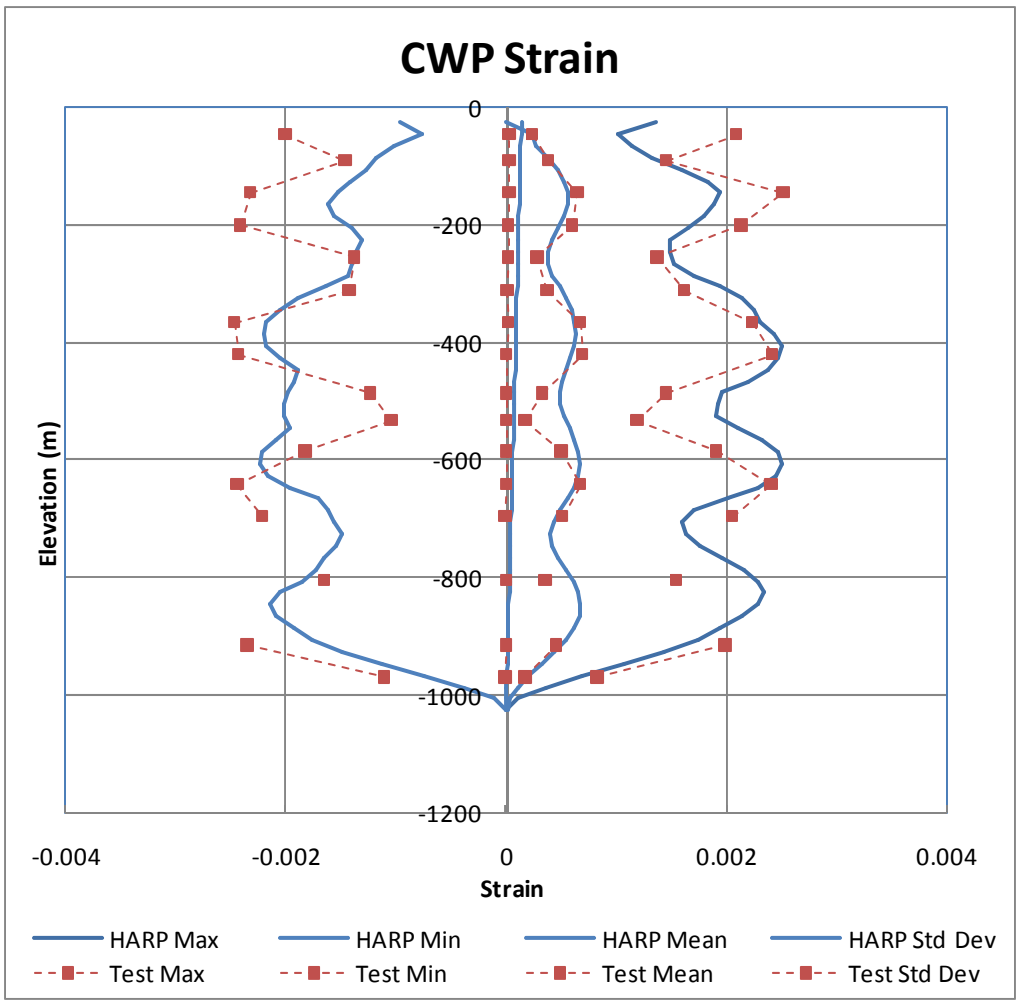

Figure 9.1-3 T600 10yr Swell CWP Strain Envelope
[Gimbal Stiffness = 3.15E+09, 3.3% Installation Stiffness, 2.5x Operation Stiffness]

T600 10yr Swell

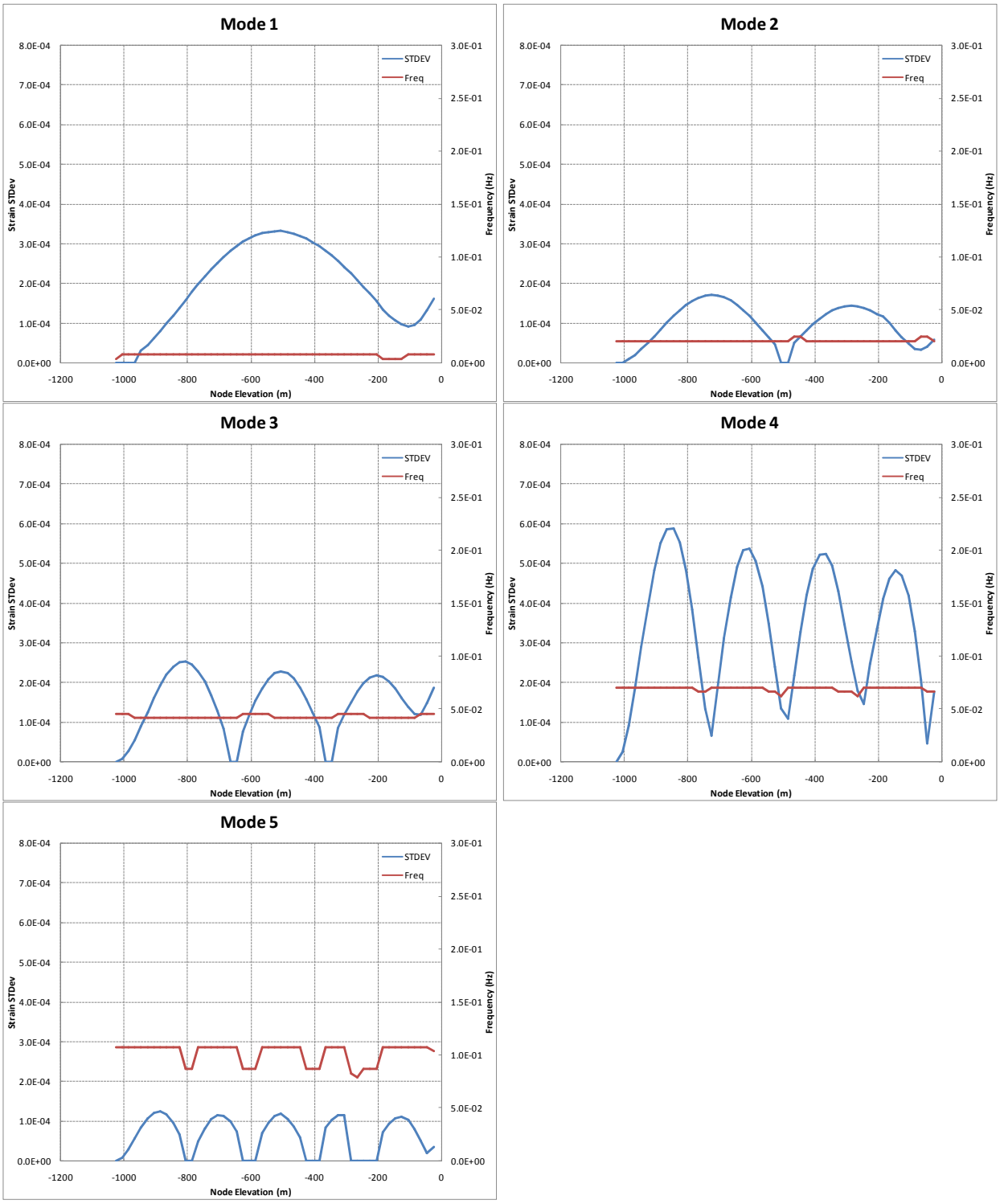

Figure 9.1-4 T600 10yr Swell Mode Shapes Using HARP

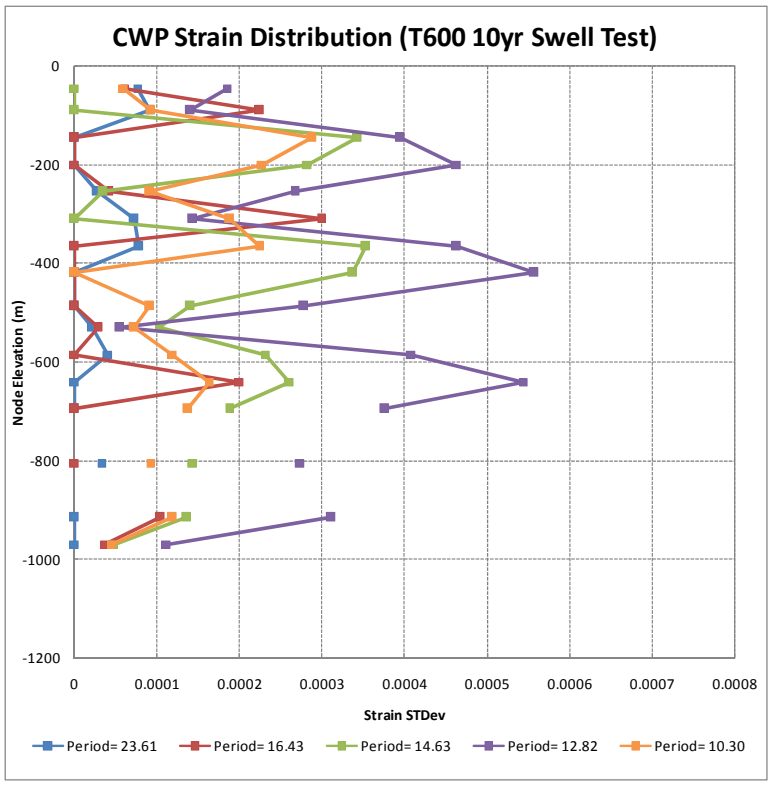

Figure 9.1-5 T600 10yr Swell Mode Shapes from TEST

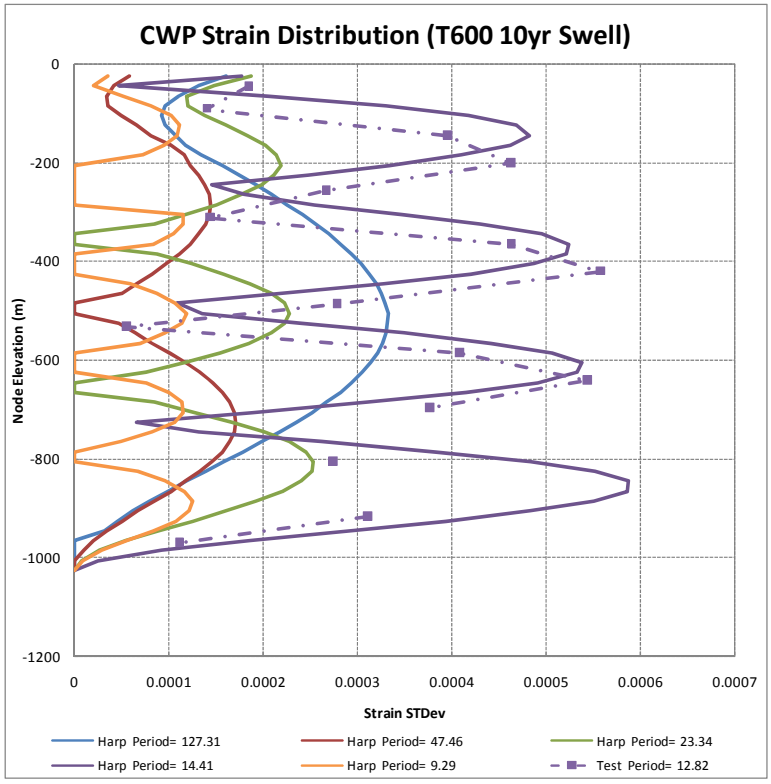

Figure 9.1-6 T600 10yr Swell Mode Shapes Comparison between HARP and TEST

Table 9.1-2 T600 10yr WindSea Calculated Motion Statistics

Summary of T600 10yr WindSea Wave					
	Surge (m)			Heave (m)	Pitch (deg)
	Original	Low-Freq	High-Freq	Original	Original
Mean	-0.53	0.00	0.00	-0.02	0.01
Max	10.90	10.62	2.29	0.93	3.24
Min	-11.37	-10.09	-1.98	-0.87	-3.38
RMS	3.31	3.22	0.56	0.21	0.92
Tz (sec)	87.49	165.19	16.72	18.68	19.75

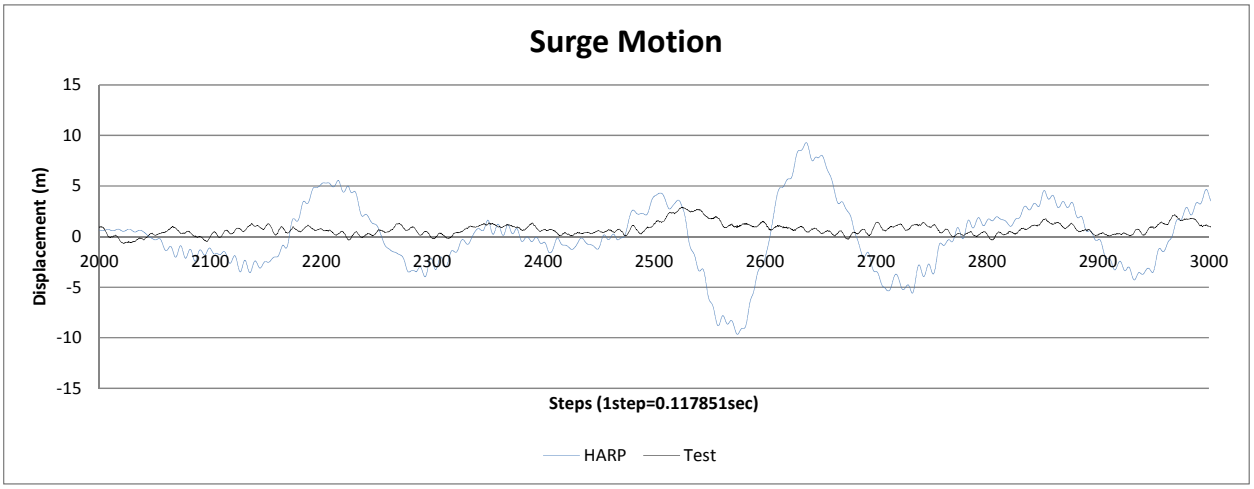

Figure 9.1-7 T600 10yr WindSea Motions

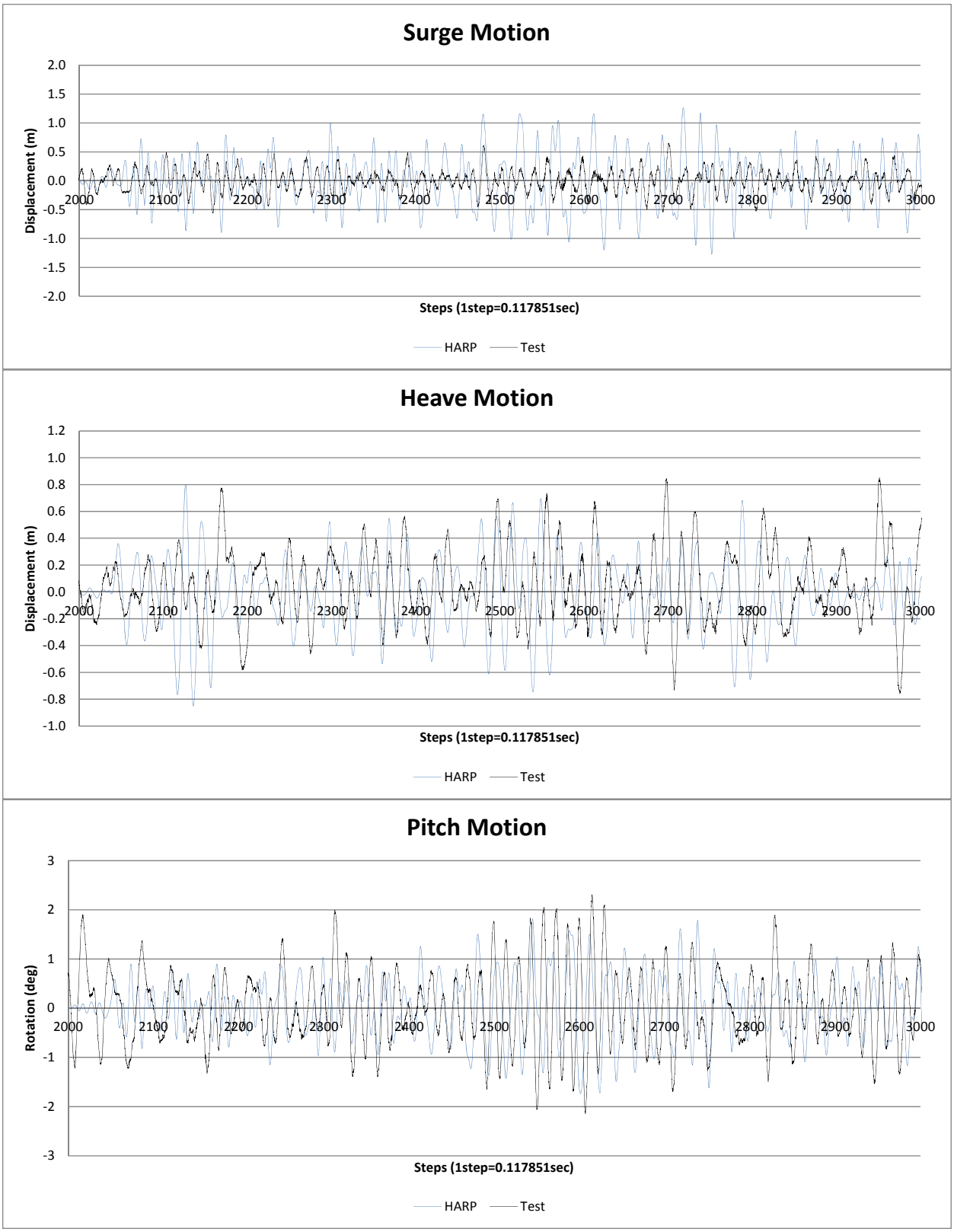

Figure 9.1-8 T600 10yr WindSea Wave Motions

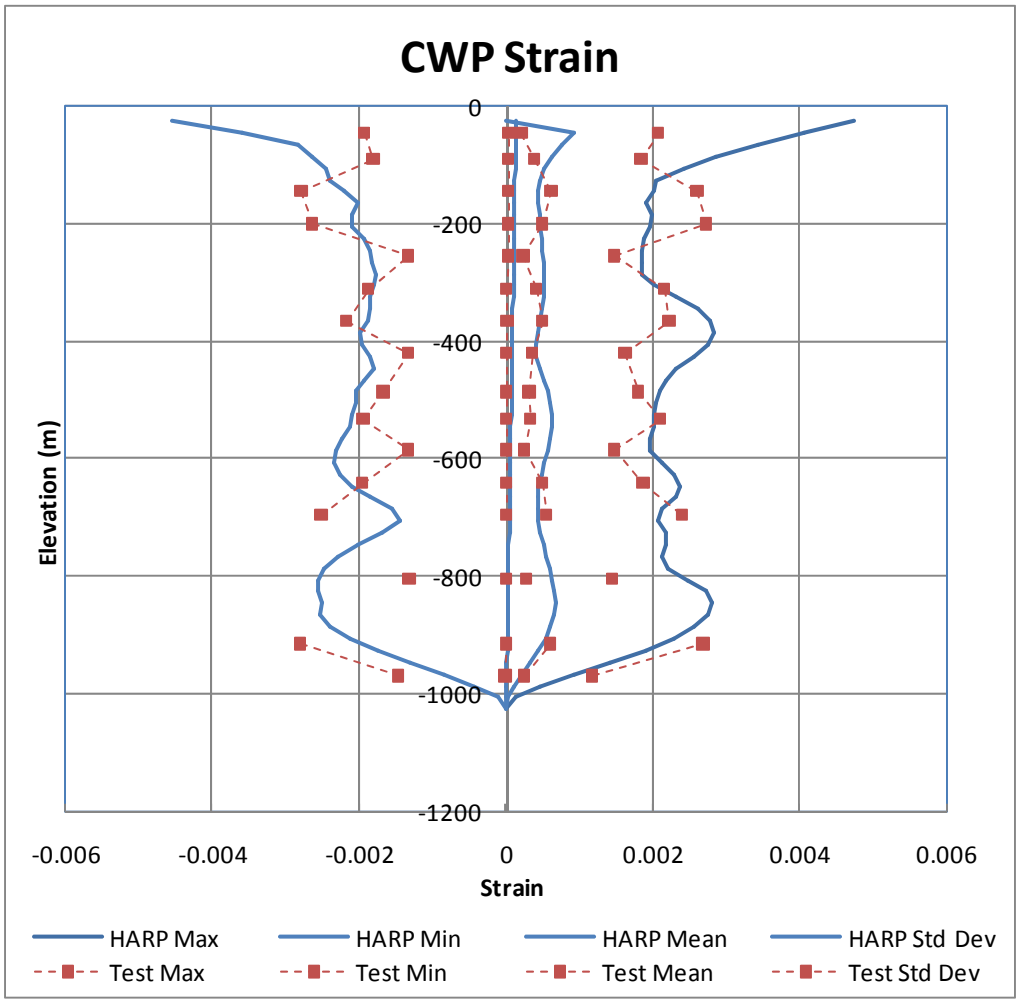

Figure 9.1-9 T600 10yr WindSea CWP Strain Envelope

Table 9.1-3 T600 WhiteNoise Calculated Motion Statistics

Summary of T600 WhiteNoise Wave					
	Surge (m)			Heave (m)	Pitch (deg)
	Original	Low-Freq	High-Freq	Original	Original
Mean	0.29	0.00	0.00	-0.01	0.02
Max	19.94	7.08	19.57	6.08	20.06
Min	-7.15	-7.31	-1.80	-1.74	-3.05
RMS	2.74	2.65	0.62	0.55	1.00
Tz (sec)	62.28	157.46	20.27	19.83	20.93

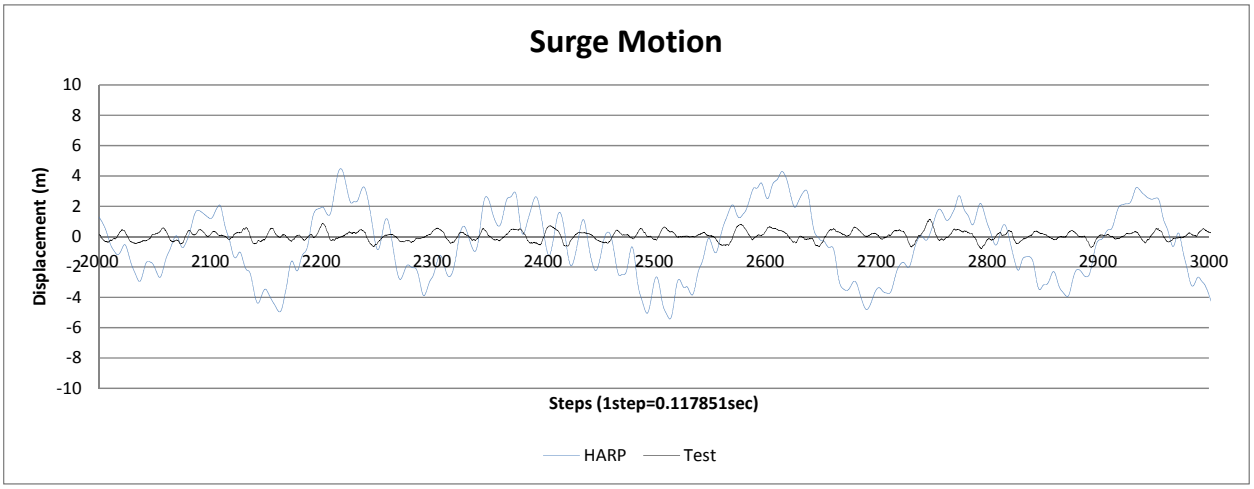

Figure 9.1-10 T600 WhiteNoise Motions

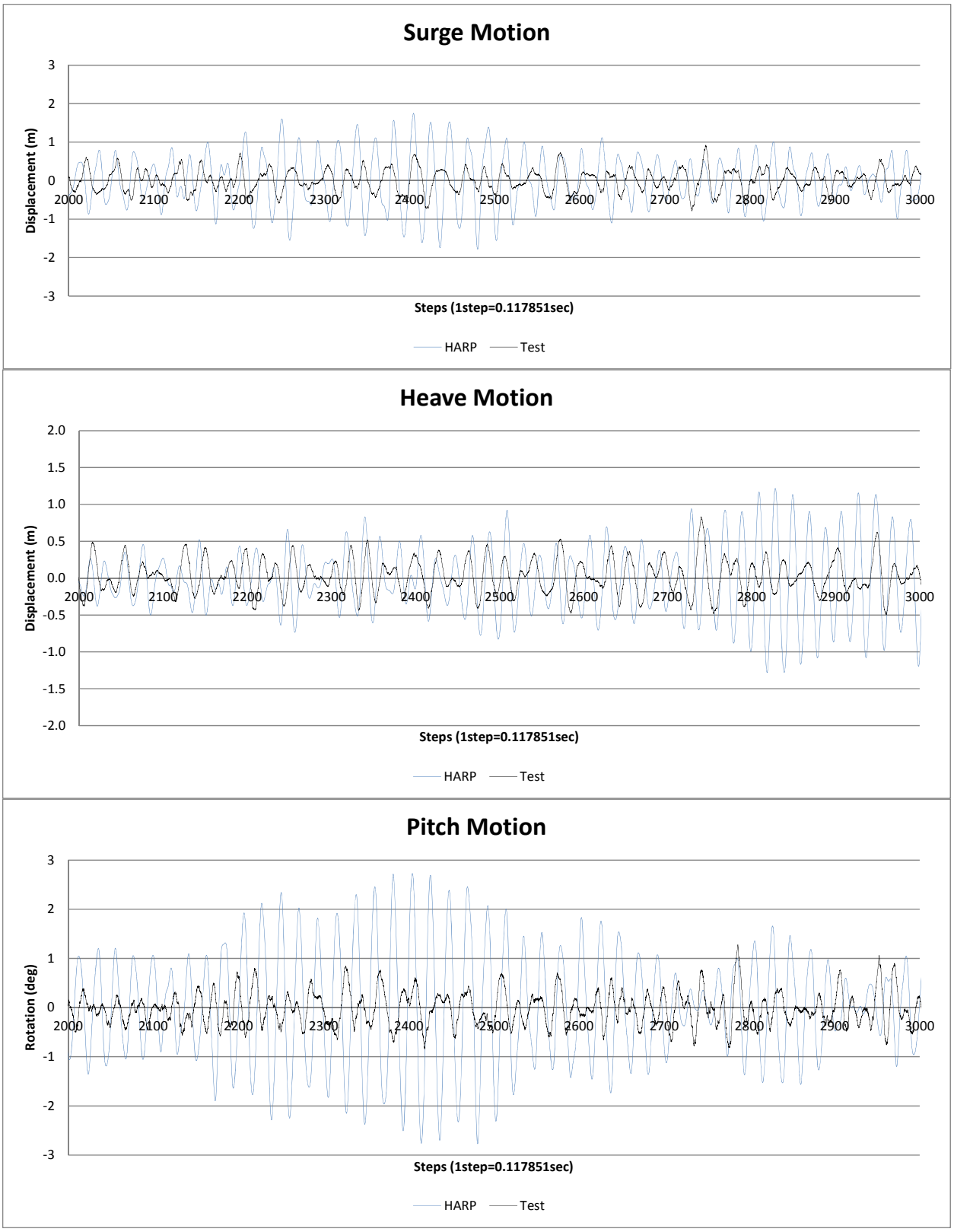

Figure 9.1-11 T600 WhiteNoise Wave Motions

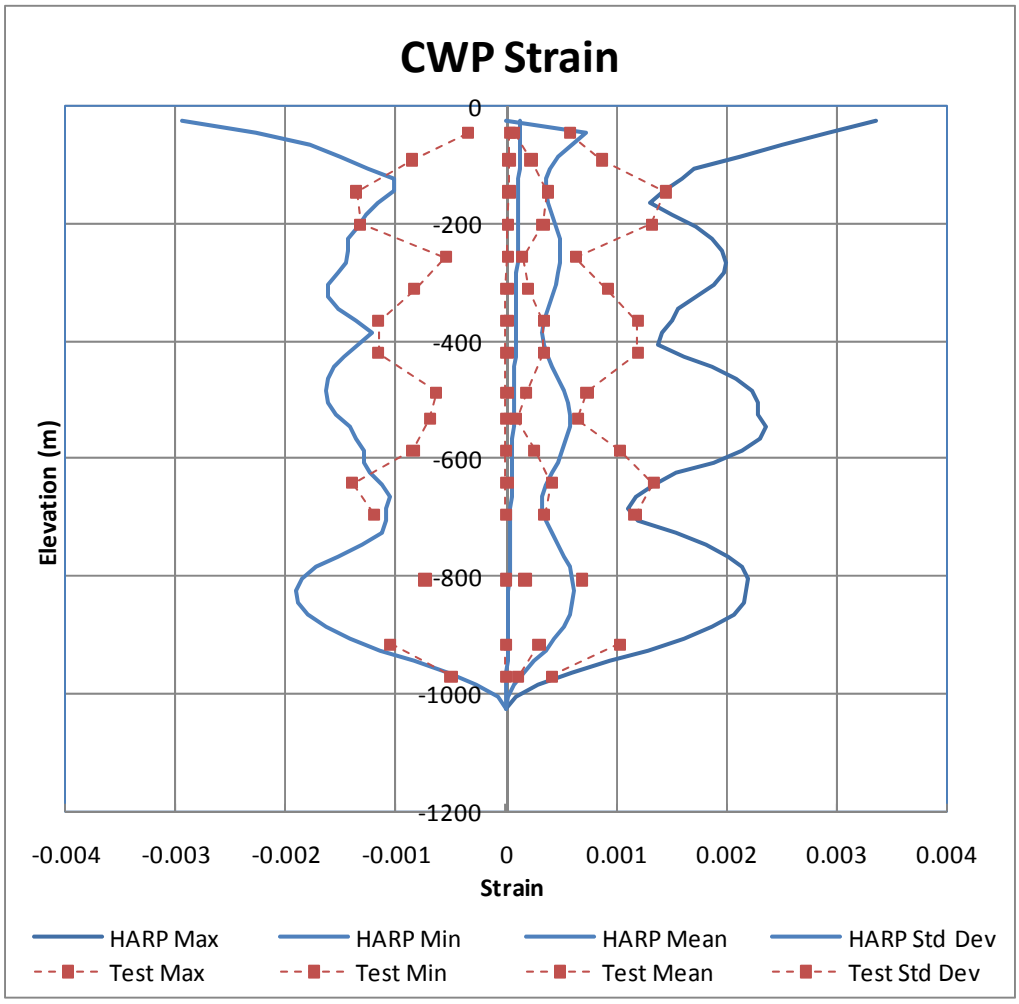

Figure 9.1-12 T600 WhiteNoise CWP Strain Envelope

10 Conclusion Remarks

The conclusions form compare the simulation and the model test results are summarized in below:

1. The numerical simulations performed by program HARP provide adequate and slightly conservative results. The simulated platform motions have very good agreement with the model test in wave frequency for testing cases: T100, T200, and T400, but not T300, T500, and T600. Time trace are off in term of period for T300, T500, and T600. This is also shown in the different of pitch period for these cases.
2. The model test shows limited slow drift motion of the platform. Larger drift motions are shown in the simulations. This is may cause by the damping of the testing system, which is difficult to simulate. This has not impact on using the program simulation for real project application, where the damping is minimum.
3. Analysis shows T400 and T300 motions are not much different. Motion time trace can overlap on each other. Model test show big different on pitch period. It is suspecting that there is something going on after T400, which is not addressed in the analysis.
4. Test results have the pitch period for T600 longer than T100. T100 pitch period is 27 sec (same as HARP) and T500 pitch period is 19.56 sec (different from HARP). For the T400 case, simulation and model test have the same pitch period of 21.28 second. Closer look of Cases after T400 test are necessary in the future.
5. Numerical simulation results show the program HARP can adequate predict CWP response modes and strains for the 10-yr swell, 100-yr cyclone, but overly conservative for 10-yr wind sea, fatigue, and white noise.
6. The model tests always show the CWP response reduced with water depth. This is suspecting that the hydrodynamic damping is increasing with water depth. In the simulation, constant damping and added mass coefficients are used. This can be the reason for larger CWP response and strains are calculated compare with the testing results. It is recommended that modify the simulation program to update the damping and added mass coefficients at each time step of simulation based on Reynolds number and Keulegan-Carpenter number for each CWP element. The following Cd and Cm vs K relationship are proposed by Sarpkaya in the book of “Wave Forces on Offshore Structures”.

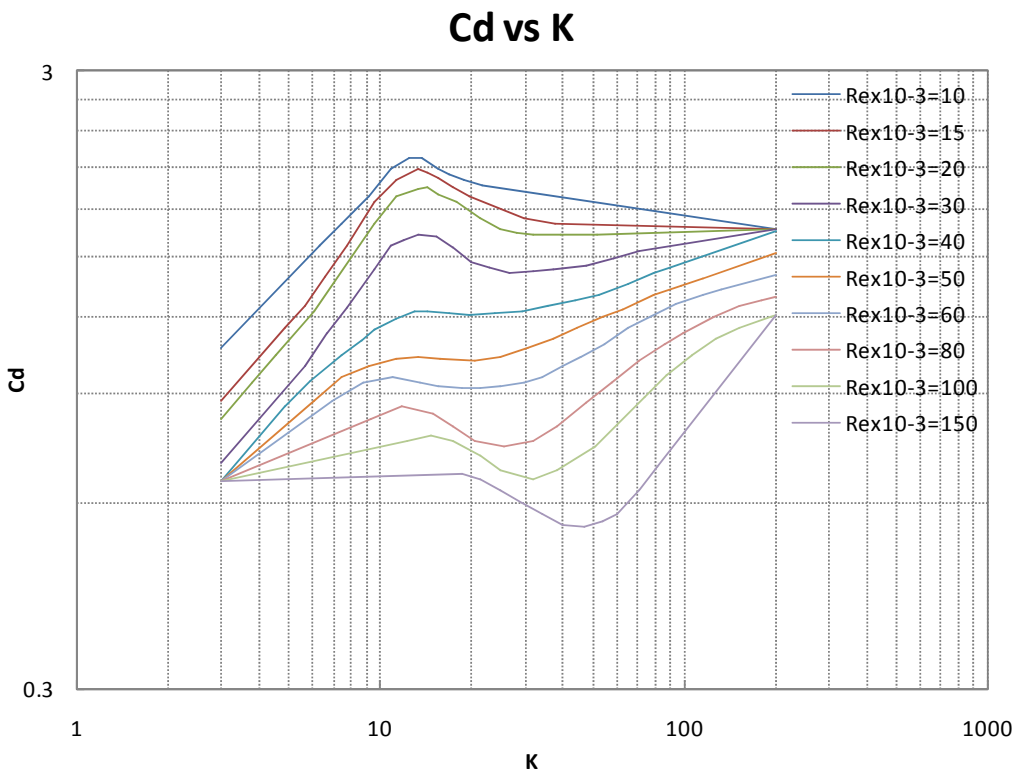

Figure 10.1 Sarpkaya Cd vs K relationship

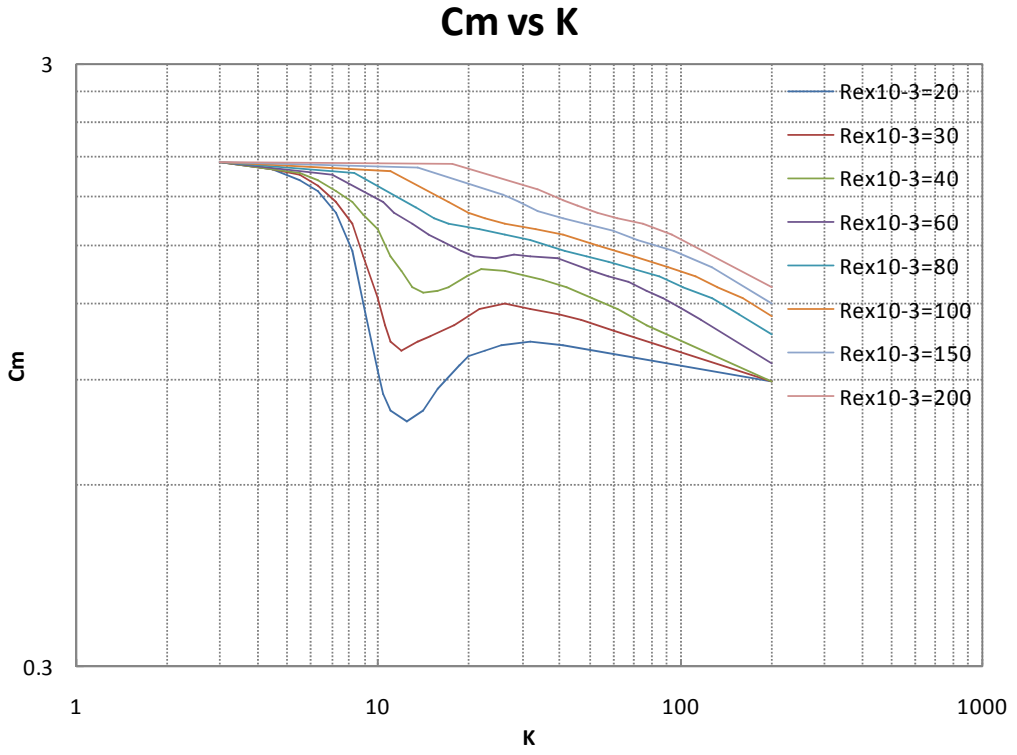

Figure 10.2 Sarpkaya Cm vs K relationship

7. For T600 and T500, discrepancy between tests and simulations are shown at the top of CWP connection. Sensitivity analyses were performed for various gimbal stiffness. Results are shown in the next 3 (three) pages. It shows the comparison of tests and HARP results for the 500m riser with semisubmersible alone for stiffness equal to 3.3% of the installation stiffness, 3.15E9 N-m/rad. The sensitivity of the T600 results (1,000m pipe) also showed good agreement near the platform with about 5 – 10% of the prescribed installation stiffness.

T600

Gimbal Stiffness = 9.55E+10
[Installation Stiffness]

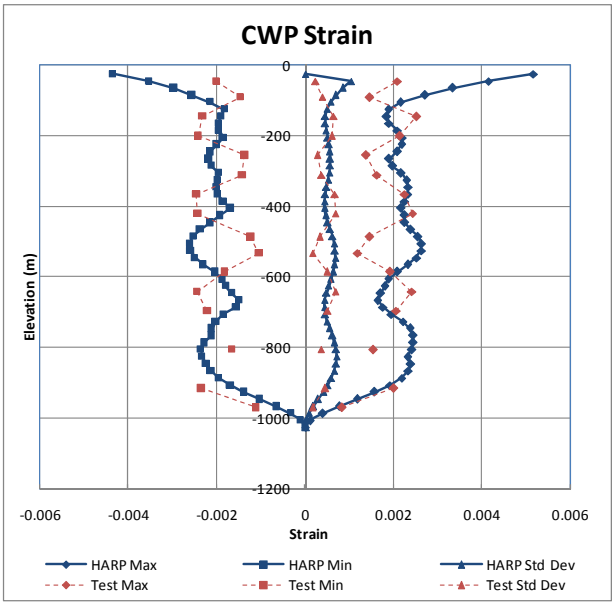

Gimbal Stiffness = 7.19E+10
[75.3% Installation Stiffness, 57.1x Operation Stiffness]

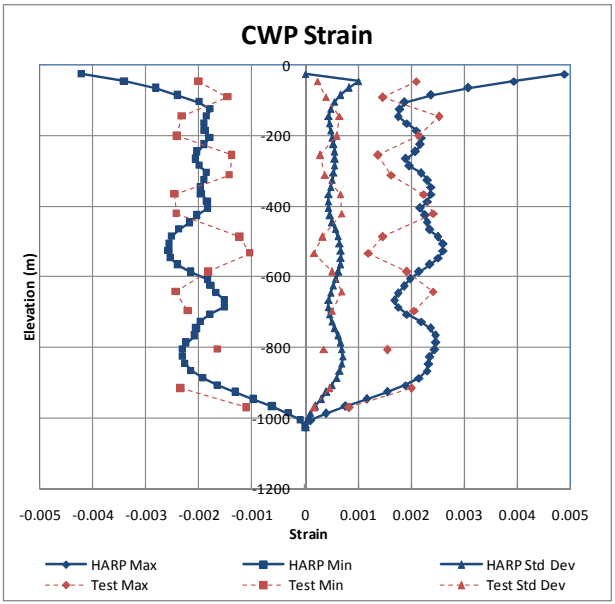

Gimbal Stiffness = 4.84E+10
[50.7% Installation Stiffness, 38.4x Operation Stiffness]

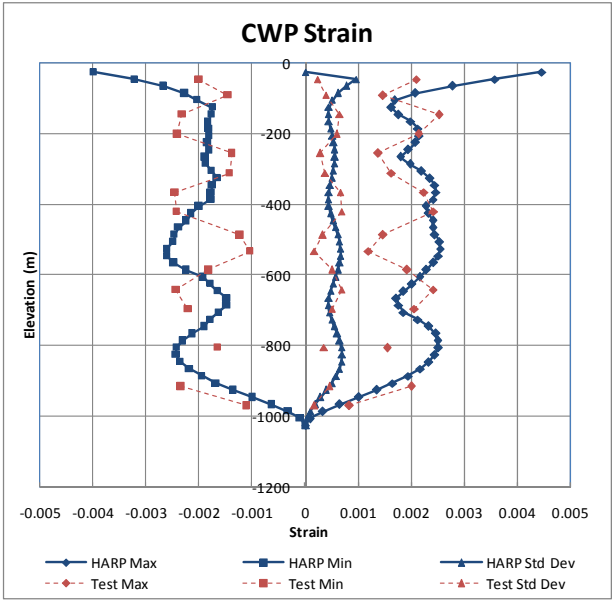

Gimbal Stiffness = 2.48E+10
[25.9% Installation Stiffness, 19.7x Operation Stiffness]

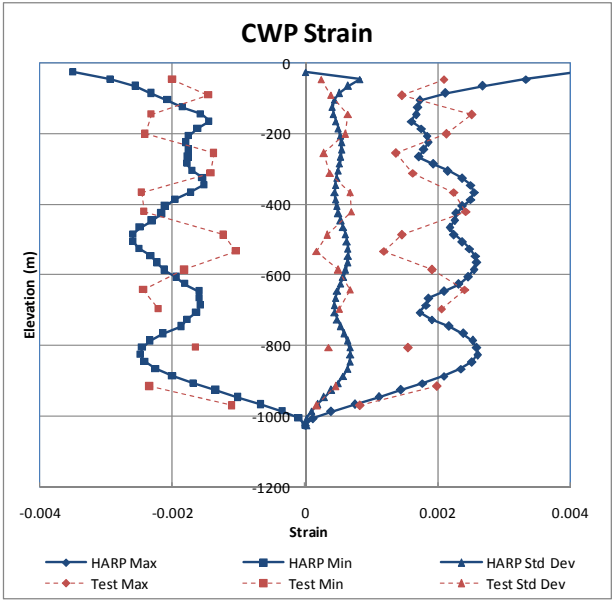

Gimbal Stiffness = 1.89E+10
[19.8% Installation Stiffness, 15x Operation Stiffness]

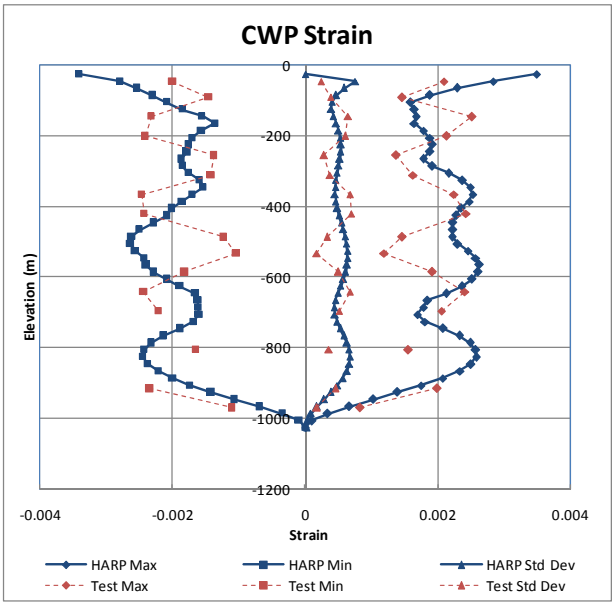

Gimbal Stiffness = 1.30E+10
[13.6% Installation Stiffness, 10.3x Operation Stiffness]

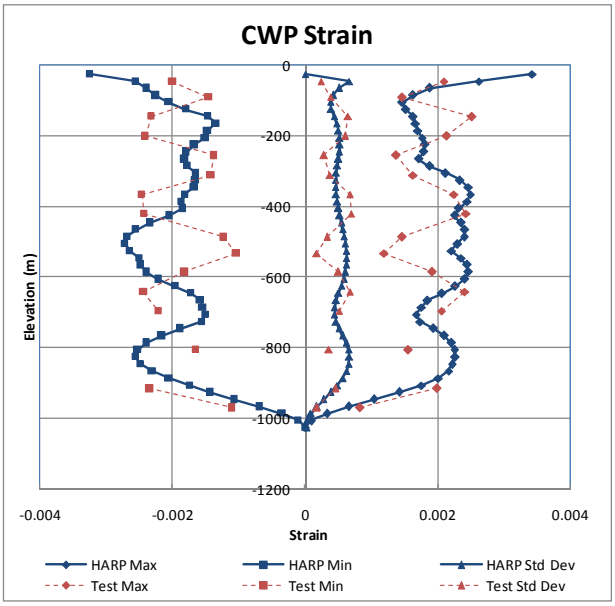

Gimbal Stiffness = 7.15E+09
[7.5% Installation Stiffness, 5.7x Operation Stiffness]
(Selected for T500 Analysis)

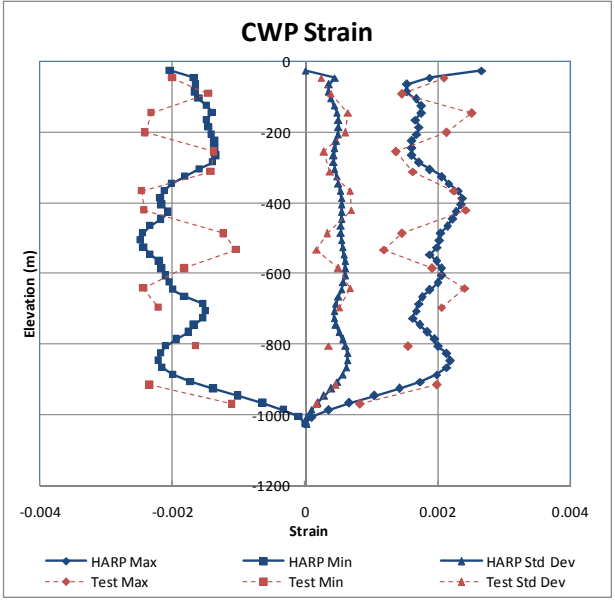

Gimbal Stiffness = 3.15E+09
[3.3% Installation Stiffness, 2.5x Operation Stiffness]
(Selected for T500 Analysis)

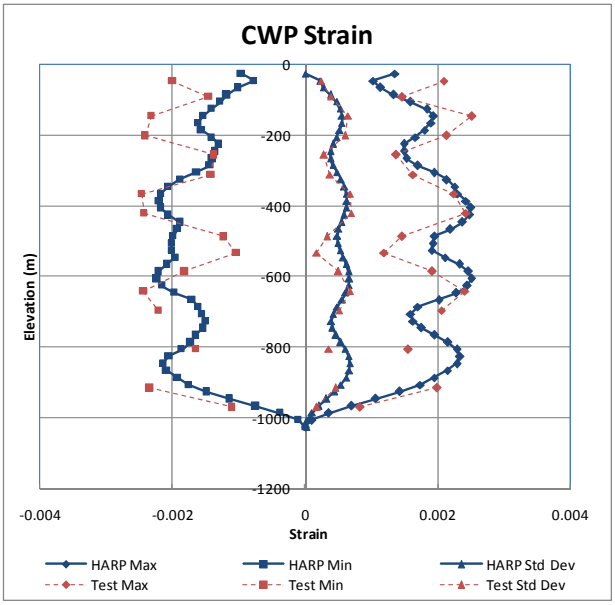

T500

Gimbal Stiffness = 7.15E+09
[7.5% Installation Stiffness, 5.7x Operation Stiffness]

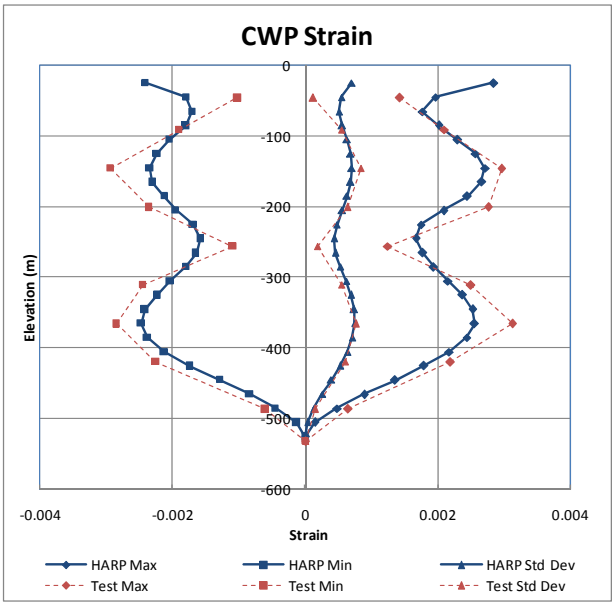

Gimbal Stiffness = 3.15E+09
[3.3% Installation Stiffness, 2.5x Operation Stiffness]

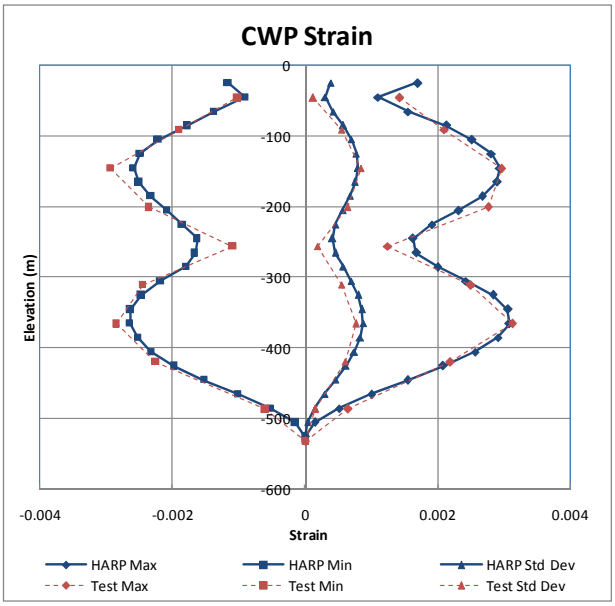

This page intentionally left blank.

F. TEST LISTING

This page intentionally left blank.

Appendix F - Table 10 Test Configurations

Configuration Description	Basin Test Group	Test Specification Reference	Test Schedule Order	Semi	Six Power Modules	CWP Length (m)	Gimbal Stiffness		Comments
							Rotation (N-m/rad)	Lateral (N/m)	
Calibrations	T000	Dry Tests	0						
Semi Installation	T100	Group 3	1	Y	N	0			
Operational Semi & Remoras	T200	Group 1	2	Y	Y	0			
Operational A	T300	Group 1	4	Y	Y	1,000	0	3.15E+08	Free Gimbal
Operational B	T400	Group 2	3	Y	Y	1,000	1.26E+09	3.33E+08	Stiff Gimbal
CWP Installation 1	T500	Group 3	6	Y	N	500	9.55E+10	3.05E+08	
CWP Installation 2	T600	Group 4	5	Y	N	1,000	9.55E+10	3.15E+08	

Appendix F - Table 11 Group T000 Tests

GROUP	T000		
DESCRIPTION	DRY-TESTS		
CLIENTS REF	DRY-TESTS		
GROUP	NUMBER	CLIENTS REF	ID
PT030	_00100	-	GIMBAL LVDT SCRIPT X
PT030	_00200	-	GIMBAL LVDT SCRIPT XY
PT030	_00300	Gimbal static friction - Pinned	GIMBAL STAT FRICTION
PT030	_00400	Gimbal dynamic friction - Pinned	GIMBAL DYN FRICTION
PT032	_00100	Gimbal horizontal stiffness Installation condition (dir. x)	GIMBAL INST HOR STIF X
PT032	_00200	Gimbal horizontal stiffness Installation condition (dir. y)	GIMBAL INST HOR STIF Y
PT032	_00300	Gimbal angular stiffness Installation condition (dir. x)	GIMBAL INST ANG STIF X
PT032	_00400	Gimbal angular stiffness Installation condition (dir. y)	GIMBAL INST ANG STIF Y
PT031	_00100	Gimbal angular and horizontal stiffness Operation condition (dir.	GIMBAL OPER SPR STIF X
PT031	_00200	Gimbal angular and horizontal stiffness Operation condition (dir.	GIMBAL OPER SPR STIF Y
PT031	_00300	Gimbal static friction - Operational	GIMBAL OPER STAT FRICTION
PT031	_00400	Operational	GIMBAL OPER DYN FRICTION
PT020	_00100	-	1/2 CWP DW & X IMPULSE
PT020	_00200	-	1/2 CWP DW & Y IMPULSE
PT020	_00300	-	1/2 CWP D PULLOUT

Appendix F - Table 12 Group T100 Tests

GROUP	T100		
DESCRIPTION	INSTALLATION SEMI ALONE		
CLIENTS REF	GROUP 3		
GROUP	NUMBER	CLIENTS REF	ID
PT100_	00100	GM l	INCLINING PITCH
PT100_	00200	GM t	INCLINING ROLL
PT100_	100100	Surge Static Offset	OFFSET SURGE
PT100_	100200	Sway Static Offset	OFFSET SWAY
PT100_	100600	Yaw Static Offset	OFFSET YAW
PT100_	200100	Surge Free Decay	DECAY SURGE
PT100_	200200	Sway Free Decay	DECAY SWAY
PT100_	200300	Heave Free Decay	DECAY HEAVE
PT100_	200400	Roll Free Decay	DECAY ROLL
PT100_	200500	Pitch Free Decay	DECAY PITCH
PT100_	200600	Yaw Free Decay	DECAY YAW
T100_	100100	Regular Wave 1	REG H2.0 T6.36
T100_	100200	Regular Wave 2	REG H2.5 T7.0
T100_	100300	Regular Wave 3	REG H3.6 T8.5
T100_	100400	Regular Wave 4	REG H5.0 T10.0
T100_	100500	Regular Wave 5	REG H6.6 T11.5
T100_	100600	Regular Wave 6	REG H8.5 T13.0
T100_	100700	Regular Wave 7	REG H11.3 T15.0
T100_	200100	100 Year Cyclone	IRR JS H10.2 T12.8 G2.0 Uw 33.8
T100_	200200	10-yr Sea	IRR JS H4.2 T8.3 G1.0 Uw 15.7
T100_	200300	10-yr Swell	IRR JS H3.8 T15.7 G6.0 Uw 14.6
T100_	500100	White Noise	WN H2.5 DT 3.5 25.0 Uw 8.0

Appendix F - Table 13 Group T200 Tests

GROUP	T200		
DESCRIPTION	OPERATIONAL SEMI & REMORAS		
CLIENTS REF	GROUP 1		
GROUP	NUMBER	CLIENTS REF	ID
PT200_	00100	GM l	INCLINING PITCH
PT200_	00200	GM t	INCLINING ROLL
PT200_	200100	Surge Free Decay	DECAY SURGE
PT200_	200200	Sway Free Decay	DECAY SWAY
PT200_	200300	Heave Free Decay	DECAY HEAVE
PT200_	200400	Roll Free Decay	DECAY ROLL
PT200_	200500	Pitch Free Decay	DECAY PITCH
PT200_	200600	Yaw Free Decay	DECAY YAW
T200_	100100	Regular Wave 1	REG H2.0 T6.36
T200_	100300	Regular Wave 3	REG H3.6 T8.5
T200_	100500	Regular Wave 5	REG H6.6 T11.5
T200_	100700	Regular Wave 7	REG H11.3 T15.0
T200_	200100	100 Year Cyclone	IRR JS H10.2 T12.8 G2.0 Uw 33.8
T200_	200200	10-yr Sea	IRR JS H4.2 T8.3 G1.0 Uw 15.7
T200_	200300	10-yr Swell	IRR JS H3.8 T15.7 G6.0 Uw 14.6
T200_	500100	White Noise	WN H2.5 DT 3.5 25.0 Uw 8.0

Appendix F - Table 14 Group T300 Tests

GROUP	T300		
DESCRIPTION	OPERATIONAL A		
CLIENTS REF	GROUP 1		
GROUP	NUMBER	CLIENTS REF	ID
PT300_	00100	GM l	INCLINING PITCH
PT300_	00200	GM t	INCLINING ROLL
PT300_	300100	Pipe bottom Surge Static offse	OFFSET TEST CWP
PT300_	400100	Pipe impulse	IMPULSE TEST CWP
PT300_	200500	Pitch Free Decay	DECAY PITCH
T300_	100100	Regular Wave 1	REG H2.0 T6.36
T300_	100200	Regular Wave 2	REG H2.5 T7.0
T300_	100300	Regular Wave 3	REG H3.6 T8.5
T300_	100400	Regular Wave 4	REG H5.0 T10.0
T300_	100500	Regular Wave 5	REG H6.6 T11.5
T300_	100600	Regular Wave 6	REG H8.5 T13.0
T300_	100700	Regular Wave 7	REG H11.3 T15.0
T300_	200100	100 Year Cyclone	IRR JS H10.2 T12.8 G2.0 Uw 33.8
T300_	200200	10-yr Sea	IRR JS H4.2 T8.3 G1.0 Uw 15.7
T300_	200300	10-yr Swell	IRR JS H3.8 T15.7 G6.0 Uw 14.6
T300_	200400	Fatigue Wave	IRR JS H2.5 T16.6 G6.0 Uw 8.0
T300_	500100	White Noise	WN H2.5 DT 3.5 25.0 Uw 8.0

Appendix F - Table 15 Group T400 Tests

GROUP	T400		
DESCRIPTION	OPERATIONAL B		
CLIENTS REF	GROUP 2		
GROUP	**NUMBER**	**CLIENTS REF**	**ID**
PT400_	00100	GM l	INCLINING PITCH
PT400_	00200	GM t	INCLINING ROLL
PT400_	300100	Pipe bottom Surge Static offse	OFFSET TEST CWP
PT400_	400100	Pipe impulse	IMPULSE TEST CWP
PT400_	200100	Surge Free Decay	DECAY SURGE
PT400_	200200	Sway Free Decay	DECAY SWAY
PT400_	200300	Heave Free Decay	DECAY HEAVE
PT400_	200400	Roll Free Decay	DECAY ROLL
PT400_	200500	Pitch Free Decay	DECAY PITCH
PT400_	200600	Yaw Free Decay	DECAY YAW
T400_	100100	Regular Wave 1	REG H2.0 T6.36
T400_	100200	Regular Wave 2	REG H2.5 T7.0
T400_	100300	Regular Wave 3	REG H3.6 T8.5
T400_	100400	Regular Wave 4	REG H5.0 T10.0
T400_	100500	Regular Wave 5	REG H6.6 T11.5
T400_	100600	Regular Wave 6	REG H8.5 T13.0
T400_	100700	Regular Wave 7	REG H11.3 T15.0
T400_	200100	100 Year Cyclone	IRR JS H10.2 T12.8 G2.0 Uw 33.8
T400_	200200	10-yr Sea	IRR JS H4.2 T8.3 G1.0 Uw 15.7
T400_	200300	10-yr Swell	IRR JS H3.8 T15.7 G6.0 Uw 14.6
T400_	200400	Fatigue Wave	IRR JS H2.5 T16.6 G6.0 Uw 8.0
T400_	500100	White Noise	WN H2.5 DT 3.5 25.0 Uw 8.0

Appendix F - Table 16 Group T500 Tests

GROUP	T500		
DESCRIPTION	CWP INSTALLATION 1		
CLIENTS REF	GROUP 3		
GROUP	NUMBER	CLIENTS REF	ID
PT500_	00100	GM l	INCLINING PITCH
PT500_	00200	GM t	INCLINING ROLL
PT500_	300100	Pipe bottom Surge Static offse	OFFSET TEST CWP
PT500_	400100	Pipe impulse	IMPULSE TEST CWP
PT500_	200500	Pitch Free Decay	DECAY PITCH
T500_	100100	Regular Wave 1	REG H2.0 T6.36
T500_	100200	Regular Wave 2	REG H2.5 T7.0
T500_	100300	Regular Wave 3	REG H3.6 T8.5
T500_	100400	Regular Wave 4	REG H5.0 T10.0
T500_	100500	Regular Wave 5	REG H6.6 T11.5
T500_	100600	Regular Wave 6	REG H8.5 T13.0
T500_	100700	Regular Wave 7	REG H11.3 T15.0
T500_	200200	10-yr Sea	IRR JS H4.2 T8.3 G1.0 Uw 15.7
T500_	200300	10-yr Swell	IRR JS H3.8 T15.7 G6.0 Uw 14.6
T500_	500100	White Noise	WN H2.5 DT 3.5 25.0 Uw 8.0

Appendix F - Table 17 Group T600 Tests

GROUP	T600		
DESCRIPTION	CWP INSTALLATION 2		
CLIENTS REF	GROUP 4		
GROUP	NUMBER	CLIENTS REF	ID
PT600_	00100	GM l	INCLINING PITCH
PT600_	00200	GM t	INCLINING ROLL
PT600_	300100	Pipe bottom Surge Static offse	OFFSET TEST CWP
PT600_	400100	Pipe impulse	IMPULSE TEST CWP
PT600_	200100	Surge Free Decay	DECAY SURGE
PT600_	200200	Sway Free Decay	DECAY SWAY
PT600_	200300	Heave Free Decay	DECAY HEAVE
PT600_	200400	Roll Free Decay	DECAY ROLL
PT600_	200500	Pitch Free Decay	DECAY PITCH
PT600_	200600	Yaw Free Decay	DECAY YAW
T600_	100100	Regular Wave 1	REG H2.0 T6.36
T600_	100200	Regular Wave 2	REG H2.5 T7.0
T600_	100300	Regular Wave 3	REG H3.6 T8.5
T600_	100400	Regular Wave 4	REG H5.0 T10.0
T600_	100500	Regular Wave 5	REG H6.6 T11.5
T600_	100600	Regular Wave 6	REG H8.5 T13.0
T600_	100700	Regular Wave 7	REG H11.3 T15.0
T600_	200200	10-yr Sea	IRR JS H4.2 T8.3 G1.0 Uw 15.7
T600_	200300	10-yr Swell	IRR JS H3.8 T15.7 G6.0 Uw 14.6
T600_	500100	White Noise	WN H2.5 DT 3.5 25.0 Uw 8.0

G. CONSOLIDATED AS-BUILT TABLES

This page intentionally left blank.

The file associated with this appendix material titled "Consolidated As-Built Tables.xlsm" is provided in a DVD attached to Appendix H. Tab names in this appendix refer to Excel© worksheet tabs.

'Scaling & Channels' Tab

Scale Factors

Multiplier (Conversion Factor) from model to full scale

Geometric Scale, λ	50	
Seawater Density, ρ_F	1025	kg/m^3
Basin Density, ρ_M	992.2	kg/m^3

OD_{Core}	1.9105	m
OD_{Sheath}	10.49	m

Froude Scaling		
length	λ	50
Mass	$\lambda^3\rho_F/\rho_M$	129132.2
Force	$\lambda^3\rho_F/\rho_M$	129132.2
Acceleration	1	1
Moment	$\lambda^4\rho_F/\rho_M$	6456612
Time	$\sqrt{\lambda}$	7.071068

Wave Probe Locations	x	y
WAVE1_C	-625	0
WAVE2_C	0	0
WAVE3_C	0	-375
WAVE4_C	27	0
WAVE5_C	27	-375

'Scaling & Channels' Tab (continued)

Derived Channels				
Channel	**Min**	**Max**	**Units**	**CF**
Airgap	-10	20	m	50
Gimbal_Fx	-10000	10000	KN	129132.2
Gimbal_Fy	-10000	10000	KN	129132.2
Gimbal_Fz	0	25000	KN	129132.2
Gimbal_Pitch	-15	15	Degrees	-
Gimbal_Roll	-15	15	Degrees	-
Mooring1	0	25000	KN	129132.2
Mooring2	0	25000	KN	129132.2
Mooring3	0	25000	KN	129132.2
Mooring4	0	25000	KN	129132.2
Pullout_Semi	0	40000	KN	129132.2
Pullout_CWP	0	40000	KN	129132.2
Runup	-15	30	m	50
SG1	-0.02	0.02	-	5.490709
SG10	-0.02	0.02	-	5.490709
SG11	-0.02	0.02	-	5.490709
SG12	-0.02	0.02	-	5.490709
SG13	-0.02	0.02	-	5.490709
SG14	-0.02	0.02	-	5.490709
SG15	-0.02	0.02	-	5.490709
SG16	-0.02	0.02	-	5.490709
SG17	-0.02	0.02	-	5.490709
SG18	-0.02	0.02	-	5.490709
SG19	-0.02	0.02	-	5.490709
SG2	-0.02	0.02	-	5.490709
SG20	-0.02	0.02	-	5.490709
SG3	-0.02	0.02	-	5.490709
SG4	-0.02	0.02	-	5.490709
SG5	-0.02	0.02	-	5.490709
SG6	-0.02	0.02	-	5.490709
SG7	-0.02	0.02	-	5.490709
SG8	-0.02	0.02	-	5.490709
SG9	-0.02	0.02	-	5.490709
CWP1_X	-50	50	m	50
CWP1_Y	-50	50	m	50
CWP1_Z	-50	50	m	50
CWP2_X	-50	50	m	50
CWP2_Y	-50	50	m	50
CWP2_Z	-50	50	m	50
CWP3_X	-50	50	m	50
CWP3_Y	-50	50	m	50
CWP3_Z	-50	50	m	50

Derived Channels				
CWP4_X	-50	50	m	50
CWP4_Y	-50	50	m	50
CWP4_Z	-50	50	m	50
CWP5_X	-50	50	m	50
CWP5_Y	-50	50	m	50
CWP5_Z	-50	50	m	50
CWP6_X	-50	50	m	50
CWP6_Y	-50	50	m	50
CWP6_Z	-50	50	m	50
Semi_X	-50	100	m	50
Semi_Y	-50	50	m	50
Semi_Z	-20	20	m	50
Semi_Pitch	-15	15	Degrees	-
Semi_Roll	-15	15	Degrees	-
Semi_Yaw	-20	20	Degrees	-
WAVE1	-15	15	m	50
WAVE3	-15	15	m	50
WAVE5	-15	15	m	50
WAVE1_C	-15	15	m	50
WAVE2_C	-15	15	m	50
WAVE3_C	-15	15	m	50
WAVE4_C	-15	15	m	50
WAVE5_C	-15	15	m	50
Wind	0	3000	KN	129132.2

'Scaling & Channels' Tab (continued)

Acquired (Raw) Channels (model scale)			
AMTI1_Fx	Raw Dynamometer forces and moments		
AMTI1_Fy			
AMTI1_Fz			
AMTI1_Mx			
AMTI1_My			
AMTI1_Mz			
AMTI2_Fx			
AMTI2_Fy			
AMTI2_Fz			
AMTI2_Mx			
AMTI2_My			
AMTI2_Mz			
AMTI3_Fx			
AMTI3_Fy			
AMTI3_Fz			
AMTI3_Mx			
AMTI3_My			
AMTI3_Mz			
AMTI4_Fx			
AMTI4_Fy			
AMTI4_Fz			
AMTI4_Mx			
AMTI4_My			
AMTI4_Mz			
Airgap			
CWP1_X			
CWP1_Y			
CWP1_Z			
CWP2_X			
CWP2_Y			
CWP2_Z			
CWP3_X			
CWP3_Y			
CWP3_Z			
CWP4_X			
CWP4_Y			
CWP4_Z			
CWP5_X			

Acquired (Raw) Channels (model scale)			
CWP5_Y			
CWP5_Z			
CWP6_X			
CWP6_Y			
CWP6_Z			
Gimbal_Fx			
Gimbal_Fy			
Gimbal_Fz			
Gimbal_Pitch			
Gimbal_Roll			
LVDT0	Raw LVDT readings		
LVDT1			
LVDT2			
LVDT3			
Mooring1			
Mooring2			
Mooring3			
Mooring4			
Pullout_CWP			
Pullout_Semi			
Pullout_YAW			
Runup			
SG1			
SG10			
SG11			
SG12			
SG13			
SG14			
SG15			
SG16			
SG17			
SG18			
SG19			
SG2			
SG20			
SG3			
SG4			
SG5			
SG6			
SG7			

Acquired (Raw) Channels (model scale)			
SG8			
SG9			
Semi_Pitch			
Semi_Roll			
Semi_X			
Semi_Y			
Semi_Yaw			
Semi_Z			
WAVE1			
WAVE3			
WAVE5			
WAVE1_C	Calibrated Wave Time Histories		
WAVE2_C			
WAVE3_C			
WAVE4_C			
WAVE5_C			
Wind			

'Tolerance" Tab

Tolerances for Semi, Gimbal, CWP and Testing.

These tolerances from the basis for dry test acceptance criteria

Hull Weight & Mass Properties - Installation Condition

	Tolerance +/-	Unit	Scale
Weight (dry)	0.50	%	
LCG	10	cm	Full
TCG	10	cm	Full
VCG	10	cm	Full
Radius of Gyration, kxx	5	%	
Radius of Gyration, kyy	5	%	
Radius of Gyration, kzz	5	%	

Hull Weight & Mass Properties - Operational Condition (combined model)

	Tolerance +/-	Unit
Weight (dry)	0.50	%
LCG	10	cm
TCG	10	cm
VCG	10	cm
Radius of Gyration, kxx	5	%
Radius of Gyration, kyy	5	%
Radius of Gyration, kzz	5	%

Cold Water Pipe

	Tolerance +/-	Unit	Scale
Length	10	cm	Full
Diameter	10	cm	Full
EI	10	%	
Wet Weight	0.5	%	

Gimbal

	Tolerance +/-	Unit	Scale
Rotational Stiffness	10	%	
Horizontal Stiffness			
Gimbal Rotational Accuracy	? (0.1)	°	
Dynamomter Accuracy	?		

'Tolerance' Tab (continued)

Waves				
	Tolerance +/-	Unit	Scale	
Hs	2	%		
Tp	0.2	s	Full	
Peak Energy (80%)	10	%		80% of energy below the peak
MPM Crest - 100yr	+10	%		
Crest Max	+10	%		
10 Successive Regular Waves				
H	2	%		
T	0.2	s	Full	

Testing			
Sampling Freq	4	Hz	Full
Incline Tests	5	%	Variance from predicted
Free decay tests	5	%	Variance from predicted

'Semi Dimensions' Tab

Semi Hull Principle Dimensions			
Item	Units	Table 2-1	As Built
Column height	m	33	33.02
Column depth	m	14	14.1
Column width	m	14	14.1
Column center to center spacing	m	56	56
Pontoon length	m	42	41.86
Pontoon height	m	8.5	9.4
Pontoon width	m	14	14.1
Deck length	m	70	70.05
Deck width	m	70	70.05
Upper deck elevation (TOS)	m	39.5	39.49
Lower deck elevation (BOS)	m	33	33.02
Installed draft	m	20	20

Semi Hydrostatics (model) from as-built dimensions				
Item	Units	Test Spec	As Built	
Draft	m	20	20	
KB	**m**	**6.81**	**6.47**	Only this value is used from this table
KMt	m	23.88	22.08	
BMt	m	17.07	15.61	
KMl	m	23.88	22.08	
BMl	m	17.07	15.61	
LCB	m	0	0	
TCB	m	0	0	
Displacement	t	37672.64	41769.06	This displacement is not accurate – based on hydrostatic model

'Semi Dimensions' Tab (continued)

Free Floating LONGITUDINAL Incline Test results	
Target	
Displacement (t)	41472
Target VCG, KG (m)	18.40
Estimated Metacentric Height, GM (m)	3.92
Results	
Calculated VCG, KG (m)	18.967
Measured Metacentric Height, GM (m)	**3.913**
Δ VCG (%)	3.09%
Δ GM (%)	-0.18%

From results provided by LabOceano 8/11/13

Note = Static tank specific gravity was 995kg/m3

Free Floating TRANSVERSE Incline Test results	
Target	
Displacement (t)	41472
Target VCG, KG (m)	18.40
Estimated Metacentric Height, GM (m)	3.92
Results	
Calculated VCG, KG (m)	19.000
Measured Metacentric Height, GM (m)	**3.880**
Δ VCG (%)	3.27%
Δ GM (%)	-1.02%

From results provided by LabOceano 8/11/13

'Remoras' Tab

Individual Remora Mass Properties (as per specification)(table 2-5)	w/ Ent. Water
Total Weight, t	30183.1
KG (ref base of Remora)	31.65
kxx, m	~~21.12~~
kyy, m	~~21.47~~
kzz, m	~~8.21~~

Remoras Buoyancy	w/ Ent. Water
Remora Buoyancy	181098
Remora KB	-16.6

'Remoras' Tab (continued)

Individual Remora Mass Properties as per MassProperties_130212.xlsx (Prototype scale)						
w/entrained water						
kxx, m	15.66	15.66	15.66	15.66	15.66	15.66
kyy, m	15.34	15.34	15.34	15.34	15.34	15.34
kzz, m	7.28	7.28	7.28	7.28	7.28	7.28

As built Mass Properties (w. entrained water) - model scale	Remora 1-1	Remora 1-2	Remora 2-1	Remora 3-1	Remora 3-2	Remora 4-1
Mass (Kg)	233.917	233.833	233.097	234.35	233.68	233.287
XCG (mm)	-1.5	-0.2	0	-1.6	-0.9	0.3
YCG (mm)	1.3	-0.5	0.5	-1.2	-2	-0.5
VCG (mm)	635.9	632.6	633.4	634.6	633.4	634.1
kxx (mm)	314.9	317.3	315.1	316.6	316.7	315.4
kyy (mm)	318.8	318.5	319.5	320.4	321.2	319.5
kzz (mm)	150.2	149.1	149.7	149.4	150	149.8
Prototype Scale						
Mass (t)	30151.5	30140.7	30045.8	30207.3	30121.0	30070.3
% error	0.10%	0.14%	0.45%	0.08%	0.21%	0.37%
VCG (m)	31.80	31.63	31.67	31.73	31.67	31.71
abs error (cm)	14.50	2.00	2.00	8.00	2.00	5.50
kxx (m)	15.75	15.87	15.76	15.83	15.84	15.77
% error	0.56%	1.32%	0.62%	1.10%	1.13%	0.72%
kyy (m)	15.94	15.93	15.98	16.02	16.06	15.98
% error	3.93%	3.83%	4.16%	4.45%	4.71%	4.16%
kzz (m)	7.51	7.46	7.49	7.47	7.50	7.49
% error	3.15%	2.39%	2.80%	2.60%	3.01%	2.87%

'Remoras' Tab (continued)

Target CG Locations

	Remora 1-1	Remora 1-2	Remora 2-1	Remora 3-1	Remora 3-2	Remora 4-1	
XCG	45.40	45.40	0.00	-45.40	-45.40	0.00	
YCG	14.30	-14.30	-45.40	14.30	-14.30	45.40	(Note: YCG was +/- 12.5)
ZCG	-41.50	-41.50	-41.50	-41.50	-41.50	-41.50	

Prototype Scale	Remora 1-1	Remora 1-2	Remora 2-1	Remora 3-1	Remora 3-2	Remora 4-1
Mass (Kg)	3E+07	3E+07	3E+07	3E+07	3E+07	3E+07
XCG (m)	-0.075	-0.01	0	-0.08	-0.045	0.015
YCG (m)	0.065	-0.025	0.025	-0.06	-0.1	-0.025
VCG (m)	31.795	31.63	31.67	31.73	31.67	31.705
kxx (m)	15.745	15.865	15.755	15.83	15.835	15.77
kyy (m)	15.94	15.925	15.975	16.02	16.06	15.975
kzz (m)	7.51	7.455	7.485	7.47	7.5	7.49
XCG (m)	45.40	45.40	0.00	-45.40	-45.40	0.00
YCG (m)	14.30	-14.30	-45.40	14.30	-14.30	45.40
ZCG (m)	-41.41	-41.57	-41.53	-41.47	-41.53	-41.50

Apply Parallel Axis Theorem							Remora I
ixx	7.5E+09	7.6E+09	7.5E+09	7.6E+09	7.6E+09	7.5E+09	
iyy	7.7E+09	7.7E+09	7.7E+09	7.8E+09	7.8E+09	7.7E+09	
izz	1.7E+09	1.7E+09	1.7E+09	1.7E+09	1.7E+09	1.7E+09	
Ixx	1.6E+10	1.6E+10	7.1E+10	1.6E+10	1.6E+10	7.1E+10	2.0E+11
Iyy	7.2E+10	7.2E+10	9.4E+09	7.2E+10	7.1E+10	9.4E+09	3.0E+11
Izz	7.0E+10	7.0E+10	6.4E+10	7.0E+10	7.0E+10	6.4E+10	4.1E+11

'Remoras' Tab (continued)

Semi Properties				
	T100	T200	Check	
m (t)	41471	220739	222535	
Rgx (m)	28.58977	35.28	32.76	
Rgy (m)	28.72559	41.19	39.04	
Rgz (m)	30.17929	44.76	44.76	
Ixx (t.m2)	33897211	2.75E+08	2.39E+08	87%
Iyy (t.m2)	34220041	3.74E+08	3.39E+08	91%
Izz (t.m2)	37771178	4.42E+08	4.46E+08	101%
XCG (m)	0.0525	-0.0405		
YCG (m)	-0.2105	-0.0325		
ZCG (m)	-1.992	-34.00	-34.14	
ZB (m)	-13.53	-32.23	-32.30	
GMx (m) (longitudinal)	3.913	20.2715		
GMy (m) (lateral)	3.88	14.1475		

'Remoras' Tab (continued)

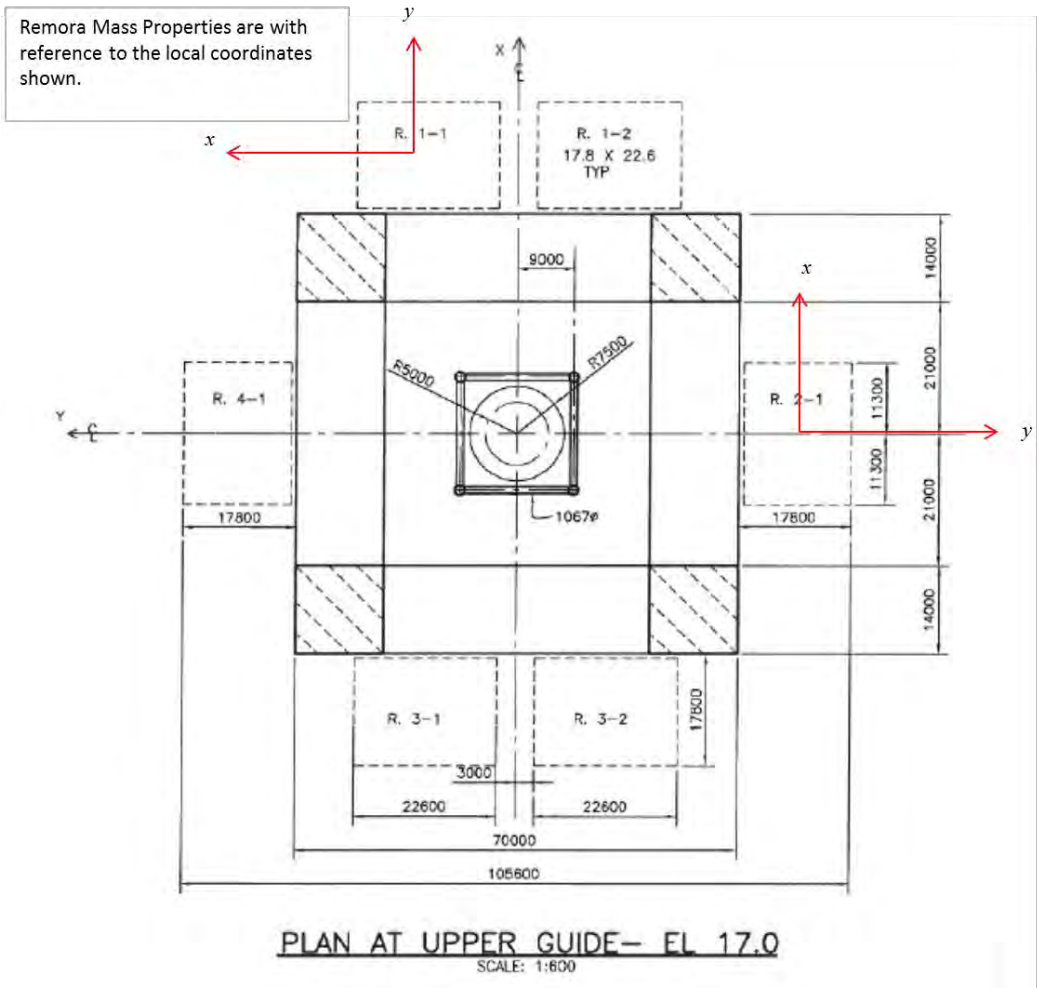

'Mass Properties' Tab

Semi Properties (T100)	Model Spec	As-built			
		Model	Prototype	Δ	
m (t)	37672.6	0.32115	41470.8	10.08	%
Rgx (m)	28.9	0.572	28.590	-1.20	%
Rgy (m)	28.9	0.575	28.726	-0.73	%
Rgz (m)	31.1	0.604	30.179	-2.82	%
Ixx (t.m2)	3.15E+07	1.05E-01	3.39E+07	7.45	%
Iyy (t.m2)	3.15E+07	0.106	3.42E+07	8.47	%
Izz (t.m2)	3.63E+07	1.17E-01	3.78E+07	3.95	%
XCG (m)	0	0.00105	0.0525	5.25	cm
YCG (m)	0	-0.00421	-0.2105	-21.05	cm
KG (m)	18.40	0.360	18.008	-38.96	cm
KB (m)	6.81	0.129	6.470	-5.04	%
GMy (m) (pitch)	5.49	0.078	3.913	-28.69	%
GMx (m) (roll)	5.49	0.078	3.880	-29.29	%

Source Mass Properties spreadsheet, Rev. 12/02/2013

	Semi Alone		As Built	
Buoyancy	Value (t)	KB	Value (t)	KB
Columns	9241.0	14.25		
Nodes	6831.0	4.25		
Pontoons	20492.0	4.25		
Guide Support	1085.6	8.04		
Guides	23.0	6.00		
Remoras (6)	0.0	0.00	0.00	0.00
Total Buoyancy	37672.6	6.81	41769.06	6.47
Mass	Value (t)	KG		
Deck	11972.0	44.00		
Hull	9761.0	9.30		
Guide Support	1737.3	8.74		
Ballast	14202.4	4.25		
Remoras	0.0	0.00		
Total Ballasted Hull Weight	37672.6	18.40		
Rgx	28.9			
Rgy	28.9			
Rgz	31.1			
Vertical Loads	0.0	0.00		
Total Weight+Vertical Loads	37672.6	18.40		
Iwpx	627461			
BMx	17.07		15.61	
GMx (incl vertical loads)	5.49			
Iwpy	627461			
Bmy	17.07			
Gmy	5.49			

'Mass Properties' Tab (continued)

Semi + Remoras Properties (T200)	Model Spec	As-built			
		Model	Prototype	Δ	
m (t)	218771.1	1.7094	220738.6	0.90	%
Rgx (m)	35.0	~~0.706~~	~~35.279~~	0.68	%
Rgy (m)	41.3	~~0.824~~	~~41.189~~	-0.32	%
Rgz (m)	44.7	~~0.895~~	~~44.762~~	0.03	%
Ixx (t.m2)	2.69E+08	~~8.51E-01~~	~~2.75E+08~~	2.28	%
Iyy (t.m2)	3.74E+08	~~1.16~~	~~3.74E+08~~	0.25	%
Izz (t.m2)	4.38E+08	~~1.37E+00~~	~~4.42E+08~~	0.96	%
XCG (m)	0	-0.00081	-0.0405	-4.05	cm
YCG (m)	0	-0.00065	-0.0325	-3.25	cm
KG (m)	-14.61	-0.280	-13.999	61.40	cm
KB (m)	-12.57	-0.245	-12.23	-2.69%	%
GMy (m) (pitch)	21.47	0.405	20.27	-5.59	%
GMx (m) (roll)	14.35	0.283	14.15	-1.43	%

See Remoras Sheet for Updated Mass Properties for T200 and T400

	Semi+Remoras	
Buoyancy	Value (t)	KB
Columns	9241.0	14.25
Nodes	6831.0	4.25
Pontoons	20492.0	4.25
Guide Support	1085.6	8.04
Guides	23.0	6.00
Remoras (6)	181098.4	-16.60
Total Buoyancy	218771.1	-12.57
Mass	Value (t)	KG
Deck	11972.0	44.00
Hull	9761.0	9.30
Guide Support	1737.3	8.74
Ballast	14202.4	4.25
Remoras	181098.4	-21.48
Total Ballasted Hull Weight	218771.1	-14.61
Rgx	35.0	
Rgy	41.3	
Rgz	44.7	
Vertical Loads	0.0	0.00
Total Weight+Vertical Loads	218771.1	-14.61
Iwpx	2626946	
BMx	12.31	
GMx (incl vertical loads)	14.35	
Iwpy	4146558	
Bmy	19.43	
Gmy	21.47	

'Mass Properties' Tab (continued)

Operational A & B (T300 & 400)	Model Spec	As-built			
		Model	Prototype	Δ	
m (t)	218771.1	1.7094	220738.6	0.90	%
Rgx (m)	35.1	~~0.706~~	~~35.279~~	0.46	%
Rgy (m)	41.4	~~0.824~~	~~41.189~~	-0.62	%
Rgz (m)	44.9	~~0.895~~	~~44.762~~	-0.22	%
Ixx (t.m2)	2.70E+08	~~8.51E-01~~	~~2.75E+08~~	1.83	%
Iyy (t.m2)	3.76E+08	~~1.16E+00~~	~~3.74E+08~~	-0.34	%
Izz (t.m2)	4.40E+08	~~1.37E+00~~	~~4.42E+08~~	0.45	%
XCG (m)	0	-0.0008	-0.04	-4.00	cm
YCG (m)	0	-0.00065	-0.0325	-3.25	cm
KG (m)	-14.70	-0.289	-14.467	23.44	cm
KB (m)	-12.57	-0.245	-12.23	-2.69%	%
GMy (m) (pitch)	21.56	0.405	20.27	-5.98	%
GMx (m) (roll)	14.44	0.283	14.15	-2.03	%

See Remoras Sheet for Updated Mass Properties for T200 and T400

	Op. A & B	
Buoyancy	Value (t)	KB
Columns	9241.0	14.25
Nodes	6831.0	4.25
Pontoons	20492.0	4.25
Guide Support	1085.6	8.04
Guides	23.0	6.00
Remoras (6)	181098.4	-16.60
Total Buoyancy	218771.1	-12.57
Mass	Value (t)	KG
Deck	11972.0	44.00
Hull	9761.0	9.30
Guide Support	1737.3	8.74
Ballast	12125.1	4.25
Remoras	181098.4	-21.48
Total Ballasted Hull Weight	216693.8	-14.79
Rgx	35.1	
Rgy	41.4	
Rgz	44.9	
Vertical Loads	2077.3	-5.00
Total Weight+Vertical Loads	218771.1	-14.70
Iwpx	2626946	
BMx	12.31	
GMx (incl vertical loads)	14.44	
Iwpy	4146558	
Bmy	19.43	
Gmy	21.56	

'Mass Properties' Tab (continued)

Installation 1 (T500)	Model Spec	As-built			
		Model	Prototype	Δ	
m (t)	37672.6	0.31879	41166.1	9.27	%
Rgx (m)	29.0	0.571	28.558	-1.51	%
Rgy (m)	29.0	0.577	28.832	-0.57	%
Rgz (m)	31.1	0.606	30.291	-2.49	%
Ixx (t.m2)	3.17E+07	1.04E-01	3.36E+07	6.00	%
Iyy (t.m2)	3.17E+07	1.06E-01	3.42E+07	8.04	%
Izz (t.m2)	3.64E+07	1.17E-01	3.78E+07	3.90	%
XCG (m)	0	0.0001	0.005	0.50	cm
YCG (m)	0	-0.00457	-0.2285	-22.85	cm
KG (m)	18.14	0.359	17.929	-21.36	cm
KB (m)	6.81			-100.00%	%
GMy (m) (pitch)	5.74			-100.00	%
GMx (m) (roll)	5.74			-100.00	%

	CWP Install 1	
Buoyancy	Value (t)	KB
Columns	9241.0	14.25
Nodes	6831.0	4.25
Pontoons	20492.0	4.25
Guide Support	1085.6	8.04
Guides	23.0	6.00
Remoras (6)	0.0	0.00
Total Buoyancy	37672.6	6.81
Mass	Value (t)	KG
Deck	11972.0	44.00
Hull	9761.0	9.30
Guide Support	1737.3	8.74
Ballast	13163.8	4.25
Remoras	0.0	0.00
Total Ballasted Hull Weight	36634.0	18.80
Rgx	29.0	
Rgy	29.0	
Rgz	31.1	
Vertical Loads	1038.6	-5.00
Total Weight+Vertical Loads	37672.6	18.14
Iwpx	627461	
BMx	17.07	
GMx (incl vertical loads)	5.74	
Iwpy	627461	
Bmy	17.07	
Gmy	5.74	

'Mass Properties' Tab (continued)

Installation 2 (T600)	Model Spec	As-built			
		Model	Prototype	Δ	
m (t)	37672.6	0.31412	40563.0	7.67	%
Rgx (m)	29.1	0.564	28.211	-2.89	%
Rgy (m)	29.1	0.578	28.908	-0.49	%
Rgz (m)	31.1	0.594	29.722	-4.35	%
Ixx (t.m2)	3.18E+07	1.00E-01	3.23E+07	1.54	%
Iyy (t.m2)	3.18E+07	1.05E-01	3.39E+07	6.61	%
Izz (t.m2)	3.64E+07	1.11E-01	3.58E+07	-1.48	%
XCG (m)	0	-0.0002	-0.01	-1.00	cm
YCG (m)	0	-0.00422	-0.211	-21.10	cm
KG (m)	17.89	0.358	17.880	-0.81	cm
KB (m)	6.81			-100.00%	%
GMy (m) (pitch)	6.00			-100.00	%
GMx (m) (roll)	6.00			-100.00	%

	CWP Install 2	
Buoyancy	Value (t)	KB
Columns	9241.0	14.25
Nodes	6831.0	4.25
Pontoons	20492.0	4.25
Guide Support	1085.6	8.04
Guides	23.0	6.00
Remoras (6)	0.0	0.00
Total Buoyancy	37672.6	6.81
Mass	Value (t)	KG
Deck	11972.0	44.00
Hull	9761.0	9.30
Guide Support	1737.3	8.74
Ballast	12125.1	4.25
Remoras	0.0	0.00
Total Ballasted Hull Weight	35595.3	19.22
Rgx	29.1	
Rgy	29.1	
Rgz	31.1	
Vertical Loads	2077.3	-5.00
Total Weight+Vertical Loads	37672.6	17.89
Iwpx	627461	
BMx	17.07	
GMx (incl vertical loads)	6.00	
Iwpy	627461	
Bmy	17.07	
Gmy	6.00	

'CWP' Tab

Summary CWP Characteristics (model spec)	Units	Prototype
Inside diameter including Resin Distribution Layer	m	10.01
Outside Diameter including Resin Distribution Layer	m	10.49
Length	m	1,000.80
Bottom Weight, wet weight	kN	-
Mass, CWP - no bottom weight - no internal water	kg	4,807,809
% wall that is void inc RDL	%	65.3
Total wet Weight including bottom weight	tonnes	2,077.30
EA	kN	7.35E+07
EI	kN-m^2	9.50E+08
Wet Weight per unit length of circumference:	tonnes/cm	0.63
Air Pressure to float:	atm	2.58
Natural frequency of CWP/pad interaction.	sec	1.21

CWP impulse test data not included here. Results from these tests deemed unreliable.

CWP Static Offset test data not included here. Results from these tests deemed unreliable.

Simply Supported Beam Test Results

Results of simply supported beam tests provided below in Model Scale

Applied Weight (kg)	y (mm) at point of loading
0	0
1.781	12.7
2.863	20.93
3.904	29.99
2.863	22.57
1.781	14.73
0	0.92

'CWP' Tab (continued)

Compute bending Stiffness using beam flexure relationship (Model scale)		
l, beam Length	4963.3	mm
a, distance to load from left support	2978	mm
b, distance to point load from right support	1985.3	mm
x, location of deflection calculation	2978	mm
dy / dP (line of best fit through above data)	0.765840979	mm/N
Calculate EI from gradient of load-displacement curve		
EI (model scale)	**3.065288036**	**kNm^2**
EI (prototype scale)	**9.90E+08**	**kNm^2**

Results from Flexcom Analysis (HOE)

Model Scale			Full Scale				Model Scale
Dead Weight of CWP (kg)	Applied Load (kg)	Vertical Displacement (mm) at point of loading	Applied Load +Weight (N)	Applied Load (N)	Vertical Displacement (m) at point of loading	Calculated EI (Nm^2)	Calculated EI (Nm^2)
10.875	0	0.46	1.3722E+07	0.0000E+00	0.02	-	-
10.875	1.781	13.72	1.3722E+07	2.2472E+06	0.69	9.92E+11	3.08E+03
10.875	2.863	21.75	1.3722E+07	3.6124E+06	1.09	9.94E+11	3.09E+03
10.875	3.904	29.99	1.3722E+07	4.9259E+06	1.50	9.77E+11	3.04E+03

'CWP' Tab (continued)

	Model Scale	Prototype Scale	
Strain Gauge	Position [mm]	Position [m]	Direction
1	916	-45.8	x
2	1816	-90.8	x
3	2916	-145.8	x
4	4016	-200.8	x
5	5116	-255.8	x
6	6216	-310.8	x
7	7316	-365.8	x
8	8396	-419.8	x
9	9736	-486.8	x
10	10636	-531.8	x
11	11716	-585.8	x
12	12816	-640.8	x
13	13916	-695.8	x
14	15016	-750.8	x
15	16116	-805.8	x
16	17216	-860.8	x
17	18316	-915.8	x
18	19396	-969.8	x
19	7186	-359.3	y
20	13846	-692.3	y

position relative to semi reference frame - z=0=MWL

CWP Dry Weight	Model Scale (g)	Prototype (tonnes)
Design 1/2 CWP Mass	22475.78	2902.35
Design Full CWP Mass	45157.68	5831.31
As-built 1/2 CWP Mass	22479.2	2902.79

'CWP(2)' Tab

	MODEL SCALE				PROTOTYPE SCALE								
Section	Start [mm]	End [mm]	Mass per Length [g/mm]	EI [N.mm²]	Start [m]	End [m]	Mass per Length [kg/m]	EI [KN.m²]	Core Tube	Con-nector	Outer Sheet 1	Outer Sheet 20	Outer Sheet 2 - 19
1	0	20	6.07	7.14E+09	0	1	15676.65289	2.31E+09	*	*			
2	20	51.1	3.14	7.14E+09	1	2.555	8109.504132	2.31E+09	*	*			
3	51.1	263.6	0.83	2.95E+09	2.555	13.18	2143.595041	9.52E+08	*				
4	263.6	328.6	3.14	7.14E+09	13.18	16.43	8109.504132	2.31E+09	*	*			
5	328.6	1010.32	2.47	2.95E+09	16.43	50.516	6379.132231	9.52E+08	*		*		
6	1010.32	1020.32	0.83	2.95E+09	50.516	51.016	2143.595041	9.52E+08	*				
7	1020.32	2000.62	2.37	2.95E+09	51.016	100.031	6120.867769	9.52E+08	*				*
8	2000.62	2010.62	0.83	2.95E+09	100.031	100.531	2143.595041	9.52E+08	*				
9	2010.62	2990.92	2.22	2.95E+09	100.531	149.546	5733.471074	9.52E+08	*				*
10	2990.92	3000.92	0.83	2.95E+09	149.546	150.046	2143.595041	9.52E+08	*				
11	3000.92	3981.22	2.3	2.95E+09	150.046	199.061	5940.082645	9.52E+08	*				*
12	3981.22	3991.22	0.83	2.95E+09	199.061	199.561	2143.595041	9.52E+08	*				
13	3991.22	4971.52	2.2	2.95E+09	199.561	248.576	5681.818182	9.52E+08	*				*
14	4971.52	5036.52	3.14	7.14E+09	248.576	251.826	8109.504132	2.31E+09	*	*			
15	5036.52	6016.82	2.21	2.95E+09	251.826	300.841	5707.644628	9.52E+08	*				*
16	6016.82	6026.82	0.83	2.95E+09	300.841	301.341	2143.595041	9.52E+08	*				
17	6026.82	7007.12	2.26	2.95E+09	301.341	350.356	5836.77686	9.52E+08	*				*
18	7007.12	7017.12	0.83	2.95E+09	350.356	350.856	2143.595041	9.52E+08	*				
19	7017.12	7997.42	2.16	2.95E+09	350.856	399.871	5578.512397	9.52E+08	*				*
20	7997.42	8007.42	0.83	2.95E+09	399.871	400.371	2143.595041	9.52E+08	*				
21	8007.42	8987.72	2.23	2.95E+09	400.371	449.386	5759.297521	9.52E+08	*				*
22	8987.72	8997.72	0.83	2.95E+09	449.386	449.886	2143.595041	9.52E+08	*				
23	8997.72	9978.02	2.4	2.95E+09	449.886	498.901	6198.347107	9.52E+08	*				*
24	9978.02	10008.02	3.14	7.14E+09	498.901	500.401	8109.504132	2.31E+09	*	*			
25	10008.02	10043.02	3.14	7.14E+09	500.401	502.151	8109.504132	2.31E+09	*	*			
26	10043.02	11023.32	2.23	2.95E+09	502.151	551.166	5759.297521	9.52E+08	*				*
27	11023.32	11033.32	0.83	2.95E+09	551.166	551.666	2143.595041	9.52E+08	*				
28	11033.32	12013.62	2.21	2.95E+09	551.666	600.681	5707.644628	9.52E+08	*				*
29	12013.62	12023.62	0.83	2.95E+09	600.681	601.181	2143.595041	9.52E+08	*				
30	12023.62	13003.92	2.23	2.95E+09	601.181	650.196	5759.297521	9.52E+08	*				*
31	13003.92	13013.92	0.83	2.95E+09	650.196	650.696	2143.595041	9.52E+08	*				
32	13013.92	13994.22	2.22	2.95E+09	650.696	699.711	5733.471074	9.52E+08	*				*
33	13994.22	14004.22	0.83	2.95E+09	699.711	700.211	2143.595041	9.52E+08	*				
34	14004.22	14984.52	2.28	2.95E+09	700.211	749.226	5888.429752	9.52E+08	*				*
35	14984.52	15049.52	3.14	7.14E+09	749.226	752.476	8109.504132	2.31E+09	*	*			
36	15049.52	16029.82	2.24	2.95E+09	752.476	801.491	5785.123967	9.52E+08	*				*
37	16029.82	16039.82	0.83	2.95E+09	801.491	801.991	2143.595041	9.52E+08	*				
38	16039.82	17020.12	2.34	2.95E+09	801.991	851.006	6043.38843	9.52E+08	*				*
39	17020.12	17030.12	0.83	2.95E+09	851.006	851.506	2143.595041	9.52E+08	*				
40	17030.12	18010.42	2.33	2.95E+09	851.506	900.521	6017.561983	9.52E+08	*				*
41	18010.42	18020.42	0.83	2.95E+09	900.521	901.021	2143.595041	9.52E+08	*				
42	18020.42	19000.72	2.25	2.95E+09	901.021	950.036	5810.950413	9.52E+08	*				*
43	19000.72	19010.72	0.83	2.95E+09	950.036	950.536	2143.595041	9.52E+08	*				
44	19010.72	19980.72	2.29	2.95E+09	950.536	999.036	5914.256198	9.52E+08	*			*	
45	19980.72	20016.02	0.83	2.95E+09	999.036	1000.801	2143.595041	9.52E+08	*				
Half CWP Mass	22475.78 g												
Full CWP Mass	45157.68 g												

'Gimbal' Tab

Gimbal stiffness and rotational properties			
Model Test Specification	Installation	Operation B	Operation A
Gimbal Angular Stiffness [N.m/rad]	4.93E+10	1.00E+09	0.00E+00
Gimbal Lateral Stiffness [N/m]	2.00E+08	2.00E+08	2.00E+08
Maximum angular offset [^{o}]	0.7	12	12
As built stiffness and gimbal rotation accuracy	Installation	Operation B	Operation A
Gimbal Angular Stiffness [N.m/rad]	9.55E+10	1.26E+09	0.00E+00
Gimbal Lateral Stiffness [N/m]	3.15E+08	3.36E+08	3.15E+08
Gimbal Rotation Accuracy [^{o}]	0.62^o	0.62^o	0.62^o
Δ (%)			
Gimbal Angular Stiffness	93.75%	25.84%	
Gimbal Lateral Stiffness	57.67%	67.87%	57.67%

Dynamometer Cross Talk Validation

	Direction of applied load		
Applied Force (zero offset) - Stage 1	x	y	z
Measured Fx / Applied Load (%)	**95.98**	4.46	-1.20
Measured Fz / Applied Load (%)	-3.40	**95.40**	-0.66
Measured Fz / Applied Load (%)	7.70	3.64	**95.92**
Applied Force (zero offset) - Stage 2	x	y	z
Measured Fx / Applied Load (%)	**97.07**	5.13	-1.49
Measured Fz / Applied Load (%)	-3.84	**97.13**	-0.99
Measured Fz / Applied Load (%)	9.47	3.61	**95.37**
Applied Force (y & z offset) - Stage 1	x	y	z
Measured Fx / Applied Load (%)	-	7.65	-1.50
Measured Fz / Applied Load (%)	-	**94.75**	-2.31
Measured Fz / Applied Load (%)	-	3.04	**95.85**
Applied Force (y & z offset) - Stage 2	x	y	z
Measured Fx / Applied Load (%)	-	8.45	-1.86
Measured Fz / Applied Load (%)	-	**95.71**	-2.04
Measured Fz / Applied Load (%)	-	4.56	**94.74**

'Mooring' Tab

SEMI MOORING: Taut Mooring stiffness: 650 kN/m

Pretension 13735 KN

Mooring Line Numbering

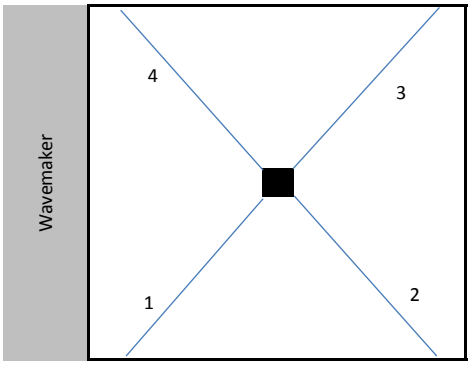

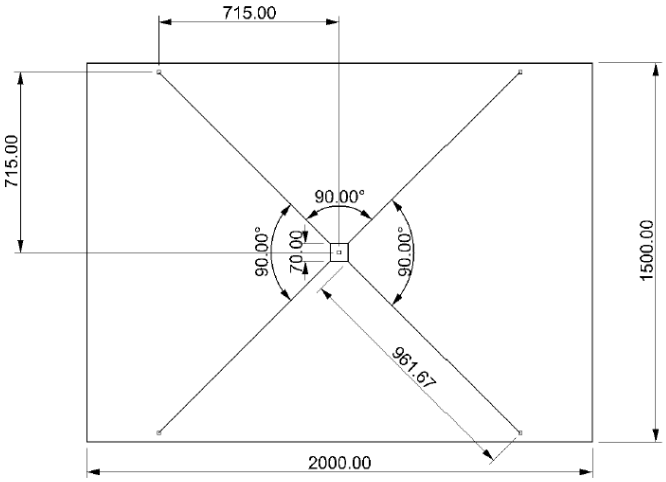

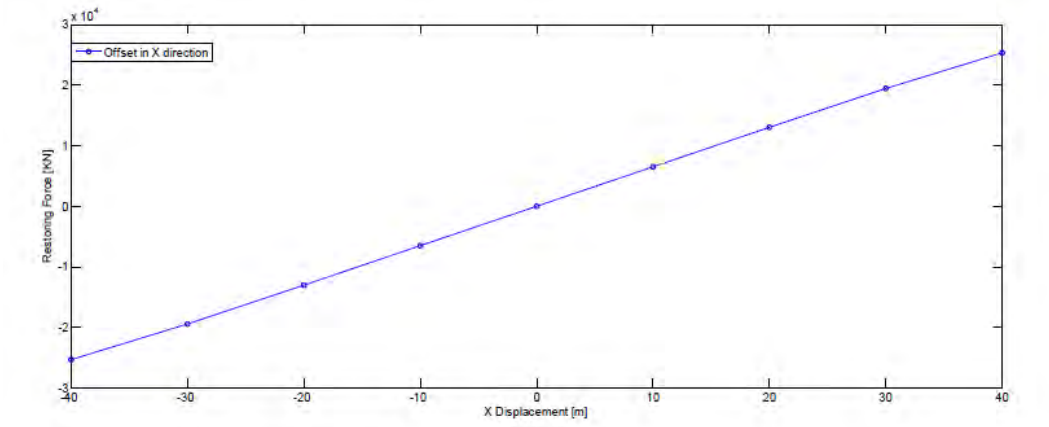

'Mooring' Tab (continued)

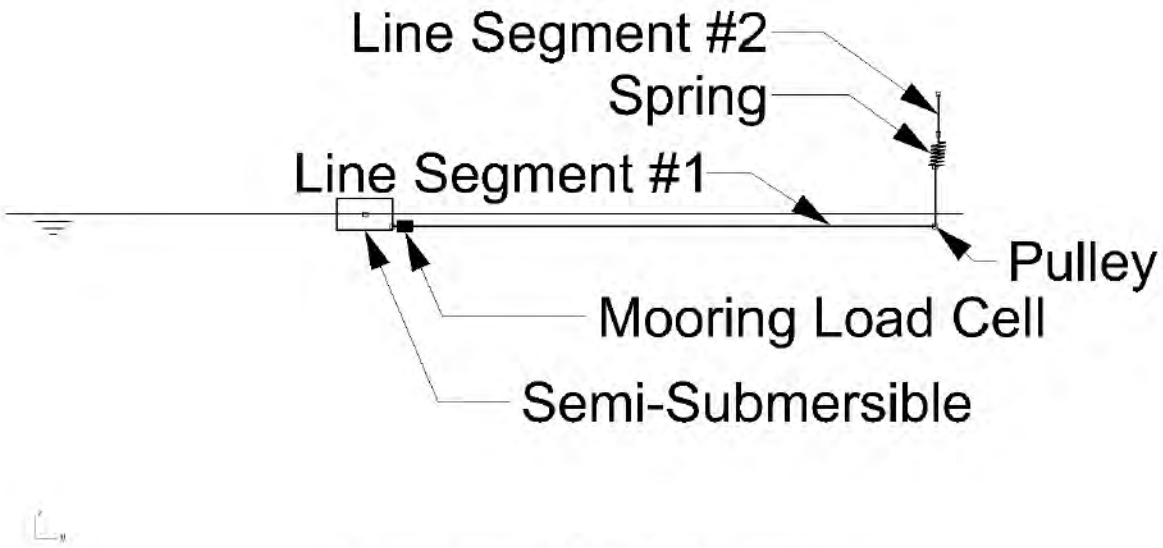

Figure 10. Model Mooring Elements

Those elements are described on table 2.

Table 4. Model Elements Description

Item	Description (Model - Full)	Length [m] (Prototype)	Weight (Prototype)	Length [mm] (Model)	Weight (Model)
Semi Fairleads	Eye bolt on model	See figure 5			
Fairlead Fixture	Shackle	See figure 6			
Mooring Load Cell	FUTEK 50lb	-	2.3 ton	-	18g
Line Segment #1	1.5 - 75mm Steel cable	1035	dry: 26 kg/m wet:21 kg/m	20,700	dry: 10g/m wet: 8g/m
Spring	126.5 g/cm - 320 KN/m	41.1 [unstreched]	-	821 [unstreched]	-
Line Segment #2	Adjustable length 16x9x2 chain	50	144 kg/m	1000	56 g/m
Line Fixture	Shackle on vertical strut	-			

'Waves' Tab

Model Test Spec (Table 3-1)	100 Year Cyclone	10-Yr Sea	10-Yr Swell	Fatigue Wave	White Noise
Uw, m/sec	33.8	15.7	14.6	8	8
Hs, m	10.2	4.2	3.8	2.5	2
Tp, sec	12.8	8.3	15.7	16.6	2 - 26
Gamma	2	1	6	6	
Hmax, m	16.9	8	7.1		
Amax, m	9.4	4.5	4		
Wind Force, kN (w/ remoras)	2002.2	432	373.6	112.2	112.2
Center of Pressure (w/ remoras)	14.3	14.3	14.3	14.3	14.3
Wind Force, kN (w/o remoras)	1547.2	333.8	288.7	86.7	86.7
Center of Pressure (w/o remoras)	16.6	16.6	16.6	16.6	16.6

Model Test Spec (Table 3-2)	H (m)	T (s)	Pre-test calibration	Post-test calibration
Regular Wave 1	1.5	5.5	*	
Regular Wave 2	2.5	7	*	
Regular Wave 3	3.6	8.5	*	
Regular Wave 4	5.0	10	*	
Regular Wave 5	6.6	11.5	*	
Regular Wave 6	8.5	13	*	
Regular Wave 7	11.3	15	*	

Cases correspond to constant steepness $H=0.05T^2$

2.02248

'Waves' Tab (continued)

Wave Calibration Results				
Irregular Waves	Parameter	Required	Measured	% Error
100-yr Cyclone	Hs	10.2	10.4	1.98%
	Tp	12.8	12.7	-0.10
	Hmax	16.9	17.69	4.68%
10-yr Sea	Hs	4.2	4.16	-1.00%
	Tp	8.3	8.47	0.17
	Hmax	8	7.51	-6.13%
10-yr Swell	Hs	3.8	3.78	-0.45%
	Tp	15.7	15.57	-0.13
	Hmax	7.1	6.74	-5.01%
Fatigue Wave	Hs	2.5	2.54	1.74%
	Tp	16.6	16.65	0.05

Regular Waves	H	Error	T	Error
Regular Wave 1	2.13		6.35	
Regular Wave 2	2.60	6.3%	7.00	0.00
Regular Wave 3	3.65	1.1%	8.50	0.00
Regular Wave 4	5.19	3.8%	10.00	0.00
Regular Wave 5	6.83	3.3%	11.49	-0.01
Regular Wave 6	8.36	-1.1%	13.02	0.02
Regular Wave 7	11.56	2.7%	15.00	0.00

Mean H & T from 15 consecutive regular waves after transient

Data from probe 2 - model centre

'Drawings' Tab

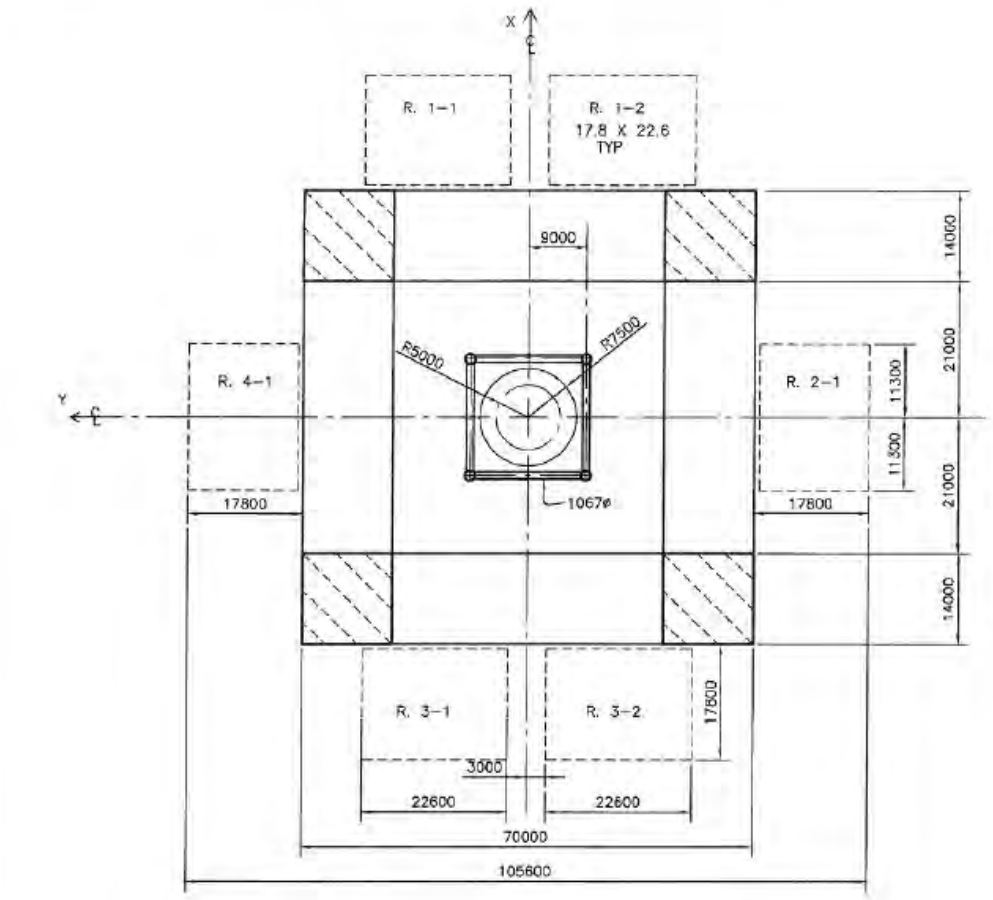

PLAN AT UPPER GUIDE– EL 17.0
SCALE: 1:600

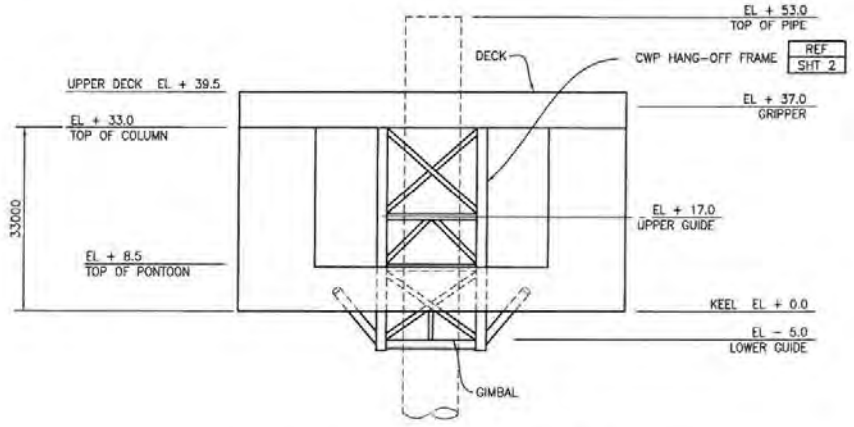

PLATFORM OUTBOARD PROFILE
SCALE: 1:600

'Drawings' Tab, continued

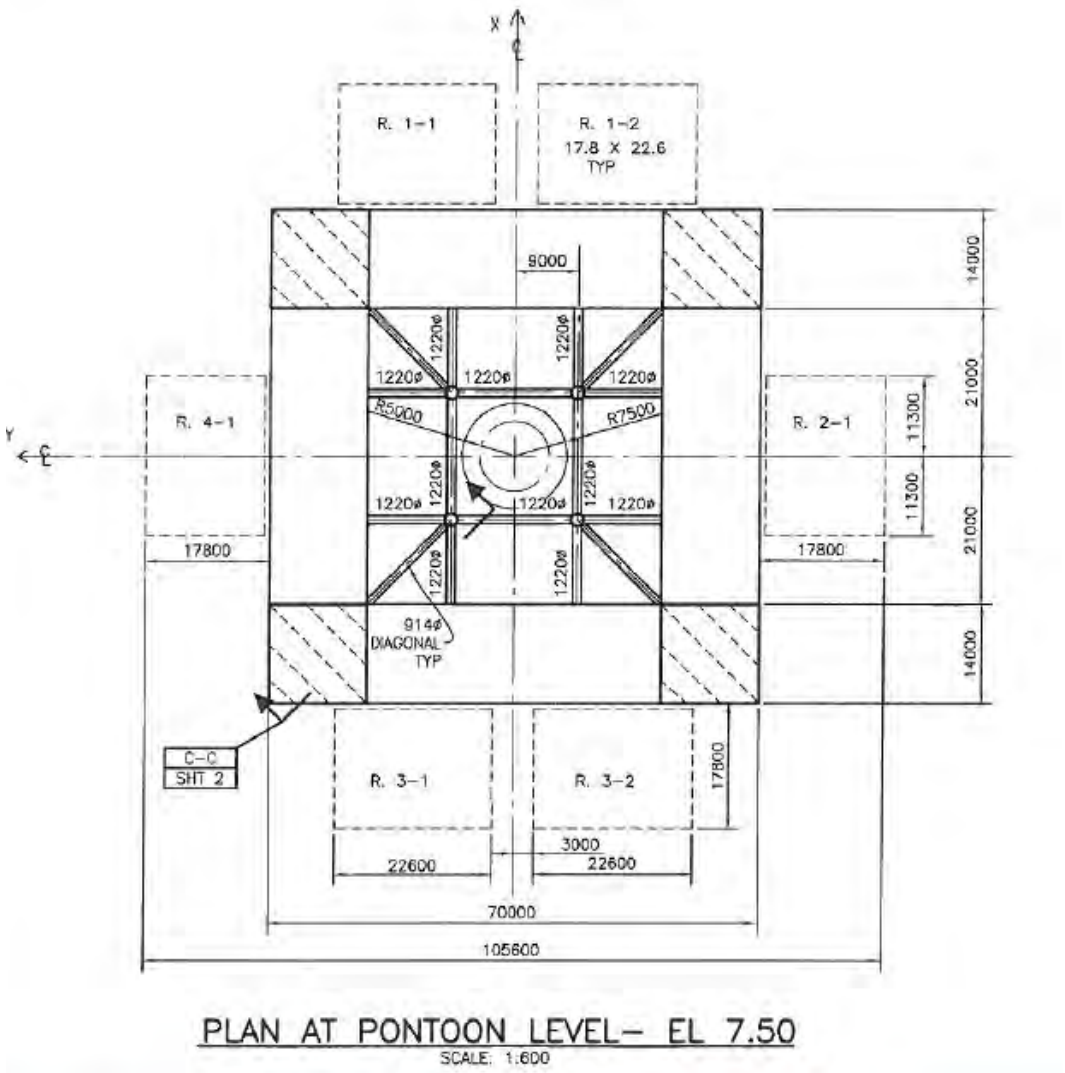

PLAN AT PONTOON LEVEL- EL 7.50
SCALE: 1:600

This page intentionally left blank.

H. REGULAR WAVE CALIBRATION SUMMARY

This page intentionally left blank.

The file associated with this appendix material titled “Regular Wave Calibration Summary.xlsm” is provided in a DVD attached to Appendix H. Tab names in this appendix refer to Excel© worksheet tabs.

‘Reg (1)’ Tab

Model Test Spec (Table 3-2)	H (m)	T (s)
Regular Wave 1	1.5	5.5
Regular Wave 2	2.5	7
Regular Wave 3	3.6	8.5
Regular Wave 4	5.0	10
Regular Wave 5	6.6	11.5
Regular Wave 6	8.5	13
Regular Wave 7	11.3	15

Regular Wave Verification	using WAVE3_C	
Num Waves	15	
Start Time	37.55	s

Prototype	Min	Mean	Max
H (m)	2.0143	2.1293	2.2774
A (m)	1.0505	1.1007	1.1725
T (s)	6.2978	6.3449	6.3812

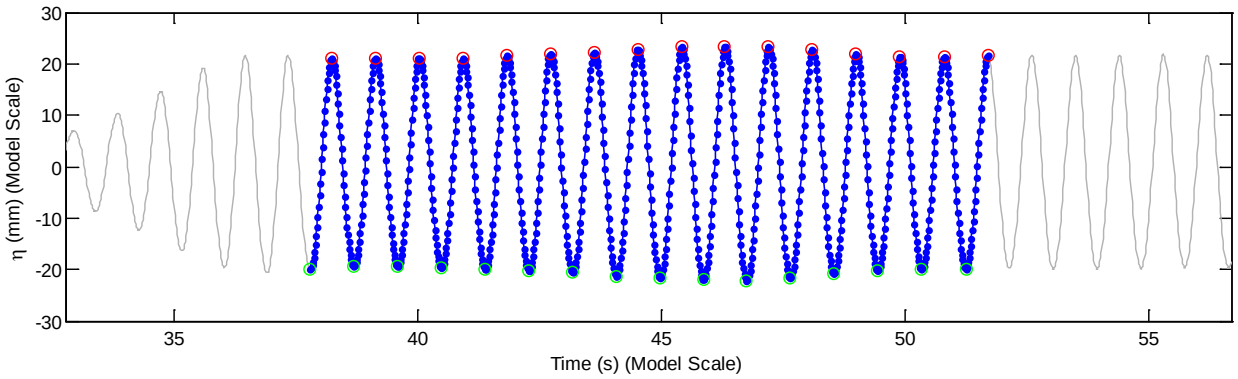

'Reg (2)' Tab

Model Test Spec (Table 3-2)	H (m)	T (s)
Regular Wave 1	1.5	5.5
Regular Wave 2	2.5	7
Regular Wave 3	3.6	8.5
Regular Wave 4	5.0	10
Regular Wave 5	6.6	11.5
Regular Wave 6	8.5	13
Regular Wave 7	11.3	15

Regular Wave Verification	using WAVE2_C	
Num Waves	15	
Start Time	37.55	s

Prototype	Min	Mean	Max
H (m)	2.58	2.60	2.64
A (m)	1.37	1.38	1.39
T (s)	6.99	7.00	7.01

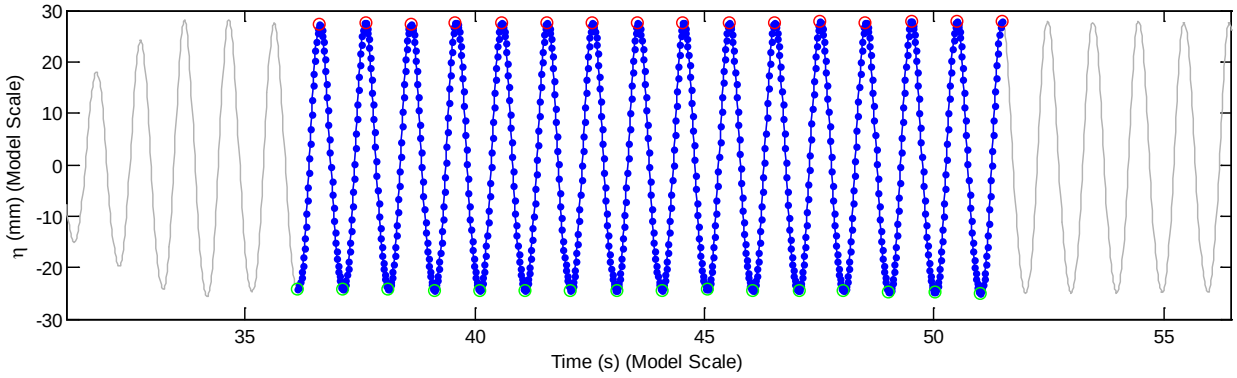

'Reg (3)' Tab

Model Test Spec (Table 3-2)	H (m)	T (s)
Regular Wave 1	1.5	5.5
Regular Wave 2	2.5	7
Regular Wave 3	3.6	8.5
Regular Wave 4	5.0	10
Regular Wave 5	6.6	11.5
Regular Wave 6	8.5	13
Regular Wave 7	11.3	15

Regular Wave Verification

Num Waves	15	
Start Time	34	s

Prototype	Min	Mean	Max
H (m)	3.6283	3.6527	3.6913
A (m)	1.8987	1.9173	1.9316
T (s)	8.4861	8.5047	8.5183

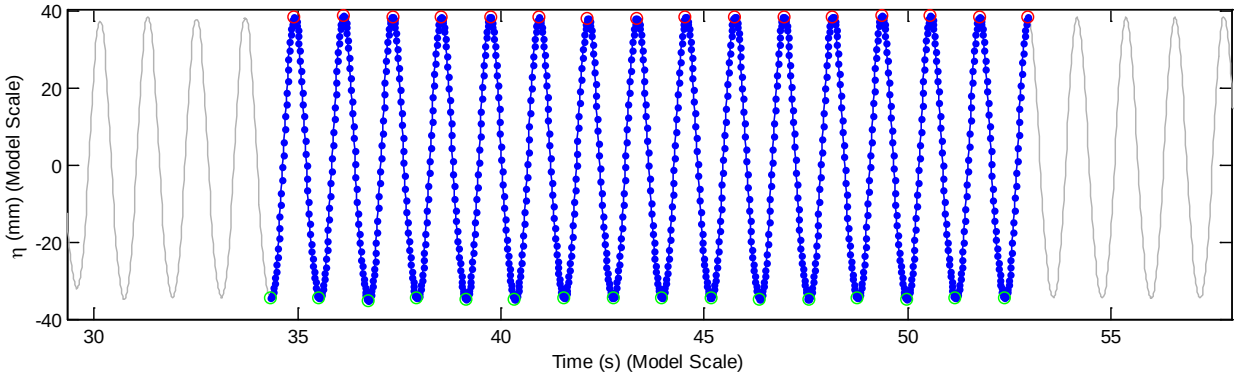

'Reg (4)' Tab

Model Test Spec (Table 3-2)	H (m)	T (s)
Regular Wave 1	1.5	5.5
Regular Wave 2	2.5	7
Regular Wave 3	3.6	8.5
Regular Wave 4	5.0	10
Regular Wave 5	6.6	11.5
Regular Wave 6	8.5	13
Regular Wave 7	11.3	15

Regular Wave Verification

Num Waves	15	
Start Time	30	s

Prototype	Min	Mean	Max
H (m)	5.0954	5.1903	5.3311
A (m)	2.6293	2.6847	2.7458
T (s)	9.9797	9.9999	10.0305

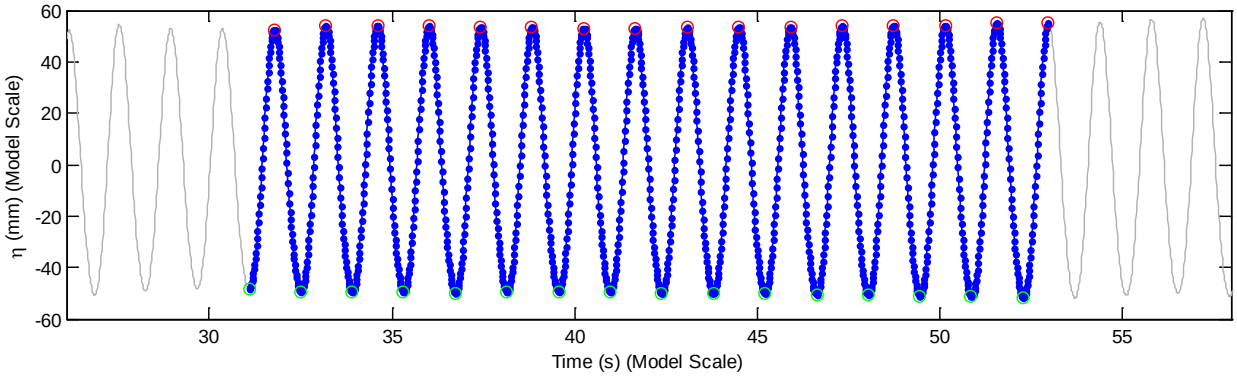

'Reg (5)' Tab

Model Test Spec (Table 3-2)	H (m)	T (s)
Regular Wave 1	1.5	5.5
Regular Wave 2	2.5	7
Regular Wave 3	3.6	8.5
Regular Wave 4	5.0	10
Regular Wave 5	6.6	11.5
Regular Wave 6	8.5	13
Regular Wave 7	11.3	15

Regular Wave Verification

Num Waves	15	
Start Time	28	s

Prototype	Min	Mean	Max
H (m)	6.7032	6.8308	6.9864
A (m)	3.5032	3.5441	3.6017
T (s)	11.4822	11.4932	11.5132

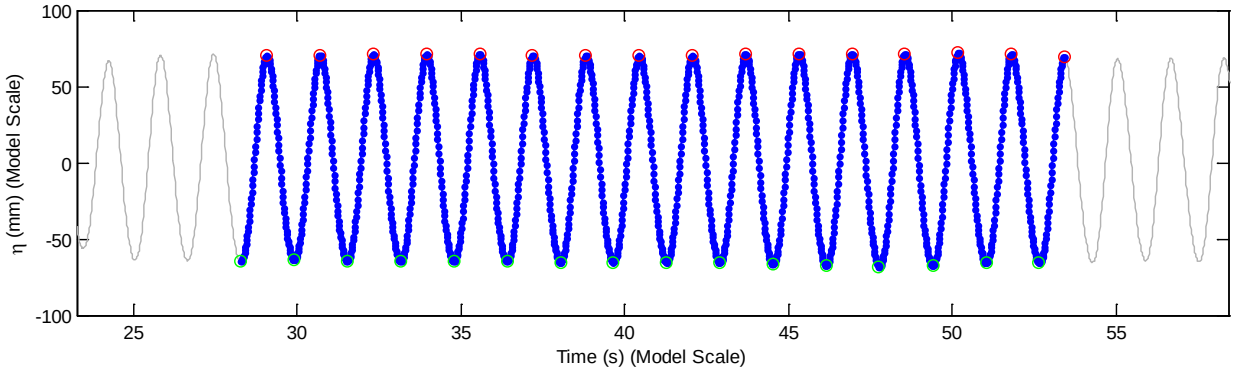

'Reg (6)' Tab

Model Test Spec (Table 3-2)	H (m)	T (s)
Regular Wave 1	1.5	5.5
Regular Wave 2	2.5	7
Regular Wave 3	3.6	8.5
Regular Wave 4	5.0	10
Regular Wave 5	6.6	11.5
Regular Wave 6	8.5	13
Regular Wave 7	11.3	15

Regular Wave Verification

Num Waves	15	
Start Time	28	s

Prototype	Min	Mean	Max
H (m)	8.1192	8.3568	8.5002
A (m)	4.2543	4.3419	4.4602
T (s)	12.9532	13.0229	13.086

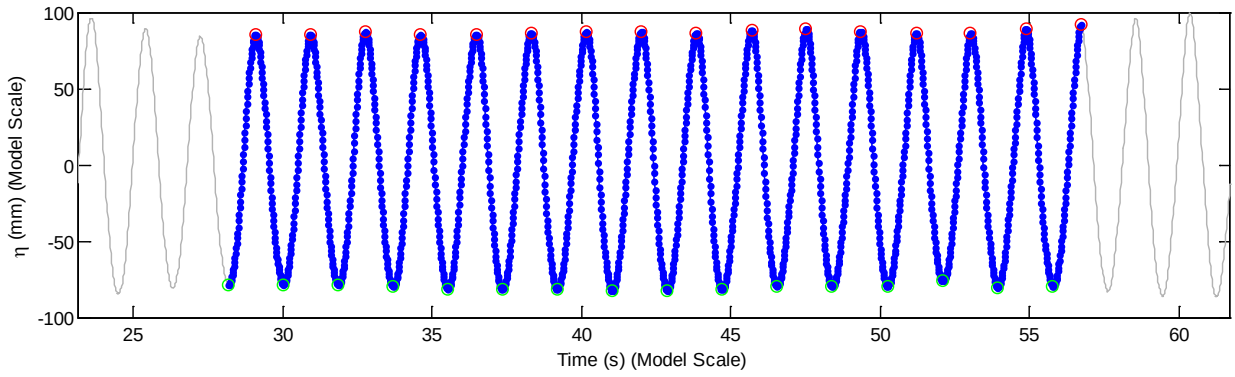

'Reg (7)' Tab

Model Test Spec (Table 3-2)	H (m)	T (s)
Regular Wave 1	1.5	5.5
Regular Wave 2	2.5	7
Regular Wave 3	3.6	8.5
Regular Wave 4	5.0	10
Regular Wave 5	6.6	11.5
Regular Wave 6	8.5	13
Regular Wave 7	11.3	15

Regular Wave Verification

Num Waves	15	
Start Time	26	s

Prototype	Min	Mean	Max
H (m)	10.469	11.5593	12.3619
A (m)	5.604	6.1154	6.5273
T (s)	14.8536	15.0028	15.1955

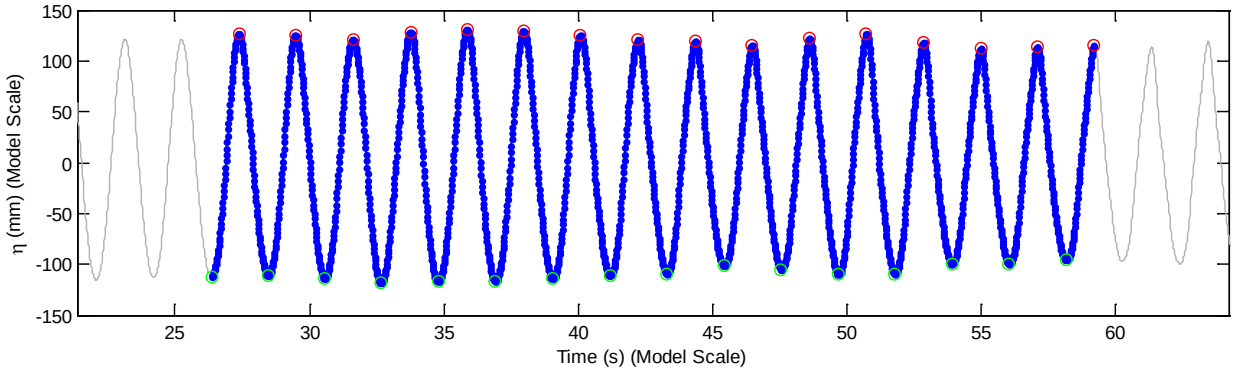

This page intentionally left blank.

I. IRREGULAR WAVE CALIBRATION SUMMARY

This page intentionally left blank.

The file associated with this appendix material titled “Irregular Wave Calibration Summary.xlsm” is provided in a DVD attached to Appendix H. Tab names in this appendix refer to Excel© worksheet tabs.

Irregular Wave Calibration Summary: 100-Year Cyclone

Spectra based on calibrated wave signal measured at model origin (Probe 2). FFT, Hanning window, size =2^{11}, 50% overlap. Digital data is available on the DVD file, Appendix K.

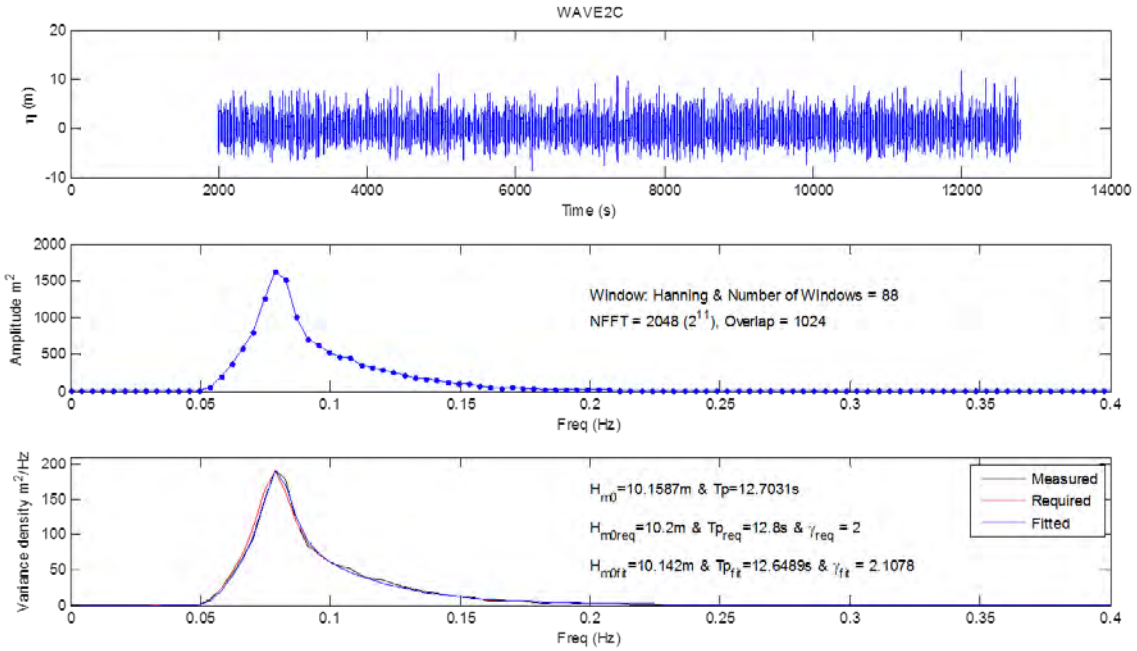

Spectral Density	
f (Hz)	Sηη (m^2s)
m0	6.45
m1	0.6218
m2	0.0688
m3	0.0099
m4	0.0024

Irregular Wave Calibration Summary: 10-Year Sea

Spectra based on calibrated wave signal measured at model origin (Probe 2). FFT, Hanning window, size =2^{11}, 50% overlap. Digital data is available on the DVD file, Appendix K.

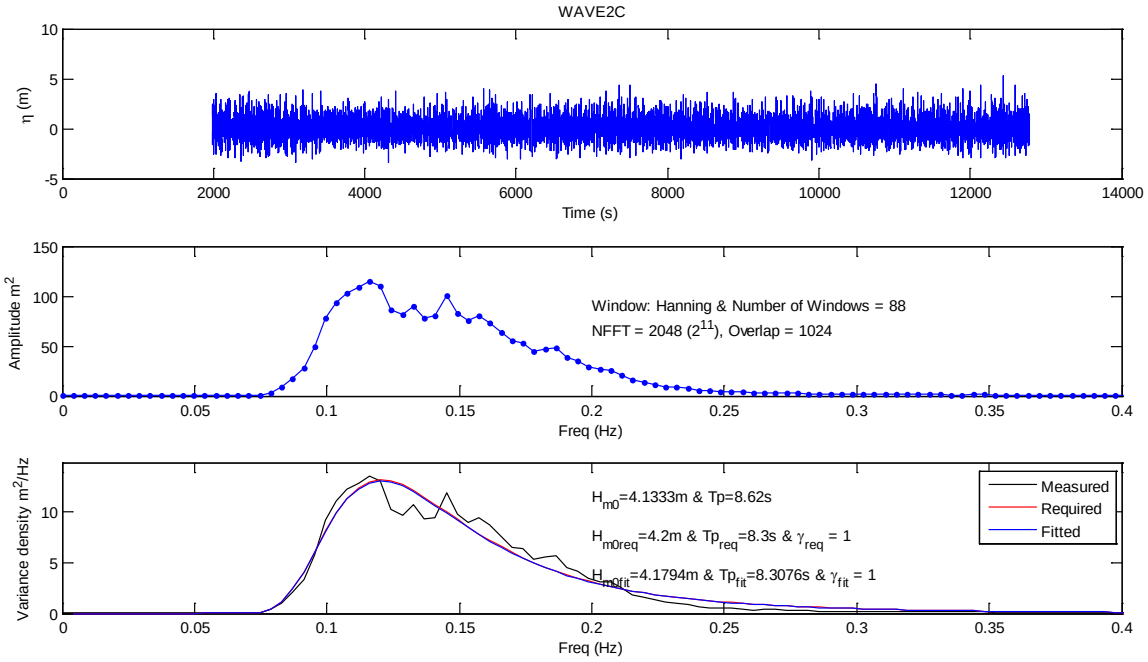

Spectral Density	
f (Hz)	Sηη (m^2s)
m0	1.0678
m1	0.1592
m2	0.0265
m3	0.0052
m4	0.0014

Irregular Wave Calibration Summary: 10-Year Swell

Spectra based on calibrated wave signal measured at model origin (Probe 2). FFT, Hanning window, size =2^{11}, 50% overlap. Digital data is available on the DVD file, Appendix K.

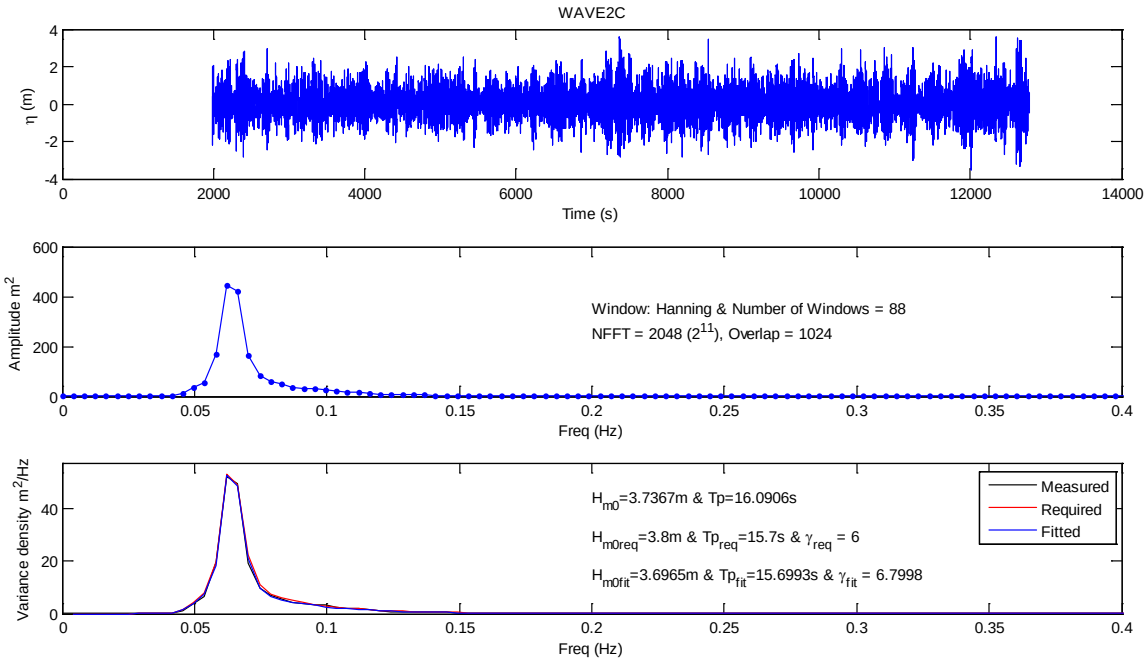

Spectral Density	
f (Hz)	Sηη (m^2s)
m0	0.8727
m1	0.0657
m2	0.006
m3	0.0008
m4	0.0002

Irregular Wave Calibration Summary: Fatigue Wave

Spectra based on calibrated wave signal measured at model origin (Probe 2). FFT, Hanning window, size =2^{11}, 50% overlap. Digital data is available on the DVD file, Appendix K.

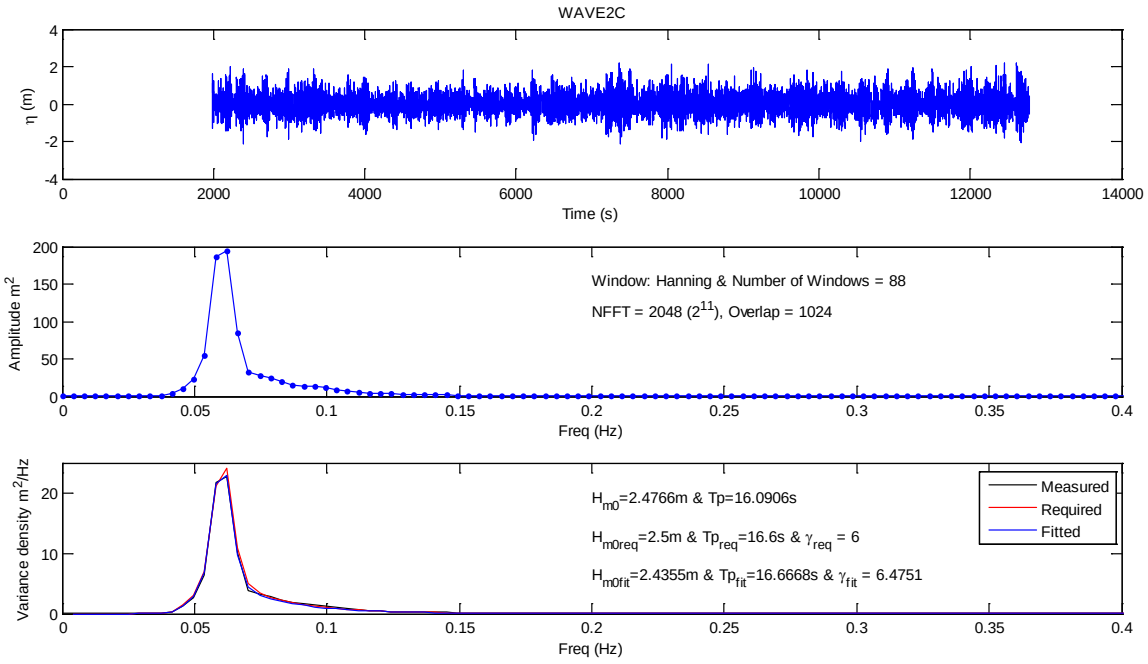

Spectral Density	
f (Hz)	Sηη (m^2s)
m0	0.3834
m1	0.0278
m2	0.0025
m3	0.0003
m4	0.0001

Irregular Wave Calibration Summary: White Noise

Spectra based on white noise calibrated wave signal measured at model origin. FFT, Hanning window, size =2^{11}, 50% overlap. Digital data is available on the DVD file, Appendix K.

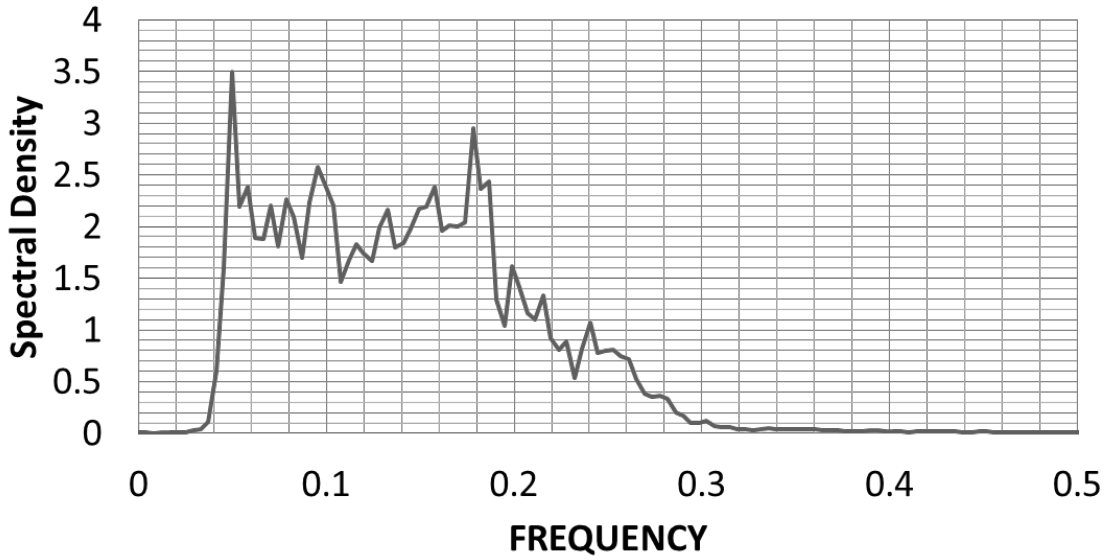

Spectral Density	
f (Hz)	$S\eta\eta$ (m^2s)
m0	0.399
m1	0.0572
m2	0.0101
m3	0.0021
m4	0.0005

Hs (m) = 2.53

This page intentionally left blank.

J. NUMERICAL MODEL PARAMETERS

This page intentionally left blank.

OTEC Model Dry-Tests Report
November, 08th, 2013
By: Thiago Marinho

1 T100 - Semi Alone

1.1 Model As-Built Dimensions

The main as-built dimensions are summarized on table.

Item	units	Specified	As-Built
Column heigth	m	33	33.02
Column depth	m	14	14.1
Column width	m	14	14.1
Column center to center spacing	m	56	56
Pontoon length	m	42	41.86
Pontoon heigth	m	8.5	9.4
Pontoon width	m	14	14.1
Deck length	m	70	70.05
Deck width	m	70	70.05
Upper deck elevation	m	39.5	39.49
Lower deck elevation	m	33	33.02
Installed draft	m	20	-

1.2 Mass Properties

The model summarized mass properties and ballast plan are presented on table.

Final Inertial Properties									
Prototype Target Values			Model Target Values		Model Obtained Values			deviation	
rho_{agua}	1025.0	kg/m³	-	kg/m³	rho_{agua}	992.2	kg/m³		
m	4.177E+04	ton	323.450	kg	m	321.15	kg	-0.71	%
Ixx	3.498E+07	ton.m²	1.08E+08	kg.mm²	Ixx	1.05E+08	kg.mm²	-3.49	%
Iyy	3.498E+07	ton.m²	1.08E+08	kg.mm²	Iyy	1.06E+08	kg.mm²	-1.95	%
Izz	4.029E+07	ton.m²	1.25E+08	kg.mm²	Izz	1.17E+08	kg.mm²	-6.18	%
Xcg	0.000	m-SM	0.00	mm	Xcg	1.05	mm-SM	1.05	mm
Ycg	0.000	m-LC	0.00	mm	Ycg	-4.21	mm-LC	-4.21	mm
Zcg	18.400	m-LB	368.00	mm	Zcg	360.16	mm-LB	-2.13	%

1.3 Model Hydrostatics

The updated hydrostatic properties, based on a numerical model with as-built dimensions and the observed model draft are summarized on table.

Semi Hydrostatics	units	Specified	As-Built
Draft	m	20	20
KB	m	6.81	6.47
KMt	m	23.88	22.08
BMt	m	17.07	15.61
KMl	m	23.88	22.08
BMl	m	17.07	15.61
LCB	m	0	0.00
TCB	m	0	0.00
TPC	t/cm	-	8.36
Displacement	t	37672.64	41769.06

1.4 Longitudinal Metacentric Height - GM l

	Model Scale	Full Scale
R6.1 Displacement, Δ [kgf; t]:	321.15	**41472**
R6.2 Target VCG, KG_{req} [mm; m]:	368	**18.400**
R6.3 Estimated Metacentric Height, GM_{req} [mm, m]	78	**3.920**
R6.4 Calculated VCG, KG_{obt} [mm; m]:	**379**	**18.967**
R6.5 Measured Metacentric Height, GM_{obt} [mm, m]	**78**	**3.913**
R6.6 VCG deviation [mm, %]:	**11**	**3.1%**
R6.7 GM deviation [mm, %]:	**0**	**-0.2%**

1.5 Transversal Metacentric Height - GM t

	Model Scale	Full Scale
R6.1 Displacement, Δ [kgf; t]:	321.15	**41472**
R6.2 Target VCG, KG_{req} [mm; m]:	368	**18.400**
R6.3 Estimated Metacentric Height, GM_{req} [mm, m]	78	**3.920**
R6.4 Calculated VCG, KG_{obt} [mm; m]:	**380**	**19.000**
R6.5 Measured Metacentric Height, GM_{obt} [mm, m]	**78**	**3.880**
R6.6 VCG deviation [mm, %]:	**12**	**3.3%**
R6.7 GM deviation [mm, %]:	**-1**	**-1.0%**

2 T200 - Semi & Remoras

2.1 Model As-Built Dimensions

The Remora model dimensions deviation were small and within tolerance, for this reason the specified dimensions were used on the hydrostatic model. Refer to section 1.1.

2.2 Mass Properties

The model summarized mass properties and ballast plan are presented on table.

Final Inertial Properties									
Prototype Target Values			Model Target Values		Model Obtained Values			deviation	
rho_{agua}	1025.0	kg/m³	-	kg/m³	rho_{agua}	992.2	kg/m³		
m	2.226E+05	ton	1723.918	kg	m	1725.55	kg	0.09	%
Ixx	0.000E+00	ton.m²	0.00E+00	kg.mm²	Ixx	8.72E+08	kg.mm²	#DIV/0!	%
Iyy	0.000E+00	ton.m²	0.00E+00	kg.mm²	Iyy	1.19E+09	kg.mm²	#DIV/0!	%
Izz	0.000E+00	ton.m²	0.00E+00	kg.mm²	Izz	1.38E+09	kg.mm²	#DIV/0!	%
Xcg	0.000	m-SM	0.00	mm	Xcg	-0.81	mm-SM	-0.81	mm
Ycg	0.000	m-LC	0.00	mm	Ycg	-0.65	mm-LC	-0.65	mm
Zcg	-14.610	m-LB	-292.20	mm	Zcg	-279.98	mm-LB	-4.18	%

2.3 Model Hydrostatics

The updated hydrostatic properties, based on a numerical model with as-built dimensions and the observed model draft are summarized on table.

Semi Hydrostatics	units	Target	As-Built
Draft	m	20	20
KB	m	-12.23	-12.23
KMt	m	0.26	0.26
BMt	m	12.49	12.49
KMl	m	6.31	6.31
BMl	m	18.54	18.54
LCB	m	0	0
TCB	m	0	0
TPC	t/cm	33.10	33.10
Displacement	t	222620.07	222620.07

2.4 Longitudinal Metacentric Height - GM l

	Model Scale	Full Scale
R6.1 Displacement, Δ [kgf; t]:	1709.4	220745311
R6.2 Target VCG, KG_{req} [mm; m]:	-292	-14.610
R6.3 Estimated Metacentric Height, GM_{req} [mm, m]	413	20.640
R6.4 Calculated VCG, KG_{obt} [mm; m]:	-285	-14.242
R6.5 Measured Metacentric Height, GM_{obt} [mm, m]	405	20.272
R6.6 VCG deviation [mm, %]:	7	-2.5%
R6.7 GM deviation [mm, %]:	-7	-1.8%

2.5 Transversal Metacentric Height - GM t

	Model Scale	Full Scale
R6.1 Displacement, Δ [kgf; t]:	1709.4	**220745311**
R6.2 Target VCG, KG_{req} [mm; m]:	-292	**-14.610**
R6.3 Estimated Metacentric Height, GM_{req} [mm, m]	295	**14.759**
R6.4 Calculated VCG, KG_{obt} [mm; m]:	**-280**	**-13.998**
R6.5 Measured Metacentric Height, GM_{obt} [mm, m]	**283**	**14.148**
R6.6 VCG deviation [mm, %]:	**12**	**-4.2%**

3 T400 - Operations B

3.1 Model As-Built Dimensions

Refer to section 1.1.

3.2 Mass Properties

The model summarized mass properties and ballast plan are presented on table X. The model target mass has been updated in order to achieve the required draft with an additional vertical load equivalent to the CWP design wet weight, 2077.3 tonf.

Final Inertial Properties									
Prototype Target Values			Model Target Values		Model Obtained Values			deviation	
rho_{agua}	1025.0	kg/m³	-	kg/m³	rho_{agua}	992.2	kg/m³		
m	2.205E+05	ton	1707.832	kg	m	1709.40	kg	0.09	%
Ixx	0.000E+00	ton.m²	0.00E+00	kg.mm²	Ixx	8.51E+08	kg.mm²	#DIV/0!	%
Iyy	0.000E+00	ton.m²	0.00E+00	kg.mm²	Iyy	1.16E+09	kg.mm²	#DIV/0!	%
Izz	0.000E+00	ton.m²	0.00E+00	kg.mm²	Izz	1.37E+09	kg.mm²	#DIV/0!	%
Xcg	0.000	m-SM	0.00	mm	Xcg	-0.80	mm-SM	-0.80	mm
Ycg	0.000	m-LC	0.00	mm	Ycg	-0.65	mm-LC	-0.65	mm
Zcg	-14.610	m-LB	-292.20	mm	Zcg	-289.33	mm-LB	-0.98	%

3.3 Model Hydrostatics

Refer to section 2.3

K. VIDEO TRANSCRIPT

This page intentionally left blank.

OTEC Coupled Physical Model Tests conducted October-November 2013

Video Script

Introduction

00:00 Every day the sun transmits millions of gigawatts of solar energy to the surface of the Earth. This is thousands of times more energy than all the power consumed daily by mankind.

00:17 Much of this incoming solar energy is absorbed by the oceans which act as a massive heat sink – a kind of enormous heat battery.

00:27 Ocean Thermal Energy Conversion, or OTEC, - a bold, yet simple, way to tap this heat and convert it into electricity without any additional fuel … has the potential to significantly reduce the global consumption of fossil fuels.

00:45 The OTEC concept uses the temperature difference between warm surface seawater and the deeper cold water. In tropical waters, this temperature difference can be 20 degrees Celsius, about 36 degrees Fahrenheit, or more.

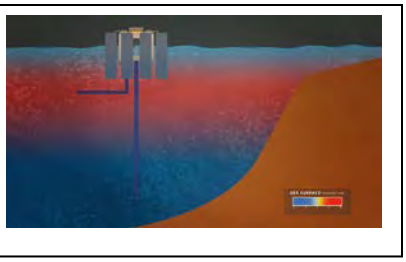

01:02 In this design, a semi-submersible platform is moored several miles offshore. The platform supports a kilometer long pipe that conveys the cold seawater to the platform. Simultaneously warm water enters the platform from the surface.

01:20 The warm water passes through an evaporator which boils a liquid working fluid, such as anhydrous ammonia, contained within a closed circuit. The now gaseous ammonia drives a turbine to generate electricity. The gas then enters a condenser where it is cooled by frigid seawater from the cold water pipe, returns to a liquid and is pumped back to the evaporator to continue the cycle.

01:49 A Lockheed Martin Corporation led team of subcontractors has designed a 100-megawatt OTEC system capable of fabricating the 1,000-meter cold water pipe, or CWP, directly from the platform.

02:05 Once the cold water pipe is completed, the fabrication facility is removed, and the Power Modules containing the seawater pumps and heat exchangers are installed.

02:16 The United States Department of Energy and Lockheed Martin jointly sponsored model tests of the semi-submersible platform, the cold water pipe, and the connection between the two. These tests examined each of this marine structure's many configurations for motions, forces, and pipe bending behavior. The project's test data will be used to validate the numerical predictions of platform and pipe responses to operational and extreme waves.

02:46 Testing at the relatively large scale of 50 to 1 was conducted at one of the few hydrodynamic research basins in the world that can accommodate such a deep model, LabOceano.

03:01 Located near Rio de Janeiro on Ilha do Fundao, a sort of Silicon Valley of deep-water petroleum technology, this exceptional facility is operated by the Federal University of Rio de Janeiro. Nearby are the headquarters of Petrobras, the Brazilian oil company, and a host of the leading companies in the deep-water oil industry.

03:25 The model test program at the LabOceano examined three of the major components of the OTEC system.

03:35 The Platform

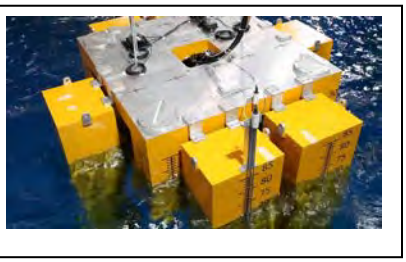

03:40 Based on the proven semi-submersible design common to the offshore oil industry, the platform is well understood from decades of development and operations.

03:51 The fiberglass covered aluminum model is 1.4 meters square and 800 centimeters high, roughly four and a half feet square by two and a half feet high. The semi-submersible was tested in four configurations:

1. The platform by itself, ballasted to include the weight of the pipe fabrication facility.
2. The platform with 6 power modules.

3. The platform in the cold water pipe fabrication phase, without power modules, with two different pipe lengths of 500 and 1,000 meters.
4. And the platform in the operational mode with 6 power modules and the 1,000 meter CWP.
04:35 The total full-scale weight of an operational OTEC system and platform is 217,000 tons.

04:45 The Cold Water Pipe

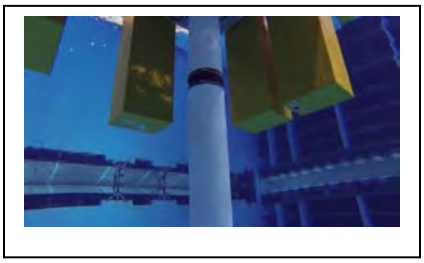

04:50 The fiberglass reinforced cold water pipe has a full-scale diameter of 10 meters, which is two meters larger than one of the railway tunnels in the England to France Chunnel. The total cold seawater flow rate is about a third that of Victoria Falls in Zimbabwe.

05:10 Here, two technicians stand beside a four-meter prototype model of the cold water pipe built by Lockheed.

05:18 The mass of the cold water pipe, including the entrained seawater, is greater than the mass of the semi-submersible platform.

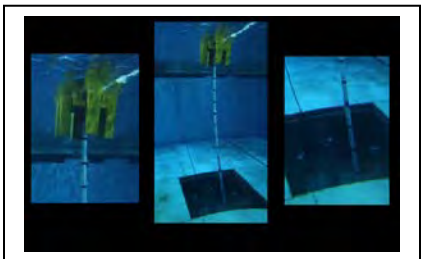

05:28 The CWP is significantly larger than typical pipes used in the offshore industry, so determining the model scale pipe's loads and the behavior of the coupled system are vital to assessing the entire project's feasibility.

05:45 A previous investigation of large-diameter composite pipe was an extensive 1983 NOAA-sponsored at-sea trial of a 2.5-meter diameter, 130 meter-long reinforced-fiberglass composite pipe. These trials yielded important data about the pipe's behavior, bending characteristics, and fatigue life.

06:09 The cold water pipe model has a core tube consisting of four sections of 38 millimeter or 1.5" diameter aluminum pipe. This models the bending stiffness of the CWP. The outside diameter is modeled by twenty discontinuous tubular sheets made of composite material, which represents the pipe's hydrodynamic diameter. The outer sections are centered on the inner core, and adjacent sections are sealed with rubber strips so that bending stiffness is not affected.

06:44 The pipe core is instrumented with 20 sensitive strain gauges. Here one-half of the assembled pipe is suspended from the lab's rafters for a Pipe Impulse Response test. The impulse is applied to the core with a common hammer to determine the natural frequencies of the pipe. The strain gage data is displayed for each channel as a time line.

07:12 The pipe's spatial location is measured with an underwater optical tracking system.

07:18 The CWP is floated into the water and divers install the 20-meter model in the LabOceano test basin. The depth at the bottom of the center pit is 25 meters, deep enough that the divers must decompress before emerging. Because so little is known about the behavior of the cold water pipe in the physical world, the loads, motions and bending test data is invaluable.

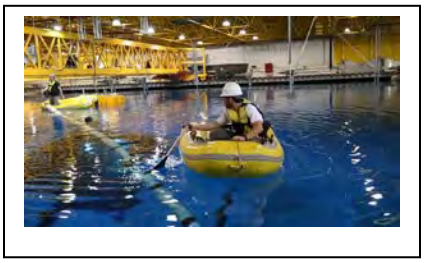

07:50 The Coupling

07:56 During fabrication the cold water pipe is almost rigidly connected to the platform. As the fabricated length becomes longer, the pipe's response to waves and currents increases and begins to affect the platform.

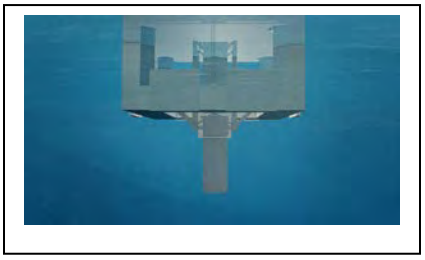

08:12 Because there is no way to accommodate its motions relative to the platform the coupled structure is particularly vulnerable to storms with the largest loads and forces concentrated at the lower location.

08:27 In operation, the CWP is coupled to the platform by a huge gimbal which acts like a universal joint to accommodate the motions and lessen bending strains on the pipe. The model gimbal was carefully instrumented to record forces and angles. Two different gimbals were tested: a free gimbal and a restrained gimbal.

08:54 The Sea States

09:00 The ideal locations for OTEC systems are in tropical waters with a thousand meter water depth within several kilometers of shore. Within the United States, Hawaii and Puerto Rico are of prime interest. Internationally, there are many candidates from the

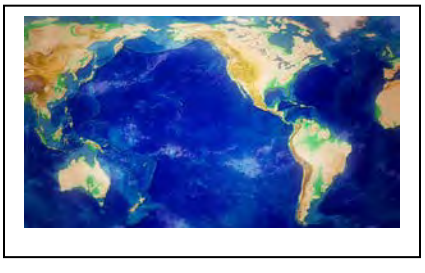

South Pacific to the South China Sea as far as the Indian Ocean.

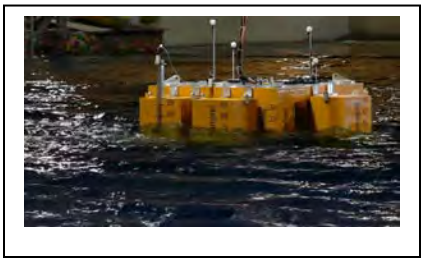

09:24 The wave conditions selected for the tests cover a range of likely design conditions for these locations, from monsoonal storms to large swells to tropical cyclones.

09:38 The tests shown here were conducted on the coupled OTEC model in the operational stage with a free gimbal. To appreciate the motions of the model, as they would appear in real time this video footage has been slowed by a factor of seven to represent its full-scale behavior.

09:59 Here the pipe is seen flexing during a ten-year swell. If we superimpose a frame of the structure in calm water as a reference, you can see the relative differences in the pipe's shape as the sea state develops.

10:20 However if we speed up the footage it is much easier to appreciate just how much the pipe flexes in model scale time.

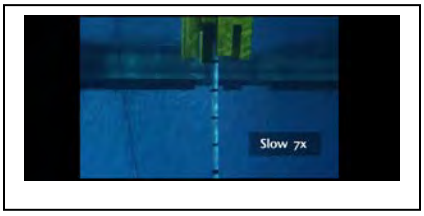

10:35 The bending of the pipe dynamically affects the loads and angles at the gimbal. This constant flexing determines the pipe's fatigue life - so it is imperative that the CWP's bending properties are fully understood.

10:52 Here the pipe is seen being excited by regular waves with a significant height of 8.5 meters and a period between peaks of 13 seconds. Though such a series of waves are never seen in the real ocean, they offer invaluable base-line data. Once again when the footage is speeded up you can see the regular rhythm of the pipe's undulations.

11:30 The coupled OTEC system is designed for a twenty-year or more life span. For these permanent systems, it is common to design for an event with a likelihood of occurring only once in one hundred years.

11:45 Therefore, it is vital to understand the total system's behavior in a 100-year cyclone, first to see if it can survive a maximum strength cyclone, and

secondly to understand what are the forces imposed on the unified structure … and which specific points might be especially vulnerable.

12:07 Because the gimbal couples the cold water pipe to the platform, it is of extreme interest. In the 100-year cyclone as seen here, the gimbal seems to handle the various angles of force quite smoothly.

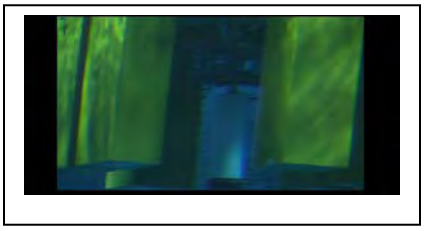

12:24 Throughout the cyclone - waves and wind excite the platform inducing loads and motions on the pipe's much larger mass.

12:34 The OTEC coupled model tests carefully examined a unique marine concept that has never before been studied in the physical world. Nearly a hundred sensitive instruments measured the loads, forces and motions of the coupled system in a variety of sea states. This data set will allow benchmarking of future theoretical analyses of the 100-megawatt OTEC concept as well as other applications of the cold water pipe technology.

13:05 OTEC offers an enormous amount of benefit to humanity and the environment… and these model tests are a big step forward in understanding the behavior of such a complex marine structure.

13:21 Engineers working with this test program's data over the next months and years will find the answers to a range of technical problems… and it is almost certain, that they will also discover the questions that have not yet been asked.

13:45 Credits:

U.S. Department of Energy
Lockheed Martin
Petrobras
LabOceano
John Halkyard & Associates
BMT Scientific Marine Services
Houston Offshore Engineering
Group 1 Production

L. DVD CONTENT

This page intentionally left blank.

Appendix L – DVD Content

The following files are provided on the attached DVD.

- OTEC CWP-Platform Subsystem Dynamic Interaction Validation Final Report DE-EE0003637.pdf
- Consolidated As-Built Tables.xlsm
- Regular Wave Calibration Summary.xlsx
- Irregular Wave Calibration Summary.xlsx
- Four versions of the project video:
    - The OTEC Model Basin Test Video.mov (2,167,994 KB)
    - The OTEC Model Basin Test Video-HD.mp4 (283,088 KB)
    - The OTEC Model Basin Test Video-SD.mp4 (92,152 KB)
    - The OTEC Model Basin Test Video-Mobile.mp4 (44,080 KB)